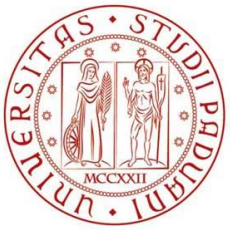

UNIVERSITÀ DEGLI STUDI DI PADOVA

Sede Amministrativa:

UNIVERSITÀ DEGLI STUDI DI PADOVA

DIPARTIMENTO DI INGEGNERIA INDUSTRIALE

CORSO DI DOTTORATO DI RICERCA IN: Ingegneria Industriale

CURRICOLO: Ingegneria Chimica ed Ambientale

CICLO: XXX

EXPLOITATION OF MICROALGAL BIOMASS AS AN ALTERNATIVE SOURCE TO BIOETHANOL PRODUCTION

Direttore della Scuola: Ch.mo Prof. Paolo Colombo

Coordinatore di Indirizzo: Ch.mo Prof. Matteo Strumendo

Supervisore: Ch.mo Prof. Alberto Bertucco

Dottorando: Carlos Eduardo de Farias Silva

2017

Contents

Abstract

This research project aimed to collect the information available regarding microalgal ethanol and to expand/study the real applicability of microalgae to this purpose. A literature review and theoretical analysis of an ethanolic biorefinery using microalgal biomass revealed lacking information regarding the maximum carbohydrate productivity achievable using this source, the hydrolysis and fermentation steps and the issue of nutrient recovery/recycling. Experimental procedures and process simulation were carried out as well. The entire work was divided in two parts: 1) microalgal cultivation and 2) hydrolysis and fermentation steps.

In the cultivation step, three species were used: *Synechococcus* PCC 7002 (in batch mode), *Chlorella vulgaris* and *Scenedesmus obliquus* (in continuous mode). Batch experiments optimized carbon source and pH stabilization of *S.* PCC 7002 developing an inorganic buffer CO_2-bicarbonate as the best strategy. In addition, this species was cultivated in urban wastewater and was able to remove chemical oxygen demand, nitrogen and phosphorous below the law limits to discharge into hydric bodies, thus representing an environmental gain with valorisation of the biomass produced, where a high carbohydrate content was achieved. About the continuous cultivation of *C. vulgaris* and *S. obliquus*, the effect of a combination between nitrogen inlet concentration, light intensity and residence time was studied and remarkable values of carbohydrate productivity were obtained under both constant and seasonal light irradiation regimes. To complement the study, the simulation of a two-unit system (reactor + settler) based on a steady-state model was done to understand the influence of the operating variables in biomass production and to highlight the crucial role of the recycle ratio.

Both acidic and enzymatic hydrolysis were investigated. For the first one the operating conditions of time, temperature and acid concentration were optimized, proposing a kinetic model for biomass solubilization and sugars hydrolysis. This model was successful applied within the concept of severity factor. Enzymatic hydrolysis was focused on the role of enzyme type/concentration and on the use of ultrasonication as a pretreatment method in order to improve enzyme accessibility. A suitable amylase, pectinase and cellulase mix was efficient to de-structure the carbohydrates present in the biomass. Both hydrolytic methods reached more than 90% of sugars recovery. Yeast fermentation of the hydrolysates were eventually carried out and the presence of inhibition with respect to a control condition showed that further studies are necessary to improve this step.

Foreword

This research project was a collaboration between CNPq (Conselho Nacional de Desenvolvimento Científico e Tecnológico do Brasil – Brazilian Council of Scientific and Technological Development) and University of Padova through the Project number 249182/2013-0 (Doutorado Pleno no Exterior) – Cultivo e exploração de biomassa de microalgas como uma alternativa para a produção de bioetanol (Exploitation of microalgal biomass as an alternative to bioethanol production).

The research work was completely performed at Department of Industrial Engineering (DII) under the supervision of Prof. Alberto Bertucco.

As a tangible result of the work completed during the Ph. D. school, a number of publications and presentations to conferences has been produced, as listed below.

Publications in Referred Journals

1. **De Farias Silva**, C.E., Gris, B., Sforza, E., Rocca, N., Bertucco, A. Effects of sodium bicarbonate on biomass and carbohydrate production in *Synechococcus* PCC 7002. Chemical Engineering Transactions, 49, 241-246, 2016.
2. **De Farias Silva**, C.E., Bertucco, A. Bioethanol from microalgae and cyanobacteria: a review and technological outlook. Process Biochemistry, 51, 1833-1842, 2016.
3. **De Farias Silva,** C.E., Gris, B., Bertucco, A. Simulation of microalgal growth in a continuous photobioreactor with sedimentation and partial biomass recycling. Brazilian Journal of Chemical Engineering, 33(4), 773-781, 2016.
4. **De Farias Silva**, C.E., Sforza, E. Carbohydrate productivity in continuous reactor under nitrogen limitation: Effect of light and residence time on nutrient uptake in *Chlorella vulgaris*. Process Biochemistry, 51, 2112-2118, 2016.
5. **De Farias Silva**, C.E., Sforza, E., Bertucco, A. Effects of pH and carbon source on *Synechococcus* PCC 7002 cultivation: biomass and carbohydrate production with different strategies for pH control. Applied Biochemistry and Biotechnology, 181, 682-698, 2017.
6. **De Farias Silva**, C.E., Sforza, E., Bertucco, A. Stability of carbohydrate production in continuous microalgal cultivation under nitrogen limitation: Effect of irradiation regime and intensity on *Scenedesmus obliquus*. Journal of Applied Phycology, in Press, 2017.
7. **De Farias Silva**, C.E., Bertucco, A. Dilute acid hydrolysis of microalgal biomass for bioethanol production: an accurate kinetic model of biomass solubilization, sugars hydrolysis and nitrogen/ash balance. Reaction Kinetics, Mechanisms and Catalysis, 122, 1095-1114, 2017.
8. **De Farias Silva**, C.E., Bertucco, A. Bioethanol from microalgal biomass: a promising approach in biorefinery. Brazilian Archives of Biology and Technology, in Press, 2018.

Book Chapters

1. **De Farias Silva**, C.E., Sforza, E., Bertucco, A. Enhancing carbohydrate productivity in photosynthetic microorganism production: A comparison between cyanobacteria and microalgae and the effect of cultivation systems. Chapter 22 – Advanced Bioprocessing for Alternative Fuels, Biobased Chemicals and Bioproducts. Elsevier, in Press, 2017.
2. **De Farias Silva**, C.E., Barbera, E., Bertucco, A. Bio-refinery as a promising approach to promote ethanol industry from microalgae and cyanobacteria. Chapter 17 – Bioethanol Production from Food Crops. Elsevier, in Press, 2017.

Papers submitted for publication in Referred Journals

1. **De Farias Silva**, C.E., Bertucco, A. A two-stage system for the continuous cultivation of biomass: An analytical analysis and development of a limiting operative variables approach to process control assessment. BioEnergy Research, 2017.
2. **De Farias Silva**, C.E., Bertucco, A. Severity factor as an efficient control parameter to predict biomass solubilization and saccharification during acidic hydrolysis of microalgal biomass: An accurate phenomenological kinetics and discussion regarding literature simplifications. BioEenergy Research, 2017.
3. **De Farias Silva,** C.E., Meneghello, D., Abud, A.K.S., Bertucco, A. Ultrasonication intensity in the enzymatic hydrolysis of microalgal sugars. Fuel, 2017.
4. **De Farias Silva,** C.E., Meneghello, Bertucco, A. A systematic study regarding hydrolysis and ethanol fermentation from microalgal biomass. Biocatalysis and Agricultural Biotechnology, 2017.

Paper or abstracts in Conference Proceedings

1. Gris, B., **De Farias Silva**, C.E., Sforza, E., La Rocca, N., Bertucco, A. Evaluation of the effects of different light intensities and carbon sources on growth of two species of cyanobacteria. Algology Reunion. Riunione Annuale del Gruppo di Algologia, 6 – 7 Novembre – 2015 – Venice – Italy (http://www.societabotanicaitaliana.it/uploaded/2547.pdf). Oral presentation.
2. **De Farias Silva**, C.E., Sforza, E., Bertucco, A. Continuous cultivation of *Chlorella vulgaris* to improve the carbohydrate production. EABA – European Algae Biomass Association – Congress, 1 – 3 December – 2015 – Lisbon – Portugal (http://algaecongress.com/). Poster presentation.
3. **De Farias Silva**, C.E., Gris, B., Sforza, E., La Rocca, N., Bertucco, A. Effects of sodium bicarbonate on biomass and carbohydrate production in *Synechococcus* PCC 7002. IBIC – International Conference on Industrial Biotechnology, 10 – 13 April – 2016 – Bologna – Italy (http://www.aidic.it/ibic2016/). Oral presentation.
4. **De Farias Silva**, C.E., Sforza, E., Bertucco, A. Improving carbohydrate productivity in a continuous system for microalgal cultivation to biotechnological applications. 1st Forum Italiano sulle Tecnologie Microalgali, 6 – 7 April – 2017 - Palermo – Italy. Poster presentation.

5. **De Farias Silva**, C.E., Sforza, E., Bertucco, A. Continuous cultivation of microalgae as an efficient method to improve productivity and biochemical stability. 25th European Biomass Conference and Exhibition, 12 – 15 June – 2017 – Stockholm – Sweden (http://www.eubce.com/home.html). Poster presentation.

Riassunto

L'obiettivo generale di questo progetto di ricerca è stato di verificare la potenzialità delle microalghe come fonte alternativa di biomassa per la produzione di etanolo. In particolare, sono state discusse teoricamente, sperimentalmente e tramite simulazione di processo la coltivazione, l'idrolisi e la fermentazione della biomassa microalgale.

Inizialmente, grazie ad un'ampia ricerca bibliografica ed a prove preliminari effettuate nel Laboratorio Microalghe del Dipartimento di Ingegneria Industriale della Università di Padova si è dimostrato che le specie più promettenti da studiare erano *Synechococcus* PCC 7002, *Chlorella vulgaris* e *Scenedesmus obliquus*, grazie alle loro elevate velocità di crescita e capacità di accumulo di carboidrati, che costituiscono le materia-prima per la produzione di etanolo (fino al 50-60% del peso secco).

In particolare, l'attenta analisi della letteratura riguardo a queste specie ha consentito di verificare che:

- per la produzione di carboidrati è preferibile sviluppare un processo continuo, perché richiede un solo step, mentre il processo batch ne richiede due, e perciò consente di ottenere produttività significativamente inferiori;
- sono disponibili pochi lavori sulla possibilità di usare le microalghe in un processo continuo di questo tipo, mentre sono parecchi i riferimenti al processo batch;
- mancano informazioni sulla capacità di produrre carboidrati da parte di *S.* PCC 7002.

In una prima parte del lavoro sono stati quindi pianificati e condotti esperimenti in modalità batch con *S.* PCC 7002, per studiare come mantenere la stabilità e vitalità della coltura durante tutto il periodo di coltivazione. Si sono rilevati problemi con il controllo del pH, ed é stato approfondito l'uso di bicarbonato come fonte di carbonio assieme ad un tampone inorganico, dimostrando in un primo lavoro che il suo impiego è efficiente per la produzione di biomassa ma insufficiente per accumulare un alto contenuto di carboidrati, a causa di una significativa inibizione osmotica causata dall'alta concentrazione di sodio in soluzione. D'altro canto, l'applicazione di un tampone con sostanze organiche, generalmente usato nella coltivazione di microalghe e cianobatteri, ha evidenziato notevoli fenomeni di tossicità per questa specie. Al contrario, il tampone inorganico CO_2-bicarbonato messo a punto successivamente è stato capace di garantire la stabilità del pH durante 12 giorni di

coltivazione, ed ha consentito di ottenere 6 g L^{-1} di biomassa (peso secco) con circa il 60% di contenuto di carboidrati.

La coltivazione in continuo di *C. vulgaris* in un fotobioreattore piatto e sottile è stata studiata per verificare la produzione di carboidrati secondo questa modalità operativa. Il lavoro ha evidenziato l'importanza della riduzione della concentrazione di azoto in entrata al reattore, che va rapportata ai valori di intensità di luce e tempo di residenza per massimizzare la produzione di carboidrati. Si sono misurati valori massimi per la produttività di biomassa e di carboidrati pari a 0.7 e 0.37 g L^{-1} $giorno^{-1}$. La stessa procedura é stata usata nello studio del comportamento di *S. obliquus*, per vedere se l'approccio era valido anche durante la coltivazione all'aperto, simulando la fornitura della luce in modo stagionale. *S. obliquus* ha mostrato una produttività quasi tre volte maggiore che *Chlorella*, raggiungendo valori di 0.8 g L^{-1} $giorno^{-1}$ (con luce costante) e di 0.71 g L^{-1} $giorno^{-1}$ (nell'estate). Questa produttività di carboidrati, se estrapolata a dimensioni industriali, consentirebbe di ottenere tra 45–100 $ton_{biomass}$ ha^{-1} $anno^{-1}$, ben di più di quanto prodotto con le fonti tradizionali di carboidrati.

Un sistema reattore-sedimentatore con riciclo parziale di biomassa è generalmente usato a livello industriale in processi di coltivazione e/o fermentazione. Questo sistema fornisce semplicità e diversi vantaggi per la produzione su larga scala. É stato quindi messo a punto un modello per la simulazione di tale processo, nel caso specifico delle microalghe, per verificare l'influenza dei gradi di libertà (tempo di residenza, rapporto di riciclo della biomassa, età della biomassa e sua velocità di sedimentazione) sulle prestazioni. I principali risultati sono:

- la definizione di un rapporto di riciclo minimo R_{min}, di un intervallo operativo per la stessa variabile, e di un valore massimo per la portata di spurgo di biomassa Fw_{max};
- la dimostrazione che la perdita di biomassa dalle sommità del sedimentatore abbassa significativamente le prestazioni del sistema;
- la costruzione di grafici adimensionali che legano R a $\theta c/\theta$ e F_I/F_W (età della biomassa/tempo di residenza, e rapporto tra le portate di ingresso e di spurgo);
- il confronto fra il modello rigoroso messo a punto ed il modello semplificato generalmente considerato in letteratura.

Synechococcus è stata coltivata in acque reflue urbane (sintetiche e reali, con valori di COD pari a 340.0 ± 14.1 mg L^{-1}, di azoto totale pari a 31.0 ± 1.4 mg L^{-1}, e di fosforo totale a 8.20 ± 0.99 mg L^{-1}), con l'obbiettivo di ottenere la depurazione da questi inquinanti. Questa specie è stata molto efficiente nella rimozione di COD, azoto e fosforo totale, raggiungendo valori sotto i limiti di legge in due giorni di coltivazione. L'acqua reflua sintetica ha evidenziato una

limitazione dei micronutrienti quando la concentrazione di COD era elevata, differentemente dell'acqua reflua reale, in cui *Synechococcus* è cresciuta più velocemente.

Successivamente, l'idrolisi e la fermentazione di biomassa microalgale sono state studiate con riferimento ai processi di saccarificazione acida ed enzimatica, e con riferimento ai microorganismi *Saccharomyces cerevisiae* e *Pichia stipitis*, rispettivamente. L'idrolisi acida, con acido solforico 0-5% v/v, è stata condotta a diverse temperature (110-130 °C) e tempi di reazione (0-60 min) partendo da 100 g L^{-1} di concentrazione di biomassa (*Chlorella vulgaris*). Gli zuccheri idrolizzati sono stati recuperati con un valore massimo pari al 92%, ottenuto con il 3% di acido e 20 min di reazione a 120 °C. La solubilizzazione di biomassa ha esibito un ordine di reazione n = 3.63 ± 0.18 ed un'energia di attivazione pari a 41.19 ± 0.18 kJ/mol. Questi valori sono significativamente diversi di quelli trovati per l'idrolisi di matrici lignocellulosiche, generalmente considerata di primo ordine con *Ea* = 100-200 kJ/mol, e dimostrano che la biomassa microalgale è più suscettibile al trattamento termico catalizzato all'acido in confronto ai lignocellulosici. Un'equazione basata sulla cinetica di Michaelis-Menten modificata per tenere conto della concentrazione di acido è riuscita a modellare tutti i risultati sperimentali, con un valore della costante di semi-saturazione per la biomassa Pol_{KM} pari al 42% della concentrazione iniziale, e con una resa di fermentazione di circa il 60%.

Prima di realizzare l'idrolisi enzimatica, si é reso necessario procedere ad un'ottimizzazione del pretrattamento della biomassa. È stata studiata l'ultrasonicazione applicando un piano statistico di sperimentazione su tre livelli con 3 esperimenti centrali (in tutto si sono condotte 11 prove). Le variabili ottimizzate sono state l'intensità, il tempo di pretrattamento e la concentrazione di biomassa. I risultati hanno dimostrato che l'intensità e il tempo di trattamento sono più importanti e consentono di ottenere un recupero degli zuccheri superiore al 90%, in 4-8 ore. Si é visto che l'energia spesa nel processo di ultrasonicazione non è direttamente collegata con l'efficienza dell'idrolisi, per cui questa può essere condotta efficientemente anche riducendo il consumo di energia nel pretrattamento.

Infine, si sono eseguiti esperimenti di fermentazione dell'idrolizzato ad etanolo con le due specie menzionate (*S. cerevisiae* e *P. stipitis*). Si sono ottimizzati la concentrazione di inoculo (7.5 g L^{-1}) ed il consorzio (25% *Pichia* + 75% *Saccharomyces*) per avere una produttività tra 5 e 10 g L^{-1} ora^{-1} (prossimo al valore industriale). Si è però visto che le velocità di fermentazione sono però più basse a causa di una inibizione dovuta alla accresciuta salinità dell'idrolizzato, un fattore. Per questo motivo, la parte di fermentazione necessita di essere più approfondita al fine di validare l'impiego di questo tipo di biomassa a livello industriale.

Introduction

The use of natural sources in economic activities can aid in the resource saving and recycling and reuse of wastes, contributing for a more sustainable world by providing clean technologies in the industrial and agricultural sector in both developed and developing countries.

In general, increased and improved global strategies for energy safety, security and mitigation of CO_2 emissions from energy production processes are required, especially those aimed at maximizing the energy efficiency by expanding the use of clean energy. This means using fuels that are able to implement the carbon cycle without changing the atmospheric balance (renewable fuels), by developing energy resources in CO_2 reduced/neutral systems (Brennan and Owende, 2011; Moraes et al., 2017).

The expansion of biofuels production and use is an important issue since it plays primary role in reducing global the climate change. But, in order to insert a new source/technology in the market, several factors are involved such as industrial aspects and economic feasibility, legal restrictions and incentives, international trade, land use, raw material availability and management techniques.

At present, ethanol is the main biofuel produced worldwide. Between 2007 and 2015 bioethanol throughput practically doubled, reaching 25 billion gallons per year, even though after 2010 the production was stagnant (AFDC, 2016). This is the result of a number of reasons, to cite:

- high dependency on the first-generation crops which need a lot of arable land and compete directly with food/feed production;
- need for a complete validation of the lignocellulosic ethanol industry due to unsuitability of the large-scale process because of corrosion problems (mainly in the pretreatment), cost of enzymes, difficult/inhibition of the fermentation step;
- difficulty to utilize all lignocellulosic fractions, according to a biorefinery approach, because each biomass has its biological complexity and the related lignocellulosic content/arrangement/recalcitrance changes significantly;
- Lacking of investments/incentives (mainly, governmental) after the decrease of petroleum prices occurred at the end of 2014.

In fact, based on the type of biomass, bioethanol production is classified as first (raw material saccharine or starch-based – sugarcane and corn); second (lignocellulosic materials); third (microalgal/macroalgal biomass) and fourth (genetically modified cyanobacteria) generation.

Sugar cane ensures the lowest bioethanol production costs. In spite of its significant advantage, it is not a viable option for all the regions of the planet owing to climatic and soil limitations (Belincanta et al., 2016). Consequently, countries of the northern hemisphere have been incessantly looking for new technological routes that permit the efficient production of biofuels while respecting environmental and economic sustainability issues, and 'new' generations of biomass-to-ethanol processes are proposed. In addition, countries as Brazil have their sugarcane cultivation saturated, i.e., there is no new extensions of arable land to expand significantly the Brazilian ethanol industry.

Low production costs are the advantage of first generation bioethanol, with the exception of corn-based one, which has a well-established and economically sustainable technology, while second generation still requires more investigations to become economically competitive, with pretreatment and hydrolysis processes needing to be more effective and largely scalable (Gupta and Verna, 2015). On the other hand, micro and macroalgae have not reached a maturity for designing and operating industrial scale plants yet. Therefore, in the case of third and fourth generation bioethanol, further studies are required to develop a competitive and consolidated technology, taking into account also issues other than technological ones.

In third generation bioethanol, microalgae and/or macroalgae biomass are used, which do not have lignin in their cellular structure, and are cultivated with higher growth rates when compared to higher plants. As for this biomass, a suitable process is not available yet, and the related costs cannot be properly estimated. Researchers are currently trying for microalgae: to optimize microalgal productivity and cultivation conditions, as this represents the highest production costs, considering that hydrolysis and fermentation are instead easier compared with lignocellulosics and macroalgae (Jonh et al., 2011; Wei et al., 2013; Hong et al., 2014).

Thanks to their high growth rate, and relatively simple biochemical composition (partitioned among carbohydrates, lipids and proteins), microalgae are acknowledged as very promising feedstock for bioethanol production (Chen et al., 2013). Main aspects needing to be developed in this respect are: carbohydrate cultivation (productivity), hydrolysis and ethanolic fermentation and nutrient recycling/recovery from residual medium/biomass.

With regard to the open issues recalled above, the aim of this research project has been to address and study how to improve the knowledge and discuss the real potentiality of microalgal biomass as a feedstock for an effective bioethanol production, from a perspective

of biomass/carbohydrate productivity (microalgal cultivation) and bioconversion process (hydrolysis and fermentation) in a context of a biorefinery concept. In fact, experimental values about fermentation applications from microalgae are not expanded yet in literature. The topics addressed by this thesis are organized and subdivided in twelve chapters as follows.

In **Chapter 1**, a literature survey to collect and discuss the available information about bioethanol from photosynthetic microorganisms, and to delimit the main lacks to be developed, is done.

Chapter 2 shows a basic analysis of an ethanol biorefinery scheme aimed to include microalgal biomass, discussing the main bottlenecks and the processes which must be developed to adequately evaluate the potentiality of this type of biomass for industrial fermentation proposes.

Chapter 3 treats specifically of the carbohydrate-rich biomass cultivation from microalgae utilizing nutritional and environmental techniques. Operation mode of microalgae cultivation is discussed as well, and the importance to consider semi-continuous and continuous processes is shown, because batch mode is extensively used but less efficient.

Chapter 4 develops a design procedure of a two-unit system composed by a reactor and settler, discussing the influence of operating variables and their limiting values. Specifically, recycle ratio and purge flow rate concepts and effects are extensively studied.

In **Chapter 5**, the carbohydrate cultivation with *Synechococcus* PCC 7002 is optimized with respect to the carbon source and pH, because a stable pH (greatly influenced by the carbon source) is necessary for this strain and organic buffers exhibit toxicity. An inorganic buffer study (CO_2-bicarbonate) is developed and detailed.

Chapter 6 shows *S.* PCC 7002 treating urban wastewater to remove chemical oxygen demand, nitrogen and phosphorous content, thus ensuring a double gain: environmental enhancement and valorization of cyanobacterial biomass.

In **Chapter 7**, continuous cultivation of *Chlorella vulgaris* in flat-plate photobioreactors to improve carbohydrate productivity is assessed and evaluated using nitrogen limitation as a combination between nitrogen concentration inlet, light intensity and residence time under constant light intensity.

Chapter 8 demonstrates that a similar approach used for the continuous cultivation of *C. vulgaris* is applicable also to *Scenedesmus obliquus*. Additionally, it is proved that under outdoor conditions (seasonal regime of illumination – summer and winter), a high carbohydrate content can be produced as well.

In **Chapter 9**, the kinetics regarding acidic hydrolysis to biomass solubilization and sugars depolymerization is studied with *Chlorella vulgaris* biomass. An n order kinetics for biomass solubilization and m order for acid concentration is applied for biomass solubilization, providing values of reaction order and activation energy for microalgae. In addition, a saccharification model based on the Michaelis-Menten model is proposed and validated.

Chapter 10 demonstrates how the kinetics considerations determined in the previous chapter can be efficiently applied with the concept of severity factor – CSF (combination between time, temperature and acid concentration). A literature discussion about some assumptions so far considered and the importance to know the biomass nature to determine a coherent range of CSF is provided.

Chapter 11 reports ultrasonication as an effective pretreatment method to improve enzyme accessibility and promote a high rate of hydrolysis from *Scenedesmus obliquus* biomass. Pretreatment time, ultrasonication intensity and biomass concentration are specifically studied in order to minimize the energy consumption since the bottleneck of the pretreatment method is a high energy dissipation.

In **Chapter 12**, ethanolic fermentation is addressed with acidic and enzymatic hydrolysates. A systematic optimization of inoculum concentration and consortium between *Saccharomyces cerevisiae* and *Pichia stipitis* is determined. Then, the influence of salinity/matrix characteristics was evaluated to understand possible interferences during fermentation process and exhibited lower biochemical yields than the control conditions. Thus, further fermentations experiments are necessary.

REFERENCES

AFDC. Ethanol production in the world. 2016. Available in: http://www.afdc.energy.gov/data/

Belincanta, J., Alchorne, J.A., Silva, M.T., 2016. The Brazilian experience with ethanol fuel: aspects of production, use, quality and distribution logistics. Brazilian Journal of Chemical Engineering 33(4), 1091-1102.

Brennan, L., Owende, P., 2010. Biofuels from microalgae – a review of technologies for production, processing, and extractions of biofuels and co-products. Renew. Sust. Energy Rev. 14(2), 557–577.

Chen, C., Zhao, X., Yen, H., Ho, S., Cheng, C., Lee, D., Bai, F., Chang, J., 2013. Microalgae-based carbohydrates for biofuel production. Biochem. Eng. J. 78, 1-10.

Gupta, A., Verna, J.P., 2015. Sustainable bio-ethanol production from agroresidues: a review. Renew. Sust. Energ. Rev. 41, 550 – 567.

Hong, I.K., Jeon, H., Lee, S.B., 2014. Comparison of red, brown and green seaweeds on enzymatic saccharification process. J. Ind. Eng. Chem. 20, 2687-2691.

Jonh, R.P., Anisha, G.S., Nampoothiri, K.M., Pandey, A., 2011. Micro and macroalgal biomass: A renewable source for bioethanol. Bioresource Technol. 102, 186-193.

Moraes, B.S., Petersen, S.O., Zaiat, M., Sommer, S.G., Triolo, J.M., 2017. Reduction in greenhouse gas emissions from vinasse through anaerobic digestion. *Appl. Energ.* 189, 21-30.

Wei, N., Quaterman, J., Jin, Y., 2013. Marine macroalgae. An untapped resource for producing fuels and chemicals. Trends Biotechnol 31(2), 70-77.

Chapter 1

Bioethanol from microalgae and cyanobacteria: state of the art

The increasing global demand for energy and advances in new biofuel production routes have increased the research on the potential of microalgae and cyanobacteria as a third generation of biofuels. The majority of research has been focused on using this type of biomass for producing biodiesel and biogas; however, more recent developments have indicated the potential of microalgae and cyanobacteria for the production of bioethanol. There are three routes for producing bioethanol from such microorganisms: the traditional one involving hydrolysis and fermentation of biomass with bacteria or yeast, the dark fermentation route, and the use of engineered cyanobacteria or "photofermentation". In recent years, the use of engineered cyanobacteria to directly produce ethanol has gained enormous attention, mainly after the successful use of these microorganisms in industrial plants. However, only little information is available on the efficiency and the real advantages and disadvantages of these processes, and particularly, a comparison between traditional processes and engineered cyanobacteria. This study compiles the main publications on the production of bioethanol from microalgae and cyanobacteria, and summarizes the main features, advantages, and key aspects for each type of process. The industrial implementation of these technologies depends on the capability of reducing production costs through more scientific research and technical development, to become competitive with the lower cost of fossil fuels also thanks to public subsidies[•].

[•] *Part of this chapter was published in Process Biochemistry (**Silva, C.E.F.**, Bertucco, A., 51, 1833-1842, 2016).*

1.1 INTRODUCTION

The fact that the future of transportation is associated with the exploitation of liquid biofuels and the development of their production process is widely recognized (Brennan and Owende, 2010). However, biofuels can be an effective replacement for traditional fuels only when their production costs are lower or energetically equivalent to the drilling and oil-refining costs.

At present, the biofuel sustainability is limited by the cost of production with a significant dependency on fossil fuels. As can be seen in **Figure 1.1**, the global energy matrix is composed of fossil carbon sources (about 87%), "with about 33% of oil, 30% of coal and 24% of natural gas". Renewable energy accounts for only 10% of the global energy. In particular, the "growing need to expand the use of renewable energy sources in a sustainable" way has boosted biofuel production worldwide (Moraes et al., 2015; Moraes et al., 2017).

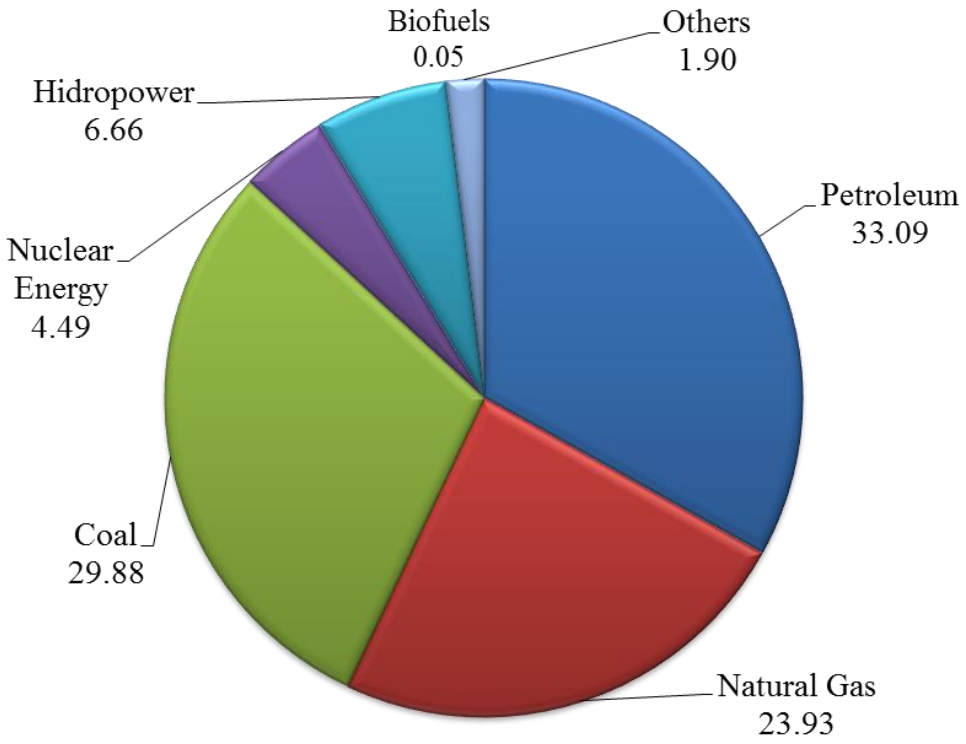

Figure 1.1: Energetic matrix worldwide. Adapted from BP Global 2015 and EPE, 2015.

In this study, the development of new cellular processes or enhancement of preexisting metabolic pathways in host microorganisms, and the production of rapid prototypes for testing are considered as crucial steps to convert biofuels into more feasible alternatives to the traditional fuels (Lee et al., 2008; Gupta and Verna, 2015).

The use of algae, microalgae, and cyanobacteria for the production of third-generation biofuels has many advantages over higher plants in view of producing first- and second-generation biofuels. This is due to their faster growth; capability of growing under several conditions, including in wastewater; reduced need for water and other resource inputs; and the possibility of not occupying arable lands for their cultivation.

The biochemical composition of microalgae grown under normal conditions, that is, without nutrient limitation, primarily encompasses proteins (30–50%), carbohydrates (20–40%), and lipids (8–15%) (Hu, 2004; Cardoso et al., 2011; Ho et al., 2013a). Effort to increase yields of biofuels produced by microalgae is underway, including the optimization of light technologies to modify the carbon uptake pathways, aimed at a higher accumulation of biomass or specific compounds such as carbohydrates and lipids (Gimpel et al., 2013) or, more recently, the use of genetic engineering for producing bioethanol, biohydrogen, and other special fermentation products (Beer et al., 2009; Angermayr et al., 2009; Ducat et al., 2011).

Photosynthetic organisms are favorable for the production of biofuels, mainly because of their low cost of cultivation, but biofuel yields obtained under normal conditions are not satisfactory (Desai and Atsumi, 2013). In addition to the production of biodiesel, microalgae and cyanobacteria serve as attractive feedstock for the production of bioethanol, although the scientific and technological knowledge on this context is still scarce (Harun et al., 2010; Ducat et al., 2011; John et al., 2011; Zhu et al., 2014). On the contrary, numerous studies have documented that the contents of oil and carbohydrates in microalgae cells can be increased under stress conditions, resulting, for instance, in a decrease of the protein content under nitrogen depletion (Ho et al., 2013a; Wang et al., 2013). This approach could be applied to cultivate microalgae biomass richer in carbohydrates, thereby leveraging their use for the production of bioethanol, which is currently the most widely used biofuel in the world.

Technologies for the first (sugar or starch feedstock) and second generation (lignocellulosic feedstock) of bioethanol basically involve two stages:

(i) the conversion of sunlight into chemical energy (such as carbohydrates and lipids) and; (ii) the conversion of chemical energy into biofuel.

(ii) These two stages are related to each other and result in increased production costs. As an improvement of this process, the use of a single-stage system that is capable of capturing sunlight directly and converting it into biofuel (bioethanol) would avoid one step, thereby reducing the cost of production and increasing the sustainability of the bioethanol production process.

Three possible routes involving the use microalgae and cyanobacteria biomass for bioethanol production are discussed in the literature. The first one is the traditional process in which the biomass undergoes pretreatment steps, enzymatic hydrolysis, and yeast fermentation. The second route is the use of metabolic pathways in dark conditions, redirecting photosynthesis to produce hydrogen, acids, and alcohols (such as ethanol). The third way is via "photofermentation", which is impracticable in nature. The last route requires the use of genetic engineering to redirect the preexisting biochemical pathways of microalgae for a more subjective and efficient production of bioethanol.

The aim of this chapter is to compile the main publications about the production of bioethanol from microalgae and cyanobacteria and to summarize the main features, advantages, and key aspects for each type of process. The open literature has been thoroughly examined, and published information is analyzed and discussed as from the source. In order to simplify the presentation of data from different sources, the units of measures have been converted as follows: volumes in L, biomass concentration in g L^{-1} (based on dry cell weight), temperature in °C, time of reaction in min, homogenous catalyst concentration in N (normality), yield of hydrolysis in % (respect to carbohydrates) and yield of fermentation in %, based on the maximum stoichiometric conversion of sugar into ethanol and carbon dioxide.

1.2 MICROALGAE AND CYANOBACTERIA FOR BIOFUELS

Photosynthesis is a vital process that drives the synthesis of all biofuels, by converting light energy into biomass, carbon storage products (e.g., carbohydrates and lipids), and a small amount of H_2. In green algae, the light-harvesting complex (LHC) (chlorophylls and carotenoids) absorbs photons from sunlight as chemical energy. This energy is used by the photosystem II (PS II) for the catalytic oxidation of water to form protons, electrons, and molecular oxygen. Low-potential electrons are transferred to the electron transport chain for the reduction of ferredoxin and then the formation of nicotinamide adenine dinucleotide phosphate (NADPH). An electrochemical gradient is formed, and the release occurs after oxidation of water in the thylakoid lumen, which is used to produce adenosine triphosphate (ATP) by ATP synthase. Photosynthetic products (NADPH and ATP) are substrates for the Calvin–Benson cycle, where CO_2 is fixed as C_3 molecules that are assimilated to form sugars, lipids, and other biomolecules essential for cell growth (Hu et al., 2004).

Biofuels from microalgae has been the subject of intense research mainly focused on the production of biodiesel and biogas, although bioethanol and biohydrogen are also considered (**Figure 1.2**). The production pathways and operating conditions vary for each biofuel. Several studies have already demonstrated the viability of industrial processes for the production of biodiesel, some of them suggesting the anaerobic digestion after extraction of lipid from algal biomass (Tercero et al., 2013; Santander et al., 2014; Sawaengsak et al., 2014; Tercero et al., 2014). However, studies aimed at consolidating suitable process for the production of bioethanol are still ongoing.

On the contrary, cyanobacteria strains have been shown to produce relevant amount of bioethanol (Markou et al., 2013; Mollers et al., 2014). The phylum Cyanobacteria or division Cyanophyta comprises a group of oxygenic bacteria that allow to obtain energy by photosynthesis. They are commonly referred to as blue-green algae, although the term algae is usually associated with eukaryotic organisms (such as the divisions Chlorophyta, Rhodophyta, and Heterokontophyta). It is currently known that these microorganisms are not phylogenetically related to any group of eukaryotic algae. Most species of cyanobacteria are terrestrial, but there are some marine species as well. *Spirulina*, *Chlorococcus*, *Gloeocapsa*, *Synechocystis*, and *Synechococcus* are some examples of genera grouped into the cyanobacteria phylum.

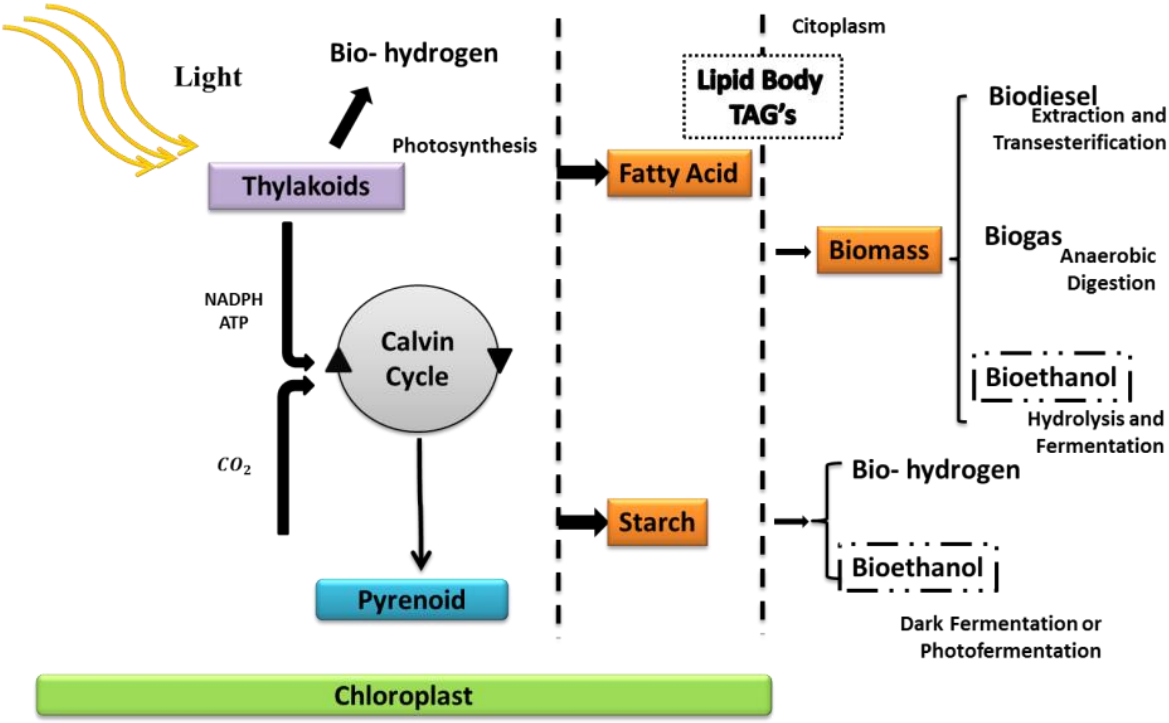

Figure 1.2: Biofuels potential from microalgae.

The production of bioethanol from microalgae and cyanobacteria is a feasible technological development, as they showed higher productivity than certain crops such as sugarcane and corn (already consolidated as feedstock for bioethanol production). Microalgae and cyanobacteria can reach 50% of their dry weight (DW) in carbohydrates, which can then be hydrolyzed and fermented with high yields. This fact will be better discussed later. They can also be easily concentrated, but the costs of cultivation are still high (Acién et al., 2012; Slade and Bauen, 2013; Tercero et al., 2014, Silva and Bertucco, 2016).

As described earlier, three routes exist for the production of bioethanol from microalgae:

(i) hydrolysis and fermentation of biomass;

(ii) dark fermentation and;

(iii) "photofermentation".

Each route has its own peculiarities, as discussed in the following sections and summarized in **Figure 1.3**.

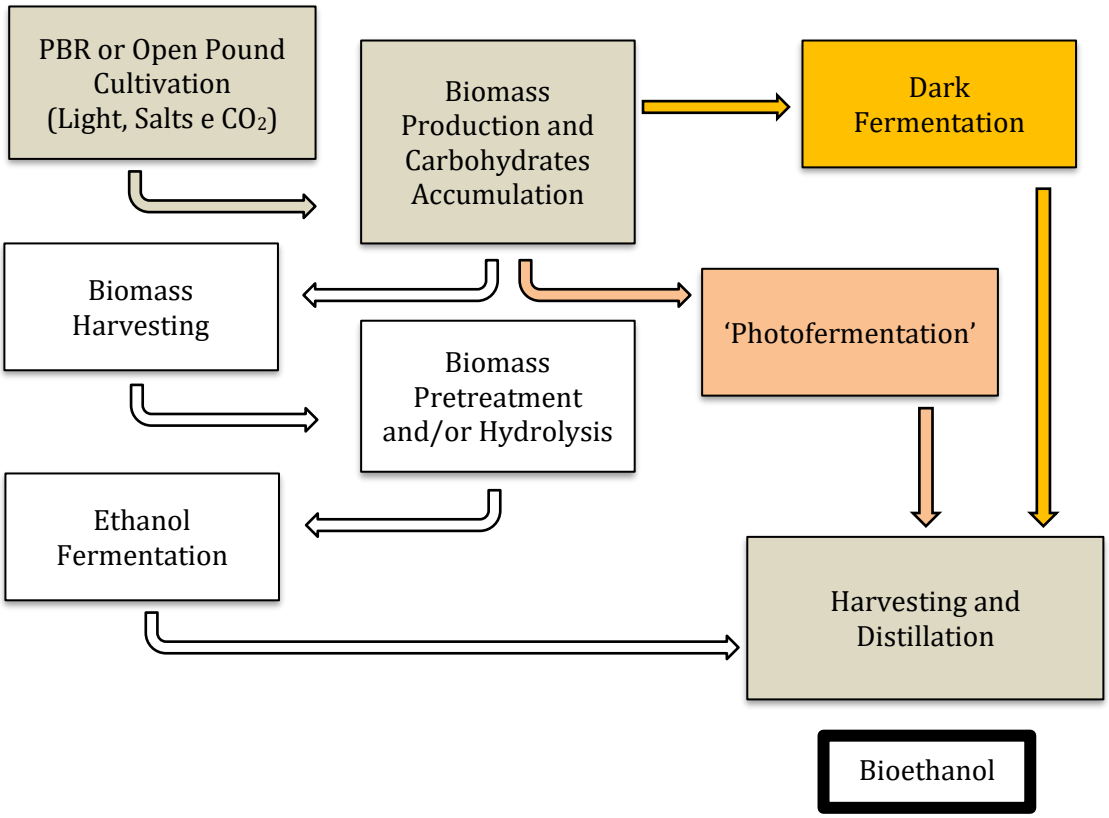

Figure 1.3: Routes for production of ethanol from microalgae.

1.3 BIOETHANOL PRODUCTION BY HYDROLYSIS AND FERMENTATION

This route is based on the production of microalgae biomass in photobioreactors succeeded by pretreatment steps (breakdown of the cell structure and hydrolysis of the biomass), and frequently by the addition of enzymes. The treated biomass is then fermented with yeasts or bacteria to obtain ethanol. The main drawbacks of this route are the multistep processes required, which demands more energy, and the use of enzymes and yeasts, which accounts for a considerable proportion of the costs. On the contrary, the hydrolysis/fermentation process converts biomass at the highest rate, because of the well-known high efficiency of enzymes and yeasts in converting biomass into products.

1.3.1 Microalgae cultivation and carbohydrate accumulation

Microorganisms with potential for bioethanol production in this way are selected primarily in accordance with their ability to accumulate carbohydrates, which depends on environmental and nutritional conditions. The main environmental factors are light intensity, pH, salinity, and temperature, while the nutritional factors include availability and source type for nitrogen, carbon, phosphorus, sulfur, and iron (Markou et al., 2012; Chen et al., 2013). The genera *Scenedesmus*, *Chlorella*, *Chlorococcum*, and *Tetraselmis* of the Clorophyta division and *Synechococcus* among other cyanobacteria have been extensively studied as feedstock for this type of bioethanol production. In general, the cultivation in a high light intensity ranged from 150 to 450 $\mu m^{-2}s^{-1}$ using a mix of CO_2 in air between 2% and 5% and mesophilic temperatures (20–30°C) achieves around 50% of carbohydrate content under nutrient starvation, mainly nitrogen (**Table 1.1**).

The positive effect of increasing light intensity on the accumulation of starch and lipids is feasible only up to a point, usually equal to saturation of photosynthesis under given conditions in a particular species (Vitovà et al., 2015).

Nutritional factors directly or indirectly influence the rate of photosynthesis and biochemical composition of microalgae. Macroelement (nitrogen, sulfur, or phosphorous) limitation is the most widely used and so far the most successful strategy for enhancing starch accumulation (Vitovà et al., 2015). For example, availability of nitrogen enhances the synthesis of proteins, pigments, and DNA (Markou et al., 2012; Chen et al., 2013); the amount of iron affects the photosynthetic electron transport, nitrite/nitrate and sulfate reduction, nitrogen fixation, and/or detoxification of reactive oxygen species (ROS) (Sunda and Huntsman, 1997). Sulfur involves in the formation of sulfolipids, polysaccharides, and proteins, as well as in the electron transport chain. When sulfur is present at limiting concentrations, it inhibits cell division, whereas high concentrations inhibit the photosynthetic assimilation of carbon-rich compounds, such as carbohydrates (Markou et al., 2012). CO_2 is the most common source of carbon (autotrophic condition), and under N depletion conditions, the supplementation of CO_2 in conjunction with light intensity causes the carbon to be absorbed and converted into carbohydrates more efficiently (Chen et al., 2013).

Table 1.1: Carbohydrate content in some microalgae and cyanobacteria.

Microorganism	Growth Conditions	Dry Cell Weight (gL^{-1})	Carbohydrates Accumulation (%)	Reference
Anthrospira platensis	150 $\mu molm^{-2}s^{-1}$, 30 °C, Bubbling air	2-2.2	58	Markou et al. (2013)
***Chlamydomonas fasciata* Ettl 437**	3000 lux, 25 °C - 0.4 $vvm^{(CO_2\text{-air})}$	-	43.5	Asada et al. (2012)
***Chlamydomonas reinhardtii* UTEX 90**	450$\mu molm^{-2}s^{-1}$, 23°C, 4 days and 130 rpm	12.4	59.7	Choi et al. (2010)
Chlorella sokoniana	-	-	40.3	Lorente et al. (2015)
***Chlorella variabilis* NC64A**	150 $\mu molm^{-2}s^{-1}$, 25°C, and 2% CO_2 $^{(CO_2\text{-air})}$	0.43	37.8	Cheng et al. (2013)
***Chlorella vulgaris* P12**	70 $\mu molm^{-2}s^{-1}$, 30°C and 2% CO_2 $^{(CO_2\text{-air})}$	-	41	Dragone et al. (2011)
***Chlorella vulgaris* FSP-E**	60 $\mu molm^{-2}s^{-1}$ and 2% CO_2 $^{(CO_2\text{-air})}$	7.5	52	Ho et al. (2013c)
***Chlorella vulgaris* KMMCC-9 UTEX26**	150 $\mu molm^{-2}s^{-1}$, 20-22°C, Bubbling air	-	22.4	Kim et al. (2014)
***Chlorella sp.* KR-1**	80 $\mu molm^{-2}s^{-1}$,30 °C and 10% CO_2 $^{(CO_2\text{-air})}$	-	49.7	Lee et al. (2013)
Chlorococcum humicola	Outdoor and bubbling CO_2 34.5 kPa	-	32.0	Harun and Danquah (2013a,b)
Chlorococcum infusionum	-	-	32.0	Harun et al. (2011)
***Dunaliella tertiolecta* LB999**	60 $\mu molm^{-2}s^{-1}$, 20-25°C and 2% CO_2 $^{(CO_2\text{-air})}$	-	37.8	Lee et al. (2013)
***Dunaliella tertiolecta* LB999**	60 $\mu molm^{-2}s^{-1}$ and 20-25°C	-	40.5	Kim et al. (2015)
Scenedesmus dimorphus	50-1200, 25°C and 2% CO_2.	5	45-50	Wang et al. (2013)
Scenedesmus obliquus	150 $\mu molm^{-2}s^{-1}$, 25°C, Bubbling air	-	30	Miranda et al. (2012)
***Scenedesmus obliquus* CNW-N**	210-230 $\mu molm^{-2}s^{-1}$, 28°C, 300rpm and 2.5% CO_2 $^{(CO_2\text{-air})}$	4.5	51.8	Ho et al. (2011b)
Scenedesmus bijugatus	Outdoor	-	26	Ashokkumar et al. (2015)
***Synechococcus elongatus* PCC 7942**	200 $\mu molm^{-2}s^{-1}$, 28°C, and 5 % CO_2 $^{(CO_2\text{-air})}$	-	28	Chow et al. (2015)
***Synechococcus sp.* PCC 7002**	250 $\mu molm^{-2}s^{-1}$ and 1% CO_2 $^{(CO_2\text{-air})}$	3.0	59	Mollers et al. (2014)
Tetraselmis subcordiformis	200 $\mu molm^{-2}s^{-1}$, 25°C and 3% CO_2 $^{(CO_2\text{-air})}$	6.0	45-50	Yao et al. (2012)
***Tetraselmis subcordiformis* FACHB-1751**	150 $\mu molm^{-2}s^{-1}$, 25°C and 3% CO_2 $^{(CO_2\text{-air})}$	4.5	40	Yao et al (2013a)
Tribonema sp.	-	-	31.2	Wang et al. (2014)

It was shown that *Scenedesmus obliquus* CNW-N grown in normal medium accumulated about 50% of its DW in carbohydrates after exhaustion of the nitrogen source. It was observed that as the amount of protein was significantly decreased, the carbohydrate content largely increased in the *S. obliquus* cells (Ho et al., 2013b). The growth of *Synechococcus* sp. PCC 7002 was studied for various concentrations of nitrate, and it was found that after depletion of nitrate (in the first days of cultivation), there was a significant accumulation of carbohydrates in the microalgae cell, reaching about 60% of DW (Mollers et al., 2014). *Tetraselmis subcordiformis* cells cultivated under phosphorus depletion conditions (0.5–6.0 mM) did not show significant differences in the accumulation of carbohydrates (~45% of content, 4.6–5.3 g L^{-1} DW), and that despite the similar carbohydrate content, there was a lower cellular productivity for phosphorus depletion than for nitrogen (nitrate 3–11 mM) or sulfur (sulfate 0.4–0.8 mM) depletions (45–50%, 5–6 g L^{-1} of DW) (Yao et al., 2012; Yao et al., 2013a). This same microalga using salinity (5.4–67.5 g L^{-1} of NaCl) reached 2.7–4.2 g L^{-1} of DW with 30–40% of carbohydrate content, mainly under N starvation (Yao et al., 2013b). *Chlorella vulgaris* FSP-E and ESP-6 cultivated under N depletion conditions exhibit an increase in the carbohydrate content from 15–20% to 49–54%, whereas *Chlamydomonas orbicularis* Tai-04 from 34% to 47% (Ho et al., 2013c). *C. vulgaris* Beijerinck, strain CCALA 924, was also cultivated under phosphorus, nitrogen, and sulfur depletion conditions, and it was noted that the limitation of sulfur imparts the highest percentage of accumulated starch in the microalgae (~60% of DW), 50% higher than without sulfur starvation (Branyikova et al., 2011). *Chlorella sorokiniana*, after a short period of N starvation, accumulated starch as the main source of carbon storage (Li et al., 2015).

The drawback of using nitrogen, phosphorus, and sulfur depletion strategies is that the viability of the process decreases substantially due to the reduced biomass yield, although a larger accumulation of carbohydrates is achieved (Branyikova et al., 2011).

The interaction between nutritional factors is another important aspect to be examined in the cultivation of microalgae. It has been expected that only one factor should be responsible for imparting both larger biomass yield and high accumulation of carbohydrates. For instance, *C. vulgaris* P12 was cultivated with limiting concentration of Fe (III) (FeNa–EDTA) and/or urea, and it was found that only the depletion of

nitrogen source (urea) significantly increased the starch content in the cells (up to about 40%) (Dragone et al., 2011). *T. subcordiformis* was cultivated by studying the relationship between the limitations of nitrogen (nitrate 0–11 mM) and sulfur (sulfate 0–0.8 mM). It was found that limitation of nitrogen played a more significant role on starch accumulation than sulfur limitation or even than the combination of both (Yao et al., 2012). The same microalgae was also cultivated under osmotic stress (NaCl – salinity), and the effect on starch accumulation was still higher than for nitrogen depletion conditions (Yao et al., 2013b). It was found that in almost all cases, the nitrogen limitation was significant for carbohydrate accumulation, probably because it suppresses the synthesis of nitrogen compounds, particularly proteins.

1.3.2 Hydrolysis and fermentation of microalgal biomass

The most common carbohydrates present in the microalgae and cyanobacteria that are used for the production of bioethanol are starch, glycogen, and cellulose. Starch is one of the largest microalgal sources of carbon, and it is an important feedstock for the production of bioethanol (starch-rich cereals are mainly used in the United States for producing bioethanol after enzymatic hydrolysis and fermentation). The cellulose present inside the microalgae cell wall is also suitable as a feedstock for bioethanol production (Ho et al., 2013d). The most common microorganisms used for ethanolic fermentation are yeasts of the genus *Saccharomyce*s or bacteria of the genus *Zymomonas*. Glycogen is a glucose polymer synthesized as an energy storage compound by cyanobacteria, and named cyanophycean starch. It has several interesting characteristics similar to starch, such as higher solubility in water and shorter polymer chains, apart from the fact that cyanobacteria can be easily hydrolyzed for producing bioethanol (Mollers et al., 2014).

Regarding the process operating conditions, the microalgae biomass appears to require mild conditions for hydrolysis as well as for fermentation. Moreover, the acid and enzyme hydrolysis of microalgal biomass requires low amount of reactants, particularly in the case of enzymatic hydrolysis, to achieve high yields of conversion. A summary is given below.

Acid hydrolysis of *S. obliquus* at 120°C with 2–3 N sulfuric acid for 30 min resulted in practically full hydrolysis of all carbohydrate content (71–97% of the carbohydrate

content), of which 65% was made up of glucose using solid concentration between 20 and 500 g L^{-1} (Miranda e al., 2012). *Scenedesmus bijugatus* (26% of carbohydrate content after lipid extraction), after acid hydrolysis with H_2SO_4 (0.36–1.08 N) at 130°C, 45 min, and 20 g L^{-1} solid concentration, saccharified 84% of biomass sugars and resulted in 70% of ethanol conversion (Ashokkumar et al., 2015). Enzymatic hydrolysis and fermentation of *Chlamydomonas reinhardtii* (50 g L^{-1} of biomass concentration and 59.7% of carbohydrate content) by separated hydrolysis and fermentation (SHF) using amylases (0.005% α-amylase from *Bacillus licheniformis* at 90°C and 30 min to liquefaction and 0.2% glucoamylase from *Aspergillus niger* at 55°C and 30 min to saccharification, pH 4.5) achieved hydrolysis of 94% of the carbohydrates present in the microalgae, and further fermentation using *Saccharomyces cerevisiae* S288C achieved a yield of 60% (Choi et al., 2010). *Chlamydomonas fasciata* Ettl 437, using an ultrasonic homogenizer (30 W and 20 kHz, 40 min), extracted 98% of the carbohydrates (starch), hydrolyzed with glutase-AN (from *A. niger*) and fermented with *S. cerevisiae* AM12, achieving a fermentation yield of 80% (Asada et al., 2012).

Acidic treatment of *C. vulgaris* FSP-E with sulfuric acid is a more efficient hydrolysis method than enzymatic treatment (complex of amylases and cellulases). Ho et al. (2013a) reported that hydrolysis performed with H_2SO_4 (0.036–1.8 N at 121°C for 20 min) using 10–80 g L^{-1} of biomass concentration led to 95% saccharification of the glucose content of the biomass, and that approximately 90% of the theoretical fermentation yield was achieved in 12 h, after further fermentation with *Zymomonas mobilis* ATCC 29191. *C. vulgaris* was also subjected to different methods of cell disruption (autoclave, beadbeating, and sonication), and it was found that the use of beadbeating combined with pectinase (from *Aspergillus aculeatus*) treatment (an more effective enzyme compared with cellulases, amylases, and xylanases) increased the extraction of sugars from 45% to 70%, further resulting in a fermentation yield of 89% after 12 h with *S. cerevisiae* KCTC 7906. This finding also indicated the occurrence of significant amounts of pectin in the *C. vulgaris* cell wall (Kim et al., 2014). *Chlorella* sp. KR-1 (49.7% carbohydrate content) attained >98% of saccharification using HCl 0.3 N at 121°C in 15 min and achieved 80% fermentation yield with *S. cerevisiae* (Lee et al., 2015a). *Dunaliella tertiolecta* (original carbohydrate content of 37.8%, and 51.9% of DW after lipid extraction) was acid hydrolyzed with HCl and H_2SO_4 (0.1–1 N at

121°C for 15 min) and enzyme hydrolyzed (e.g., amyloglucosidase, cellulase, and Viscozyme L) under a biomass concentration of 50 g biomass/L. The highest efficiency was observed for the amyloglucosidase + HCl 0.5 N treatment (chemo-enzymatic treatment), where a biomass hydrolysis level of 80% in terms of theoretical sugar content and a fermentation yield of 82% with *S. cerevisiae* YPH500 were achieved (Lee et al., 2013).

The potential of *Chlorococcum humicola* biomass as a feedstock for bioethanol has also been investigated. Harun et al. (2011a) studied the acid hydrolysis of the microalgae (acid concentrations between 0.36 and 3.6 N) at 120–160°C, and obtained a final ethanol concentration of 7.2 g L^{-1} with *S. cerevisiae*. The same microalgae was also alkali hydrolyzed with NaOH (0.2–0.5 N) at 60–120°C, and 26% of ethanol yield (based on $g_{ethanol}/g_{biomass}$) was achieved (Harun et al., 2011). Another study reported that 70% of the sugars (based on glucose) present in *C. humicola* biomass can be hydrolyzed by cellulases of *Trichoderma reesei* ATCC 26921, thereby demonstrating the potential of the enzymatic treatment to convert the microalga into inputs for bioethanol (Harun et al., 2011b). The cyanobacteria *Synechococcus* sp. PCC 7002 accumulated 60% of the carbohydrate content (3 g L^{-1} of biomass concentration) under nitrate depletion conditions, and after enzymatic treatment (lysozyme, and α-glucanases Liquozyme® SC DS and Spirizyme® Fuel), a hydrolysis yield of 80% was achieved. Further fermentation with *S. cerevisiae* resulted in an ethanol yield of 86%, in relation to the theoretical maximum value (Mollers et al., 2014). *Arthrospira platensis* was hydrolyzed using H_2SO_4, HNO_3, HCl, and H_3PO_4, or the combined use of H_2SO_4 (0.25–2.5 N) and HNO_3 (0.5 N) at 100°C obtained the best results with 80% saccharification and 55% fermentation yield using *S. cerevisiae* MV 92081 (Markou et al., 2013).

All the findings reported so far demonstrate that microalgae and cyanobacteria are diverse in terms of their cellular structure, and that each species requires a specific enzyme to be efficiently saccharified. In general, the use of amylase contributes significantly to the hydrolysis of microalgae grown under nutrient-limiting conditions. Accordingly, glucose has been the most frequently identified sugar after saccharification of biomass. Another important aspect is that chemical hydrolysis methods may also facilitate the solvent extraction of lipids, thereby serving to recover both fermentable sugars and lipids from microalgae biomass. *Nannochloropsis*

gaditana, C. sorokiniana, and *Phaeodactylum tricornutum* have been treated by steam explosion with sulfuric acid (H_2SO_4, 0–3.6 N at 120–150°C for 5 min), and approximately 96% of the sugar content was hydrolyzed using 0.6 N of the acid at 150°C. The acid hydrolysis of these microalgae biomasses also increased the efficiency of lipid extraction (Lorente et al., 2015) Wang and coworkers (2014) reported the difference between the lipid contents obtained before and after hydrolysis of the microalgae *Tribonema* sp. with H_2SO_4 1N, that is, an increase of 25%. The carbohydrate content was hydrolyzed to 80% for a biomass concentration of 50 g L^{-1} of solution at 121°C and 45 min, and 70% of the theoretical yield was achieved after fermentation with *S. cerevisiae*.

In summary, acid hydrolysis (sulfuric, nitric, or chloridric acid) at temperatures between 120 and 140°C for 15–30 min results in >80% saccharification and fermentation. However, the use of high catalyst concentrations (acids and alkalis) can inhibit the fermentation step because of the formation of salts after neutralization of the liquor (Markou et al., 2013). For enzymatic hydrolysis, amylases, cellulases, and/or pectinanes are used, depending upon the specie and cultivation conditions according to the biochemical composition and type of carbohydrates (**Table 1.2**).

1.4 BIOETHANOL PRODUCTION BY DARK FERMENTATION

Dark fermentation has been referred to as the conversion of organic substrates into biohydrogen. Fermentative and hydrolytic microorganisms hydrolyze complex organic polymers into monomers, which are subsequently converted into a mixture of organic acids of low molecular weight and alcohols, mainly acetic acid and ethanol. Various microalgae and cyanobacteria that are capable of expelling ethanol through the cell wall by means of intracellular process in the absence of light (Ueno et al., 1998), include *C. reinhardtii, Chlamydomonas moewusii, C. vulgaris, Oscillatoria limnetica, Oscillatoria limosa, Gleocapsa alpícola, Cyanothece* sp., *Chlorococcum littorale*, and *Spirulina* sp. *e Synechococcus* sp. (Ueno et al., 1998; Deng and Coleman, 1999). However, dark fermentation is disadvantageous in terms of hydrogen productivity, because approximately 80–90% of the initial chemical oxygen demand (COD) remains in the form of acids and alcohols after the process. Even under optimal operating conditions, typical yields vary only between 1 and 2 mol H_2 per mol of glucose (Ueno et al., 1998).

The production of ethanol is favored by the accumulation of carbohydrates in the microalgae cells through photosynthesis, and then the microalgae are forced to synthesize ethanol through fermentative metabolism directly from their carbohydrate and lipid reserves when switching the growth to dark conditions Beer et al., 2009; Abo-hashesh et al., 2011). However, it can be concluded that dark fermentation of microalgae is not an efficient process for the production of bioethanol.

1.5 BIOETHANOL PRODUCTION BY PHOTOFERMENTATION

Photofermentation is a process of growing interest principally after the announcement of the installation of industrial plants where modified cyanobacteria are used to produce bioethanol directly (ABO, 2014; Algenol, 2015).

The "photofermentative" route (simply, Photanol) is a natural mechanism of converting sunlight into products of fermentation through a highly efficient metabolic pathway (Hellingwerf and Mattos, 2009). Photanol is not only limited to ethanol production, but it is also used for a large number of naturally occurring products resulting from glycolysis-based fermentation. Thus, several cyanobacteria species can be genetically modified by introducing specific fermentation cassettes through molecular engineering procedures, and then tested as a fermentative organism (Angermayr et al., 2009).

Many studies have been performed on two models of cyanobacteria, *Synechocystis* sp. PCC 6803 and *Synechococcus elongatus* sp. PCC 7992. In addition to these *Synechococcus* sp., PCC 7002 and *Anabaena* sp. PCC 7120 have received much attention (Savakis and Hellingwerf, 2015). *Synechococcus* sp. is a unicellular cyanobacterium that lives in freshwater that has been relatively well characterized. It is capable of tolerating insertion of foreign DNA to be transformed and replicated using shuttle vectors between *Escherichia coli* and cyanobacteria, or insertion of foreign DNA into the chromosome through homologous recombination at selected active sites (Golden et al., 1987; Thiel, 1995; Angermayr et al., 2011; Ducat et al., 2011). *Synechocystis* sp. PCC 6803 was the first photosynthetic organism that had its genome sequenced, and one of the best characterized cyanobacteria. *Thermosynechococcus* is also naturally transformable (Rosgaard et al., 2012).

The metabolic pathway of ethanol synthesis is briefly summarized: after fixation of inorganic carbon by Calvin cycle, it forms phosphoglycerate that is converted into

piruvate by two enzymes (pyruvate decarboxylase (PDC) and alcohol dehydrogenase (ADH)), and finally into ethanol:

$$CO_2 \xrightarrow[Calvin\ Cycle]{} GAP \xrightarrow[Intermediate\ (PEP)]{} Pyruvate \xrightarrow{PDC} Acetaldehyde \xrightarrow{ADH} Ethanol$$

GAP – phosphoglycerate, PEP – phosphoenolpyruvate, PDC – pyruvate decarboxylase, ADH – alcohol dehydrogenase.

Therefore, the "photofermentation" process for obtaining ethanol includes two stages: photosynthesis and fermentation. Each stage has its key factors that determine the efficiency of the process and the metabolic needs of the cyanobacteria. In any case, this route requires the use of genetically modified microorganisms.

Table 1.2: Hydrolysis and fermentation of microalgal biomass.

Microorganism	Biomass Concentration ($g/L_{dry\ cell\ weight}$)	Productivity ($g_{ethanol}$/ (L day))	Lipid Extracted	Type and Conditions of Hydrolysis	Yield of Hydrolysis (%)	Yield of Fermentation (%)	Reference
Antrosphira platensis	12-13	-	no	Acid (sulfuric and nitric acid 0.5 N and 100°C)	80	56	Markou et al. (2013)
Chlamydomonas fasciata Ettl 437	100	14.4	no	Enzymatic (glutase)	80	69	Asada et al. (2012)
Chlamydomonas reinhardtii	50	~7	no	Enzymatic (α-amylase and glucoamylases)	94	60	Choi et al. (2010)
Chlorella sp. KR-1	50	12-14	yes	Acid (HCl 0.3 N, 15 min and 121 °C) and Enzymatic (pectinases)	98 (acid) and 76 (enzymatic)	80	Lee et al. (2015a)
Chlorella vulgaris	10	0.58	no	Enzymatic (pectinases)	45-70	89	Kim et al. (2014)
Chlorella vulgaris FSP-E	10-80	-	no	Acid (Sulfuric acid 0.36 N, 20 min and 121°C)	95	90	Ho et al. (2013a)
Chlorococcum sp.	15	-	no	Acid 0.36 N, 15 min and 140 °C	-	-	Harun et al. (2011), Harun and Danquah (2011a,b)
	15	-	no	Alkaline (NaOH 0.2-0.5 N and 60-120°C)	-	78	
		-		Enzymatic (cellulases)	70	-	
Dunaliella tertiolecta	50	8-9	yes	Chemeo-enzymatic (amyloglucosidase and after HCl 0.5 N, 15 min and 121 °C)	80	82	Lee et al. (2013)
Scenedesmus bijugatus	20	-	yes	Acid (Sulfuric acid 0.36-1.08 N, 45 min and 130°C)	84	70	Ashokkumar et al. (2015)
Scenedesmus obliquus	20-500	-	no	Acid (Sulfuric acid 2-3 N, 30 min and 120°C)	71-96	-	Ho et al. (2013d)
Synechococcus PCC 7002	100	30	no	Enzymatic (lysozyme and α-glucanases)	80	86	Mollers et al. (2014)

1.6 GENETIC ENGINEERING OF CYANOBACTERIA FOR BIOETHANOL PRODUCTION

Recently, there has been a rapid expansion of products obtained by "photofermentation" metabolism of engineered cyanobacteria. This has been facilitated by the knowledge acquired on conventional fermentation, in particular, of *E. coli* and *S. cerevisiae,* which have been genetically engineered to produce several products (Savakis and Hellingwerf, 2015).

Algae are a highly diverse set of organisms with largely unexplored genetic potential. The number of novel genes identified among different species indicates that although microalgae may be morphologically similar single-celled photosynthetic organisms, the functional genetic diversity is very large. This functional diversity is being exploited to develop elite algal strains for biofuel production (Gimpel et al., 2013). On the contrary, two properties of cyanobacteria make them excellent candidates for bio-industrial applications: their photosynthetic capacity and potential to genetic engineering, that is, the short life cycle and possibility of being modified by genetic engineering procedures (Ducat et al., 2011).

As the underlying aspect of photosynthesis is the use of CO_2 and sunlight for assimilation and conversion of carbon into organic molecules, CO_2 and light are the foremost factors determining the enhancement of productivity. Regarding intensity of light, the microalgae photosynthetic efficiency generally spans from 6% to 10%, which is consequently much higher than that with higher plants (1–2%) (Peccia et al., 2013; Sforza et al., 2014). This result has been obtained by the improvement of geometry, study of optimal growing conditions, and capacity of the photosynthetic apparatus to absorb light.

Considering the fixation of CO_2, the main aspect is related to RuBisCO (ribulose bisphosphate carboxylase/oxygenase), which is inefficient to drive the core enzyme through the Calvin cycle. RuBisCO has been the main obstacle in the production of biomass, as its catalytic activity does not appear to be increased by improvements of environmental and nutritional conditions as well as enhancement of illumination conditions and temperature.6 There are naturally occurring mutant forms of RuBisCO that possess high catalytic activity, but are less capable of recognizing CO_2 and require

higher rates of photorespiration. Currently, there are no examples of genetically engineered RuBisCO with higher photosynthetic efficiency (Ducat et al., 2011).

Biological approaches such as metabolic engineering, synthetic biology, evolution and reverse engineering, and multi-omics (e.g., proteomics, transcriptomics, and metabolomics) can form microbial cellular factors for the production of biofuels or compounds of chemical or biological interest (e.g., intermediates, proteins, isoprene, and amino acids) (Lu, 2010), providing a better understanding of the biological apparatus and how these biochemical routes work at biological and molecular levels.

Some works involving the techniques for characterization of omics have reported the behavior of cyanobacteria in the presence of ethanol, aiming at clarifying metabolic, structural, and genetic modifications in the microorganism and using these data for improving the resistance/production of bioethanol. The transcriptomic response of *Synechocystis* sp. PCC 6803 was studied in extended periods of bioethanol synthesis reaching 0.6% (v v^{-1}) after 19 days (Dienst et al., 2014). The same cyanobacterium was treated with various concentrations of ethanol, and its proteomic response was examined in terms of digestion. It was found that ethanol alters the cell membrane, activates transport and specific proteins, and diminishes the mobility and metabolism of the microbial cells (Qiao et al., 2012). Other reports on genetic engineering of cyanobacteria have cited commercially important substances that are difficult to be produced by natural biological mechanisms (e.g., isoprene, mannitol, glycerol, low- and high-molecular-weight hydrocarbons, isopropanol, and isobutyraldehyde) or that are produced in conjunction with secondary routes, for instance, 1-butanol in the acetone–butanol–ethanol (ABE) fermentation (Lan and Liao, 2011; Tan et al., 2011; Machado and Atsumi, 2012; Desai and Atsumi, 2013; Jacobsen and Frigaard, 2014; Kusakabe et al., 2014; Savakis and Hellingwerf, 2015; Savakis et al., 2015; Lee et al., 2015b); *Synechocystis* sp. PC 6803 for the production of higher alcohols such as pentadecanol, hexadecanol, and octadecanol and higher hydrocarbons such as pentadecane, heptadecane, 8-heptadecene, and eicosane (Tan et al., 2011); *S. elongatus* PCC 7942 for the production of 1-butanol (12–14 mg L^{-1} between 4 and 6 days) (Lan and Liao, 2011) or isopropanol (~20 mg L^{-1} in 6 days (Kusakabe et al., 2013) and 2 mM in 10 days (Hirakawa et al, 2015)); and *Synechococcus* sp. PCC 7002 for the production of mannitol (0.7 g L^{-1} in 175 h) (Jacobsen and Frigaard, 2014).

The main aim of genetic modification of microorganisms for the production of ethanol is to increase the activity of PDC and ADH, so that the conversion of fixed carbon into ethanol can be efficiently increased, and improve the growth conditions of microorganisms. Ethanol-producing cells grow slower than the nonproducing cells, but rapid growth is desirable only in the scale-up phase and not during bioethanol synthesis stages (ABO, 2014).

Another unexplained aspect is how and at what rates the molecules formed in the Calvin cycle can be driven to the synthesis of ethanol. The regulatory factors and genetic structure involved in this metabolic pathway have not been elucidated yet, and only few studies have been devoted to this topic.

Synechococcus sp. PCC 7942 was modified with a *Z. mobilis* gene by a plasmid grown in *E. coli* with the aim of increasing the PDC and ADH activities and consequently the yield of ethanol. This finding was reported by Deng and Coleman (1999), who proposed the use of *Synechococcus* sp. PCC 7942 as an ethanol-producing microorganism, yielding approximately 0.025 mg L^{-1} after 6 days. *Synechocystis* sp. PC 6803 has also been recognized as an ethanol-producing genetically modified organism (GMO), and Dexter and Fu (2009) used the same genes in *Synechocystis* sp. PCC 6803, which resulted in a larger ethanol yield of 0.55 g L^{-1} after 6.25 days, a value still insufficient for industrial purposes.

In a recent and innovative report, *S. elongatus* PCC 7942 has been genetically modified to accumulate carbohydrates for the production of bioethanol. After genetic adjustment, the percentage of carbohydrates increased from 28% to 35% (DW), and the microalgae productivity increased four times (144–564 mg L^{-1} day^{-1}). The genetically modified *S. elongatus* biomass further achieved yields of >95% by hydrolysis with H_2SO_4 (0.36–0.72) N and 91% of the theoretical fermentation yield after fermentation by *Z. mobilis* ATCC 29191 (Chow et al., 2015).

The microorganisms *E. coli*, *Z. mobilis*, and *S. cerevisiae* produce bioethanol with high efficiency and have consolidated industrial activity, in particular, *Saccharomyces*. Furthermore, the aforementioned three microorganisms are still being genetically modified to increase their tolerance to ethanol, productivity, and capability of using different sugars for the synthesis of ethanol, (Jang et al., 2012) mainly hexoses and pentoses. This has been achieved in natural genera such as *Pichia*, *Candida*, and

Kluyveromyces that are well known for their ability to use hexoses and pentoses, at low rates, to synthesize ethanol (Kuhad et al., 2011).

A final aspect that must be considered is the environmental impact of GMOs. Genetically modified microalgae and cyanobacteria may compete with naturally occurring microbial species, change biota composition (dominance and diversity) in several environments, or even involve in GM gene exchange with natural organisms via horizontal gene transfer (HGT) mechanisms (Henley et al., 2013).

1.7 SOME INDUSTRIAL APPLICATIONS

An American company, named Algenol (Bonita Springs, FL, USA: http://www.algenol.com/), owner of the first industrial plant for bioethanol production from engineered microorganisms, has attracted much attention in relation to its numbers, such as ethanol productivity (>60,000 L ha^{-1} $year^{-1}$) and the maximum efficiencies of 3,700 and 9,100 L ha^{-1} $year^{-1}$ for corn and sugarcane, respectively. An Algenol patent was filed in 2013 and published in 2014, mentioning the *Cyanobacterium* sp. and reporting tolerance of 1% of bioethanol in 16 weeks. This cyanobacterium received plasmids of a heterologous alcohol dehydrogenase gene (from *Synechocystis*) and pyruvate decarboxylase gene (from *Zymomonas*) (ALGENOL, 2015).

These high photosynthetic efficiency values can be ascribed not only to the species used but also to the geometrical characteristics of the photobioreactors (vertical bags) and to the cultivation under continuous conditions. The main limitations are the fixed carbon/ethanol ratio, incidence of light (problems with photosaturation and photoinhibition must be avoided), contaminants, and supply time (correct quantity of nutrients and CO_2) (ABO, 2014). Reportedly, Algenol has tested about 2300 species, but there is no much information on the specific specie used in its scaled-up bioethanol production process. It has been reported that Algenol is experiencing some financial problems that culminated in the dismissal of part of the employees and its founder and current president by the executive council (Walcher, 2015).

On the other hand, in 2011, Joule Unlimited (Bedford, MA, USA: http://www.jouleunlimited.com/news) started a project to build an industrial plant using an engineered cyanobacterium, which produces bioethanol directly from light, carbonic

gas, water, and salts. In 2014, the company obtained authorization from the Environmental Protection Agency (EPA: http://www.epa.gov/) to explore this cyanobacterium.

This company claims to have an efficient system to directly produce biofuels such as alkanes and ethanol from CO_2. It was reported that a photosynthetic efficiency of 6–7% was achieved, in comparison to algal open-pond values of 1.5%, both in outdoor conditions. The system proposed by Joule Unlimited, called Helioculture® Platform, is based on a reactor called SolarConverter® (a horizontal thin film plastic using CO_2 in a closed system and outdoor), where the mixing, culture density, and geometry (depth and surface area) have been studied to optimize the capture and conversion of CO_2 by an appropriate combination of the light and dark areas with the reactor (Robertson et al., 2011; Lane, 2015). The company estimated ethanol productivity >230,000 L ha^{-1} $year^{-1}$ with a production cost of $0.16/L of ethanol with subsidies ($0.32/L without subsidies). The announcement for a plant start-up in 2017 was made (Lane, 2015; Frost and Sulivan, 2015).

Furthermore, other scientists and companies such as Bill Sims (AGSOLVE, 2011) proposed industrial-scale photobioreactors for direct production of ethanol; in addition, China University of Petroleum/University of Hawaii (FAPESP, 2008; Dexter and Fu, 2009) has a patent on a plant on a laboratory scale, using genetically modified cyanobacteria.

However, Algenol and Joule Unlimited appears in recent years (2015-2017) to be discouraged with this genetically modified cyanobacterium approach, because no news have been updated and their company sites have not emphasized this technology anymore.

The costs of bioethanol production from sugarcane (Brazil, 0.16–0.22 US$/L) are lower than those from corn (USA, 0.25–0.40 US$/L), sugar beet (Europe, 0.43–0.73 US$/L), and lignocellulosic materials (USA, 0.43–0.93 US$/L) (Gupta and Verna, 2015). It is quite difficult to estimate the economics of bioethanol from genetically engineered cyanobacteria. Algenol announced a production cost of approximately 0.79 US$/L, and potential application of this method of bioethanol production will be increased with the continuously decrease in costs (ABO, 2014). An industrial plant of microalgal ethanol from biomass hydrolysis and yeast/bacteria fermentation was not proposed yet.

1.8 CONCLUSIONS AND OUTLOOK

On the basis of the available information from open literature, it is clear that the traditional fermentation should focus on not only the increase of the carbohydrate content but also the higher productivity of biomass. Technical and economic evaluations are necessary to verify the gains and losses of energy involved in the production of ethanol from microbiological biomass.

On the contrary, the use of engineered cyanobacteria still needs careful investigation on structural, metabolic, and genetic bases to understand not only its use for industrial bioethanol processes, but also the latent environmental risks associated with the use of genetically modified microorganisms. Notably, the relevance of genetically engineered microorganisms with traditional processes must also be discussed, as it is well known that enzymes and yeasts can efficiently produce bioethanol (hydrolysis and fermentation) with high productivity. A numerical comparison of production costs is however necessary, particularly for the production of ethanol by hydrolysis and fermentation as well as by "photofermentation", which appears indeed a highly promising technological application in future.

The major bottlenecks for an industrial implementation appear to be more research to be done about hydrolysis and fermentation technologies, and lack of knowledge about genetically modified cyanobacteria. In any case, the biofuel production costs, mainly related to microalgae/cyanobacteria cultivation (Tercero et al., 2014), are to be compared with those of fossil fuels which are, at present, so low (U.S. Department of Prices, 2015) to discourage both investments and public subsidies, although the environmental and climatic factor are in great favor of biofuels.

REFERENCES

ABO., 2014. Photosyntetic production of biofuels from CO_2 by cyanobacteria using Algenol's Direct to Ethanol® Process – Strain development aspects. Algal Biomass Summit.

Abo-hashesh, M., Wang, R., Hallenbeck, P.C., 2011. Metabolic engineering in dark fermentative hydrogen production: theory and pratice. Bioresource Technology 102, 8414-8422.

Acién, F.G., Fernandez, J.M., Magàn, J.J., Molina, E., 2012. Production cost of a real microalgae production plant and strategies to reduce it. Biotechnology Advances 30, 1344-1353.

AGSOLVE., 2011. Cyanobacteria make fuel using water, sunlight and CO_2. (Original Title: Cianobactéria produz combustível apenas com agua, sol e CO_2).

ALGENOL. Piven, I., Friedrich, A., Duhring, U., Baier, K., Inaba, M., Shi, T., Wang, K., Enke, H., Kramer, D., 2015. Cyanobacterium sp. host cell and vector for production of chemical compounds in cyanobacterial cultures. Patent. US 8846369 B2. [01.15.2015].

Angermayr, S.A., Hellingwerf, K.J., Lindblad, P., Mattos, M.J.T., 2009. Energy biotechnology with cianobactéria. Current Opinion in Biotechnology 20, 257-263.

Asada, C., Doi, K., Sasaki, C., Nakamura, Y., 2012. Efficient extraction of starch from microalgae using ultrasonic homogenizer and its conversion into ethanol by simultaneous saccharification and fermentation. Natural Resources 3, 175–179.

Ashokkumar, V., Salam, Z., Tiwari, O.N., Chinnasamy, S., Mohammed, S., Ani, F.N., 2015. An integrated approach for biodiesel and bioethanol production from *Scenedesmus bijugatus* cultivated in a vertical tubular photobioreactor. Energy Conversion and Management 101, 778–786.

Beer, L.L., Boyd, E.S., Peters, J.W., Posewitz, M.C., 2009. Engineering algae for biohydrogen and biofuel production. Current Opinion in Biotechnology 20, 264-271.

BP GLOBAL – BP Statistical Review of World Energy, 2011. Available in: <www.bp.com>

Branyikova, I., Marsalkova, B., Doucha, J., Branyik, T., Bisova, K., Zachleder, V., Vitova, M., 2011. Microalgae – Novel Highly Efficient Starch Producers. Biotechnology and Bioengineering 108(4), 766-776.

Brennan, L., Owende, P., 2010. Biofuels from microalgae – a review of technologies for production, processing, and extractions of biofuels and co-products. Renew. Sust. Energ. Rev. 14 (2), 557–577.

Cardoso, A.S., Vieira, G.E.G., Marques, A.K., 2011. O uso de microalgas para a obtenção de biocombustíveis. Revista Brasileira Biociencias 9(4), 542-549.

Chen, C., Zhao, X., Yen, H., Ho, S., Cheng, C., Lee, D., Bai, F., Chang, J., 2013. Microalgae-based carbohydrates for biofuel production. Biochemical Engineering Journal 178, 1-10.

Cheng, Y., Zheng, Y., Labavitch, J.M., Vandergheynst, J.S., 2013. Virus infection of *Chlorella variabilis* and enzymatic saccharification of algal biomass for bioethanol production. Bioresource Technology 137, 326-331.

Choi, S.P., Nguyen, M.T., Sim, S.J., 2010. Enzymatic pretreatment of *Chlamydomonas reinhardtii* biomass for ethanol production. Bioresource Technology 101, 5330-5336.

Chow, T., Su, H., Tsai, T., Chou, H., Lee, T., Chang, J., 2015. Using recombinant cyanobacterium (*Synechococcus elongatus*) with increased carbohydrate productivity as feedstock for bioethanol production via separate hydrolysis and fermentation process. Bioresource Technology 184, 133 – 141.

Deng, M., Coleman, J.R., 1999. Ethanol Synthesis by Genetic Engineering in Cyanobacteria. Applied and Environmental Microbiology 65(2), 523-528.

Desai, S.H., Atsumi, S., 2013. Photosynthetic approaches to chemical biotechnology. Current Opinion in Biotechnology 24, 1031-1036.

Dexter, J., Fu, P., 2009. Metabolic engineering of cyanobacteria for ethanol production. Energy & Environmental Sciences 2, 857-864.

Dienst, D., Georg, J., Abts, T., Jakorew, L., Kuchmina, E., Borner, T., Wilde, A., Duhring, V., Enke, H., Hess, W.R., 2014. Transcriptomic response to prolonged ethanol production in the cyanobacterium *Synechocystis sp.* PCC 6803. Biotechnology and Biofuels 7(21), 1-11.

Dragone, G., Fernandes, B.D., Abreu, A.P., Vicente, A.A., Teixeira, J.A., 2011. Nutrient limitation as a strategy for increasing starch accumulation in microalgae. Applied Energy 88, 3331-3335.

Ducat, A.C., Way, J.C., Silver, P.A., 2011. Engineering cyanobacteria to generate high-value products. Applied Microbiology 29(2), 95-103.

EMPRESA DE PESQUISA ENERGÉTICA – EPE., 2015. Balanço Energético Nacional – 2015 Relatório Síntese – Ano Base 2014. Available in: <www.epe.gov.br>

Frost & Sulivan., 2015. Frost & Sullivan Honors Joule for its Helioculture Platform, a Breakthrough Photosynthetic System for the CO_2-to-Fuels Market. Published online in July.

Gimpel, J.A., Specht, E.A., Georgianna, D.R., Mayfield, S.P., 2013. Advances in microalgae engineering and synthetic biology applications for biofuel production. Current Opinion in Chemical Biology 17, 489-495.

Golden, S.S., Brussian, J., Haselkorn, R., 1987. Genetic engineering of the cyanobacterial chromosome. Methods Enzymol. 153, 215-231.

Gupta, A., Verna, J.P., 2015. Sustainable bio-ethanol production from agroresidues: a review. Renewable and Sustainable Energy Reviews 41, 550-567.

Harun, R., Danquah, M.K., Forde, G.M., 2010. Microalgal biomass as a fermentation feedstock for bioethanol production. J. Chem. Technol. Biotechnol. 85, 199-203.

Harun, R., Jason, W.S.Y., Cherrington, T., Danquah, M.K., 2011. Exploring alkaline pre-treatment of microalgal biomass for bioethanol production. Applied Energy 88, 3464-3467.

Harun, R., Danquah, M.K., 2011. Influence of acid pre-treatment on microalgal biomass for bioethanol production. Process Biochemistry 46, 304-309. (a)

Harun, R., Danquah, M.K., 2011. Enzymatic hydrolysis of microalgal biomass for bioethanol production. Chemical Engineering Journal 168, 1079-1084. (b)

Hellingwerf, K., Mattos, M.J.T., 2009. Alternative routes to biofuels: light driven biofuel formation from CO_2 and water based on the "Photanol" approach. J. Biotechnol. 142, 87-90.

Henley, W.J., Litaker, R.W., Novoveska, L., Duke, C.S., Quemada, H.D., Sayre, R.T., 2013. Initial risk assessment of genetically modified (GM) microalgae for commodity-scale biofuel cultivation. Algal Research 2, 66-77.

Hirakawa, Y., Suzuki, I., Hanai, T., 2015. Optimization of isopropanol production by engineered cyanobacteria with synthetic metabolic pathway. Journal of Bioscience and Bioengineering 119(5), 585-590.

Ho, S., Huang, S., Chen, C., Hasunuma, T., Kondo, A., Chang, J., 2013. Bioethanol production using carbohydrate-rich microalgae biomass as feedstock. Bioresource Technology 135, 191–198. (a)

Ho, S., Kondo, A., Hasunuma, T., Chang, J., 2013. Engineering strategies for improving the CO_2 fixation and carbohydrate productivity of *Scenedesmus obliquus* CNW-N used for bioethanol fermentation. Bioresource Technology 143, 163-171. (b)

Ho, S., Huang, S., Chen, C., Hasunuma, T., Kondo, A., Chang, J., 2013. Characterization and optimization of carbohydrate production from and indigenous microalga *Chlorella vulgaris* FSP-E. Bioresource Technology 135, 157–165. (c)

Ho, S., Chen, C., Chang, J., 2012. Effect of light intensity and nitrogen starvation on CO_2 fixation and lipid/carbohydrate production of an indigenous microalga *Scenedesmus obliquus* CNW-N. Bioresource Technology 113, 244–252. (d)

Hu, Q., 2004. Environmental effects on cell composition. Oxford: Blackwell Science Ltd, 83 - 93.

Jacobsen, J.H., Frigaard, N., 2014. Engineering of photosynthetic mannitol biosynthesis from CO_2 in a cyanobacterium. Metabolic Engineering 21, 60-70.

Jang, Y., Park, J.M., Choi, S., Choi, Y.J., Seung, D.Y., Cho, J.H., Lee, S.Y., 2012. Engineering of microorganisms for the production of biofuels and perspectives based on systems metabolic engineering approaches. Biotechnology Advances 30, 989 – 1000.

John, R.P., Anisha, G.S., Nampoothiri, K.M., Pandey, A., 2011. Micro and macroalgal biomass: a renewable source for bioethanol. Bioresource Technology 102, 186 – 193.

Kim, K.H., Choi, I.S., Kim, H.M., Wi, S.G., Bae, H., 2014. Bioethanol production from the nutriente stress-induced microalga *Chlorella vulgaris* by enzymatic hydrolysis and immobilized yeast fermentation. Bioresource Technology 153, 47-54.

Kim, S., Ly, H.V., Kim, J., Lee, E.Y., Woo, H.C., 2015. Pyrolysis of microalgae residual biomass derived from *Dunaliella tertiolecta* after lipid extraction and carbohydrate saccarification. Chemical Engineering Journal 263, 194-199.

Kuhad, R.C., Gripta, R., Khasa, Y.P., Singh, A., Zhang, Y.H.P., 2011. Bioethanol production from pentose sugars: Current status and future prospects. Renewable and Sustainable Energy Reviews 15(9), 4950-4962.

Kusakabe, T., Tatsuke, T., Tsuruno, K., Hirokawa, Y., Atsumi, S., Liao, J.C., Hanai, T., 2013. Engineering a synthetic pathway in cyanobacteria for isopropanol production directly from carbon dioxide and light. Metabolic Engineering 20, 101-108.

Lan, E.I., Liao, J.C., 2011. Metabolic engineering of cyanobacteria for 1-butanol production from carbon dioxide. Metabolic Engineering 13, 353-363.

Lane, J., 2015. Joule Unlimited: Biofuels Digest's 2015 5-Minute Guide. BiofuelsDigest. Published in Februray.

Lee, S.K., Chou, H., Ham, T.S., Lee, T.S., Keasling, J.D., 2008. Metabolic engineering of microorganisms for biofuels production: from bugs to synthetic biology to fuels. Current Opinion in Biotechnology 19, 556-563.

Lee O.K., Kim, A.L., Seong, D.H., Lee, C.G., Jung, Y.T., Lee, J.W., Lee, E.Y., 2013. Chemo-enzymatic saccharification and bioethanol fermentation of lipid-

extracted residual biomass of the microalga, *Dulaliella tetriolecta*. Bioresource Technology 132, 197-201.

Lee O.K., Oh, Y., Lee, E.Y., 2015. Bioethanol production from carbohydrate-enriched residual biomass obtained after lipid extraction of *Chlorella sp.* KR-1. Bioresource Technology 196, 22–27. (a)

Lee, S.Y., Kim, H.M., Cheon, S., 2015. Metabolic engineering of the production of hydrocarbon fuels Current Opnion in Biotechnology 33, 15-22. (b)

Li, T., Gargouri, M., Feng, J., Park, J., Gao, D., Miao, C., Dong, T., Gang, D.R., Chen, S., 2015. Regulation of starch and lipid accumulation in a microalga *Chlorella sorokiniana*. Bioresource Technology 180, 250–257.

Lorente, E., Farriol, X., Salvado, J., 2015. Steam explosion as a fractionation step in biofuel production. Fuel Processing Technology 131, 93-98.

Lu, X., 2010. A perspective: photosynthetic production of fatty acid-based biofuels in genetically engineered cyanobacteria. Biotechnology Advances 28, 742-746.

Machado, I.M.P., Atsumi, S., 2012. Cyanobacterial biofuel production. Journal of Biotechnology 162, 50-56.

Markou, G., Angelidaki, I., Georgakakis, D., 2012. Microalgal carbohydrates: na overview of the factors influencing carbohydrates production, and of main bioconversion technologies for production of biofuels. Appl. Microbiol. Biotechnol. 96, 631-645.

Markou, G., Angelidaki, I., Nerantzis, E., Georgakakis, D., 2013. Bioethanol production by carbohydrate-enriched biomass of *Antrospira (Spirulina) platensis*. Energies 6, 3937–3950.

Miranda, J.R., Passarinho, P.C., Gouveia, L., 2012. Pre-treatment optimization of *Scenedesmus obliquus* microalga for bioethanol production. Bioresource Technolgy 104, 342-348.

Mollers, K.B., Cannella, D., Jorgensen, H., Frigaard, N., 2014. Cyanobacterial biomass as carbohydrate and nutrient feedstock for bioethanol production by yeast fermentation. Biotechnology for Biofuels 7, 1-11.

Moraes, B.S., Zaiat, M., Bonomi, A., 2015. Anaerobic digestion of vinasse from sugarcane ethanol production in Brazil: challenges and perspectives. Renewable and Sustainable Energy Reviews 44, 888-903.

Moraes, B.S., Petersen, S.O., Zaiat, M., Sommer, S.G., Triolo, J.M., 2017. Reduction in greenhouse gas emissions from vinasse through anaerobic digestion. Applied Energy 189, 21-30.

Peccia, J., Haznebaroglu, B., Gutierrez, J., Zimmerman, J.B., 2013. Nitrogen supply is an important driver of sustainable microalgae biofuel production. Trends in Biotechnology 31(3), 134-138.

PESQUISA FAPESP., 2008. Ethanol from algae (Original Title: Álcool de algas).

Qiao, J., Wang, J., Chen, L., Tian, X., Huang, S., Ren, X., Zhang, W., 2012. Quantitative iTRAQLC-MS/MS proteomics reveals metabolic responses to biofuel ethanol in cyanobacterial *Synechocystis sp.* PCC 6803. Journal of Proteome Research 11, 5286-5300.

Robertson, D.E., Jacobson, S.A., Morgan, F., Berry, D., Church, G.M., Afeyan, N.B., 2011. A new dawn for industrial photosynthesis. Photosynthesis Research 107, 269 – 277.

Rosgaard, L., Porcellinis, A.J., Jacobsen, J.H., Frigaard, N., Sakuragi, Y., 2012. Bioengineering of carbon fixation, biofuels, and biochemical in cyanobacteria and plants. Journal of Biotechnology 162, 134-147.

Santander, C., Robles, P.A., Cisternas, L.A., Rivas, M., 2014. Technical-economic feasibility study of the installation of biodiesel from microalgae crops in the Atacama Desert of Chile. Fuel Processing Technology 125, 267-276.

Savakis, P., Hellingwerf, K.J., 2015. Engineering cyanobacteria for direct biofuel production from CO_2. Current Opnion in Biotechnology 33, 8-14.

Savakis, P., Tan, X., Du, W., Santos, F.B., Lu, X., Hellingwerf, K.J., 2015. Photosynthetic production of glycerol by a recombinant cyanobacterium. Journal of Biotechnology 195, 46-51.

Sawaengsak, W., Silalertruksa, T., Bangviwat, A., Gheewala, S.H., 2014. Life cycle cost of biodiesel production from microalgae in Thailand. Energy for Sustainable Development 18, 67-74.

Sforza, E., Gris, B., De Farias Silva, C.E., Morosinotto, T., Bertucco, A., 2014. Effects of light on cultivation of *Scenedesmus obliquus* in batch and continuous Flate Plate photobioreactor. Chemical Engineering Transactions 38, 211-216.

Slade, R., Bauen, A., 2013. Micro-algae cultivation for biofuels: cost, energy balance, environmental impacts and future prospects. Biomass and Bioenergy 53, 29-38.

Sunda, W.G., Huntsman, S.A., 1997. Interrelated influence of iron, light and cell size on marine phytoplakton growth. Nature 390, 389–392.

Tan, X., Yao, L., Gao, Q., Wang, W., Qi, F., Lu, X., 2011. Photosynthesis driven conversion of carbon dioxide to fatty alcohols and hydrocarbons in cyanobacteria. Metabolic Engineering 13, 169-176.

Tercero, E.A.R., Sforza, E., Bertucco, A., 2013. Energy profitability analysis for microalgal biocrude production. Energy 60, 373-379.

Tercero, E.A.R., Domenicali, G., Bertucco, A., 2014. Autotrophic production of biodiesel from microalgae: An update process and economic analysis. Energy 76, 807–815.

Thiel, T., 1995. Genetic analysis of cyanobacteria. In: BRYANT, D.A. (ed.), The molecular biology of cyanobacteria. Dordrecht: Kluwer Academic Press, 581-611.

Ueno, Y., Kurano, N., Miyachi, S., 1998. Ethanol production by dark fermentation in the marina green alga, *Chlorococcum littorale*. Journal of Fermentation and Bioengineering 86(1), 38-43.

U.S. Department of Energy., 2015. Fuel Prices. Published online in October.

Vitovà, M., Bisova, K., Kawano, S., Zachleder, V., 2015. Accumulation of energy reserves in algae: from cell cycles to biotechnological applications. Biotechnology Advances 33, 1204-1218.

Walcher, M., 2015. Algenol CEO resigns, company lays off employees. WINKNEWS. Published online in October.

Wang, L., Li, Y., Sommerfeld, M., Hu, Q., 2013. A flexible culture process for production of the green microalga *Scenedesmus dimorphus* rich in protein, carbohydrate or lipid. Bioresource Technology 129, 289–295.

Wang, H., Ji, C., Bi, S., Zhou, P., Chen, L., Liu, T., 2014. Joint production of biodiesel and bioethanol from filamentous oleaginous microalgae *Tribonema sp*. Bioresource Technology 172, 169-173.

Yao, C., Ai, J., Cao, X., Xue, S., Zhang, W., 2012. Enhancing starch production of a marine green microalga *Tetraselmis subcordiformis* through nutrient limitation. Bioresource Technology 118, 438-444.

Yao, C., Ai, J., Cao, X., Xue, S., 2013. Characterization of cell growth and starch production in the marine green microalga *Tetraselmis subcordiformis* under extracellular phosphorous-deprived and sequentially phosphorous-replete conditions. Appl. Microbiol. Biotechnol. 97, 6099-6110. (a)

Yao, C., Ai, J., Cao, X., Xue, S., 2013. Salinity manipulation as an effective method for enhanced starch production in the marine microalga *Tetraselmis subcordiformis*. Bioresource Technology 146, 663-671. (b)

Zhu, L.D., Hiltunen, E., Antila, E., Zhong, J.J., Yuang, Z.H., Wang, Z.M., 2014. Microalgal biofuels: flexible bioenergies for sustainable development. Renewable and Sustainable Energy Reviews 30, 1035-1046.

Chapter 2

Bio-refinery as a promising approach to promote ethanol industry from microalgae and cyanobacteria

The development of new technologies to increase the production of biofuels without directly competing with food production is a must. Microalgal biomass has recently been in the highlight in this regard. In this chapter, the role of this biomass for bioethanol production is discussed within a biorefinery approach, in view to promote industrial sustainability. A cultivation aimed at accumulating around 50-60% of carbohydrates in the biomass (dry weight) and the importance of water and nutrient recycling are reviewed. Saccharification of biomass using enzymes or acids is addressed together with alternative operations (such as hydrothermal liquefaction and flash hydrolysis) that aim at recovering additional products (i.e. biocrude). Since the main monosaccharide in microalgal biomass is glucose, high rates of hydrolysis and fermentation are possible achieving more than 80% of the efficiency as a sum of these two operations. Anaerobic digestion to treat vinasse after distillation and the recycling of CO_2 from the ethanolic fermentation and from biogas combustion could increase the process sustainability. Finally, the advantage of using microalgae rather than other sources of biomass in bioethanol production is estimated with reference to the production rate, even though the cultivation costs remain still high•.

•*Part of this chapter was published in Brazilian Archives of Biology and Technology, in Press (2018) and has been accepted as a Book Chapter in Bioethanol Production from Food Crops. Elsevier, in Press, 2017.*

2.1 INTRODUCTION

In both developed and developing countries, exploiting natural resources in economic activities to provide clean technologies, especially in the industrial and agricultural sectors, has numerous advantages, including those related to resource saving, recycling and reuse of wastes. Therefore, exploitation of natural resources in industrial processes is essential to achieve a more sustainable world (Uenojo and Pastore, 2007; Gupta and Verna, 2015).

In general, increased and improved global strategies for energy security and mitigation of CO_2 emissions from energy production processes are required, especially those aimed at maximizing the energy efficiency by expanding the use of clean energy. This means using of fuels that promote the carbon cycle without changing the atmospheric balance (renewable fuels), and developing energy resources in CO_2 neutral systems (Brennan and Owende, 2010; Moraes et al., 2017).

In particular, biofuels play an important role in reducing global climate change. Their impact will depend on several aspects related to the selection of new technologies, legal restrictions, international trade, land use, choice of raw materials and management techniques (Worldwatch Institute, 2007; Silva and Bertucco, 2016). This is one of the main goals of what is known as a biorefinery approach.

Among other definitions, according to the International Energy Agency (IEA Bioenergy) biorefining is "the sustainable processing of biomass into a spectrum of marketable products and energy" (IEA, 2008). The National Renewable Energy Laboratory (NREL) comments that "biorefinery is a facility that integrates biomass conversion processes and equipment to produce fuels, power and chemicals from biomass" (NREL, 2015). As a rule, biorefinery is the integration of a given biomass, with all its components separated, to produce energy and chemicals. Biorefineries enlarge and spread the concept of biofuels, energy and chemicals from a renewable source and promote the concept of carbon cycle, aiming at sustainability, while helping in the reduction of production costs.

Ethanol is the main biofuel produced worldwide. Between 2007 and 2015, bioethanol throughput practically doubled, reaching 25 billion gallons per year, even though after 2010 the production was stagnant due the limitations of arable land for biomass

cultivation ('Food *vs.* Fuel') (AFDC, 2016). United States and Brazil are the main contributors in the field, using corn and sugarcane, respectively (**Figure 2.1**).

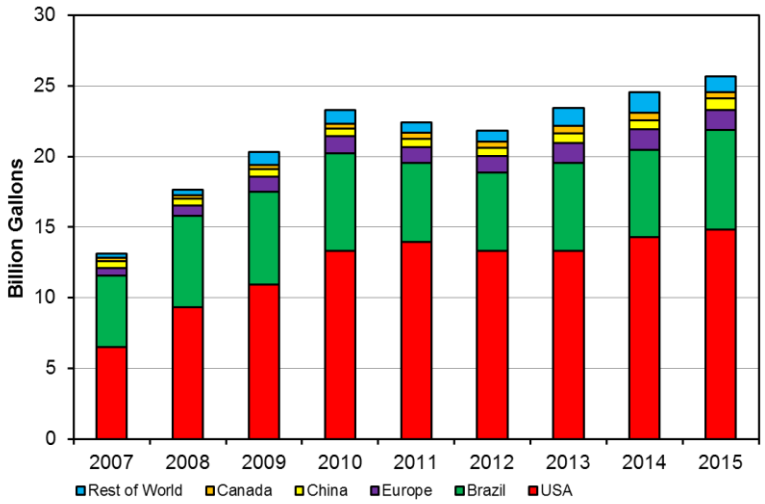

Figure 2.1: Global Ethanol Production by Country/Region and Year. Source: Adapted from AFDC, 2016. (http://www.afdc.energy.gov/data/).

Sugar cane ensures the lowest bioethanol production costs. In spite of its significant advantage, it is not a viable option for all the regions of the planet. Consequently, countries of the northern hemisphere have been incessantly looking for new technological routes that permit the efficient production of biofuels while respecting environmental and economic sustainability issues (BNDS, 2008), and 'new' generations of biomass-to-ethanol are proposed. In fact, based on the type of biomass, bioethanol production is classified as first (raw material saccharine or starch-based); second (lignocellulosic materials); third (microalgal/macroalgal biomass) and fourth (genetically modified cyanobacteria) generation.

Figure 2.2 represents a scheme of the four generations and the advantages/disadvantages of each one of them. The main concerns are about the land use, food *vs.* fuel competition, recalcitrance of the lignocellulosics/macroalgae, high cultivation costs of microalgae and little information in literature about genetically modified cyanobacteria.

Low costs are proper to first generation bioethanol (with the exception of corn-based one) which has a well-established and economically sustainable technology, while second generation still requires a decrease in production costs to become competitive,

with pretreatment and hydrolysis processes needing to be more effective and largely scalable (Gupta and Verna, 2015). On the other hand, micro and macroalgae have not reached an industrial scale operating plant yet. In the case of third and fourth generation bioethanol, further studies are required to develop a competitive and consolidated technology, taking into account also issues other than technological ones.

In addition, bioethanol based on lignocellulosic biomass (2nd generation) has greater saccharification difficulties, due to hemicellulose-cellulose-lignin tridimensional structure. In particular, lignin is a recalcitrant and non-fermentable component. High production rates associated with violent pretreatments and the use of a number of enzymes, in order to improve the productivity, make this process difficult for large scale consolidation with acceptable production costs, even if new lignocellulosic-based industrial plants in the last decade have been trying to stimulate this approach and to increase significantly the ethanol production worldwide.

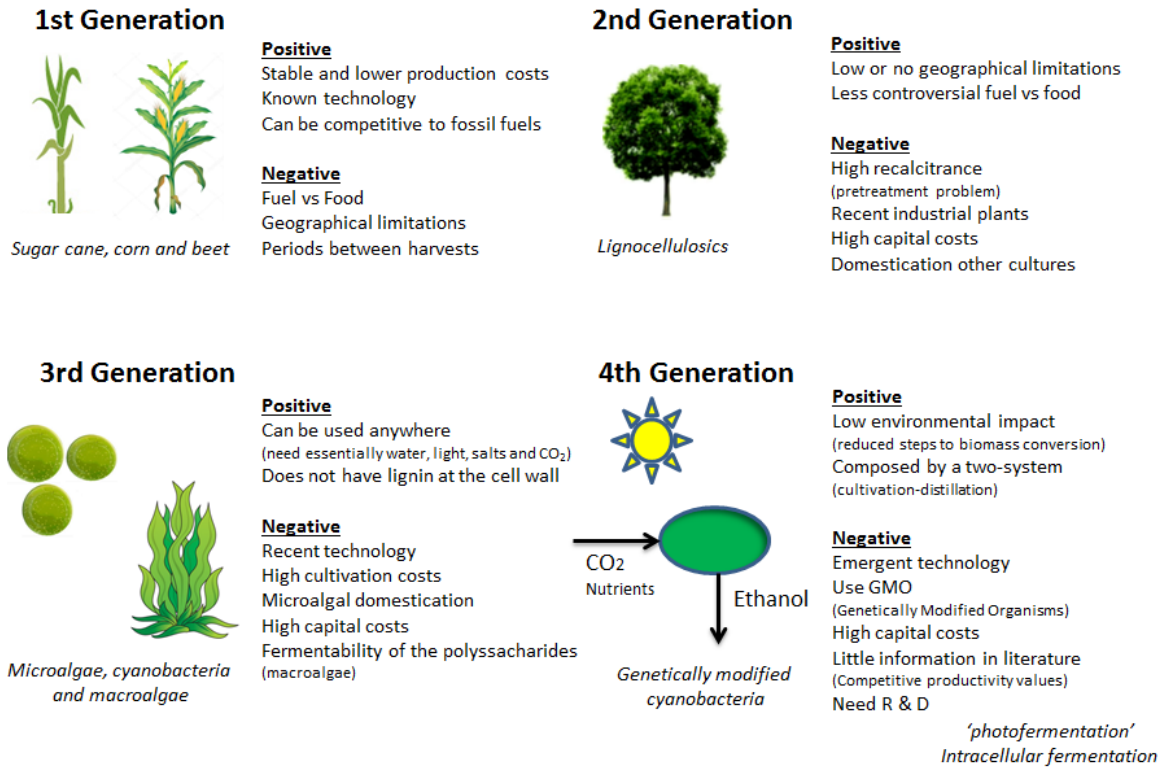

Figure 2.2: Biomass generations aimed to bioethanol production.

In third generation bioethanol, microalgae/macroalgae biomass is used, which does not have lignin in its cellular structure, and is cultivated with higher growth rates when compared to higher plants (John et al., 2011; Harun and Danquah, 2011; Ho et al., 2013; Wei et al., 2013; Hong et al., 2014). As for this biomass, a suitable process is not available yet, and the related costs cannot be properly estimated, researchers are trying:

- **for microalgae**: to optimize microalgal productivity and cultivation conditions, as this represents the highest production costs, considering that hydrolysis and fermentation are instead easier compared with lignocellulosics and macroalgae (Silva and Bertucco, 2016).
- **for macroalgae**: to increase the polysaccharide fermentability, considering that when the entire biomass (and not only the cellulose-rich residue remaining after hydrocolloid extraction) is saccharified, some residual sugars, such as mannitol, are not fermented by *S. cerevisiae* (Wei et al. 2013; Daroch et al., 2013; Enquist-Newman et al., 2014). Genetically modified microorganisms are proposed to this aim (Wei et al., 2013).

At last, fourth generation bioethanol is still an emerging technology and refers to the process in which ethanol is produced without need of biomass breakdown, i.e., using genetically modified cyanobacteria able to capture sunlight, water and nutrients and convert them directly into ethanol by 'photofermentation' (A representation of the steps for each technology is represented in **Figure 2.3**). It has a limited use protected by patents in the USA issued by Algenol® and Joule Unlimited® and little information is shared, which makes a real validation of the potentiality for these microorganisms quite difficult (Silva and Bertucco, 2016). Data available in the literature report a production of 0.025 mg L^{-1} in 6 days (*Synechococcus* PCC 7942) and 0.55 g L^{-1} after 6.25 days (*Synechocystis* PCC 6803) (Deng and Coleman, 1999; Angermayr et al., 2009; Tan et al., 2011), values indeed much lower than those divulgated by the companies (Silva and Bertucco, 2016). Because of their high growth rate, and relatively simple biochemical composition (partitioned among carbohydrates, lipids and proteins), microalgae are acknowledged as very promising feedstock for bioethanol production, and are the focus of this chapter.

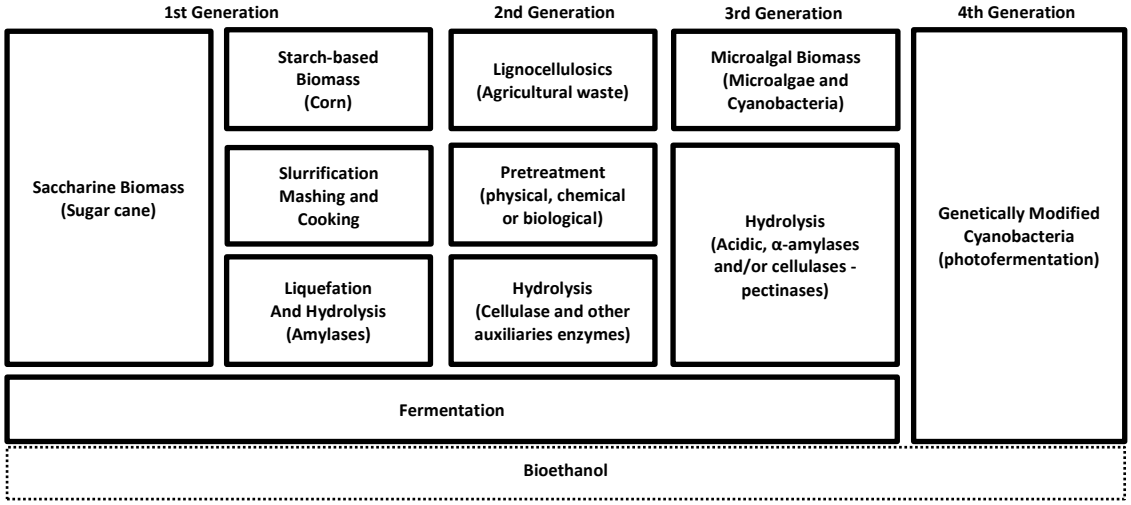

Figure 2.3: Main steps of the four generations to bioethanol production.

However, in order for this process to be economically and environmentally sustainable, it is essential to fully exploit the microagal biomass, by carefully recovering from it all the possible products as well as energy. Accordingly, in this chapter, we suggest the idea that it should be more correct to address the issue of microalgal bioethanol production from a biorefinery standpoint, with the main focus directed towards maximizing production of biofuels (ethanol/biodiesel) and energy (power generation), while at the same time promoting nutrients (nitrogen, phosphorous and other micronutrients) and CO_2 recovery/recycle integrated approach.

This concept can be applied to bioethanol production processes from microalgal biomass as proposed in the block-flow diagram of **Figure 2.4**. The different units of this flowsheet will be discussed separately in the following sections. In our opinion, the main challenges of microalgae-based ethanol biorefinery are related to: cultivation and carbohydrate production, hydrolysis and fermentation, CO_2/water/salts recycling and nutrient recovery by anaerobic digestion. Fine chemicals were excluded from the currently discussed process because they generally use carbohydrate or lipid fractions, and we focused on the biofuel-based biorefinery (bioethanol).

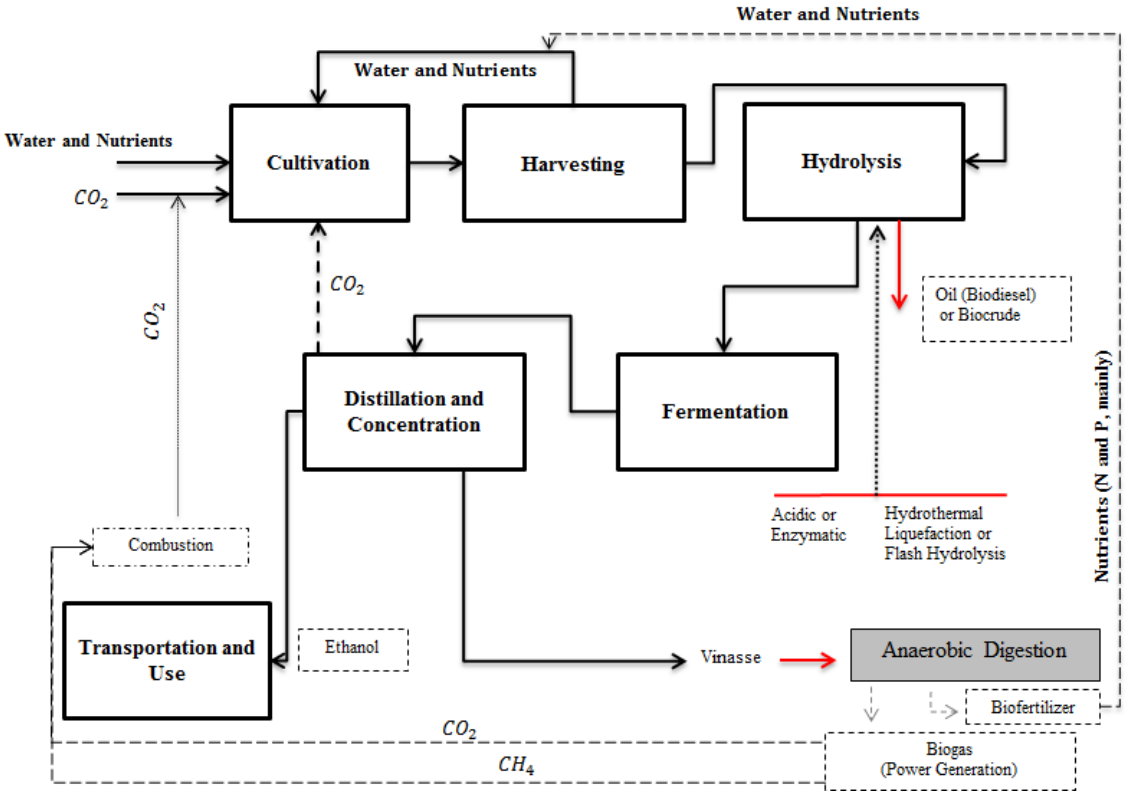

Figure 2.4: Flow chart of bio-ethanol production from microalgae biomass within the concept of biorefinery.

2.2 MICROALGAL BIOMASS CULTIVATION AND CARBOHYDRATE PRODUCTION: Screening of species and operation mode

Microalgae (eukaryote) and cyanobacteria (prokaryote) are photosynthetic microorganisms, exploited for their biochemical plasticity, i.e. the ability to change the biochemical composition as an adaptation to environmental and nutritional changes, and consequently to produce energy-reserves (carbohydrates and lipids). Even though applications as foods, food additives, animal feed, fertilizers and biochemicals are under investigation, this chapter is focused on microalgal biomass for biofuels. *Scenedesmus*, *Chlorella*, *Chlamydomonas*, *Tetraselmis* and *Nannochloropsis* are examples of industrial microalgae for carbohydrate/lipid production. As to cyanobacteria species, *Spirulina*, *Chlorococcus*, *Gloeocapsa*, *Synechocystis* and *Synechococcus* can be cited.

Photosynthesis represents a unique process of sunlight energy conversion. In this process, inorganic compounds and sunlight energy are converted to organic matter by photoautotrophs. Oxygenic photosynthesis can be expressed as a redox reaction driven

by light energy, in which carbon dioxide and water are converted to carbohydrates (not complex molecules) and oxygen.

When nitrogen limitation is used, according to the main method currently applied, it shifts the carbon fixed by Calvin's Cycle to produce substances other than nitrogen-based compounds (proteins), i.e. carbohydrates (polysaccharides) and lipids. Starch and glycogen are examples of polysaccharides accumulated as energetic reserves. Most of green algae accumulate starch as primary energy and carbon reserve, whereas lipids serve as a secondary storage, while cyanobacteria preferentially produce glycogen (Gonzalez-Fernandez and Ballesteros, 2012; Vitovà et al., 2015). On the other hand, some species, such as chrysolaminarin-producers (Heterokotophyta, Bacillariophyceae) and some oleaginous algae (*Nannochloropsis*, *Trachydiscus*) are apparently unable to produce polyglucans, thus they are not applicable in the context of this chapter (Vitovà et al., 2015).

Microalgae must ensure a high production rate of carbohydrates if bioethanol from fermentation is desired. Namely, nutritional techniques (nutrient starvation and carbon source), saline stress, light intensity and temperature (Chen et al., 2013, Silva and Bertucco, 2016) can be applied to this purpose. For instance, these are efficiently used for *Scenedesmus*, *Chlorella*, *Chlamydomonas* and *Tetraselmis*. Under proper conditions, microalgae/cyanobacteria species can accumulate carbohydrates with a fraction of dry cell weight up to 60%. For this reason, an adequate screening in order to find the faster species that can produce high amount of biomass and accumulate a good carbohydrate content is necessary. As shown in **Figure 2.6**, after nitrogen starvation several microalgae species accumulate carbohydrates with a maximum fraction of dry cell weight between 50-55%.

Cultivation can be carried out in batch, fed-batch or continuous systems. These operating modes, with their characteristics and procedure to accumulate carbohydrates, including pros and cons, are represented in **Figure 2.7**.

Chlorella vulgaris

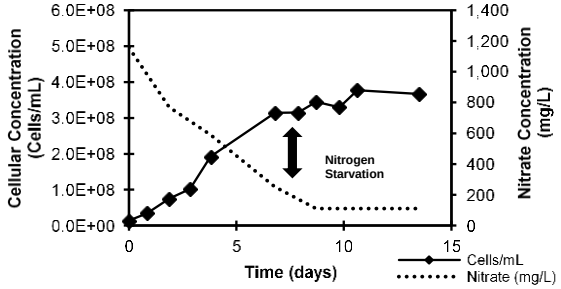

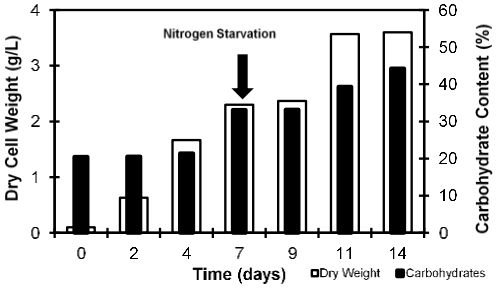

Chlorella prothotecoides

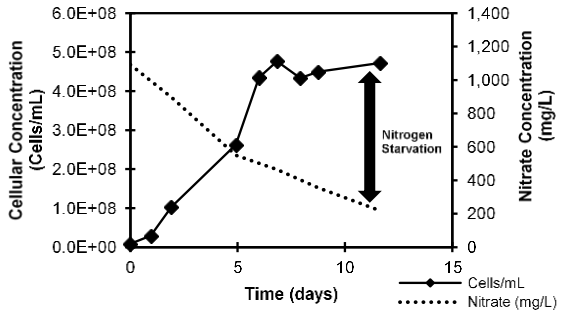

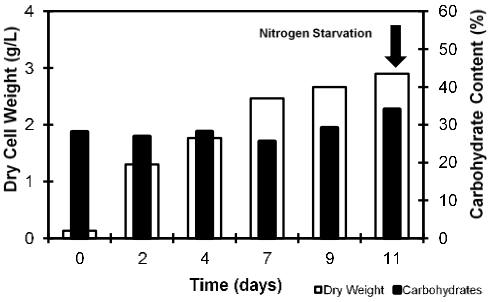

Muriella zoofigiensis

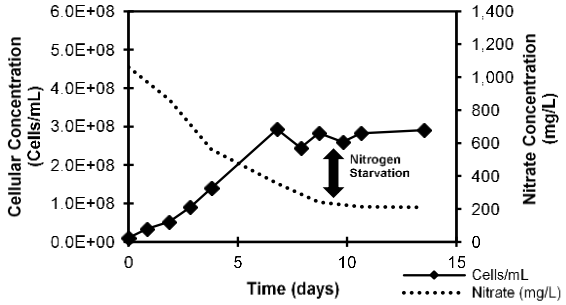

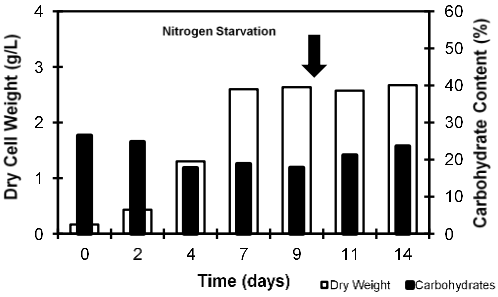

Scenedesmus obliquus

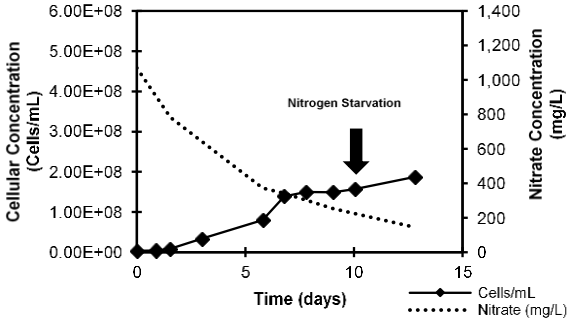

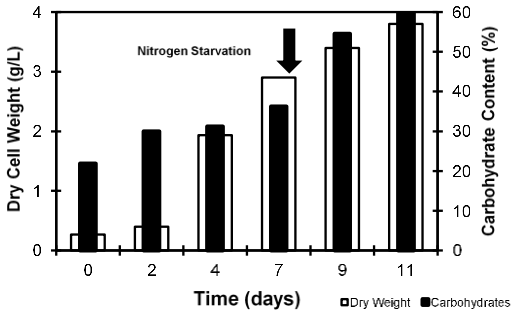

Figure 2.6: Screening of Microalgae Species with respect to Carbohydrate Accumulation. Species grown at 150 µmol photons/(m^2 s) and 28°C. *Chlorella vulgaris* and *Scenedesmus obliquus* were more promising to bioethanol application. Species were grown in medium BG-11 (Rippka et. al., 1979). Dry cell weight (DCW) or dry weight was measured by using 0.45 µm cellulose acetate filters (Whatman®) by gravimetry. The carbohydrate content was measured by the anthrone method (Trevelyan and Harrison, 1952). Nitrate concentration (used as reference substrate) was determined by Kit Idrimetre St. Carlo Erba Reagenti®.

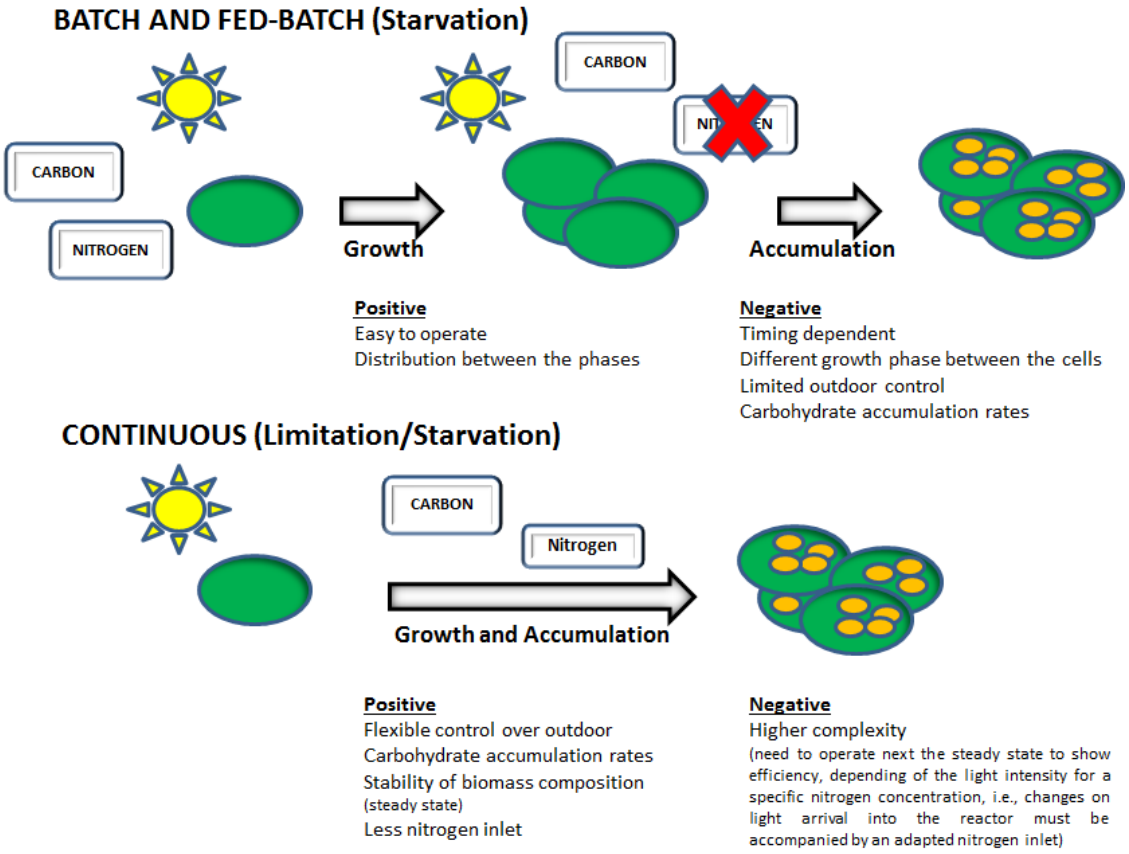

Figure 2.7: Mechanism of carbohydrate accumulation under nitrogen starvation/limitation at different operating systems.

In batch mode, the main concern is related to biomass productivity, as a two-steps operation is required: a first one (excess of nutrients), where biomass grows until nutrient starvation, and a second one (accumulation) where carbon continues to be fixed but it is converted in energy-reserves, like carbohydrates and lipids. In this second step, biomass is not produced anymore and, although the carbohydrate productivity slightly increases, the biomass productivity considerably decreases (generally between 40-60%). When continuous mode is carried out, using lower nitrogen concentration in the feed it is possible to obtain growth and carbohydrate accumulation simultaneously, thus achieving a steady state with 2-3 times higher carbohydrate productivity, even though biomass productivity decreases by 0-20% in comparison with a steady state performed with excess of nutrients. When the stress is moderate, carbohydrate is generally accumulated, but if it is strong, lipids are preferred, because these metabolisms (carbohydrate and lipids) are interconnected to the environmental/nutritional stresses.

2.3 HARVESTING AND WATER/NUTRIENT RECYCLE STEPS

In microalgae and cyanobacteria cultivation units a biomass concentration of not more than a few grams per liter can be achieved. In order to remove water, the most applied harvesting methods comprise flocculation (both pH induced and bioflocculation), coagulation, gravitational sedimentation, electric-based processes, filtration and centrifugation (Barros et al., 2015). Gravitational sedimentation, flocculation and centrifugation usually have higher yields and lower costs with respect to the others. It was shown that a carbohydrate-rich microalgal biomass (N stressed) increases its settling velocities up to 10 times in comparison with a control condition (N replete) (Depraetere et al., 2015).

Since the amounts of fertilizers and carbon dioxide required to microalgal cultivation represents a significant portion of production costs (Acién et al., 2012; Slade and Bauen, 2013), it is mandatory to minimize the waste of nutrients due to process purges. With respect to water/nutrient/CO_2 recycling, two process streams are discussed in this chapter (see **Figure 2.4**): the culture medium after cultivation and the exausted/solubilized biomass/organic matter at the end of ethanolic production step (the latter will be specifically discussed in **sections 2.5.1 and 2.5.2**).

Water and nutrient recycling after cultivation is an essential stage to make biofuels processes environmentally and economically sustainable, as it warrants a better use of available resources, with an increase in the process yield.

Microalgae biomass production has been estimated to consume water in a ratio 200-1000 kgwater/kg of dry biomass, with closed systems clearly losing less water than open raceways (Farooq et al., 2015; Béchet et al., 2016). For this reason, a reliable low-cost water supply is critical to the success of biofuel production from microalgae (Slade and Bauen, 2013). In particular, freshwater needs to be added to raceway ponds systems to compensate evaporation, while some PBR designs require high water consumption for heating/cooling. In addition, cleaning and purge water are examples of water use in an industrial plant and need be accurately quantified. A water balance of the system can be written according to (Guieysse et al., 2013):

$$V_{total,input} = V_{fill}F_{req} + V_{evap} + V_{blowdown} + V_{photo} + V_{harvest} + V_{drying} + V_{biomass} + V_{gray\ water} \quad (2.1)$$

where:
$V_{total,input}$ = water volume that needs to be added to the cultivationsystem annualy ($m^3/(m^2year)$);
V_{fill} – nominal water required to fill the cultivation system (m^3/m^2)
F_{req} – frequency of emptying the cultivation system for cleaning ($year^{-1}$)
V_{evap} – water loss due to evaporation ($m^3/(m^2year)$);
$V_{blowndown}$ – water removed during cultivation to maintain stable salinity and culture control ($m^3/(m^2year)$);
V_{photo} – water loss due the photosynthesis($m^3/(m^2year)$);
$V_{harvest}$ – water removal during the harvesting process ($m^3/(m^2year)$);
V_{drying} – water removed if the biomass is dried ($m^3/(m^2year)$);
$V_{biomass}$ – water in biomass (moisture content) ($m^3/(m^2year)$);
$V_{gray\ water}$ – water with nutrients or contaminants non-recycled in the process of cultivation ($m^3/(m^2year)$);
V_{photo} is a less amount and $V_{gray\ water}$ if the water is recycled can be neglected. The values of evaporation and water supply cost is geographic dependent.

This water requirement of the system can be significantly reduced by recycling the cultivation medium after harvesting. For example, it was reported that the water consumption to produce 1 L of biodiesel with C*hlorella vulgaris* would be reduced from 1500-3700 L to a range between 500-800 L (Yang et al., 2011; Farroq et al., 2015). Quantitative data related to specific water consumption for bioethanol in literature is lacking, but clearly recycling water after cultivation would allow significant savings also in this case.

Water recycling is not an issue for microalgal cultivation. For instance, *Chlorella zoofigiensis* was cultivated twice in water harvested and totally recycled, being adjusted the nitrogen and phosphorous content only (Zhu et al., 2013).

In relation to nutrients, it is necessary specially to control the correct use of macronutrients such as nitrogen, phosphorus, magnesium and sulfur, i.e., to quantify their concentrations in the effluent after cultivation, together with those of a number of micronutrients, such as, Fe, Al and Cu. Nutrient recycling is the only alternative to promote their maximum utilization.

However, water/nutrient recycling after cultivation can cause a number of problems:

- Salinity of the medium increases as a result of water evaporation (mainly Na, Ca, Mg and Cl) and strategies to monitorate them are necessary, in view of an economic and ecological viability, because saline stress is a problem for biomass productivity in microalgal systems;
- Aluminum and ferric salts used as bioflocculant deteriorate the water quality, because they can show inhibitory effects, which are species-dependent;
- The presence of organic molecules/particulate released from microalgae (extracellular compounds or from died cells) can inhibit the growth, even though the productivity can be improved due to mixotrophy;

- Higher bacterial, fungi and virus contamination is likely to occur (Slade and Bauen, 2013; Farooq et al., 2015).

Reverse osmosis and dilution are methods proposed to control water salinity, the latter being more feasible. To prevent contamination some techniques are suggested, such as filtration, ozonation, chlorination, treatment with hydrogen peroxide or heating. Also, centrifugation reduces significantly the content of contaminant microorganisms (Farooq et al., 2015).

Eventually, it is noteworthy that, when nitrogen limitation/starvation is applied, this nutrient is used efficiently, maximizing the carbohydrate/lipid production. Phosphorous content in the biomass can increase in nitrogen limitation/starvation conditions. An example is presented in **Figure 2.8,** which shows the remarkable difference between biomass production under nitrogen excess and limited/starved conditions, corresponding to around 50 g N/kg of microalgal biomass for nitrogen limited, instead of 130 g N/kg in nitrogen excess condition, thus reducing significantly the requirement of this fertilizer.

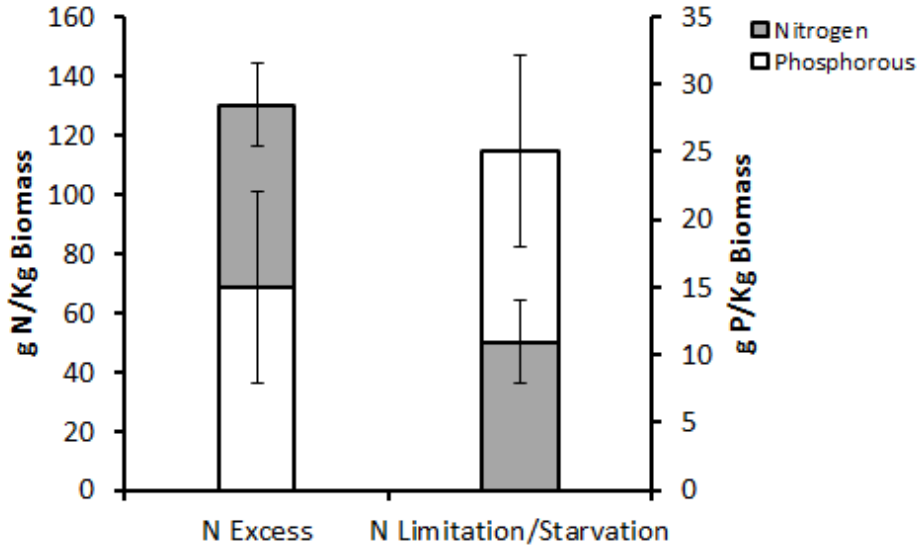

Figure 2.8: Difference between the nitrogen and phosphorous supplied to cultivate microalgae under excess and limitation/starvation of nitrogen. Data from Silva and Sforza (2016).

2.4 HYDROLYSIS AND FERMENTATION

Once biomass is harvested and a concentration of about 50-200 g/L is achieved, the carbohydrate fraction needs to be converted into simple sugars and fermented to produce bioethanol. The conventional saccharification-fermentation process is described below, followed by possible alternative processing routes aiming at a more strategic fractionation and recovery of products from the biomass.

2.4.1 Traditional methods

The main routes to saccharify microalgae are chemical (thermochemical) or enzymatic hydrolysis, each one with its own advantages. In any case, microalgae and cyanobacteria present lower recalcitrance in comparison to lignocellulosics/macroalgae, so that no pretreatment is needed, and hydrolysis can be performed in one step.

Concerning the **thermochemical process**, sulfuric, hydrochloric and nitric acid are effective in chemical saccharification, although more aggressive conditions than the enzymatic process are required for hydrolysis, generally ranging between 120 and 140 °C of temperature and between 15 and 30 min of reaction time, if > 80% saccharification and > 80% of theoretical fermentation yield are desired. If acid is not added, a hydrothermal process can be performed with the natural acidity of biomass but it requires higher temperature, between 160-220 °C (**See section 2.4.2**).

A few examples of acidic hydrolysis on microalgal biomass reported in the literature include:

- *Scenedesmus obliquus* when hydrolyzed at 120 °C using 2–3 N sulfuric acid for 30 min (biomass concentration between 20-500 g/L) yielded an almost total transformation of the carbohydrate content in reducing sugars (between 71–97% of hydrolysis extension), of which 65% was made of glucose (Miranda et al., 2012).
- *Scenedesmus bijugatus* with 26% carbohydrate content after lipid extraction, after acid hydrolysis (H_2SO_4 (0.36–1.08 N) at 130 °C, 45 min, and 20 g/L solid concentration) achieved 84% of sugars solubilization and was 70% converted in bioethanol (Ashokkumar et al., 2015).
- sulfuric acid hydrolysis was more efficient than enzymatic treatment with pectinases, amylases and cellulases (Kim et al., 2014) for *Chlorella vulgaris* FSP-E. In fact, Ho et al. (2013) reported that this acidic process, with H_2SO_4 (0.036–1.8 N) at 121 °C for 20 min and 10–80 g/L of biomass concentration, ensured 95% of glucose saccharification, and reached approximately 90% of the theoretical fermentation yield in 12 h with *Zymomonas mobilis* ATCC 29191.
- *Arthrospira platensis* was hydrolyzed using different acids (H_2SO_4, HNO_3, HCl and H_3PO_4, alone or combined) at a concentration of 0.25–2.5 N, and a temperature

between 60-100°C. The best result was 80% saccharification and 55% fermentation yield using *Saccharomyces cerevisiae* MV 92081 (Markou et al., 2013).

Enzymatic hydrolysis features mild temperatures and lower degradation risks. Enzymes used for the saccharification of microalgal biomass normally include amylases (glucoamylases and alfa-amylases), cellulases (endo-beta-glucanase, exo-beta-glucanase and beta-glucosidase) and pectinases, although hemicellulase can be required (separate or together). In this case, cell disruption is a crucial step. However, the major drawbacks of this treatment are related to the cost of enzymes, together with the necessity to control pH (generally using buffers) and to optimize temperature, according to the optimum conditions required by the specific enzyme. The performances obtained with enzymatic hydrolysis on different microalgal/cyanobacterial species can be summarized as follows:

- *C. vulgaris* was subjected to different methods of cell disruption, with beadbeating combined with pectinase (from *Aspergillus aculeatus*), resulting in sugars extraction increased between 45% and 70% and a subsequent fermentation yield of 89% after 12 h with *S. cerevisiae* KCTC 7906. For this species, pectinase appears as a more effective enzyme if compared with cellulases, amylases and xylanases (Kim et al., 2014).
- *Chlamydomonas reinhardtii* (50 g/L of biomass concentration and 59.7% of carbohydrate content) treated by separated hydrolysis and fermentation (SHF) using amylases (0.005% α-amylase from *Bacillus licheniformis* at 90 °C and 30 min to liquefaction and 0.2% glucoamylase from *Aspergillus niger* at 55 °C and 30 min to saccharification, pH 4.5) resulted in 94% hydrolysis efficiency and 60% of fermentation yield with *Saccharomyces cerevisiae* S288C (Choi et al., 2010).
- *Synechococcus* sp. PCC 7002 (with 3 g/L of biomass concentration and 60% of carbohydrate content), hydrolyzed 80% of sugars after enzymatic treatment (lysozyme, and α-glucanases Liquozyme® SC DS and Spirizyme® Fuel). After fermentation with *S. cerevisiae*, an ethanol yield of 86% with respect to the theoretical maximum rate was reached (Mollers et al., 2014).

2.4.2 Alternative processes

As an alternative to conventional acid or enzymatic hydrolysis, different processes have been proposed in the literature to fractionate the algal biomass by exploiting the solvent-like, tunable properties of water under hydrothermal conditions (high T and P). These processes (namely, hydrothermal liquefaction and flash hydrolysis) have been originally developed with the aim of converting microalgal biomass into biocrude, hence

exploiting mostly the oil fraction. They are particularly suitable for microalgae/cyanobacteria systems, considering that this type of biomass brings along a high-water content and its slurry is relatively easy to pump in continuous-flow systems.

Typically, **HTL** (hydrothermal liquefaction) is carried out in a temperature range between 220°C-374°C (i.e. subcritical water conditions), and the residence time is in the order of a few minutes (10-30 min) (López-Barreiro et al., 2013). It leads to the production of gaseous, aqueous and solid by-products. Under such conditions, sugars are degraded to furfurals, hydroxymethylfurfural (HMF), and other complex aromatic compounds (Martinez-Fernandez and Chen, 2017). However, by properly acting on the operating variables (i.e. temperature and residence time) carbohydrates can be extracted/hydrolyzed without being degraded. In addition, with respect to HTL applied to lignoscellulosic biomass, microalgal carbohydrates are easier to extract/hydrolyze, being present mostly as starch and without the presence of lignin.

As an example, a two-step Sequential Hydrothermal Liquefaction (SHTL) process has been proposed, which consists in a first extraction of polysaccharides under milder temperatures (140°C-200°C), followed by a second step of bio-oil production under typical HTL conditions (Miao et al., 2012; Chakraborty et al., 2013; Martinez-Fernandez and Chen, 2017). It has been reported that, under a temperature T = 160°C and 20 min of residence time, a maximum yield of 32% wt. polysaccharides could be extracted from *C. sorokiniana* biomass into the aqueous phase (Miao et al., 2012). That was characterized to be mainly a linear 1-4 linked glucan with only minor branching, which can be easily hydrolyzed to simple sugars (97.5% glucose) (Chakraborty et al., 2013). Similar results have been reported by Yuan et al. (2016), who obtained a recovery of sugars in the aqueous phase of 84.15% at 200°C and 60 min with *Scenedesmus* sp., even though only 1% was present as glucose, the rest being mostly oligosaccharides. By slightly increasing the temperature, polysaccharides could be, at least partially, directly hydrolyzed to monosaccharides (i.e. glucose), even though the formation of protein-sugar interaction compounds might also start to occur, so the conditions need to be specifically optimized to maximize sugars recovery.

Alternatively, a process called **Flash Hydrolysis** (FH) is also promising in this regard. It consists in treating the wet algal biomass under temperatures similar to those of HTL (210-350°C), but with extremely short residence times (less than 10 s), in a continuous-

flow system. Because of the fast reaction time, mainly proteins along with carbohydrates are extracted in the aqueous phase, while the rest ends up in a solid product (Garcia-Moscoso et al., 2013). This process looks very promising, considering that for crystalline cellulose treated at 335°C and 4.7 s, a 66.8% yield of hydrolysis products (mainly glucose and some oligomers) is obtained (Kumar and Gupta, 2008). In addition, a recovery of reducing sugars between 4% and 40% is reported for *Scenedesmus* sp. treated under temperatures between 205°C-325°C and 9-10 s of residence time (with the highest value reported for the highest temperature) (Garcia Moscoso et al., 2013). Controlling the residence time and ensuring rapid cooling is a key aspect to minimize degradation of glucose into undesired products, such as aldehydes, furfurals etc. A great advantage of FH is related to the rapid residence time, which allows easily working in continuous-flow systems, so that it appears more suitable for industrial scale plants.

One of the main advantages of these two hydrothermal processes is that they allow fractionation of the whole algal biomass with simultaneous recovery of different co-products: most importantly, the lipid fraction is converted into fuel products (see **Section 2.4.3**). Additionally, nutrients (mainly N, P, but also other inorganics such as S, Mg, K, etc.) are also extracted in the aqueous phase (Martinez-Fernandez and Chen, 2017, Teymouri et al., 2017), which can therefore be suitable for the subsequent fermentation step, by providing nutrients for yeasts growth. Alternatively, other high-value bio-products might be recovered by inducing precipitation of minerals from the aqueous phase: for example, Barbera et al. (2017) showed how Magnesium Ammonium Phosphate ($MgNH_4PO_4$) could be precipitated from the hydrolysate after FH and recycled as a slow-release fertilizer for algae cultivation or other applications. The hydrolysate itself has shown to be a good substrate for algal growth, suggesting that part of it could be recycled to the cultivation system. For instance, *Scenedesmus obliquus* was grown in the hydrolysate obtained from the same species for flash hydrolysis at 280 °C and 9 s of residence time. This species ensured better performance in batch cultivation than the standard medium for autotrophic growth, thanks to the combination with mixotrophy. In continuous mode, the productivities ranged between 0.62-0.72 g L^{-1} day^{-1}, showing satisfactory performances (Barbera et al., 2016).

Clearly, a solid residue is also left over by both of these processes: such biochar could however find applications in heavy metals removal from polluted water or as soil amendment (Abdel-Fattah et al., 2015). The removal of heavy metals such as copper, cadmium, chromium and lead has already been proven feasible with biochar obtained from switchgrass and other terrestrial biomasses (Abdel-Fattah et al., 2015, Regmi et al., 2012). Alternatively, even though it is not the preferable solution, the solid char could be combusted as a low-value fuel to supply a portion of the heat energy required by the process (Martinez-Fernandez and Chen, 2017).

The main disadvantage of hydrothermal processes is the high energy duty, caused by the rather strong temperature and pressure operating conditions. These might hinder the convenience of applying such a technology to exploit the useful fraction of microalgae. However, as water acts as both reaction medium and reactant, they allow avoiding the costs associated with chemicals (acids) or enzymes, provided that the conditions and fermentable sugars recovery yields are optimized. A comparison between the operating process conditions and main limitations are presented in **Table 2.1**.

Table 2.1: Comparison between the main discussed process for microalgal biomass hydrolysis.

Process of Hydrolysis	Range of Temperature (°C)	Operation Time	Limitations/Particularities
Acidic	110-140	5-60 min	Neutralization after hydrolysis (increase the salinity of the broth); Additional cost with chemicals.
Enzymatic	50-80	24-72 hours	Cellular rupture is necessary; Necessity to find an average value of pH and temperature (enzymatic mix – each enzyme has an optimum value); Accurately control of pH and temperature (sensibility of enzymes); Use of buffers to control the pH; Cost of enzymes.
HTL	160°C-200°C	10-30 min	High energy duty; Incomplete hydrolysis of polysaccharides;
Flash Hydrolysis	250-350	Less than 10 seconds	New technology (scale-up to pilot scale is needed to obtain more reliable results).

2.4.3 Lipid utilization

In view of a biorefinery concept, it has been stressed how the importance to recover products from the algal biomass needs to be maximized. In particular, the lipid fraction

should also be exploited for the production of additional liquid biofuels. When considering the traditional saccharification process, this is particularly important because chemical hydrolysis methods may also facilitate the subsequent solvent extraction of lipids, thereby recovering both fermentable sugars and lipids from the microalgal biomass.

Nannochloropsis gaditana, *Chlorella sorokiniana* and *Phaeodactylum tricornutum* have been treated by steam explosion with sulfuric acid (H_2SO_4, 0–3.6 N at 120–150°C for 5 min), and approximately 96% of the sugar content was hydrolyzed using 0.6 N of the acid at 150°C. The acid hydrolysis of these microalgae biomasses also increased the efficiency of lipid extraction (Lorente et al., 2015). Wang and coworkers (2014) reported a 25% increase in lipid contents obtained before and after hydrolysis of the microalgae *Tribonema* sp. with H_2SO_4 1 N. The carbohydrate content was hydrolyzed to 80% for a biomass concentration of 50 g/L in suspension at 121°C and 45 min, and 70% of the theoretical yield was achieved after fermentation with *S. cerevisiae*. Recent studies on wet lipid extraction from algal biomass are also promising (Naghdi et al., 2016), encouraging the recovery of oil, to be then converted into biodiesel via transesterification, by eliminating the extremely high cost otherwise associated with biomass drying.

The FH process described in the previous section also allows recovering the lipid fraction from the starting microalgal feedstock, which could be subsequently converted into biodiesel. In fact, from experiments carried out at 280°C and 9 s residence time, using different algal species (e.g., *Scenedesmus* sp. and *Nannochloropsis gaditana*) it was found that roughly 90% of initial lipids are preserved in the solid fraction (Garcia-Moscoso 2013,2015; Teymouri et al., 2017). In particular, Teymouri et al. (2017) verified that the FAME profile of the lipids retained in the solid was consistent with that of the starting algal biomass. Moreover, thanks to the fact that the solid product is already partially degraded, and that its lipid content can be as high as 70% (Teymouri et al., 2017), lipids extraction will also be facilitated.

If the SHTL approach is followed, instead, the residual biomass remaining after the first step is then converted into biocrude. Compared to direct HTL, the biocrude produced with the two-step approach is reported to have lower oxygen, nitrogen and sulfur contents, thanks to the prior extraction of proteins along with polysaccharides. In

addition, the production of solid char residues is also reduced, while biocrude yields of roughly 30% and Higher Heating Values (HHV) between 33-37 MJ kg^{-1} are reported for different *Chlorella* species (Martinez-Fernandez and Chen, 2017).

2.5 NUTRIENT RECOVERY

The possibility of nutrients recovery is of tremendous importance when large-scale biomass cultivation is desired for biofuels production. In fact, standard mediums, which are recipes providing an optimized mixture of nutrients to support microalgae growth, are very expensive. Thus, in a biorefinery approach, recycling carbon, nitrogen, phosphorous and other micronutrients is mandatory, and could definitely increase the sustainability of the proposed ethanol process from photosynthetic microorganisms (Barreiro et al., 2015). While the recycling of cultivation medium after harvesting was discussed in section 19.3, nutrients can also be recovered from the residual biomass, since only little amounts of them end up in the biofuels products. In this regard, the recycling of nutrients (N and P) and CO_2 by anaerobic digestion and from fermentation is discussed in the following.

2.5.1 Anaerobic digestion of vinasse

After the operations of sugars fermentation and subsequent bioethanol distillation, all the remaining organic matter from biomass and yeasts together with large amounts of macro and micronutrients (especially K, N and P) end up in a wastewater effluent, the so-called vinasse. Vinasse produced from sugar cane or sugar beet biorefineries is typically employed as field fertilizer for crop production, or as an additive animal feed (Moraes et al., 2017). However, considering the high organic content, this application does not appear as a good one in terms of environmental impacts (CO_2 and CH_4 emissions, for example).

In agreement with the concept of biorefinery, treating this effluent by anaerobic digestion (AD) looks like a promising option (**Figure 2.4**). Through anaerobic digestion, in fact, the organic matter can be converted into biogas (i.e., a mixture of mainly CH_4 and CO_2, with volumetric amounts of roughly 55-70% and 45-30% respectively). The biogas produced can then be used for combined heat and power generation, to be integrated in any of the energy consuming operations within the

industrial process. The CO_2 so obtained could, on the other hand, be reused in loco for the cultivation of the microalgae/cyanobacteria (Thiansathit et al., 2015), together with that derived from the fermentation process (**see section 2.5.2**).

In addition to biogas, anaerobic digestion also produces a liquid digestate in which nutrients are mineralized: for example, organic nitrogen is converted into ammonium (i.e., the most preferred form for microalgae to uptake) (Markou et al., 2014), while phosphorus into phosphate salts. Specifically, for stillage which has a good C/N for AD, after the digestion nitrogen and phosphorous content in liquid phase are higher, since these fractions are not left in gaseous phase (Moraes et al., 2015; Silva and Abud, 2016).

Such a digestate can indeed be employed as a nutrient source for microalgal cultivation: for instance, *Chlorella vulgaris* was successfully cultivated in anaerobically digested sugarcane stillage, showing good consumptions of N and P from the effluent (Marques et al., 2013). Thanks to nutrients recycling into the microalgal cultivation system by anaerobic digestion of vinasse, the supply of fresh fertilizers required would be greatly reduced, thus increasing the sustainability of the process, as well as its economicity.

So far, anaerobic digestion of vinasse from microalgal bioethanol production has not been investigated much. However, a few reports carried out on AD of sugar cane vinasse, which is starting to be considered a promising approach in the Brazilian area, show that promising results can be obtained, provided that the operating parameters are properly considered (Koyana et al., 2016). Among the aspects to be investigated are the likely better suitability of employing thermophilic rather than mesophilic conditions (given the temperature of the effluent from the distillation process); also, the high amount of proteinaceous material (after the extraction of both carbohydrates and lipids from the microalgal biomass), may lead to low C/N ratios in the vinasse, which could hinder the anaerobic digestion process, so that co-digestion with other C-richer substrates may be advisable (Moraes et al., 2017). Overall, given all the promising aspects related to nutrients and CO_2 recovery together with energy generation, the possibility of integrating anaerobic digestion of vinasse in microlagal/cyanobacterial bioethanol production certainly deserves further attention and investigation.

2.5.2 CO_2 recycling

Since in the next future it might not be permissible for industrial applications to emit CO_2 in large amount at ground level (Slade and Bauen, 2013), recycling carbon streams in the process is important, especially in microalgal systems.

The re-use of carbon dioxide in ethanol biorefineries is a must (Moncada et al., 2014). Generally, 1 kg of dry algal biomass requires at least 1.83 kg of CO_2. In practical terms, the efficiency of CO_2 fixation in open raceways may be less than 10%; for a thin layer cultivation, it can achieve 35%. In closed tubular photobioreactors (PBRs) CO_2 fixation efficiencies of around 75% are reported (Slade and Bauen, 2013).

Almost half of initial sugars mass during the fermentation is 'lost' as carbon dioxide (CO_2) (Glucose → Ethanol + $2CO_2$). This carbon has a market value and can be used in several processes, such as food industry or chemical synthesis, or be stored as value added product and softener the environmental impact (CO_2 emissions), thus decreasing energy losses and process costs (Kheshgi and Prince, 2005; Xu et al., 2010).

In this sense, the development of a technology able to capture carbon dioxide becomes important, being essential in view a sustainable/economic/environmental aspect of the whole process (Mollersten et al., 2003; Rhodes and Keiter 2005; Xu et al. 2010).

Another application is to use this carbon dioxide to cultivate microalgae, because at industrial level supply and maintenance of this gas can correspond up to 50% of production costs (Chisti, 2013; Silva et al., 2016). As an example, *Dunaliella teriolecta* was cultivated with CO_2 from beer fermentation, reaching a growth rate of 0.58 day^{-1} and biomass productivity 0.18 g L^{-1} day^{-1} (18 klx, 28°C and airflow rate of 1 L min^{-1}), which can represent a valuable contribution even to integrate first and second with third ethanol generation (Chagas et al., 2015).

2.6 POTENTIAL BIOETHANOL PRODUCTIVITY FROM MICROALGAE

Thanks to the higher growth rates and, consequently, biomass productivities, microalgae/cyanobacteria have a good potential for bioethanol extensive production. Maximum ethanol throughput is estimated to be between 46-140 thousand L bioethanol/(ha year), between 5-14 times higher than sugarcane (**Table 2.2**) (Cheryl, 2008). Actually, in continuous mode for *Chlorella vulgaris* and *Scenedesmus obliquus* under constant and day-night light cycles ethanol productivities of 11 and 30 thousand L

bioethanol/(ha year) were calculated (Silva et al., 2017), which are between 2-5 times higher than sugarcane (average of 6 thousand L bioethanol/(ha year)).

An economic/energetic analysis exclusively for an ethanol biorefinery from microalgae is lacking in the literature, and real figures of the feasibility of this process cannot be provided, so that it is presently not possible to compare with a biodiesel plant (first objective of microalgae exploitation for biofuels). However, cultivating microalgae for biofuels is still expensive and new developments are necessary.

Table 2.2: Comparison between plants and microalgae productivities for biofuels.

Raw Material	Carbohydrate Content (% dry biomass)	Yield ($L_{bioethanol}$ /$ton_{biomass}$)	Land Use ((m^2 year) /$L_{bioethanol}$)	Productivity ($L_{bioethanol}$ / (ha year))	Reference
Corn	–	460	2.5	3,450–4,600	BNDS, 2008
Beet	–	100	1.3	5,000–10,000	
Sugarcane	–	90	1.2	5,400–10,800	
Lignocellulosic Biomass (Sugarcane)	50–70	~400	1.0	~10,000	Santos et al., 2012; Santos et al., 2014
Microalgae (LCC)	20	129	1.40–0.47	7,093–21,279	Acién et al., 2012
Microalgae (MCC)	35	227	0.80–0.27	12,413–37,286	
Microalgae (HCC)	50	324	0.56–0.19	17,733–53,199	
Maximum Expectative for Microalgae	–	–	–	46,760–140,290	Cheryl, 2008

LCC – low carbohydrate content, MCC – medium carbohydrate content, HCC – high carbohydrate content.

2.7 CONCLUDING REMARKS AND FUTURE OUTLOOK

Research on microalgae and cyanobacteria cultivation, hydrolysis and fermentation are, as a rule, the object of many investigations even though they are not currently consolidated within a continuous process, as cultivation costs are still high (Tercero et al., 2014). The stage of water and nutrient recycles and the reuse of lipids in the biomass saccharification process of sugars/lipid extraction, anaerobic digestion and energy-economic analysis of viability still lack technical information. Further investigations should be undertaken to consolidate and guarantee the viability for the production of bioethanol from microalgae, but they are more likely to be successful if addressed within a biorefinery approach. Thus, a valuable analysis for this adapted technology is

necessary, because most of the data available are related to other processes, such as microalgal biomass for food or biodiesel.

REFERENCES

Abdel-Fattah, T.M., Mahmoud, M.E., Ahmed, S.B., Huff, M.D., Lee, J.W., Kumar, S., 2015. Biochar from woody biomass for removing metal contaminants and carbon sequestration. J. Ind. Eng. Chem. 22, 103-109.

Acién, F.G., Fernandez, J.M., Magan, J.J., Molina, E., 2012. Production cost of a real microalgae production plant and strategies to reduce it. Biotechnol. Adv. 30, 1344-1353.

AFDC. Ethanol production in the world. 2016. Available in: http://www.afdc.energy.gov/data/

Angermayr, S.A., Hellingwerf, K.J., Lindblad, P., Mattos, M.J.T., 2009. Energy biotechnology with cianobactéria. Curr. Opin. Biotech. 20, 257-263.

Ashokkumar, V., Salam, Z., Tiwari, O.N., Chinnasamy, S., Mohammed, S., Ani, F.N., 2015. An integrated approach for biodiesel and bioethanol production from *Scenedesmus bijugatus* cultivated in a vertical tubular photobioreactor. Energ. Convers. Manage. 101, 778 – 786.

Barbera, E., Sforza, E., Kumar, S., Morosinotto, T., Bertucco, A., 2016. Cultivation of *Scenedesmus obliquus* in liquid hydrolysate from flash hydrolysis for nutrient recycling. Bioresource Technol. 207, 59-66.

Barbera, E., Teymouri, A., Bertucco, A., Stuart, B.J., Kumar, S., 2017. Recycling minerals in microalgae cultivation through a combined flash hydrolysis – precipitation process. ACS Sustain. Chem. Eng. 5, 929-935.

Barreiro, D.L., Bauer, M., Hornung, U., Posten, C., Kruse, A., Prins, W., 2015. Cultivation of microalgae with recovered nutrientes after hydrothermal liquefaction. Algal Res. 9, 99-106.

BNDS, 2008. Banco Nacional de Desenvolvimento Econômico e Social. Bioetanol de cana-de-açúcar: Energia para o desenvolvimento sustentável. Rio de Janeiro: BNDS.

Barros, A.I., Gonçalves, A.L., Simoes, M., Pires, J.C.M., 2015. Harvesting techniques applied to microalgae: A review. Renew. Sust. Energ. Rev. 41, 1489-1500.

Béchet, Q., Shilton A., Guieysse, B., 2016. Maximizing productivity and reducing environmental impacts of full-scale algal production through optimization of open pond depth and hydraulic retention time. Environm. Sci. 50, 4102-4110.

Brennan, L., Owende, P., 2010. Biofuels from microalgae – a review of technologies for production, processing, and extractions of biofuels and co-products. Renew. Sust. Energy Rev..14(2), 557–577.

Chakraborty, M., McDonald, A.G., Nindo, C., Chen, S., 2013. An α-glucan isolated as a co-product of biofuel by hydrothermal liquefaction of *Chlorella sorokiniana* biomass. Algal Res. 2, 230-236.

Chagas, A.L., Rios, A.O., Jarenkow, A., Marcilio, N.R., Ayub, M.A.Z., Rech, R., 2015. Production of carotenoids and lipids by *Dunaliella tertiolecta* using CO_2 from beer fermentation. Process Biochem 50, 981-988.

Chen, C., Zhao, X., Yen, H., Ho, S., Cheng, C., Lee, D., Bai, F., Chang, J., 2013. Microalgae-based carbohydrates for biofuel production. Biochem. Eng. J. 78, 1-10.

Cheryl, 2008. Algae becoming the new biofuel of choice. Available in: http://duelingfuels.com/biofuels/non-food-biofuels/algae-biofuel.php

Chisti, Y., 2013. Constraints to commercialization of algal fuels. J. Biotechnol. 167, 201-214.

Choi, S.P., Nguyen, M.T., Sim, S.J., 2010. Enzymatic pretreatment of *Chlamydomonas reinhardtii* biomass for ethanol production. Bioresource Technol. 101, 5330-5336.

Daroch, M., Geng, S., Wang, G., 2013. Recent advances in liquid biofuel production from algal feedstocks. Appl. Energ. 102, 1371-1381.

Deng, M., Coleman, J.R., 1999. Ethanol Synthesis by Genetic Engineering in Cyanobacteria. Appl. Environ. Microb. 65(2), 523-528.

Depraetere, O. et al., 2015. Harvesting carbohydrate-rich *Arthrospira platensis* by spontaneous settling. Bioresource Technol. 180, 16-21.

Enquist-Newman, M. et al., 2014. Efficient ethanol production from brown macroalgae sugars by a synthetic yeast platform. Nature 505, 239-243.

Farooq, W., Suh, W.I., Park, M.S., Yang, J., 2015. Water use and its recycling in microalgae cultivation for biofuel application. Bioresource Technol. 184, 73-81.

Garcia-Moscovo, J.L., Obeid, W., Kumar, S., Hatcher, P.G., 2013. Flash hydrolysis of microalgae (*Scenedesmus sp.*) for protein extraction and production of biofuels intermediates. J. Supercrit. Fluids 82, 183-190.

Garcia-Moscovo, J.L., Teymouri, A., Kumar, S., 2015. Kinetics of peptides and arginine production from microalgae (*Scenedesmus sp.*) by flash hydrolysis. Ind. Eng. Chem. 54, 2048-2058.

Gonzalez-Fernandez, C., Ballesteros, M., 2012. Linking microalgae and cyanobacteria culture conditions and key-enzymes for carbohydrate accumulation. Biotechnol. Adv. 30, 1655-1661.

Guieysse, B., Béchet, Q., Shilton, A., 2013. Variability and uncertainty in water demand and water footprint assessment of fresh algae cultivation based on case studies from five climatic regions. Bioresource Technol. 128, 317-323.

Gupta, A., Verna, J.P., 2015. Sustainable bio-ethanol production from agroresidues: a review. Renew. Sust. Energ. Rev. 41, 550 – 567.

Harun, R., Danquah, M.K., 2011. Enzymatic hydrolysis of microalgal biomass for bioethanol production. Chem. Eng. J. 168, 1079-1084.

Ho, S., Huang, S., Chen, C., Hasunuma, T., Kondo, A., Chang, J., 2013. Bioethanol production using carbohydrate-rich microalgae biomass as feedstock. Bioresource Technol. 135, 191–198.

Hong, I.K., Jeon, H., Lee, S.B., 2014. Comparison of red, brown and green seaweeds on enzymatic saccharification process. J. Ind. Eng. Chem. 20, 2687-2691.

IEA., 2008. IEA Bioenergy Task 42 on biorefineries: co-production of fuels, chemicals, power and materials from biomass. Copenhagen, Denmark, 25-26, March 2007.

Jonh, R.P., Anisha, G.S., Nampoothiri, K.M., Pandey, A., 2011. Micro and macroalgal biomass: A renewable source for bioethanol. Bioresource Technol. 102, 186-193.

Kheshgi, H., Prince, R.C., 2005. Sequestration of fermentation CO_2 from ethanol production. Energy 30, 1865-1871.

Kim, K.H., Choi, I.S., Kim, H.M., Wi, S.G., Bae, H., 2014. Bioethanol production from the nutrient stress-induced microalga *Chlorella vulgaris* by enzymatic hydrolysis and immobilized yeast fermentation. Bioresource Technol. 153, 47-54.

Koyama, M.H., Junior, M.M.A., Zaiat, M., Junior, A.D.N.F., 2016. Kinetics of thermophilic acidogenesis of typical Brazilian sugarcane vinasse. Energy 116, 1097-1103.

Kumar, S., Gupta, R.B., 2008. Hydrolysis of microcrystalline cellulose in subcritical and supercritical water in a continuous flow reactor. Ind. Eng. Chem. Res. 47(23), 9321-9329.

Lopez-Barreiro, D., Prins, W., Ronsee, F., Brilman, W., 2013. Hydrothermal lioquefaction (HTL) of microalgae for biofuel production: state of the art review and future prospects', Biomass Bioenerg. 53, 113-127.

Lorente, E., Farriol, X., Salvado, J., 2015. Steam explosion as a fractionation step in biofuel production. Fuel Process. Technol. 131, 93-98.

Markou, G., Angelidaki, I., Nerantzis, E., Georgakakis, D., 2013. Bioethanol production by carbohydrate-enriched biomass of *Antrospira (Spirulina) platensis*. Energies 6, 3937 – 3950.

Markou, G., Vandamme, D., Muylaert, K., 2014. Microalgal and cyanobacterial cultivation: the supply of nutrients. Water Res. 65, 186-202.

Marques, S.S.I., Nascimento, I.A., Almeida, P.F., Chinalaia, F.A., 2013. Growth of *Chlorella vulgaris* on sugarcane vinasse: the effect of anaerobic digestion pretreatment. Appl. Biochem. Biotechnol. 171, 1933-1943.

Martinez-Fernandez, J.S., Chen, S., 2017. Sequential hydrothermal liquefaction characterization and nutrient recovery assessment. Algal Res. 25, 274-284.

Miao, C., Chakraborty, M., Chen, S., 2012. Impact of reaction conditions on the simultaneous production of polysaccharides and bio-oil from heterotrophically grown by a unique sequential hydrothermal liquefaction process. Bioresource Technol. 110, 617-627.

Miranda, J.R., Passarinho, P.C., Gouveia, L., 2012. Pre-treatment optimization of *Scenedesmus obliquus* microalga for bioethanol production. Bioresource Technol. 104, 342-348.

Mollers, K.B., Cannella, D., Jorgensen, H., Frigaard, N., 2014. Cyanobacterial biomass as carbohydrate and nutrient feedstock for bioethanol production by yeast fermentation. Biotechnol. Biofuels 7, 1-11.

Mollersten, K., Yan, J., Moreira, J.R., 2003. Potential market niche for biomass energy with CO_2 capture and storage – opportunities for energy supply with negative CO_2 emissions. Biomass Bioenerg. 25, 273-285.

Moncada, J., Tamayo, J.A., Cardona, C.A., 2014. Integrating first, second, and third generation biorefineries: incorporating microalgae into the sugarcane biorefinery. Chem. Eng. Sci. 118, 126-140.

Moraes, B.S., Zaiat, M., Bonomi, A., 2015. Anaerobic digestion of vinasse from sugarcane ethanol production in Brazil: Challenges and perspectives. Renew. Sust. Energ. Rev. 44, 888-903.

Moraes, B.S., Petersen, S.O., Zaiat, M., Sommer, S.G., Triolo, J.M., 2017. Reduction in greenhouse gas emissions from vinasse through anaerobic digestion. *Appl. Energ.* 189, 21-30.

Naghdi, F.G., Gonzalez, L.M., Chan, W., Schernk, P.M., 2016. Progress on lipid extraction from wet algal biomass for biodiesel production. Microb. Biotechnol. 9(6), 718-726.

NREL. What is a biorefinary? U. S. Department of Bioenergy. Available in: http://www.nrel.gov/biomass/biorefinery.html

Regimi, P., Moscovo, J.L.G., Kumar S., Cao X., MaO J., Schafran, G., 2012. Removal of copper and cadmium from aqueous solution using switchgrass biochar produced via hydrothermal carbonization process. J. Environ. Manage. 109, 61-69.

Rippka, R., Deurelles, J., Waterbury, J.B., Herdman, M., Stainer, R.Y., 1979. Generic assignments, strain histories and properties of pure cultures of cyanobacteria. J. Gen. Microb. 111, 1-61.

Santos, F.A., Queiroz, J.H., Colodette, J.L., Fernandes, A.S., Guimaraes, V.M., Rezende, S.T., 2012. Potencial da palaha da cana-de-açucar para a produçao de etanol. Quimica Nova 35(5), 1004-1010.

Santos, F.A., Queiroz, J.H., Colodette, J.L., Manfredi, M., Queiroz, E.L.R., Caldas, C.S., Soares, F.E.F., 2014. Otimizaçao do pré-tratamento hidrotérmico da palha de cana-de-açuca visando à produçao de etanol celulosico. Quimica Nova 37(1), 56-62.

Silva, C.E.F., Bertucco, A., 2016. Bioethanol from microalgae and cyanobacteria. Process Biochem. 51, 1833-1842.

Silva, C.E.F., Sforza, E., 2016. Carbohydrate productivity in continuous reactor under nitrogen limitation: effect of light intensity and residence time on nutrient uptake in *Chlorella vulgaris.* Process Biochem. 51, 2112-2118.

Silva, C.E.F., Gris, B., Sforza, E., La Rocca, N., Bertucco, A., 2016. Effects of sodium bicarbonate on biomass and carbohydrate production in *Synechococcus* PCC 7002. Chem. Engineer. Trans. 49, 241-246.

Silva, C.E.F., Abud, A.K.S., 2016. Anaerobic biodigestion of sugarcane vinasse under mesophilic conditions using manure as inoculum. Revista Ambiente e Agua 11(4), 763-777.

Silva, C.E.F., Sforza, E., Bertucco, A., 2017. Continuous cultivation of microalgae as an efficient method to improve carbohydrate productivity and biochemical stability. 26th European Biomass Conference and Exhibition, Stockholm, Sweden.

Slade, R., Bauen, A., 2013. Micro-algae cultivation for biofuels: cost, energy balance, environmental impacts and future prospects. Biomass Bioenerg. 53, 29-38.

Vitovà, M., Bisova, K., Kawano, S., Zachleder, V., 2015. Accumulation of energy reserves in algae: from cell cycles to biotechnological applications. Biotechnol. Adv. 6, 1204-1218.

Tan, X., Yao, L., Gao, Q., Wang, W., Qi, F., Lu, X., 2011. Photosynthesis driven conversion of carbon dioxide to fatty alcohols and hydrocarbons in cyanobacteria. Metabolic Engineering 13, 169-176.

Tan, I.S., Lee, K.T., 2014. Enzymatic hydrolysis and fermentation of seaweed solid wastes for bioethanol production: an optimization study. Energy 78, 53-62.

Tercero, E.A.R., Domenicali, G., Bertucco, A., 2016. Autotrophic production of biodiesel from microalgae: An update process and economic analysis. Energy 76, 807 – 815.

Teymouri, A., Kumar, S., 2017. Integration of biofuels intermediates production and nutrients recycling in the processing of a marine algae. Alche Journal 63(5), 1494-1502.

Thiansathit, W., Keesser, T.C., Khang, S., Ratpukdi, T., Hovichitr, P., 2015. The kinetics of *Scenedesmus obliquus* microalgae growth utilizing carbon dioxide gas from biogas. Biomass Bioenerg. 76, 79-85.

Trevelyan, W.E., Harrison, J.S., 1952. Studies on yeast metabolism. 1. Fractionation and microdetermination of cell carbohydrates. Biochem J. 50(3), 298-303.

Uenojo, M., Pastore, G.M., 2007. Pectinases: applications and perspectives [Pectinases: aplicações e perspectivas]. Revista Química Nova 30(2), 388-394.

Wang, H., Ji, C., Bi, S., Zhou, P., Chen, L., Liu, T., 2014. Joint production of biodiesel and bioethanol from filamentous oleaginous microalgae *Tribonema sp*. Bioresource Technol. 172, 169-173.

Wei, N., Quaterman, J., Jin, Y., 2013. Marine macroalgae. An untapped resource for producing fuels and chemicals. Trends Biotechnol 31(2), 70-77.

WORLDWATCH INSTITUTE, 2007. Biofuels for Transport. Washington, D.C.: Earthscan.

Xu, Y., Isom, L., Hanna, M.A., 2010. Adding value to carbon dioxide from ethanol fermentations. *Bioresource Technol.* 101, 3311-3319.

Yang, J., Xu, M., Zhang, X., Hu, Q., Sommerfeld, M., Chen, Y., 2011. Life-cycle analysis on biodiesel production from microalgae: water footprint and nutrients balance. Bioresource Technol. 102, 159-165.

Yuan, T., Li, X., Xiao, S., Guo, Y., Zhou, W., Xu, J., Yuan, Z., 2016. Microalgae pretreatment with liquid hot water to enhance enzymatic hydrolysis efficiency. Bioresource Technol. 220, 530-536.

Zhu, L.D., Takala, J., Hiltunen, E., Wang, Z.M., 2013. Recycling harvest water to cultivate Chlorella zoofigiensis under nutrient limitation for biodiesel production. Bioresource Technol. 144, 14-20.

Chapter 3

Carbohydrate production from microalgae and cyanobacteria: the effect of cultivation systems and nutritional factors

Photosynthetic microorganisms have received enormous attention due to their fast growth rate, higher photosynthetic efficiency and productivity, and high carbohydrates content (up to 60% DW). Microalgae and cyanobacteria are the organisms investigated, but some differences should be discussed between them, regarding carbohydrates composition, light utilization, growth rates, and biomass productivity. The common batch method to evaluate growth capabilities is strongly limited by a number of factors, such as the acclimation of preinoculum and a changing biomass concentration over time, which makes it more difficult to explain the results. Conversely, in a continuous system operated at steady-state, biomass production is constant and is well acclimated to the reactor adapting to environmental conditions. In this chapter, a brief comparison between cyanobacteria and microalgae based on composition, productivity and photosynthetic efficiency is completed and the effectiveness of the continuous system as a method to exploit these organisms for carbohydrate production is discussed•.

•*Part of this chapter is a Book Chapter in Advanced Bioprocessing for Alternative Fuels, Biobased Chemicals and Bioproducts. Elsevier, in Press (2018) and was presented as a conference paper in 25th European Biomass Conference and Exhibition, 12-15 June, Stockholm, Sweden, 2017.*

3.1 INTRODUCTION

Ethanol production from microalgae and cyanobacteria is still a matter under investigation and the related technology has not been fully realized commercially so far. The process of obtaining ethanol from microalgae is similar of the one used when producing ethanol from starch and cellulosic biomass (Cardoso et al., 2011; Silva and Bertucco, 2016). The cell wall of microalgae is composed by cellulosic and hemicellulosic structures. In addition, as storage of polysaccharides, microalgae and cyanobacteria have starch and glycogen, respectively. The absence of lignin, which is a recalcitrant compound present in higher plants, allows a faster and more effective hydrolysis and conversion of sugars.

In the last two decades, microalgae have been extensively studied as a complement to biodiesel production due to high levels of lipids accumulated in dry biomass (15-70%). However, the related cultivation costs are still quite high (Acién et al., 2012; Slade and Bauen, 2013) and most of the international research community unanimously comply with a systemic approach for microalgae production, where the production of fuels and high value-added compounds are combined to boost the feasibility of microalgae-based processes. So, in a biorefinery concept, carbohydrates and lipids could be extracted efficiently from microalgae biomass and used to produce biofuels, with the concomitant extraction of some valuable compounds. It is noteworthy that the chemical rupture of the biomass to obtain fermentable sugars can improve the solvent extraction of lipids. *Nannochloropsis gaditana*, *Chlorella sookiniana* and *Phaedactylum tricormutum* have been treated by steam explosion with sulfuric acid (0–10 % H_2SO_4, 120–150 °C for 5 min), so that sugars were efficiently recovered (almost 100%) and lipid extraction from the biomass was also increased (Lorente et al., 2015). Significant differences between the lipid content obtained before and after acidic hydrolysis of the microalga *Tribonema sp.*, were also reported, with an increase of about 25% of the extraction efficiency (Wang et al., 2014a).

In addition, microalgae carbohydrate exploitation is not limited to ethanol fermentation, as other products such as butanol, acetone, hydrogen, methane or a variety of high added value molecules can be obtained. For instance, butanol was produced with a concentration of 8.05 g/L (Gao et al., 2016) and 3.74 g/L (Castro et al., 2015) by using the residues of microalgal biomass after lipid extraction, which may still have a good

carbohydrate content. Moreover, butanol was obtained from *Chlorella vulgaris* JSC-6 hydrolyzate (mixed of glucose and xylose) with a productivity of 0.9 g L^{-1} d^{-1} (Wang et al., 2014b). Hydrogen can also be obtained between 38–97 mL g^{-1} VS using several microalgae species, such as *Scenedesmus* and *Chlorella* species (Kumar et al., 2016a), *Chlorella pyrenoidosa*, *Nannochloropsis oceanica* (Ding et al., 2016), and *Arthrospira platensis* (Xia et al., 2016). In addition, methane can be produced by the anaerobic digestion of algae residues (Ding et al., 2016; Kumar et al., 2016b). Concerning high value-added compounds, 7-aminocephalosporanic acid (antibiotic) was produced by *Chorella vulgaris* lipid-extracted-biomass (Park et al., 2016).

For bioethanol, productivity is mainly determined by the sugars concentration, since a high amount of fermentable carbohydrates can be converted by yeast and bacteria (*e.g.*, *S. cerevisiae* and *Z. mobilis*). A carbohydrate-rich microalgae biomass (~50%) has a theoretical bioethanol production of around 0.26 $g_{ethanol}/g_{biomass}$ (based on Gay-Lussac stoichiometry, 1 g monomer-glucose produces 0.5111 g ethanol), but the efficiency depends on the sugars extraction and saccharification methods, which must not degrade the sugars and ensures high rates of monomer production. Another factor is the composition of sugars present in the biomass because, for example, glucose (hexose) is easily fermentable by the strains mentioned above, but xylose (pentose) is not used by *S. cerevisiae,* (which is sometimes present in considerable amount within the carbohydrate-based microalgae biomass (20-30%) (Harun and Danquah 2011; Ho et al., 2013a). Other strains are necessary in this case, such as *Pichia stipitis* (aka *Scheffersomyces stipitis*), *Pichia segobiensis*, *Kluyveromyces marxianus*, *Candida shehatae* and *Pacchysolen tannophilus,* although the ethanol production rates are slow when compared to a *Saccharomyces*-glucose fermentation system (Silva and Bertucco, 2016). In addition, glucose is the main component of the carbohydrates in the biomass, reaching values between 60-90% of total carbohydrates, which is good as this monomer is easily fermentable by *Saccharomyces* strains (**Table 3.1**).

Some experimental values of ethanol/biomass yields obtained are 0.163 $g_{ethanol}/g_{biomass}$ (*Arthrospira platensis* – chemical hydrolysis) (Markou et al., 2013), 0.140 $g_{ethanol}/g_{biomass}$ (*Dunaliella tertiolecta* - chemeoenzimatic) (Lee et al., 2013) and 0.214-0.233 $g_{ethanol}/g_{biomass}$ (*Chlorella vulgaris* FSP-E - enzymatic and chemical hydrolysis), respectively (Ho et al., 2013).

Anyway, the exploitation of photosynthetic wild type organisms is increasing worldwide, as several biotechnological processes can utilize microalgae and cyanobacteria in fermentative applications for biofuels and high value-added chemicals. The main constraint for biofuel application is obviously linked to production costs, which can be possibly overcome by a rational approach to the process variables involved. On the other hand, the problem of fossil fuel availability cannot be postponed indefinitely; therefore, finding alternative routes to fuel supply is both urgent and strictly required from an environmental point of view.

Table 3.1: Carbohydrate composition in different microalgae and cyanobacteria species.

Microorganism	Carbohydrate Content (%)	Starch or Glycogen Content (%)	Monosaccharides*							Reference
			D-glu	L-fuc	L-rha	D-ara	D-gal	D-man	xyl	
***Chlamydomonas reinhardtii* UTEX 90**	59.7	43.6	75	0.67	1.5	3.2	4.5	2.3	-	Choi et al., 2010
***Chlorella variabilis* NC64A**	53.9	37.8	2.3**	-	42.9**	13.0**	19.1**	9.0**	13.7**	Cheng et al., 2013
***Chlorella vulgaris* P12**	-	41	-	-	-	-	-	-	-	Dragone et al., 2011
***Chlorella vulgaris* FSP-E**	53	-	94.3	-	-	-		5.7***		Ho et al., 2013°
***Chlorella vulgaris* KMMCC-9 UTEX26**	17.1-22.4	-	54	-	16	4.5	27	7	4.5	Kim et al., 2014
Chlorococcum spp.	32.5	11.3	47	-	-	-	8.9	1.5	29	Harun and Danquah, 2011
Scenedesmus obliquus	21-45	-	56	-	-	5	13	19	7.2	Miranda et al., 2012
***Scenedesmus obliquus* CNW-N**	50	-	~80	-	-	-	-	-	~20	Ho et al., 2013c
***Synechococcus elongatus* PCC 7942**	28-35	-	68-87	-	-	-	-	-	-	Chow et al., 2015
Synechococcus sp. PCC 7002	59	-	60	-	-	5	4	4	5	Mollers et al., 2014
Tetraselmis subcordiformis	44.1	-	~90							Yao et al., 2013a

glu-glucose, fuc-fucose, rha-rhamnose, ara-arabnose, gal-galactose, man-mannose e xyl-xylose. * Based in total carbohydrate content. **Based in the cell wall components only. *** D-gal + xyl.

3.2 MICROALGAE AND CYANOBACTERIA: Biological aspects and strains

The advantages of exploiting photosynthetic organisms for industrial applications are relevant in achieving a sustainable future. Microalgae are a polyphyletic group, which includes a large typology of organisms, often also the cyanobacteria, even though they may have extremely different characteristics. The phylum cyanobacteria or division

Cyanophyta is a group of oxygenic bacteria (prokaryotic) able to obtain energy by photosynthesis. They are commonly referred to as blue-green algae, even though the term "algae" is usually associated with eukaryotic organisms (such as the divisions Chlorophyta, Rhodophyta, and Heterokontophyta). Most species of cyanobacteria are terrestrial or live in fresh water but there are some marine species as well. *Spirulina*, *Chlorococcus*, *Gloeocapsa*, *Synechocystis*, and *Synechococcus* are examples of genera grouped in the cyanobacteria phylum, which are usually studied in view of scientific or industrial perspectives. The most studied genera of eukaryotic microalgae are *Scenedesmus*, *Chlorella*, *Chlamydomonas*, and *Nannochloropsis*. The taxonomy of photosynthetic microorganisms is historically based on morphology, biochemical composition, and pigmentation, but is under constant revision from a genetic and evolutionary point of view. Another key point to be accounted for is the wide species variability characterizing both eukaryotic microalgae and cyanobacteria; of the about 25,000 species known worldwide, approximately 70 are commercially exploited and play an important role in the production of foods, food additives, animal feed, fertilizer and biochemicals (**Figure 3.1**).

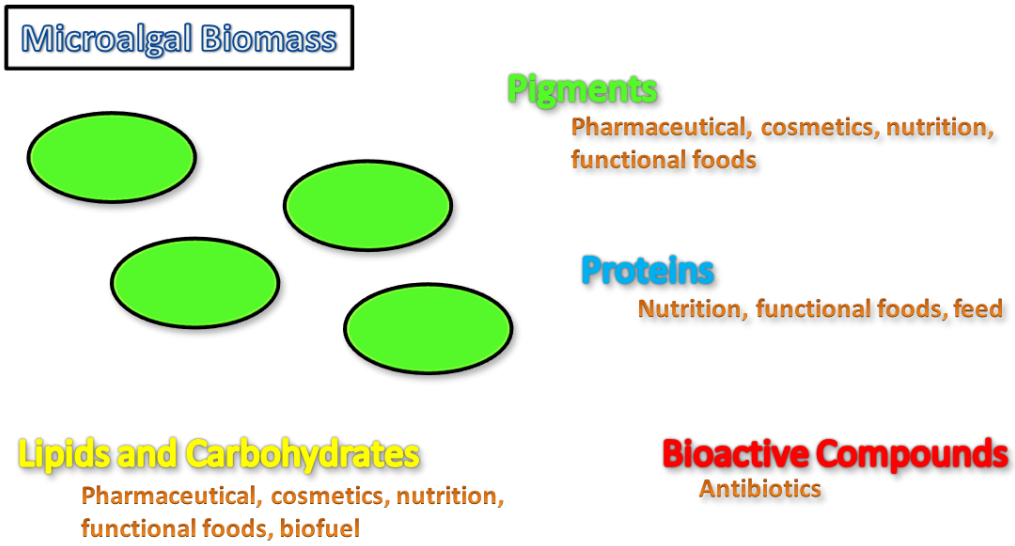

Figure 3.1: Industrial applications of microalgal components.

From a cultivation perspective, both microalgae and cyanobacteria may follow many metabolisms and are capable of a metabolic shift as a response to changes in the environmental conditions. They can grow: (i) photoautotrophically (i.e. using light as a

sole energy source which is converted to chemical energy through photosynthetic reactions); (ii) heterotrophically (i.e., exploiting only organic compounds as carbon and energy source, in the absence of light); (iii) mixotrophically or photoheterotrophically (i.e., performing photosynthesis as the main energy source for both organic compounds and CO_2 consumption). Amphitrophy (i.e., the capability of organisms to live either autotrophically or heterotrophically depending on the concentration of organic compounds and light intensity available), is commonly included in mixotrophy. The photoheterotrophic and mixotrophic metabolisms are not well distinguished, but they can be defined according to a difference in the energy source required to perform growth and specific metabolite production (Chojnacka and Noworyta, 2004; Abo-Shanab, 2015). Finally, certain microalgae species such as *Ochromonas danica* are capable of phagotrophic growth (i.e., feeding by engulfing a food cell or particle and ingesting it in a phagocytic vacuole) (Hosseini and Ju, 2015; Hosseini et al., 2016).

The main metabolism is certainly crucial in view of storage material accumulation, including carbohydrates for biofuel production. In the autotrophic process, the accumulation of carbohydrates within the cells is linked to the carbon fixation pathway during photosynthesis. If the aim is a sustainable biofuel production, sunlight must be the main energy source, as autotrophic growth is preferred. However, in a global perspective, the exploitation of wastewaters for nutrient supply in biofuel processes may also affect the carbon metabolism, as they contain organic compounds and particles that can be mixotrophically or phagotrophically used by certain microalgae and cyanobacteria species.

The types of carbohydrates present in the biomass have been reported (**Table 3.1**). Carbohydrates in microalgae are formed within the plastids as a storage product (starch) or cellular wall components, such as cellulose, pectin and sulfated polysaccharides (Chen et al., 2013). Conversely, cyanobacteria generally accumulate glycogen as a storage product. Glucose-based polysaccharides are more suitable since once hydrolyzed, they can be easily fermented by *S. cerevisiae* (the species most used at industrial level). In addition, from a chemical point of view the peptidoglycane-based cell wall of cyanobacteria can be degraded by lysozymes, as it has a lower complexity and diversity of polysaccharides than microalgae. Moreover, glycogen is soluble in water (while starch is not) which is another advantage of cyanobacteria when enzymatic

systems are applied (Mollers et al., 2014). Cyanobacteria can also accumulate polyhydroxybutyrate, which is very interesting for industrial applications (Gonzalez-Fernandez and Ballesteros, 2012).

On the other hand, a reliable comparison about carbohydrate production between microalgae and cyanobacteria is not possible yet, as little information about the stability of cyanobacterial production in industrial systems is available at present.

In terms of productivity, common values of growth rate constants are between 0.3–1.2 day^{-1} depending on the optimum environmental and nutritional conditions and reactor design for Chlorophytes and Cyanobacteria (Lurling et al., 2013), although these values can be increased by nutritional and environmental factors adaptations (Silva et al., 2016). Several species that may accumulate carbohydrates in a reasonable amount have been found, in some cases exceeding 50% of dry weight (**Table 3.2**), but most investigations are performed in batch and/or at laboratory scale and studies in continuous mode for scale-up are still missing. The reported carbohydrate productivities are between 0.1-0.6 g^{-1} L^{-1} day^{-1} showing that *Scenedesmus*, *Chlorella*, and *Synechococcus spp*., are the best microorganisms available at the moment for this approach. Factors such as temperature, nutrient form and availability, and light intensity are species-dependent. The best species in terms of productivity, energy conversion, and carbohydrate accumulation require screening with respect to a specific region, and the use of native species can help to overcome acclimation problems.

Table 3.2: Carbohydrate production: productivities and carbohydrate content.

Microorganism	Growth Conditions	Reactor Type	Operation Mode	Type of Stress	Dry Weight ($g\ L^{-1}$)	Carbo. Accumulation (%)	Carb. Productivity ($g\ L^{-1}day^{-1}$)	Reference
***Chlamydomonas reinhardtii* UTEX 90**	450µmol$m^{-2}s^{-1}$, 23°C, 4 days and 130 rpm	-	Fed-batch with acetate	NS	2.40	59.7	0.360	Choi et al., 2010
***Chlorella variabilis* NC64A**	150 µmol$m^{-2}s^{-1}$, 25°C, and 2% CO_2 (CO_2-air)	Glass bottle	Batch 16/8 light-dark cycle	NS	0.43	53.9	-	Cheng et al., 2013
***Chlorella vulgaris* P12**	70 µmol$m^{-2}s^{-1}$, 30°C and 2% CO_2 (CO_2-air)	Column PBR	Batch	NS and IS	-	41	0.199	Dragone et al., 2011
***Chlorella vulgaris* FSP-E**	60 µmol$m^{-2}s^{-1}$ and 2% CO_2 (CO_2-air)	Glass bottle	Batch	NS	5.51	51.3	0.631	Ho et al., 2013b
***Chlorella vulgaris* KMMCC-9 UTEX26**	150 µmol$m^{-2}s^{-1}$, 20-22°C, Bubbling air	Plastic containers	Batch 16/8 light-dark cycle	NS and SS	-	17.1–22.4	-	Kim et al., 2014
Chlorococcum spp.	Outdoor and bubbling CO_2 34.5 kPa	Bag PBR	Fed-batch	-	-	32.0	-	Harun and Danquah, 2011
***Dunaliella tertiolecta* LB999**	60 µmol$m^{-2}s^{-1}$, 20-25°C and 2% CO_2 (CO_2-air)	Plate PBR	-	-	-	37.8	-	Lee et al., 2013
***Dunaliella tertiolecta* LB999**	60 µmol$m^{-2}s^{-1}$ and 20-25°C	Plate PBR	-	-	-	40.5	-	Kim et al., 2015
Scenedesmus dimorphus	50 – 1200, 25°C and 2% CO_2.	Glass Column	Batch	NS	5	45-50	0.510	Wang et al., 2013
Scenedesmus obliquus	150 µmol$m^{-2}s^{-1}$, 25°C, Bubbling air	Tubular Bubble Column Open pound	- - -	- - -	0.37 0.41–0.68 0.81	24 45 29	- - -	Miranda et al., 2012
***Scenedesmus obliquus* CNW-N**	210-230 µmol$m^{-2}s^{-1}$, 28°C, 300rpm and 2.5% CO_2 (CO_2-air)	-	-	-	4.5	51.8	-	Ho et al., 2013c
***Scenedesmus obliquus* CNW-N**	220-240 µmol$m^{-2}s^{-1}$, 28°C, 300rpm and 2.5% CO_2 (CO_2-air)	Glass vessel	Batch Fed-Batch Continuous	NS NS HRT	- - -	49.4 52.9 35.6	0.273 0.467 0.312	Ho et al., 2013d
***Synechococcus elongates* PCC 7942**	200 µmol$m^{-2}s^{-1}$, 28°C, and 5 % CO_2 (CO_2-air)	-	Batch	-	2.9-3.7	28-35	0.144-0.564	Chow et al., 2015
***Synechococcus sp.* PCC 7002**	400 µmol$m^{-2}s^{-1}$ and 1% CO_2 (CO_2-air)	Vessels	Batch	NS	3.0	59	0.590	Mollers et al., 2014
Synechococcus sp. PCC 7002	150 µmol$m^{-2}s^{-1}$ and sodium bicarbonate (5.5-88 $g\ L^{-1}$)	Glass bottle	Batch	NS	6.0	30	0.360	Silva et al., 2016
Tetraselmis subcordiformis	200 µmol$m^{-2}s^{-1}$, 25°C and 3% CO_2 (CO_2-air)	Bubble Column	Batch	PS	2.5-5.6	24.8-44.1	0.180-0.310	Yao et al., 2013b
***Tetraselmis subcordiformis* FACHB-1751**	150 µmol$m^{-2}s^{-1}$, 25°C and 3% CO_2 (CO_2-air)	Bubble Column	Batch	Salinity and NS	1.7-4.5	30-40	0.070-0.420	Yao et al., 2013a
Tribonema sp.	-	-	-	-	-	31.2	-	Wang et al., 2014a

Carb. – Carbohydrates. NS – nitrogen starvation, IS – Iron starvation, SS – sulfur starvation, PS – phosphorous starvation, HRT – hydraulic retention time or residence time.

3.3 CULTIVATION OF MICROALGAE AND CYANOBACTERIA TOWARDS LARGE SCALE APPLICATION

When considering the possible exploitation of photosynthetic organisms for bioethanol production, a large-scale approach is the only way to assess the technical and economic feasibility of the whole process. Thus, moving from lab to industrial scale, the impact of variables involved in the cultivation step increases. Even not considering the technical challenges of downstream processes, which are currently under in-depth investigation, some critical aspects concerning the cultivation are not overcome yet. The main key issues still needing improvement are related to photosynthetic efficiency, CO_2 and nutrient supply, and the management of cultivation conditions to stimulate the accumulation of the target product of interest. Other aspects which are not considered in this chapter (i.e., the water supply, regulation of a suitable temperature, pH, salinity, and mixing), should be carefully considered as well.

However, data from large scale production is still limited, due to the high costs involved. Therefore, in order to limit investment risk a deeper comprehension of the variables and mechanisms involved in the cultivation step is necessary. Based on lab measurements, the dependence of growth parameters on key variables can be obtained, and can be then applied in reliable models useful to develop large scale process by simulation. Of course, the experimental approach, even at lab scale, must be carefully designed and performed, if the aim is to understand the effect of variables in view of large scale application.

3.3.1 Cultivation system and operation mode

The cultivation systems generally considered for the production of microalgae biomass are open and closed ones, generally ponds and photobioreactors (PBR), respectively.

Raceway ponds are the simplest alternative. These “systems are usually 30 cm deep and are relatively easy to construct and operate” (Slegers, 2014). Here, microalgae/cyanobacteria are grown under the same conditions of their natural environment, and the operation may be carried out continuously; however, open pounds are prone to contamination and evaporation.

In PBR's there is no direct contact with the atmosphere, so that they can be an alternative to avoid the problems of open ponds, and usually obtain a higher productivity (**Figure 3.2**).

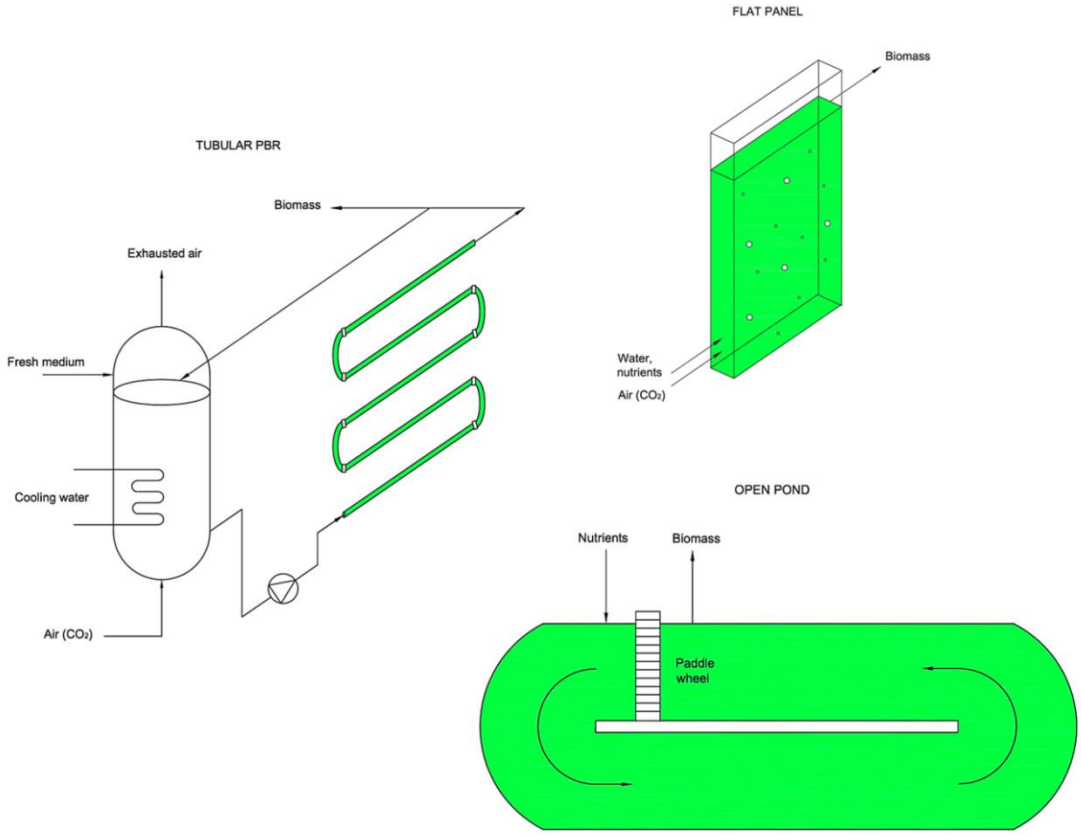

Figure 3.2: Operation mode of different photobioreactor configurations.

Closed reactors are more technologically advanced, with a past proposed example being "flat panel PBRs, which are rectangular reactors with light paths between 0.02-0.10 m, or tubular PBRs, which have usually a light path of 0.06 m" (Slegers, 2014). "The tubes can be placed horizontally next to each other ("horizontal" tubular PBR), or can be stacked vertically (resulting in a "vertical" tubular PBR)" (Slegers, 2014). Each type of reactor has a particular operation mode.

Closed systems have the greatest advantage of ensuring stable process productivity, while open systems are highly dependent on external conditions. On the other hand, the costs associated with closed reactors should be carefully considered, because they strongly affect the economical sustainability of the whole process. In **Table 3.3,** a comparison and the differences between open and closed systems are summarized. The discussion about open versus closed systems is currently fervent, but the productivity

advantages of PBRs should boost the research towards cheaper solutions. Some of the currently proposed solutions are based on a concept of a "closed pond", with a simple covering of the pond surface, or the allocation of the pond inside greenhouses (Cossu et al., 2014). Other solutions, specifically designed for marine environments, include floating permeable bags offshore (OMEGA Project) (NASA, 2012).

Table 3.3: Comparison between open and closed systems for microalgal cultivation.

Culture System	**Open Systems**	**Closed Systems**
Contamination control	Hard	Easy
Contamination risk	High	Reduced
Sterility	Does not have	Achievable
Process control	Hard	Easy
Species control	Hard	Easy
Mixing	Very poor	uniform
Operating System	Batch or semi-continuous	Batch or semi-continuous
Required space	PBR's ~ ponds	Depend of productivity
Area/volume ratio	Low (5 – 10 m^{-1})	High (20 – 200 m^{-1})
Cellular density	Low	High
Investments	Low	High
Operation costs	Low	High
Capital costs	PBR's > ponds	ponds 3 – 10 times cheaper
Light use efficiency	Poor	High
Temperature control	Hard	More uniform
Productivity	Low	3 to 5 times more productive
Water losses	PBR's ~ ponds	Depend cooling
Hydrodynamic stress to algae	Very low	High – Low
Culture medium evaporation	High	Low
Gas transfer control	Low	High
CO_2 Losses	Pbr's ~ ponds	depend of Ph, alkalinity ecc.
O_2 inhibition	Pbr's > ponds	A big problem to Pbr's
Biomass concentration	Pbr's > ponds	3 -5 times higher
Parameters reproducibility	not, depend of the climatic conditions	possible, depend of control conditions
Dependence of Temperature	High, does not have production in rainy periods, photihnibition	have an efficient control
Operating period	long, 6-8 weeks	short, 2-4 weeks
Scale-up	Hard	Hard

Source: Adapted from Pulz (2001) and Mata et al. (2010). PBR -photobioreactor.

Beside the geometry of the cultivation system, the major constraint towards industrial application is the operation mode of the reactor. Batch production is not suitable in an industrial perspective, while continuous processes could noticeably improve the performances, as a steady state production is generally more efficient, has lower costs and is easier to operate (Ho et al., 2014). At lab scale, cultivation of microalgae in

continuous systems is well established and has been studied for several species and different approaches (biomass production, lipid production, wastewater treatment and growth modelling development) (Sobczuk et al., 2000; Tang et al., 2012; Ruiz et al., 2013; Klok et al., 2013), but less information is available on carbohydrate accumulation under continuous operation (Ho et al., 2013d). The role of limitation/starvation in the accumulation of these substances in batch cultures is extensively proved for microalgae and cyanobacteria, reaching values of 60-65% (carbohydrate or lipids content, depending of the specie in optimized conditions) (Vitovà et al., 2015; Silva ad Sforza, 2016; Silva et al., 2017). As a result, in this case, a first step is required for growth and a second one for an efficient accumulation, according to the metabolic pathway to produce carbohydrates and lipids (**Figure 3.3**).

Unfortunately, the batch method requires more time, reducing significantly the productivity, and a more complex process, which results in higher capital and operating costs. In addition, a possible biomass degradation or the formation of secondary metabolite should be carefully considered, affecting the stability of biochemical biomass and a not guaranteed biochemical reproducibility over time due the instability/variability of the system.

For this reason, a proper study of the stress conditions that influence not only the carbohydrate content but biomass and carbohydrate productivity (light intensity, residence time and nitrogen availability, mainly), with respect to a control condition (no nutrient limitation/starvation condition) is necessary to confirm if energetic-reserve (carbohydrates) production is associated with substantial decreasing of biomass productivity.

As aforementioned, continuous cultivation of energetic reserves is still in development. Continuous production of lipids from microalgae was studied by a number of authors (Zhang et al., 2014; San Pedro et al., 2014), but they used a two-step system to increase the lipid content in the cells even reducing the productivity. Less literature information can be found to cultivate a carbohydrate-rich biomass in a continuous system. Ho et al. (2013d), continuous cultivation of *Scenedesmus obliquus*, but using the residence time as driver to carbohydrate accumulation, reached a carbohydrate productivity of 0.31 g L^{-1} day^{-1} at 240 µmol photons m^{-2} s^{-1}.

Cheng et al. (2017) used a two-stage system to accumulate carbohydrate with *Chlorella sp.* AE10. In the first step, the cultivation achieved 1 g L^{-1}, then the second step was performed diluting the culture to 0.1 g L^{-1} and reducing 75% of the nitrogen in the medium. A carbohydrate productivity of 0.27 g L^{-1} day^{-1} was achieved. Guccione et al. (2014), after a strain selection (*Chlorella spp*.) and optimization condition under nitrogen deprived experiments, showed carbohydrates productivities between 0.12-0.19 g L^{-1} day^{-1}, with a biomass productivity reduction higher than 50% (detail: this cultivation used an inoculum concentration of 0.4 g L^{-1}). *Neochloris oleabundans* was cultivated in continuous mode with a nitrogen inlet of 45 mg N L^{-1} day^{-1} (nitrogen starvation), and a reduction of more than 50% of biomass produced (De Winter et al., 2014).

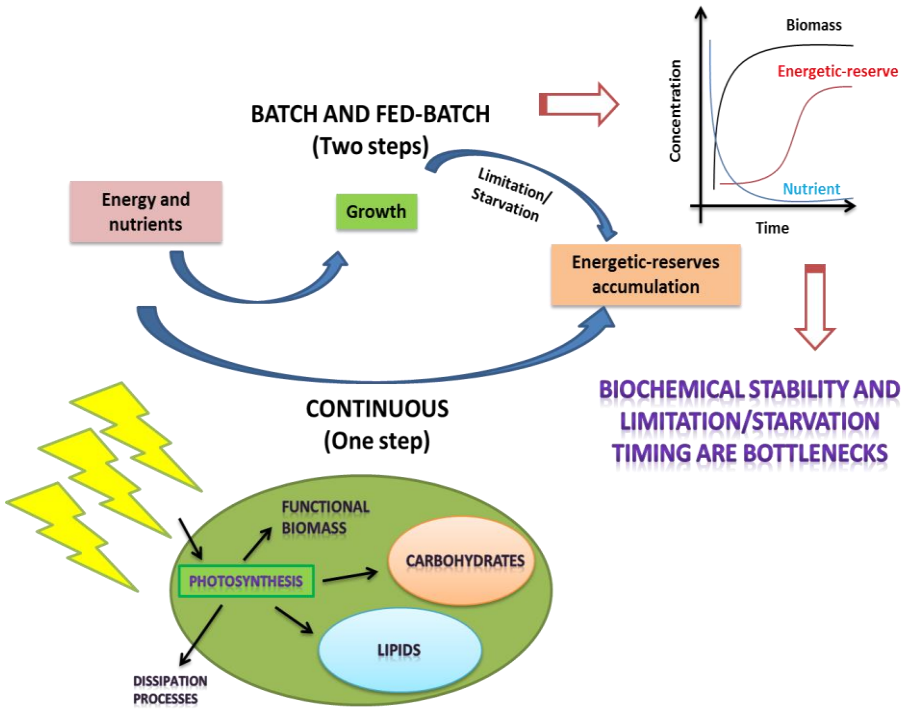

Figure 3.3: Proposal of chapter's discussion.

The hypothesis of the relation between biomass/carbohydrate productivity under nutrient limitation is represented by the **Figure 3.4**, where the peaks of productivity for biomass and the energetic reserves are different, been regulated by residence time (**Fig. 3.4A**), or nutrient source (**Fig. 3.4B**) when nutrient limitation/starvation is applied. Three areas are outlined, i.e., area 1, when the nutrient is provided in excess, and the energetic reserve can be increased slightly. After that, a second zone (area 2) with

limitation/beginning of starvation, where the peak of energetic-substances is theoretically reached, and a last zone (area 3), of strong starvation. In view of carbohydrate production (primary energetic-reserve produced by microalgae) (Klok et al., 2014), it is necessary to work in the range of area 2. In fact, it is already known that an excessive stress condition shifts metabolism to lipid production, as the two metabolic pathways can interact (Vitovà et al., 2015), and lipid is obtained instead of carbohydrate. Therefore, it is important to study specific stress conditions depending of the product of interest.

Generally, in the continuous cultivation of microalgae and cyanobacteria, the main operative/environmental variables are nutrient availability (nitrogen), light availability/intensity, temperature and residence time. Not considering the influence of temperature, light intensity, nitrogen limitation and residence time are the most influent variables to accumulate carbohydrate. Nitrogen limitation can be applied by using a suitable inlet concentration depending of light intensity and, if necessary, by changing the residence time (**Figure 3.5**). A N inlet must be accurately optimized to a specific light, and this combination should be suitable to achieve a high carbohydrate content (45-55%) in continuous mode. The residence time is the last variable to be considered because it influences directly the biomass and carbohydrate productivity, and for this reason it is desired not to be increased too much.

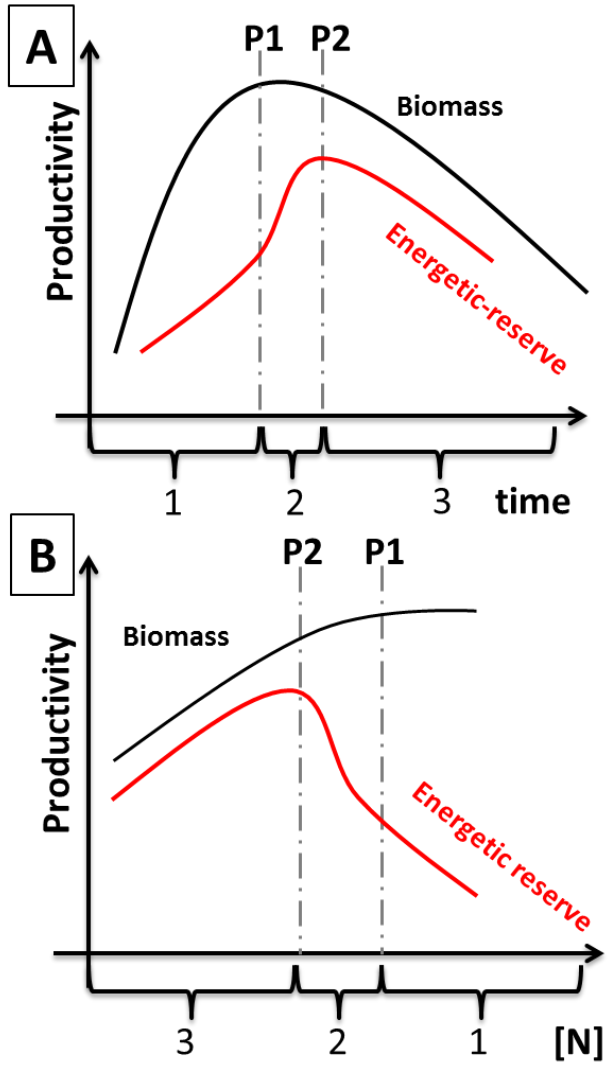

Figure 3.4: Productivity behavior of biomass and energetic reserve from microalgae as a function of residence time (A) and N_{outlet} (B). P1 – Peak of functional biomass productivity, P2 – Peak of energetic-reserve productivity. 1 - excess of nutrients, 2 - limitation/beginning of starvation and 3 - starvation of nutrients.

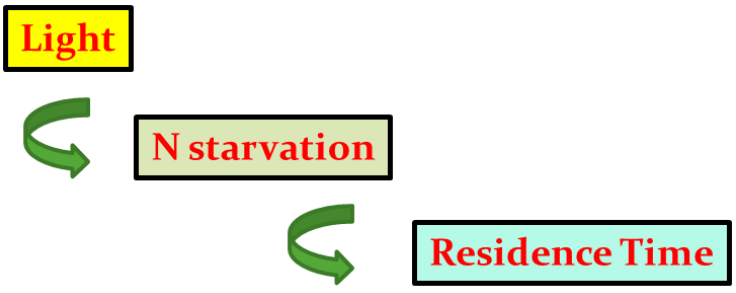

Figure 3.5: Order of the environmental/operative variables studied.

Concerning cyanobacteria productivity in continuous systems, only a few papers are available in literature (Touloupakis et al., 2015; Touloupakis et al., 2016), and the actual feasibility of a continuous production of these organisms is not proven yet.

In addition, it is noteworthy that continuous systems working at steady-state are a viable tool to study the biomass' physiological response to environmental condition since light intensity, residence time and nitrogen concentration can be managed for an efficient carbohydrate accumulation (Ho et al., 2011; Chen et al., 2013; Silva and Sforza, 2016).

In a perfectly mixed continuous system at steady state, the apparent growth rate μ is equal to the dilution rate, which is the inverse of the residence time τ (Kliphius et al., 2012; Sforza et al., 2015a):

$$\mu = 1/\tau \tag{3.1}$$

Thus, by changing the residence time, different growth rates can be studied. This means that microalgae population is somehow selected by the residence time set, and they grow with a rate which is fixed by the operating conditions. This also has another biological implication; if the residence time is low enough all the biomass contained in the reactor is composed of living organisms, as the dead cells are continuously removed from the reactor (Klok et al., 2014). Only the cells actually acclimated to the operating/environmental conditions can survive in a continuous system. So, working in a lab scale continuous system is essential even from a biological point of view, because once steady state is reached, all the transient acclimation phenomena are achieved, allowing a more reliable measure of physiological parameters (Sforza et al., 2015b).

Thus, if the crucial point is to understand the feasibility of large scale carbohydrate production from microalgae and cyanobacteria, continuous cultivation should be recognized as the best method to deeply understand the effect of key operating variables on microalgae acclimation and physiology.

On the other hand, at industrial scale, the possibility of cultivating microalgae in a continuous industrial system is still challenging, particularly due to the variability of environmental parameters in outdoor cultivation, which change significantly light availability and temperature. Productivity varies from species to species, as well as the geometry of the reactor and lighting conditions (i.e., the location in the world). In **Table**

3.4 some examples of outdoor productivities as a function of the countries and using different types of reactors are reported.

Table 3.4: Overview of some reported outdoor culture productivities observed during one year of production. Four reactor systems are considered: raceway pound, horizontal tubular and vertically stacked horizontal 'vertical' tubular PBR's and flat panels. The areal productivity is based on one-hectare ground surface area.

Reactor System	Location	Light Path (m)	Algae species	Productivity (ton ha^{-1} $year^{-1}$)	Reference
Raceway Pond	Hawaii	0.12	*Haematococcus pluvialis*	37.2	Slegers, 2014
Raceway Pond	Tucson, Arizona	0.08 – 0.20	*Nannochloropsis salina*	12.2 – 12.7	
Raceway Pond	La Jolla, California	0.28	*Phaeodactylum tricornutum*	59.1	
Raceway Pond	Poole, England	0.40	*Phaeodactylum tricornutum*	10.6 – 27.3	
Raceway Pond	Perth, Australia	0.16	*Pleurochrysis carterae*	60	
Raceway Pond	La Mancha, Mexico	0.1 – 0.25	*Spirulina platensis*	43.1	
Raceway Pond	Malaga, Spain	0.30	*Spirulina platensis*	23.6 – 30	
Raceway Pond	China	10	*Grasiella sp.* WBG-1	43.8 – 69	Wen et al., 2016
Raceway Pond	Florence, Italy	25	*Nannochloropsis*	52.9	Pushparaj et al., 1997
Horizontal Tubular	Hawaii	0.38	*Haematococcus pluvialis*	55.1	Slegers, 2014
Horizontal Tubular	Netherlands	0.03	*Nannochloropsis*	20	
Horizontal Tubular	Florence, Italy	0.06	*Spirulina platensis*	30	
Horizontal Tubular	Hawaii	0.41	*unknown*	47.5	
Vertical Tubular	Almeria, Spain	0.09	*Scenedesmus almeriensis*	90	Acién et al., 2012
Vertical Tubular	Cadiz, Spain	0.30	*unknown*	73	Slegers, 2014
Flat Panel	Sede-Boquer, Israel	0.10	*Nannochloropsis*	22.1	
Flat Panel	Florence, Italy	1.5	*Nannochloropsis*	88.69	Pushparaj et al., 1997
Flat Panel	Eilat, Israel	1.3-17	*Nannochloropsis*	20 – 44	Amos and Cheng-Wu, 2001

3.3.2 CO_2 availability

Carbon may represent between 17.5 to 65% of the dry weight of microalgae and cyanobacteria biomass, usually around 50% (Markou et al., 2014). In their natural

environment, microalgae usually absorb carbon from the CO_2 dissolved in an aqueous solution, which maintains a balance with the bicarbonate and carbonate ions (pH-dependent, $pK_1 = 3.6$, $pK_2 = 6.3$, and $pK_3 = 10.3$).

$$CO_{2(aq)} + H_2O \overset{pK1}{\longleftrightarrow} H_2CO_3^* \overset{pK2}{\longleftrightarrow} HCO_3^- + H^+ \overset{pK3}{\longleftrightarrow} CO_3^{2-} + 2H^+ \quad (3.2)$$

Most microalgae and cyanobacteria are cultivated in the pH range of 6.5 to 10, and the dominant form of carbon, in the aqueous phase, is the bicarbonate ion. Since the amount of dissolved inorganic carbon (DIC) depends on pH, salinity, pressure and temperature, microalgae have developed uptake mechanisms for each specific environment and depending on the carbon source. These mechanisms include diffusion, active transport, carbonic anhydrase, phosphorylation (Markou et al., 2014).

The main ways to supply carbon to the culture media are: pumping air, pumping air enriched with CO_2, using bicarbonate salts, and using organic compounds (in the case of heterotrophy and mixotrophy).

Usually, the carbohydrate-rich microalgae systems use inorganic carbon supplied by CO_2 in excess (2-5% mix air-CO_2) to conduct photosynthesis, increasing the rates of carbon fixation to maximum, and consequently, maximizing the conversion of CO_2 in carbohydrates. Some authors applied high concentrations of bicarbonate salts (*Euhalotece* ZM 001 14–160 gL^{-1}) (Chi et al., 2013), while lower concentrations (< 15 gL^{-1}) were studied on *Chlorella prothotecoides* (Lohman et al., 2015), *Scenedesmus sp.* (Pancha et al., 2015) *Scenedesmus obliquus* (Guagmin et al., 2014), *Thermosynechococcus sp.* (Su et al., 2012). Not all the species of microalgae and cyanobacteria are able to exploit large amounts of bicarbonate; despite having the necessary carriers, they are often inhibited by the substrate concentration (Qiao et al., 2015). Silva et al. (2016) used sodium bicarbonate (5.5–88 g L^{-1}) to cultivate *Synechococcus* PCC 7002, in order to specifically produce carbohydrates, in batch conditions with automatic pH control, and noticed that these values were not efficient to obtain high amounts of carbohydrates, reaching around 30% only (in dry weight) with 88 g L^{-1} of sodium bicarbonate. In addition, growth inhibition was shown above 22 g L^{-1} of sodium bicarbonate, so that a fraction of bicarbonate was wasted as CO_2 when 88 g L^{-1} were used. Selecting and optimizing the growth conditions of these tolerant

bicarbonate species is a recent approach and can substantially reduce cultivation production costs because the cost of gaseous CO_2 supply is too high (Silva et al., 2016).
When microalgae are cultivated in organic substrates (both mixotrophic and heterotrophic cultivation), they tend to grow faster, with higher biomass and lipids yields than with conventional autotrophic cultivation (Liang, 2013).
This concept finds applications to treat several effluents and wastes, such as whey protein concentrate (*Spirulina platensis* using lactose 7.18% and producing 60 mg L^{-1} d^{-1} of carbohydrate productivity) (Salla et al., 2016), cheese whey permeate (40% of culture medium – 1.9–3.0 g L^{-1} in 13 days of cultivation) (Girard et al., 2014), dark fermentation effluents (*Chlorella vulgaris* ESP6 – 0.25–0.3 g L^{-1} of lactate, formate, butyrate and acetate – 0.2 g L^{-1} d^{-1} of biomass productivity) (Liu et al., 2013), (*Scenedesmus subspicatus* GY-16, *Chlorella vulgaris* FSP-E and *Anistrodesmus gracilis* GY-09 – 2 g L^{-1} – sodium acetate – 0.498 g L^{-1} d^{-1} of carbohydrate productivity) (Chen et al., 2016) and (*Chlorella sorokiniana* -0.2–0.3 g_{carbon} L^{-1} of acetate and butyrate – 1.14 g L^{-1} in 10 days of cultivation) (Turon et al., 2015), glucose (*Chlorella sorokiniana* - 0.5–2 g L^{-1} – 0.1–0.6 g L^{-1} of biomass in 10 days of cultivation) (Juntilla et al., 2015), human urine (*Spirulina platensis* – urea 75 mg L^{-1} and acetate 200 mg L^{-1} – 1.7 g L^{-1} of biomass in 5 days) (Chang et al., 2013) and glycerol (*Chlorella pyrenoidosa* – 1% – 1.2 g L^{-1} of maximum biomass production with 60 % of carbohydrate content) (Bajwa et al., 2016).
However, this approach of carbohydrate production is not discussed in literature enough, which is more focused on lipid accumulation. In addition, from a biofuel perspective, autotrophic cultivation is quite essential for the process to be sustainable, but the effect of organic source on carbohydrate accumulation could become a relevant issue in the case of waste stream exploitation.

3.3.3 Nutrients supply

To efficiently produce microalgae at large scale, all the essential elements have to be supplied in a cultivation medium with appropriate ratios, adequate quantities and bioavailable chemical forms, so that the growth of microalgae will not be limited by anything else but light (Markou et al., 2014). Common phytoplankton elemental composition is based on the universal Redfield C:N:P of 106:16:1. In some conditions,

algae stoichiometry may diverge from this canonical ratio, thus suggesting that the cultivation media should be flexible and must be adapted to the microalgae metabolic needs (Markou et al., 2014). The standard biochemical composition of microalgae includes proteins (30-50%), carbohydrates (20-40%) and lipids (8-15%) (Cardoso et al., 2012; Hu, 2004), but several studies have shown that lipids and carbohydrates can be accumulated under stress conditions (mainly under nitrogen starvation), thus decreasing the protein content (Ho et al., 2013a; Ho et al., 2013c; Mollers et al., 2014). The mechanism of nutrient starvation or limitation can be applied to obtain carbohydrate-rich biomass with the potential to produce bioethanol.

Nitrogen is the second most abundant element in microalgae biomass, as its fraction may vary from 1 to 14% (Markou et al., 2014). Microalgae can use various forms of inorganic nitrogen like nitrite, nitrate, ammonia and N_2 (in some cyanobacterial species), but also organic forms such as urea and amino acids. They are essential in the formation of genetic material, pigments and proteins. Nitrate is usually used as the culture media for microalgae and cyanobacteria (Markou et al., 2014), although the preferred source of microalgae and cyanobacteria is the ammonium ion by intracellular uptake; in terms of energy expenditure, nitrate needs two more reduction steps to provide ion ammonium before being processed by the cells (Gonzalez-Fernandez and Ballesteros, 2012).

Nutrient starvation is a strategy for macromolecules accumulation (mainly lipids and carbohydrates) (Gonzalez-Fernandez and Ballesteros, 2012). A standard growth curve for batch conditions under nutrient starvation is shown in **Figure 3.6**. At the beginning, the carbohydrate content is low (5-20%) and increases after nutrient exhaustion and CO_2 in excess, driving the assimilated carbon to produce energetic substances (carbohydrates and lipids), almost as an exponential function although the biomass production does not increase significantly. Generally, the maximum carbohydrate content may reach 50-60% of dry weight.

As examples, C*hlorella vulgaris* FSP-E, decreases the protein content from 60 to 20% of protein, while the carbohydrate content increased from 12 to 54% and lipids 11 to 20%, when the cultivation status changed from nitrogen in excess to nitrogen starvation (Ho et al., 2013a). In similar way, the composition of *Scenedesmus obliquus* CNW-N moved from 50 to 25% of proteins, 20 to 50% for carbohydrates and 7 to 14% for lipids

(Ho et al., 2013c). A recent work where carbohydrates were produced from microalgae using nitrogen starvation (in outdoor conditions) to grow *Chlorella spp.* (four strains), a maximum protein, carbohydrate and lipid content of about 25, 51 and 40, respectively, was reached instead of 41, 25, and 26 in nitrogen excess (Guccione et al., 2014), confirming that nitrogen starvation is a great strategy to carbohydrate accumulation in closed and open systems. The disadvantage of using nutrient depletion strategies is that the viability of the process decreases substantially due to the reduced yield of biomass, even though a larger accumulation of carbohydrates is reached (Branyikova et al., 2011). Moreover, carbohydrate accumulation in a batch system is not stable, and under extreme N starvation, carbohydrates content may actually decrease (Branyikova et al., 2011), while N limitation seems a viable alternative (Vitovà et al., 2015).

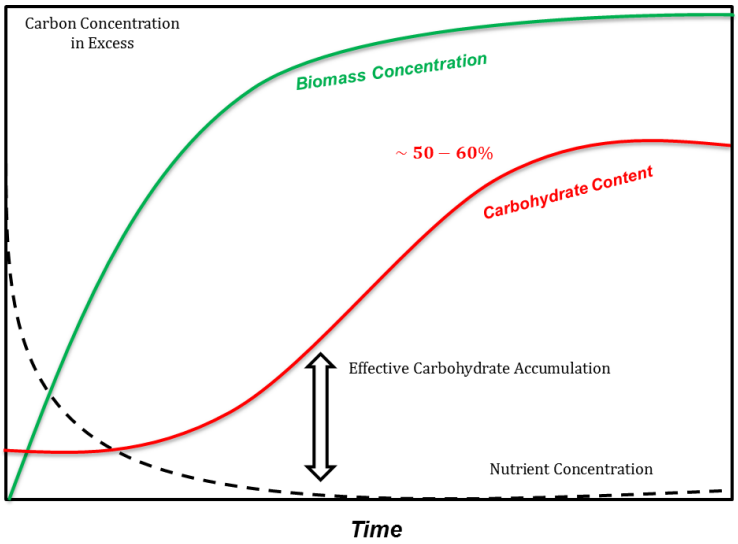

Figure 3.6: Carbohydrate accumulation under nutrient starvation in batch mode.

Again, a continuous system approach can be the solution to this issue (Klok et al., 2013), where a nitrogen limitation was applied to a continuous system, to find an optimum carbohydrates productivity without affecting much the overall biomass productivity.

Understanding in detail the influence of each nutrient's availability on algae productivity is thus seminal to optimize the productivity of both biomass and carbohydrates. Studying the nutrient uptake and yield on biomass in a continuous system allows a better application of mass balance and a reliable evaluation of the capability of microalgae to adapt their composition to the environment. It was found

that N and P concentrations in biomass depend on the specific growth rate and specific light supply rate (Quigg and Beardall, 2003; Sforza et al., 2015a; Silva and Sforza, 2016). Again, it is possible to investigate these phenomena by working in a continuous system at different residence times. As stated previously, different growth rates correspond to different residence times. For instance, it was observed that N- and P-biomass composition increased at higher residence time values. This corresponds to the overall specific growth rate fixed by the dilution rate (Sforza et al., 2015a), and appears to be a common behavior for many species. In **Figure 3.7** a linear correlation is highlighted between $Y_{N/X}$ and μ, for a few species and under different conditions, suggesting that at higher growth rates an accumulation of nitrogen occurs. In fact, a change in N- and P-biomass ratio was observed by various authors (Marrtinez-Sancho et al., 1999; Quigg and Beardall, 2003; Sforza et al., 2015a; Silva and Sforza, 2016). As an example, in the case of *Scenedesmus* (Martinez-Sancho et al., 1999) a higher P/X ratio (i.e., P content in biomass), was found at higher growth rate, suggesting that P is stored as a result of increasing cellular nucleic acids and high energy compounds under high-growth rate conditions.

More complex is the effect of light on nutrient yields. Even though the relation between light and nutrient uptake under non-limiting concentration is mostly unknown, some authors have suggested that light inhibition can affect the elemental composition of microalgae (Clark et al., 2002; Quigg and Beardall, 2003). In fact, a reduction in nutrient content under strong irradiances can be observed.

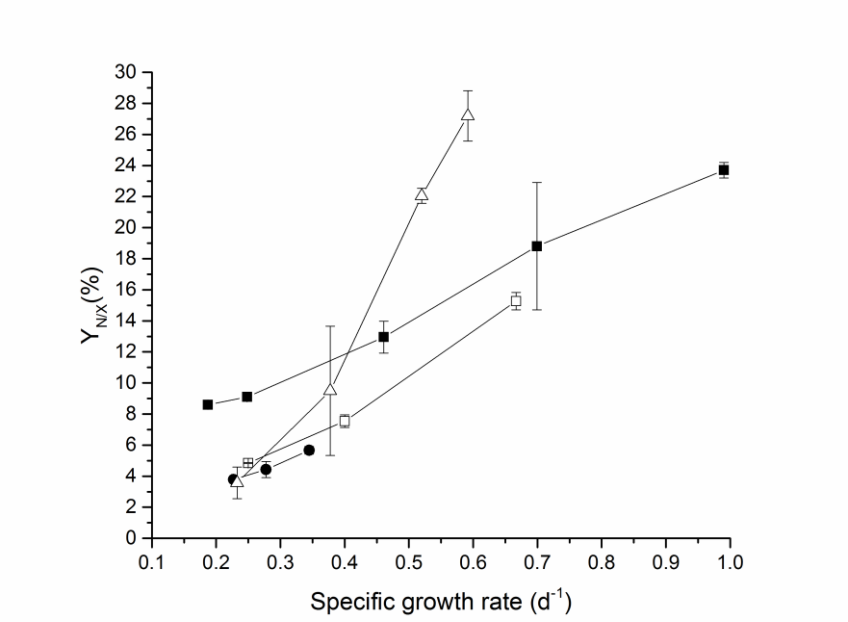

Figure 3.7: Nitrogen content in microalgal biomass as a function of specific growth rate as a results of different residence time in continuous system for *Chlorella vulgaris* (dark circles, data from Silva and Sforza et al., 2016), *Scenedesmus obliquus* (dark squares from Sforza et al., 2015a, open squares, data adapted from Barbera et al., 2015) and *Nannochloropsis salina* (open triangles, unpublished data from experiments reported in Sforza et al., 2015b).

The effect of light on nutrient uptake is particularly interesting in the case of P uptake, whose assimilation is directly linked to light intensity, as algae may transform P into high energy organic compounds by photophosphorylation, where light energy is transformed and incorporated into ATP (Martinez-Sancho et al., 1999; Silva and Sforza et al., 2016). Generally, phosphorus is an important nutrient for the growth of microalgae and its content in the biomass ranges from 0.05 to 3.3% (Markou et al., 2014). It participates in the synthesis of various substances including RNA and DNA, phospholipids and ATP. Unlike the sources of N and C, it can be provided by fossil feedstock-rocks only, such as sodium, ammonium and potassium salts.

Microalgae and cyanobacteria can accumulate intracellular phosphorus when it is in excess in the medium as polyphosphate granules (luxury uptake) (Markou et al., 2014). Moving to a large-scale system, this phenomenon referred as P luxury uptake should be carefully accounted for. In fact, as P is a finite resource, luxury uptake represents an actual nutrient loss. Even when recycling nutrients, it is essential to minimize their make up to avoid luxury uptake phenomena that, from a process point of view, represent a loss. In addition, moving to large scale, where continuous production is required, the

effect of residence time on nutrient uptake, resulting in different P- and light-biomass ratio, should be carefully accounted for in order to maximize the productivity and photosynthetic efficiency, as well as to minimize P consumption.

3.3.4 Light exploitation and photosynthetic efficiency

An efficient light exploitation is the key to any industrial process based on photosynthetic organisms. Under phototrophic conditions, the increasing of the turbidity associated with microalgae concentration usually becomes a significant growth-limiting factor due to the self-shading effect (Ho et al., 2014). On the other hand, high sunlight irradiances may produce reactive oxygen species (ROS), and damage the photosynthetic apparatus, thus causing growth inhibition (photo-inhibition) as the photosystems are not able to efficiently exploit the high flow rate of absorbed photons. If photosaturation is a reversible process, photoinhibition causes damages in the reaction centers, mainly PSII (Taiz and Zeiger, 2009), which affects the process efficiency. Some cellular defenses can be activated against photooxidation, such as the synthesis of enzyme superoxide dismutase and carotenoids, although these mechanisms are not sufficient with prolonged exposition. Therefore, a suitable light supply is necessary to avoid these phenomena and to optimize biomass productivity.

In addition, the natural changes of sunlight intensity along with the day and the seasons should be considered, as well as the in homogeneous light distribution in a photobioreactor or pond, which is a complex environment with different regions where light limitation, light saturation or light inhibition may simultaneously occur. Effective engineering strategies to face this complex phenomenon are still lacking and should be developed as soon as possible, to allow successful biofuel production from photosynthetic organisms (Sforza et al., 2015a).

Providing optimal irradiation flux is also essential for the accumulation of storage compounds such as carbohydrates and lipids (Chen et al., 2013). In general, increasing light intensity leads to a higher carbohydrate content in photosynthetic microorganisms (Markou et al., 2012), although this can happen in combination with other operative and nutritional parameters as well (Chen et al., 2013). Generally, the positive effect of increasing light intensity on the accumulation of starch and lipids is feasible only below the saturation of photosynthesis under the given conditions of a particular species,

ranging between 150-450 µmol photons m^{-2} s^{-1} for carbohydrate accumulation (Silva and Bertucco, 2016), as shown in **Table 3.2**.

At present, biomass productivity and photosynthetic efficiency in outdoor conditions need to be improved because the instability of the climatic conditions (low or excess light and rain) changes the temperature in the photobioreactor significantly, and consequently, the biomass production rate.

Outdoor data for carbohydrate production is not available at present. Some remarks can be based on the biomass productivity range for *Scenedesmus* sp. (Acién et al., 2012) of 47–160 ton biomass ha^{-1} $year^{-1}$ (90 can be referred as a medium value). Supposing a carbohydrate content of 50%, it is possible to estimate a bioethanol productivity from 50 to 140 L bioethanol ha^{-1} $year^{-1}$. This range means 5–15 times more biomass production than first and second generation biomass from sugar cane, corn, beet, and lignocellulosic material, showing a promising approach for this type of biomass.

Optimizing photoconversion is the key of a sustainable process, and this can be obtained not only by selecting a proper reactor geometry (i.e., an optimal light path), but also operating the reactor appropriately. For instance, when setting the residence time, the concept of specific light supply rate should be carefully considered (Sforza et al., 2015a). As mentioned before, the possibility to account for the light actually perceived by the cells allows not only for the understanding of the physiology of adaptation, but also the application of the energy balance in the photoconversion process.

At steady-state, a stable specific light supply per unit mass of cell r_{Ex} (mmol g^{-1} d^{-1}) (Kliphuis et al., 2012; Sforza et al., 2015a) can be calculated as:

$$r_{Ex} = \frac{PFD_{abs} * A_{pbr}}{c_x * V_{pbr}} \tag{3.3}$$

Looking at the efficiency of the photoconversion from sunlight to biomass energy, the photosynthetic efficiency (PE) can be calculated as:

$$PE\ (\%) = \frac{C_x * Q * LHV}{PFD_{abs} * E_p * A_{PBR}} \tag{3.4}$$

where LHV is the Lower Heating Value (assumed equal to 20 kJ g^{-1}), Ep is the energy of photons (kJ μmol^{-1}), C_X is the biomass concentration (DW) at steady state and A_{PBR} is the irradiated surface of the reactor (m^2). The photon flux density absorbed by the algae (PFD_{abs}) can be measured at steady state as:

$$PFD_{abs} = I_{in} - B_I - I_0 \quad (3.5)$$

where I_{in} is the incident light (mmol m^{-2} d^{-1}), B_I the back irradiance (mmol m^{-2} d^{-1}), and I_0 the light absorbed by the medium and the panel walls (mmol m^{-2} d^{-1}).

From equations (3.3) and (3.4), that the following equation can be obtained:

$$PE\ (\%) = \frac{\mathrm{LHV}}{E_p} \cdot \frac{1}{\tau} \cdot \frac{1}{r_{Ex}} \quad (3.6)$$

So, for a given species, LHV as well as Ep are constants, and a clear relation between photosynthetic efficiency and the specific light supply rate is found, depending on residence time as reported in **Figure 3.8A**. In this figure, different data series are reported together in the cases of limiting or saturating irradiances. Clearly, both PE and r_{EX} depend on the light actually absorbed by the biomass (PFD_{abs}), which is strongly affected by the incident light, as the biomass-light yield is strongly reduced under photosaturating and inhibiting irradiances (Zijffers et al., 2010; Sforza et al., 2015a). The effect of light intensity is clear when, at same residence time, the r_{EX} is modified by changing both the biomass concentrations and incident light. In one case, different biomass concentrations were obtained by reducing the N supply in the inlet are displayed in **Figure 3.8B** (Silva and Sforza, 2016). Thus, a direct relation can be observed between PE and r_{EX}. On the other hand, as reported in **Figure 3.8A**, it appears that the trends obtained by changing the residence time are similar for both irradiances, suggesting that by managing this operating variable, the specific supply rate can be adjusted so to obtain a higher photoconversion efficiency.

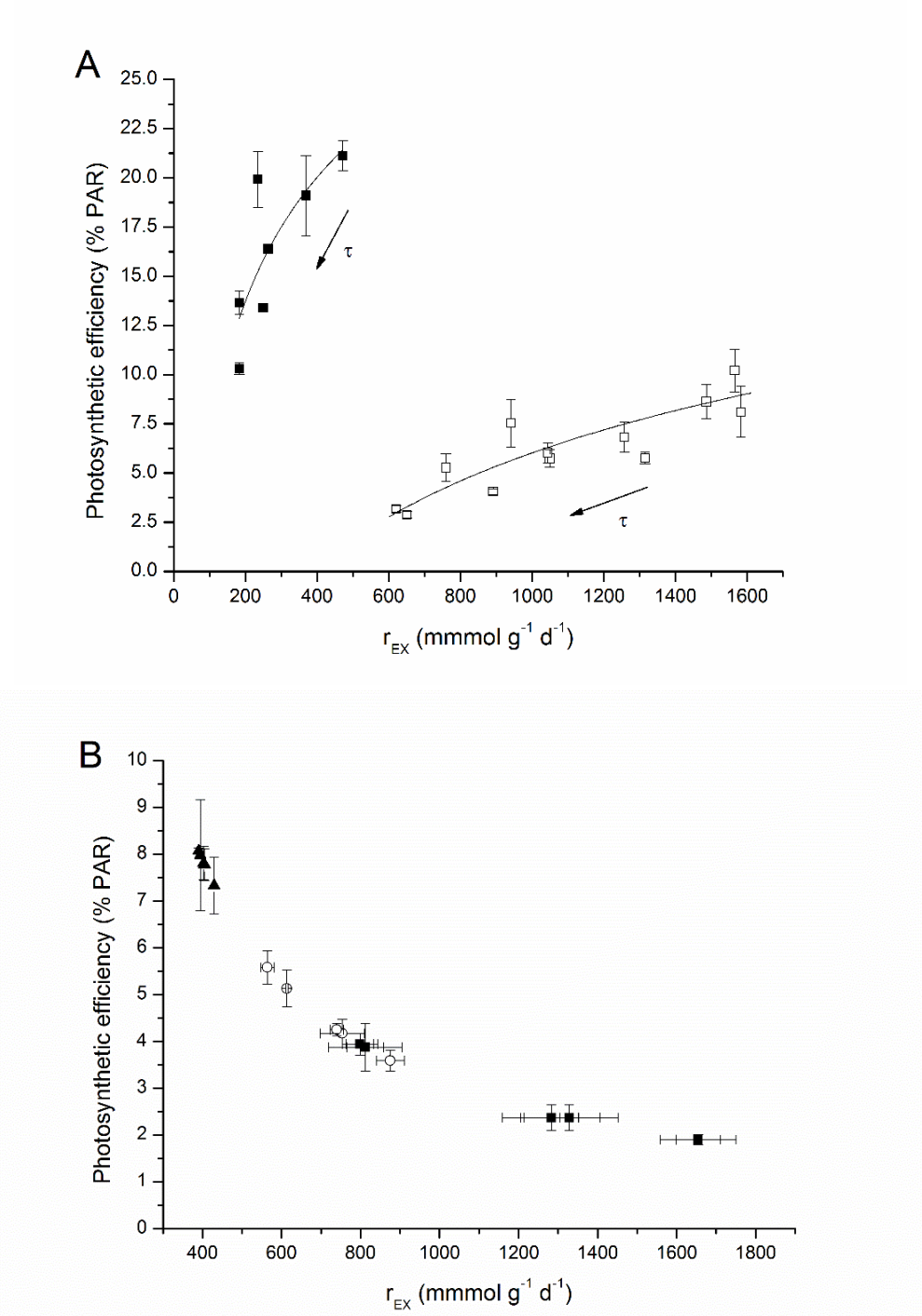

Figure 3.8: Photosynthetic efficiency as a function of specific supply rate. In figure 6A the trends obtained by changing the residence time under low (black squares) and high (open squares) light intensities (150 and about 650 µmol m^{-2} s^{-1} respectively) are reported. Data are an elaboration of those reported in (Sforza et al., 2015a) per *Scenedesmus obliquus* under no limiting nutrient condition. In 6B data obtained under limiting N supply, resulting in different biomass concentration and specific light supply rate are reported, under different incident light intensities (black triangles for 150, open circles for 300 and black squares for 450 µmol m^{-2} s^{-1}). Data are an elaboration of those reported in (Silva and Sforza, 2016) for *Chlorella vulgaris*.

3.4 FINAL REMARKS

In conclusion, the specific light supply rate is a quantitative measurement allowing for the understanding of light conversion efficiency in the cultivation of microalgae and cyanobacteria. In fact, photoconversion efficiency was found to decrease if the specific light supply rate per cell was not optimized (Sforza et al., 2015b). Thus, the specific light supply rate is the main variable that affects photosynthetic productivity, as it affects both photosynthetic efficiency and the state of the photosynthetic apparatus, resulting in a lower light/biomass yield and high energy requirement for maintenance because of photoinhibition. The key factor to obtain stable biomass productivity in a continuous system is the ability to set a proper light supply rate, which depends on the incident light and residence time applied, the reactor depth and geometry, and the biomass concentration.

REFERENCES

Abo-Shanab, R.A.I., 2015. Green Renewable energy for sustainable socio-economic development. Proceedings of the 14th International Conference on Environmental Science and Technology, Greece.

Acién, F.G., Fernandez, J.M., Magan, J.J., Molina, E., 2012. Production cost of a real microalgae production plant and strategies to reduce it. Biotechnol. Adv. 30, 1344-1353.

AFDC Energy, 2016. Bioethanol production. Available in: http://www.afdc.energy.gov/data/

Amos, R., Cheng-Wu, Z., 2001. Optimization of a flat plate glass reactor for mass production of *Nannochloropsis sp.* outdoors. Journal of Biotechnology 85 (2001) 259-269.

Bajwa, K., Silambarasan, T., Bishnoi, N.R., 2016. Effect of glucose supplementation and mixotrophic effects of glycerol and glucose on the production of biomass, lipid yield and different physiological, biochemical attributes of *Chlorella pyrenoidosa*. Journal of Algal Biomass Utilization 7(1), 93-103.

Barbera, E., Sforza, E., Bertucco, A., 2015. Maximizing the production of Scenedesmus obliquus in photobioreactors under different irradiation regimes: experiments and modeling. Bioprocess. Biosyst. Eng. 38, 2177-2188.

Branyikova, I., Marsalkova, B., Doucha, J., Branyik, T., Bisova, K., Zachleder, V., Vitova, M., 2011. Microalgae – Novel Highly Efficient Starch Producers. Biotechnology and Bioengineering 108(4), 766-776.

Cardoso, A.S., Vieira, G.E.G., Marques, A.K., 2011. O uso de microalgas para a obtenção de biocombustíveis. Revista Brasileira Biociencias 9(4), 542-549.

Castro, Y.A., Ellis, J.T., Miller, C.D., Sims, R.C., 2015. Optimization of wastewater microalgae saccarification using dilute acid hydrolysis for acetone, butanol, and ethanol fermentation. Applied Energy 140, 14-19.

Chang, Y., Wu, Z., Bian, L., Feng, D., Leung, D.Y.C., 2013. Cultivation of *Spirulina platensis* for biomass production and nutrient removal from synthetic human urine. Applied Energy 102 (2013) 427-431.

Chen, C., Zhao, X., Yen, H., Ho, S., Cheng, C., Lee, D., Bai, F., Chang, J., 2013. Microalgae-based carbohydrates for biofuel production. Biochem. Eng. J. 78, 1-10.

Chen, C., Chang, H., Chang, J., 2016. Producing carbohydrate-rich microalgae biomass grown under mixotrophic conditions as feedstock for biohydrogen production, International Journal of Hydrogen Energy 41, 4413-4420.

Cheng, D., Li, D., Yuan, Y., Zhou, L., Li, X., Wu, T., Wang, L., Zhao, Q., Wei, W., Sun, Y., 2017. Improving carbohydrate and starch accumulation in *Chlorella sp.* AE10 by a novel two-stage process with cell dilution. J. Appl. Phycol. 27(4), 1453-1462.

Chi, Z., Xie, Y., Elloy, F., Zheng, Y., Hu, Y., Chen, S., 2013. Bicarbonate-based integrated carbon capture and algae production system with alkalihalophilic cyanobacterium. Bioresource Technology 133, 513-521.

Chojnacka, K., Noworyta, A., 2004. Evaluation of Spirulina sp. growth in photoautotrophic, heterotrophic and mixotrophic cultures. Enzyme and Microbial Technology 34, 461-465.

Choi, S.P., Nguyen, M.T., Sim, S.J., 2010. Enzymatic pretreatment of *Chlamydomonas reinhardtii* biomass for ethanol production. Bioresource Technology 101, 5330-5336.

Chow, T., Su, H., Tsai, T., Chou, H., Lee, T., Chang, J., 2015. Using recombinant cyanobacterium (*Synechococcus elongatus*) with increased carbohydrate productivity as feedstock for bioethanol production via separate hydrolysis and fermentation process. Bioresource Technology 184, 133 – 141.

Clark, D.R., Flynn, K.J., Owens, N.J.P., 2002. The large capacity for dark nitrate-assimilation in diatoms may overcome nitrate limitation of growth. New Phytologist 155, 101-108.

Cossu, M., Murgia, L., Ledda, L., Deligios, P.A., Sirigu, A., Chessa, F., Pazzona, A., 2014. Solar irradiation distribution inside a greenhouse with south-oriented photovoltaic roofs and effects on crop productivity. Applied Energy 133, 89-100.

De Winter, L., Schepers, L.W., Cuaresma, M., Barbosa, M.J., Martens, D.E., Wijffels, R.H., 2014. Circadian rhythms in the cell cycle and biomass composition of *Neochloris oleobundans* under nitrogen limitation. Journal of Biotechnology 187, 25-33.

Ding, L., Cheng, J., Xia, A., Jacob, A., Voelklein, M., Murphy, J.D., 2016. Co-generation of biohydrogen and biomethane through two-stage batch co-fermentation of macro- and micro-algal biomass. Bioresource Technology 218, 224-231.

Dragone, G., Fernandes, B.D., Abreu, A.P., Vicente, A.A., Teixeira, J.A., 2011. Nutrient limitation as a strategy for increasing starch accumulation in microalgae. Applied Energy 88, 3331-3335.

Gao, K., Orr, V., Rehmann, L., 2016. Butanol fermentation from microalgae-derived carbohydrates after ionic liquid extraction. Bioresource Technology 206, 77-85.

Girard, J., Roy, M., Hafsa, M.B., Gagnon, J., Faucheux, N., Heitz, M., Tremblay , R., Deschenes, J., 2014. Mixotrophic cultivation of green microalgae *Scenedesmus obliquus* on cheese whey permeate for biodiesel production. Algal Research 5, 241-248.

Gonzalez-Fernandez, C., Ballesteros, M., 2012. Linking microalgae and cyanobacteria culture conditions and key-enzymes for carbohydrate accumulation. Biotechnol. Adv. 30, 1655-1661.

Guagmin, L., Lina, Q., Hong, Z., Shumei, X., Dan, Z., 2014. The capacity of bicarbonate capture of a continuous microalgae photo-bioreactor system. Energy Procedia 61, 361-364.

Guccione, A., Biondi, N., Sampietro, G., Rodolfi, L., Bassi, N., Tredici, M.R., 2014. *Chlorella* for protein and biofuels: from strain selection to outdoor cultivation in a green wall panel photobioreactor. Biotechnology for Biofuels 7(84), 1-12.

Harun, R., Danquah, M.K., 2011. Enzymatic hydrolysis of microalgal biomass for bioethanol production. Chem. Eng. J. 168, 1079-1084.

Ho, S., Chen, C., Lee, D., Chang, J., 2011. Perspectives on microalgal CO_2-emissions mitigation systems – a review. Biotechnology Advances 29, 189-198.

Ho, S., Huang, S., Chen, C., Hasunuma, T., Kondo, A., Chang, J., 2013. Characterization and optimization of carbohydrate production from an indigenous microalga *Chlorella vulgaris* FSP-E. Bioresource Technology 135, 157-165. (a)

Ho, S., Huang, S., Chen, C., Hasunuma, T., Kondo, A., Chang, J., 2013. Bioethanol production using carbohydrate-rich microalgae biomass as feedstock. Bioresource Technology 135, 191–198. (b)

Ho, S., Chen, C., Chang, J., 2012. Effect of light intensity and nitrogen starvation on CO_2 fixation and lipid/carbohydrate production of an indigenous microalga *Scenedesmus obliquus* CNW-N. Bioresource Technology 113, 244–252. (c)

Ho, S., Kondo, A., Hasunuma, T., Chang, J., 2013. Engineering strategies for improving the CO_2 fixation and carbohydrate productivity of *Scenedesmus obliquus* CNW-N used for bioethanol fermentation. Bioresource Technology 143, 163-171. (d)

Ho, S., Ye, X., Hasunuma, T., Chang, J., Kondo, A., 2014. Perspectives on engineering strategies for improving biofuel production from microalgae – A critical review. Biotechnology Advances 32, 1448-1459.

Hosseini, M., Ju, L.-K., 2015. Use of phagotrophic microalga *Ochromonas danica* to pretreat waste cooking oil for biodiesel production. Journal of the American Oil Chemists' Society 92(1), 29-35.

Hosseini, M., Starvaggi, H.A., Ju, L.-K., 2016. Additive-free harvesting of oleaginous phagotrophic microalga by oil and air plotation. Bioprocess and Biosystems Engineering 39(7), 1181-1190.

Hu, Q., 2004. Environmental effects on cell composition, Blackwell Science Ltd, Oxford, 83-93.

Juntilla, D.J., Bautista, M.A., Monotilla, W., 2015. Biomass and lipid production of a local isolate *Chlorella sorokiniana* under mixotrophic growth conditions. Bioresource Technology 191, 395-398.

Kim, K.H., Choi, I.S., Kim, H.M., Wi, S.G., Bae, H., 2014. Bioethanol production from the nutriente stress-induced microalga *Chlorella vulgaris* by enzymatic hydrolysis and immobilized yeast fermentation. Bioresource Technology 153, 47-54.

Kim, S., Ly, H.V., Kim, J., Lee, E.Y., Woo, H.C., 2015. Pyrolysis of microalgae residual biomass derived from *Dunaliella tertiolecta* after lipid extraction and carbohydrate saccarification. Chemical Engineering Journal 263, 194-199.

Kliphuis, A.M.J., Klok, A.J., Martens, D.E., Lamers, P.P., Janssen, M., Wijffels, R.H., 2012. Metabolic modeling of *Chlamydomonas reinhardtii* energy requirements for photoautotrophic growth and maintenance, J. Appl. Phycol. 24, 253-266.

Klok, A.J., Verbaiaderd, J.A., Lamers, P.P., Martens, D.E., Rinzena, A., Wijffels, R.H., 2013. A model for customising biomass composition in continuous microalgae production. Bioresource Technology 146, 89-100.

Klok, A.J., Lamers, P.P., Martens, D.E., Draaisma, R.B., Wijffels, R.H., 2014. Edible oils from microalgae: insights in TAG accumulation. Trends in Biotechnology 32(10), 521-528.

Kumar, G., Sivagurunathan, P., Thi, N.B.D., Zhen, G., Kobayashi, T., Kim, S., Xu, K., 2016. Evaluation of different pretreatments on organic matter solubilization and

hydrogen fermentation of mixed microalgae consortia. International Journal of Hydrogen Energy 41, 21628-21640. (a)

Kumar, G., Zhen, G., Kobayashi, T., Sivagurunathan, P., Kim, S.H., Xu, K.Q., 2016. Impact of pH control and heat pre-treatment seed inoculum in dark H2 fermentation: A feasibility report using mixed microalgae biomass as feedstock. International Journal of Hydrogen Energy 41, 4382-4392. (b)

Lee O.K., Kim, A.L., Seong, D.H., Lee, C.G., Jung, Y.T., Lee, J.W., Lee, E.Y., 2013. Chemo-enzymatic saccharification and bioethanol fermentation of lipid-extracted residual biomass of the microalga, *Dulaliella tetriolecta*. Bioresource Technology 132, 197-201.

Liang, Y., 2013. Producing liquid transportation fuels from heterotrophic microalgae, Applied Energy 104, 860-868.

Liu, C., Chang, C., Liao, Q., Zhu, X., Liao, C., Chang, J., 2013. Biohydrogen production by a novel integration of dark fermentation and mixotrophic microalgae cultivation. International Journal of Hydrogen Energy 38, 15807-15814.

Lorente, E., Farriol, X., Salvado, J., 2015. Steam explosion as a fractionation step in biofuel production. Fuel Processing Technology 131, 93-98.

Lohman, E.J., Gardner, R.D., Pedersen, T., Peyton, B.M., Cooskey, K.E., Gerlach, R., 2015. Optimized inorganic carbon regime for enhanced growth and lipid accumulation in *Chlorella vulgaris*. Biotechnology for Biofuels 8:82, 1-13.

Lurling, M., Eshetu, F., Faassen, E.J., Kosten, S., Huszar, V.L.M., 2013. Comparison of cyanobacterial nad algal growth rates at different temperatures. Freshwater Biology 58, 552-559.

Markou, G., Chatzipavlidis, I., Georgakakis, D., 2012. Effects of phosphorus concentration and light intensity on the biomass composition of *Arthrospira* (*Spirulina*) *platensis*. World J. Microbiol. Biochnol. 28, 2661-2670.

Markou, G., Angelidaki, I., Nerantzis, E., Georgakakis, D., 2013. Bioethanol production by carbohydrate-enriched biomass of *Antrospira (Spirulina) platensis*. Energies 6, 3937 – 3950.

Markou, G., Vandamme, D., Muylaert, K., 2014. Microalgal and cyanobacterial cultivation: the supply of nutrients. Water Res. 65, 186-202.

Martinez-Sancho, M.E., Jimenez Castillo, J.M., Yousfi, F.E., 1999. Photoautotrophic consumption of phosphorous by *Scenedesmus obliquus* in a continuous culture. Influence of light intensity. Process Biochemistry 34, 811-818.

Mata, T.M., Martins, A.A., Caetano, N.S., 2010. Microalgae for biodiesel production and other applications: a review. Renewable and Sustainable Energy Reviews 14, 217-232.

Miranda, J.R., Passarinho, P.C., Gouveia, L., 2012. Pre-treatment optimization of *Scenedesmus obliquus* microalga for bioethanol production. Bioresource Technolgy 104, 342-348.

Mollers, K.B., Cannella, D., Jorgensen, H., Frigaard, N., 2014. Cyanobacterial biomass as carbohydrate and nutrient feedstock for bioethanol production by yeast fermentation. Biotechnol. Biofuels 7, 1-11.

NASA, 2012. Ômega Project. Available in: http://www.nasa.gov/centers/ames/research/OMEGA/#.V-uNkSGLQdU

Pancha, I., Chokshi, K., Ghosh, T., Paliwal, C., Maurya, R., Mishra, S., 2015. Bicarbonate supplementation enhanced biofuel production potential as well as nutritional stress mitigation in the microalgae *Scenedesmus sp.* CCNM 1077. Bioresource Technology 193, 315-323.

Park, C., Heo, K., Oh, S., Kim, S.B., Lee, S.H., Kim, Y.H., Kim, Y., Lee, J., Han, S.O., Lee, S., Kim, S.W., 2016. Eco-design and evaluation for producing of 7-aminocephalosporanic acid from carbohydrate wastes discharged after microalgae-based biodiesel production. Journal of Cleaner Production 133, 511-517.

Pulz, O., 2001. Photobioreactors: production systems for phototrophic microorganisms, Appl. Microbiol. Biotechnol. 57, 287-293.

Pushparaj, B., Pelosi, E., Tredici, M.R., Pinzani, E., Materassi, R., 1997. An integrated culture system for outdoor production of microalgae and cyanobacteria. Journal of Applied Phycology 9 (1997) 113-119.

Qiao, K., Takano, T., Liu, S., 2015. Discovery two novel highly tolerant $NaHCO_3$ Treuboxiophytes: Identification and characterization of microalgae from extreme saline-alkali soil. Algal Research 9, 245-253.

Quigg, A., Beardall, J., 2003. Protein turnover in relation to maintenance metabolism at low photon flux in two marine microalgae. Plant, Cell and Environment 26, 693-703.

Ruiz, J., Alvarez-Dias, P.D., Arbib, Z., Garrido-Perez, C., Barragan, J., Perales, J.A., 2013. Performance of a flat panel reactor in the continuous culture of microalgae in urban wastewater: prediction from a batch experiment. Bioresource Technology 127, 456-463.

Salla, A.C.V., Margarites, A.C., Seibel, F.I., Holz, L.C., Briao, V.B., Bertolin, T.E., Colla, L.M., Costa, J.A.V., 2016. Increase in the carbohydrate content of the microalgae *Spirulina* in culture by nutrient starvation and the addition of residues of whey protein concentrate, Bioresource Technology 104, 133-141.

San Pedro, A., Gonzalez-Lopez, Z.V., Acién, F.G., Molina-Grima, E., 2014. Outdoor pilot-scale production of *Nannochloropsis gaditana*: influence of culture

parameters and lipid production rates in tubular photobioreactors. Bioresource Technology 169, 667-676.

Sforza, E., Urbani, S., Bertucco, A., 2015. Evaluation of maintenance energy requirements in the cultivation of *Scenedesmus obliquus*: Effect of light intensity and regime. J. Appl. Phycol. 27(4), 1453-1462. (a)

Sforza, E., Calvaruso, C., Meneghesso, A., Morosinotto, T., Bertucco, A., 2015. Effect of specific supply rate on photosynthetic efficiency of *Nannochloropsis salina* in a continuous flat plate photobioreactor. Appl. Microbiol. Biotechnol. 99, 8309-8318. (b)

Silva, C.E.F., Bertucco, A., 2016. Bioethanol from microalgae and cyanobacteria. Process Biochem. 51, 1833-1842.

Silva, C.E.F., Gris, B., Sforza, E., La Rocca, N., Bertucco, A., 2016. Effects of sodium bicarbonate on biomass and carbohydrate production in *Synechococcus* PCC 7002. Chem. Engineer. Trans. 49, 241-246.

Silva, C.E.F., Sforza, E., 2016. Carbohydrate productivity in continuous reactor under nitrogen limitation: effect of light intensity and residence time on nutrient uptake in *Chlorella vulgaris.* Process Biochem. 51, 2112-2118.

Silva, C.E.F., Sforza, E., Bertucco, A., 2017. Continuous cultivation of microalgae as an efficient method to improve productivity and biochemical stability. 25th European Biomass Conference and Exhibition, Stockholm, Sweden, 319-324.

Slade, R., Bauen, A., 2013. Micro-algae cultivation for biofuels: cost, energy balance, environmental impacts and future prospects. Biomass Bioenerg. 53, 29-38.

Slegers, P.M., 2014. Scenario studies for algae production. Thesis submitted in fulfilment of the requirements for the degree of doctor at Wargeningen University. Available in: http://edepot.wur.nl/294573

Sobczuk, T.M., Camacho, F.G., Rubio, F.C., Acién Fernandez, F.G., Molina Grima, E., 2000. Carbon dioxide uptake efficiency by outdoor microalgal cultures in tubular airlift photobioreactors, Biotechnology and Bioengineering 67(4), 465-475.

Su, C.M., Hsueh, H.T., Chen, H.H., Chu, H., 2012. Effects of dissolved inorganic carbon and nutrient levels on carbon fixation and properties of *Thermosynechococcus sp*. in a continuous system. Chemosphere 88, 706-711.

Tang, H., Chen, M., Ng, K.Y.S., Salley, S.O., 2012. Continuous microalgae cultivation in a photobioreactor. Biotechnology and Bioengineering 109(10), 2468-2474.

Taiz, L., Zeiger, E., 2009. Fisiologia Vegetal. 5th ed., Artmed.

Touloupakis, E., Cicchi, B., Torzillo, G., 2015. A bioenergetic assessment of photosynthetic growth of *Synechocystis sp.* PCC 6803 in continuous cultures. Biotechnology for Biofuels 8:133, 1-11.

Touloupakis, E., Cicchi, B., Benavides, A.M.S., Torzillo, G., 2016. Effect of pH on growth of *Synechocystis sp.* PCC 6803 cultures and their contamination by golden algae (*Poteioochromonas* sp.). Appl. Microbiol. Biotechnol. 100, 1333-1341.

Turon, V., Trobly, E., Fouilland, E., Steyer, J.P., 2015. Growth of *Chlorella sorokiniana* on a mixture of volatile fatty acids: The effects of light and temperature. Bioresource Technology 198, 852-860.

Vitovà, M., Bisova, K., Kawano, S., Zachleder, V., 2015. Accumulation of energy reserves in algae: from cell cycles to biotechnological applications. Biotechnology Advances 33, 1204-1218.

Wang, L., Li, Y., Sommerfeld, M., Hu, Q., 2013. A flexible culture process for production of the green microalga *Scenedesmus dimorphus* rich in protein, carbohydrate or lipid. Bioresource Technology 129, 289–295.

Wang, H., Ji, C., Bi, S., Zhou, P., Chen, L., Liu, T., 2014. Joint production of biodiesel and bioethanol from filamentous oleaginous microalgae *Tribonema sp*. Bioresource Technology 172, 169-173. (a)

Wang, Y., Guo, W., Lo, Y., Chang, J., Ren, N., 2014. Characterization and kinetics of bioi-butanol production with Clostridium acetobutylicum ATCC824 using mixed sugar medium simulating microalgae-based carbohydrates. Biochemical Engineering Journal 91, 220-230. (b)

Wen, X., Du, K., Wang, Z., Peng, X., Luo, L., Tao, H., Xu, Y., Zhang, D., Geng, Y., Li, Y., 2016. Effective cultivation of microalgae for biofuel production: a pilot-scale evaluation of a novel oleaginous microalga *Grasiella sp.* WBG-1. Biotechnology for biofuels 9:123, 1-12.

Xia, A., Jacob, A., Tabassum, M.R., Hermann, C., Murphy, J.D., 2016. Production of hydrogen, ethanol and volatile fatty acids through co-fermentation of macro- and micro-algae. Bioresource Technology 205, 118-125.

Yao, C., Ai, J., Cao, X., Xue, S., 2013. Salinity manipulation as an effective method for enhanced starch production in the marine microalga *Tetraselmis subcordiformis*. Bioresource Technology 146, 663-671. (a)

Yao, C., Ai, J., Cao, X., Xue, S., 2013. Characterization of cell growth and starch production in the marine green microalga *Tetraselmis subcordiformis* under extracellular phosphorous-deprived and sequentially phosphorous-replete conditions. Appl. Microbiol. Biotechnol. 97, 6099-6110. (b)

Zhang, D., Xue, S., Sun, Z., Liang, K., Wang, L., Zhang, Q., Cong, W., 2014. Investigation of continuous-batch mode of two-stage culture of *Nannochloropsis sp.* for lipid production. Bioprocess. Biosystem. Engineering 37, 2073-2082.

Zijffers, J.F., Schippers, K.J., Zheng, K., Janssen, M., Tramper, J., Wijffels, R., 2010. Maximum photosynthetic yield of green microalgae in photobioreactors. Mar. Biotechnol. 12, 708-718.

Chapter 4

A two-stage system for the large-scale cultivation of biomass: a design and operation analysis based on a simple steady-state model tuned on laboratory measurements

The optimal design and operation at large scale of a continuous fermentation process including a biological reactor/photobioreactor and a gravity settler with partial recycle and purge of the biomass is addressed. The proposed method is developed with reference to microalgae (*Scenedesmus obliquus*) cultivation, but it can be applied to any fermentation process as well as to activated sludge wastewater treatment. A procedure is developed to predict the effect of process variables, mainly the recycle ratio (R), the solid retention time (θ_c), the reactor residence time (θ) and the ratio between feed and purge flow rates (F_I/F_W). It includes a simple steady-state model of the two units coupled in the process and the experimental measurement of basic kinetic data, in both the bioreactor and the settler, for the tuning of model parameters. The bioreactor is assumed as perfectly mixed and a rigorous gravity-flux approach is used for the settler. The process model is solved in terms of dimensionless variables, and plots are given to allow sensitivity analyses and optimization of operating conditions. A discussion about washout is presented, and a simple method is outlined for the calculation of the minimum values of residence time (θ_{min}) and recycle ratio (R_{min}), and of the maximum allowed recycle ratio ($R_{max,operating}$) and biomass purge rate (F_{Wmax}). In particular, it is shown that the system is sensitive to the concentration of biomass lost from the top of the settler (C_X^S). The proposed method can be useful for the design and analysis of large scale processes of this type•.

•*Part of this chapter was published in Brazilian Journal of Chemical Engineering (**Silva, C.E.F.**, Gris, B., Bertucco, A., 33(4), 773-781, 2016). The full paper was submitted to BioEnergy Research, 2017.*

4.1 INTRODUCTION

Biotechnology is becoming more and more important in process industries, and bioprocess control is an issue of increasing interest, which is receiving extensive attention. The main engineering motivation in applying control methods to living processes is to increase their operational stability and production efficiency (Peter and Selisteanu, 2013). However, simple and efficient methods to achieve this goal are still under development. In particular, characteristics such as highly non-linear behavior, high sensitivity to operating variables, often poor understanding of the system dynamics, and the difficulty of measuring biological variables by online sensors (i.e. costs vs. reliability) make it difficult to design and operate a bioprocess where the production and harvesting sections are strongly interconnected.

Biomass production by continuous fermentation is a must of any bioprocess aimed to ensure time-cost-effective gains and energy efficiency. Main applications, in respect to this, are the activated sludge wastewater treatment (D'Antonio and Carbone, 1987; Sardo and Indelicato, 1995; Yuan et al., 2009; Alcantara et al., 2015; Amanatidou et al., 2015), the biogas production (Nges and Liu, 2010; Lee et al., 2011), the ethanolic fermentation (Narodolawsky et al., 1988; Oliveira et al., 2015), the ABE fermentation (Meyer and Papoutsakis, 1989), the hydrogen production (Lee et al., 2010), α-amylases and proteinases (Grøn et al., 1995; Grøn et al., 1996), and microalgae cultivation (Park et al., 2011; Sforza et al., 2014; Sing et al., 2014).

The simplest flowsheet of a bioprocess of this type is sketched in **Figure 4.1**: it includes a fermenter, a gravity settler, a recycle of the concentrated suspension and a purge of biomass. The relevant operating variables, or degrees of freedom, are the hydraulic retention time (θ), the solids retention time or biomass age (θ_c), the recycle ratio (R) and the flow rate of the solids removal purge stream (F_W). So far, the effect of these variables has usually been studied separately, i.e., with respect to the reactor (Narodolawsky et al., 1988; Meyer and Papoutsakis, 1989) or to the settler (D'Antonio and Carbone, 1987; Sardo and Indelicato, 1995; Depraetere et al., 2015) alone, neglecting that the two of them are interrelated and strongly dependent from each other, thus affecting the overall bioprocess performance.

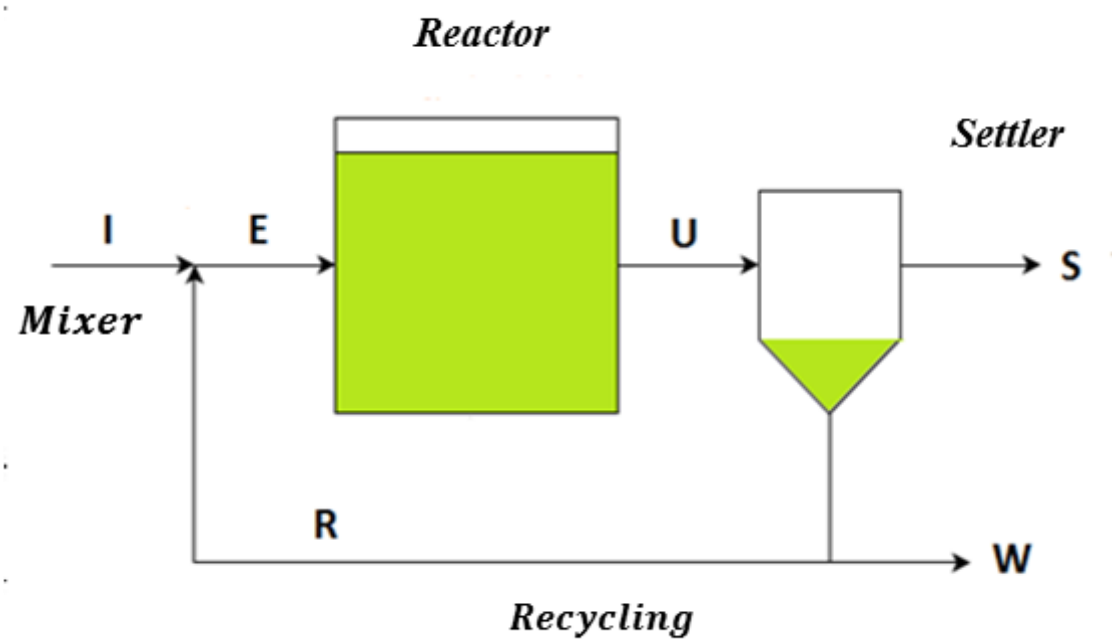

Figure 4.1: Schematic of the continuous cultivation process investigated.

For instance, a partial biomass recycling is used to reduce the costs associated to the inoculum preparation, ensures a shorter production time as well as allows to maintain high cellular concentration in the reactor. On the other hand, the recycle flow rate and concentration heavily affect the settler behavior. Therefore, the recycle rate must be carefully designed. Some articles experimentally show the advantages of optimizing the biomass recycle, which increases the productivity in alcoholic fermentation (Narodolawsky et al., 1988), the nutrient removal in wastewater treatment (Kosinska and Miskiewicz, 2009; Uduman et al., 2010), enhances the process energy efficiency, stabilizes dominant colonies in open systems and improves sedimentation rates for microalgae production systems (Park et al., 2011; Park et al., 2013; Sing et al., 2014).
Although the method we are proposing is applicable in general to fermentation processes, our interest, and the example we refer as well, is focused on this last application. Microalgae and cyanobacteria are photosynthetic microorganisms that have received much attention as a source of biomass for use in the production of third-generation biofuels, as well as of high value-added products such as pharmaceuticals, nutraceuticals and exopolysaccharides (Zhu, 2015), so that engineering procedures for effective large-scale cultivation of microalgae are of utmost importance.

In a multistage interconnected bioprocess, nutritional and environmental issues during the cultivation step do not determine alone the maximization of energy recovery and biomass production. In the case addressed an effective harvesting method combined with suitable operating variables is essential (Park et al., 2013; Barros et al., 2015). So, the harvesting units have to be designed together with the photobioreactor, according to the characteristics of target micro-organisms and also to the type and value of the end product. Among other methods (Barros et al., 2015), gravitational sedimentation is largely applied (Lund, 1951; Salim et al., 2011; Smith and Davis, 2012; Depraetere et al., 2015), both separately and in combination with flocculation/coagulation (Smith and Davis, 2012; Liu et al., 2014). Gravitational sedimentation has a number of advantages in comparison to other techniques, for instance a low cost for achieving a controlled process, margin for scaling-up, and ease to splitting supernatant with minimum operating cost, mainly when pumping is involved. Conversely, it is a time-consuming operation that gives rise to a probability of biomass deterioration during the process (Rawat et al., 2013; Barros et al., 2015).

So far, little work has been done to couple the dynamic parameters of the cultivation and harvesting steps, and separate laboratory studies on each one of them are not sufficient for an optimal process design, as well as for process scale-up to the industrial scale. For instance, the wash-out time has been experimentally determined by tentative methods, or the inoculum concentration in the system has been optimized by a lengthy trial-and-error procedure, or the problem of a local optimum for the solid retention time has been discussed (Yuan et al., 2009; Nges and Liu, 2010; Lee et al., 2011). On the other hand, the use of larger recycle ratios (between 150-600%) to improve nitrate concentration in the anoxic tank of wastewater treatment or to increase sedimentation rate are reported in the literature without explaining how these values were selected, most likely based on empirical evidences (Alcantara et al., 2015; Amanatidou et al., 2015). It was also shown that increasing the recycle rate may not improve the biomass/product throughput (Du et al., 2012; Bertucco et al., 2014); in addition, the determination of the critical recycle ratio has been based on the settler performance only, without taking into account the simultaneous effect it has on the bioreactor performance (D'Antonio and Carbone, 1987; Sardo and Indelicato, 1995).

Unfortunately, publications about a process of the type sketched in **Figure 4.1** applied to microalgae cultivation are apparently missing in the literature, even though strong interest is currently paid to microalgae continuous cultivation processes, so that quite a lot of information is available (Sforza et al., 2014; Fernandes et al., 2015; Silva et al., 2016). A number of papers discuss the use of a recycle stream coupled with the reactor, but without accounting for the effect of a settler (Du et al., 2012; Bertucco et al., 2014; Barbera et al., 2015; Oliveira et al., 2015; Silva et al., 2016). Sedimentation is indeed a common process to recover microalgal biomass but, generally, it is applied in batch mode (Barros et al., 2015).

The aim of this chapter is to develop a simplified model of a steady-state continuous process composed by a bioreactor and a gravity settler with partial biomass recycling, in order to increase the biomass production for a given plant size, or to minimize the equipment size for a desired throughput. The model includes simple material balances and a number of adjustable parameters that can be readily measured at the laboratory level. The proposed procedure allows to better understand the role of process operating variables in view of optimizing their values to maintain a proper biomass concentration in both the reactor and the settler, and can be applied to a plant of this type, irrespective to the plant size.

The cultivation of the microalga *Scenedesmus obliquus* has been chosen as a reference system to show the proposed procedure, but the approach can be applied to any fermentation processes, as well as to biological wastewater treatment ones.

4.2 MATERIAL AND METHODS

In order to evaluate the parameters of the process model, the microalga *Scenedesmus obliquus* was cultivated in a flat-plate lab-scale photobioreactor, according to the methods reported below.

4.2.1 Experimental part

4.2.1.1 Microorganism and culture medium

S. obliquus cultivation was performed using BG-11 medium (Rippka et al., 1979) with doubled concentration. Microalgae cultures were sustained in solid medium by adding

agar (10 g L^{-1}) to the BG-11 medium. Pre-inoculum of *S. obliquus* were prepared in flasks at approximately 100 µE m^{-2} s^{-1} and held in exponential phase. The plant was fed with CO_2 in excess conditions (5 % in air), while maintaining pH at 8 with 10 mM HEPES buffer in order to prevent the culture medium from acidification. *S. obliquus* growth was monitored every 24 h by means of optical density measurements at λ = 750 nm (UV-visible Spectro, Spectronic Unicam), cell counting in a counting chamber Burker (HGB®, Germany), and dried weight determinations.

Inoculum cellular concentration within the reactor tank had an optical density of 0.5 at λ = 750 nm. The reactor was illuminated with a LED lamp (Light Source SL 3500, Photon System Instruments) whose effective light intensity was measured for both continuous and batch operations with a radiometer DeltaOhm HD2102.1.

4.2.1.2 Cultivation System and Nutrient Analysis

The photobioreactor used in the experiments had a flat-plate layout, which is shown in **Figure 4.2**. The experimental values of the operating variables are summarized in **Table 4.1**. The light intensity was kept constant at 300 µmol photons m^{-2} s^{-1}, a value at which it does not interfere negatively on the growth, i.e. photoinhibition is not occurring. For more details, see Sforza et al. (2014).

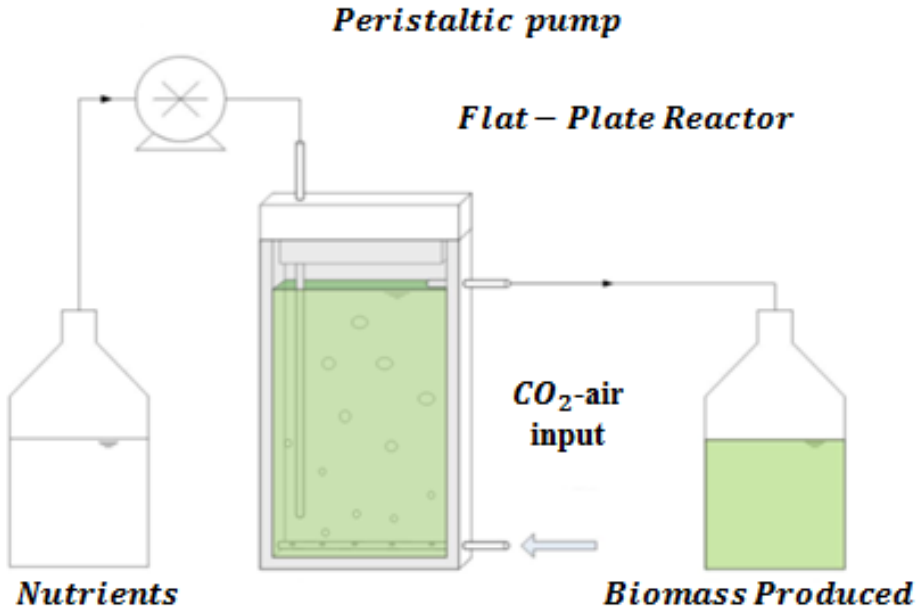

Figure 4.2: Schematic of the flat-plate photobioreactor used.

Table 4.1: Operating variables of the laboratory photobioreactor (steady state).

Variables	Values
V_R (cm^3) – Reactor Volume	250
θ (day) - Residence Time in the Reactor	1.66
I (µE m^{-2} s^{-1}) - Lighting	300
Fg (m^3 day^{-1}) – Gas volume flow rate	$1.2x10^{-3}$
C_{CO2}^{g} (%) – Concentration of CO_2 (Mixed- CO_2-air)	5
T - Reactor Temperature (°C)	22-24

The experimental procedure involved a specific condition (constant light intensity and culture medium concentration) to obtain the values of the growth kinetic parameters of the model. Nitrate was used as the reference substrate because carbon was provided in excess by bubbling a CO_2-air mix at 5%, whereas nitrogen sensitively limits the microalgal growth at the concentration used.

The nitrate concentration was measured by an Idrimetre Kit (Carlo Erba Reagenti®). The colorimetric reaction consists in an initial reduction of nitrate to nitrite, which forms a diazo after reacting with sulfuric acid. The succeeding reaction between diazonium salt and gentisic acid (2,5-dihydroxybenzoic acid) forms a diazo dye. The absorbance of the samples was measured spectrophotometrically at selected wavelength of λ = 445 nm. The calibration curve was based on different $NaNO_3$ solutions.

4.2.2 Simulation model

A continuous system including a photobioreactor and a gravity settler with partial mass recycle was simulated (**Figure 4.1**). Operating conditions at steady-state were calculated according to a simple model (Sundstrom and Klei, 1979), which was here modified, extended and generalized.

In all the simulations performed by the equations reported below, the growth parameters for *S. obliquus* were fitted to experimental data of Cs^I, Cs^U and $C_X{}^U$, measured at steady-state with suitable values of residence time. The gravity settling parameters for *S. obliquus* were derived from literature data. Alternately, they can be fitted from experimental data of settling velocity.

The model assumes that $C_X{}^I = Cp^I = 0$, i.e., there are no product nor biomass in the feed. The flat-plate photobioreactor was modeled as a continuous stirred tank reactor (CSTR),

which reproduces our experimental conditions as shown by Sforza et al. (2013). For a CSTR the mass balance takes the general form:

$$\frac{\Delta C}{\theta} = r \tag{4.1}$$

$$\theta = \frac{V_R}{F_I} \tag{4.2}$$

where ΔC is the difference of concentration (C) of the species under investigation between the reactor inlet (C^{in}) and outlet (C^{out}), $\Delta C = C^{out} - C^{in}$, r is the rate of production or consumption of the species of interest and θ is the residence time (or Hydraulic Retention Time, HRT), given by the ratio of the reactor volume V_R and the feed volumetric flow rate F_I.

The net biomass production rate is assumed to be equal to the growth rate (r_X), expressed by the Monod's equation, minus the cellular death rate ($r_{X,d}$), which is linearly proportional to the cell concentration (Borzani, 2001), according to the following relationships:

$$r_{X,t} = r_X - r_{X,d} \tag{4.3}$$

$$r_X = \frac{kC_X C_s}{K_M + C_s} \tag{4.4}$$

$$r_{X,d} = k_d C_X \tag{4.5}$$

where K_M is the Monod semi-saturation constant for substrate S (g L^{-1}), k is the maximum growth rate (day^{-1}), k_d is the specific rate of cell death (day^{-1}), whereas C_S and C_X represent the concentrations of a generic substrate and of biomass, respectively.

The apparent yield coefficient for substrate-to-biomass conversion ($Y_{X/S}$) is defined by:

$$Y_{x/s} = \frac{\Delta C_X}{-\Delta C_S} = \frac{C_{X,out}}{(C_{s,in} - C_{s,out})} \tag{4.6}$$

According to the definition of $Y_{X/S}$, a relationship can be set between the biomass growth rate and substrate consumption rate:

$$r_S = -\frac{1}{Y_{x/s}} \left(\frac{k.C_X.C_s}{K_M + C_s}\right) \tag{4.7}$$

Two important operating variables are the recycle ratio (R), which is the ratio between the recycle flow rate (F_R) and the feed flow rate (F_I):

$$R = \frac{F_R}{F_I} \tag{4.8}$$

and the biomass age (θ_c), or solid retention time (SRT), defined as:

$$\theta_c = \frac{Biomass\ amount\ in\ the\ reactor\ tank}{Biomass\ removed\ from\ the\ system\ per\ unit\ time} = \frac{V_{reactor} C_X^U}{F_w\ C_X^R + F_s\ C_X^S} \tag{4.9}$$

The value of θ_c is considered to be adequate when it warrants high process efficiency, i.e., there is sufficient time for the microorganisms to metabolize the nutrients fed to the reactor and the light energy, with the given residence time. The concept of wash-out time (θ_c^{wo}) is crucial in continuous bioprocesses. θ_c^{wo} is defined as the minimum solid retention time that allows the biomass to be present in the system. Therefore θ_c^{wo} is an operating limit, below which the biomass is washed out from the reactor, as its removal rate is higher than its production rate (Bertucco et al., 1990). From the biomass balance over the whole system, it results:

$$\frac{1}{\theta_c} = \frac{r_X}{C_X} - k_d \tag{4.10}$$

The wash-out time θ_c^{wo} can be determined when θ_c is minimum, i.e. when $\mu = \frac{r_X}{C_X}$ is maximum, which occurs when $C_S = C_S^I$. It can be obtained:

$$\theta_c^{wo} = \frac{(K_M + C_s^I)}{((k - k_d) C_S^I - K_M k_d)} \tag{4.11}$$

Corresponding to θ_c^{wo}, a minimum recycle ratio, R_{min}, can be calculated (**see Section 4.3.2.1 below**).

Two cases have to be considered: $C_X^S = 0$ (no loss of biomass from the top of the settler) and $C_X^S \neq 0$.

- If $C_X^S = 0$, when θ and F_I/F_W are known, θ_c is a function of R. Alternately, if θ_c and F_I/F_W are known, θ is a function of R. These relations can be expressed in dimensionless form.
- If $C_X^S \neq 0$ the biomass loss from the settler overflow influences the concentration of biomass in the process streams: in this case, besides θ and F_I/F_W, also the value of C_X^S/C_X^U is needed to express the dependence of θ_c on R. It is also

important to evaluate the biomass loss from the settler overflow ($F_S\ C_X^S$) as a function of R and C_X^S/C_X^U.

4.2.2.1 Model if $C_X^S = 0$

By writing the mass balances around the system and around the settler, and by using the definition of biomass age (Eq. 4.9), θ_c, C_S^U, C_X^U and C_X^R can be calculated as follows:

$$\theta_c = \frac{V_r C_X^U}{F_w\ C_X^R} = \frac{\theta}{1+R}\left(1 + \frac{RF_I}{F_w}\right) \tag{4.12}$$

$$C_s^U\left(\frac{g}{L}\right) = \frac{K_M(1+k_d\theta_c)}{((k-k_d)\theta_c - 1)} \tag{4.13}$$

$$C_X^U\left(\frac{g}{L}\right) = \frac{Y_{x/s}(\,C_s^I - C_s^U)}{(1+k_d\theta_c)}\frac{\theta_c}{\theta} \tag{4.14}$$

$$C_X^R\left(\frac{g}{L}\right) = \frac{\left(1+R-\frac{\theta}{\theta_c}\right)C_X^U}{R} \tag{4.15}$$

Equations (4.12) to (4.15) can be used sequentially to calculate these four variables, once θ, R and F_I/F_W are defined as data of the problem.

4.2.2.2 Model if $C_X^S \neq 0$

In analogy with the previous case, the mass balances around the system and the settler allow to calculate θ_c, C_S^U, C_X^U and C_X^R. Equations (4.13) and (4.14) for C_S^U and C_X^U still hold, whereas the expressions for θ_c and C_X^R become:

$$\theta_c = \frac{\theta}{(1+R)+\left(\frac{F_I}{F_w}-1\right)R\frac{C_X^S}{C_X^U}}\left(1 + \frac{RF_I}{F_w}\right) \tag{4.16}$$

$$C_X^R\left(\frac{g}{L}\right) = \frac{\left(\frac{(1+R)F_I}{F_w} - \frac{C_X^S}{C_X^U}\left(\frac{F_I}{F_w}-1\right)\right)C_X^U}{\left(1+\frac{RF_I}{F_w}\right)} = \frac{\left(1+R-\frac{\theta}{\theta_c}\right)C_X^U}{R} \tag{4.17}$$

It can be easily seen that Eq. (4.17) reduces to Eq. (4.15), so that also the expression for C_X^R remains unchanged. On the other hand, the value of θ_c is different in the two cases considered.

4.2.2.3 Sedimentation Model

The well-known gravity solid flux theory (D'Antonio and Carbone, 1987) was applied to model the gravity settler, as analytically summarized in the **Appendix** in combination with **Figures A4.1** and **A4.2**. It can be seen that the analysis of the settler performance results in four conditions (Eq. A4.10, A4.11, A4.15 and A4.24) which provide constraints for the system operating variables. It is worth noting that, with respect to the literature reference, a rigorous expression was derived, Eq. (A4.39), which allowed to compare the rigorous and approximate model solution.

4.3 RESULTS AND DISCUSSION

4.3.1 Measurement and fitting of cultivation data

The *S. obliquus* cultivation experiments were carried in a continuous photobioreactor, and **Table 4.2** displays the measured steady-state values of NO_3^- concentration at the inlet and outlet of the reactor tank (C_S^I and C_S^U, respectively) and the biomass concentration (dry weight) at the reactor exit (C_X^U). The NO_3^- consumption resulted to be approximately 79%. The cellular concentration at steady state was found to be 198.6 million of cells mL^{-1}. In **Table 4.2** also the fitted values of the growth rate constant (k), half-saturation constant (K_M) and effective yield ($Y_{X/S}$) are reported. In this work, the maintenance term (k_d) was assumed equal to zero, even though it could be easily included in the calculation, if needed (the dependence of this two-stage process to the k_d might be significant, as shown in Silva et al. (2016)).

Table 4.2: Experimental data and parameter values for the *S. obliquus* cultivation process.

Parameter	Value	Parameter	Value
C_S^I $(g\ L^{-1})$	1.78 ± 0.18	$k\ (day^{-1})$	0.49
C_S^U $(g\ L^{-1})$	0.38 ± 0.07	$K_M\ (g\ L^{-1})$	0.80
C_X^U $(g\ L^{-1})$	5.19 ± 0.47	$Y_{x/s} = \frac{c_x^U}{(c_s^I - c_s^U)}$	3.86
		θ_c^{wo}	2.86

4.3.2 Relations among operating variables

The model outlined in **section 4.2.2** was applied to predict the behavior of the two-stage system as a function of the operating variable. The recycle ratio R was varied between R_{min} and 1, which is a reasonable upper limit value.

4.3.2.1 How θ_c depends of R when θ and F_I/F_W are known

In the two-stage system considered, the SRT (θ_c) is extensively used as the key variable, but in most cases, it is the only variable investigated, without considering the coupled effects between the settler and the reactor. For instance, Yuan et al. (2009) studied the effect of SRT in wastewater treatment to find the best inoculum concentration in a semi-continuous mode. The biomass recycle rate could be used to optimize the inoculum inlet in the system. Nges and Liu (2010) and Lee et al. (2011) found the wash-out time of a wastewater treatment process by tentative method performing experiments between 3-35 days, which required a lot of time and solved partially the problem of a local optimum for θc without considering other operating variables. The effect of recycle rate appears underestimated by most authors, as it is generally simpler to keep it constant in the system while changing the solid retention time. However, R interferes directly in the productivity, and can be an interesting variable to work on. The wrong setting of recycle ratio can lead at least to two undesired behaviors: (i) the decreased productivity in comparison with a control condition without recycle, and (ii) the selection of unnecessarily high recycle ratios. About the first point, Bertucco et al. (2014) studied the continuous cultivation of *Scenedesmus obliquus* under seasonal day-night irradiation achieving biomass productivities of 1.34 (April conditions) and 1.04 g L^{-1} (October ones) with recycle rate of 50%, in comparison to 1.85 and 1.54 g L^{-1} without recycle, respectively. Other results for *S. obliquus* cultivation modeling using recycle ratios between 0.3–3 (and neglecting the settler) required higher SRT values to improve biomass productivity (Barbera et al., 2015). Fermentation with *Clostridium tyrobutyricum* showed an increased productivity of butyric acid as a result of the recycle rate only at higher fermentation time (called long-term strategy) (Du et al., 2012). About the second point, by using an extremely high recycle ratio (R = 600%), Amanatidou et al. (2015) performed a forced sedimentation, but the biomass concentration could not be

optimized, as well as the process operating (energy) costs. Alcantara et al. (2015) used a recycle to provide nitrate and nitrite in the anoxic tank, but set it to a fixed value of R = 1.5, probably by means of an empirical procedure.

In **Figure 4.3** θ_c is plotted as a function of R at different F_I/F_W values for a given SRT (θ). When $\theta_c = \theta_c^{wo}$, which can be calculated from Eq. (4.11), the intersection of the corresponding horizontal line with the curve gives the value of R_{min} for the selected F_I/F_W ratio. This is the minimum recycle ratio needed for maintaining the system in operation with the selected θ. When F_W increases, i.e., the removal rate of biomass from the system is larger, R_{min} increases to counteract the decreased concentration of biomass. From **Figure 4.3** it can be seen that, if F_W increases significantly (as in the case $F_W = 0.3F_I$), the minimum recycle ratio gets quite high, making the system unfeasible in practice. It is important to guarantee that $R > R_{min}$ for the selected operating conditions.

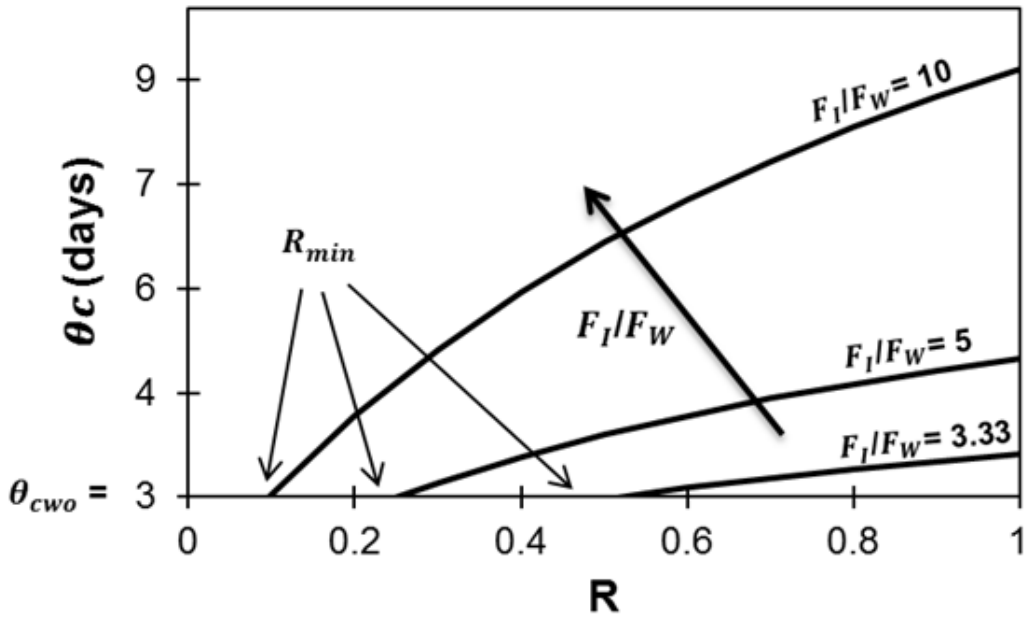

Figure 4.3: Dependence of θ_c on R as a function of F_I/F_W. θ=1.66 day.

Alternately, the value of the minimum recycle ratio (R_{min}) can be obtained from the value of θ_c^{wo} and Eq. (4.12), or Eq. (4.16):

$$R_{min} = \frac{(\theta - \theta_c^{wo})}{(\theta_c^{wo} - \theta\frac{F_I}{F_W})} \qquad (C_X^S/C_X^U = 0) \qquad (4.18)$$

$$R_{min} = \frac{(\theta - \theta_c^{wo})}{(\theta_c^{wo} + \theta_c^{wo}\frac{C_X^S}{C_X^U}\left(\frac{F_I}{F_W}-1\right) - \theta\frac{F_I}{F_W})} \qquad (C_X{}^S/C_X{}^U \neq 0) \qquad (4.19)$$

Therefore, when setting θ it is important to determine the corresponding values of both $\theta_c{}^{wo}$ and R_{min}.

4.3.2.2 Dimensionless relationships among the operating variables

By solving Eq. (4.12) with respect to θ, we have:

$$\theta = \theta_c \frac{1+R}{1+\frac{RF_I}{F_W}} \qquad (4.20)$$

It is clear from Eq. (4.20) that that $\theta < \theta_c$, always. In addition, there is a limiting value of the residence time θ_{min}, similarly to R_{min}, which can be calculated from Eq. (4.20) as well:

$$\lim_{R\to\infty} \theta = \theta_{min} = \theta_c \frac{F_W}{F_I} \qquad (4.21)$$

As an example, in **Figure 4.4** this value is represented as the horizontal asymptote of the curves. However, working near θ_{min} means needing high recycle rates and this makes the process not effective. So, using a proper value of θ to decrease the recycle rate is crucial for maintaining a suitable system operation and biomass production. This value will be larger if the system removes less biomass in the overflow stream. Therefore, using smaller R and larger F_I/F_W values can improve the viability of the reactor operation, as by lowering F_W more biomass is recirculated and remains in the system, thus reducing θ_{min}.

Experimental evidence of what is predicted by our simulation can be found in the literature. For proteinase production by *Saccharomyces cerevisiae* in a cell-recycling fermenter it was verified that higher recycle rate provided higher cell concentration, and the minimum residence time (θ_{min}) decreased from 2.5 to 0.30 h when moving from R = 0 to R = 0.9 (Grøn et al., 1996). A similar behavior was found for α-amylase production by *Bacillus amyloliquefaciens*, where θ_{min} was reduced from 0.83 to 0.25 when increasing R from 0 to 1 (Grøn et al., 1995). Both articles found the peak of productivity far from θ_{min}, (4 versus 0.66 h for *S. cerevisiae* and 4 versus 0.41 h for *B.*

amyloliquefaciens, i.e., lower cultivation time (θ). Also, the continuous cultivation of *Clostridium tycobutyricum* showed a similar performance of biomass productivity with much less minimum residence time, when recycle was used, which was equal to 0.01 h instead of 0.05 h without recycling (extrapolated) (Du et al., 2012).

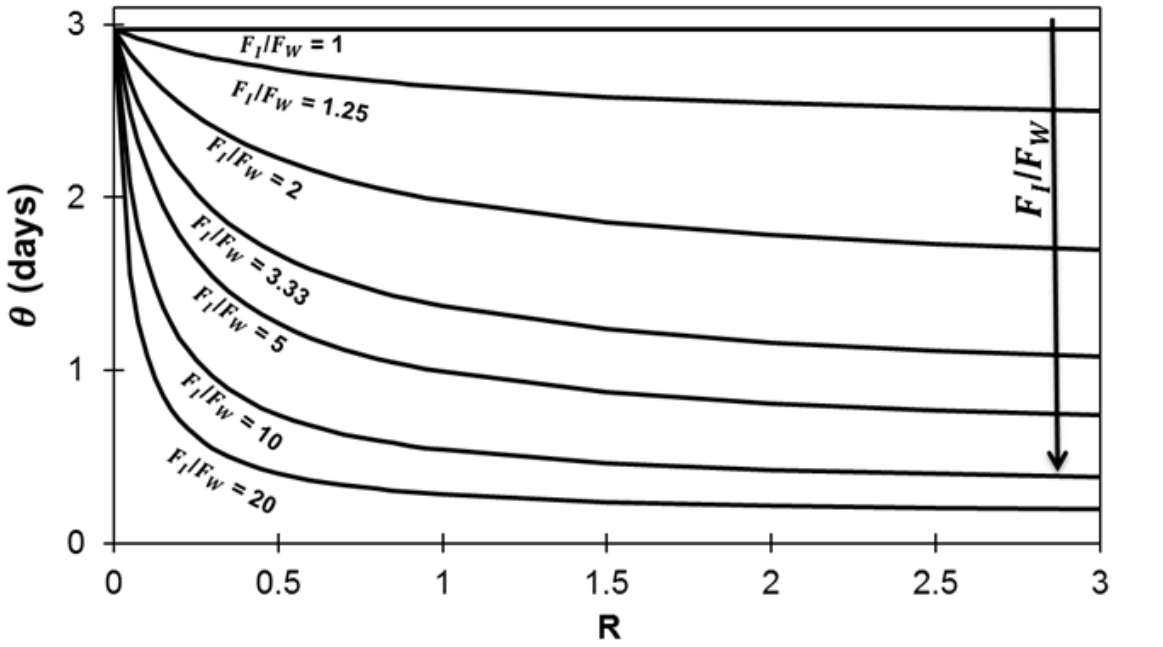

Figure 4.4: Relation between θ and R when θ_c = 2.98 days.

Eq. (4.12) can be written in a dimensionless form, with respect to either θ_c/θ:

$$\frac{\theta_c}{\theta} = \frac{\left(1+\frac{RF_I}{F_W}\right)}{(1+R)} \tag{4.22}$$

or with respect to R:

$$R = \frac{1-\frac{\theta_c}{\theta}}{\frac{\theta_c}{\theta}-\frac{F_I}{F_W}} \tag{4.23}$$

Eq. (4.22) is plotted in **Figures 4.5A** (θ_c/θ as a function of R, and parametric in F_I/F_W) and **4.5B** (θ_c/θ as a function of F_I/F_W, and parametric in R), whereas **Figure 4.5C** displays Eq. (4.23), with R depending on F_I/F_W, parametric in θ_c/θ.

With the use of **Figures 4.5**, if two of the three variables (R, θ_c/θ and F_I/F_W) are known, the third one can be readily obtained. These plots can be profitably applied to any

bioprocess based on the scheme of **Figure 4.1**, when its operating variables are expressed in dimensionless form.

It is also clear that:

$$\lim_{\frac{\theta_c}{\theta}\to 1} R = 0 \tag{4.24}$$

i.e. SRT and HRT have the same value when there is no recycle.

4.3.3 Calculation of θ_c, C_S^U, C_X^U, C_X^R as a function of R for given θ, F_I/F_W, and C_X^S/C_X^U

As an application of the currently proposed model, the values of θ_c, C_S^U, C_X^U and C_X^R as a function of R for two conditions of F_I/F_W are displayed in **Figure 4.6**.

It is noteworthy that C_X^U and C_X^R are quite sensitive to the loss of biomass in the overflow stream from the settler. For instance, with $C_X^S/C_X^U = 0.05$ at $F_I/F_W = 20$, their values decrease by around 30-40%, and θ_c is substantially lowered, with respect to the situation where $C_X^S = 0$ (**Figure 4.6**, **left column**). However, when using $F_I/F_W = 10$ no significant differences in biomass concentrations are found (**Figure 4.6**, **right column**).

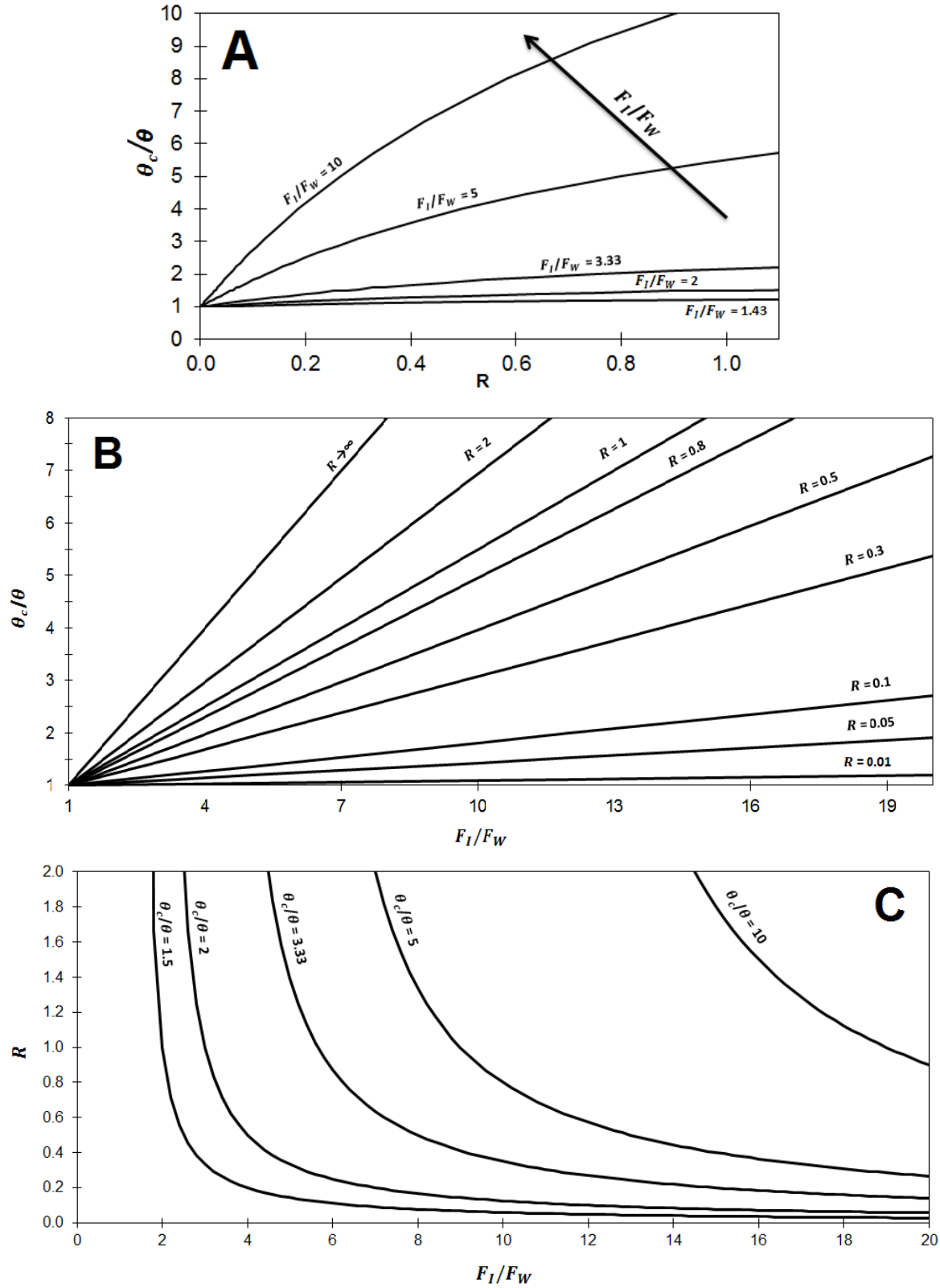

Figure 4.5: Dimensionless curves: θ_c/θ vs R (**A**), θ_c/θ vs F_I/F_W (**B**), R vs F_I/F_W (**C**).

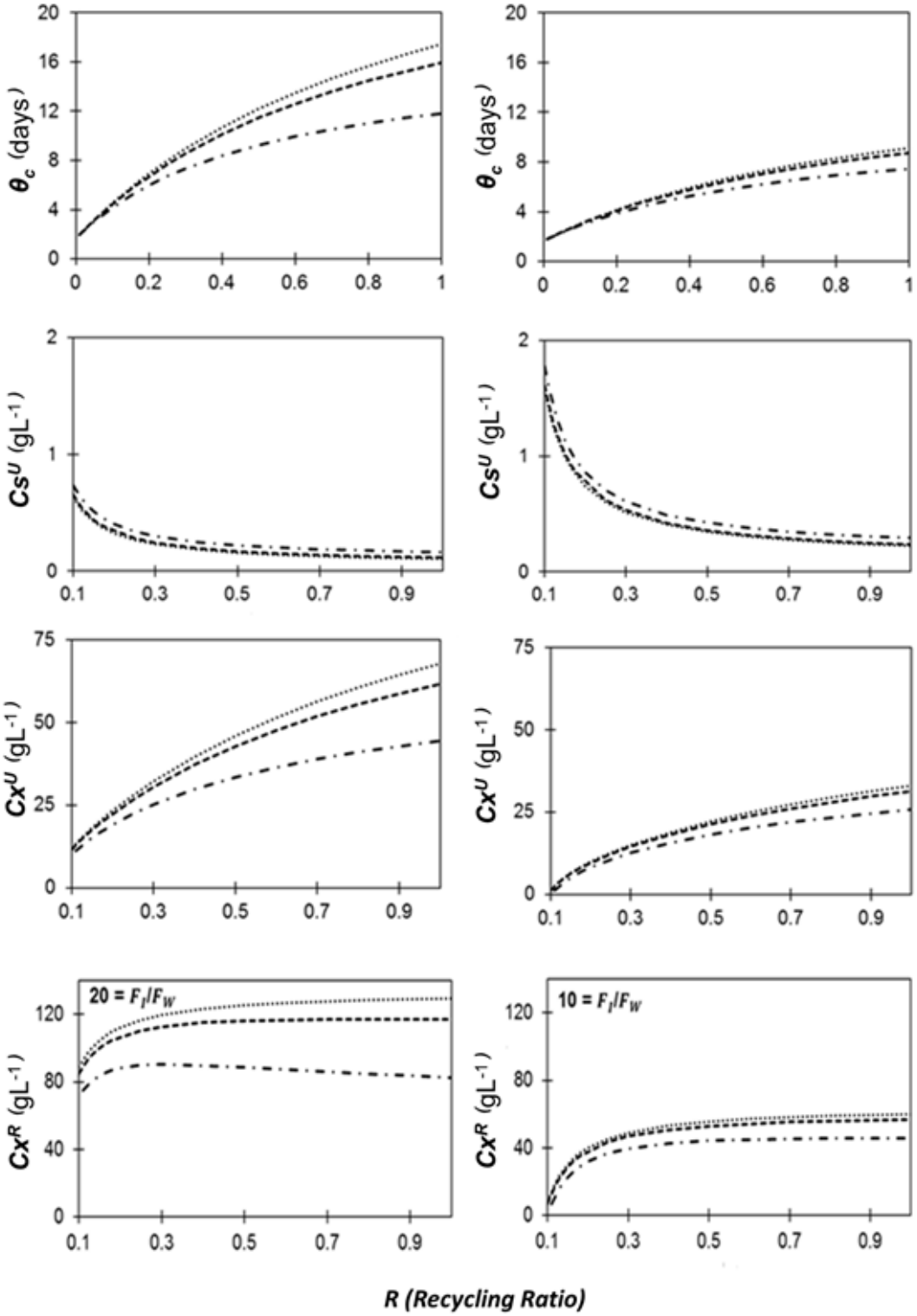

Figure 4.6: Steady-state values of θ_c, Cs^U, and Cx^R at different F_I/F_W and C_X^S/C_X^U ratios:

(...) C_X^S/C_X^U= 0, (---) C_X^S/C_X^U=0.01 and (-•-) C_X^S/C_X^U= 0.05;
F_I/F_W = 10 (left column) and F_I/F_W = 20 (right column).

4.3.4 Loss of biomass in the settler overflow as a function of R and C_X^S/C_X^U

Finally, it is interesting to see how much biomass is lost in the overflow stream from the settler as a function of *R* and C_X^S/C_X^U. To this purpose we define:
Percent of biomass lost with respect to the total biomass produced in the reactor:

$$\frac{M_S}{M_U}\,(\%) = \frac{F_S C_X^S}{F_U C_X^U} 100 \tag{4.25}$$

Percent of biomass lost with respect to biomass purged from the system:

$$\frac{M_S}{M_W}\,(\%) = \frac{F_S C_X^S}{F_W C_X^R} 100 \tag{4.26}$$

Percent of biomass purged from the system with respect to the total biomass produced in the reactor:

$$\frac{M_W}{M_U}\,(\%) = \frac{F_W C_X^R}{F_U C_X^U} 100 \tag{4.27}$$

As shown by the comparison between **Figures 4.7A** and **4.7B**, at lower F_I/F_W, M_S/M_W decreases (34 to 20% and 9 to 5%, when F_I/F_W changes from 20 to 10, respectively), so that the biomass loss in the overflow stream is decreased by almost 50%. It is also worth mentioning the highly sensitive dependence of M_S/M_W on C_X^S/C_X^U: the ratio between biomass loss and biomass removed from the system increases from 20 to 34% and 5 to 20%, when C_X^S/C_X^U changes from 0.01 to 0.05, respectively. In the case considered, also if C_X^S as little as 1% of the biomass concentration in the reactor (C_X^U) the biomass recovered and the efficiency of the two-stage process can change significantly. This confirms the importance of removing efficiently the biomass produced from the system, to avoid both washout conditions and loss of biomass.

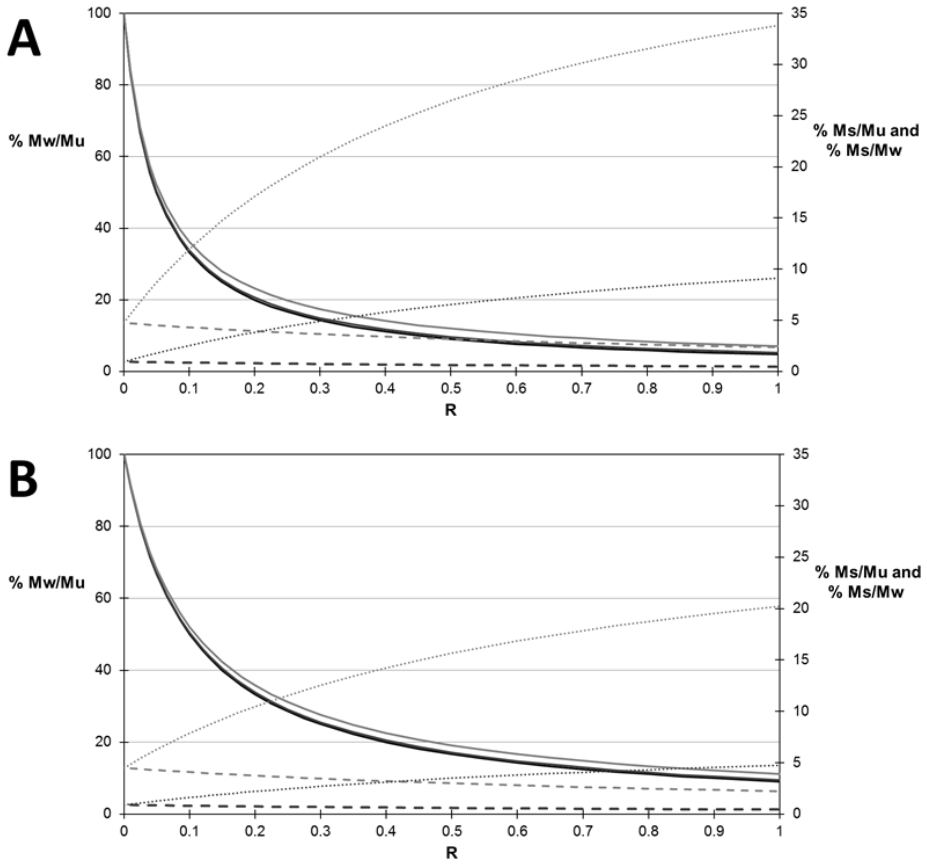

Figure 4.7: Loss of biomass in the settler overflow stream:
(**—**) $\%M_W/M_U$; (---) $\%M_S/M_U$; (…) $\%M_S/M_W$;
Ratio between feed and purge rates. $F_I/F_W = 20$ **(**A**)** and $F_I/F_W = 10$ **(**B**)**;
$C_X^S/C_X^U = 0$ (black lines), $C_X^S/C_X^U = 0.01$ (dark grey lines), $C_X^S/C_X^U = 0.05$ (grey lines).

4.3.5 Simulations accounting for the gravity settler kinetics

To model the gravity settler behavior, the settling velocity must be known. In our case, it was expressed by the following equation:

$$v = v_0\, e^{-\alpha C_x} = 8e^{-0.26C_x} \qquad (m\ day^{-1}) \qquad (4.28)$$

The initial settling velocity v_0, 8 m/day, is an acceptable value for our microalga, according to other works and personal experience (data not shown). For instance, Peperzak et al. (2003) found values between 0.4-2.2 m/day for phytoplankton in natural environment, and Depraetere et al. (2015), 1.15-3.65 m/day for *Arthrospira platensis* (0.6 g L^{-1} of dry cell weight - DW). The differences among these values mainly depend on cellular concentration and size because, according to Peperzak et al. (2003), a significant increase of settling velocity is expected when biomass concentration is

higher. It is important to mention that these values were measured for gravitational settling and can be potentially raised by the use of flocculants/coagulants (Barros et al., 2015).

The same data used in the first analysis with an ideal settler are now considered to account for the settler behavior. First of all, θ_c^{wo} and R_{min} are calculated from Eqs. (4.11), (4.18) and (4.19). With F_I/F_W = 10 it can be obtained θ_c^{wo} = 2.96 day and R_{min} = 0.0952. Using the dimensionless graphs of **Figures 4.5** we find θ_{min} = 0.5912 day. Now the values of θ_c and R more suited to the process can be chosen: first a θ_c larger than θ_c^{wo} is set, then a value for R is assumed. It is important that:

$$R_{min} < R < R_c \qquad \text{(Condition } V\text{)} \qquad (4.29)$$

where R_{min} is the minimum recycle ratio to maintain the active biomass in the reactor, while R_c is the maximum value required to promote biomass sedimentation.

With reference to the **Appendix**, on the base of the maximum operating value expressed by Eq. (A4.25), this relation can be improved:

$$R_{min} \leq R \leq R_{max,operating} < R_c \qquad \text{(Condition } V \text{ improved)} \qquad (4.30)$$

In addition, to ensure that both the clarification ($C_x^S \sim 0$) and thickening functions are fulfilled, applying Conditions *I, II, III* in the **Appendix** (Eq. A4.10, A4.11 and A4.15) leads to the results summarized in **Table 4.3**.

Table 4.3: Operating values according to conditions.

Condition	Values
(*I*) $\boldsymbol{C_L > \frac{2}{\alpha}}$	7.69 *g L*$^{-1}$
(*II*) $\boldsymbol{u < v_0 e^{-2}}$	1.08 *m day*$^{-1}$
(*III*) $\boldsymbol{C_x^R > \frac{4}{\alpha}}$	15.38 *g L*$^{-1}$

As an example, three values of θ_c were considered, and the sensitivity of R to θ_c is reported in **Table 4.4**. If a θ_C near to θ_C^{wo} (3.30 days) is chosen, an accurate control of safe system operation is required because the operating range for recycle ratio is 0.0952 < R < 0.1579 < 0.1859. On the other hand, with a higher θ_c (3.80 days), the operating range is much larger (0.0952 < R < 0.5398 < 0.7623).

In **Table 4.4** and **Figure 4.8** the limiting conditions (i.e. the tangent curves) for these three θ_c values are displayed. When R decreases a higher C_X^R is obtained at the settler bottom, as the gravitational solid flux is shifted to the right the graph of G_V, so that v is lower. Accordingly, F_I/A decreases and larger area is required. For this reason it is better to work near $R_{max,operating}$ ($C_X{}^R{}_{min,operating}$). In any case, the recycle ratio must lie between the R_{min} and $R_{max,operating}$ (Eq. A4.25) to ensure appropriate thickening of the biomass.

Table 4.4: Points of operating range at different θ_C.

Parameter	Value		
θ (days) = 1.66 and $\theta_C{}^{wo}$(days) = 2.96			
θ_C (days)	3.30	3.80	4.20
$C_X{}^U$ (g/L)	3.71	7.53	9.99
R_{min}	0.0952		
$R_{max,operating}$	0.1579	0.5398	1.1199
$C_{Lmin,operating}$	7.6923		
F_I/A_{max}	3.8941	1.4365	0.7865
R_C	0.1859	0.7623	1.5710

It is also possible to verify how the area of the settler changes as a function of θ_c. The minimum thickening and clarification area can be calculated by:

$$A_{thickening} = \frac{F_I(1+R)C_X^U}{G_{app}} \tag{4.31}$$

$$A_{clarification} = \frac{F_S}{v_{(C_X^U)}} \tag{4.32}$$

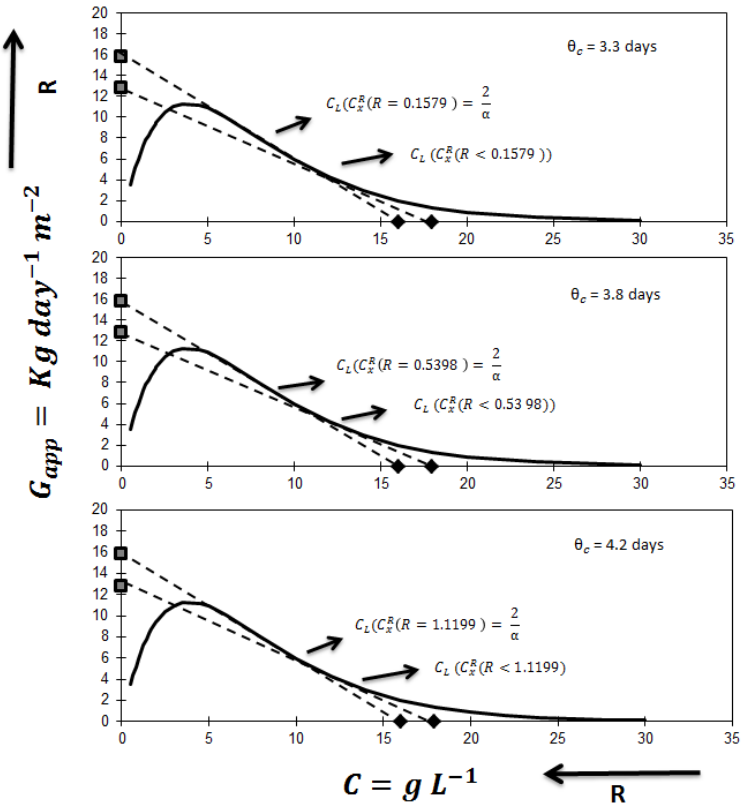

Figure 4.8: Tangent lines as a function of θ_C and R values. ($C_X{}^R{}_{min,operating}$ = 15.38 g L^{-1}, θ = 1.66 day).

In **Table 4.5** an example is shown with F_I = 1000 m^3/day. When θ_C increases, F_I/A decreases, so that the required area is larger.

Finally, we would like to point out that the assumption $v \sim 0$ is insufficient when R gets larger: if the rigorous model (Eq. A4.26) is applied instead of the simplified one (Eq. A4.13) a significantly different value is calculated for F_I/A and show the importance of the considerations presented in this manuscript. In **Figure 4.9** the rigorous and the approximate models are compared for the three values of θ_c considered. The results for R are quite different, especially near the value of $R_{max,operating}$, which is indeed a general reference. It is also clear that, when θ_c increases, F_I/A decreases because the biomass concentration is higher, and consequently the effects of sedimentation are higher too, and more settling area is necessary with respect the case with $v \sim 0$.

Critical recycle ratio (R_c) has already been discussed in literature, but considering the settler only, and no connection with the reactor was made. Further, the condition of v = 0 is always assumed (D'Antonio and Carbone, 1987; Sardo and Indelicato, 1995). In this paper, we propose a range of R useful for properly running both the reactor and the

settler, and we show how the assumption of v = 0 may influence significantly the calculation.

Table 4.5: Area required for clarification and thickening.

Variables	R_{min} = 0.0952		
	θ_C (days) = 3.30	θ_C (days) = 3.80	θ_C (days) = 4.20
F_I/A_{max} *(m day^{-1})*	3.89	1.44	0.79
A_{min} *(m^2)*	256.79	696.13	1271.45
Thichening Area min (m^2)	258.00	817.09	996.14
Clarification Area min (m^2)	288.14	695.74	1251.01

**considering F_I = 1000 m^3 day^{-1}.*

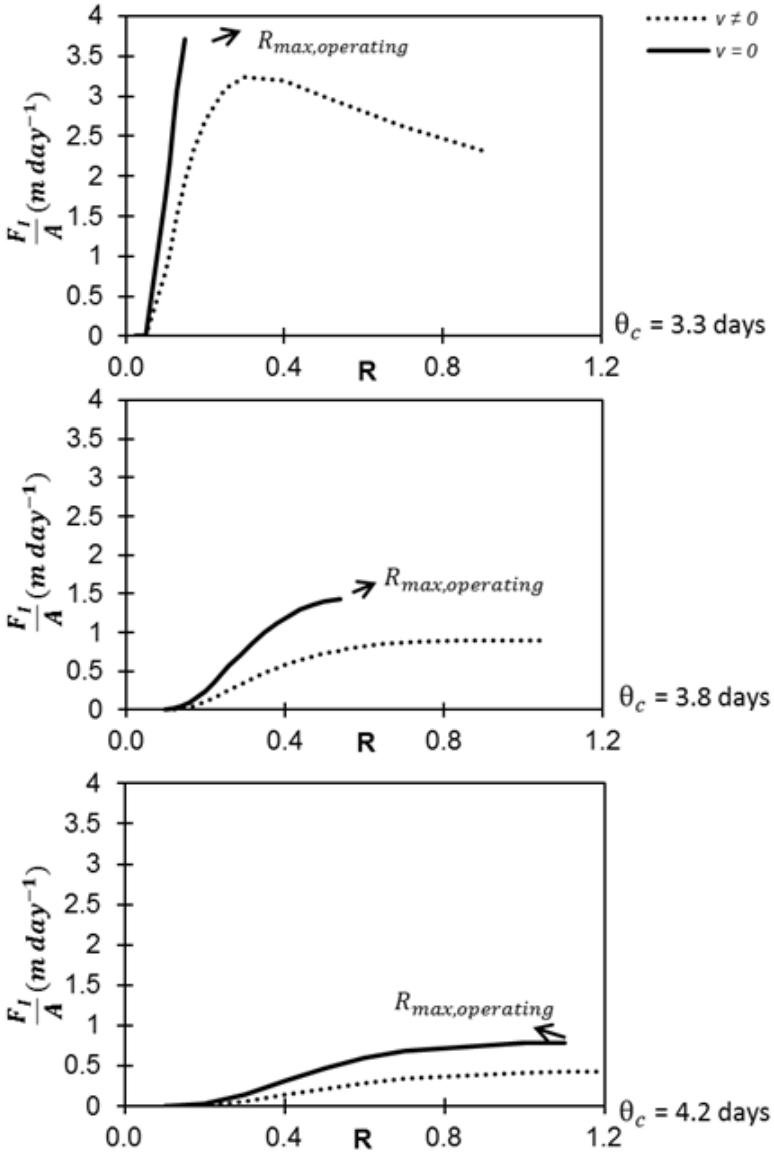

Figure 4.9: Comparison between F_I/A values when v = 0 (simplified model) and $v \neq 0$ (rigorous model).

Eventually, the effect of F_W is discussed. As the F_I/F_W ratio affects both θ_c/θ and R, (Eq. 4.22 and 4.23), F_W needs to be adequately set once R is decided. Both expressions of R_c and R_{min} depend of F_I/F_W (Eq. 11, A22 and A23), and their behavior is plotted as a function of F_I/F_W in **Figure 4.10**. Here, a minimum value of F_I/F_W is evidenced for which $R_{min} = R_c$. Above it, all values of $R_{min} < R_c$, satisfy condition *V*.

By equating the two expressions of R_{min} and R_c, we obtain:

$$F_I/F_{W\,min} = \frac{4\theta_C^{wo}}{\alpha\theta C_x^U} \qquad (C_X{}^S/C_X{}^U = 0) \qquad \text{(Condition } VI\text{)} \qquad (4.33)$$

which exactly gives this intersection value (for example, F_I/F_W = 3.66 with θ_c = 3.8 days).

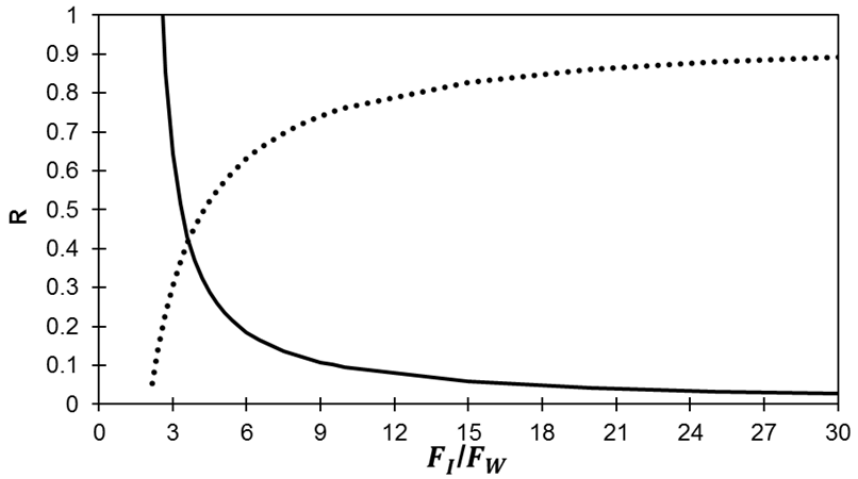

Figure 4.10: Intersection point between R_{min} **(–)** and R_c **(•••)** as function of F_I/F_W.

The calculation of F_I/F_W corresponding to $R_{max,operating}$ can be performed by Eq. (4.22) or (4.23) (i.e. the dimensionless curves in **Figures 4.5**). In **Table 4.6** results are shown for the same θ_c values examined above, where the maximum F_W is reported as well. The purge flow rate (F_W) is another variable that must be paid attention to, as far as the settler performance is concerned, because it can increase the convective flow rate and make the settler collapse.

At our knowledge, the concepts of R_{min} and $F_I/F_{W\,min}$ when both the reactor and settler kinetics are accounted for, have not been discussed in the literature so far.

Table 4.6: Settling area and maximum purge flow rate.

Variables	R_{min} = 0.0952		
	θ_C (days) = 3.30	θ_C (days) = 3.80	θ_C (days) = 4.20
$R_{max,operating}$	0.16	0.54	1.12
F_I/F_{Wmin} $(m\ day^{-1})$	7.44	3.67	2.76
$F_I/F_{Wmin,operating}$ $(m\ day^{-1})$	8.24	4.68	3.90
$F_{Wmax,operating}$ $(m^3\ day^{-1})$	121.28	213.80	256.65

**considering $F_I = 1000\ m^3\ day^{-1}$.*

A summary of viable (i.e. respecting all the conditions proposed in this work) values for the operating variables of *S. obliquus* continuous cultivation in the two-stage system presently considered is reported in **Table 4.7**.

Table 4.7: Reference operating parameters for *S. obliquus* cultivation.

Parameters	**Value**
θ *(days)*	1.66
θc *(days)*	3.80
F_I/F_W	4.67
R	0.53
C_X^U (gL^{-1})	7.52
C_X^R (gL^{-1})	16.95

4.4 CONCLUSIONS

The optimal design of a bioprocess made up by a biological reactor (or a photobioreactor) and a gravity settler with partial recycle and purge of the biomass was addressed in this work, using microalgae cultivation as a reference for simulation.

A simple steady-state model was developed, taking into account the kinetics in both the reactor and the gravity settler. The kinetic parameters values were measured in a lab scale apparatus. The proposed model allows to investigate the effect of process variables, mainly the solid retention time (θ_c), the recycle ratio (R), the reactor residence time (θ) and the ratio between feed and purge flow rates (F_I/F_W), on the outlet streams concentrations, in order to optimize the operation of the two-stage system. Dimensionless plots were given as a guide to process design and simulation.

It was shown that the recycle ratio strongly influences the cultivation and the sedimentation steps, and that it exists a range between R_{min} (defined by the reactor to avoid wash-out) and $R_{max,operating}$ (defined by the settler to achieve effective thickening) where the system can be operated properly. It was also shown that the process is quite

sensitive to the loss of biomass from the top of the settler (C_X^S), which should be accurately monitored and controlled; and a rule was given to calculate $F_I/F_{W\,min}$ (the maximum biomass purge flow rate).

The proposed procedure is able to provide indications in the design and operation of large scale bioreactor-settler systems. It is applicable to any fermentation system, and to activated sludge wastewater treatment, in order to optimize, for instance, the throughput of microalgal biomass or the production of sludge. In the case of microalgae more experimental results from large scale plants would be useful for a thorough validation of the proposed procedure.

REFERENCES

Alcantara, C., Dominguez, J.M., Garcia, D., Blanco, S., Perez, R., Garcia-Encina, P.A., Munoz, R., 2015. Evaluation of wastewater treatment in a novel anoxic-aerobic algal-bacterial photobioreactor with biomass recycling through carbon and nitrogen mass balances. Bioresource Technology 191, 173-186.

Amanatidou, E., Samiotis, G., Bellos, D., Pekridis, G., Trikoilidou, E., 2015. Net biomass production under complete solids retention in high organic load activated sludge process. Bioresource Technology 182, 193-199.

Barbera, E., Sforza, E., Bertucco, A., 2015. Maximizing the production of *Scenedesmus obliquus* in photobioreactors under different irradiation regimes: experiments and modeling. Bioprocess. Biosyst. Eng. 38, 2177-2188.

Barros, A.I, Gonçalves, A.L.; Simoes, M.; Pires, J.C.M., 2015. Harvesting techniques applied to microalgae: a review, Renewable and Sustainable Energy Reviews 41, 1489-1500.

Bertucco, A., Beraldi, M., Sforza, E., 2014. Continuous microalgal cultivation in a laboratory-scale photobioreactor under seasonal day-night irradiation: experiments and simulation. Bioprocess. Biosyst. Eng. 37, 1535-1542.

Bertucco, A., Volpe, P., Klei, H.E., Anderson, T.F., Sundstrom, D.W., 1990. The stability of activated sludge reactors with substrate inhibition kinetics and solids recycle, Water Research 24(2), 169-174.

Borzani, W., 2001. In: W. Borzani, W. Schmidell, U.A. Lima, E. Aquarone (Coords.) Biotecnologia Industrial: VOLUME 2 – Biotecnologia Industrial., Bluche, Sao Paulo, 560 p.

D'Antonio, G., Carbone, P., 1987. Verifica sperimentale della teoria del flusso solido. Ingegneria Sanitaria, 325-336.

Depraetere, O., Pierre, G., Deschoenmaeker, F., Bodri, H., Foubert, I., Leys, N., Markou, G., Wattiez, R., Michaud, P., Muylaert, K., 2015. Harvesting carbohydrate-rich *Arthrospira platensis* by spontaneous settling. Bioresource Technology 180, 16-21.

Du, J., McGraw, A., Lorenz, N., Beitle, R.R., Clausen, E.C., Hestekin, J.A., 2012. Continuous fermentation of Clostridium tyrobutyricum with partial cell recycle as a long-term strategy for butyric acid production. Energies 5, 2835-2848.

Fernandes, B.D., Mota, A., Teixeira, J.A., Vicente, A.A., 2015. Continuous cultivation of photosynthetic microorganisms: approaches, applications and future trends. Biotechnology Advances 33(6), 1228-1245.

Grøn, S., Morcel, C., Emborg, C., Biedermann, K., 1995. Cell recycling studies for α-amylase production by Bacillus amyloliquefaciens. Bioprocess Engineering 14, 23-31.

Grøn, S., Biedermann, K., Emborg, C., 1996. Production of proteinase A by *Saccharomyces cerevisiae* in a cell-recycling fermentation system: experiments and computer simulations. Appl. Microbiol. Biotechnol. 44, 724-730.

Kosinska, K., Miskiewicz, T., 2009. Performance of an anaerobic bioreactor with biomass recycling continuously removing COD and sulphate from industrial wastes. Bioresource Technology 100, 86-90.

Lee, D., Li, V., Noike, T., 2010. Influence of solids retention time on continuous H_2 production using membrane bioreactor. International Journal of Hydrogen Energy 32, 52-60.

Lee, I., Parameswan, P., Rittmann, B.E., 2011. Effects of solid retention time on methanogenesis in anaerobic digestion of thickened mixed sludge. Bioresource Technology 102, 10266–10272.

Liu, J., Tao, Y., Wu, J., Zhu, Y., Gao, B., Tang, Y., Li, A., Zhang, C., Zhang, Y., 2014. Effective flocculation of target microalgae with self-flocculating microalgae induced by pH decrease. Bioresource Technology 167, 367-375.

Lund, J.W.G., 1951. A sedimentation technique for counting algae and other organisms, Hydrobiologia 3(4), 390-394.

Meyer, C.L., Papoutsakis, E.T., 1989. Continuous and biomass recycle fermentations of *Clostridium acetobutylicum*. Bioprocess Engineering 4, 49-55.

Narodolawsky, M., Mittmannsgruber, H., Nagl, W., Moser, A., 1988. Modelling of alcohol fermentation in a tubular reactor with high biomass recycle. Bioprocess Engineering 3, 135-140.

Nges, I.A., Liu, J., 2010. Effects of solid retention time on anaerobic digestion of dewatered-sewage sludge in mesophilic and termophilic conditions. Renewable Energy 35, 2200-2206.

Park, J.B.K., Craggs, R.J., Shilton, A.N., 2011. Recycling algae to improve species control and harvest efficiency from a high rate algal pond. Water Research 45, 6637-6649.

Park, J.B.K., Craggs, R.J., Shilton, A.N., 2013. Enhancing biomass energy yield from pilot-scale high rate algal ponds with recycling. Water Research 47, 4422-4432.

Peperzak, L., Coliin, F., Koeman, R., Grieskes, W.W.C., Joordens, J.C.A., 2003. Phytoplankton sinking rates in the Rhine region of freshwater influence. Journal of Plankton Research 25(4), 365-383.

Petre, E., Selisteanu, D., 2013. A multivariable robust-adaptative control strategy for a recycled wastewater treatment bioprocess. Chemical Engineering Science 90, 40-50.

Oliveira, S.C., Castro, H.F., Visconti, A.E.S., Giudici, R., 2015. Mathematical modeling of a continuous alcoholic fermentation process in a two-stage tower reactor cascade with flocculating yeast recycle. Bioprocess Biosyst. Eng. 38, 469-479.

Rawat, R., Ranjith, R., Kumar, Mutanda, T., Bux, F., 2013. Biodiesel from microalgae: A critical evaluation from laboratory to large scale production. Applied Energy 103, 444-467.

Rippka, R., Deurelles, J., Waterbury, J.B., Herdman, M., Stainer, R.Y., 1979. Generic assignments, strain histories and properties of pure cultures of cyanobacteria. J. Gen. Microb. 111, 1-61.

Salim, S., Bosma, R., Vermué, M.H., Wijffels, R.H., 2011. Harvesting of microalgae by bio-flocculation. Journal of Applied Phycology 23, 849-855.

Sardo, F., Indelicato, S., 1995. Verifica della teoria del flusso solido in un impianto a fanghi attivi a portata costante. Ingegneria Ambientale 24(10), 584-587.

Sforza, E., Enzo, M., Bertucco, A., 2013. Design of microalgal biomass production in a continuous photobioreactor: An integrated experimental and modeling approach. Chemical Engineering Research and Design 92(6), 1153-1162.

Sforza, E., Gris, B., Silva, C.E.F., Morosinotto, T., Bertucco, A., 2014. Effects of light on cultivation of *Scenedesmus obliquus* in bacth and continuous flat plate photobioreactor. Chemical Engineering Transactions 38, 211-216.

Silva, C.E.F., Gris, B., Bertucco, A., 2016. Simulation of microalgal growth in a continuous photobioreactor with sedimentation and partial biomass recycling. Brazilian Journal of Chemical Engineering 33(4), 773-781.

Sing, S.F., Isdepsky, A., Borowitzka, M.A., Lewis, D.M., 2014. Pilot-scale continuous recycling of growth medium for the mass culture of a halotolerant *Tetraselmis sp.* In raceway ponds under increasing salinity: a novel protocol for commercial microalgal biomass production. Bioresource Technology 161, 47-54.

Smith, B.T., Davis, R.H., 2012. Sedimentation of algae flocculated using naturally-avaliable magnesium-based flocculants, Algal Research 1(1), 32-39.

Sundstorm, D.W., Klei, H.E., 1979. Wastewater Treatment, The University of Connecticut - Prentice- Hall - Englewood Cliffs, New Jersey.

Uduman, N., Qi, Y., Danquah, M.K., Forde, G.M., Hoadley, A., Dewatering of microalgal cultures: a major bottleneck to algal-based fuels. J. Renewable Sustainable Energy 2, 12701-12715.

Yuan, Q., Sparling, R., Oleszkiewicz, J.A., 2009. Waste activated sludge fermentation: effect of solids retention time and biomass concentration. Water Research 43, 5180-5186.

Zhu, L., 2015. Biorefinery as a promising approach to promote microalgae industry: An innovative framework. Renewable and Sustainable Energy Reviews 41, 1376-1384.

APPENDIX: Gravity solid flux theory

The total flux of solids in a gravity settler (G_T) is given by:

$$G_T = G_v + G_u \quad \text{(A4.1)}$$

$$G_u = C_X u \quad \text{(A4.2)}$$

$$u = \frac{RF_I + F_W}{A} \quad \text{(A4.3)}$$

$$G_v = C_X v \quad \text{(A4.4)}$$

$$v = v_0 e^{-\alpha C_X} \quad \text{(A4.5)}$$

where:
G_u = Convective solid flux (kg m^{-2} day^{-1});
G_v = Gravitational solid flux (kg m^{-2} day^{-1});
C = Solid concentration (in this case, biomass concentration) kg/m^3;
u = Convective settling velocity;
A = settler surface area;
v = Settling velocity by gravity.

In the settler, the value of C_X increases from C_X^U to C_X^R. The solid fluxes are a function of the solid concentration according to **Figure A4.1**, where the occurrence of a minimum value is evidenced.

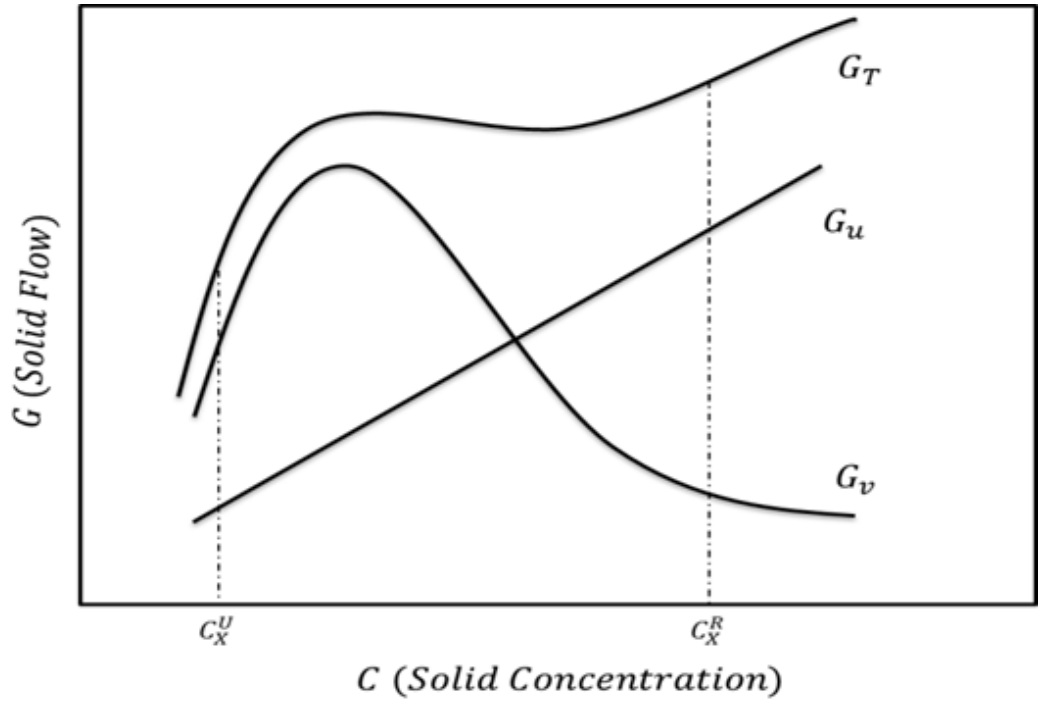

Figure A4.1: Relation between G_T, G_v and G_u.

The solid flux applied to the settler is given by:

$$Gapp = \frac{C_X^U(1+R)F_I}{A} \quad \text{(A4.6)}$$

For a correct settler operation it is necessary that $G_{app} < G_T$, whatever the value of C_X within the settler (between C_X^U and C_X^R). The dependence of G_T on C_X, for a pre-established u value is given by:

$$G_T = C_X v_0 e^{-\alpha C_X} + C_X u \quad \text{(A4.7)}$$

Applying the first and second derivatives analysis to find the minimum point, we obtain:

$$\frac{\partial G_T}{\partial C_L} = u + v_0 e^{-\alpha C_L} - v_0 C_L e^{-\alpha C_L} = 0 \quad \text{(A4.8)}$$

$$\frac{\partial^2 G_T}{\partial {C_L}^2} = v_0 \alpha^2 C_L e^{-\alpha C_L} - 2 v_0 \alpha C_L e^{-\alpha C_L} > 0 \quad \text{(A4.9)}$$

where C_L indicates the critical biomass concentration corresponding to the maximum, or limiting, solid flux (G_L) ensured by the settler.

Eq. (A4.8) cannot be resolved analytically, however using Eq. (A4.9) a relationship easier to work can be found:

$$C_L > \frac{2}{\alpha} \quad \text{(Condition } I\text{)} \quad \text{(A4.10)}$$

By replacing Eq. (A10) in Eq. (A8), we have:

$$u < v_0 e^{-2} \quad \text{(Condition } II\text{)} \quad \text{(A4.11)}$$

The value of the limiting flow of solids (G_L) can be calculated from Eq. A4.7 with u given by Eq. A4.3:

$$G_L = C_L v_0 e^{-\alpha C_L} + C_L u \quad \text{(A4.12)}$$

According to the literature (D'Antonio and Carbone, 1987), if it is assumed that $v = 0$ at the bottom of the settler, Eq. (A4.12) in combination with Eq. (A4.1) yields:

$$C_X^R = C_L + \frac{C_L v_0 \, e^{-\alpha C_L}}{u} \quad \text{(A4.13)}$$

By expressing *u* from Eq. (A4.8) and introducing it in Eq. (A4.13), it can be obtained:

$$C_X^R = \frac{\alpha C_L^2}{\alpha C_L - 1} \quad \text{(A4.14)}$$

Using condition *I* above (Eq. A10) it results:

$$C_X^R > \frac{4}{\alpha} \qquad \text{(Condition } III\text{)} \quad \text{(A4.15)}$$

Eq. (A4.14) is a 2nd degree equation in C_L:

$$C_L^2 - C_X^R C_L + \frac{C_X^R}{\alpha} = 0 \quad \text{(A4.16)}$$

whose roots are:

$$C_L' = \frac{C_X^R}{2} + \sqrt{\left(\frac{C_X^R}{4}^2 - \frac{C_X^R}{\alpha}\right)} \quad \text{(A4.17)}$$

$$C_L'' = \frac{C_X^R}{2} - \sqrt{\left(\frac{C_X^R}{4}^2 - \frac{C_X^R}{\alpha}\right)} \quad \text{(A4.18)}$$

Only C_L' is the useful root, as C_L'' does not respect conditions *I* and *III*. A correct operation of the settler requires that:

$$G_{app} = G_L \quad \text{(A4.19)}$$

according to which it can be finally obtained:

$$\frac{F_I}{A} = \frac{v_0 \alpha C_L^2 e^{-\alpha C_L}}{(1+R) C_X^U} \quad \text{(A4.20)}$$

where C_L can be expressed by Eq. (A4.17) as a function of C_X^R, which is in turn a function of C_X^U, *R*, θ and θ_C according to Eq. (4.15). In summary, if F_I, *A*, C_X^U, θ and θ_C are known, a single value of R can be calculated from Eq. (A4.20).

The recycle ratio is indeed the key variable: if *R* value is too high, the convective velocity will be dominant in the settler and will not allow to thicken the solid enough for the sedimentation. A limiting situation will be reached when $C_X^U = C_X^R$ (rupture of the reactor operation). To calculate this value, which is called critical recycle ratio (R_c), it is sufficient to express C_X^R from a mass balance around the settler:

$$F_I R C_X^R + F_W C_X^R + F_S C_X^S = F_I(1+R)C_X^U \tag{A4.21}$$

and to apply Eq. (A15) (condition *III*).

Two cases can be considered to calculate the R_c value:

1. When $C_X^S = 0$, it results:

$$R_C = \left(\frac{C_X^U - \frac{4F_W}{\alpha F_I}}{\frac{4}{\alpha} - C_X^U}\right) \tag{A4.22}$$

2. When $C_X^S \neq 0$, we have:

$$R_C = \left(\frac{1+\left(\frac{F_W}{F_I}-1\right)\frac{C_X^S}{C_X^U} - \frac{4F_W}{\alpha F_I}\frac{1}{C_X^U}}{\frac{C_X^S}{C_X^U}+\frac{4}{\alpha C_X^U}-1}\right) \tag{A4.23}$$

In any case the system must be operated with:

$$R \leq R_C \qquad \text{(Condition } IV\text{)} \tag{A4.24}$$

and Eq. (A4.20) holds under this condition only.

The value of $C_X^{R}{}_{min,operating}$, i.e., the minimum biomass concentration to correctly operate the settler, is given by Eq. (A4.15) (condition *III*), then from Eq. (4.15) $R_{max,operating}$ can be calculated:

$$R_{max,operating} = \frac{C_X^U\left(1-\frac{\theta}{\theta_c}\right)}{\left(\frac{4}{\alpha} - C_X^U\right)} \tag{A4.25}$$

It is noteworthy that the procedure outlined above assumes $v = 0$ at the bottom of the settler. If this condition is not verified, Eq (A4.13) does not hold any more. Instead, by combining Eq. (A4.12) with Eq. (A4.3), where the value of *u* is expressed by Eq. (A4.8), it can be obtained:

$$C_X^R v_0 e^{(-\alpha C_X^R)} - C_X^R v_0 e^{(-\alpha C_L)}(1 - \alpha C_L) - \alpha C_L^2 v_0 e^{(-\alpha C_L)} = 0 \quad \text{(A4.26)}$$

This equation can be solved numerically for C_L, because v_0, α and $C_X^R(\theta_c)$ are fixed values, depending on C_L, only. In this case, the value of $C_X{}^R{}_{min,operating}$ cannot be expressed analytically as for Eq. (A4.14). These concepts are qualitatively shown in **Figure A4.2**.

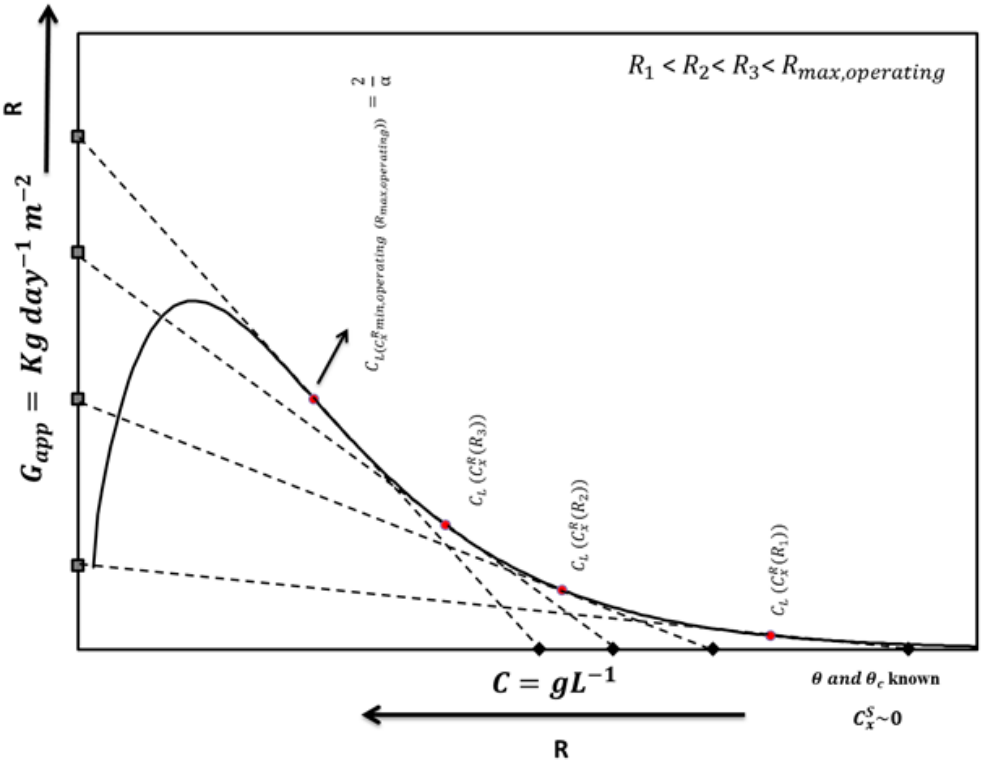

Figure A4.2: Graphical meaning of the operating range of *R*, according to the settler behavior.

Chapter 5

Effect of pH and carbon source on *Synechococcus* PCC 7002: Biomass and carbohydrate production with different strategies for pH control

Synechococcus PCC 7002 is an interesting species in view of industrial production of carbohydrates. The cultivation performances of this species are strongly affected by the pH of the medium, which also influences the carbohydrates accumulation. In this chapter, different methods of pH control were analyzed, in order to obtain a higher production of both *Synechococcus* biomass and carbohydrates. To better understand the influence of pH on growth and carbohydrates productivity, manual and automatic pH regulation in CO_2 and bicarbonate system were applied. The pH value of 8.5 resulted the best to achieve both of these goals. To use bicarbonate as a carbon source was effective to produce biomass but still limiting to accumulate carbohydrate. From an industrial point of view an alternative way to maintain the pH practically constant during the entire period of cultivation is the exploitation of the bicarbonate-CO_2 buffer system, with the double aim to maintain the pH in the viability range and also to provide the amount of carbon required by growth. In this condition, a high concentration of biomass (6 g L^{-1}) and carbohydrate content (around 60%) were obtained, which are promising in view of a potential use for bioethanol production. The chemical equilibrium of C-N-P species was also evaluated by applying the ionic balance equations and a relation between the sodium bicarbonate added in the medium and the equilibrium value of pH was discussed•.

•*Part of this chapter was published in Chemical Engineering Transactions (**Silva, C.E.F**., Gris, B., Sforza, E., La Rocca, N., Bertucco, A., 49, 241-246, 2016) and in Applied Biochemistry and Biotechnology (**Silva, C.E.F.**, Sforza, E., Bertucco, A., 181, 682-698, 2017).*

5.1 INTRODUCTION

The research on microalgae and cyanobacteria for biofuel applications has increased in the last decade and the potential of bioethanol production from microalgal biomass has been considered. Several authors published on this topic, mainly dealing with carbohydrate accumulation in microalgae species, such as *Scenedesmus obliquus* (Miranda et al., 2012; Ho et al., 2013a), *Chlorella vulgaris* (Dragone et al., 2011; Ho et al., 2013b) and *Chlamydomonas reinhardtii* (Choi et al., 2010), as well as some cyanobacteria, as *Arthrospira platensis* (Markou et al., 2013) and *Synechococcus elongatus* (Chow et al., 2015) which are promising microorganisms.

By means of photosynthesis, using only light and nutrients, microalgae and cyanobacteria synthetize lipids, proteins and carbohydrates. The relative amounts of these metabolic products are tightly linked to environmental and nutrient conditions, including the intensity of sunlight, the CO_2 levels, pH, temperature, available nutrients and the presence/absence of other competitive/symbiotic organisms (Juneja et al., 2013).

Biomass production and carbohydrate accumulation are highly dependent on the growth environment, and pH is one of the most important operating condition for the cultivation of photosynthetic microorganisms, with a species-specific range of viability of 7.5-9 (Chen et al., 2013). To avoid an unfavorable growth condition, organic buffers are typically used (Bernstein et al., 2014; Sforza et al., 2014) but these compounds may be toxic for some species (Morales et al., 2002) and alternatives must be studied, in particular from an industrial point of view.

Another important factor is the carbon available for fixation by the microorganism in the culture medium. Generally, CO_2 is provided in the medium by gas bubbling and dissolved carbon is available as different species: carbonic acid (H_2CO_3), bicarbonate (HCO_3^-) and carbonate (CO_3^{2-}) ions. The ratio among the three forms is pH dependent. From them, carbon can be assimilated by microalgae either in the form of dissolved CO_2 or via a direct bicarbonate import by specific carriers. For some cyanobacterium species, the bicarbonate ion is the most important one for algae growth, and the maximum dissociation occurs in the pH range from 7 to 9 (Vitovà et al., 2015). This range of pH is the same which is suitable for algae cultivation and has to be used to maximize the capture of inorganic carbon.

In addition, CO_2 concentration in atmospheric air is low to sustain cyanobacteria growth, about 0.04%, so that the amount of air need to aerate the culture is quite a lot, resulting in a high energetic consumption associated with the large amount of energy for pumping (Markou et al., 2014). These costs are related to technological aspects of capture, compression, transportation, temporary storage problems and loss of gas (Chi et al., 2011) and can reach up to 50% of biomass production costs (Chisti, 2013).

An alternative would be to use bicarbonate salts as a carbon source, according to a process called Bicarbonate-based Integrated Carbon Capture and Algae Production System (BICCAPS) (Chi et al., 2013). Bicarbonate salts have high solubility in water compared to CO_2 (for example, $NaHCO_3$ solubility > 90 g L^{-1} at 25 °C) and it is expected that their use efficiency is higher than CO_2 (Markou et al, 2014). The use of aqueous solutions of bicarbonate for algal cultivation should result in lower costs than CO_2, which requires intensive energy for compression (Chi et al., 2011). But this approach needs to be validate for each species.

In this chapter, the effect of the pH value on biomass production was investigated, with particular attention to carbohydrate accumulation in the cyanobacterium. A stable and efficient method for *Synechococcus* PCC 7002 growth during the entire period of cultivation is proposed and discussed. Eventually, the chemical equilibrium of C-N-P species is also evaluated by applying ionic balance equations and a relation between the sodium bicarbonate added in the medium and the equilibrium value of pH is obtained.

5.2 MATERIAL AND METHODS

5.2.1 Culture media and apparatus

Synechococcus PCC 7002 was cultivated using a modified Basal A medium: 18 g L^{-1} NaCl, 0.6 g L^{-1} KCl, 0.9 g L^{-1} NH_4Cl, 5.0 g L^{-1} $MgSO_4 \cdot 7H_2O$, 50 mg L^{-1} KH_2PO_4, 266 mg L^{-1} $CaCl_2$, 30 mg L^{-1} $Na_2EDTA \cdot 2H_2O$, 3.89 mg L^{-1} $FeCl_3 \cdot 6H_2O$ (pH 8.2), 34.26 mg L^{-1} H_3BO_3, 4.32 mg L^{-1} $MnCl_2 \cdot 4H_2O$, 0.315 mg L^{-1} $ZnCl_2$, 0.03 mg L^{-1} MoO_3, 12.15 μg L^{-1} $CoCl_2 \cdot 6H_2O$, 3 μg L^{-1} $CuSO_4 \cdot 5H_2O$, and 4 μg L^{-1} vitamin B_{12} (Bernstein et al., 2014). Preinoculum was cultivated into Erlenmeyer flasks at 100 ± 5 μE m^{-2} s^{-1} and held in exponential phase, at pH 8-9 using CO_2 5% (mix air-CO_2 % v v^{-1}, 1 L h^{-1}). Growth experiments were conducted in batch operation mode in 250 mL-working-volume glass vertical cylinders (5 cm diameter), continuously mixed by a stirring magnet placed at

the bottom of the bottle. The temperature was set at 28°C and the light intensity provided by fluorescent lamp was 100 μE m^{-2} s^{-1}, measured with a radiometer DeltaOhm HD2102.1. Each batch experiment started with an initial microalgae inoculation of OD_{750} = 0.3-0.4.

Different sets of experiments were carried out, with the aim to assess the effect of pH and carbon source on growth and carbohydrates content. The first set was carried out using CO_2 (5% v/v CO_2-air) or bicarbonate (5.5 g L^{-1}) without pH control and with manual pH control twice a day by adjusting it to values between 8.0-8.5, through addition of NaOH.

A second set of experiments was performed using sodium bicarbonate (5.5-88 g L^{-1} at pH 8.0-8.5) as a carbon source and with an automatic pH control, in order to better verify the effect of pH and bicarbonate concentration to *Synechococcus* cultivation and carbohydrate content. Several growth curves were carried out at pH values of 7.0-8.5-9.0 and 9.5 (5.5 g L^{-1} of sodium bicarbonate). The pH control was realized by an automatic system which was activated when the pH in the reactor exceeded the set point, by adding a HCl solution (2M) by a chromatographic pump (LC-20AT Prominence). The HCl concentration was chosen to avoid substantial volume changes in the reactor.

In order to verify the efficiency of organic buffers to control the pH, a third set of experiments was carried out, by using HEPES (10 and 20 mM) and Tris-HCl (5 and 10 mM) in the cultivation with the same culture medium (5.5 g L^{-1} of sodium bicarbonate as a carbon source).

In a fourth set of experiments, a buffered system using both CO_2 and bicarbonate was evaluated in order to verify the effect of such a system on biomass production and carbohydrate accumulation. Several sodium bicarbonate concentrations (5.5, 7, 11, 22 and 30 g L^{-1}) and CO_2 5% (mix air-CO_2 % v v^{-1}, 1 L h^{-1}) were used. All experiments were performed in at least two-three independent biological replicates.

5.2.2 Analytical methods

In all growth experiments, carbohydrate content and nutrients consumption were measured. The carbonate ions concentration was measured when sodium bicarbonate was used. *Synechococcus* PCC 7002 growth was monitored once a day by means of

optical density measurements at λ = 750 nm (UV-visible Spectro, Spectronic Unicam®). The dry weight was measured by filtration through cellulose acetate filters of 0.45 μm (Whatman®). Filters were pre-dried for 10 min at 105 °C in order to remove any moisture. Biomass filtered was dried for 2 h at 105 °C and then weighed to calculate the dry weight in terms of grams per liter. The growth rate constant μ (day^{-1}) was calculated by the slope of the semilogarithmic graph of cell concentration on time.
The carbonate species concentrations were measured daily by using a common titration method, based on the exploitation of two dyes, phenolphthalein, and bromocresol green (Sigma-Aldrich ®), pH-sensitive, allowing to determinate CO_3^{2-} and HCO_3^- concentrations in the solution (Warder's Method). The carbohydrate content was determined by Anthrone method (Trevelyan and Harrison, 1952). The nutrients measured were ammonium ($N–NH_4$) and phosphate ($P–PO_4$), assessed daily using standard methods in water and wastewater (APHA, 1992). Samples of culture were filtered (0.2 μm) in order to measure only dissolved nutrients. Ammonium was measured by test kits provided by St. Carlo Erba Reagenti® (Italy) where it is indirectly measured by the absorbance (at 420 nm) of an indophenolic complex produced by the reaction of ammonia with phenolic derivatives. Orthophosphates were measured by ascorbic acid method (at 706 nm).

5.2.3 Growth and bicarbonate assimilation model

To evaluate the kinetics of absorption of bicarbonate (bicarbonate ion, carbonate, total) and also the cell growth, a first order kinetics represented by Eq. (5.1) and (5.2):

$$dS/dt = -kt \quad \text{(Bicarbonate consumption)} \tag{5.1}$$

$$dX/dt = \mu t \quad \text{(Biomass production)} \tag{5.2}$$

where dS/dt is the substrate consumption rate (g L^{-1} day^{-1}), k is the absorption rate (day^{-1}), dX/dt is the cell production rate (g L^{-1} day^{-1}) and μ is the growth rate (day^{-1}).

The kinetic constant *k* (or μ) was expressed by substrate inhibition model:

$$k \; or \; \mu = (k \; or \; \mu)_{max} \cdot \frac{S}{\left(K_S + S + \frac{S^2}{K_I}\right)} \tag{5.3}$$

where *Ks* is the semi-saturation constant (g L^{-1}) and K_I is the substrate-inhibition constant (g L^{-1}). Experimental data were fitted to calculate the parameters values. The values of *k*, K_S and K_I were correlated to experimental data.

5.2.4 Model of ion balance

Although the inorganic carbon needed for growth can be absorbed either as atmospheric CO_2 or as bicarbonate salts, the compounds which are actually available in the solution are highly pH-dependent because of the equilibrium relations:

$$CO_{2(aq)} + H_2O \overset{k1}{\leftrightarrow} H_2CO_3^* \overset{k2}{\leftrightarrow} HCO_3^- + H^+ \overset{k3}{\leftrightarrow} CO_3^{2-} + 2H^+ \quad (5.4)$$

with dissociation constants $k_1 = 10^{-3.6}$, $k_2 = 10^{-6.381}$ and $k_3 = 10^{-10.377}$.

In lab-scale microalgae cultivation, carbon dioxide is generally fed to the system. However, when sodium bicarbonate is used together with CO_2, it dissociates in water, and bicarbonate ions neutralize H^+ ions, clearly changing (in this case, increasing) the pH of the medium. Therefore, varying the concentrations of sodium bicarbonate added (at constant temperature) is a way to modify the pH equilibrium value of the solution. Importantly, the pH is a parameter that depends also on the ionic status of the solution, since the counter-ions presence affects the water dissociation as well.

Counter-ions do not actively participate in the biochemical process of biomass conversion, but they are usually required to maintain the salinity of the medium. This is the case, for instance, of Cl^- ion, when using NH_4Cl, $CaCl_2$ and KCl for Cl^-, where only the cations are the species used for growth as micronutrients. Then, in order to promote the stability of the pH, a complete ion balance between anions and cations in the solution is reported to stabilize the charges:

$$[H^+(aq)] + [counter-ions]^+ = [OH^-(aq)] + [HCO_3^-(aq)] + 2.[CO_3^{2-}(aq)] + [counter-ions]^- \quad (5.5)$$

By using equation 5.5 and the parameters values of equation 5.4, it is possible to obtain the following relation between the bicarbonate ion at equilibrium and the corresponding pH value and counter-ions concentrations:

$$[HCO_3^{-*}(aq)] = \frac{(10^{-pH^*} + [counter-ions]^+ - [counter-ions]^- - 10^{pH^*-14}).10^{-pH^*}}{10^{-pH^*} + 2.10^{-10.377}} \quad (5.6)$$

where "*" means that the calculation is done at chemical equilibrium.

In addition, the ionic balance between carbonate species and N and P salts supplied can be modeled by the following equation:

$$NaHCO_3(aq) + CO_2(aq) + KH_2PO_4(aq) + NH_4Cl(aq) \leftrightarrow$$

$$\leftrightarrow CHONP - biomass\ (s) + H_2O(l) + O_2(g) + K^+(aq) + Na^+(aq) + Cl^-(aq) \quad (5.7)$$

This equation was based in the salts provided by the basal medium and sodium bicarbonate added.

5.3 RESULTS

5.3.1 Effect of CO_2 and sodium bicarbonate addition on growth

Two batch control experiments were first carried out, as reported in **Figure 5.1**. Here, it can be observed a cyanobacterial growth in the first two days, with a growth rate of μ=1.69 day^{-1} using CO_2 (**Fig. 5.1A**) and μ=0.55 day^{-1} with bicarbonate (**Fig. 5.1B**). However, after two days, inhibition occurs so that the growth is stopped, in the presence of both carbon dioxide and bicarbonate. This trend is probably due to the pH changes caused by the addition of these carbon sources which also change their concentration during the growth curve, due to consumption. In particular, in the case of CO_2 addition, the pH drops to values around 5-6, which is too low for growth. On the other hand, when using bicarbonate, the pH increases during growth up to 9-10, with a similar inhibitory effect. So, it is clear and well known that pH has to be controlled, but this is particularly true in the case of this species, which is very sensitive to it. Even though a possible effect of salinity may occurs in the case of bicarbonate addition (8.5 g L^{-1} of total Na, instead of 7 g L^{-1} of standard medium), this can be excluded by considering the euryhaline nature of the species, which is tolerant to a wide range of salinity (Ludwig and Bryant, 2012). Thus, the effect of changed pH values due to CO_2 and bicarbonate additions may be the main variable which affects growth.

To verify the effect of pH on growth inhibition, a number of experiments with pH adjustment were performed, with CO_2 as carbon source. By manually controlling the pH (once or twice a day depending of the needs) the cyanobacterium achieved a high final value of OD_{750} corresponding to about 20 (**Figure 5.2A**), which is 5 times higher than

that obtained without pH control (**Figure 5.1A**). Thus, maintaining the pH between 8-8.5 remarkably increased *Synechococcus* PCC 7002 biomass production.

In fact, at the end of the stationary phase high concentration of biomass (about 5 g L^{-1}) was obtained, with a remarkable carbohydrate content (57%) (**Figure 5.2B**). These results show the potential of this species for carbohydrate production, and consequently for bioethanol applications. By measuring the carbohydrates content during the growth period, it was verified that the accumulation of these macromolecules was more pronounced when the nutrients (ammonium and phosphate) were almost completely consumed (**Figure 5.2C**), i.e. in the last days of growth.

5.3.2 Effect of pH control on growth with sodium bicarbonate as carbon source

5.3.2.1 pH sensitivity

When bicarbonate was used as the carbon source, and automatic pH control was applied by HCl, a higher growth was obtained, in comparison to the control (**Figure 5.1B**). The growth rate depended on the pH set-point value, as reported in **Figure 5.3A**. The maximum growth rate (about 1.4 ± 0.2 day^{-1}) was observed at pH 8.5 (**Figure 5.3B**), which is comparable to that obtained with CO_2 bubbling. Thus, it seems that under alkaline environments *Synechococcus* growth can be enhanced (**Figure 5.3A**) when neutral or slightly-alkaline pH is used. This is a general indication for photosynthetic organism cultivation, i.e. working with pH between 7.5-9.0, as reported in the literature (Moreno et al., 1995; Berge et al., 2012).

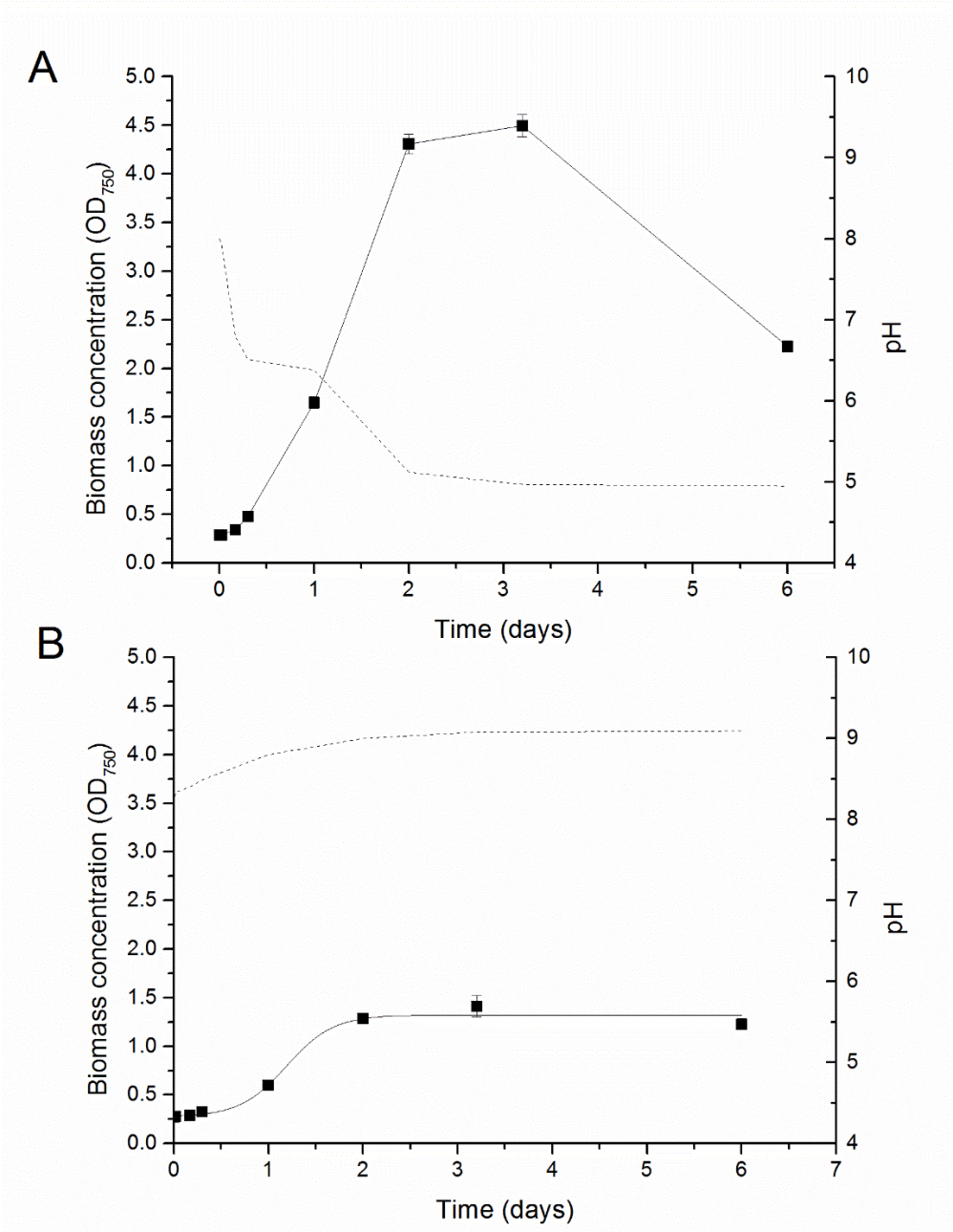

Figure 5.1: Control experiments without pH control supplying carbon as CO_2 (5.1A) and sodium bicarbonate (5.1B). Dots refer to biomass concentration, solid lines are eye guide only while dotted lines refer to pH values.

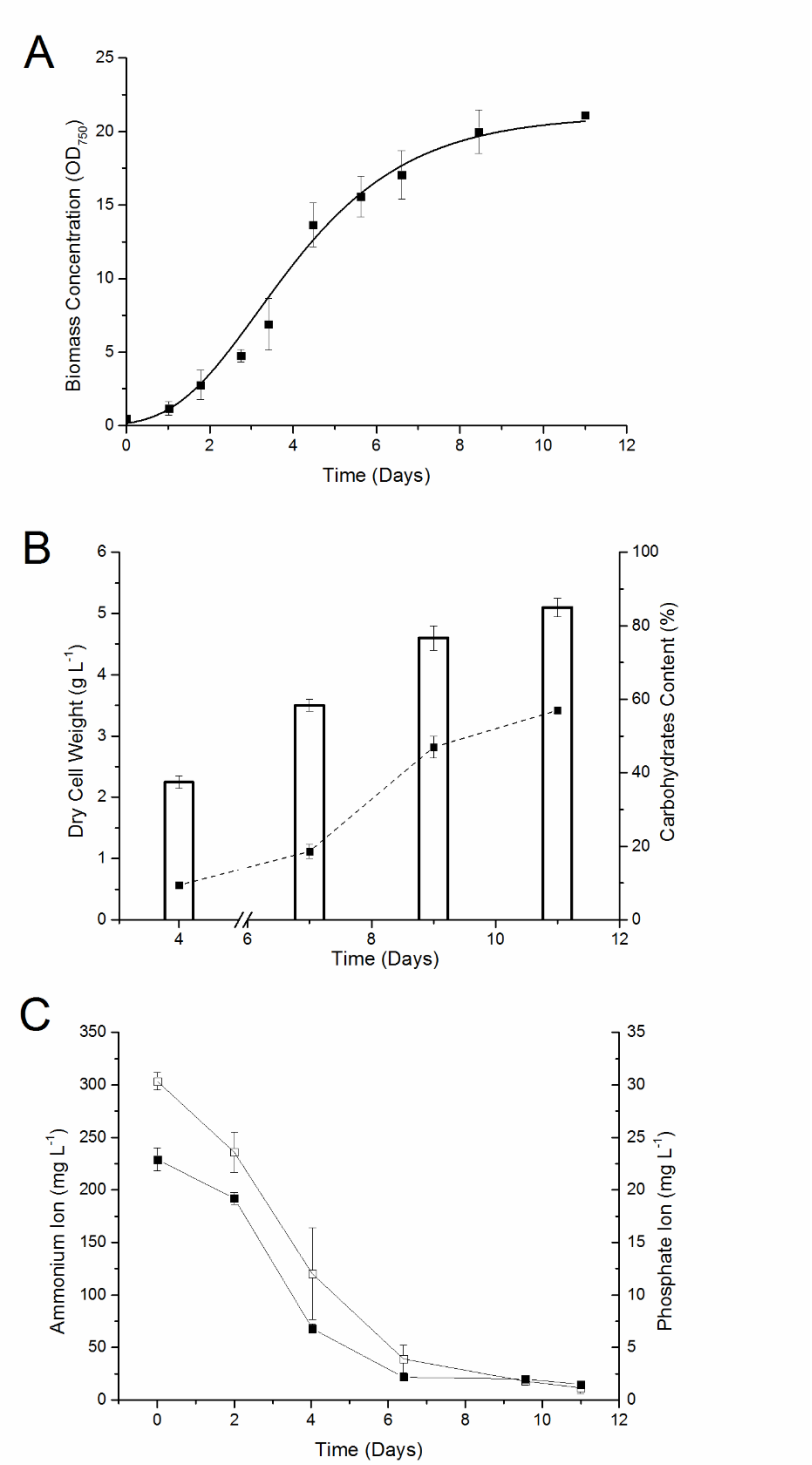

Figure 5.2: In Figure 5.2A *Synechococcus* PCC 7002 cultivation using manual pH control is reported. Biomass (bars) and carbohydrate content (dots) (Figure 5.2B) and nutrient consumption (5.2C, open squares refer to ammonium and black squares to phosphate) to the *Synechococcus* PCC 7002 using manual pH control.

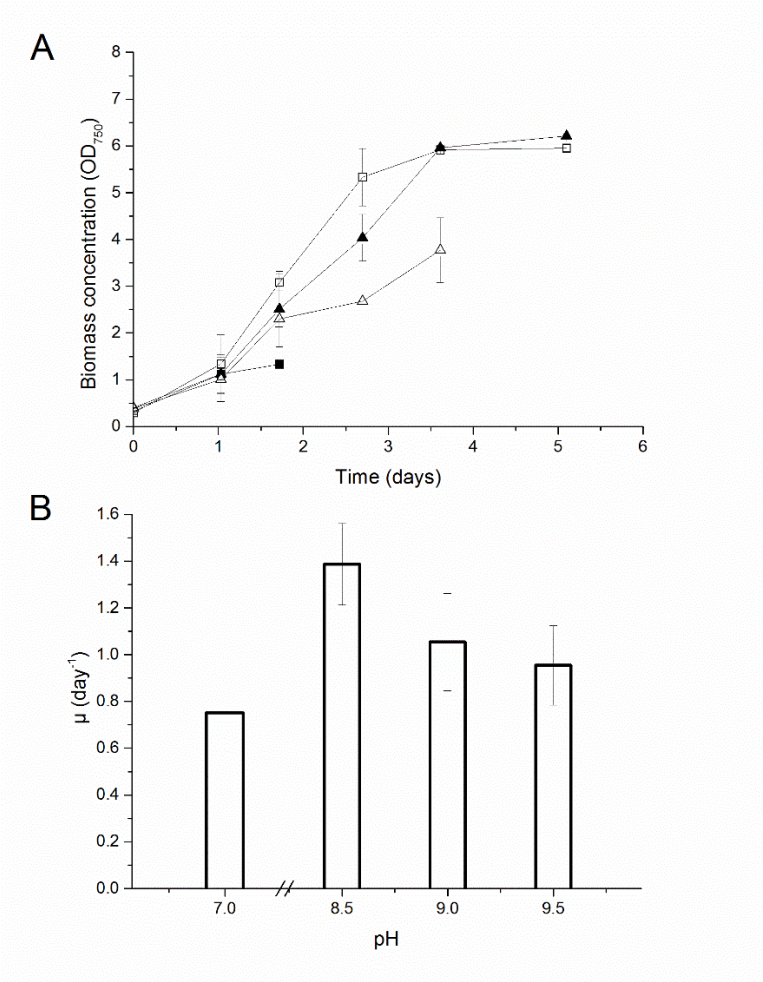

Figure 5.3: Growth curve (5.3A) and growth rates (5.3B) at different pH. In 4A dark squares correspond to pH 7, open squares to pH 8.5, dark triangles to pH 9 and open triangles to pH 9.5.

On the other hand, even though the growth rate was high, the biomass production was maximum for pH between 8.5-9.0, achieving a value of 1.4 ± 0.1 g L^{-1}, which is lower than that obtained by CO_2 bubbling (Figure 4A). In addition, the carbohydrate accumulation was lower (10-15%). These two results are probably related to the concentration of bicarbonate added to the medium (5.5 g L^{-1} of sodium bicarbonate) which may be a limiting value for biomass production. According to the measurement of the bicarbonate in solution we found that it was completely consumed in the experiments at pH range of 8.5-9.0) (**Figure 5.4A-B**). At pH 7.0 the growth rate was slower, because bicarbonate was probably lost as CO_2 (**Figure 5.4B**) according to bicarbonate equilibrium (Equation 5.4).

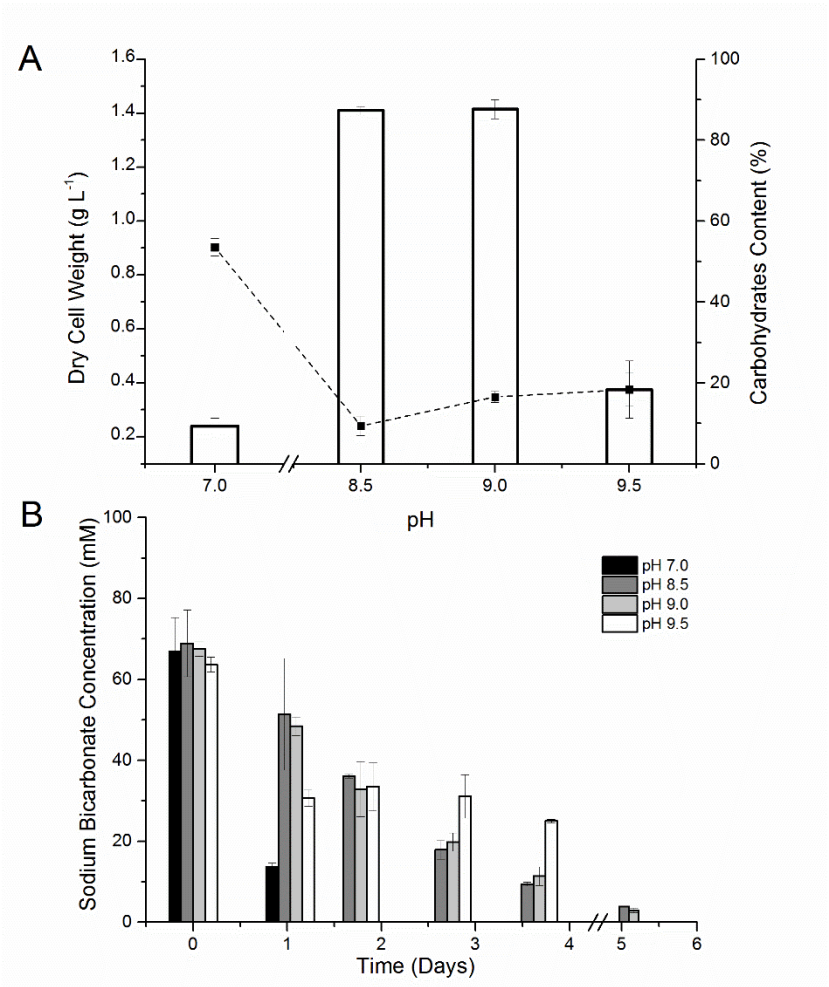

Figure 5.4: Biomass concentrations (bars) and carbohydrate production (dots) are reported in figure 5.4A. In 5.4B Sodium bicarbonate consumption is reported at each pH value.

Due to the limitation of the carbon source, nitrogen at the end of cultivation was not totally consumed (**Table 5.1**), so explaining the low carbohydrate content measured in these runs.

Table 5.1: Nutrient concentration in experiments with sodium bicarbonate as carbon source.

Nutrient	Time (days)											
	0				1.80				3.71			
	pH											
	7	8.5	9	9.5	7	8.5	9	9.5	7	8.5	9	9.5
Ammonium (mg L^{-1})	343.0 ± 14.14	329.66 ± 8.80	322.8 ± 14.78	332.9 ± 6.99	297.4 ± 6.58	242.8 ± 18.24	290.1 ± 23.57	261.8 ± 25.64	-	161.4 ± 25.19	189.4 ± 25.07	221.9 ± 50.26
Phosphate (mg L^{-1})	21. 06 ± 1.28	23.54 ± 3.03	21.84 ± 0.66	22.19 ± 1.27	2.19 ± 0.45	21.15 ± 3.13	17.83 ± 3.23	7.92 ± 0.04	-	4.42 ± 1.81	4.08 ± 2.84	3.85 ± 1.06

5.3.2.2 Sodium bicarbonate concentration sensitivity

Under constant pH, cyanobacteria were able to grow, suggesting a direct absorption of bicarbonate ion (dominant carbon specie in the pH range 7.5–9.0). Maximum values of OD_{750} around 10–12 were reached (**Figure 5.5**). The use of high concentrations of sodium bicarbonate decreased the cell growth (especially at 88 g L^{-1} of sodium bicarbonate), probably due to substrate inhibition or unbalanced osmotic pressure.

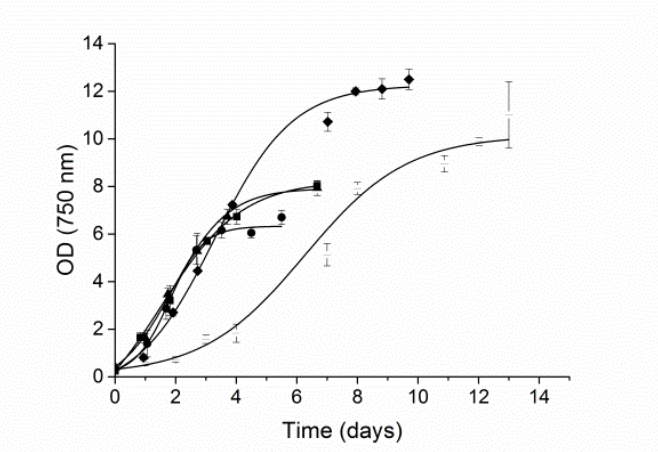

Figure 5.5: Growth curves of *Synechococcocus* PCC 7002 under different concentration of sodium bicarbonate: (●) 5.5 g L^{-1}, (■) 11 g L^{-1}, (▲) 22 g L^{-1}, (♦) 44 g L^{-1} and (▬) 88 g L^{-1}.

In our experiment, higher values of DCW were obtained with 44 and 88 g L^{-1} but the highest specific growth rate was found between 5.5–22 g L^{-1} of sodium bicarbonate, indicating that around 22–44 g L^{-1} substrate inhibition started (**Figure 5.6A** and **5.6B**).

As regards carbohydrates accumulation, it was clear that while the concentration of nitrogen was not limiting (between 5.5 and 22 g L^{-1}) few carbohydrates were formed (**Figure 5.6C** and **5.6D**). However, when the amount of N in the stationary phase was low or limiting (22, 44 and 88 g L^{-1} of sodium bicarbonate), the accumulation of carbohydrates started, reaching values around 25%. However, it is known that *Synechococcus sp* can accumulates up to 50% (% DCW) of carbohydrates with CO_2 as a carbon source (Mollers et al., 2014), and using 88 g L^{-1} of sodium bicarbonate is apparently not a satisfactory condition for carbohydrates production. This is an operational limitation due to the solubility of this salt in water.

The use of N starvation is one of the most common methods for accumulation of high energetic value substances in microalgae (both lipids and carbohydrates) (Gonzales-

Fernandez and Ballesteros, 2012). On the other hand, phosphorus was completely absorbed during the cultivation in all experiments (data not shown).

In all of our experiments, final concentrations of bicarbonate in the medium were approximately 0 (**Figure 5.6D**), but in the experiment at 88 g L^{-1} loss of gas bubbles was observed, probably due to the conversion of bicarbonate into CO_2 at high salt concentrations.

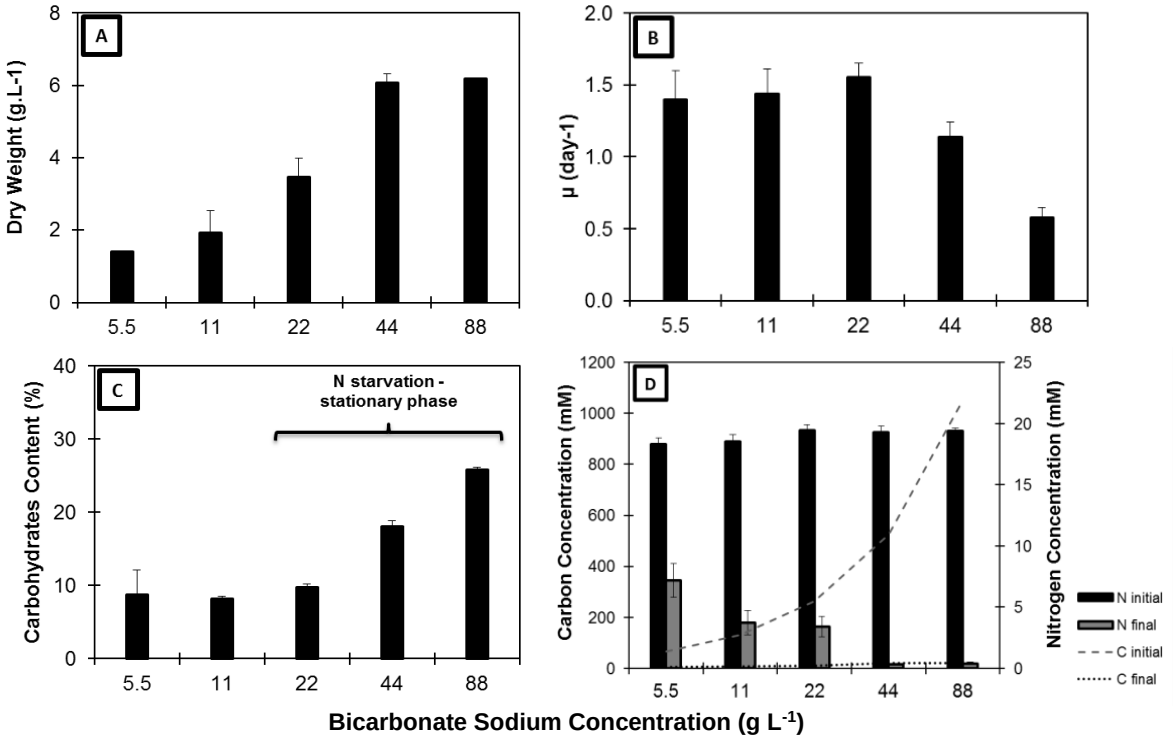

Figure 5.6: Parameters of *Synechococcus* Cultivation. A) Dry cell weight, B) Growth rate, C) Carbohydrates content and D) Nutrient consumption.

Synechococcoccus sp. PCC 7002 showed high bicarbonate absorption, growing well between 5.5 and 88 g L^{-1}, although at 88 g L^{-1} longer cultivation times were necessary. Productivity values ranged between 0.43–1.12 g L^{-1} day^{-1} (**Table 5.2**), with maximum productivity achieved at 22 g L^{-1}, 1.12 g L^{-1} day^{-1}, which is quite high and makes it very attractive in view of biofuel applications.

The kinetic results are shown in **Table 5.3**. In summary, it was observed that when increasing concentration of sodium bicarbonate, the assimilation rate of bicarbonate and the cell growth rate decreased above 22 gL^{-1}, showing that growth inhibition was occurring.

Looking at the inhibition constant values (**Table 5.3**), it is noticed that at 21.69 g L^{-1} the absorption of sodium bicarbonate becomes to be difficult, and above the 28 g L^{-1} cell growth was compromised. Stoichiometric relationships found were: 6.9 g sodium bicarbonate → 1 g biomass and 5.1 g bicarbonate ion → 1 g biomass, showing high potential of microalgae for fixation of ion bicarbonate and production of biomass. However, when using sodium bicarbonate in batch conditions for carbohydrates production we did not find the maximum value mentioned in literature (Mollers et al., 2015), which probably requires optimizations and adaptations of cultivation (fed-batch or continuous cultivation).

Table 5.2: Productivities of *Synechococcocus* PCC 7002 cultivation in batch using sodium bicarbonate.

Bicarbonate Sodium Concentration (g L^{-1})	Productivity (g L^{-1} day^{-1})	Days to reach stationary phase
5.5	0.4375	3.6
11	0.4825	3.7
22	1.1229	3.3
44	0.9059	6.6
88	0.6155	9.8

*Productivities were calculated in a time space between the starting of cultivation and the first day of the stationary phase.

Table 5.3: Kinetics constants for substrate consumption and cellular growth.

Bicarbonate Sodium Concentration (g L^{-1})	$k_{carbonate}$ (day^{-1})	R^2	$k_{bicarbonate}$* (day^{-1})	R^2	k** (day^{-1})	R^2	μ (day^{-1})	R^2
5.5	0.6406	0.9883	0.5357	0.9424	0.6196	0.9671	1.510	0.9783
11	0.6632	0.8510	0.5766	0.9871	0.6817	0.9851	1.611	0.9787
22	0.7889	0.9181	0.748	0.9632	0.6855	0.8873	1.552	0.9938
44	0.3191	0.7464	0.3188	0.8419	0.4516	0.9659	1.210	0.9977
88	0.3134	0.8948	0.2911	0.9738	0.2951	0.977	0.733	0.949

*ion bicarbonate, **total = carbonate + ion bicarbonate.

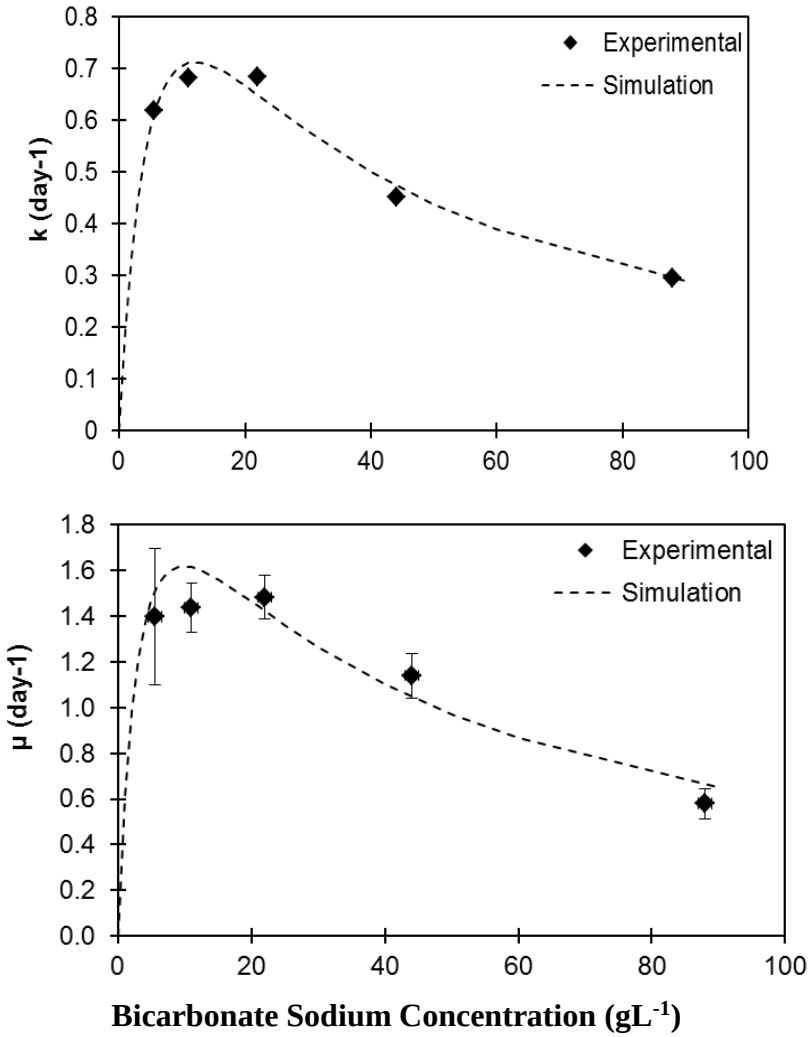

Figure 5.7: Fitting of Substrate Inibition for Sodium Bicarbonate by *Synechococcocus* PCC 7002.

Experimental data plotted in **Figure 5.7** were correlated by equations (5.8) and (5.9) obtaining:

$$k = k_{max} \cdot \frac{S}{\left(K_S + S + \frac{S^2}{K_I}\right)} = 1.5071 \cdot \frac{S}{\left(6.7346 + S + \frac{S^2}{21.6887}\right)} \qquad R^2 = 0.9525 \qquad (5.8)$$

$$\mu = \mu_{max} \cdot \frac{S}{\left(K_S + S + \frac{S^2}{K_I}\right)} = 2.7401 \cdot \frac{S}{\left(3.4336 + S + \frac{S^2}{28.5306}\right)} \qquad R^2 = 0.9766 \qquad (5.9)$$

5.3.3 Organic compounds as buffering system

When HEPES and Tris-HCl were used to control the pH, a sensitivity of *Synechococcus* PCC 7002 to these organic buffers was detected, as lower growth rates were measured (0.3-0.6 day^{-1}) in comparison to the control (data not shown). Thus, even though the buffering effect was achieved and values between 8.5-9.0 were maintained during 8 days of cultivation, an inhibition of cyanobacteria growth was observed. This result is in agreement to what was evidenced for *Anabaena sp.* PCC 7120, which exhibited toxicity to several organic buffers such as HEPES, TRICINA, Tris-HCl and CAPS (Morales et al., 2002). Accordingly, more than more 50% of sodium bicarbonate remained in the solution at the end of cultivation (8 days), showing inhibition to growth and carbon assimilation, thus confirming buffer toxicity also for *Synechococcus* genus.

5.3.4 Buffered system using CO_2-bicarbonate method

By considering the toxicity of the organic buffer, a combined CO_2-bicarbonate system was eventually tested as pH control system in view of industrial application. Several concentrations of sodium bicarbonate (5.5–30 g L^{-1}) were used under non-limiting bubbling of CO_2. *Synechococcus* was able to grow in all experiments, even though some growth inhibition was evidenced when increasing the bicarbonate concentration (**Figure 5.8A**-**B**). Also, the final biomass concentration after 11 days of cultivation decreased when sodium bicarbonate concentration was increased (**Figure 5.8A**).

Looking at the carbonate equilibria, by continuously bubbling CO_2 to the system, after 2-3 days of cultivation until its end (11^{th} day), both the bicarbonate species concentration in solution (**Figure 5.8C**) and the pH (**Figure 5.8D**) were stabilized, showing the efficiency of CO_2-bicarbonate buffer in the pH control and in *Synechoccocus* growth, with an equilibrium value which depends on the sodium bicarbonate added to the system. The range of pH reached (between 7.7 and 8.6) is close to the one previously found and can be suitable for cyanobacterial growth. The presence of growth inhibition when increasing the bicarbonate concentration may be alternatively explained by the increased salinity of the culture medium. This may also explain the effect of bicarbonate addition on biomass and carbohydrate accumulation (**Figure 5.9A-B**), with high final concentration (maximum of 6 g L^{-1}) and (60%) carbohydrate content, both achieved at 5.5 g L^{-1} of sodium bicarbonate. These values decreased when sodium

bicarbonate concentration was increased, evidencing its significative inhnibition to biomass production and carbohydrate accumulation.

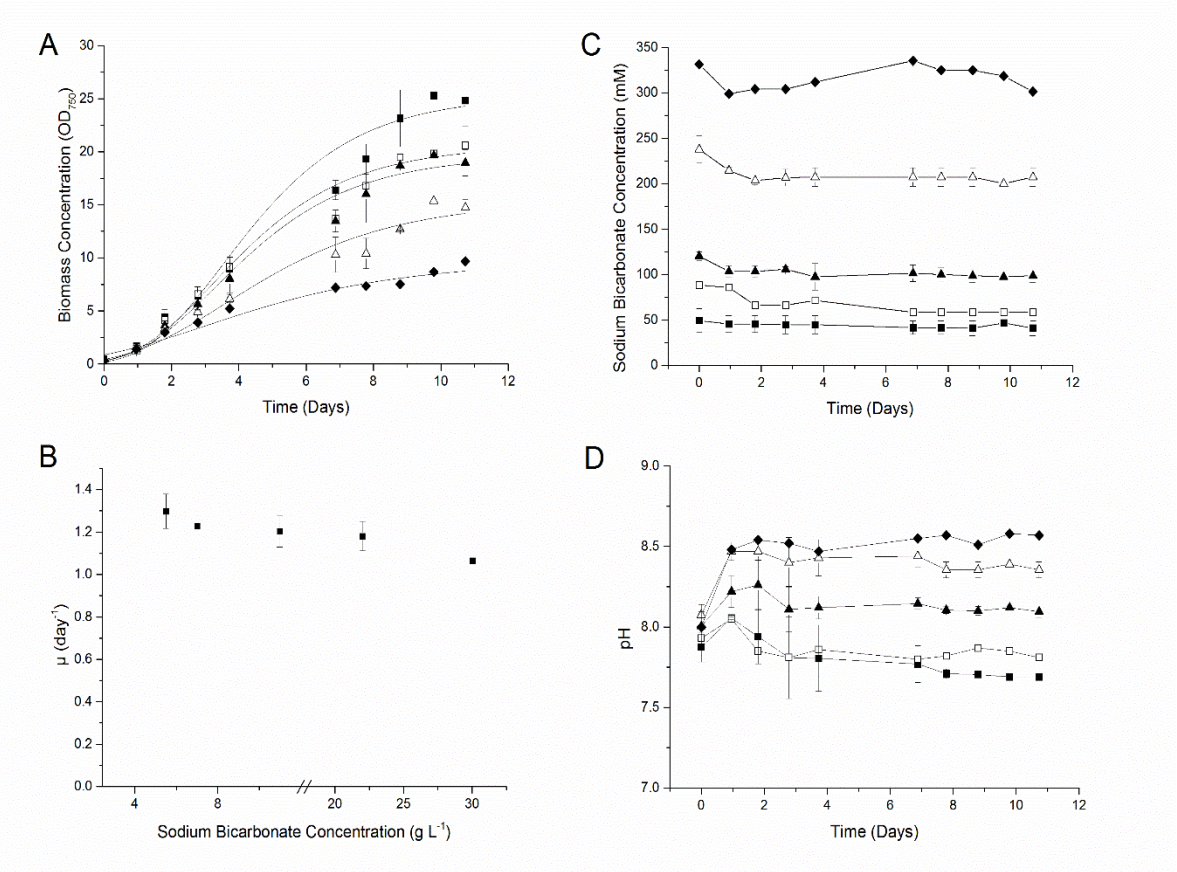

Figure 5.8: *Synechococcus* growth at different sodium bicarbonate concentration. A) Growth curve, B) growth rate, C) Bicarbonate concentration in solution and D) pH. Black squares refer to 5.5, open squares to 7, black triangles to 11, open triangles to 22 and black diamonds to 30 g L^{-1} of sodium bicarbonate.

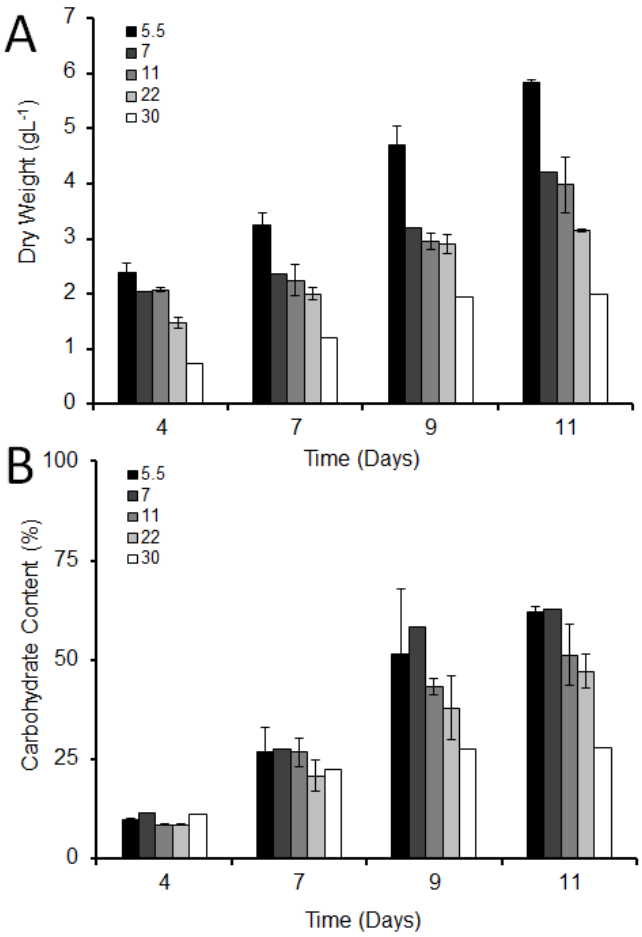

Figure 5.9: Biomass and carbohydrate production. A) Dry weight and B) Carbohydrate accumulation.

The effect of bicarbonate addition on nutrient consumption was also assessed. Some differences in nutrient assimilation were observed (**Table 5.4**). When increasing sodium bicarbonate concentration, nutrients were consumed at a slower rate, even though the same overall consumption was reached at the end of cultivation. Also in this case the high salinity is a possible explanation, as the salt may cause an osmotic stress thus affecting the absorption of nutrients (Pahirar et al., 2015). In fact, the Na added to the medium ranged from 1.5 to 8.2 g L^{-1}, which can partially explain the lower growth performances.

On the other hand, the complete consumption of ammonium at the end of the growth curves caused a nitrogen starvation, explaining the accumulation of carbohydrates in all experiments (**Figure 5.9B**) (25 to 60% depending on salt concentration).

In summary, the pH values were maintained during the entire period of cultivation (11 days) using a relatively simple buffering method. The best condition occured with 5.5 g L^{-1} of sodium bicarbonate and pH value stabilized around 7.7, obtaining about 60% of carbohydrates content and 6 g L^{-1} of dry cell wieght, showing a potential for the cultivation of this specie to obtain bioethanol by subsequent fermentation.

Table 5.4: Nutrient concentration of buffered system using CO_2-bicarbonate method.

Time (days)	Nutrient Concentration									
	Ammonium (mg L^{-1})					Phosphate (mg L^{-1})				
	Sodium Bicarbonate Concentration g L^{-1}									
	5.5	7	11	22	30	5.5	7	11	22	30
0	353.6 ± 44.98	358.4 ± 12.48	342.8 ± 29.72	351.0 ± 27.82	359.2 ± 11.79	21.79 ± 0.69	22.76 ± 0.64	22.19 ± 0.32	22.15 ± 0.37	22.64 ± 0.32
1.80	159.8	191.2 ± 14.57	185.8	237.8	243.6 ± 6.94	10.89	14.09 ± 0.25	15.07	19.29	19.27 ± 0.68
3.73	88.3 ± 0.91	56.3 ± 6.94	109.3 ± 39.58	123.1 ± 50.69	180.9 ± 12.48	2.19 ± 1.15	2.15 ± 0.07	1.87 ± 0.35	4.45 ± 1.97	12.73 ± 0.68
6.88	33.9 ± 2.63	11.96 ± 2.57	28.55 ± 9.16	25.46 ± 14.51	132.7 ± 5.13	2.02 ± 1.03	1.82 ± 0.18	1.62 ± 0.21	1.63 ± 0.01	4.58 ± 0.18
8.79	19.13	9.80 ± 0.76	18.64	6.38	94.35 ± 1.60	2.40	1.82 ± 0.18	1.32	1.57	2.04 ± 0.21
10.73	10.03 ± 3.79	5.29 ± 1.32	11.53 ± 4.50	15.02 ± 7.88	16.86 ± 0.21	1.67 ± 0.57	1.64 ± 0.07	1.31 ± 0.02	1.50 ± 0.04	1.64 ± 0.07

5.3.5 Ionic balance and the pH control into the system

Experimental nutrient and counter-ion concentrations values are summarized in **Table 5.5**. It is seen that, when adding higher concentrations of sodium bicarbonate, the concentration of counter-ion Na^+ (present in greater quantities in relation to the other ones) increases leading to a higher value of the equilibrium pH.

Table 5.5: Experimental Nutrients and Counter-ions Concentration

$NaHCO_3$ ($g\ L^{-1}$)	Initial Concentration (mM)			Final Concentration* (mM)		Counter-ions (mM)			pH*
	HCO_3^-	HPO_4^{2-}	NH_4^+	HCO_3^-	CO_3^{2-}	Na^+	K^+	Cl^-	
5.5	57.6	0.368	16.82	42.79	1.0	57.6	0.368	16.82	7.70
7.0	73.3	0.368	16.82	60.67	1.0	73.3	0.368	16.82	7.84
11	115.2	0.368	16.82	86.67	11.1	115.2	0.368	16.82	8.11
22	230.4	0.368	16.82	187.85	19.5	230.4	0.368	16.82	8.39
30	314.1	0.368	16.82	274.05	39.0	314.1	0.368	16.82	8.54

HCO_3^- - represent the total of the carbon species (bicarbonate and carbonate ion). *in the chemical equilibrium. NH_4^+ and HPO_4^- had % consumption > 95% and were not considered in the ion balance (**Eq. 3**) of the system in equilibrium.

The relations between pH and concentration of sodium bicarbonate and carbon ions in equilibrium is evidenced in **Figure 5.10A-B**, where continuous lines represent fitting curves.

The value of pH* as a function of sodium bicarbonate in equilibrium was also calculated from equation 3 and **Figure 5.10A**, obtaining the curve shown in **Figure 5.11**. Clearly, the simple model proposed is able to predict the pH control of the system (data points are experimental values and the 10% confidence range is plotted).

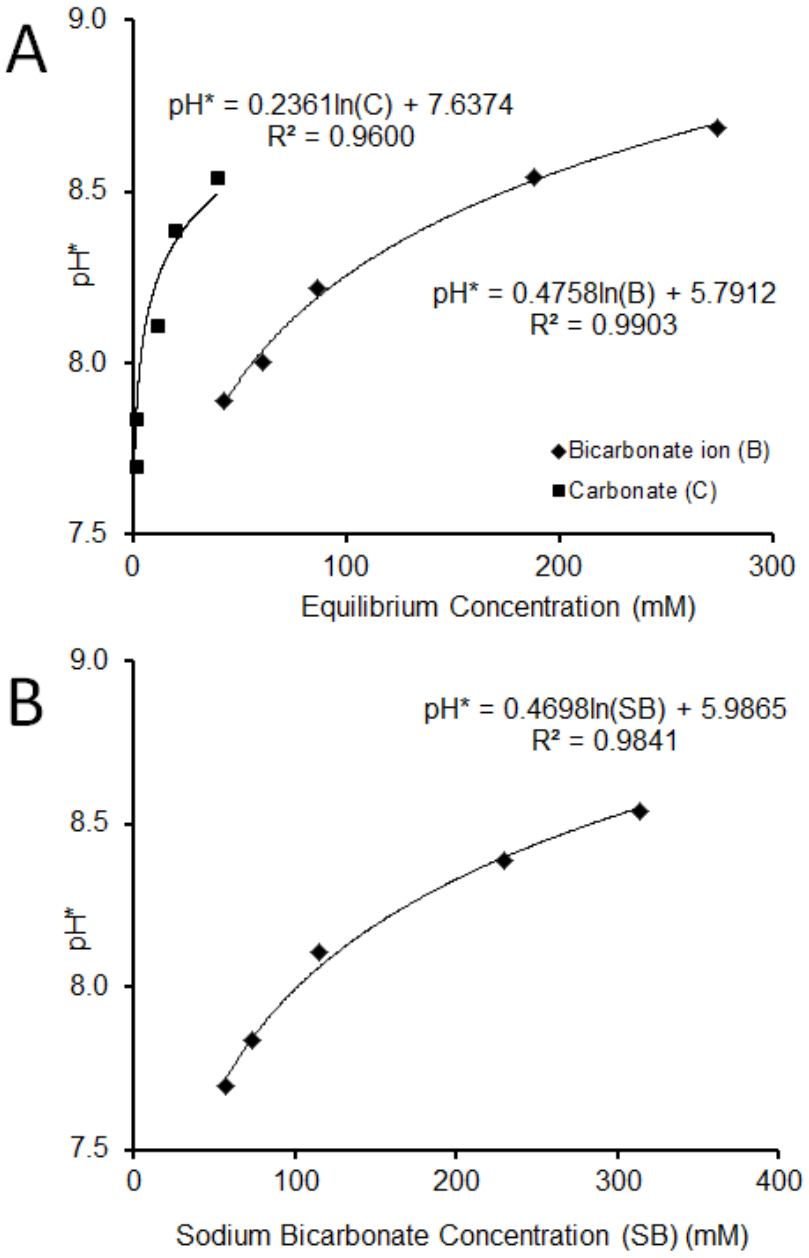

Figure 5.10: Correlations between the equilibrium pH and carbon species. (A) Bicarbonate ion and carbonate* vs pH* and (B) Sodium Bicarbonate Added vs pH*.

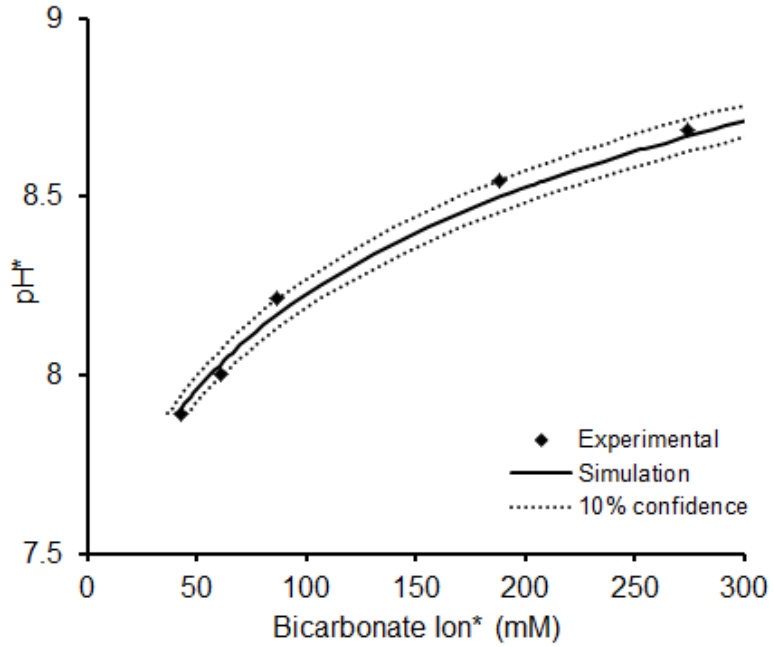

Figure 5.11: Bicarbonate ion* simulation vs pH*.

5.4 DISCUSSION

In order to evaluate the pH changes and the productivity in the cultivation of *Synechococcus* PCC 7002, batch experiments were carried out using CO_2, sodium bicarbonate or a combination of them, to find out the best condition for both high productivity/carbohydrate accumulation and a stable pH value in the culture. In fact, cyanobacteria cells are able to import both HCO_3^- and CO_2 using specific cellular transporters or by direct diffusion through cell membrane (Badge and Price, 2003): in the cells HCO_3^- is concentrated within the carboxysome, where it is converted to CO_2 by the activity of different carbonic anhydrases (CA) (Price, 2011; Kamennaya et al., 2015).

A number of authors (i.e., Chi et al., 2013) applied high concentrations of bicarbonate salts (*Euhalotece* ZM 001 14 – 160 g L^{-1}), while lower concentrations (< 15 g L^{-1}) were studied on *Chlorella prothotecoides* (Gris et al., 2014), *Scenedesmus sp.* (Pancha et al., 2015a) *Scenedesmus obliquus* (Guangmin et al., 2014), *Thermosynechococcus sp.* (Su et al., 2012). Not all the species of microalgae and cyanobacteria are able to exploit large amounts of bicarbonate: despite they have the necessary carriers, they are often inhibited by the substrate concentration (Qiao et al., 2015). Selecting and optimizing the

growth conditions of these tolerant bicarbonate species is a recent approach and can substantially reduce the process complexity and therefore production costs.

An important issue is the pH-value of the culture, because *Synechococcus* has a high sensitivity to the pH medium. It was found that a pH control system by adding soda/acid was effective, but it would not be feasible in an industrial perspective. Sodium bicarbonate ensured a good biomass productivity but carbohydrate content was not significantly increased due to carbon limitation in the cellular accumulation process. On the other hand, organic buffers exhibited toxicity to this species as also found for other species of cyanobacteria (Tindall et al., 1978). The CO_2-bicarbonate buffer is one of the most know in nature and is also exploited in lab culture systems (Azov, 1982; Su et al., 2012; Ying et al., 2013; Ying et al., 2014; Silva et al., 2014; Pancha et al., 2015a).

In this work, the CO_2-bicarbonate buffer system was found to be highly effective and beneficial both to biomass production and carbohydrate accumulation, also in the case of *Synechococcus* cultivation. An adequate pH control was achieved by adding 5.5 g L^{-1} of sodium bicarbonate to a CO_2 bubbled culture, thus obtaining a remarkable growth rate of 1.4 d^{-1} and a carbohydrate accumulation up to 60%. The maximum carbohydrate content in *Synechcoccocus* PCC 7002 found in the literature is around 50% in nitrogen starvation, with a biomass concentration around 4 g L^{-1}, but using nitrate as a source of nitrogen (Mollers et al., 2014). By increasing the bicarbonate concentration to values about 7 g L^{-1} an inhibitory effect was observed for both biomass and carbohydrate accumulation. In fact, the salinity of culture media for microalgae and cyanobacteria may have inhibitory or toxic levels which can significantly alter the growth rate and the biochemical composition of cells (Juneja et al., 2013; Scherholz and Curtis, 2013). For this reason, the bicarbonate addition has to be optimized in order to avoid salt stress: high salinity may cause the accumulation of ROS (Reactive Oxygen Species) in the cells and decreases the photosynthetic efficiency of microorganisms by peroxidation of thylakoids and damage to the PSII Complex (Vorshak and Torzillo, 2007; Liu et al., 2012; Pancha et al., 2015b). ROS are extremely toxic and degrade proteins, lipids, DNA and other cellular macromolecules, inhibiting the cell growth and leading the organism to death (Pancha et al., 2015b; Kumar et al., 2015). In the open literature, several species of microalgae were exposed to salt stress using NaCl (Tagaki et al., 2006; Duan et al., 2012; Liu et al., 2012; Pancha et al., 2015b), as well as some cyanobacteria

species (*Nostoc muscorum*, 1.7–5.25 g L^{-1} (Kumar et al., 2015), *Phormidium foveolarum* 1.7–5.25 g L^{-1} (Kumar et al., 2015) and *Synechocystis sp.* CCNM 2501, 11–58.5 g L^{-1} (Paliwal et al., 2015). In all of these works the accumulation of carbohydrates and lipids under salt-stress was emphasized, although lower biomass concentration was always obtained in comparison to the control experiment (no salt-stress). Similar results were obtained in our work where less biomass was produced when higher salt concentrations were used (7–30 g L^{-1}) (**Figure 5.9A**). This can be explained by the fact that the production of biomass depends on carbon fixation, but the photosynthesis is reduced and the pigments damaged in salt-stress conditions (Vorshak and Torzillo, 2007; Parihar et al., 2015; Kumar et al., 2015). Another reason could be the excess of sodium ion in solution, as Na^+ competes with K^+ for its uptake, and excess Na^+ causes nutrient imbalances (for example, K^+, Ca^{2+} and N) within the cytosol, and leading to inhibition of some reactions (Vorshak and Torzillo, 2007; Singh et al., 2014; Kumar et al., 2015).

Last, we would like to point out the effect of counter-ions, which are high-reactive ions and can form buffers for the carbonic acid-bicarbonate system (weak acid and its salt). The cation shifts the equilibrium of equation 5.5 to the right until an equilibrium is achieved according to equation 5.7. As CO_2 is supplied continuously in excess, bicarbonate ion is formed (HCO_3^-), which is the carbon dominant species (> 90% of carbon species) in if the pH ranges between 7.5 – 9, an optimum value for growth. This ion is neutralized by the charges of counter cation and is then absorbed by microalgae, together with ions of P and N to produce biomass, as sketched in **Figure 5.12**. Here, it is represented the importance of maintaining a suitable counter-ions concentration level to equilibrate the charges and consequently the pH while cyanobacterium absorbs inorganic carbon. As shown by **Figure 5.11**, this hypothesis, expressed by equation 5.6, is able to simulate pH values correctly, so that the addition of bicarbonate can be used to control pH in autotrophic microorganisms cultivation.

In summary, applying this process scheme eliminates the need of using a pH control system with *in situ* sensors, and the consumption of acids/bases or organic buffers, thus reducing the process costs. However, it is necessary to further investigate the recycling of sodium ions after cultivation, in order to increase the process sustainability.

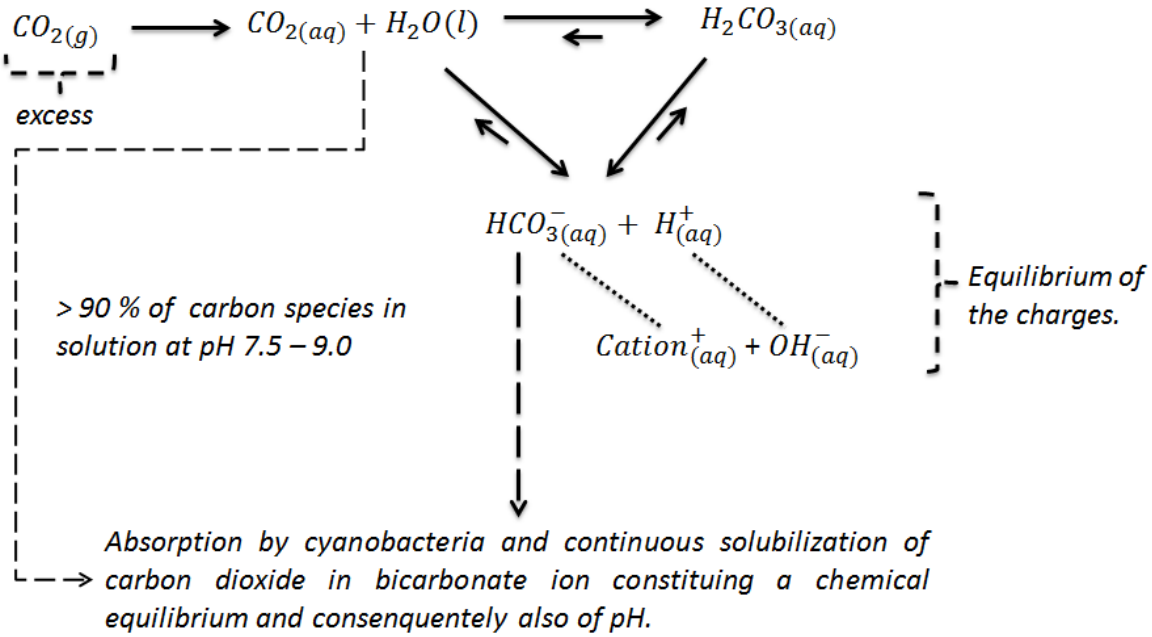

Figure 5.12: Scheme of the buffering of the culture medium of cyanobacteria.

REFERENCES

American Public Health Association, A.W.W.A., 1992. Water Environment Federation Standard Methods for the Examination of Water and Wastewater. 18th ed. APHA-AWWA-WEF, Washington, DC.

Azov, Y., 1982. Effect of pH on inorganic carbon uptake in algal cultures. Applied and Environmental Microbiology 43(6), 1300–1306.

Badge, M.R., Price, D., 2003. CO_2 concentrating mechanisms in cyanobacteria: molecular components, their diversity and evolution. Journal of Experimental Botany 54(383), 609-622. doi: 10.1093/jxb/erg076

Berge, T., Daugbjerg, N., Hansen, P.J., 2012. Isolation and cultivation of microalgae select for low growth rate and tolerance to high pH. Harmful Algae 20, 101–110. doi: 10.1016/j.hal.2012.08.006

Bernstein, H.C., Konopka, A., Melnicki, M. R., Hill, E. A., Kucek, L. A., Zhang, S., Shen, G., Bryant, D. A. & Beliaev, A. S. (2014). Effects of mono- and dichromatic light quality on growth rates and photosynthetic performance of *Synechococcus* sp. PCC 7002. *Frontiers in Microbiology*, *5*, 1–9. doi: 10.3389/fmicb.2014.00488

Chen, C., Zhao, X., Yen, H., Ho, S., Cheng, C., Lee, D., Bai, F., Chang, J., 2013. Microalgae-based carbohydrates for biofuel production. Biochemical Engineering Journal 78, 1–10. doi: 10.1016/j.bej.2013.03.006

Chi Z., O'Fallon J. V., Chen S., 2011. Bicarbonate produced from carbon capture for algae culture. Trends in Biotechnology 29(11), 537–541. DOI: *10.1016/j.tibtech.2011.06.006*

Chi Z., Xie Y., Elloy F., Zheng Y., Hu Y., Chen S., 2013. Bicarbonate-based integrated carbon capture and algae production system with alkalihalophilic cyanobacterum. Bioresource technology 133, 513–521. DOI: *10.1016/j.biortech.2013.01.150*

Chisti, Y., 2013. Constraints to commercialization of algal fuels. Journal of Biotechnology 167, 201–214. DOI: *10.1016/j.jbiotec.2013.07.020*

Choi, S.P., Nguyen, M.T., Sim, S.J., 2010. Enzymatic pretreatment of *Chlamydomonas reinhardtii* biomass for ethanol production. Bioresource Technology 101, 5330–5336. doi: 10.1016/j.biortech.2010.02.026

Chow, T., Su, H., Tsai, T., Chou, H., Lee, T., Chang, J., 2015. Using recombinant cyanobacterium (*Synechococcus elongatus*) with increased carbohydrate productivity as feedstock for bioethanol production via separate hydrolysis and fermentation process. Bioresource Technology 184, 133–141. doi: 10.1016/j.biortech.2014.10.065

Dragone, G., Fernandes, B.D., Abreu, A.P., Vicente, A.A., Teixeira, J.A., 2011. Nutrient limitation as a strategy for increasing starch accumulation in microalgae. Applied Energy 88, 3331–3335. doi: 10.1016/j.apenergy.2011.03.012

Duan, X., Ren, G.Y., Liu, L.L., Zhu, W.X., 2012. Salt-induced osmotic stress for lipid overproduction in batch culture of *Chlorella vulgaris*. African Journal of Biotechnology 11(27), 7072–7078. doi: 10.5897/AJB11.3670

Gonzales-Fernandez C., Ballesteros M., 2012. Linking microalgae and cyanobacteria culture conditions and key-enzymes for carbohydrate accumulation. Biotechnology Advances 30, 1655–1661.

Gris B., Sforza E., Vecchiato L., Bertucco A., 2014. Development of a process for an efficient exploitation of CO_2 captured from flue gases as liquid carbonates for *Chlorella protothecoides* cultivation. Industrial & Engineering Chemistry Research 53, 16678–16688. doi: *dx.doi.org/10.1021/ie502336d*

Guangmin L., Lina Q., Hong Z., Shumei X., Dan Z., 2014. The capacity of bicarbonate capture of a continuous microalgae photo-bioreactor system. Energy Procedia 61 361–364.

Ho, S., Kondo, A., Hasunuma, T., Chang, J., 2013. Engineering strategies for improving the CO_2 fixation and carbohydrate productivity of *Scenedesmus obliquus* CNW-N used for bioethanol fermentation. Bioresource Technology 143, 163–171. (a) doi: 10.1016/j.biortech.2013.05.043

Ho, S., Huang, S., Chen, C., Hasunuma, T., Kondo, A., Chang, J., 2013. Characterization and optimization of carbohydrate production from and indigenous microalga *Chlorella vulgaris* FSP-E. Bioresource Technology 135, 157–165. (b) doi: 10.1016/j.biortech.2012.10.100

Juneja, A., Ceballos, R.M., Murthy, G.S., 2013. Effects of environmental factors and nutrient availability on the biochemical composition of algae for biofuels production: a review. Energies 6, 4607–4638. doi: 10.3390/en6094607

Kamennaya, N.A., Ahn, S., Park, H., Bartal, R., Sasoki, K.A., Holman, H., Jansson, C., 2015. Installing extra bicarbonate transporters in the cyanobacterium *Synechocystis* sp. PCC 6803 enchances biomass production. Metabolic Engineering 29, 79–85. doi: 10.1016/j.ymben.2015.03.002

Kumar, J., Singh, V.P., Prasad, S.M., 2015. NaCl-induced physiological and biochemical changes in two cyanobacteria *Nostoc muscorum* and *Phormidium foveolarum* acclimatized to different photosynthetically active radiation. Journal of Photochemistry and Photobiology B: Biology 151, 221–232. doi: 10.1016/j.jphotobiol.2015.08.005

Liu, W., Ming, Y., Li, P., Huang, Z., 2012. Inhibitory effects of hypo-osmotic stress on extracellular carbonic anhydrase and photosynthetic efficiency of green alga *Dunaliella salina* possibly through reactive oxygen species formation. Plant Physiol. Biochem. 54, 43–48. doi: 10.1016/j.plaphy.2012.01.018

Ludwig, M., Bryant, D.A., 2012. *Synechococcus* sp. Strain PCC 7002 Transcriptome: Acclimation to Temperature, Salinity, Oxidative Stress, and Mixotrophic Growth Conditions. Front. Microbiol. 3, 1–14. doi: 10.3389/fmicb.2012.00354. eCollection 2012

Miranda, J.R., Passarinho, P.C., Gouveia, L., 2012. Pre-treatment optimization of *Scenedesmus obliquus* microalga for bioethanol production. Bioresource Technolgy 104, 342–348. doi: 10.1016/j.biortech.2011.10.059

Markou, G., Angelidaki, I., Nerantzis, E., Georgakakis, D., 2013. Bioethanol production by carbohydrate-enriched biomass of *Antrospira (Spirulina) platensis*. Energies 6, 3937–3950. doi: 10.3390/en6083937

Markou G., Vandamme D., Muylaert K., 2014. Microalgal and cyanobacterial cultivation: the supply of nutrients. Water Research 65, 186–202. DOI: *10.1016/j.watres.2014.07.025*

Morales, E., Rodriguez, M., Garcia, D., Loreto, C., Marco, E., 2002. Crecimento, produccion de pigmentos y exopolisacaridos de la cianobactéria *Anabaena sp*. PCC7120 em funcion del pH y CO_2. Interciencia 27(7), 373–378.

Mollers, K.B., Cannella, D., Jorgensen, H., Frigaard, N., 2014. Cyanobacterial biomass as carbohydrate and nutrient feedstock for bioethanol production by yeast fermentation. Biotechnology for Biofuels 7, 1–11. doi: 10.1186/1754-6834-7-64

Moreno, J., Rodriguez, H., Vargas, A., Rivas, J., Guerrero, G., 1995. Nitrogen-fixing cyanobacteria as source of phycobiliproteins pigments. Composition and growth performance on ten filamentous heterocystous strains. J. Appl. Phycol. 7, 17–23.

Parihar, P., Singh, S., Singh, R., Singh, V.P., Prassad, S.M., 2015. Effect of salinity stress on plants and its tolerance strategies: a review. Environ. Sci. Pollut. Res. 22, 4056–4075. doi: 10.1007/s11356-014-3739-1

Price, G.D., 2011. Inorganic carbon transporters of the cyanobacterial CO_2 concentrating mechanism. Photosynth. Res. 109, 47–57. doi: 10.1007/s11120-010-9608-y

Pancha, I., Chokshi, K., Ghosh, T., Paliwal, C., Maurya, R., Mishra, S., 2015. Bicarbonate supplementation enhanced biofuel production potential as well as nutritional stress mitigation in the microalgae *Scenedesmus sp.* CCM 1077. Bioresource Technology 193, 315–323. (a) doi: 10.1016/j.biortech.2015.06

Pancha, I., Chokshi, K., Maurya, R., Trivedi, K., Patidar, S.K., Ghosh, A., Mishra, S., 2015. Salinity induced oxidative stress enchanced biofuel production potential of microalgae *Scenedesmus sp.* CCNM 1077. Bioresource Technology 189, 341–348. (b) doi: 10.1016/j.biortech.2015.04.017

Paliwal, C., Pancha, I., Ghosh, T., Maurya, R., Chokshi, K., Bharadwaj, S.V.V., Ram, S., Mishra, S., 2015. Selective carotenoid accumulation by varying nutrient media and salinity in *Synechocystis sp.* CCNM 2501. Bioresource Technology 197, 363–368. doi: 10.1016/j.biortech.2015.08.122

Qiao K., Takano T., Liu S., 2015. Discovery of two novel highly tolerant $NaHCO_3$ Trebouxiophytes: identification and characterization of microalgae from extreme saline-alkali soil. Algae Research 9, 245–253.

Scherholz, M.L., Curtis, W.R., 2013. Achieving pH control in microalgal cultures through fed-batch addition of stoichiometrically-balanced growth media. BMC Biotechnology 13(39), 1–15. doi: 10.1186/1472-6750-13-39

Sforza, E., Gris, B., Silva, C.E.F., Morosinotto, T., Bertucco, A., 2014. Effects of Light on Cultivation of *Scenedesmus Obliquus* in Batch and Continuous Flat Plate Photobioreactor. Chemical Engineering Transactions 44, 211–216. doi: 10.3303/CET1438036

Silva, C.S.P., Silva-Stenico, M.E., Fiore, M.F., Castro, H.F., Da Ròs, P.C.M., 2014. Optimization of the cultivation conditions for *Synechococcus sp.* PCC 7942 (cyanobacterium) to be used as feedstock for biodiesel production. Algal Research, 3, 1–7. doi: 10.1016/j.algal.2013.11.012

Singh, M., Kumar, J., Singh, V.P., Prassad, S.M., 2014. Plant tolerance mechanism against salt stress: the nutrient management approach. Biochemistry & Pharmacology 3(5), 1–2. doi: 10.4172/2167-0501.1000e165

Su, C.M., Hsueh, H.T., Chen, H.H., Chu, H., 2012. Effects of dissolved inorganic carbon and nutrient levels on carbon fixation and properties of *Thermosynechococcus sp.* In a continuous system. Chemosphere 88, 706–711. doi: 10.1016/j.chemosphere.2012.04.011

Tagaki, M., Karseno, Yoshida, T., 2006. Effect of salt concentration on intracellular accumulation of lipids and triacylglyceride in marine microalgae *Dunaliella* cells. Journal of Bioscience and Bioengineering 101(3), 223–226. doi: 10.1263/jbb.101.223

Tindall, D., Yopp, J., Miller, D., Chimid, W., 1978. Physico-chemical parameters governing the growth of *Aphanothece halophytica* in hypersaline media. Phycologia 17, 179–185.

Trevelyan, W.E., Harrison, J.S., 1952. Studies on yeast metabolism. 1. Fractionation and microdetermination of cell carbohydrates. Biochem J. 50(3), 298–303.

Vitovà, M., Bisova, K., Kawano, S., Zachleder, V., 2015. Accumulation of energy reserves in algae: from cell cycles to biotechnological applications. Biotechnology Advances 33(6), 1204–1218. doi: 10.1016/j.biotechadv.2015.04.012

Vorshak, A., Torzillo, G., 2007. Handbook of Microalgal Culture: cap.4 – Environmental Stress Physiology. Ed. By Amos Richmond. 4° Ed. Blackwell Science, Oxford, 57–82.

Ying, K., Al-mashhadani, M.K.H., Hanotu, J.O., Gilmour, D.J., Zimmerman, W.B., 2013. Enchanced mass transfer in microbubble driven airlift bioreactor for microalgal culture. Engineering 5, 735–743. doi: 10.4236/eng.2013.59088

Ying, K., Gilmour, D.J., Rimmerman, W.B., 2014. Effects of CO_2 and pH on growth of the microalgae *Dunaliella salina*. Microbiol & Biochemical Technology 6(3), 167–173. doi: 10.4172/1948-5948.1000138

Chapter 6

Synechococcus PCC 7002 as a potential species to produce carbohydrate while removing chemical oxygen demand, nitrogen and phosphorous from urban wastewater

In this chapter, *Synechococcus* PCC 7002 was cultivated in synthetic and real urban wastewater and its depurative capacity was evaluated to remove chemical oxygen demand (COD), nitrogen (N) and phosphorus (P) content. Preliminary studies demonstrated that 28°C and no injection of concentrated CO_2 are suitable conditions to perform the biological treatment and to obtain a depurated water with characteristics below the law limit for COD, N and P, with more than 80% of removal fraction. Using concentrated synthetic wastewater to verify the extended capacity to treat several range of wastewaters, *Synechococcus* proportionally decreased the capacity of pollutants removal showing that probable an environmental/nutritional factor such as lacking micronutrients was not completely simulated by the synthetic wastewater. Real wastewater experiments validated the potentiality of this strain to wastewater bioremediation also reaching values of COD, N and P, below the law limit (> 80% of removal rate) and producing a carbohydrate-rich biomass (more than 50% of carbohydrate content in dry cell weight), ensuring a double gain: environmental and biomass valorization•.

•*A paper based on this chapter is in preparation.*

6.1 INTRODUCTION

The demand for clean water is currently a worldwide priority (Cabanelas et al., 2013; Cuellar-Bermudez et al., 2017). In addition, bioenergy production should be significantly progressed to compete with the cost of energy production from other resources, specially petroleum based ones (Cho et al., 2013). Thus, the combination between wastewater treatment, algae and biofuel production could represent at moment an important alternative for nutrient recovery and valorization of the biomass produced.

In microalgal cultivation the main expenditure is to cover the costs of larger amount of water, nutrients supplement and additional illumination for enhancing biomass production as well as those related to the extraction of carbohydrates and lipids, and to the biofuel production steps (fermentation and biodiesel) (Cho et al., 2013; Silva and Bertucco, 2016). On the other hand, biological wastewater treatment has as bottlenecks the elevated cost of air injection in the aerobic step, the need of denitrification and, generally, an inefficient phosphorous removal (Cuellar-Bermudez et al., 2017). With respect to this, it is well known that microalgae/cyanobacteria can remove nitrogen, phosphorous and organic matter efficiently (Markou and Georgakakis, 2011; Cabanelas et al., 2015; Markou, 2015; Karn, 2016; Cuellar-Bermudez et al., 2017).

At present, a number of issues should be understood and controlled more practically for stable application of wastewaters as a nutrient source for mass culture of microalgae/cyanobacteria (Cho et al., 2013). Generally, there are two approaches of algae investigation for wastewater treatment: i) to evaluate the depurative capacity of a specific strain, or the combination (co-cultivation) of more algae species for exploiting their capacity to perform mixotrophy with simultaneous removal of nitrogen, phosphorous and organic matter, and ii) to apply consortia between algae and bacteria, thus improving the efficiency of gas exchange (CO_2 and O_2), and the velocity of the bacteria to remove chemical oxygen demand (COD) with respect to algae alone (Markou and Georgakakis, 2011; Markou, 2015; Cuellar-Bermudez et al., 2017).

The first approach is important because the depurative capacity heavily depends on the microalgal/cyanobacterial species. Several species have been studied, most of them are freshwater strains to avoid interference due to the reduced/no salinity of urban wastewater. Examples of this type are *Chlorella vulgaris* (Cabanelas et al., 2013; Markou, 2015; Gonçalves et al., 2016a; Gonçalves et al., 2016b), *Scenedesmus* spp.

(Lynch et al., 2015), *Microcystis aeruginosa*, *Pseudokirchneriella subcapitata* (Dong et al., 2012; Gonçalves et al., 2016a; Gonçalves et al., 2016b), *Synechocystis* PCC 6803 (Cai et al., 2013), *Arthrospira platensis* (Markou, 2015) and *Synechococcus* spp. (Lynch et al., 2015). However, also a number of saline species are cited: *Nannochloropsis salina* (Cai et al., 2013) and *Synechocystis salina* (Gonçalves et al., 2016a; Gonçalves et al., 2016b).

In particular, *Synechococcus* sp. strain PCC 7002 is a unicellular, euryhaline cyanobacterium. It has potentiality for several biotechnological applications, exhibiting an exceptional tolerance of high light irradiation, showing fast growth. The habitats from which this, and closely related strains were isolated are subjected to changes in several environmental factors, including light, nutrient supply, temperature, and salinity, an attractive possibility to produce carbohydrates (up to 60% of dry matter weight) (Ludwig and Bryant, 2012; Silva et al., 2016; Silva et al., 2017). However, its application to wastewater treatment is still lacking in the literature, so that the genus *Synechococcus* has been rarely considered, such as: *Synechococcus sp.* 1TU2155, 1TU3951 and OTU2454 (Lynch et al., 2015) and *Synechococcus elongatus* (Aguilar-May and Sanchez-Saavedra, 2009; Ruiz-Guereca and Sanchez-Saavedra, 2016). Moreover, this species is not cited in recent review articles (Markou and Georgakakis 2011; Cuellar-Bermudez et al., 2017; Guldhe et al., 2017).

In this chapter, the capacity to treat urban wastewater of *Synechococcus* PCC 7002 was evaluated using synthetic and real urban wastewater, and COD, nitrogen and phosphorous removal were validated. Carbohydrate accumulation was quantified in each experiment in order to provide an alternative valorization of the biomass produced as a possible source for fermentative processes.

6.2 MATERIAL AND METHODS

6.2.1 Strain and culture medium

Synechococcus PCC 7002 was cultivated using a modified Basal A medium: 18 g L^{-1} NaCl, 0.6 g L^{-1} KCl, 0.9 g L^{-1} NH_4Cl, 5.0 g L^{-1} $MgSO_4 \cdot 7H_2O$, 50 mg L^{-1} KH_2PO_4, 266 mg L^{-1} $CaCl_2$, 30 mg L^{-1} $Na_2EDTA \cdot 2H_2O$, 3.89 mg L^{-1} $FeCl_3 \cdot 6H_2O$ (pH 8.2), 34.26 mg L^{-1} H_3BO_3, 4.32 mg L^{-1} $MnCl_2 \cdot 4H_2O$, 0.315 mg L^{-1} $ZnCl_2$, 0.03 mg L^{-1} MoO_3, 12.15 μg L^{-1} $CoCl_2 \cdot 6H_2O$, 3 μg L^{-1} $CuSO_4 \cdot 5H_2O$, and 4 μg L^{-1} vitamin B_{12} (Bernstein et al. 2014).

Preinoculum was cultivated in Erlenmeyer flasks at 100 ± 5 μE m^{-2} s^{-1} and held in its exponential growth phase, at pH 8-9 using CO_2 5% (mix air-CO_2 % v v^{-1}, 1 L h^{-1}) and 5.5 g L^{-1} of sodium bicarbonate (inorganic buffer) (Silva et al. 2017).

The real wastewater was sampled from the full scale activate sludge municipal wastewater treatment plant of Montebello Vicentino (Vicenza, Italy, 47000 PE served), before the primary treatment. It was then filtered with laboratory paper to remove the suspended solids and was subdivided into aliquots of 0.4 L that were stored at -20°C. The main wastewater pollutants had the following composition: NH_4^+-N 21.0 mg L^{-1}, total nitrogen (Ntot) 33.1 mg L^{-1} PO_4^{3-}-P, 5 mg L^{-1} and chemical oxygen demand (COD) 496 mg L^{-1}.

Due to the high variability of real wastewater characteristics, also a synthetic one was formulated to obtain a medium with constant quality to improve the reproducibility of the experiments. The concentration of a standard synthetic wastewater (OECD, 2001) was slightly modified in order to have a medium similar to common wastewaters. The synthetic wastewater was prepared using the following chemicals: peptone 80 mg L^{-1}, meat extract 110 mg L^{-1}, NH_4Cl 40 mg L^{-1}, CH_3COONa 159 mg L^{-1}, K_2HPO_4 23 mg L^{-1}, NaCl 7 mg L^{-1}, $CaCl_2 \bullet 2H_2O$ 4 mg L^{-1} and $Mg_2SO_4 \bullet 7H_2O$ 2 mg L^{-1}. The final characterization of the synthetic sewage is: NH_4^+-N 13 mg L^{-1}, total nitrogen (Ntot) 29.5 mg L^{-1}, $PO4^{3-}$-P 8.2 mg L^{-1} and COD 313 mg L^{-1}. All the initial and final concentrations of the pollutants in all experiments present in this article are reported in the **Appendix**, better represented in this chapter in terms of removal rate (%).

6.2.2 Cultivation system and set of experiments

Growth experiments were carried out in batch operation mode in 250 mL-working-volume glass vertical cylinders (5 cm diameter), continuously mixed by a stirring magnet placed at the bottom of the bottle. The light intensity provided by a fluorescent lamp was 100 μE m^{-2} s^{-1}, measured with a radiometer DeltaOhm HD2102.1. Each batch experiment started with an initial microalgae inoculation of OD_{750} = 0.3-0.4.

Different sets of experiments were performed:

1) Preliminary experiments at two temperatures and with/without CO_2 supply were made at 24 and 28°C and with CO_2 bubbling (5% mix CO_2-air and 1 L

h^{-1}) to verify the capacity of *Synechococcus* to treat the synthetic wastewater and the need to add CO_2 in the process;

2) A number of concentrations of the synthetic wastewater (1x, 3x and 5x) were tested (without CO_2 supply at 28°C) to understand the depurative capacity of *Synechococcus*, as urban/industrial wastewaters can present a significative variation of nitrogen, phosphorous and organic matter. A reduced depurative capacity with the increasing of wastewater concentration was found;
3) Nutritional and environmental factors were adjusted to understand their influences in the strain performance (without CO_2 supply at 28°C). It was evaluated the influence of salinity (NaCl), salinity + vitamin B_{12} and micronutrients (at fixed concentrations, except for nitrogen and phosphorous). These concentrations were based on the Basal medium used to prepare the preinoculum, which was efficient in the cultivation of this specie (Silva et al., 2016; Silva et al., 2017);
4) A comparison between the synthetic and real wastewater was made (without CO_2 supply at 28°C).

6.2.3 Analytical procedures

In all growth experiments, carbohydrate content and nutrients consumption were measured. *Synechococcus* PCC 7002 growth was monitored by means of optical density measurements at λ = 750 nm (UV-visible Spectro, Spectronic Unicam®). The dry weight was measured by filtration through cellulose acetate filters of 0.2 μm (Whatman®). Filters were pre-dried for 10 min at 105°C in order to remove any moisture. Biomass filtered was dried for 2 h at 105°C and then weighed to calculate the dry weight in terms of grams per liter. The growth rate constant μ (day^{-1}) was calculated by the slope of the semilogarithmic graph of cell concentration on time.

The carbohydrate content was determined by the Anthrone method (Trevelyan and Harrison, 1952). Samples of culture were filtered (0.2 μm) in order to measure only dissolved nutrients. The nutrients measured were nitrate, nitrite, ammonium and ortophosphate analysed using HYDROCHECK SPECTRATEST kits by Reasol®. The chemical oxygen demand was determined by AQUANAL® kit purchased from Sigma-Aldrich®. Total nitrogen was measured as nitrate after persulfate digestion in autoclave

for 1 h (reagent - 40 g L^{-1} of sodium persulfate and 8 g L^{-1} of sodium hydroxide). Reactions based on the standard methods for wastewater analysis (AOAC, 1992). Nitrogen (N/X) and phosphorous content (P/X) were calculated at the end of growth curve from a relation between their removed contents (g/L) and dry cell weight (g/L).

6.3 RESULTS AND DISCUSSION

Synechococcus sp. PCC 7002 was cultivated in synthetic and real urban wastewater. Firstly, to find an effective cultivation temperature and the need of CO_2 supply, experiments in mixotrophy with/without CO_2 injection and in the absence of light (heterotrophy) were carried out. Then, the evaluation of depurative capacity at different concentrations of the synthetic wastewater was done. Some environmental/nutritional factors were also verified to try an improvement of strain performance at high concentration of COD, nitrogen and phosphorous content. Finally, a comparison between a real and synthetic wastewater was made to approximate the experimental condition with a real application. The carbohydrate content of the biomass produced was determined in all cases.

6.3.1 Preliminary validation of the cultivation temperature and effect of CO_2 supply

As verified in the **Figure 6.1**, *Synechococcus* growth was favored at 28°C, mainly in the condition without CO_2 supply (**Figure 6.1A-B**). At 28 °C no significant differences were found in the conditions with or without CO_2. This is important, because the cost of carbon supply as CO_2 is relevant in the cultivation step of microalgae/cyanobacteria, regardless the environmental gain involved, as in the case of treatment/bioremediation treated in this paper (Silva et al., 2016; Cuellar-Bermudez et al., 2017). In the completely absence of light and external CO_2 (heterotrophy) no growth was detected at both temperatures (24 and 28°C) (**Figure 6.1C**), emphasizing that this cyanobacteria strain is able to perform autotrophy/mixotrophy only.

This experimental evidence agrees with literature reports about the biochemical behavior of cyanobacteria strains and their mixotrophic metabolism. In fact, according to Feng et al. (2015) and Wan et al. (2015):

1) Calvin cycle and the oxidative pentose phosphate (OPP) can operate simultaneously to regulate mixotrophic and autotrophic metabolism;

2) Cyanobacteria, generally, cannot grow heterotrophically in complete darkness;
3) Cyanobacteria can close their TCA cycle by 2-oxoglutarate decarboxylase and succinic semialdehyde dehydrogenase;
4) Some reactions such as the glyoxylate production via photorespiration and employment of malic enzymes (malic enzymes) for balancing NADPH/NADH and re-synthetizing pyruvate.

Thus, cyanobacteria is a group of microorganisms prepared/evolved to perform mixotrophy.

Using organic carbon sources (such as glucose or acetate), their metabolism is improved in terms of photosynthesis efficiency and higher growth rate, becoming stronger in terms of cellular synthesis. Under limiting conditions of light or CO_2, cyanobacteria up-regulate their OPP pathway to consume more glucose and reduce their net CO_2 fixation rate (Wan et al., 2015).

In relation to the temperature, *Synechococcus* is a strain generally cultivated at 28-30°C (Bernstein et al., 2014), but this value depends on the species origin or the isolation region (Mackey et al., 2013). *Synechococcus* WH8103 performed better with respect to growth rate between 28-32°C, and a significative decrease was observed at 17-20°C (Moore et al., 1995). *Synechococcus* PCC 7002 exhibited a strong increase in the growth rate, considering the temperature range of 15-27°C: At 21°C the value of growth rate was 35% lower in comparison to the 27°C experiment (Mackey et al., 2013).

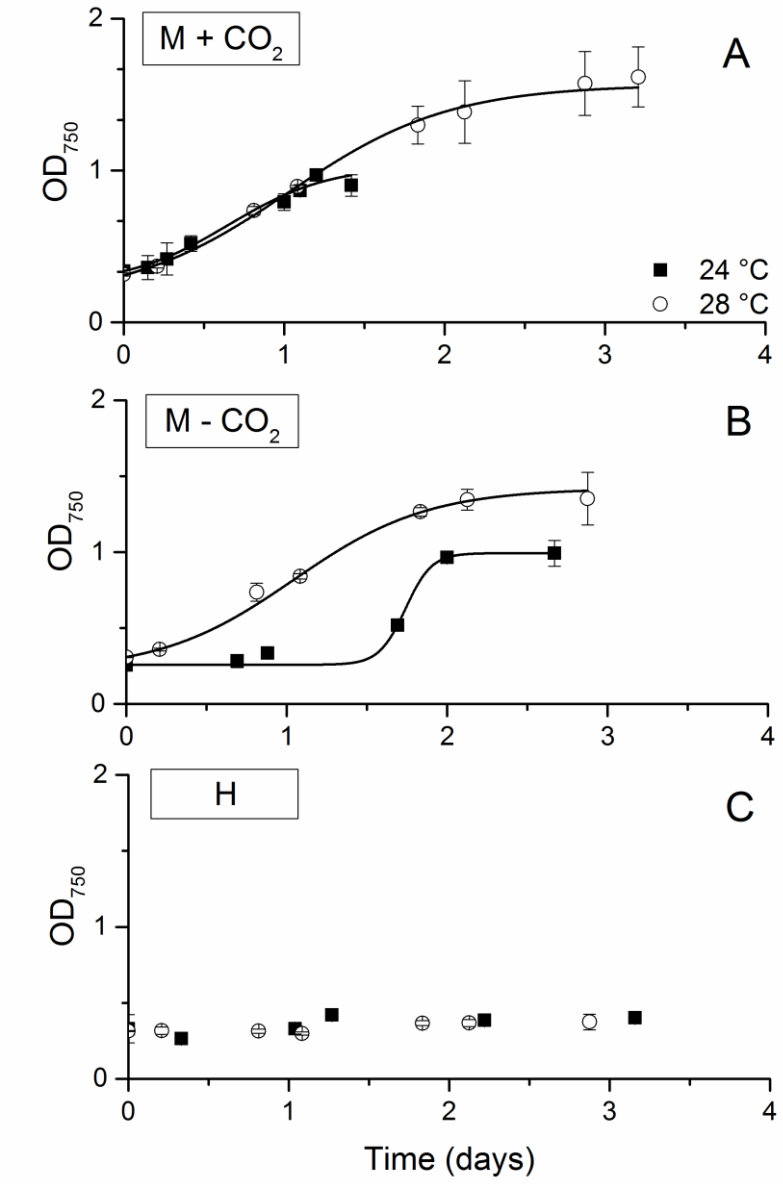

Figure 6.1: Growth curve with synthetic wastewater at different temperatures (Optical density at 750 nm). A) (M + CO_2) – Mixotrophy with carbon dioxide injection, B) (M – CO_2) – Mixotrophy without carbon dioxide and C) H – heterotrophy (absence of light and CO_2 supply). Closed squares refer to 24°C and open circles to 28°C experiments.

As aforementioned, CO_2 input was not necessary for this species, at the experimental conditions tested in this paper, so that, it was not considered in the following experiments. Gonçalves et al. (2016c) tested different concentrations of CO_2 (3-10%) and air to remove nitrogen and phosphorous. The removal of these nutrients was slightly higher when using air, making it unfeasible to use concentrated CO_2. The good performance of *Synechococcus* without CO_2 confirms that the combination

autotrophy/mixotrophy in CO_2 limiting conditions can be successfully performed, and represents an important information towards a large-scale operation.

In **Table 6.1**, it is seen that lower growth rates were achieved at 24°C, and consequently lower biomass concentration. Nitrogen and phosphorous content varied according to the experiment but without a clear trend. The important finding was the carbohydrate content at 28 °C, when apparently the growth was performed adequately, and it reached 55-60% of dry weight. In some literature works mixotrophy and carbohydrate accumulation are related: *Scenedesmus subspicatus* GY-16, *Chlorella vulgaris* FSP-E, *Anestrodesmus gracilaris* GY-09 achieved between 40-55% of carbohydrate content after performing mixotrophy with urea (1 g/L) and sodium acetate (1-3 g/L) (Chen et al., 2016). *Chlorella vulgaris* grown in industrial dairy waste showed higher carbohydrate and lipid content when glucose and galactose concentrations were increased in the medium (Abreu et al., 2012).

Table 6.1: Growth parameters and carbohydrate content.

Temp. (°C)	Experiment	Dry Weight ($g\ L^{-1}$)	Carbohydrate Content (%)	Growth Rate (day^{-1})	N/X	P/X
24	Mixotrophic (with CO_2)	0.28 ± 0.01	33.25 ± 1.06	0.876 ± 0.137	8.60 ± 0.80	1.80 ± 0.12
	Mixotrophic (Whitout CO_2)	0.27 ± 0.03	49.00 ± 7.07	0.976 ± 0.200	6.83 ± 1.34	0.70 ± 0.05
28	Mixotrophic (with CO_2)	0.58 ± 0.03	60.97 ± 3.75	1.063 ± 0.005	5.65 ± 0.19	1.48 ± 0.05
	Mixotrophic (Whitout CO_2)	0.39 ± 0.12	56.12 ± 4.42	1.091 ± 0.108	8.02 ± 1.42	2.03 ± 0.36

Pollutants removal performance is demonstrated in **Figure 6.2**. It is evident that at 24°C the cyanobacterial growth was inhibited. Even though COD was removed (~80%), *Synechococcus* was unable to remove nitrogen and phosphorous efficiently. At 28°C, the process was completely different with a removal fraction larger than 90% for COD, nitrogen and phosphorous, whose concentrations were below the law limits for these parameters to discharge the treated water into hydric bodies (COD = 125 mg L^{-1}, Total Nitrogen = 15 mg L^{-1} and Phosphorous = 2 mg L^{-1}, EEC, 1991).

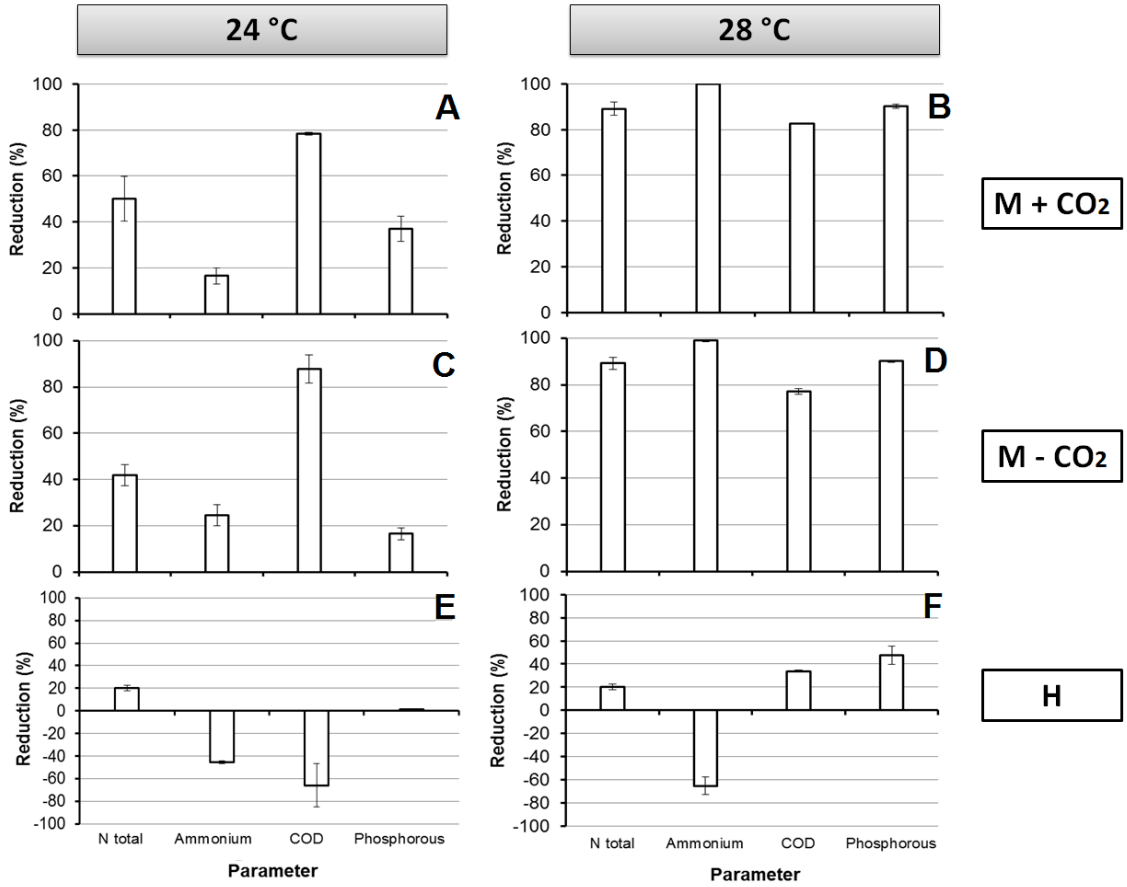

Figure 6.2: % Reduction of pollutants parameters of the synthetic wastewater at different temperatures. Initial concentration (mg L^{-1}): COD 340.0 ± 14.1, Total Nitrogen - 31.0 ± 1.4 and Phosphorous - 8.20 ± 0.99. A) and B) - (M + CO_2) (Mixotrophy with CO_2), C) and D) - (M – CO_2) (Mixotrophy without CO_2) and E) and F) – H (Heterotrophy).

Synechocystis salina and *M. aeruginosa* removed 49.8-52.3% of nitrogen and 77-81.3% of phosphorous while *C. vulgaris*, *P. subcapitata* 62.9-70.6% and 50.4-80.2%, respectively, from a culture medium with 41 mg N L^{-1} and 9 mg P L^{-1} (synthetic wastewater). Co-cultures of *S. salina* and these species improved the removal efficiency, reaching between 72-84.5% of N and 85.9-97.2% of P (experiments conducted at 24 °C, 120 µmol m^{-2} s^{-1} and bubbling atmospheric air for 7 days) (Gonçalves et al., 2016a). *Synechocystis* sp. PCC 6803 and *Nannochloropsis salina* cultivated in f/2 medium replaced with anaerobic digestion wastewater 3% (v/v) providing a culture medium with 80 of COD, 80 of total N and 11.43 of P (mg L^{-1}), and removed 100% of these parameters (f/2 medium – saline ~20 g L^{-1} of NaCl - culture medium with vitamin B_{12} and other micronutrients, 200 µmol m^{-2} s^{-1} at 25 °C for 17

days) (Cai et al., 2013). *Chlorella vulgaris* cultivated in different types of domestic wastewater (90-180 of COD, 9.79-88.47 of total N and 0.75-9.07 of P, mg L^{-1} for 17 days), ensured good removal of these nutrients (14:10 light:dark cycle of illumination, 150 µmol m^{-2} s^{-1} at 20°C for 12 days) (Cabanelas et al., 2013). Nitrogen removal as ammonium was evaluated with *C. vulgaris* and *Arthrospira platensis* using an agricultural wastewater (anaerobic digestion of poultry) with 550-2000 mg COD L^{-1}, 2-7.5 mg P L^{-1} and 5-30 mg N L^{-1} and practically 100% of N and P were removed, with a COD removal ranged between 60-70% (16:8 h light: dark cycle of illumination at 30 °C for 12 days) (Markou, 2015). *Chlorella sp.* ADE5 treating urban wastewater (15 of COD, 50 of total N and 5 of P, mg L^{-1}) (200 µmol m^{-2} s^{-1}, 1% of CO_2 at 30°C for 6 days) removed efficiently all N and P content, but increased COD to 40 mg L-1, probably, the COD was low and autotrophy was dominant since CO_2 in excess was provided (Cho et al., 2013). *Synechococcus elongatus* and *Azospirillum brasiliense* were cultivated for 7 days in synthetic aquaculture wastewater (22 of nitrate and 8.2 of P, mg L^{-1}) removed 52.93, 25.86 and 44.87% of P to free *S. elongatus*, free *A. brasiliensis* and immobilized co-culture, respectively (Ruiz-Guereca and Sanchez-Saavedra, 2016).

With respect to the cited papers, we have shown that *Synechococcus* PCC 7002 has a number of advantages as a potential strain to treat urban wastewater:

1) Removal of COD, nitrogen and phosphorous below the legislation limit;
2) Faster growth of *Synechococcus* PCC 7002, 2-3 days to conclude the treatment;
3) no need of CO_2 supply to perform efficiently the wastewater treatment;
4) No additional costs with nutrient supply (vitamin or micronutrients) was necessary;
5) No co-cultures or complex operational techniques were required to improve its depurative capacity;
6) High carbohydrate content (more than 50%) was achieved.

6.3.2 Influence of wastewater concentration

In order to verify if the preliminary results can be efficiently exploited at higher wastewater concentration, it is necessary to change significantly the COD, nitrogen and phosphorous content, so as to simulate different types of urban/industrial/agricultural wastewater. In **Figure 6.3**, for instance it is evident that some limitation occurred which did not permit the growth of *Synechococcus* in the synthetic wastewater concentrated 5x.

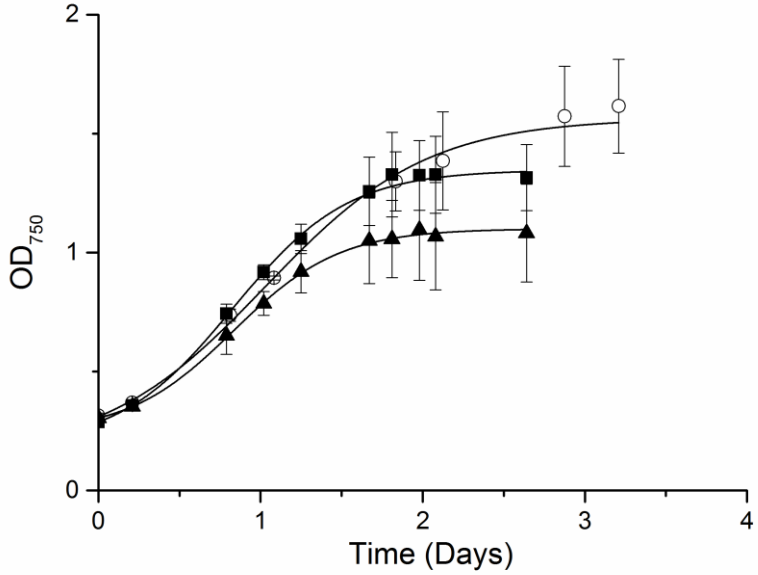

Figure 6.3: Growth curve at different synthetic wastewater concentrations. 1x (■), 3x (o) and 5x (▲).

A similar behavior is evidenced by the dry cell weight and growth rate (**Table 6.2**). In addition, with the experiments 3x and 5x, the carbohydrate content was not increased, as a possible consequence of nitrogen in excess due the inefficient treatment of this concentrated wastewater. It can also be seen that carbohydrate accumulation in *Synechococcus* is easily triggered by the combination of carbon assimilation and nitrogen depletion (Silva et al., 2016; Silva et al., 2017).

Table 6.2: Growth parameters and carbohydrate content.

Experiment	Dry Weight ($g\ L^{-1}$)	Carbohydrate Content (%)	Growth Rate (day^{-1})	N/X	P/X
1x	0.39 ± 0.12	56.12 ± 4.42	1.091 ± 0.108	8.02 ± 1.42	2.03 ± 0.36
3x	0.64 ± 0.11	16.73 ± 3.51	1.167 ± 0.003	10.2 ± 1.74	1.71 ± 0.29
5x	0.57 ± 0.02	14.38 ± 5.46	0.942 ± 0.134	7.90 ± 0.16	3.70 ± 0.08

As shown in **Figure 6.4**, the depurative capacity of *Synechococcus* decreased proportionally with the increase of wastewater concentration. Apparently, the organic nitrogen was converted to ammonium and could not to be assimilated. COD and phosphorous were not efficiently used by the microorganism.

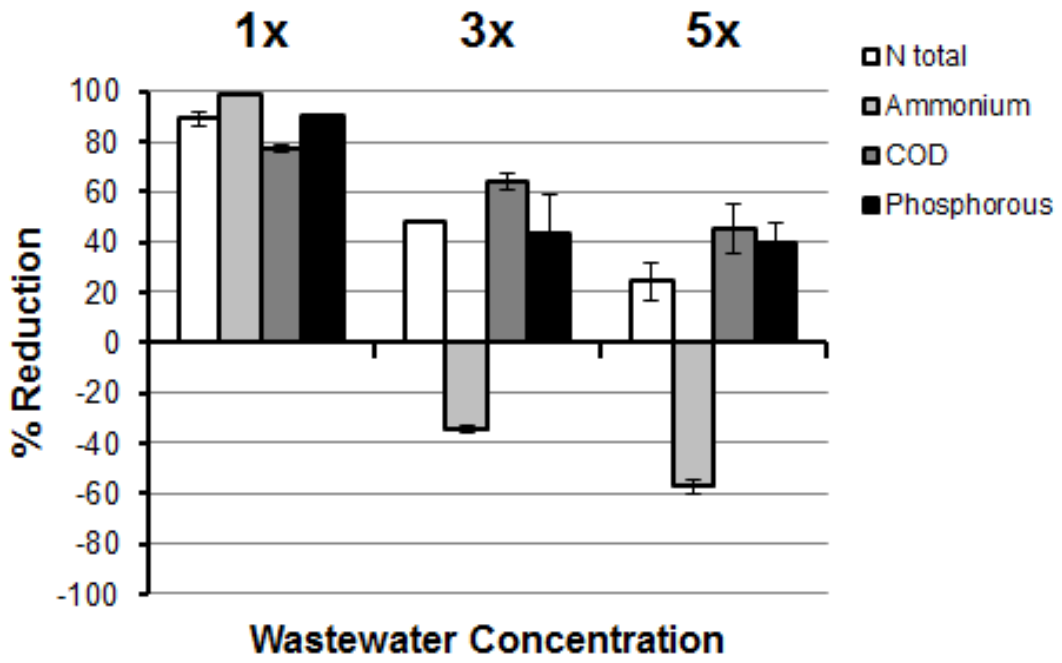

Figure 6.4: % Reduction of pollutant parameters at different synthetic wastewater concentrations.

Low nitrogen removal was also observed by Cabanelas et al. (2013) using *Chlorella vulgaris* when domestic wastewater contained a large amount of COD, nitrogen and phosphorous content; 675, 130-909 and 60-180, respectively (experimental conditions: 14:10 light:dark cycle of illumination, 150 µmol m^{-2} s^{-1} at 20°C for 12 days). However, P content was almost completely removed (92%) in all of these experiments.

Chlorella sp. ADEE5 was cultivated in municipal wastewater with several concentrations of nitrogen (50-250 mg L^{-1}) and phosphorous (6-17 mg L^{-1}) (200 µmol m^{-2} s^{-1}, 1% of CO_2 at 30°C for 6 days). With the exception of the 250 mg N L^{-1} and 17 mg P L^{-1} conditions, all experiments removed almost 100 % of these contaminants. The aforementioned condition (250 of N and 17 of P, mg L^{-1}) removed around 80% of N and 70% of P (Cho et al., 2013). In contrast, *Synechocystis salina* and *Nannochloropsis salina* were cultivated in f/2 medium replaced with anaerobic digestion effluent (3-24% v/v) having a final concentration of COD 80-639, total N 80-640 and P 11.43-91.44, mg L^{-1}. The efficiency of these nutrients removal was between 70-100 % for N and 83.6-100 for P – *S. salina* and 87.6-100 for N and 99.3-100% for P – *N. salina*, decreasing with the increase of nutrients load, but retaining still good values of efficiency respect to the initial values (Cai et al., 2013).

The presently reported results emphasize that some environmental/nutritional problem are occurring. For this reason, different conditions considering Basal A (standard medium to *Synechococcus* cultivation) were evaluated in the following: salinity (19 g L^{-1} NaCl), vitamin B_{12} and micronutrients presence.

6.3.3 Influence of salinity, vitamin and micronutrients supplementation

The experiments with salinity and vitamin adjustment did not improve the microorganism performance (**Figure 6.5A**). On the other hand, the experiment with micronutrient addition enhanced the growth by almost 3 times, revealing that this nutritional factor is the main problem of the concentrated synthetic wastewater (**Figure 6.5B**).

In fact, even though more biomass was produced in the experiments of salinity and vitamin supplementation, the carbohydrate content was still low because organic nitrogen was almost totally converted into ammonium but not incorporated efficiently by *Synechococcus*. Total nitrogen in the biomass increased as a function of medium adjustments, resulting in higher nitrogen assimilation (**Table 6.3** and **Figure 6.6**). The combination of high removal rate of nitrogen and COD resulted in more than 40% of carbohydrate content (5x Micronutrients condition) showing that it is possible to treat a wastewater with high content of pollutants using *Synechococcus*.

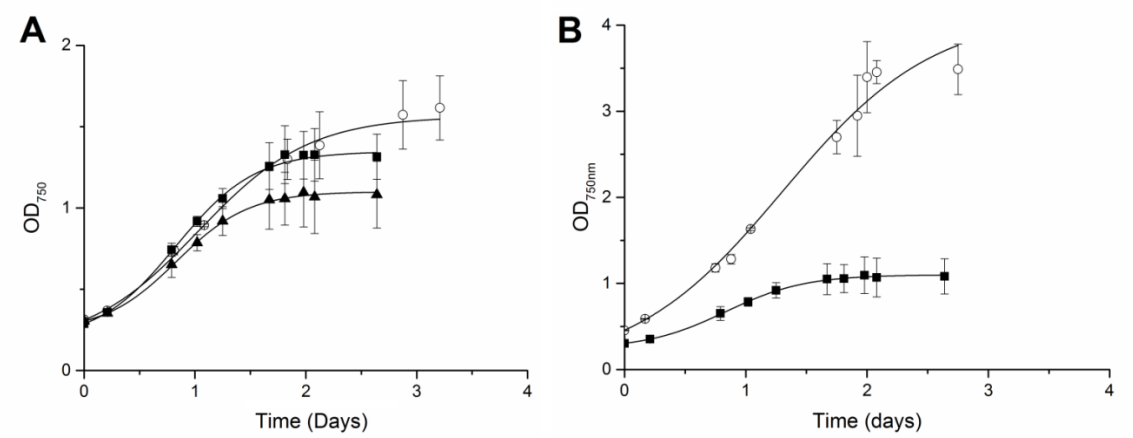

Figure 6.5: Growth curve at different nutritional/environmental techniques. A) 5x (wastewater) (■), 5x + S (Salinity) (o) and 5x + S + V (Salinity + Vitamin) (▲). B) 5x (■) and (o) 5x + Micronutrients.

Table 6.3: Growth parameters and carbohydrate content.

Experiment	Dry Weight ($g\ L^{-1}$)	Carbohydrate Content (%)	Growth Rate (day^{-1})	N/X	P/X
5x	0.57 ± 0.02	14.38 ± 5.46	0.942 ± 0.134	7.90 ± 0.16	3.70 ± 0.08
5x S	0.94 ± 0.06	12.89 ± 3.56	1.180 ± 0.155	8.68 ± 0.65	2.19 ± 0.16
5x S + V	0.95 ± 0.08	13.02 ± 2.79	0.923 ± 0.031	8.35 ± 0.35	0.67 ± 0.05
5x + M	1.20 ± 0.05	41.84 ± 4.40	1.061 ± 0.125	10.37 ± 0.58	2.30 ± 0.13

S – salinity, V – vitamin and M – micronutrients.

After medium adjustment according to salinity and vitamin presence, the COD was removed close to 80% representing a good efficiency value, but nitrogen and phosphorous assimilations were not significantly improved. On the other hand, when micronutrients were supplied, 70-80% of nitrogen and phosphorous removal was achieved (**Figure 6.6**). Thus, clearly micronutrients were not enough in the concentrated synthetic wastewater, emphasizing that a real application is necessary to validate the strain performance.

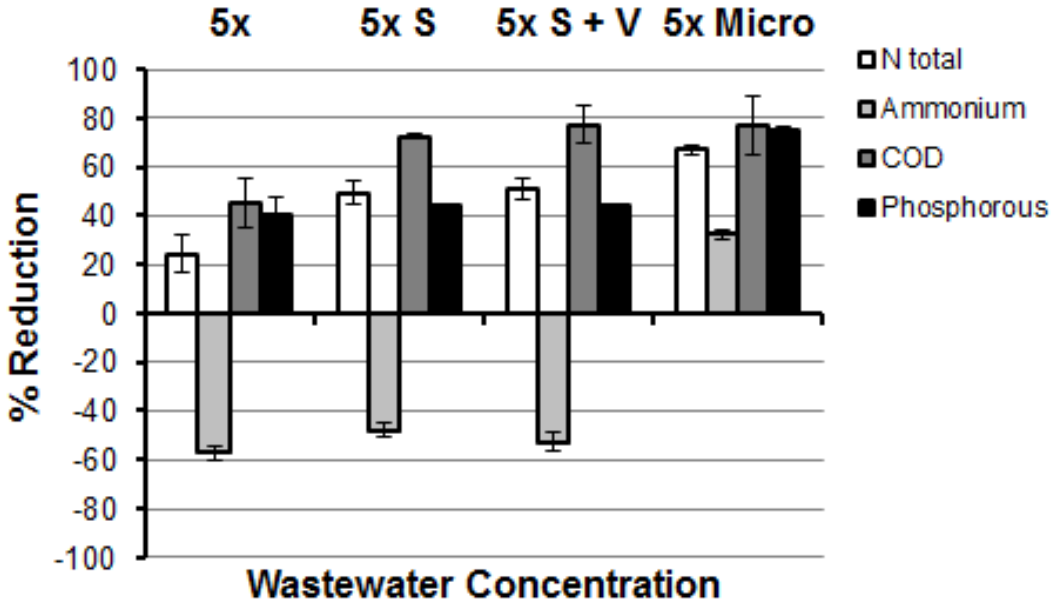

Figure 6.6: % Reduction of main parameters of concentrated synthetic wastewater (5x). Experiments with adjusted synthetic wastewater for salinity (S), presence of vitamin B_{12} (V) and micronutrients (Micro).

Cho et al. (2013), using *Chlorella sp.* ADEE5, were able to remove in almost all experiments 100% of nitrogen and phosphorous content when wastewater was combined with f/2 medium (3-24% v/v) (salinity, vitamin and micronutrients addition, mainly). Ammonia-rich wastewater with several contents of phosphorous and COD was treated with *Chlorella vulgaris* and *Arthospira platensis*, and practically all ammonia

and phosphate was removed, with COD removal values ranging between 60-80% (Markou, 2015). Cabanelas et al. (2013) using *Chlorella vulgaris* in a domestic wastewater containing much COD, nitrogen and phosphorous (675, 130-909 and 60-180, mg L^{-1}, respectively), were able to remove efficiently P content (92%) in all experiments, but the treatment of nitrogen and COD was insufficient. These literature results showed that high pollutants concentrated wastewater can be treated efficiently by photosynthetic microorganisms but nutritional and environmental factors are important to determine this efficiency, because pollutant toxicity or nutrients content cannot be simulated in approximately by the synthetic wastewater.

6.3.4 Real versus synthetic wastewater

Several authors use synthetic or supplemented wastewater (Cai et al., 2013; Lynch et al., 2015; Gonçalves et al., 2016a), and for this reason a validation is necessary because good better performance can be obtained with real wastewater due the possible presence of all nutrients required to cyanobacterial growth.

In **Figure 6.7** is possible to see that *Synechococccus* growth in the real urban wastewater was faster, reaching the stationary phase in two days (40% lower cultivation time in comparison to the synthetic effluent).

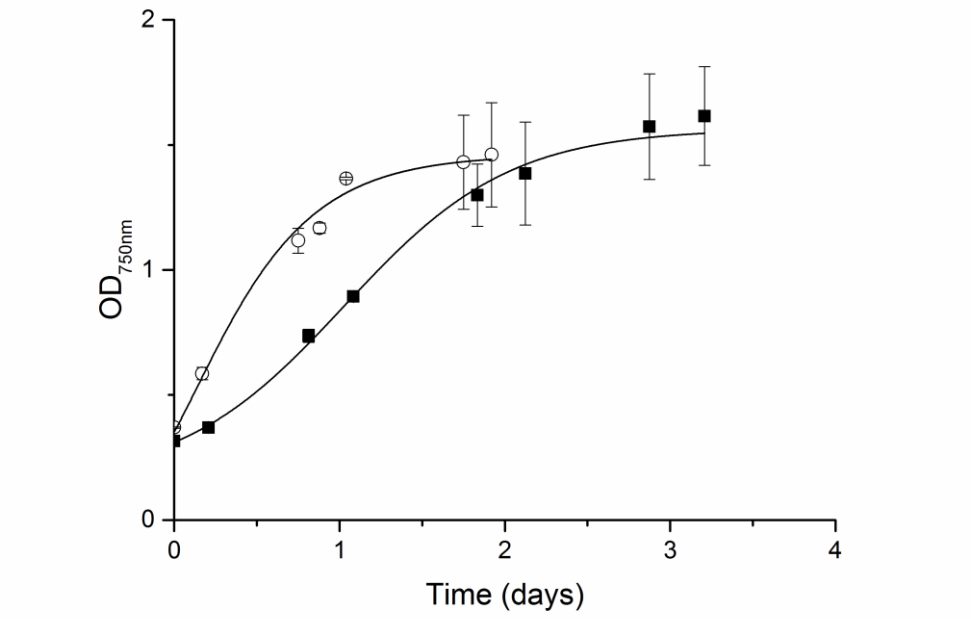

Figure 6.7: Growth curve with synthetic (■) and real wastewater (o).

The productivity indexes (dry weight, carbohydrate content, growth rate, nitrogen content) were practically the same (with the exception of P content) (**Table 6.4**). The pollutant removal profile did not have significant differences between the wastewaters types: it was always efficiently removed the COD, the total nitrogen and the phosphorous, with final values below the law limits (COD – 125, Total Nitrogen – 15 and Phosphorous – 2 mg L^{-1}, EEC 1991) (**Figure 6.8**).

Table 6.4: Growth parameters and carbohydrate content.

Experiment	Dry Weight (g L^{-1})	Carbohydrate Content (%)	Growth Rate (day^{-1})	N/X	P/X
1x synthetic	0.39 ± 0.12	56.12 ± 4.42	1.091 ± 0.108	7.90 ± 0.16	3.70 ± 0.08
1x real	0.45 ± 0.04	56.1 ± 12.9	1.061 ± 0.125	6.21 ± 0.43	0.37 ± 0.03

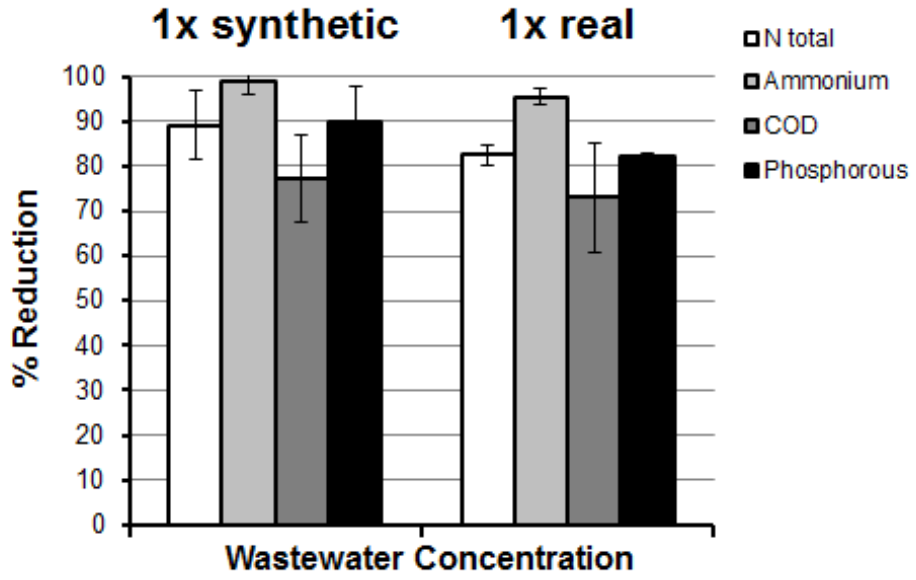

Figure 6.8: % Reduction of main pollutant parameters for synthetic and real wastewater. Initial concentration (mg L^{-1}): COD - 340.0 ± 14.1, Total Nitrogen - 31.0 ± 1.4 and Phosphorous - 8.20 ± 0.99.

6.4 CONCLUSIONS

Synechococcus sp. PCC 7002 demonstrated be a potential strain to treat urban wastewater reaching more than 80% of COD, nitrogen and phosphorous removal (below the law limit) and without CO_2 injection what decreases production costs. Concentrated

synthetic wastewater cannot simulate efficiently the real wastewater and show limitations on the strain performance, and for this reason a validation with a real effluent is always necessary. It was possible to produce a biomass with a carbohydrate content higher than 50% in dry cell weight.

REFERENCES

Abreu, A.P., Fernandes, B., Vicente, A. A., Teixeira, J., Dragone, G., 2012. Mixotrophic cultivation of Chlorella vulgaris using industrial dairy waste as organic carbon source. Bioresource Technology 118, 61-66.

Aguillar-May, B., Sanchez-Saavedra, M.P., 2009. Growth and removal of nitrogen and phosphorous by free-living and chitosan-immobilized cells of the marine cyanobacterium *Synechococcus elongatus*. Journal of Applied Phycology 21(3), 353-360.

AOAC – APHA, 1992. Standard methods for the examination of water and wastewater. 18th edn. American Public Health Association, Washington, DC, USA.

Bernstein, H.C., Konopka, A., Helnicki, M.R., Hill, E.A., Kucek, L.A., Zhang, S., Shen, G., Bryant, D.A., Beliarv, A.S., 2014. Effects of mono- and dichromatic light quality on growth rates and photosynthetic performance of *Synechococcus* sp. PCC 7002. Frontiers in Micorbiology 5, 1-9.

Cabanelas, I.T.D., Ruiz, J., Arbib, Z., Chinalia, F.A., Garrido-Pérez, C., Rogalla, F., Nascimento, I.A., Perdes, J.A., 2013. Comparing the use of diferente domestic wastewaters for coupling microalgal product ion and nutrient removal. Bioresource Technology 131, 429-436.

Cai, T., Ge, X., Park, S.Y., Li, Y., 2013. Comparison of *Synechococystis* sp. PCC 6803 and *Nannochloropsis salina* for lipid production using artificial seawater and nutrients from anaerobic digestion effluent. Bioresource Technology 144, 255-260.

Chen, C., Chang, H., Chang, J., 2016. Producing carbohydrate-rich microalgal biomass grown under mixotrophic conditions as feedstock for biohydrogen production. International Journal of Hydrogen Energy 41, 4413-4420.

Cho, S., Lee, N., Park, S., Yu, J., Luong, T.T., Oh, Y., Lee, T., 2013. Microalgae cultivation for bioenergy production using wastewaters from a municipal WWTP as nutritional sources. Bioresource Technology 131, 515-520.

Cuellar-Bermudez, S.P., Aleman-Nava, G.S., Chandra, R., Garcia-Perez, J.S., Contreras-Ângulo, J.R., Markou, G., Muylaert, K., Rittmann, B.E., Parra-Saldivan, R., 2017. Nutrients utilization and contaminants removal: a review of two approaches of algae and cyanobacteria in wastewater. Algal Research 24(Part B), 438-449.

Dang, T.C., Fujii, M., Rose, A.L., Bligh, M., Waite, T.D., 2012. Characteristics of the freshwater Cyanobacterium *Microcystis aeruginosa* grown in iron-limited continuous culture. Applied and Environment Microbiology 78(5), 1574-1583.

EEC Council. 1991. 91/271/EEC of 21 May 1991 concerning urban waste-water treatment. EEC Counc. Dir. 10. doi: http://eur-lex.europa.eu/legal-content/en/ALL/?uri=CELEX:31991L0271

Feng, X., Bandyapaghyay, A., Bisla, B., Page, L., Wu, B., Pakrasi, H.B., Tang, Y.J., 2010. Mixotrophic and photoheterotrophic metabolism in *Cyanothece* sp. ATCC 51142 under continuous light. Microbiology 156, 2566-2574.

Gonçalves, A.L., Pires, J.C.M., Simoes, M., 2016. Biotechnological potential of *Synechocystis salina* co-cultures with selected microalgae and cyanobacteria: nutrients removal, biomass and lipid production. Bioresource Technology 200, 279-286. (a)

Gonçalves, A.L., Abreu, A.C., Coqueiro, A., Gaspar, A., Borges, F., Choi, Y.H., Pires, J.C.M., Simoes, M., 2016. Co-cultivation of *Synechocystis salina* and *Pseudokirchneriella subcapitata* under varying phosphorous concentrations evidences and allelopathic competition scenario. RSC Adv. 6, 56091-56100. (b)

Gonçalves, A.L., Rodrigues, C.M., Pires, J.C.M., Simoes, M., 2016. The effect of increasing CO_2 concentrations on its capture, biomass production and wastewater bioremediation by microalgae and cyanobacteria. Algal Research 14, 127-136. (c)

Guldhe, A., Kumari, S., Ramanna, L., Ramsundar, P., Singh, P., Rawat, I., Bux, F., 2017. Prospects, recent advancements and challenges of different wastewater streams for microalgal cultivation. Journal of Environmental Management 203, 299-315.

Kam, S.K., 2016. Application of cyanobacteria for bioremediation of wastewaters. Journal of Cleaner Production 135, 819-820.

Ludwig, M., Bryant, D.A., 2012. *Synechococcus sp*. strain PCC 7002 transcriptome: acclimation to temperatures, salinity, oxidative stress, and mixotrophic growth conditions. Front. Microbiol. 3, 1-14.

Lynch, F., Santana-Sànchez, A., Jamsa, M., Sivonenk, Aro, E., Allahverdiyeva, Y., 2015. Screening native isolates of cyanobacteria and a green alga for integrated wastewater treatment, biomass accumulation and neutral lipid production. Algal Research 11, 411-420.

Mackey, K.R.M., Paytan, A., Caldeira, K., Grossman, A.R., Moran, D., McIlvin, M., Saito, M.A., 2013. Effect of temperature on photosynthesis and growth in marine *Synechococcus* spp. Plant Physiology 163, 815-829.

Markou, G., Georgakakis, D., 2011. Cultivation of filamentous cyanobacterium (blue-green algae) in agro-industrial wastes and wastewaters: a review. Applied Energy 88, 3389-3401.

Markou, G., 2015. Fed-batch cultivation of *Arthrospira* and *Chlorella* in ammonia-rich wastewater: Optimization of nutrient removal and biomass production. Bioresource Technology 193, 53-41.

Moore, L.R., Goericke, R., Chisholm, S.W., 1995. Comparative physiology of *Synechococcus* and *Prochlorococcus*: influence of light and temperature on growth, pigments, fluorescence and absorptive properties. Marine Ecology Progress Series 116, 259-275.

OECD. 2001. Available in: http://www.oecd.org/chemicalsafety/testing/oecdguidelinesforthetestingofchemicals.htm

Ruiz-Guereca, D.A., Sanchez-Saavedra, M.P., 2016. Growth and phosphorous removal by Synechococcus elongatus co-immobilized in alginate beads with *Azospirillum brasiliense*. Journal of Applied Phycology 28(9), 1501-1507.

Silva, C.E.F., Bertucco, A., 2016. Bioethanol from microalgae and cyanobacteria: A review and technological outlook. Process Biochemistry 51, 1833-1842.

Silva, C.E.F., Sforza, E., Bertucco, A., 2016. Effects of sodium bicarbonate on biomass and carbohydrate production in *Synechococcus* PCC 7002. Chemical Engineering Transactions 49, 241-246.

Silva, C.E.F., Sforza, E., Bertucco, A., 2017. Effects of pH and carbon source on *Synechococcus* PCC 7002 cultivation: biomass and carbohydrate production with different strategies for pH control. Applied Biochemistry and Biotechnology 181, 682-698.

Trevelyan, W.E., Harrison, J.S., 1952. Studies on yeast metabolism. 1. Fractionation and microdetermination of cell carbohydrates. The Biochemical Journal 50(3), 208-303.

Wan, N., Abernathy, M., Tang, J.K., Tang, Y.J., You, L., 2015. Cyanobacterial photo-driven mixotrophic metabolism and its advantages for biosynthesis. Front. Chem. Sci. Eng. 9(3), 203-216.

APPENDIX

Table 6.S1: Initial and final contaminants concentration.

Synthetic Wastewater (Initial)			**24 °C**				**28 °C**			
			Without CO_2		**With CO_2**		**Without CO_2**		**With CO_2**	
			Final		**Final**		**Final**		**Final**	
Nutrient	**[ ]**	**Dev St**	**[ ]**	**Dev St**	**[ ]**	**Dev St**	**[ ]**	**Dev St**	**[ ]**	**Dev St**
Total Nitrogen (mg N L^{-1})	31.0	1.4	18.0	1.41	16.86	3.39	3.44	0.84	3.44	0.84
Nitrate (mg NO_3 L^{-1})	0.55	0.07	0.0	0.0	7.8	2.1	0.2	0.1	0.4	0.3
Nitrite (mg NO_2 L^{-1})	0.04	0.01	0.20	0.03	0.06	0.02	0.05	0.01	0.08	0.01
Ammonium (mg NH_4^+ L^{-1})	15.25	0.35	11.5	0.71	15.05	0.30	0.15	0.07	0.00	0.00
COD (mg O_2 L^{-1})	340.0	14.1	45.5	14.8	65.0	1.0	68.7	3.5	56.0	1.1
Phosphate (mg P L^{-1})	8.20	0.99	6.9	0.2	5.9	0.1	0.78	0.05	0.78	0.05

Table 6.S2: Initial and final contaminants concentration.

Synthetic Wastewater												
	1x				**3x**				**5x**			
	Initial		**Final**		**Initial**		**Final**		**Initial**		**Final**	
Nutrient	**[ ]**	**Dev St**	**[ ]**	**Dev St**	**[ ]**	**Dev St**	**[ ]**	**Dev St**	**[ ]**	**Dev St**	**[ ]**	**Dev St**
Total Nitrogen (mg N L^{-1})	31.0	1.4	3.44	0.84	116.6	0.6	60.03	5.18	158.2	4.8	119.76	12.05
Nitrate (mg NO_3 L^{-1})	0.55	0.07	0.2	0.1	1.0	0.7	4.3	0.9	1.4	0.5	1.7	0.3
Nitrite (mg NO_2 L^{-1})	0.04	0.01	0.05	0.01	0.05	0.00	0.54	0.66	0.05	0.01	0.09	0.04
Ammonium (mg NH_4^+ L^{-1})	15.25	0.35	0.15	0.07	40.75	3.57	54.68	4.62	69.94	3.97	110.03	1.92
COD (mg O_2 L^{-1})	340.0	14.1	68.7	3.5	1167.78	11.12	420.3	35.2	1405.31	72.24	770.0	136.9
Phosphorous (mg P L^{-1})	8.20	0.99	0.78	0.05	21.93	2.67	12.43	3.39	44.93	0.94	26.95	3.59

Table 6.S3: Initial and final contaminants concentration.

Synthetic Wastewater										
	5x				5x + S		5x + S + V		5x + Micro	
	Initial		Final		Final		Final		Final	
Nutrient	**[ ]**	**Dev St**	**[ ]**	**Dev St**	**[ ]**	**Dev St**	**[ ]**	**Dev St**	**[ ]**	**Dev St**
Total Nitrogen (mg N L^{-1})	158.2	4.8	119.76	12.05	80.10	7.21	77.62	6.36	57.47	3.98
Nitrate (mg NO_3 L^{-1})	1.4	0.5	1.7	0.3	4.9	0.0	5.7	0.7	2.6	0.4
Nitrite (mg NO_2 L^{-1})	0.05	0.01	0.09	0.04	0.08	0.01	0.08	0.01	0.16	0.03
Ammonium (mg NH_4^+ L^{-1})	69.94	3.97	110.03	1.92	103.46	1.89	106.73	2.74	38.34	0.93
COD (mg O_2 L^{-1})	1405.31	72.24	770.0	136.9	387.8	10.8	319.5	105.6	327.7	170.0
Phosphorous (mg P L^{-1})	44.93	0.94	26.95	3.59	25.25	0.45	25.26	0.40	11.2	0.7

Table 6.S4: Initial and final contaminants concentration.

	1x synthetic				1x real			
	Initial		Final		Initial		Final	
Nutrient	**[ ]**	**Dev St**	**[ ]**	**Dev St**	**[ ]**	**Dev St**	**[ ]**	**Dev St**
Total Nitrogen (mg N L^{-1})	31.0	1.4	3.44	0.84	27.6	0.1	4.83	1.70
Nitrate (mg NO_3 L^{-1})	0.55	0.07	0.2	0.1	0.0	0.0	0.0	0.0
Nitrite (mg NO_2 L^{-1})	0.04	0.01	0.05	0.01	0.04	0.01	0.04	0.01
Ammonium (mg NH_4^+ L^{-1})	15.25	0.35	0.15	0.07	23.52	0.41	1.04	0.04
COD (mg O_2 L^{-1})	340.0	14.1	68.7	3.5	495.92	8.60	133.9	44.4
Phosphorous (mg P L^{-1})	8.20	0.99	0.78	0.05	5.0	0.2	1.1	0.2

Chapter 7

Carbohydrate productivity in continuous reactor under nitrogen limitation: Effect of light and residence time on nutrient uptake in *Chlorella vulgaris*

Chlorella vulgaris is commonly recognized as an interesting species for bioethanol production due to its carbohydrate content. Carbohydrates accumulation is often obtained under nitrogen starvation, which on the other hand may lead to a reduced biomass production. In this work, the effect of nitrogen limitation in a continuous system was assessed, with the aim of finding an optimal value where biomass productivity and carbohydrate content are well balanced. The effect of light intensity was also investigated, and it was highlighted that in a continuous system light stress is the main variable affecting the carbohydrate content and productivity. It was also evidenced that increasing the residence time is a way to boost nitrogen starvation: the biomass yield on nitrogen noticeably changes with the residence time, thus modifying the elemental composition of the microalgal biomass, and resulting in an accumulation of carbohydrates•.

•*Part of this chapter was published in Process Biochemistry (**Silva, C.E.F**., Sforza, E., 51, 2112-2118, 2016).*

7.1 INTRODUCTION

Fossil carbon sources account for about 85% of the global energetic consumption, with about 33% of oil, 29% of coal and 24% of natural gas. Renewable energy accounts for only 10% of the total. The growing need to expand the use of renewable energy sources in a sustainable manner has boosted, in particular, the production of biofuels worldwide (Moraes et al., 2015).

In this scenario, bioethanol is one of the main biofuels produced. The global ethanol production corresponds to approximately 25 billion gallons per year (over 100 million m^{-3} y^{-1}). It is perceived that the US and Brazil hold hegemony in production accounting for almost 85%, using corn and sugarcane, respectively (RFA, 2016). On the other hand, the production of bioethanol is expected to largely increase, leading to an unsustainable competition for arable land. In this perspective, microalgae and cyanobacteria are a source of biomass that can complement the agricultural raw materials and help to increase the global demand for food, biofuels and chemical production (Markou et al., 2014; Silva and Bertucco, 2016). The biochemical composition of microalgae mainly includes proteins (30-50%), carbohydrates (20-40%) and lipids (8-15%) (Cardoso et al., 2011), but several studies have shown that lipids and carbohydrates can be accumulated under stress conditions thus decreasing the protein content (Ho et al., 2012; Wang et al., 2014). It is important to mention that carbohydrates and lipids are energy rich molecules, which constitute reserves in microalgae, and they are an indispensable buffer against varying external growth conditions, allowing to survive for periods of light-energy absence (Vitova et al., 2015).

In view of bioethanol production, an efficient accumulation of carbohydrates is the key factor: carbohydrates in microalgae are mainly composed of starch or glycogen, depending on the species, which can be hydrolyzed and easily fermented to produce bioethanol. Several studies report an increase of carbohydrate content up to 50%, for many microalgal and cyanobacterial species, such as *Chlorella vulgaris* (Kim et al., 2014), *Dunaliella tertiolecta* (Kim et al., 2015), *Scenedesmus* spp. (Ho et al., 2013a; Ashokkumar et al., 2015), *Tribonema* sp. (Wang et al., 2014), *Arthrospira platensis* (Markou et al., 2013) and *Synechococcus* sp. (Mollers et al., 2014), mainly cultivated under nitrogen starvation or limitation occurring at the stationary phase in batch cultivation. In fact, nitrogen plays a key role in the redirection of algal metabolism, for

both carbohydrate and lipid accumulation. Both carbohydrate and lipid metabolism start with a common initial pool of molecules consisting of three carbons and, even though some species produce preferentially one of the two macromolecules as reserve, other organisms can produce both, with ratios that differ depending on growth conditions. If nitrogen starvation is a commonly recognized method to trigger lipid accumulation, its effect on carbohydrates is still under investigation, in particular because it usually results in lower biomass productivity, thus affecting the efficiency of the whole process. Carbohydrates and lipid accumulation also depends on many other variables (or their interactions), such as light intensity, temperature, carbon source, growing time, nutrients availability, salinity and pH, as recently reviewed by Vitova et al (2015).

In addition, carbohydrates accumulation in batch system is not stable, and under extreme N starvation carbohydrates content may actually decrease (Branyikova et al., 2011), while N limitation seems a viable alternative (Vitova et al., 2015).

Moreover, from an industrial perspective, batch systems are not suitable, while continuous processes could noticeably improve the productivity: steady state production is generally more efficient, has lower costs and is easier to operate (Ho et al., 2014). The possibility of cultivating microalgae in continuous industrial system is still challenging, particularly due to the variability of environmental parameters in outdoor cultivation. On the other hand, at lab scale, cultivation of microalgae in continuous systems is quite established and studied for several species (Sobczuk et al., 2000; Tang et al., 2012; Ruiz et al., 2013; Ramos-Tercero et al., 2013), but less information is available on the carbohydrate accumulation under continuous mode (Ho et al., 2013b), in particular for *Chlorella vulgaris*. In addition, continuous systems working at steady-state are a viable tool to study physiological response to environmental condition since light intensity, residence time and nitrogen concentration can be managed for an efficient carbohydrate accumulation (Gonzalez-Fernandez and Ballesteros, 2012; Ho et al., 2013a).

In this chapter *Chlorella vulgaris* was grown in a flat panel continuous photobioreactor (PBR), under different light intensities. The residence time and nitrogen inlet concentrations were changed, in order to assess their effect on biomass steady state concentration, carbohydrate productivity and photosynthetic efficiency. A N limitation approach in continuous system was used, to boost carbohydrate accumulation without strongly affecting the biomass productivity.

7.2 MATERIAL AND METHODS

7.2.1 Microalgae and media composition

The microalgal species *Chlorella vulgaris* was maintained and cultured in modified BG11 medium (buffered with 10 mM HEPES pH 8), sterilized in an autoclave for 20 min at 121°C. The P and N content of the medium, in the form of K_2HPO_4 and $NaNO_3$, were optimized to study the nutrient starvation, and concentrations for each condition are reported in the corresponding sections.

7.2.2 Equipment

Batch experiments were performed in 250 mL working-volume glass vertical cylinders (5 cm diameter), continuously mixed by a stirring magnet placed at the bottom of the bottle.

Continuous experiments were performed in vertical flat-plate polycarbonate CSTR (continuously stirred tank reactor) PBR (see Sforza et al. (2014a) and Bertucco et al. 2014, for the schematic of the experimental setup), with a working volume of 300 mL, a depth of 1.2 cm, and a surface exposed to light of 250 cm^2. CO_2 in excess is provided by a CO_2–air (5% v/v) bubbling at the reactor bottom (1 L h^{-1} of total gas flow rate), which also provided mixing. A magnetic stirrer was also used to prevent any deposition of biomass and thus ensuring a good mixing of the reactor (Bertucco et al., 2014). The fresh medium was fed at a constant rate by a peristaltic pump (Watson-Marlow sci400, flow rate range: 25-250 mL d^{-1}). Light was provided by a LED lamp (Photon System Instruments, SN-SL 3500-22) both for continuous and batch experiments. Photon Flux Density (PFD) was measured on both the front and back panels of the reactor using a photoradiometer (HD 2101.1 from Delta OHM), which quantifies the photosynthetically active radiation (PAR).

7.2.3 Experimental procedures

In steady state continuous experiments, *C. vulgaris* was inoculated into the reactor with the culture medium. At the beginning, batch operation mode was set to prevent the occurring of washout. Once a significant concentration (10^8 cells mL^{-1}) was reached, the operation was switched to continuous, feeding the fresh medium from a tank, through

the peristaltic pump. The working volume (V_{PBR}) was controlled by an overflow tube, and the outlet flow rate Q (mL d^{-1}) was collected in another tank. The hydraulic residence time (τ) in the reactor was directly controlled by the peristaltic pump, according to:

$$\tau = \frac{V_{PBR}}{Q} \quad (7.1)$$

When steady-state operation was achieved, biomass was sampled and analyzed at least for 3-7 days. For each steady state the biomass density C_x, the carbohydrates content, as well as the N and P consumptions were measured. The volumetric biomass productivity P_X (g L^{-1} d^{-1}) was calculated as:

$$P_X = \frac{C_X}{\tau} \quad (7.2)$$

where C_X is the biomass concentration (DW) at steady state.

To assess the effect of nutrients ratios on biomass and carbohydrates concentrations, the inlet medium was changed and transient conditions were observed, until a new steady state was reached.

The photon flux density absorbed by the algae (PFD_{abs}) was also measured at steady state. This was calculated as:

$$PFD_{abs} = I_{in} - B_I - I_0 \quad (7.3)$$

where I_{in} is the incident light (mmol m^{-2} d^{-1}), B_I the back irradiance (mmol m^{-2} d^{-1}), and I_0 the light absorbed by the medium and the panel walls (mmol m^{-2} d^{-1}).

The photosynthetic efficiency (PE), i.e. the fraction of PAR converted to biomass, was calculated as:

$$\%PAR = \frac{C_x * Q * LHW}{PFD_{abs} * E_p * A_{PBR}} \quad (7.4)$$

where *LHV* is the Lower Heating Value (assumed equal to 20 kJ g^{-1}), E_p the energy of photons (kJ μmol^{-1}), and A_{PBR} is the irradiated surface of the reactor (m^2).

In addition, at steady-state a stable specific light supply per unit mass of cell r_{Ex} (mmol g^{-1} d^{-1}) (Kliphius et al., 2012; Sforza et al., 2014b) was calculated as:

$$r_{Ex} = \frac{PFD_{abs} * A_{pbr}}{c_x * V_{pbr}} \quad (7.5)$$

7.2.4 Analytical methods

The biomass concentration was monitored daily by spectrophotometric analysis of the optical density (OD_{750}) using a UV-Visible spectrophotometer (UV 500, Spectronic Unicam, UK) correlated to cell concentration, measured with a Bürker Counting Chamber (HBG, Germany). The concentration of biomass was also gravimetrically measured as dry weight (DW) in terms of g L^{-1} in cells previously harvested with a 0.22 μm filter, and then dried for 4 h at 80 °C in a laboratory oven. The nutrients analyzed were nitrate ($N\text{-}NO_3$) and phosphate ($P\text{-}PO_4$), assessed at least three different times for each steady state. Culture samples were filtered in order to measure only dissolved nutrients (0.2 μm): $N\text{-}NO_3$ concentration was measured by an analytical test kits provided by St. Carlo Erba Reagenti, Italy, (code 0800.05482) and orthophosphates were measured by the ascorbic acid method described in APHA-AWWA-WEF (1992). Nutrient concentrations were measured at the reactor inlet and outlet and the nutrient/biomass yields $Y_{i/X}$ ($mg_i\ mg_{biomass}^{-1}$) were calculated as:

$$Y_{i/X} = \frac{C_{i_{in}} - C_{i_{out}}}{C_X} \quad (7.6)$$

where subscript i indicates N or P, and $C_{i_{in}}$ and $C_{i_{out}}$ are the concentrations of i at the reactor inlet and outlet, respectively.

The total carbohydrate content of biomass was determined by the Anthrone method (Trevelyan and Harrison, 1952).

The lipid content was determined by solvent extraction using chloroform: methanol (1:2) and measured gravimetrically after solvent removal by rotary evaporator at 50 ± 2 °C and dried at 105 ± 2 °C for 1 h to remove residual moisture.

7.2.5 Statistical analysis

Student's t tests were applied to ascertain significant differences in carbohydrate ratio under different inlet nitrogen concentration in continuous experiments. The level of statistical significance was $p<0.05$.

7.3 RESULTS AND DISCUSSION

7.3.1 Carbohydrate accumulation in batch cultures

A first batch control growth curve was carried out to assess the growth rate and carbohydrate accumulation of *Chlorella vulgaris*, under an irradiance of 150 µmol photons m^{-2} s^{-1}. Results are reported in **Figure 7.1** and **7.2**. This species showed a remarkable growth rate of 0.89 day^{-1} and a final biomass concentration of 3.6 g L^{-1}. At the beginning of the growth curve the carbohydrates content was about 20% DW, which started to increase when the external nitrogen source was consumed, reaching a value of about 43% DW at the end of the stationary phase. These results are in agreement with those obtained by Ho and coworkers (Ho et al., 2013b), who cultivated *C. vulgaris* FSP-E in batch mode reaching a carbohydrates content of about 50% when the external nitrogen source was exhausted.

It is well known that N starvation/limitation is one of the most common methods for accumulation of high energetic value substances in microalgae (Gonzalez-Fernandez and Ballesteros, 2012), including carbohydrates (Ho et al., 2013b): nitrogen limitation shifts the carbon fixed by Calvin's Cycle to produce other substances instead of nitrogen-based compounds (proteins), i.e. carbohydrates and lipids (Vitova et al., 2015). Most of green algae (*Chlorophyta*, as *Chlorella*) accumulate starch as primary energy and carbon reserve, whereas lipids serve as a secondary storage. In addition, if N starvation seems a viable way to trigger lipid accumulation, N limitation can be responsible of carbohydrate synthesis for industrial application (Vitova et al., 2015).

However, moving to large-scale cultivation in industrial applications, a continuous process may be more suitable (Sobczuk et al., 2000; Tang et al., 2012; Ruiz et al., 2013). In addition, working in continuous systems has also interesting physiological implications because, at steady-state, biomass with constant biochemical composition is produced, which is particularly relevant when a specific product is targeted.

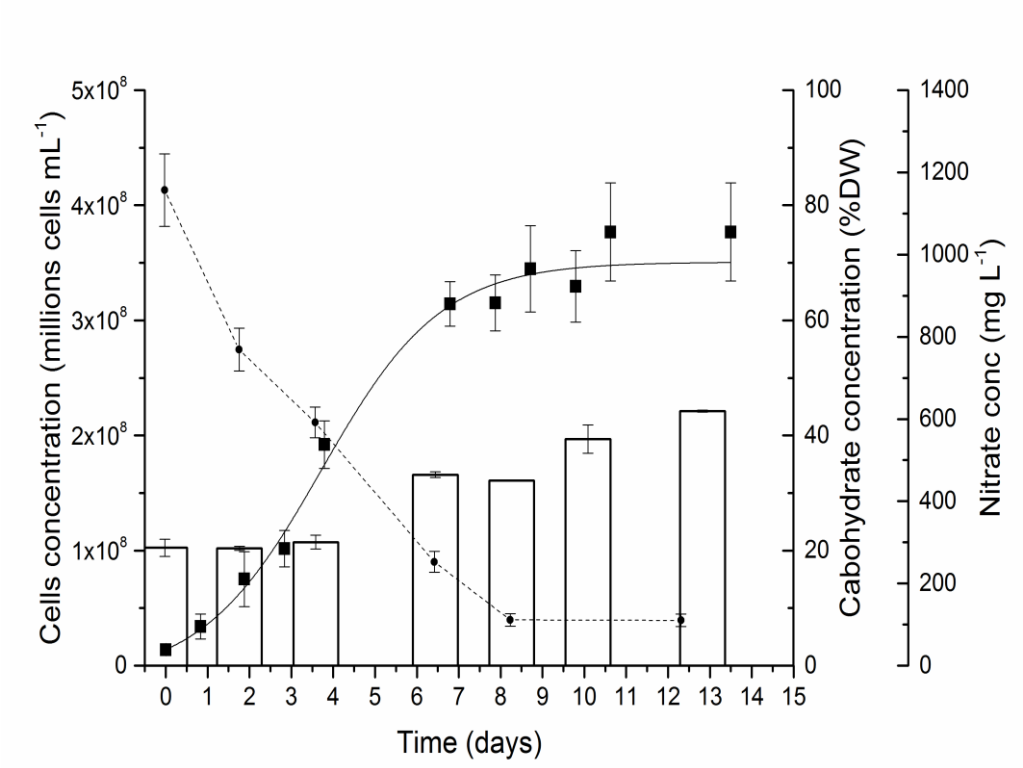

Figure 7.1: Cell concentration (black squares) of batch growth curve of *C. vulgaris*. White bars refer to the carbohydrate content (%DW) while black circles correspond to the NO_3^- concentration in the culture medium, measured during the growth curve.

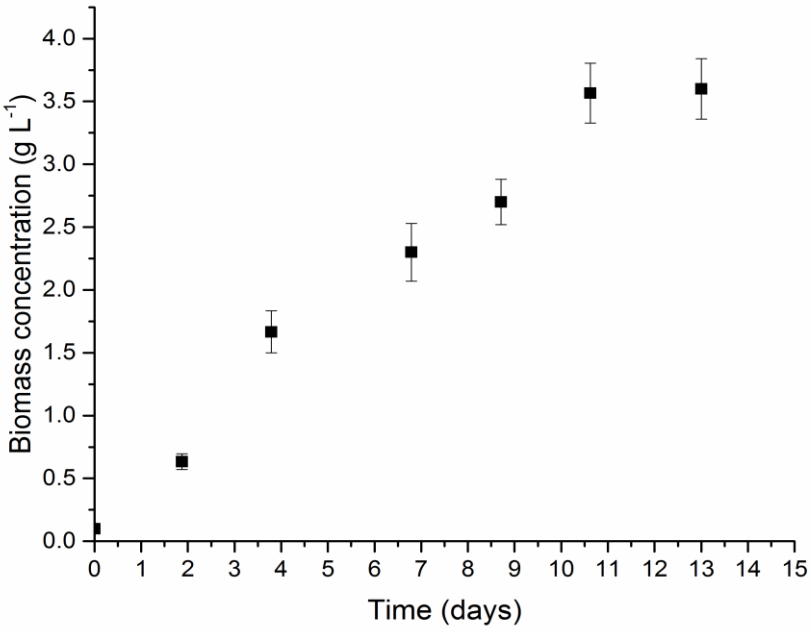

Figure 7.2: Batch growth curve of *Chlorella vulgaris*, data reported as DW in terms of g/L.

7.3.2 Effect of nitrogen limitation in continuous system

A first experiment in continuous system was carried out as a control, by supplying nitrogen and phosphorus in non-limiting conditions (at 150 µmol photons m^{-2} s^{-1}) [26], in order to measure the maximum value of biomass concentration and productivity, as well as to assess nutrients consumption and carbohydrates content. A residence time of 2.9 days was set and a steady state biomass concentration of about 1.9 g L^{-1} was obtained (**Figure 7.3**). Under excess of nutrients, a carbohydrate content of about 18% DW was measured. Concerning nutrient consumption, a ΔN and ΔP of about 150 and 50 mg L^{-1} were measured respectively. Therefore, the inlet concentration of these nutrients was modified accordingly in the following experiments. The same biomass and carbohydrate concentration of the control were measured after the steady state was reached. After that, the P content of the inlet stream was then kept constant, while the nitrogen concentration in the feed was progressively reduced, with the aim to assess the effect of N limitation as a single variable on steady-state concentration and productivity. The idea was to find out an optimum value of both biomass and carbohydrate productivity: under nitrogen limitation, even though the biomass concentration may slightly decrease, a possible increase of carbohydrate content could compensate the loss of biomass production, and might increase the overall carbohydrate productivity.

Three nitrogen concentrations in the feed were tested (100, 75 and 70 mg L^{-1} of $N\text{-}NO_3$). In all conditions tested, the nitrogen concentration inside the PBR, which in a continuously stirred tank reactor (CSTR) (Bertucco et al., 2014) corresponds to the outlet one, was measured and reported as supplementary materials (**Table 7.1**). Since nitrogen was found not totally consumed, a regime of nitrogen limitation was obtained. The steady state biomass concentration remained substantially stable at 100 and 75 mg L^{-1}, while a decrease of 13% was observed with 70 mg L^{-1}. Accordingly, biomass productivity decreased only with this last nitrogen concentration. On the other hand, carbohydrate content was found to be slightly increased with 75 and 70 mg L^{-1} of nitrogen, corresponding to 27.8 and 27.1% DW respectively. Concerning the carbohydrate productivity, a maximum of 0.18 g L^{-1} d^{-1} was found at 75 mg L^{-1}, i.e. at the condition where biomass is limited by nitrogen availability, but not enough to decrease the biomass concentration and productivity.

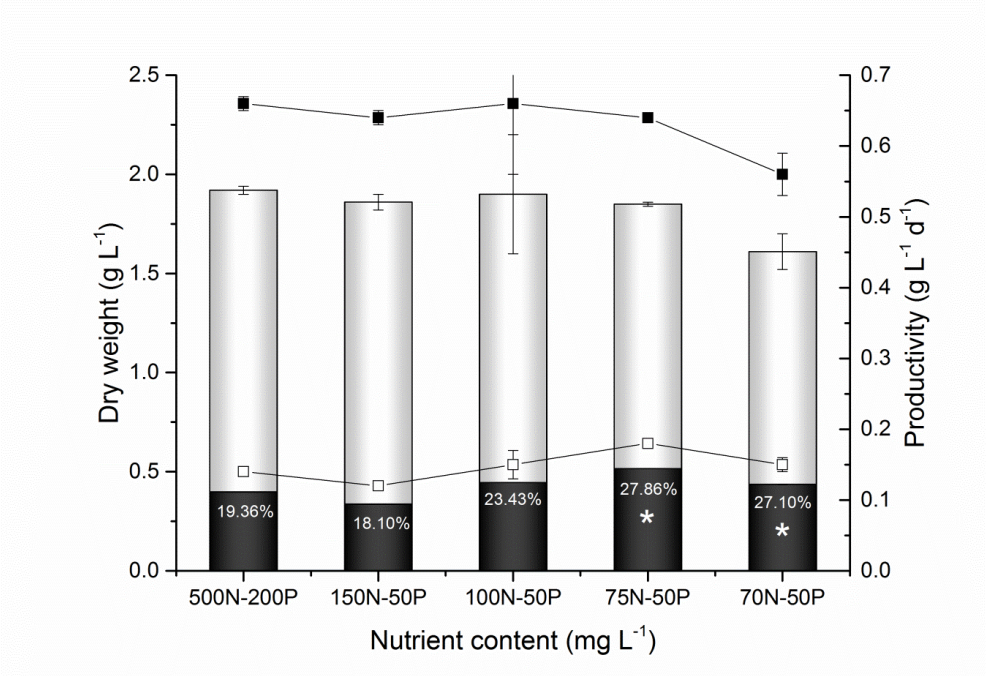

Figure 7.3: Biomass concentration (gray bars) and carbohydrate concentration (DW) (dark bars) of *C. vulgaris* at steady state under 150 µmol photons m^{-2} s^{-1}, 2.9 days of residence time and with different inlet concentration of nutrients, reported as elemental concentrations. Dark and open squares refer to biomass and carbohydrates productivity, respectively. Numbers on the bars report the carbohydrate-biomass ratio (%DW). Statistically significant results with respect to the control are marked with an asterisk.

Table 7.1: Nitrogen and phosphorus outlet concentrations from the reactor at different nitrogen supply concentrations and 2.9 days of residence time.

Light Intensity (µmol m^{-2} s^{-1})	**N/P Concentration (mg L^{-1})**	**N out (mg L^{-1})**		**P out (mg L^{-1})**	
		Avg	StD	Avg	StD
150	500N/200P	325.98	3.65	153.65	31.53
	150N/50P	9.94	10.15	35.81	6.73
	100N/50P	10.76	1.25	37.68	2.99
	75N/50P	10.45	2.14	28.94	1.94
	70N/50P	9.42	1.98	29.98	2.28
300	500N/200P	300.73	41.58	154.55	10.37
	320N/50P	5.63	0.78	9.45	0.50
	175N/50P	1.35	0.69	15.67	0.69
	125N/50P	1.00	0.60	6.21	1.02
	75N/50P	1.28	0.34	6.62	0.53
450	500N/200P	261.20	39.06	129.73	4.38
	380N/50P	56.63	1.47	13.62	0.66
	250N/50P	32.72	2.46	14.91	1.77
	150N/50P	2.48	0.65	9.81	2.26
	75N/50P	3.82	0.90	6.00	1.10

Nevertheless, the carbohydrate content was found generally lower than that obtained at the end of the stationary phase of batch experiments. A possible explanation can be related to a limitation of some other nutrient, that limits biomass accumulation, or to the absence of stressing conditions, which are well known to trigger the accumulation of high energy content molecules in microalgae. Moreover, it has to be noticed that in batch conditions an actual N starvation occurred, while in continuous system only a nutrient limitation was applied (**Tables 7.1-7.2**), to avoid a negative effect on biomass productivity.

Table 7.2: Lipid content under nitrogen excess or limitation in continuous cultivation, at 2.9 days of residence time.

Light Intensity ($\mu E\ m^{-2}\ s^{-1}$)	**Excess of Nutrient 500N/200 P**		**Nitrogen Limitation 75N/50P**	
	Lipid		**Lipid**	
	Avg	StD	Avg	StD
150	24.15	1.3	28.06	4.6
300	24.97	0.4	31.66	3.2
450	20.56	2.2	37.37	4.7

Finally, since micronutrients and CO_2 were provided in excess, the major role in the accumulation of carbohydrates could be played by light. For this reason, further continuous experiments were carried out under higher light intensities.

7.3.3 Combined effect of light intensity and nitrogen limitation

Two set of experiments were carried out under incident light intensities of 300 and 450 µmol photons $m^{-2}\ s^{-1}$ and by changing inlet nitrogen concentration (keeping the same residence time of 2.9 days). Results of biomass and carbohydrates concentrations and productivities are reported in **Figure 7.4**.

Similarly, to what reported in section 3.2, a first experiment under N and P excess was carried out for both light intensities. In these conditions a general increase of both biomass and carbohydrates accumulation was observed, with respect to 150 µmol photons $m^{-2}\ s^{-1}$. The carbohydrates content was found to be about 23% DW, even under nutrients excess conditions, suggesting that high light intensity itself is able to trigger the synthesis of carbohydrates. This is also confirmed by Ho et al. (2013b): using 450 µmol $m^{-2}\ s^{-1}$ of light intensity more than 50% of dry weight of carbohydrates was accumulated in *C. vulgaris* FSP-E. Generally, a light intensity between 250-450 µmol

photons m^{-2} s^{-1}, close to the saturation point, is the best range for carbohydrates accumulation in microalgae (Silva and Bertucco, 2016).

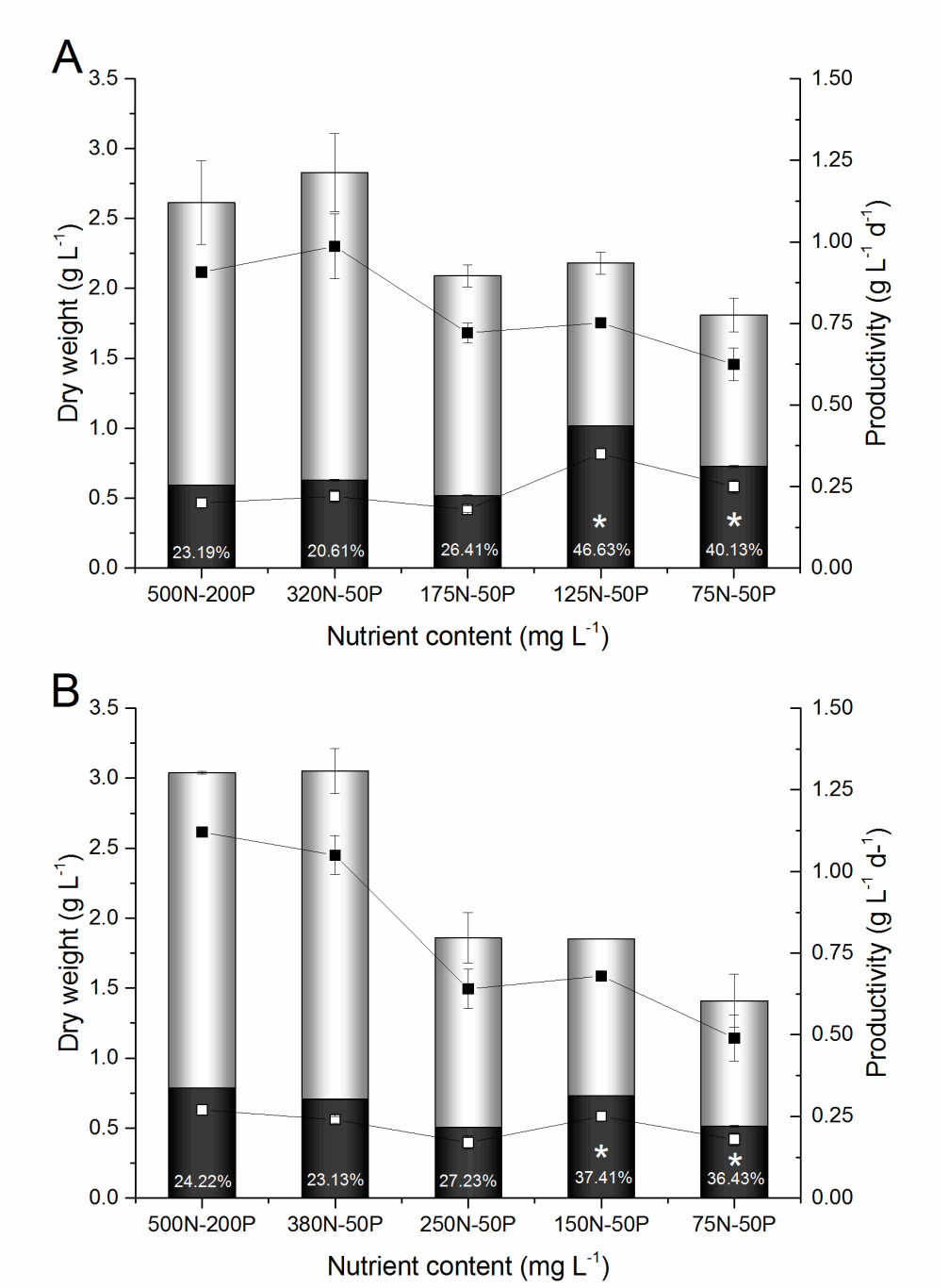

Figure 7.4: Biomass concentration (gray bars) and carbohydrate fraction (DW) (dark bars) of *C. vulgaris* at steady state under 300 µmol photons m^{-2} s^{-1} (A) and 450 µmol photons m^{-2} s^{-1} (B), with different inlet concentration of nutrients, reported as elemental concentrations and 2.9 days of residence time. Dark and open squares refer to biomass and carbohydrates productivity, respectively. Numbers on the bars report the carbohydrate-biomass ratio (%DW). Statistically significant results with respect to the control are marked with an asterisk.

After that, the nutrients consumption was measured and subsequently only the amount of N and P needed were provided in the inlet, obtaining biomass and carbohydrates concentrations comparable to those of the control, similarly to what previously found under 150 µmol photons m^{-2} s^{-1}. Also, as in the case of 150 µmol photons m^{-2} s^{-1}, the nitrogen in the inlet stream was then reduced to assess the effect of starvation on steady state cultures. Under higher intensities the biomass concentration decreased faster than in the previous case, suggesting that the uptake of nutrient is strongly affected by light as already reported for other species (Clark et al., 2002; Quigg and Beardall, 2003; Sforza et al., 2015b). On the other hand, even if biomass concentration decreased, the carbohydrates accumulation was triggered by a combined high light and N starvation stress with a maximum of 46.4 % DW at 300 µmol m^{-2} s^{-1} and 125 mg L^{-1} of N in the inlet. At this point a maximum carbohydrates productivity of 0.35 g L^{-1} d^{-1} was found, which is a remarkable value, comparable to that obtained by Ho et al. (2013a) by cultivating *Scenedesmus obliquus* in continuous mode and 240 µmol m^{-2} s^{-1} with carbohydrates productivities between 0.287-0.312 g L^{-1} d^{-1}.

The photosynthetic efficiency was also evaluated for all intensities and nitrogen concentration tested, as reported in F**igure 7.5**. Obviously, the PE increased with nitrogen concentration, but much more relevant was the effect of light intensity. Clearly, cells exposed to 300 and 450 µmol m^{-2} s^{-1} resulted to be photosaturated or photoinhibited, with a strongly reduced PE, suggesting that the effect of light is stressful and is the reason of the increased carbohydrates content. Such an effect on carbohydrate production is a complex phenomenon: the increasing light favors carbohydrates accumulation up to the saturation point of photosynthesis, which is species dependent. On the opposite, at higher intensities strong photoinhibition occurred, leading to a decreased carbon fixation and consequent accumulation of energy reserves molecules (Cardoso et al., 2011; Ho et al., 2012; Wang et al., 2014; Vitova et al., 2015; Silva and Bertucco, 2016). This may explain the lower carbohydrate content of cells grown under 450 µmol m^{-2} s^{-1} found in our experiments.

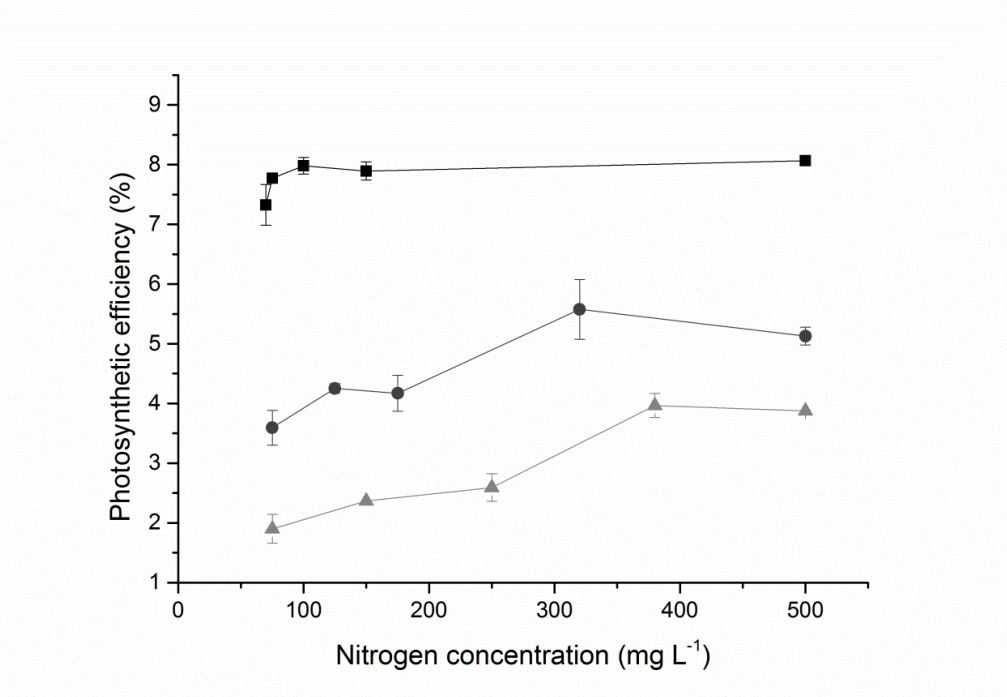

Figure 7.5: Photosynthetic efficiency calculated by eq. 7.4, as a function of inlet nitrogen concentration, for 150 (dark squares), 300 (gray circles) and 450 µmol photons m^{-2} s^{-1} (gray triangles).

As a small amount of nitrogen was always found in the reactor outlet (see **Table 7.1**), nitrogen limitation always occurred instead of starvation, which is commonly responsible of a lipid accumulation. Lipid content was measured in *Chlorella vulgaris* growth under both nitrogen excess and limitation (75N/50P) (see **Table 7.2**). It was observed that, while under nitrogen excess no accumulation of lipid was measured (ranging from 20 to 24 % DW depending on light availability), a slight increase was obtained under nitrogen limitation (from 28% under 150, to 37% under 450, confirming that light is a key parameter also in the case of lipid accumulation).

7.3.4 Effect of residence time on carbohydrate accumulation

The effect of residence time on carbohydrate accumulation was assessed under all irradiance values and under nitrogen limitation in order to evaluate the combined effect on biomass composition (the optimal value for each irradiance, as reported in previous section, i.e. 75, 125 and 150 mg L^{-1} of N for 150, 300 and 450 µmol photons m^{-2} s^{-1} respectively). As shown in **Figure 7.6**, an increased biomass concentration with the residence time was observed, as already reported for many other species, even under

inlet nitrogen limitation (data of inner nitrogen concentration are reported in **Table 7.3**). The carbohydrate fraction was found slightly increased with residence time, in particular, the case of 450 µmol photons m^{-2} s^{-1} at 4.4 days of residence time, with a value of about 52% DW. It confirms that at higher residence times the carbohydrate accumulation is enhanced, as a result of the lower apparent growth rate which is imposed by the dilution rate (Kliphuis et al., 2012; Sforza et al., 2014b). In fact, in a continuously stirred biological reactor working at steady state, the average growth rate corresponds to the dilution rate. As a consequence, at low residence time cells undergo faster duplication, while at higher residence time the average growth rate is slower, and cells are able to accumulate reserve materials (Sforza et al., 2014b).

On the other hand, even though the biomass and carbohydrate concentration increased with residence time, the biomass productivity showed a different trend. As reported before (Barbera et al., 2015), it shows a maximum when plotted against the residence time, after which the biomass productivity decreases. Accordingly, in our experiments, a decrease of biomass productivity was observed while increasing the residence time, which was apparently not compensated by the increased carbohydrate content. Thus, the carbohydrate productivity remained almost stable for all the residence times tested.

Table 7.3: Nitrogen and phosphorus outlet concentration from the reactor at different residence times (N/P inlet concentrations under each light intensity: 150 – 75N/50P, 300 – 125N/50P and 450 – 150N/50P).

Light Intensity (µmol m^{-2} s^{-1})	**Residence Time (days)**	**N_{out} (mg L^{-1})**		**P_{out} (mg L^{-1})**	
		Avg	StD	Avg	StD
150	2.9	10.45	2.14	28.94	1.94
	3.6	8.08	0.38	28.08	0.93
	4.4	5.92	0.22	27.35	0.90
300	2.9	1.00	0.01	6.21	1.02
	3.6	0	--	11.65	1.26
	4.4	0	--	9.56	3.10
450	2.9	2.48	0.65	9.81	2.26
	3.6	1.70	0.94	11.51	2.49
	4.4	2.08	0.20	6.40	0.20

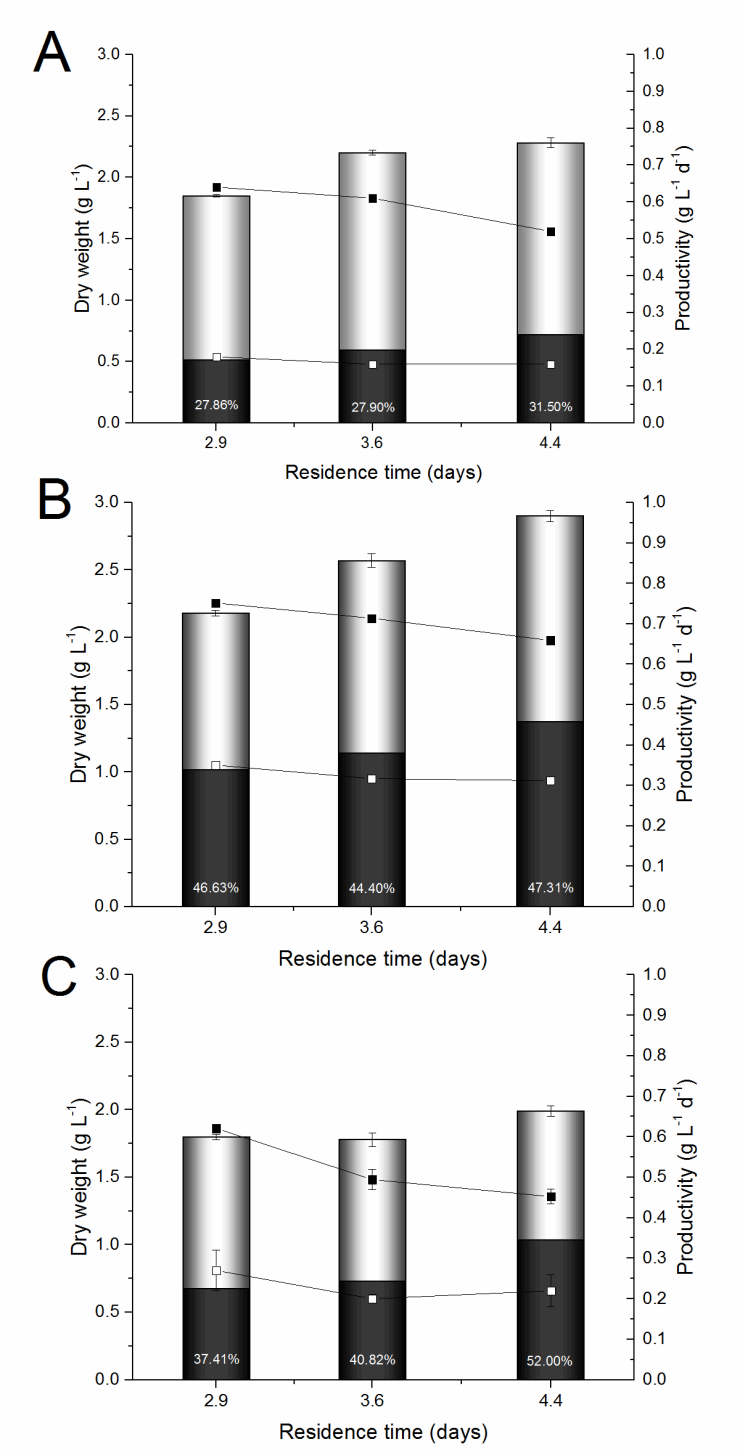

Figure 7.6: Biomass concentration (gray bars) and carbohydrate fraction (DW) (dark bars) of *C. vulgaris* at steady state under 150 (A) - 300 (B) – 450 (C) µmol photons m^{-2} s^{-1}, as a function of residence time. Dark and open squares refer to biomass and carbohydrates productivity, respectively. Numbers on the bars report the carbohydrate-biomass ratio (%DW).

7.3.5 Discussion on nutrient consumption in continuous system

By measuring the nitrogen and phosphorus consumed by the biomass at steady state, different nutrient/biomass yields were found under different operating conditions, suggesting that the elemental biomass composition of microalgae may change. In particular, as reported in **Figure 7.7A**, the nitrogen content of biomass increased together with the inlet nitrogen concentration, but it was found to be independent with respect to light intensity. In addition, a plateau was found at about 12 % N X^{-1}, suggesting that, even though *C. vulgaris* is able to adapt its composition to that of the external environment, a maximum N content is reached, and that no luxury uptake of this nutrient is occurring, even under high external concentrations.

Also, the residence time played a role on the nitrogen content of biomass, as reported in **Figure 7.7B**. Even though the inlet nitrogen concentration was kept constant (75, 125 and 150 mg L^{-1} of N for 150, 300 and 450 µmol photons m^{-2} s^{-1} respectively), the N/biomass ratio decreased with the residence time, as already observed in Sforza et al. (2013b) for *S. obliquus*.

Noteworthy, a different trend was observed in the case of phosphorus, with a very wide range of yield data (from 0.5 to about 4 %), suggesting that *C. vulgaris* is able to accumulate phosphorus inside the cell. The luxury uptake of phosphorus in a common response in many species of microalgae, and accumulation of internal polyphosphates was already observed in *Chlorella* genus (Atchinson and Butt, 1973).

On the other hand, our results showed that the P content decreases when increasing the inlet concentration of nitrogen. This is quite surprising, but can be explained by focusing on the effect of light on P uptake. In fact, as it can be seen by figure 7A, the P content is always higher under higher irradiances. This is a common phenomenon for microalgae (Sanchez et al., 1999; Powell et al., 2009), because P uptake is linked to light intensity, showing that algae may transform P into high energy organic compounds by photophosphorylation, where light energy is transformed and incorporated into ATP (Sanchez et al., 1999).

This is also probably the reason of trends reported in **Figure 7.8A**, where it seems that P content is inversely related to nitrogen concentration in the feed. Thus, this is simply a side effect of nitrogen limitation on biomass concentration at steady state. The higher the limitation of nitrogen, the lower is the biomass concentration at steady state.

Accordingly, at the same incident light, the specific light supply rate, i.e. the light effectively perceived by the cells, increases, thus affecting the P uptake rate, which is light dependent. This is confirmed by data reported in **Figure 7.8B**, where the P content is depicted as a function of specific light supply rate, for all incident lights and residence times tested: data were found, with a good approximation, linearly correlated to the r_{EX}. This can also be due to the fact that P was always provided in excess, thus allowing the microalgae to change its composition depending on light availability only. This is not the case of nitrogen content, which was instead driven directly by the nutrient limitation.

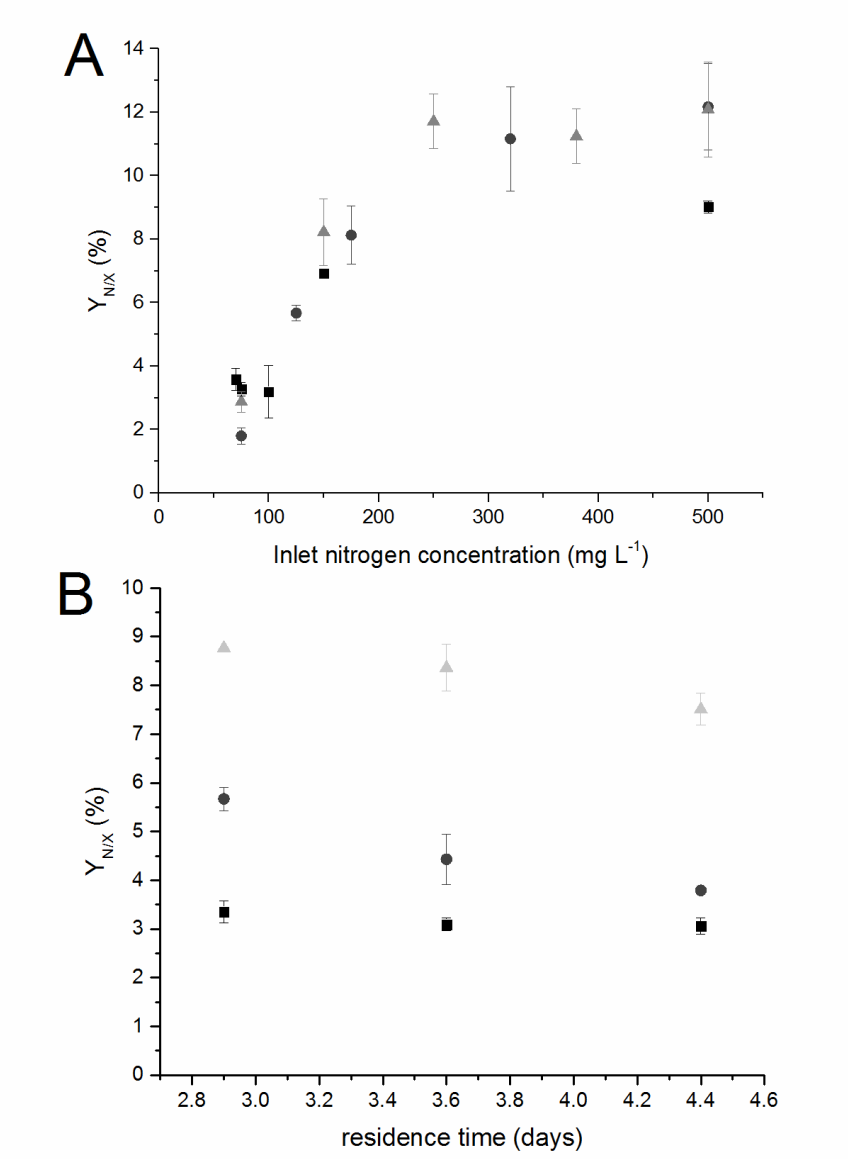

Figure 7.7: Nitrogen content of biomass at steady state as a function of inlet nitrogen concentration (A) and residence time (B), Dark squares refer to 150 µmol photons m^{-2} s^{-1} while gray circles and gray triangles to 300 and 450 µmol photons m^{-2} s^{-1}, respectively.

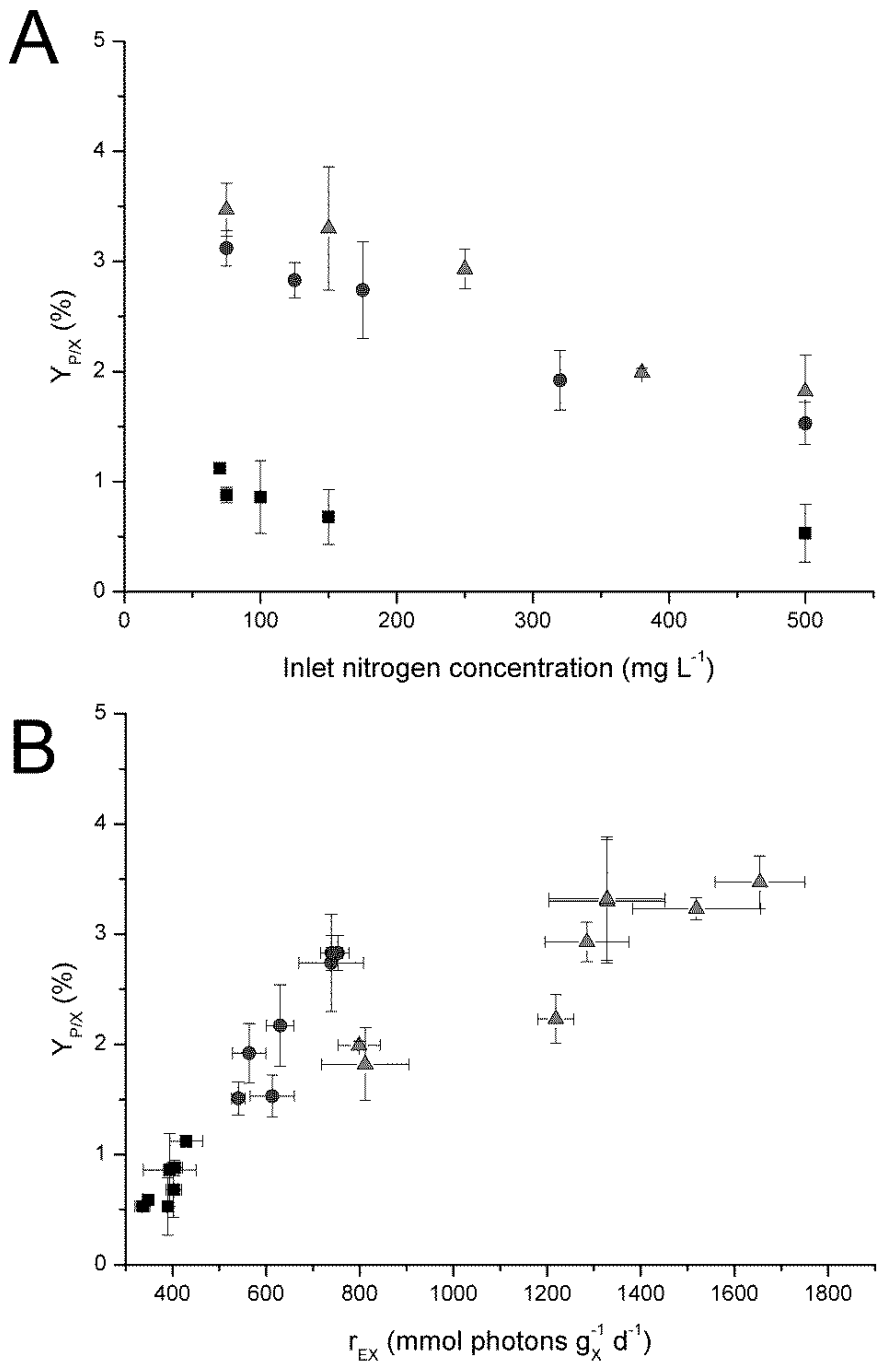

Figure 7.8: Phosphorus content of biomass at steady state as a function of inlet nitrogen concentration (A) and specific light supply rate (B). Dark squares refer to 150 µmol photons m^{-2} s^{-1} while gray circles and gray triangles to 300 and 450 µmol photons m^{-2} s^{-1}, respectively. In 7B results obtained at different residence times are also reported.

7.4 CONCLUSIONS

Chlorella vulgaris is able to accumulate carbohydrate under nitrogen starvation, which however may affect the biomass productivity. In this work it was shown that, by properly managing the inlet nitrogen concentration, an optimum value can be found where carbohydrate accumulation compensates the loss of biomass due to starvation, thus leading to a higher overall carbohydrate productivity. In addition, working at higher residence times is a valid strategy to increase the carbohydrate ratio in biomass. N/biomass yield is directly related to the nitrogen availability, while P was strongly affected by the specific light supply rate.

REFERENCES

Ashokkumar, V., Salam, Z., Tiwari, O.N., Chinnasamy, S., Mohammed, S., Ani, F.N., 2015. An integrated approach for biodiesel and bioethanol production from Scenedesmus bijugatus cultivated in a vertical tubular photobioreactor. Energy Convers. Manag. 101, 778–786. doi:10.1016/j.enconman.2015.06.006.

Atchinson, P.A., Butt, V.S., 1973. The relation between the synthesis of inorganic ployphosphate and phosphate uptake by *Chlorella vulgaris*. J. Exp. Bot. 24, 497–510.

Barbera, E., Sforza, E., Bertucco, A., 2015. Maximizing the production of *Scenedesmus obliquus* in photobioreactors under different irradiation regimes: experiments and modeling. Bioprocess Biosyst. Eng. 38, 2177–2188. doi:10.1007/s00449-015-1457-9.

Bertucco, A., Beraldi, M., Sforza, E., 2014. Continuous microalgal cultivation in a laboratory-scale photobioreactor under seasonal day-night irradiation: experiments and simulation. Bioprocess Biosyst. Eng. 37, 1535–1542. doi:10.1007/s00449-014-1125-5.

Brányiková, I., Maršálková, B., Doucha, J., Brányik, T., Bisova, K., Zachleder, V., Vitovà, M., 2011. Microalgae-novel highly efficient starch producers. Biotechnol. Bioeng. 108, 766–776. doi:10.1002/bit.23016.

Cardoso, A.S., Eliza, G., Vieira, G., Kappes, A., 2011. O uso de microalgas para a obtenção de biocombustíveis. Rev. Bras. Biociência. 9, 542–549.

Clark, D.R., Flynn, K.J., Owens, N.J.P., 2002. The large capacity for dark nitrate-assimilation in diatoms may overcome nitrate limitation of growth. New Phytol. 155,101–108.

Gonzalez-Fernandez, C., Ballesteros, M., 2012. Linking microalgae and cyanobacteria culture conditions and key-enzymes for carbohydrate accumulation. Biotechnol.

Adv. 30, 1655–1661. doi:10.1016/j.biotechadv.2012.07.003.

Ho, S.H., Chen, C.Y., Chang, J.S., 2012. Effect of light intensity and nitrogen starvation on CO 2 fixation and lipid/carbohydrate production of an indigenous microalga Scenedesmus obliquus CNW-N, Bioresour. Technol. 113, 244–252. doi:10.1016/j.biortech.2011.11.133.

Ho, S., Kondo, A., Hasunuma, T., Chang, J., 2013. Engineering strategies for improving the CO_2 fixation and carbohydrate productivity of *Scenedesmus obliquus* CNW-N used for bioethanol fermentation. Bioresour. Technol. 143, 163–171. doi:10.1016/j.biortech.2013.05.043. (a)

Ho, S.H., Huang, S.W., Chen, C.Y., Hasunuma, T., Kondo, A., Chang, J.S., 2013. Characterization and optimization of carbohydrate production from an indigenous microalga *Chlorella vulgaris* FSP-E. Bioresour. Technol. 135, 157–165. doi:10.1016/j.biortech.2012.10.100. (b)

Ho, S.H., Ye, X., Hasunuma, T., Chang, J.S., Kondo, A., 2014. Perspectives on engineering strategies for improving biofuel production from microalgae - A critical review. Biotechnol. Adv. 32, 1448–59. doi:10.1016/j.biotechadv.2014.09.002.

Kim, K.H., Choi, I.S., Kim, H.M., Wi, S.G., Bae, H.J., 2014. Bioethanol production from the nutrient stress-induced microalga *Chlorella vulgaris* by enzymatic hydrolysis and immobilized yeast fermentation, Bioresour. Technol. 153, 47–54. doi:10.1016/j.biortech.2013.11.059.

Kim, S.S., Ly, H.V., Kim, J., Lee, E.Y., Woo, H.C., 2015. Pyrolysis of microalgae residual biomass derived from *Dunaliella tertiolecta* after lipid extraction and carbohydrate saccharification. Chem. Eng. J. 263, 194–199. doi:10.1016/j.cej.2014.11.045.

Kliphuis, A.M.J., Klok, A.J., Martens, D.E., Lamers, P.P., Janssen, M., Wijffels, R.H., 2012. Metabolic modeling of Chlamydomonas reinhardtii: energy requirements for photoautotrophic growth and maintenance. J. Appl. Phycol. 24, 253–266. doi:10.1007/s10811-011-9674-3.

Markou, G., Angelidaki, I., Nerantzis, E., Georgakakis, D., 2013. Bioethanol production by carbohydrate-enriched biomass of *Arthrospira* (*Spirulina*) *platensis*. Energies 6, 3937–3950. doi:10.3390/en6083937.

Markou, G., Vandamme, D., Muylaert, K., 2014. Microalgal and cyanobacterial cultivation: The supply of nutrients. Water Res. 65, 186–202. doi:10.1016/j.watres.2014.07.025.

Mollers, K.B., Cannela, D., Jørgensen, H., Frigaard, N.-U., 2014. Cyanobacterial biomass as carbohydrate and nutrient feedstock for bioethanol production by yeast fermentation. Biotechnol. Biofuels. 7, 64. doi:10.1186/1754-6834-7-64.

Moraes, B.S., Zaiat, M., Bonomi, A., 2015. Anaerobic digestion of vinasse from

sugarcane ethanol production in Brazil: Challenges and perspectives. Renew. Sustain. Energy Rev. 44, 888–903. doi:10.1016/j.rser.2015.01.023.

Powell, N., Shilton, A., Chisti, Y., Pratt, S., 2009. Towards a luxury uptake process via microalgae--defining the polyphosphate dynamics. Water Res. 43, 4207–4213. doi:10.1016/j.watres.2009.06.011.

Quigg, A., Beardall, J., 2003. Protein turnover in relation to maintenance metabolism at low photon flux in two marine microalgae. Plant. Cell Environ. 26, 693–703.

Renewable Fuel Association, web page, (2016). Available in: http://www.ethanolrfa.org/

Ruiz, J., Alvarez-Diaz, P.D., Arbib, Z., Garrido-Pérez, C., Barragan, J., Perales, J.A., 2013. Performance of a flat panel reactor in the continuous culture of microalgae in urban wastewater: prediction from a batch experiment. Bioresour. Technol. 127, 456–63. doi:10.1016/j.biortech.2012.09.103.

Sancho, M.M.E., Castillo, J.M.J., Yousfi, F.E., 1999. Photoautotrophic consumption of phosphorus by *Scenedesmus obliquus* in a continuous culture . Influence of light intensity. Process Biochem. 34, 811–818.

Sforza, E., Tercero, E.A.R., Gris, B., Bettin, F., Milani, A., Bertucco, A., 2014. Integration of *Chlorella protothecoides* production in wastewater treatment plant: From lab measurements to process design. Algal Res. 6, 223–233. doi:10.1016/j.algal.2014.06.002. (a)

Sforza, E., Urbani, S., Bertucco, A., 2014. Evaluation of maintenance energy requirements in the cultivation of *Scenedesmus obliquus*: effect of light intensity and regime, J. Appl. Phycol., 10811-11014. In Press. doi:10.1007/s10811-014-0460-x. (b)

Silva, C.E.F., Bertucco, A., 2016. Bioethanol from microalgae and cyanobacteria: A review and technological outlook. Process Biochem 51, 1833-1842. doi:10.1016/j.procbio.2016.02.016.

Sobczuk, T.M., Camachi, F.G., Rubio, F.C., Fernandes, F.G.A., Grima, E.M., 2000. Carbon dioxide uptake efficiency by outdoor microalgal cultures in tubular airlift photobioreactors. Biotechnol. Bioeng. 67, 465–475. http://www.ncbi.nlm.nih.gov/pubmed/10620762.

Tang, H., Chen, M., Ng, K.Y.S., Salley, S.O., 2012. Continuous microalgae cultivation in a photobioreactor., Biotechnol. Bioeng. 109, 2468–2474. doi:10.1002/bit.24516.

Tercero, E.A.R., Sforza, E., Morandini, M., Bertucco, A., 2013. Cultivation of *Chlorella protothecoides* with Urban Wastewater in Continuous Photobioreactor: Biomass Productivity and Nutrient Removal. Appl. Biochem. Biotechnol. doi:10.1007/s12010-013-0629-9.

Vitova, M., Bisova, K., Kawano, S., Zachleder, V., 2015. Accumulation of energy reserves in algae: From cell cycles to biotechnological applications. Biotechnol. Adv. 33, 1204–1218. doi:10.1016/j.biotechadv.2015.04.012.

Wang, H., Ji, C., Bi, S., Zhou, P., Chen, L., Liu, T., 2014. Joint production of biodiesel and bioethanol from filamentous oleaginous microalgae *Tribonema sp.* Bioresour. Technol. 172, 169–173. doi:10.1016/j.biortech.2014.09.032.

Chapter 8

Stability of carbohydrate production in continuous microalgal cultivation under nitrogen limitation: Effect of irradiation regime and intensity on *Scenedesmus obliquus*

In this chapter, the effect of nitrogen limitation on *Scenedesmus obliquus* cultivation was evaluated in a continuous system operated at steady-state to assess the carbohydrate productivity in a single step. Under continuous irradiance (150 and 650 µmol photons m^{-2} s^{-1}), with an optimized nitrogen limitation in the reactor inlet stream, a carbohydrate fraction of 45% was achieved, with a remarkable productivity of 0.80 g L^{-1} day^{-1}. Under simulated day-night irradiation a cyclic steady state was obtained, as a result of alternating light and dark conditions, with an average carbohydrate production of 0.71 and 0.30 g L^{-1} day^{-1} (Summer and Winter, respectively), with a biomass productivity reduced due to the photoperiod. The uptake of nutrient by the cell appeared to be regulated by the light regime, which determines the carbohydrate accumulation as well. Accordingly, it was possible to obtain a stable carbohydrate production in one-step continuous system with day-night and seasonal irradiation, by properly managing the nitrogen inlet•.

•*Part of this chapter was published in Journal of Applied Phycology (**Silva, C.E.F**., Sforza, E., Bertucco, A., in Press, 2017).*

8.1 INTRODUCTION

The energy production from renewable sources is one of the major challenge of this century, as the 85% of the global energetic consumption is still currently derived by fossil carbon sources (Moraes et al., 2015). The growing demand for alternative energy sources is increasing the interest on biofuel production: in this scenario, bioethanol is probably the main one, with a global production of approximately 25 billion gallons per year (over 100 million m^3 y^{-1}) (RFA, 2016).

Boosting ethanol production from higher plants is highly linked to land availability and climatic limitations, apart from the competition to food/feed sources. In this context, microalgae and cyanobacteria have potential advantages, such as higher growth rates, possibility of cultivation in non-arable land and higher content of carbohydrates on dry weight (DW) basis (Silva and Bertucco, 2016).

Carbohydrates accumulation in microalgae, in the form of starch and glycogen, may reach a value up to 60% DW (Pirt and Pirt, 1977; Chen et al., 2013; Silva and Sforza, 2016), depending on several variables, such as light intensity, temperature, carbon source, growing time, nutrients availability, salinity and pH. So far, several carbohydrate-rich microalgae and cyanobacteria species were studied for bioethanol production, such as *Chlorella vulgaris* (Kim et al., 2014), *Dunaliella tertiolecta* (Kim et al., 2015), *Scenedesmus* spp. (Ho et al., 2013a; Ashokkumar et al., 2015), *Tribonema* sp. (Wang et al., 2014), *Arthrospira platensis* (Markou et al., 2014) and *Synechococcus* sp. (Mollers et al., 2014; Silva et al., 2017).

Nitrogen limitation/starvation is recognized as one of the most efficient methods to trigger carbohydrate accumulation in many species, because it induces a significant decrease of protein production, so that the energy absorbed in excess is delivered to energetic reserves like carbohydrates and lipids (Chen et al., 2013; Vitovà et al., 2015; Xia et al., 2016; Mortensen and Gislerød, 2016). Generally, as nitrogen limitation also decreases biomass productivity, the cultivation of microalgal species is performed in batch conditions using a two-step cultivation, i.e. a growth step, followed by carbohydrate accumulation under nitrogen starvation, with a consequent lower productivity and higher complexity and duration of the process.

On the other hand, it is generally recognized that continuous cultivation can maximize microalgal biomass productivity, even though little information is available on steady

state production of carbohydrate-rich biomass. So far, the effect of residence time and nitrogen limitation in continuous reactors was investigated in the case of *Scenedesmus obliquus* (Ho et al. 2013b), *Neochloris oleabundans* (De Winter et al., 2014) and *Chlorella vulgaris* (Silva and Sforza, 2016) but under continuous irradiation regime. However, if the purpose of cultivation is biofuel production, the microalgal growth must be carried out outdoor, under sunlight irradiation. Consequently, as the carbohydrate fraction is a form of energy storage, they may be consumed overnight, due to respiration, at an extent which may also depend on the season. In fact, the photoperiod may strongly affect the microalgal composition, as a possible result of a circadian clock regulation (Jacob-Lopes et al., 2009; De Winter et al., 2013; De Winter et al., 2014; Krzeminska et al., 2014; De Winter et al., 2017b). Besides the day-night cycle, also the average light intensity significantly changes as a function of the season at middle latitudes (Ma et al., 1997; Boechat and Giani, 2008; Bertucco et al., 2014; Guccione et al., 2014), and little information is known about the effect of real light regime on continuous cultivation of microalgae and cyanobacteria for carbohydrate production.

In this chapter *Scenedesmus obliquus* was grown in flat panel lab-scale continuous photobioreactors (PBR), under different light intensities and light/dark regimes, applying also nitrogen limitation in the inlet stream to trigger carbohydrate accumulation. In particular, two irradiation regimes were studied to simulate Summer and Winter seasons at middle latitudes, in order to assess the effect on steady state biomass concentration and carbohydrate productivity, with particular attention on carbohydrate changes in the biomass as a result of overnight respiration phenomena.

8.2 MATERIAL AND METHODS

8.2.1 Microalgae and media composition

The microalgal species *Scenedesmus obliquus* (obtained from SAG-Goettingen) was maintained and cultured in modified BG11 medium (buffered with 10 mM HEPES pH 8), which was sterilized in an autoclave for 20 min at 121°C. The P and N content of the medium, in the form of K_2HPO_4 and $NaNO_3$, were optimized to investigate the nutrient starvation, and concentrations for each condition are reported in the corresponding section.

8.2.2 Equipment

Preliminary batch experiments were performed in 250 mL working-volume glass vertical cylinders (5 cm diameter), continuously mixed by a stirring magnet placed at the bottom of the bottle.

Continuous experiments were performed in vertical flat-plate polycarbonate (continuously stirred tank reactor) CSTR PBR (see Sforza et al. (2015) and Bertucco et al. (2014) for the schematic of the experimental setup), with a working volume of 300 mL, a depth of 1.2 cm, and a surface exposed to light of 250 cm^2. CO_2 in excess was provided by a CO_2–air (5% v/v) bubbling at the reactor bottom (1 L h^{-1} of total gas flow rate). A magnetic stirrer was also used to increase mixing in the PBR, and prevent any deposition of biomass. The fresh medium was fed at a constant rate by a peristaltic pump (Watson-Marlow sci400, flow rate range: 25-250 mL d^{-1}). Light was provided by a LED lamp (Photon System Instruments, SN-SL 3500-22) for both continuous and batch experiments. Photon Flux Density (PFD) was measured on both the reactor front and back using a photoradiometer (HD 2101.1 from Delta OHM), which quantifies the Photosynthetically Active Radiation (PAR). The light intensity as a function of time was simulated so that to provide the same PAR amount of energy received under natural conditions at the selected middle latitude (see Sforza et al., 2015), using a controller able to regulate the light-dark cycle by gradually varying the light intensity during the day, similarly to real sunlight conditions. The software PVGIS Solar Irradiation Data (http://re.jrc.ec.europa.eu/pvgis/) was the source of irradiation data for the location of Padova, Italy. Two typical days of January and July were selected as representatives of Winter and Summer seasons, respectively.

8.2.3 Experimental procedures

In steady state continuous experiments, *S. obliquus* was inoculated into the reactor with the culture medium, and batch operation mode was set at the beginning, to prevent the occurring of washout. Once reached a significant concentration (around 10^8 cells mL^{-1}), the operation was switched to continuous, feeding the fresh medium from a tank with the peristaltic pump, and simultaneously withdrawing the equivalent product flow rate. The working volume (V_{PBR}) was controlled by an overflow tube, and the outlet flow

rate Q (mL d^{-1}) was collected in a second tank. So, the hydraulic residence time (τ) in the reactor was directly controlled by the peristaltic pump, according to:

$$\tau = \frac{V_{PBR}}{Q} \quad (8.1)$$

When steady-state operation was achieved, biomass was sampled and analyzed for at least 3 to 7 days. Under day-night irradiation, biomass was sampled three times: at the beginning, at the peak and at the end of the light period, for at least 4 days consecutively. Once steady state was reached, the biomass density (C_x), the carbohydrates content (C_{Ch}) as well as the N and P consumptions were measured. The volumetric biomass productivity P_X (g $L^{-1}d^{-1}$) was calculated as:

$$P_X = \frac{C_X}{\tau} \quad (8.2)$$

where C_X is the biomass concentration (DW) at steady-state.

Carbohydrate productivity (P_{Ch}) was calculated as:

$$P_X = P_{ch}.Carbohydrate\ content\ \ (\%) \quad (8.3)$$

The nutrient yield was evaluated as:

$$Y_{i/X} = \frac{C_{i,in} - C_{i,out}}{C_X} \quad (8.4)$$

where C_i refer to nutrient concentration in the inlet and outlet (mg L^{-1}). To assess the effect of nutrients feed rate on biomass and carbohydrates concentration, $C_{i,in}$ was changed and transient conditions were observed, until a new steady state was reached.

The photon flux density absorbed by the algae (PFD_{abs}) was also measured at steady state, according to:

$$PFD_{abs} = I_{in} - B_I - I_0 \quad (8.5)$$

where I_{in} is the incident light (mmol m^{-2} d^{-1}), B_I the back irradiance (mmol m^{-2} d^{-1}), and I_0 the light absorbed by the medium and the panel walls (mmol m^{-2} d^{-1}).

The photosynthetic efficiency (PE) (Kliphuis et al., 2012; Sforza et al., 2015), i.e. the fraction of PAR converted to biomass, was calculated as:

$$\%PAR = \frac{C_x * Q * LHW}{PFD_{abs} * E_p * A_{PBR}} \quad (8.6)$$

where *LHV* is the biomass Lower Heating Value (assumed equal to 20 kJ g_{DW}^{-1}), E_p the energy of photons (kJ μmol^{-1}), and A_{PBR} is the irradiated surface of the reactor (m^2).

8.2.4 Analytical methods

The biomass concentration was monitored daily by spectrophotometric analysis of the optical density (OD_{750}) with an UV-Visible spectrophotometer (UV 500, Spectronic Unicam, UK), and correlated to cell concentration, measured with a Bürker Counting Chamber (HBG, Germany). The concentration of biomass was also gravimetrically measured as dry weight (DW) in terms of g L^{-1} in cells previously harvested with a 0.22 µm filter, and then dried for 4 h at 80 °C in a laboratory oven. The nutrients analyzed were nitrate ($N\text{-}NO_3$) and phosphate ($P\text{-}PO_4$), assessed at least three times at each steady state. Samples of culture were filtered (0.2 µm) to evaluate the dissolved nutrients: $N\text{-}NO_3$ concentration was measured by an analytical test kits provided by St. Carlo Erba Reagenti, Italy, (code 0800.05482) and orthophosphates by the ascorbic acid method described in APHA-AWWA-WEF (1992). These measurements were performed at both the reactor inlet and outlet and the nutrient/biomass yields $Y_{i/X}$ (mg_i $mg_{biomass}^{-1}$) were calculated according to equation 8.4. The carbohydrate content of biomass was determined by the Anthrone method (Trevelyan and Harrison, 1952).

8.2.5 Respirometric test

In order to evaluate the oxygen production rate of *S. obliquus*, tests based on respirometry were carried out. Dissolved oxygen (DO) concentration was continuously measured by means of a Handylab Ox 12 SCHOTT® oximeter connected to a PC by using Multi/ACHAT II software provided by WTW. The oxygen measurement was carried out in airtight flasks of 25 mL, in order to prevent oxygen transfer between the liquid and the external air. In addition, no gas headspace was left to avoid gas losses. The liquid was continuously mixed by a magnetic stirrer and the temperature was maintained constant at 25°C by a thermostatic water bath.

Each respirometric test was started with fresh culture medium (modified BG-11, 180N-100P – optimized condition), where a constant biomass inoculum (about 0.4 g L^{-1} of DW), previously centrifuged, was resuspended and 0.20 g L^{-1} of sodium bicarbonate was added. The pH of the medium was buffered at 7 with HEPES 1M to avoid pH

increase and consequent shifting of bicarbonate to carbonate ion. The biomass inoculum used was sampled from the continuous experiments, at steady-state, and at different times of the day when exposed to day-night regime.

Each test lasted about 90 min and consisted in alternating cycles of light and dark (15:15 min), obtained by a digital controller connected to a neon lamp at the final irradiation of 45 µmol photons m^{-2} s^{-1}. Each experiment started in the dark phase, and the first 15 min of data acquisition were discarded because that time was considered necessary for the acclimation of the microorganisms to the applied environmental conditions.

Based on the slope of increasing (light on) and decreasing DO values (light off) the oxygen production rate (OPR) and consumption rate (OCR, µg O_2 L^{-1} min^{-1}) were obtained. All OPR and OCR values were the average of at least three measurements.

8.2.6 Statistical analysis

Student's t tests were applied to ascertain significant differences in carbohydrate ratio under different inlet nitrogen concentration in continuous experiments. The level of statistical significance was $p<0.05$.

8.3 RESULTS

8.3.1 Carbohydrate accumulation in batch cultures

A first batch control growth curve was carried out to assess the growth rate and carbohydrate accumulation of *Scenedesmus obliquus*, under an irradiance of 150 µmol photons m^{-2} s^{-1}. Results are reported in **Figure 8.1**. This species showed a remarkable maximum growth rate constant (μ_{max}) of 0.94 day^{-1} and a final biomass concentration of 3.8 g L^{-1}. At the beginning of the growth curve the carbohydrates content was about 20% DW, which started to increase when the external nitrogen source became limiting, reaching a value of about 58% DW at the end of the stationary phase.

In **Figure 8.1**, *S. obliquus* is able to accumulate carbohydrate under N limitation (not starvation) as at the end of the growth curve, a small concentration of nitrate is still present in the external medium. Even though the nitrogen was not completely depleted, the carbohydrate percent reached remarkable values.

8.3.2 Carbohydrate production at steady-state under continuous light

The production of carbohydrate in continuous systems was firstly verified under non-limiting nitrogen supply to assess the metabolic response of this species (results are reported in **Figure 8.2**). About 25 experiments were performed (Sforza et al., 2015), at different residence times, light intensities, seasonality and excess of nutrients (500N-200P mg L^{-1}), showing a carbohydrate content between 11-28% (19 ± 4.1 as average). Accordingly, it can be concluded that *Scenedesmus obliquus*, under excess of nitrogen, produces low amount of carbohydrates at steady state.

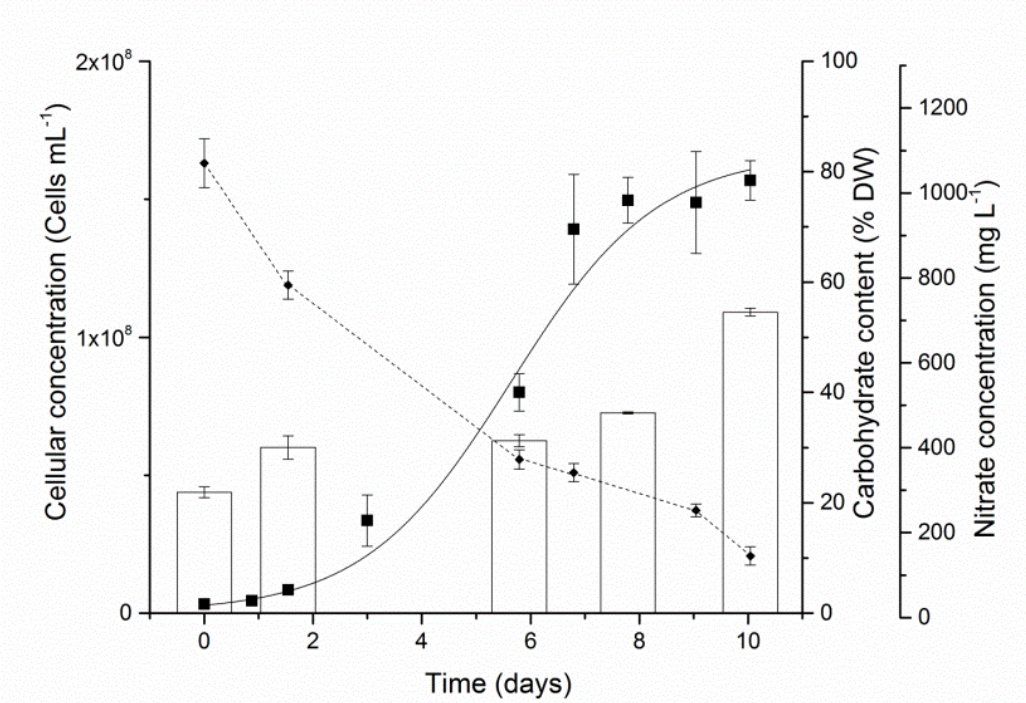

Figure 8.1: Cell concentration (black squares) of batch growth curve of *S. obliquus*. White bars refer to the carbohydrate content (%DW – dry weight) while black rhombus correspond to the NO_3^- concentration in the culture medium, measured during the growth curve. Light intensity of 150 µmol photons m^{-2} s^{-1}, DW (g L^{-1}) = 0.0192C_X (millions of cells mL^{-1}) + 0.2521 (R^2 = 0.9885). Error bars represent the standard deviation. n (independent replicates) = 2.

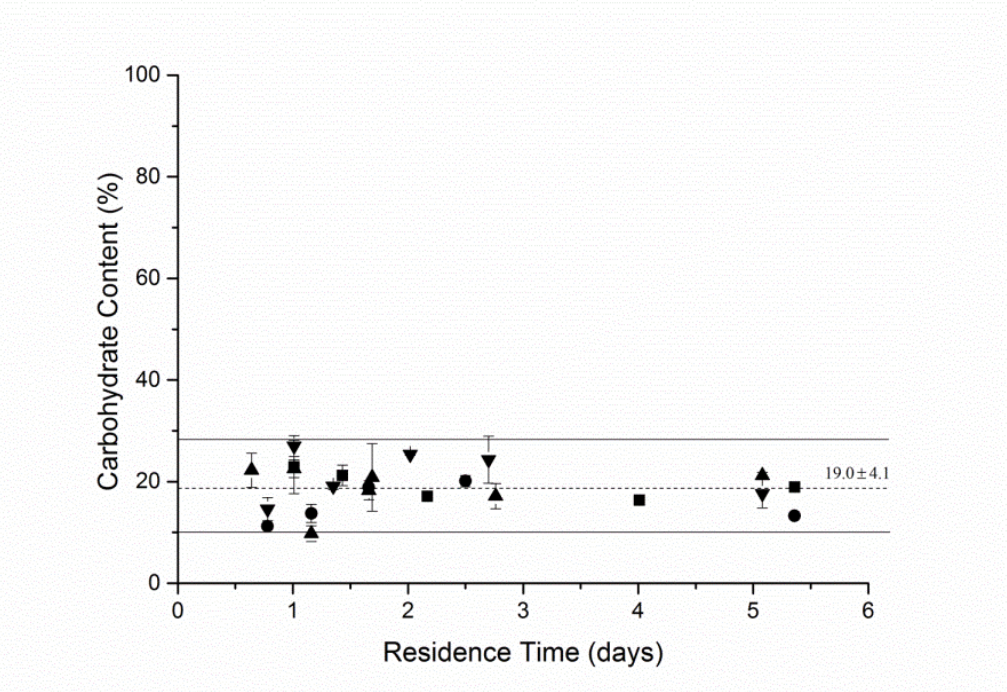

Figure 8.2: Carbohydrate content under excess of nutrients (N and P) as a function of residence time. The symbols represent: (■)150 µmol photons m^{-2} s^{-1} (●) 650 µmol photons m^{-2} s^{-1} (▲) Summer and (▼) Winter.

In this work, further experiments were carried out under nitrogen limitation, to assess the effect of this variable on steady state cultivation. Nitrogen limitation in the continuous system was performed under two different irradiances (650 and 150 µmol photons m^{-2} s^{-1}) to evaluate the relation between N limitation and light intensity and to assess the possibility of obtaining continuous carbohydrate production in the case of *S. obliquus*.

Starting from N and P excess experiments, where the biomass concentration and productivity, as well as nutrients consumption and carbohydrates content can be evaluated, the nutrients inlet were progressively decreased. The residence time was kept constant at 2.45 ± 0.25 days. Under nutrient excess, biomass concentrations of 3 and 5.5 g L^{-1} at 150 and 650 µmol photons m^{-2} s^{-1} were obtained, respectively, but the carbohydrate content was between 15-17%, with consequent low carbohydrate productivities (**Figure 8.3**).

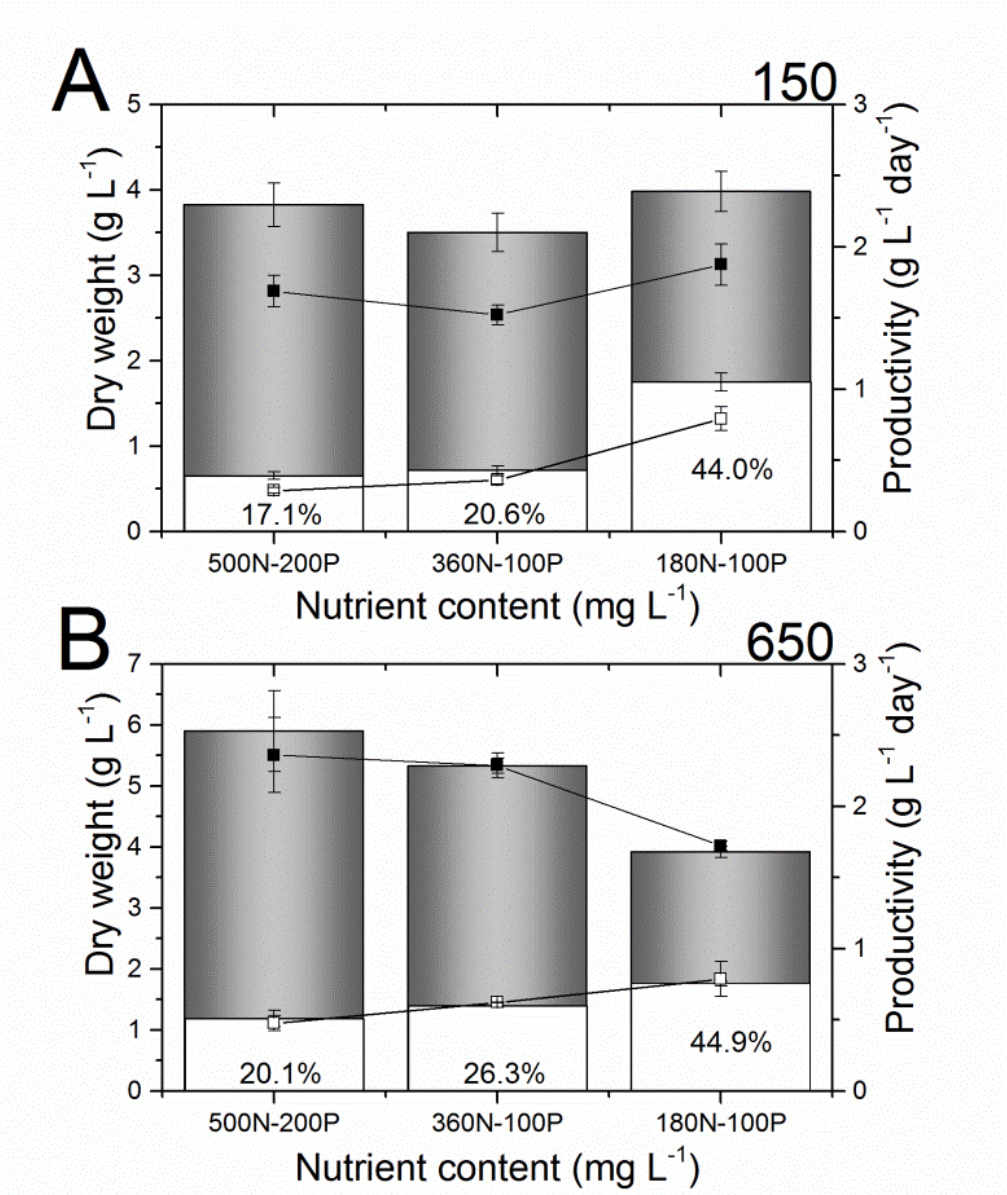

Figure 8.3: Biomass concentration (grey bars) and carbohydrate fraction (DW) (white bars) of *S. obliquus* at steady state under 150 µmol photons m^{-2} s^{-1} (A) and 650 µmol photons m^{-2} s^{-1} (B), with different inlet concentration of nutrients, reported as elemental concentrations. Dark and open squares refer to biomass and carbohydrates productivity, respectively. Numbers on the bars report the carbohydrate-biomass ratio (%DW). Error bars represent the standard deviation. n (independent replicates) ≥ 5.

A higher carbohydrate content was obtained when the nitrogen concentration outlet was almost consumed (limitation condition), reaching a remarkable value of about 45% (**Figure 8.3**). At 650 µmol photons m^{-2} s^{-1}, photosaturation/photoinhibition phenomena probably occurred, as biomass production was reduced from 2.3 to 1.7 g L^{-1} day^{-1}. Apparently, under high irradiance, cells are more susceptible to the stress due to nitrogen depletion, resulting in a faster reduction of biomass productivity. On the other hand, by looking at the carbohydrate productivity, the N-limited steady-state cultivation showed to be effective. An optimum value was shown under both light intensities, around 0.80 g L^{-1} day^{-1}.

The specific response to nitrogen limitation is also confirmed by looking at the nitrogen yield (of N into biomass): under nitrogen limitation, in fact, the biomass contained much less nitrogen, around 4%, resulting in higher carbohydrate content, while values of 12-14% were observed under excess condition. The photosynthetic efficiency was higher at low light intensity (~17% for 150), being reduced significantly at 650 up to about 4.5% (**Table 8.1**).

Table 8.1: Nutrient content in biomass and light utilization at constant irradiance.

Constant Illumination	**Irradiance (µmol photons m^{-2} s^{-1})**					
	150			**650**		
	500N/200P	360N/100P	180N/100P	500N/200P	360N/100P	180N/100P
Nutrient content (%)						
N/X	12.90 ± 0.40	9.68 ± 0.36	4.07 ± 0.29	7.82 ± 0.93	5.36 ± 0.22	4.27 ± 0.12
P/X	2.16 ± 0.24	1.84 ± 0.14	1.95 ± 0.12	1.10 ± 0.16	1.23 ± 0.09	2.06 ± 0.06
Light utilization						
PE (%)*	18.10 ± 2.42	15.12 ± 0.58	17.83 ± 0.37	5.27 ± 0.71	4.62 ± 0.15	3.41 ± 0.13

*Photosynthetic efficiency. Values in table are represented as means ± standard deviation. n (independent replicates) = 4.

8.3.3 Effect of nitrogen limitation under day-night cycle and the time of the day

Thus, experiments were carried out under seasonal irradiation, at the same average light intensity of the experiments performed with constant light intensity.

The effect of nitrogen limitation in Summer and Winter was comparable to that under continuous light, with an increased carbohydrate content, even though the biomass concentration, as well as the photosynthetic efficiency, were lower, due to the biomass

loss in the dark (**Figure 8.4**, **Table 8.2**). A smaller decrease with respect to nutrient excess condition was observed under Summer, where a carbohydrate content more than 40% and a productivity of 0.71 g L^{-1} day^{-1} (average value) were obtained, which is good if compared to 0.79 g L^{-1} day^{-1} at constant light illumination. On the other hand, under simulated Winter conditions, the biomass production remarkably decreased (by 30%) as a result of nitrogen limitation, thus decreasing carbohydrate productivity, even though the carbohydrate content remained higher (33%). This difference between the two seasons is mainly due to the duration of the photoperiod, corresponding to 9 hours in the Winter, 15 hours in Summer.

Another interesting result is the nitrogen consumption under Winter irradiation: nitrogen outlet concentration remained higher, thus preventing N limitation to occur, as a possible result of changed uptake of nutrients in Winter. This may explain the difference in the carbohydrate content between Winter and constant irradiance of 150 µmol photons m^{-2} s^{-1} (33% in Winter and 44% at constant irradiance).

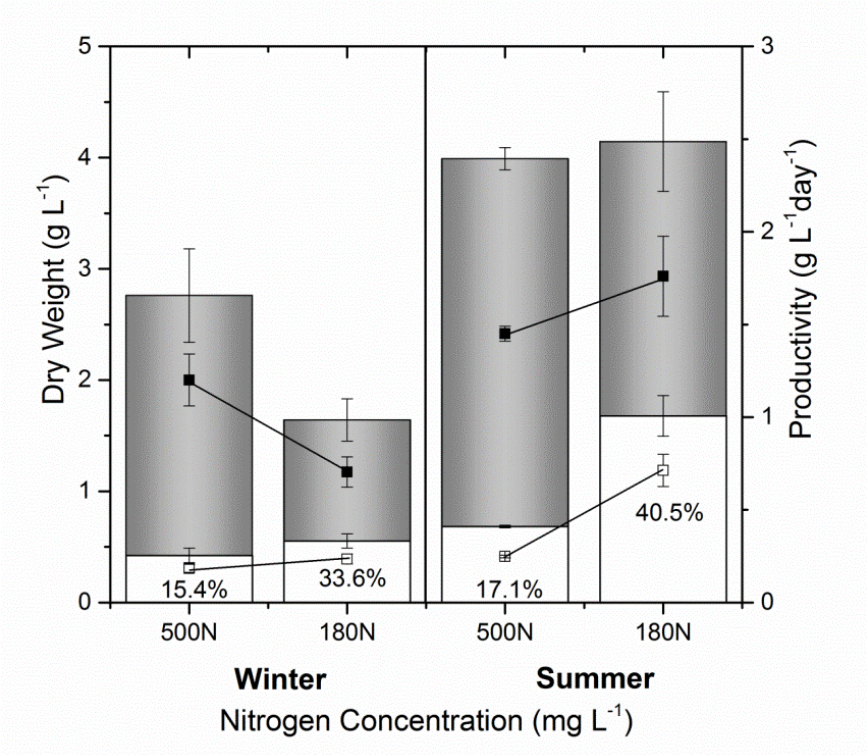

Figure 8.4: Biomass concentration (grey bars) and carbohydrate fraction (DW) (white bars) of *S. obliquus* at steady state under Winter and Summer with different inlet concentration of nutrients, reported as elemental concentrations. Dark and open squares refer to biomass and carbohydrates productivity, respectively. Numbers on the bars report the carbohydrate-biomass ratio (%DW). Error bars represent the standard deviation. n (independent replicates) ≥ 5.

Table 8.2: Nutrient content in biomass and light utilization at constant irradiance.

Constant Illumination	Irradiance (µmol photons m^{-2} s^{-1})			
	Winter		Summer	
	500N/200P	180N/100P	500N/200P	180N/100P
Nutrient content (%)				
N/X	13.8 ± 1.7	7.60 ± 0.25	11.6 ± 0.50	4.25 ± 0.59
P/X	1.0 ± 0.05	1.76 ± 0.14	1.4 ± 0.12	1.17 ± 0.20
Light utilization				
PE (%)*	18.84 ± 2.50	6.50 ± 0.96	4.06 ± 0.15	3.66 ± 0.45

*Photosynthetic efficiency. Values in table are represented as means ± standard deviation. N (independent replicates) = 4.

In summary, the effect of day-night cycles influenced significantly both biomass and carbohydrate productivity.

In **Figure 8.5**, dry weight and carbohydrate content are shown for samples taken at the beginning, at the peak and at the end of the photoperiod. It is possible to observe that the biomass production decreases significantly overnight, probably due to both respiration and washout from the system. In fact, in continuous mode, as the flowrate of inlet/outlet streams are not turned off during the night, if biomass is not actively growing the culture medium is diluted by the inlet, and a fraction of the biomass is lost in the outlet stream.

The biomass loss due to washout can be calculated as:

$$Biomass\ washed\ (\%\ day^{-1}) = \frac{\dot{V}\ (L\ day^{-1})}{V_{reactor}\ (L)} \frac{Dark\ Time\ (h)}{24\ h} . 100 \qquad (8.7)$$

A biomass reduction of about 20% was observed at night, a difference that can be attributed mainly to dilution rather than to respiration phenomena.

A different trend was observed on biomass composition: carbohydrate fraction was found significantly higher at the peak of photoperiod, in comparison to the other hours of the day (between 40-50% at the beginning and 20-38% to the end of the day). This phenomenon can take place even under decreasing illumination (second part of the day), as was observed with *S. obliquus* (**Figure 8.5**).

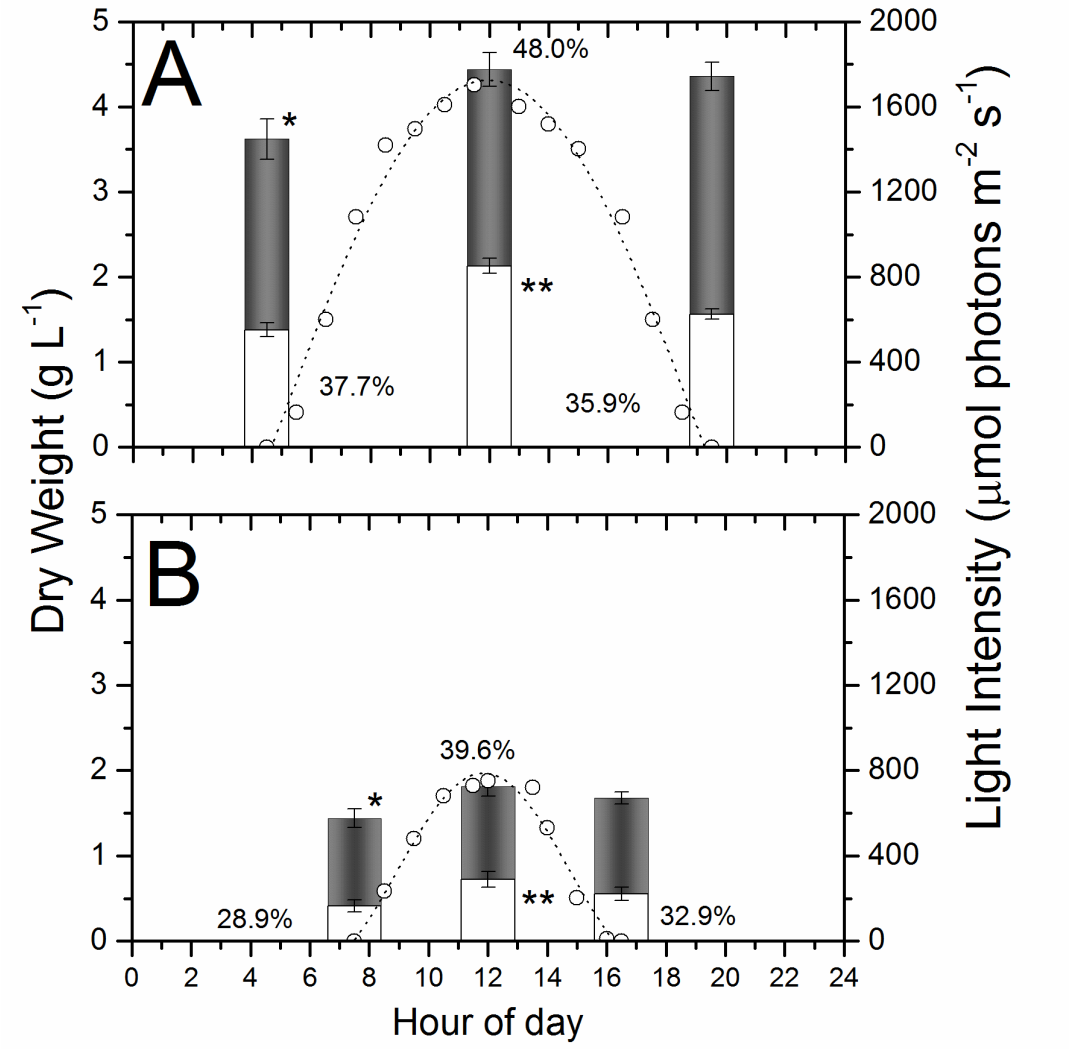

Figure 8.5: Dry weight and carbohydrate content as a function of the hour of day. The profile of illumination is shown on the right. The three values in each bar reflect beginning, peak and end of day for Summer (A) and Winter (B). Black bars refer to biomass and white to carbohydrates, both as dry weight, and the numbers represent the carbohydrate content. In both Fig. 8.5A and 8.5B: an asterisk (*) means that there is significant difference ($p < 0.05$) for biomass between the beginning and the rest of day; two asterisks (**) mean that the carbohydrate content at the peak of the day is significantly higher ($p < 0.05$) than at beginning and the end. The graph is interpreted as irradiated hours of day, for Summer 15 hours and Winter, 9 hours. Error bars represent the standard deviation. n (independent replicates) ≥ 5.

As reported in **Figure 8.6**, the nitrogen content of the biomass increased significantly between the end and beginning of day (dark period), as the same amount of nitrate was found to be absorbed during both dark and daylight (the concentration of nitrate in the medium was almost constant during all cultivation period at steady state). Thus, it was

confirmed that protein synthesis is performed at night, and carbohydrate in presence of light.

Another interesting phenomenon was observed on the nutrient content in the biomass under day-night irradiation: the uptake capacity of the nutrients was found to decrease with respect to operation with continuous light. In particular, even though the same nitrogen limitation was applied, under day-night irradiation a higher nitrogen outlet concentration was found and, as a consequence, less biomass was produced using the same inlet supply.

This can also explain the lower carbohydrate content obtained in Winter, which was a result of insufficient nitrogen limitation conditions (around 50 mg L^{-1} remained in the medium) at the outlet. In Summer, a complete nitrogen consumption occurred. Thus, the nitrogen supply should be carefully set, by also considering the effect of photoperiod on nutrient uptake capability, to allow that the limitation/starvation may take place.

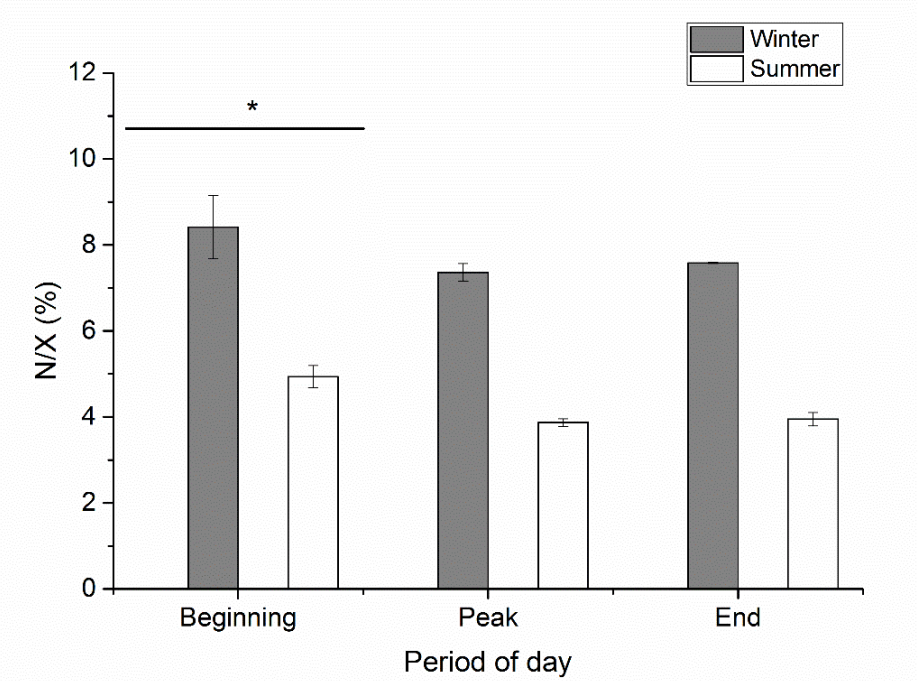

Figure 8.6: Nitrogen content per biomass. Asterisk (*) means that there is significant difference ($p < 0.05$) between the beginning and the rest of the day (both peak and end of day). Error bars represent the standard deviation. n (independent replicates) = 4.

To account for attenuation phenomena, some additional experiments were carried out, by maintaining the same photoperiod of Summer and Winter, but strongly attenuating

the average light intensity by about 66%, as a case study, according to the profiles reported in Supplementary figures (**Figure 8.7**).

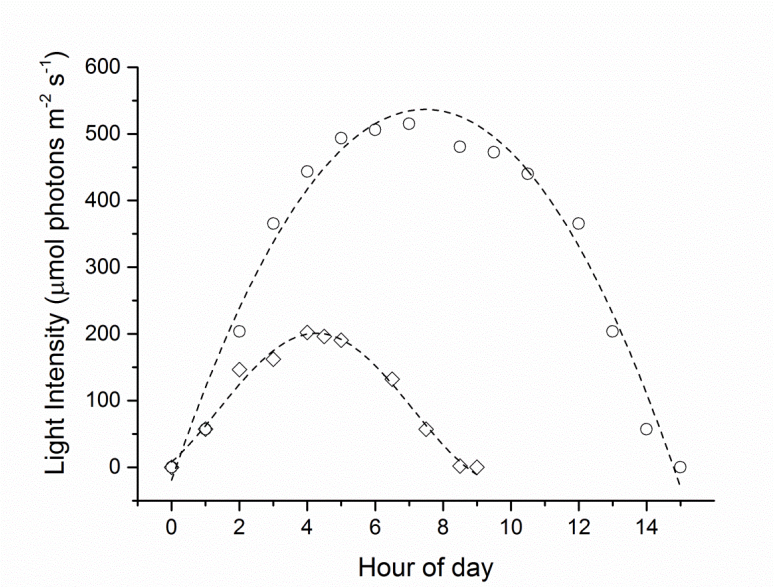

Figure 8.7: Profile of illumination of attenuated conditions. (●) Summer* (220) and (♦) Winter* (50). On the parentheses the numbers reflect the average light intensity (µmol photons m^{-2} s^{-1}).

Even though the nitrogen inlet was kept constant, the light strongly influenced the biomass productivity (**Figure 8.8A**), resulting in a lower consumption of nitrogen (**Figure 8.8B**), and, thus, in a lower carbohydrate accumulation (**Table 8.3** and **8.4**). A relation between the nitrogen content of the biomass and the average light intensity was found, as reported in **Figure 8.8B**, suggesting that the nitrogen uptake is directly regulated by light energy provided, more than the photoperiod applied. This may be a first indication about the nitrogen inlet that should be set in order to maintain an actual nutrient limitation in the system, and thus not affecting the carbohydrate production.

To better understand the process, biomass concentration and carbohydrate content change during the day, respiration rates were eventually measured as described in **section 8.2.5** (normalized by biomass concentration). The ratio between oxygen production and consumption was similar in all experiments, corresponding to about 1.162 ± 0.066 (average and standard deviation of n = 36 measurements at 4 different light irradiance).

On the other hand, the value of production/consumption rates in Summer were significantly lower with respect to both Winter and attenuated conditions (**Figure 8.9**).

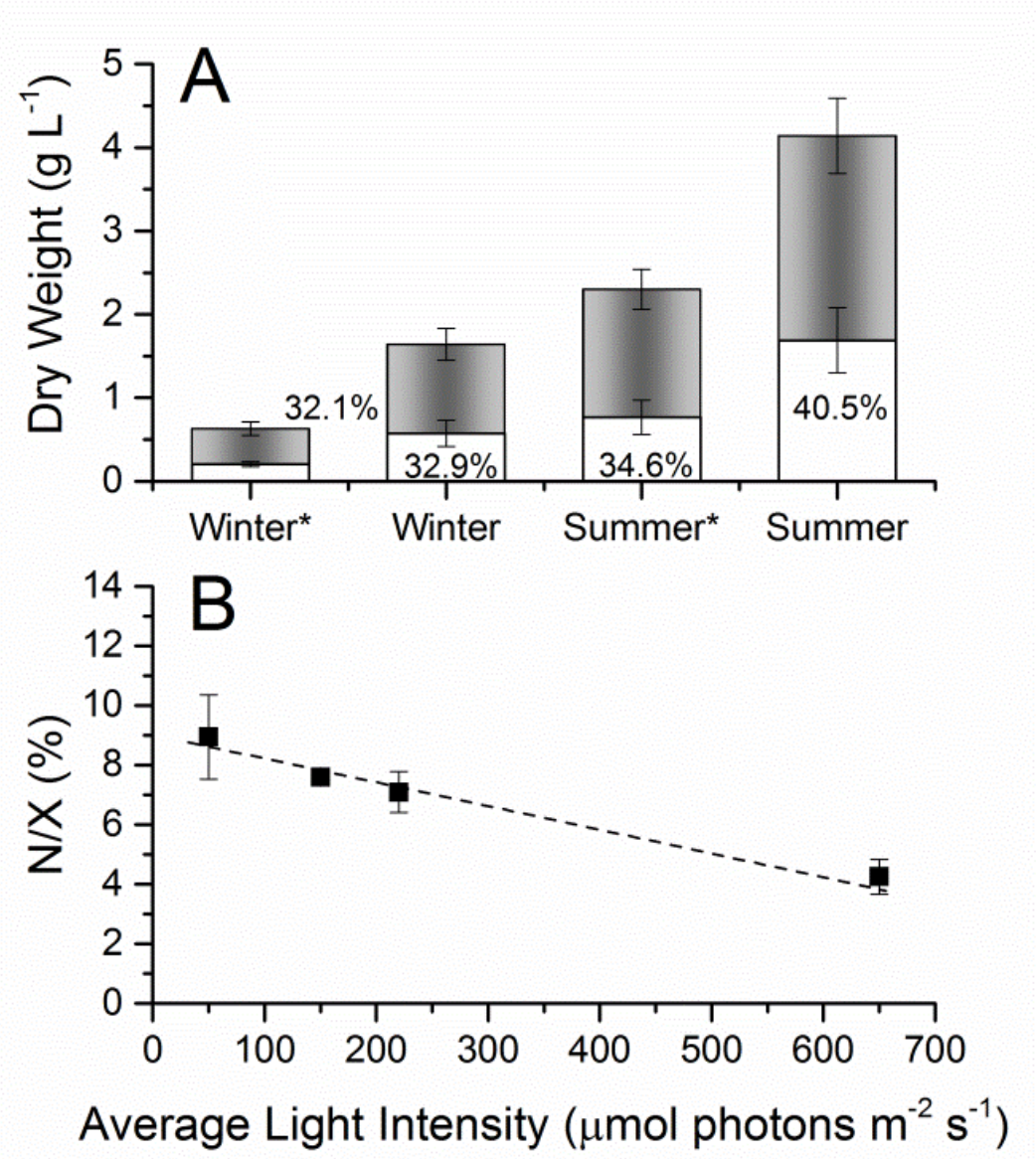

Figure 8.8: A) Biomass concentration (grey bars) and carbohydrate fraction (DW) (white bars) of *S. obliquus* at steady state under Winter and Summer with 180N-100P (Nutrient Concentration). Numbers on the bars report the carbohydrate-biomass ratio (%DW). B) Dark squares refer to nitrogen content in biomass (N/X) versus average light intensity. Nitrogen inlet concentration is the same in all experiments, i.e., 180 mg L^{-1}. The average light intensity, as specified in Fig. 6B are: Winter* = 50, Winter = 150, Summer* = 220 and Summer = 650 μmol photons m^{-2} s^{-1}. The nitrogen outlet concentration in that condition were: 125, 50, 5 and 0, mg L^{-1}, respectively. Error bars represent the standard deviation. n ≥ 5 for dry weight and n = 4 for N/X (nitrogen content in biomass) (independent replicates).

Table 8.3: Nutrient content in biomass and light utilization at constant irradiance.

Constant Illumination	Irradiance (µmol photons m^{-2} s^{-1})			
	Winter		Summer	
	500N/200P	180N/100P	500N/200P	180N/100P
Nutrient content (%)				
N/X	13.8 ± 1.7	7.60 ± 0.25	11.6 ± 0.50	4.25 ± 0.59
P/X	1.0 ± 0.05	1.76 ± 0.14	1.4 ± 0.12	1.17 ± 0.20
Light utilization				
PE (%)*	18.84 ± 2.50	6.50 ± 0.96	4.06 ± 0.15	3.66 ± 0.45

*Photosynthetic efficiency. Values in table are represented as means ± standard deviation. N (independent replicates) = 4.

Table 8.4: Nutrient content in biomass and light utilization at attenuated conditions.

Day-night cycle	Irradiance (µmol photons m^{-2} s^{-1})	
	Winter	Summer
	180N/100P	180N/100P
Biomass and carbohydrate production		
Dry weight (g/L)	0.63 ± 0.08	2.30 ± 0.24
Carbohydrate content (%)	32.19 ± 5.78	32.88 ± 5.86
Biomass productivity (g L^{-1} day^{-1})	0.27 ± 0.04	0.99 ± 0.34
Carbohydrate productivity (g L^{-1} day^{-1})	0.09 ± 0.03	0.32 ± 0.11
Nutrient content (%)		
N/X	8.94 ± 1.41	7.09 ± 0.69
P/X	2.43 ± 0.13	0.87 ± 0.08
Light utilization		
PE (%)*	11.96 ± 1.54	3.66 ± 0.45

*Photosynthetic efficiency.

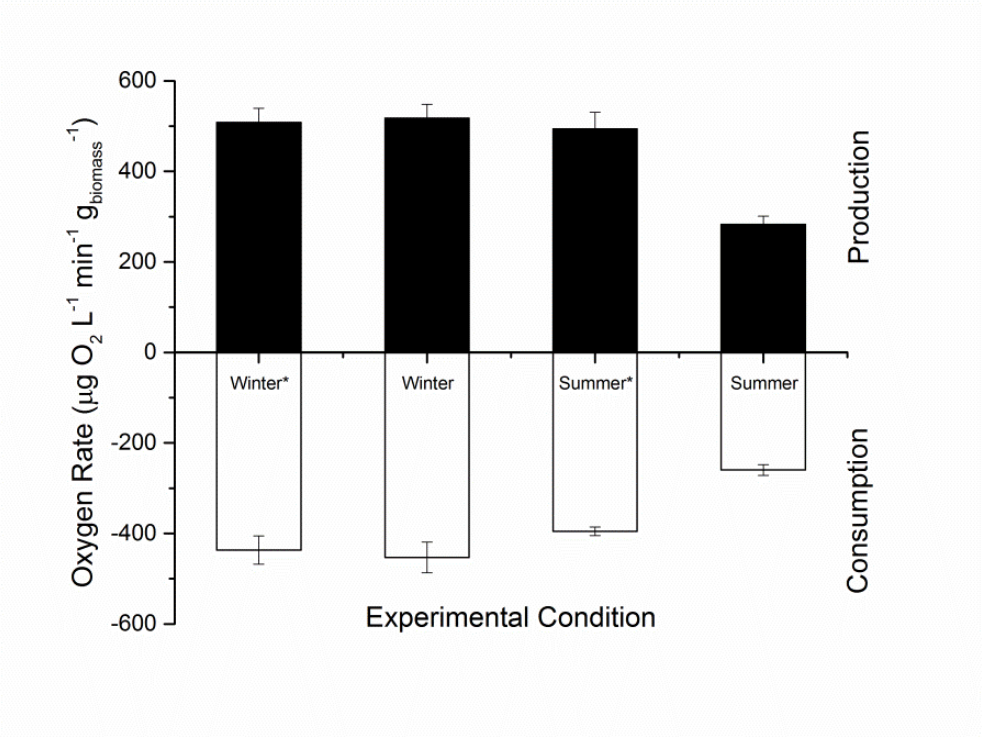

Figure 8.9: Oxygen net production (black bars) and consumption (white bars) rate of the different seasons. *Indicates the experiment with attenuation of light but the same photoperiod (~67% of attenuation). The average ratio between production and consumption in all experiments were very similar: 1.162 ± 0.066. Error bars represent the standard deviation. n (independent replicates) = 3.

8.4 DISCUSSION

Batch results are in agreement with those by Ho and coworkers (2013a), who cultivated *S. obliquus* CNW-N in batch mode reaching a carbohydrate content of about 54% when the external nitrogen source was exhausted. This is a promising behavior in view of an industrial production in a N-limited continuous system.

It is well known that N limitation is one of the most common methods for accumulation of high energetic value substances in microalgae, including carbohydrates (Silva and Bertucco, 2014): nitrogen limitation shifts the carbon fixed by Calvin's Cycle to produce other substances instead of nitrogen-based compounds (proteins), i.e. carbohydrates and lipids (Kim et al., 2014). The accumulation of carbohydrates or lipid is species dependent, and may be differentially affected by nutrient limitation or complete starvation (Kim et al., 2014; Silva and Sforza, 2016).

In continuous system, a P inlet concentration of 100 mg L^{-1} showed be sufficiently in excess, it was kept constant, while nitrogen in the feed was progressively reduced with

the aim to assess the effect of N limitation as a single variable. The idea was to find out an optimum value of both biomass and carbohydrate productivity: under nitrogen limitation, even though the biomass concentration may slightly decrease, a possible increase of carbohydrate content could compensate the loss of biomass production, and might increase the overall carbohydrate productivity, as performed with *Neochloris oleabundans* (De Winter et al., 2014); and *Chlorella vulgaris* (Silva and Sforza et al., 2016). The average value of 0.80 g L^{-1} day^{-1} found in this work for *Scenedesmus obliquus* is much higher than those obtained by Ho and coworkers (2013b), who reported 0.31 g L^{-1} day^{-1} with *Scenedesmus obliquus* CNW-N in continuous cultivation (240 µmol photons m^{-2} s^{-1} and 3.4 days of residence time).

It is noteworthy that, in the case of *S. obliquus*, carbohydrate accumulation was dependent of nitrogen concentration inlet only, while the effect of irradiance was less pronounced (considering 150 and 650 as light intensities). This is remarkably different with respect to other species such as *Chlorella vulgaris*, where carbohydrate accumulation under N limitation was preferentially triggered by high light intensities (Silva and Sforza, 2016).

Similar behavior was also obtained with *Chlorella vulgaris* (Silva and Sforza, 2016). However, the combined role of light and nutrient availability on biochemical composition is species dependent: in fact, under nitrogen excess, *S. obliquus* nitrogen yield resulted affected by light intensity, while under nitrogen limitation the yield under low or high lights are comparable, suggesting that the driving force for carbohydrate accumulation is nitrogen availability.

A significant reduction of photosynthetic efficiency when the light intensity increased between 150 to 650 µmol photons m^{-2} s^{-1} was already found for this and other species, as a result of photoinhibition and saturation effect (Sforza et al., 2014; Sforza et al., 2015; Silva and Sforza, 2016).

In order to improve the energy balance and profitability of large-scale biofuel production, sunlight exploitation is necessary. However, most of outdoor industrial and published studies looking for a carbohydrate-based biofuel are performed in batch conditions and the actual stability of the carbohydrate fraction under light/dark periods (day-night cycles) is of major concern (Ho et al., 2013a; Sforza et al., 2014; Sforza et al., 2015). In fact, the main issue is related to the dark periods, when photosynthesis is

absent, so that the productivity decreases with respect to the constant illumination experiments (Sforza et al., 2015), as well as the carbohydrate content.

The photoperiod can influence significantly also the biochemical composition of microalgae (Jacob-Lopes et al., 2009; De Winter et al., 2017). This behavior is species dependent, as the acclimation of photosynthetic apparatus can maintain/improve the efficiency under photoperiod (Sforza et al., 2012) or reduce significantly CO_2 fixation under lower photoperiods (Krzeminska et al., 2014). As a consequence of operation with a photoperiod, a cyclic steady state can also be observed (De Winter et al., 2014; De Winter et al., 2017).

The main difference of biomass concentration between the beginning and the end of the day was caused by the dilution rate, results in agreement with other data reported in the literature: for instance, De Winter et al. (2014), found that in continuous cultivation of *Neochloris oleoabundans* the biomass variation between light and dark periods was proportional to the ratio between the corresponding duration, being around 30% of biomass. In addition, it was previously reported that macroscopic loss of biomass due to respiration under dark period is small, and it can be observed only after many days under dark: according to Ogbonna and Tanaka (1996) the reduction of biomass is between 5-8% using a light:dark cycle of 48:14 (hours) with *Chlorella*, while Céron-Garcia et al. (2010) verified that *Scenedesmus almeriensis* grown at outdoor irradiation, lost 20% of biomass after 8 days only of totally dark condition. Therefore, it can be reasonably concluded that the duration of dark period set in our work did not allow a significant biomass loss due to respiration. Changes in day-night outdoor cultivation related to biomass concentration and starch content for *Chlamydomonas* HS-5 were also noticed by Mooji et al. (2015). A decrease of the energetic reserves between noon and sunset, depending of the photoperiod and the species used was observed by De Winter et al. (2014; 2017) with *Neochloris oleabundans*.

So, if the presence of both high light stress and nitrogen limitation triggers carbohydrate accumulation, it appeared that a regulation of carbohydrate metabolisms takes place as a result of circadian rhythm. In fact, during dark periods, microalgae cells usually perform protein synthesis or UV sensitive processes like DNA replication and cell division, exploiting the energy stored during the day in the form of carbohydrate and lipids (De Winter et al., 2014; De Winter et al., 2017).

Under nitrogen limitation/starvation lipids can be accumulated too, and they depend on light intensity. In our work, using *Scenedesmus obliquus*, a relevant increase of the lipid content was not observed (**Table 8.5**) in comparison to excess nutrient condition, showing an average value of 25%. The opposite was found in *Chlorella vulgaris* under constant illumination and nitrogen limitation (Silva and Sforza, 2016), a result that can be attributed to the species characteristic. In fact, Ho et al. (2013a) cultivating *Scenedesmus obliquus* CNW-N in batch mode under nitrogen starvation reached a carbohydrate content of 58%, but the content of lipids was slightly increased from 20 to 28%.

In summary, even though nitrogen limitation in the inlet is an effective way to increase the carbohydrate in continuously cultivated microalgae, it appeared that, under night day irradiation, a strict regulation should be carried out on the inlet stream. On the other hand, such a fine tuning of operating conditions can be complex in outdoor systems, where weather fluctuations may occur as well. For instance, the attenuation of light intensity is a typical problem of outdoor systems that can significantly influence microalgal productivity (Edmunson and Huesemann, 2015).

Table 8.5: Lipid content under nitrogen limitation in continuous cultivation and day-night cycles.

Light Intensity ($\mu E\ m^{-2}\ s^{-1}$)	**Excess of Nutrient 180N/100P**	
	Lipid	
	Avg	StD
Summer	25.34	0.64
Winter	22.80	0.98

Excess of nutrients: Summer: 28.0 ± 4.0 Winter: 25 ± 3.0.

A lower value of respiration/photosynthesis net ratio under nitrogen limitation condition is probably due to the acclimation to high light intensities, which results in a lower oxygen production when samples are exposed to the light intensity used in respirometric tests. However, this lower rate may have a different explanation. In fact, as mentioned before, the Summer experiment was the only one when a total nitrogen consumption occurred, thus resulting in an effective nitrogen starvation condition. As said before, this allowed a higher carbohydrate accumulation, thus suggesting that no enough nitrogen is available for protein synthesis, which may also cause a reduced photosynthesis and O_2 production rate (**Figure 8.5** and **Tables 8.3** and **8.4**) (Geider and Osbourne 1989; Langdon, 1993).

Therefore, these results suggest that under nitrogen limitation, net photosynthesis and dark respiration rates decrease significantly and this seems to be necessary to promote carbohydrate accumulation.

In conclusion, by means of steady-state continuous photobioreactor experiments, it was shown that *Scenedesmus obliquus* is able to accumulate carbohydrate under nitrogen starvation, which however may affect the biomass productivity. Thus, by properly managing the inlet nitrogen concentration, an optimum value could be found where carbohydrate accumulation compensates the loss of biomass due to starvation, thus leading to a higher overall productivity, with remarkable values of 0.8 g L^{-1} d^{-1}. This was demonstrated also with day/night cycles and seasonality, showing that attenuated light conditions and/or short photoperiods need a proper N_{inlet} to accumulate carbohydrate.

REFERENCES

Ashokkumar, V., Salam, Z., Tiwari, O.N., Chinnasamy, S., Mohammed, S., Ani, F.N., 2015. An integrated approach for biodiesel and bioethanol production from *Scenedesmus bijugatus* cultivated in a vertical tubular photobioreactor. Energy Convers. Manag. 101, 778–786.

Bertucco, A., Beraldi, M., Sforza, E., 2014. Continuous microalgal cultivation in a laboratory-scale photobioreactor under seasonal day-night irradiation: experiments and simulation. Bioprocess Biosyst. Eng. 37, 1535–1542. doi:10.1007/s00449-014-1125-5.

Boechat, I.G., Giani, A., 2008. Seasonality affects diel cycles of seston biochemical composition in a tropical reservoir. Journal of Plankton Research 30(12), 1417-1430.

Céron-Garcia, M.C., Campos-Pérez, I., Marcias-Sanchez, M.D., Bermejo-Romantz, Fernandez-Sevilla, J.M., Molina-Grima, E., 2010. Stability of carotenoids in *Scenedesmus almeriensis* biomass and extracts under various storage conditions. Journal of Agricultural and Food Chemistry 48(11), 6944–6950.

Chen, C., Zhao, X., Yen, H., Ho, S., Cheng, C., Lee, D., Bai, F., Chang, J., 2013. Microalgae-based carbohydrates for biofuels production. Biochemical Engineering Journal 78, 1-10.

De Winter, L., Klok, A.J., Franco, M.C., Barbosa, M.J., Wijffels, R.H., 2013. The synchronized cell cycle of *Neochloris oleabundans* and its influence on biomass composition under constant light conditions. Algal Research 2, 313-320.

De Winter, L., Schepers, L.W., Cuaresma, M., Barbosa, M.J., Martens, D.E., Wijffels, R.H., 2014. Circadian rhythms in the cell cycle and biomass composition of *Neochloris oleabundans* under nitrogen limitation. Journal of Biotechnology 187, 25-33.

De Winter, L., Cabanelas, I.T.D., Orfao, A.N., Vaessen, E., Martens, D.E., Wijffels, R.H., Barbosa, M.J., 2017. The influence of day length on circadian rhythms of *Neochloris oleabundans*. Algal Research 22, 31-38. (a)

De Winter, L., Cabanelas, I.T.D., Martens, D.E,, Wijffels, R.H., Barbosa, M.J., 2017. The influence of day/night cycles on biomass yield and composition of Neochloris oleoabundans. Biotechnology for Biofuels 10:104, 1-10. (b)

Edmundo, S.J., Hiesemann, M.H., 2015 The dark side of algae cultivation: chracterization night biomass loss in three photosynthetic algae, *Chlorella sorokiniana*, *Nannochloropsis salina* and *Picochlorum sp.* Algal Research 112, 470-476.

Geider, R.J., Osborne, B.A., 1989. Respiration and microalgal growth: a review of the quantitative relationship between dark respiration and growth. New Phytol. 112, 327-341.

Guccione, A., Biondi, N., Sampietro, G., Rodolfi, L., Bassi, N., Tredici, M.R., 2014. *Chlorella* for protein and biofuels: from strains selection to outdoor cultivation ina green wall panel photobioreactor. Biotechnology for Biofuels 7:84, 1-12.

Ho, S., Li, P., Liu, C., Chang, J., 2013. Bioprocess development on microalgae-based CO_2 fixation and bioethanol production using *Scenedesmus obliquus* CNW-N. Bioresource Technology 145: 142-149, (a)

Ho, S., Kondo, A., Hasunuma, T., Chang, J., 2013. Engineering strategies for improving the CO_2 fixation and carbohydrate productivity of *Scenedesmus obliquus* CNW-N used for bioethanol fermentation. Bioresour. Technol. 143, 163–171. doi:10.1016/j.biortech.2013.05.043. (b)

Jacob-Lopes, E., Scoparo, C.H.G., Lacerda, L.M.C.F., Franco, T.T., 2009. Effect of light cycles (night/day) on CO_2 fixation and biomass production by microalgae in photobioreactors. Chemical Engineering and Processing: Process Intensification 48, 306-310.

Kim, K.H., Choi, I.S., Kim, H.M., Wi, S.G., Bae, H.J., 2014. Bioethanol production from the nutrient stress-induced microalga *Chlorella vulgaris* by enzymatic hydrolysis and immobilized yeast fermentation. Bioresour. Technol. 153, 47–54. doi:10.1016/j.biortech.2013.11.059.

Kim, S.S., Ly, H.V., Kim, J., Lee, E.Y., Woo, H.C., 2015. Pyrolysis of microalgae residual biomass derived from *Dunaliella tertiolecta* after lipid extraction and carbohydrate saccharification. Chem. Eng. J. 263, 194–199. doi:10.1016/j.cej.2014.11.045.

Kliphuis, A.M.J., Klok, A.J., Martens, D.E., Lamers, P.P., Janssen, M., Wijffels, R.H., 2012. Metabolic modeling of *Chlamydomonas reinhardtii*: energy requirements for photoautotrophic growth and maintenance. J. Appl. Phycol. 24, 253–266. doi:10.1007/s10811-011-9674-3.

Kzeminska, I., Pawlik-Skowronska, B., Trzcinska, M., Tys, J., 2014. Influence of photoperiods on the growth rate and biomass productivity of green microalgae. Biosyst Eng 37, 735-741.

Langdon, C. 1993. The significance of respiration in production measurements based on oxygen. ICES mar. Sci. Symp. 197, 69-78.

Ma, X., Chen, K., Lee, Y., 1997. Growth of *Chlorella* outdoors in a changing light environment. Journal fo Applied Phycology 9, 425-430.

Markou, G., Angelidaki, I., Nerantzis, E., Georgakakis, D., 2013. Bioethanol production by carbohydrate-enriched biomass of *Arthrospira* (*Spirulina*) *platensis*. Energies. 6, 3937–3950. doi:10.3390/en6083937.

Mollers, K.B., Cannella, D., Jørgensen, H., Frigaard, N.U., 2014. Cyanobacterial biomass as carbohydrate and nutrient feedstock for bioethanol production by yeast fermentation. Biotechnol. Biofuels. 7:64. doi:10.1186/1754-6834-7-64.

Mooji, P.R., Graaff, D.R., von Loosdrecht, M.C.M., Kleerebezem, R., 2015. Starch productivity in cyclically operated photobioreactors with marine microalgae – effect of ammonium addition on regime and volume exchange ratio. Journal of Applied Phycology. 27(3), 1121-1126.

Moraes, B.S., Zaiat, M., Bonomi, A., 2015. Anaerobic digestion of vinasse from sugarcane ethanol production in Brazil: Challenges and perspectives. Renew. Sustain. Energy Rev. 44, 888–903. doi:10.1016/j.rser.2015.01.023.

Mortensen, L.M., Gislerod, H.R., 2016. The growth of *Chlorella sorokiniana* as influenced by CO2, light and flue gas. Journal of Applied Phycology. 28(2), 813-820.

Ogbonna, J.C., Tanaka, H., 1996. Night biomass loss and changes in biochemical composition of cells during light/dark cyclic culture of *Chlorella pyrenoidosa*. Journal of Fermentation and Bioengineering 82(6), 558–564.

Pirt, M.W., Pirt, S.J., 1977. Photosynthetic production of biomass and starch by *Chlorella* in chemostat culture. Journal of Chemical and Biotechnology. 27(6), 643-650.

Renewable Fuel Association, 2016. Available in: http://www.ethanolrfa.org/

Ruiz, J., Alvarez-Diaz, P.D., Arbib, Z., Garrido-Pérez, C., Barragan, J., Perales, J.A., 2013. Performance of a flat panel reactor in the continuous culture of microalgae in urban wastewater: prediction from a batch experiment. Bioresour. Technol. 127, 456–463. doi:10.1016/j.biortech.2012.09.103.

Sforza, E., Simionato, D., Giacometti, G.M., Bertucco, A., Morosinotto, T., 2012. Adjusted light and dark cycles can optimize photosynthetic efficiency in algae growing in photobioreactors. Plos One 7(6), e38675.

Sforza, E., Gris, B., Silva, C.E.F., Morosinotto, T., Bertucco, A., 2014. Effects of light on cultivation of *Scenedesmus obliquus* in batch and continuous flat plate photobioreactor. Chemical Engineering Transactions 38, 211-216.

Sforza, E., Urbani, S., Bertucco, A., 2015. Evaluation of maintenance energy requirements in the cultivation of *Scenedesmus obliquus*: effect of light intensity and regime. J. Appl. Phycol. 27(4), 1453-1462. doi: 10.1007/s10811–014–0460–x. doi:10.1007/s10811-014-0460-x.

Silva, C.E.F., Bertucco, A., 2016. Bioethanol from microalgae and cyanobacteria: A review and technological outlook. Process Biochemistry 51, 1833-1842.

Silva, C.E.F., Sforza, E., 2016. Carbohydrate productivity in continuous reactor under nitrogen limitation: Effect of light and residence time on nutrient uptake in *Chlorella vulgaris*. Process Biochemistry 51, 2112-2118.

Silva, C.E.F., Sforza, E., Bertucco, A., 2017. Effects of pH and carbon source on *Synechococcus* PCC 7002 cultivation: biomass and carbohydrate production with different strategies for pH control. Appl. Biochem. Biotehcnol. 181, 682-698.

Trevelyan, W.E., Harrison, J.S., 1952. Studies on yeast metabolism. 1. Fractionation and microdetermination of cell carbohydrates. Biochem J. 50(3), 298-303.

Vitova, M., Bisova, K., Kawano, S., Zachleder, V., 2015. Accumulation of energy reserves in algae: from cell cycles to biotechnological applications. Biotechnology Advances 3, 1204-1218.

Wang, H., Ji, C., Bi, S., Zhou, P., Chen, L., Liu, T., 2014. Joint production of biodiesel and bioethanol from filamentous oleaginous microalgae *Tribonema sp.*. Bioresour. Technol. 172, 169–173. doi:10.1016/j.biortech.2014.09.032.

Xia, L., Song, S., Hu, C., 2016. Higher temperature enhances lipid accumulation in nitrogen-deprived *Scenedesmus obtusus* XJ-15. Journal of Applied Phycology 28(2), 831-837.

Chapter 9

Dilute acid hydrolysis of microalgal biomass for bioethanol production: An accurate kinetic model of biomass solubilization, sugars hydrolysis and nitrogen/ash balance

In this chapter, acidic hydrolysis (0-5% v/v) was performed on *Chlorella vulgaris* biomass using a range of temperature (100-130 °C) and reaction time (0-60 min) with high biomass load (10% - 100 g L^{-1}), in order to characterize the kinetic of biomass solubilization, hydrolysis of sugars, proteins and ash release, and to verify the main divergences and similarities in relation to lignocellulosic biomass. More than 90% of the sugars present in the biomass was hydrolyzed and later satisfactorily fermented by *S. cerevisiae*. The inclusion of acid concentration in the kinetic model for biomass solubilization and sugars hydrolysis led to a modified Michaelis-Menten equation able to simulate efficiently the acidic extraction/hydrolysis data of all experimental runs. Main divergences in relation to lignocellulosics were related to higher reaction order and lower activation energy, reveling better susceptibility of microalgal biomass to acidic treatment. The proposed process is promising and can be easily scaled up at industrial level•.

•*Part of this chapter was published in Reaction Kinetics, Mechanisms and Catalysis (**Silva, C.E.F**., Bertucco, A., 122, 1095-1114, 2017).*

9.1 INTRODUCTION

Biomass is a highly promising fossil substitute raw material for future biofuel application owing to several reasons: abundant feedstock availability and possibility to be produced in almost all regions of the world, avoiding competition with food crops (Negahdar et al., 2016). However, its chemical structure (lignocellulose) is complex and change significantly depending on the type. For this reason, several methods of pretreatment are applied to exploit it, for example, alkaline for coconut husk fiber (Cabral et al., 2016), acidic for citric waste (Silva et al., 2015), hydrothermal for sugarcane straw (Rocha et al., 2017) or biological for wood (Song et al., 2013), becoming more complex and severe as a function of the polymeric structure recalcitrance.

A potential bio-refinery scheme, claiming an environmental gain thanks to carbon cycle and the use of renewables, aims at a controlled depolymerization of biomass which includes the following steps: (1) fractionation of biomass into biopolymers: cellulose, hemicellulose, starch and lignin; (2) depolymerization of the biopolymers and (3) transformation of the monomers into value-added products (Negahdar et al., 2016).

More recently, microalgae have been developed and proposed as a potential source of biomass, especially for biofuels applications, initially more devoted to biodiesel (lipid fraction) (Tercero et al., 2014), but then focused also on ethanol (Silva and Bertucco, 2016), methane (Ding et al., 2016), hydrogen (Kumar et al., 2016) and buthanol (Wang et al., 2014). Microalgae have a number of advantages in comparison to higher plants (i.e. lignocellulosic biomass), such as higher growth rates and less recalcitrance due to the absence of lignin and lower amount of cellulose and hemicellulose, being starch (microalgae) or glycogen (cyanobacteria) the main reserve-polysaccharides which are easily hydrolysable by acids (Chisti, 2007; Ho et al., 2013).

Kinetic studies using acidic pretreatment of lignocellulosic materials are reported in the literature, but for biomass solubilization only (Saeman, 1945; Overend and Chornet, 1987; Chum et al., 1990; Belkacemi et al., 1991; Jacobsen and Wyman, 2000; Negahdar et al., 2016). For lignocellulosic materials the acidic treatment is effective as pretreatment to remove hemicellulose and de-structure its three-dimensional arrangement, then helping the enzymatic hydrolysis of cellulose (Mosier et al., 2005; Silva and Bertucco, 2016). Thinking of microalgae and cyanobacteria (Chen et al.,

2013; Vitova et al., 2015), the potential to obtain a higher sugars hydrolysis rate by acidic hydrolysis is increased, but so far, most studies on microalgal biomass were focused to determine the best condition of hydrolysis, i.e., to find the optimized value of temperature, time of reaction, acidic concentration and biomass load (Choi et al., 2010; Miranda et al., 2012; Ashokumar et al., 2015; Silva and Bertucco, 2016). This method is faster but at the same time is not efficient to evaluate the nature of biomass hydrolysis and/or degradation processes. Kinetic and thermodynamic information are necessary to be used efficiently in the models to correctly perform process simulation and plant design. In any case, the nature of microalgal biomass is completely different from lignocellulosic biomass and the models traditionally used cannot be suitable for microalgae, so that a model of acidic sugars hydrolysis based on microalgal biomass as substrate has not been developed yet.

In addition, mass balance calculations of nutrients needed, mainly nitrogen and phosphorous, influence the global process economics, because they represent the largest costs in cultivating algae for fuels. The recycling and life cycle assessment (LCA) of these nutrients are a must (Yang et al., 2011; Biller et al., 2012; Barbera et al., 2016). Acidic hydrolysis as a non-specific process promotes not only the release of sugars but also of the other substances present in the biomass (such proteins and ash), and this additional fraction can be useful in the liquor during yeast/bacteria fermentation and needs to be quantified for an accurate investigation to close the loop of nutrients in the process.

In this chapter, ranges of temperature (100-130 °C) and reaction time (0-60 min) using high biomass load (10% - 100 g L^{-1}) were investigated in order to characterize the kinetic of biomass solubilization, hydrolysis of sugars, proteins and ash solubilization from *Chlorella vulgaris* biomass using thermochemical hydrolysis with diluted acid (0-5% v/v). Divergences and similarities with lignocellulosic biomass will be highlighted as well.

9.2 MATERIAL AND METHODS

9.2.1 Microalgal biomass and biochemical characterization

Chlorella vulgaris biomass powder was produced by Neoalgae® (Micro seaweed products B-52501749). The characterization included the determination of moisture (method 934.01), ash (method 942.05), protein (method 2001.11), lipid content (method 2003.05), carbohydrates and monomers (HPLC) (AOAC, 2002).

9.2.2 Acidic hydrolysis and analytical procedures

Acidic hydrolysis was performed with 10% of solids load (microalgal biomass), in autoclave (Autoclave vapour-line^{eco} VWR), using temperatures between 100-130 °C (P ~ 1 atm), and changing the concentration of catalyst (H_2SO_4 – 98% Sigma ®) (0, 1, 3 e 5% v v^{-1}) and the reaction time (0-60 min) in order to validate the kinetic model proposed and posteriorly discussed. The mass yield (MY) of the process was evaluated on a dry weight basis after the thermochemical treatment by gravimetry using cellulose acetate filters of 0.45 μm (Whatman®) at 105°C and 2 hours. Filters were pre-dried for 10 min at 105 °C in order to remove any moisture. The relation between solubilized biomass and mass yield is given by:

$$[Solubilized\ Biomass]\ (\%) = \frac{Initial\ biomass\ Load\ \left(\frac{g}{L}\right) - Mass\ yield\left(\frac{g}{L}\right)}{Initial\ biomass\ Load\ \left(\frac{g}{L}\right)} \bullet 100 \qquad (9.1)$$

The amount of total extracted sugars (TS) was determined by Anthrone method (Trevelyan and Harrison, 1952) and reducing sugars (monomers, RS) using the DNS method (Miller, 1959; Silva et al., 2015). The % of sugars extracted/hydrolyzed were calculated by:

$$[Sugar]\ (\%) = \frac{Sugar\ concentration\ \ in\ the\ liquor\ \left(\frac{g}{L}\right)}{Initial\ biomass\ load\ \left(\frac{g}{L}\right) \bullet\ Carbohydrates\ content} \bullet 100 \qquad (9.2)$$

where the carbohydrate content is given as a relative value between 0-0.6 (generally the maximum of carbohydrate accumulation in microalgae and cyanobacteria is 0.6 = 60% of carbohydrate content, in dry weight basis) (Silva and Bertucco, 2016; Silva and Sforza, 2016; Silva et al., 2017).

9.2.3 Kinetic Model

The reaction of acidic biomass solubilization is commonly represented by:

$$Pol - Biomass + [H^+] \xrightarrow{\Delta} Sugars + Others\ (proteic\ residue, ash\ \dots) \quad (9.3)$$

The assumption is that H^+ participates in the biomass solubilization and sugars hydrolysis as a catalyst, but interactions as reagent should be considered as well. In fact, some speculation about the effect of [H^+] only a catalyst was made, explained that it is possible of its neutralization for the biomass due the several biochemical fractions, mainly minerals (Jacobsen and Wyman, 2000).

A *n* order kinetics for biomass solubilization and an *m* order for acid hydrolysis were used, resulting in an *n* + *m* overall reaction order. The acid concentration term was incorporated in the Arrhenius equation giving a modified equation:

$$\frac{dPol}{dt} = k[Pol]^n \quad (9.4)$$

where *Pol* indicates biomass concentration, and where

$$k = k_0[H^+]^m e^{\frac{-E_a}{RT}} \quad (9.5)$$

with *n* and *m* being the orders of reactions to *Pol* and H^+, respectively.

The integration of Equation 9.4 yields:

$$Pol^{1-n} - {Pol_0}^{1-n} = (n-1)kt \quad (9.6)$$

and, consequently:

$$Pol = ({Pol_0}^{1-n} + (n-1)kt)^{\frac{1}{(1-n)}} \quad (9.7)$$

From Eq. 9.7, at constant Temperature (*T*) and *Pol* biomass concentration it is possible to find the *k* values a corresponding to the $[H^+]$ value applied. Then, using Eq. (9.5), since the values of *T* (K), *R* (J/(mol K)) and *k* (min^{-1} $(g/L)^{-m}$) are known, the values of *m* and *Ea* (kJ/mol) can be found. The Michaelis-Menten model was applied to describe the total sugars extracted from the biomass, since sugars concentration in liquid-phase depends on the substrate concentration (biomass and acid concentration):

$$\frac{d\ Sugars}{dt} = k \tag{9.8}$$

where

$k = \frac{k_{max_{[T,H^+]}}[S]}{K_M + [S]}$ (Temperature and $[H^+]$ constant, i.e., only the time (t) variable)

(9.9)

When the substrate concentration is high, the equation becomes zero order (Deichmann et al., 2014). In our work is proposed to express the *[S]* term by Equation 9.10, including the proton as a reactant and the orders of reaction. K_M ($(g/L)^{n+m}$) is the constant of half-saturation and k is the reaction rate constant (min^{-1}). Parameters estimation was performed by non-linear regression validated by the least squares method (Markovsky and Huffel, 2007).

$$[S] = [Pol]^n[H^+]^m \tag{9.10}$$

Thus, the final equation that can be obtained integrating Eq. 9.8 is:

$$[Sugar]\left(\frac{g}{L}\right) = \frac{k_{max_{[T,H^+]}}[Pol]^n[H^+]^m}{K_M + [Pol]^n[H^+]^m}\mathrm{t} \tag{9.11}$$

where t is the reaction time.

Additionally, selectivity (*S*) is defined as:

$$S = \frac{Y}{X} \tag{9.12}$$

where *Y* represents the yield of the reaction and *X* the conversion of biomass (*Pol*). The final reaction time studied in this work, 60 min was considered as the reference time.

9.2.4 Protein and ash solubilization

The extents of solubilized protein and ash were calculated by:

$$[Solubilized\ \ Component]\ (\%) = \frac{Initial\ biomass\ load\left(\frac{g}{L}\right)\bullet Initial\ component\ content - Mass\ Yield\left(\frac{g}{L}\right)\bullet Final\ component\ content}{Initial\ biomass\ load\left(\frac{g}{L}\right)\bullet Initial\ component\ content} \bullet 100$$

(9.13)

9.2.5 Ethanolic fermentation

Fermentation was performed with *S. cerevisiae* (Cameo S.p.A. ®) using the broth from acidic hydrolysis after adjustment the pH to 5.5 at 30°C for 48 hours. Reducing sugars were measured by DNS method and cellular growth by dry weight (described in the section 2.2). Ethanol was determined by gas-chromatography (Shimadzu GC-14A) injecting 5 µL of centrifugated at 5000 rpm per 10 min (Labnet, Spectrofuge 7M, bought from Sigma–Aldrich, Milan, Italy) in Eppendorf™), with a Poropak QS packed column (80/100 mesh, 1.7 m length). The carrier gas was helium with a flow rate of 20 mL/min. The injector, column oven and the detector temperatures were 150, 150 and 170 °C, respectively. The composition was computed from the GC peak areas according to a calibration curve.

Conversion factors are calculated by:

$$Y_{X/S} = \frac{\Delta X}{\Delta Sugars} \tag{9.14}$$

$$Y_{E/S} = \frac{\Delta Ethanol}{\Delta Sugars} \tag{9.15}$$

$$Y_{X/E} = \frac{\Delta X}{\Delta Ethanol} \tag{9.16}$$

where Δ is referred to the difference between time 0 and the end of fermentation, sugars indicate reducing sugars and X is the yeast concentration (g L^{-1}).

Process and fermentation yield were calculated by:

$$Yield_{Process}\ (\%) = \frac{\Delta Ethanol}{0.5111\ Initial\ Sugar} 100 \tag{9.17}$$

$$Yield_{Fermentation}\ (\%) = \frac{\Delta Ethanol}{0.5111\ \Delta Sugar} 100 \tag{9.18}$$

where 0.5111 is the glucose-ethanol conversion factor according to the stoichiometry of Gay-Lussac.

9.3 RESULTS AND DISCUSSION

The combined use of temperature, acid concentration and time was applied in order to evaluate the susceptibility of microalgal biomass to promote solubilization and, in particular, sugars extraction and hydrolysis, in order to propose a suitable model to simulate efficiently the process. Protein and ash extraction in the liquid phase were taken with account, as acid as a catalyst is not specific. Lastly, ethanolic fermentation was carried out to validate the fermentability of the hydrolyzed matter with *S. cerevisiae*, and a mass balance of industrial process flowsheet was proposed.

9.3.1 Biomass characterization

The biochemical composition of *Chlorella vulgaris* is presented in **Table 9.1**. The biomass used has a relatively high content of proteins and ash, together with carbohydrate. It is important to remember that microalgae display a biochemical plasticity able to change their composition according to the nutritional and environmental factors. Specifically, for *Chlorella vulgaris*, nitrogen availability, residence time and light intensity allow to accumulate more or less carbohydrate in the biomass (Silva and Sforza, 2016).

Carbohydrates in microalgae are present as cell wall components (generally cellulose and soluble hemicellulose) and plastids (mainly in the form of starch) (Chen et al., 2013). Glucose was found predominant monosaccharide in the biomass and accounts for more than 70% of total sugars, together with xylose (10.65%), arabinose (10.91%) and rhamnose (5.73%). These results to sugars composition in *Chlorella* are in according with literature data.

Xylose and arabinose are pentose which cannot be fermented by *Saccharomyces*, the most widely used industrial microorganism, and this deserves to be considered as they represent more than 20% of total sugars in *Chlorella vulgaris*. Genetic improvement is needed in order to increase the ethanol tolerance and ability of yeast and bacteria species to ferment pentose (Jang et al., 2012). In addition, some genders, as *Pichia*, *Candida* and *Kluyveromyces* are able to ferment pentose and hexose naturally but at lower rates in comparison to *Saccharomyces* (Kuhad et al., 2011). However, this point was not addressed here because *S. cerevisiae* was used.

Table 9.1: Macrocomponents in *Chlorella vulgaris*.

Components	This study *Chlorella vulgaris*	(Lee et al., 2015) *Chlorella sp.* KR1	(Hernandez et al., 2015) *Chlorella sorokiniana*	(Wang et al., 2016) *C. vulgaris* JSC-6
	% of dry weight			
Protein	49.5 ± 0.29	16.6	-	-
Lipid	6.3 ± 0.15	38.0	-	-
Carbohydrates	23.0 ± 2.0	36.1	18.2	54
Glucose*	**70.15**	**82.2**	**70.8**	**79**
Xylose*	**10.65**	**6.4**	**13.8**	**11.11**
Arabinose*	**10.91**	**5.54**	**-**	**9.25**
Rhamnose*	**5.73**	**5.26**	**6.5**	**-**
Other*	2.56	-	1.2	-
Ash	7.18 ± 0.01	5.9	-	-
Moisture	5.41 ± 0.05	3.6	-	-
Other	8.61	-	-	-

* % respect to the carbohydrate content.

9.3.2 Biomass solubilization

As shown in **Figure 9.1**, the range of temperature (110-130 °C) and acid concentration applied were efficient in the solubilization of microalgal biomass, reaching best values (around 20-25%) with 5% of acid and 60 min of reaction time. However, 120°C and 3% of acid was considered the best option in terms of solubilization/acid ratio used. It is noteworthy that the zero point was considered when the temperature reached 110, 120 or 130°C, i.e., the initially heating time was not included. Clearly, this had an effect in the experiments, as at zero point the initial biomass and sugar concentration are not 100% and 0, respectively (**Fig. 9.1**, but also **9.2** and **9.3** later on), but the effect is the same for all experimental runs and does not affect the kinetic model. Note that, even though most of published papers use less than 50 g L^{-1} of biomass (Nguyen et al., 2009; Ho et al., 2013; Ashokumar et al., 2015), a biomass concentration of 100 g L^{-1} was chosen to obtain a suitable sugars concentration with respect to a real process, even though higher biomass concentration increases the viscosity and can disturb the saccharification yield (Miranda et al., 2012; Wang et al., 2014; Wang et al., 2016).

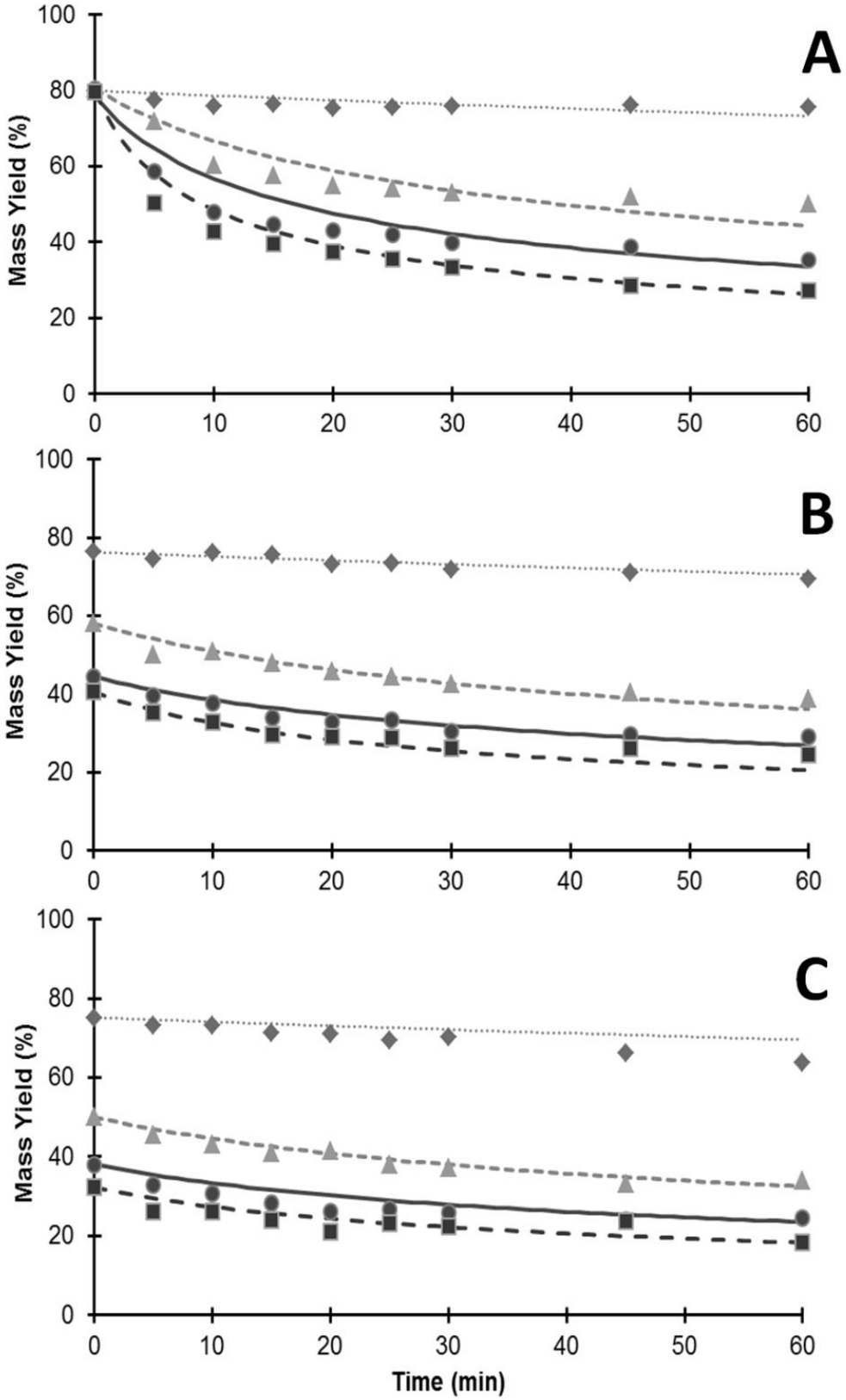

Figure 9.1: Mass yield versus time. A – 110 °C, B – 120 °C and C – 130 °C. (♦) 0, (▲) 1% (●) 3% and (■) 5% (v/v) of H_2SO_4. Lines represent model prediction. Standard deviation < 3%.

According to the **Table 9.2**, a high reaction order in comparison with lignocellulose solubilization was found: Average values were n = 3.6307 ± 0.1818 and m = 1.4161 ± 0.0649. The activation energy of the process was Ea = 41.1919 ± 0.0982 kJ/mol. These values are much lower than cellulose/lignocellulosic biomass under acidic hydrolysis (n and m are first-order and Ea range between 100-190 kJ/mol).

Therefore, microalgal biomass has higher susceptibility to acidic hydrolysis, and the currently proposed process looks promising for application as a single step one to obtain fermentable sugars from microalgal biomass, i.e., using less energy. In the case of lignocellulosic biomass, the acidic treatment is used as pretreatment to remove the hemicellulose fraction and help enzyme accessibility to cellulose fraction (de-structuration of lignocellulose) (Negahdar et al., 2016), but additional cost due to the need of specific enzymes is one of the main bottlenecks to cellulosic ethanol consolidation.

The inclusion of the acid concentration in the kinetic of biomass de-structuration during a thermochemical hydrolysis is important and was already proposed (Saeman, 1945; Negahdar et al., 2016). Solubilization of lignocellulosic biomass is usually considered as first order with respect to biomass and acid concentration (Saeman, 1945; Chum et al., 1990). This concept was also used in the case of microalgae (Nguyen et al., 2009; Zhou et al., 2011), but the same assumption was not verified in this work (n and m, **Table 9.2**), showing the importance of new development for an accurately scientific evaluation and application to process simulation and plant design.

Kinetic constants (k - (min^{-1}) $(g/L)^{-m}$) values strongly increased as a function of temperature and acid concentration, being improved by 2-3 orders of magnitude with respect to the control condition (no acid addition). A similar effect of temperature is described in several works related to both lignocellulosic and microalgal biomass (Saeman, 1945; Miranda et al., 2012; Ho et al., 2013; Ashokumar et al., 2015; Negahdar et al., 2016), but so far has not been included at kinetic level, especially for microalgae.

Table 9.2: Kinetic constants at different temperatures to biomass solubilization during acidic hydrolysis.

110°C	**Acid Concentration (% v v^{-1})**	**k (reaction rate) (min^{-1}) $(g/L)^{-m}$**	***n* (reaction order)**	**Standard Error (%)**
Mass Yield	0	5.6161×10^{-9}	3.8741	1.2597
	1	2.2092×10^{-7}	3.6457	3.8225
	3	7.1992×10^{-7}	3.5578	3.1847
	5	2.1592×10^{-6}	3.4454	3.4340
Ea Activation Energy (kJ/mol)			41.1013	
k_0 (min^{-1})			0.3682	
m (reaction order to H^+)			1.3483	
R^2			0.9993	
Standard Error (%)			1.38×10^{-7}	

120°C	**Acid Concentration (% v v^{-1})**	**k (reaction rate) (min^{-1}) $(g/L)^{-m}$**	***n* (reaction order)**	**Standard Error (%)**
Mass Yield	0	5.7161×10^{-9}	3.8741	0.9519
	1	3.3972×10^{-7}	3.6457	1.6721
	3	1.0415×10^{-6}	3.5600	2.8233
	5	3.3996×10^{-6}	3.4843	1.9537
Ea Activation Energy (kJ/mol)			41.2962	
k_0 (min^{-1})			0.3702	
m (reaction order to H^+)			1.4221	
R^2			0.9946	
Standard Error (%)			4.07×10^{-7}	

130°C	**Acid Concentration (% v v^{-1})**	**k (reaction rate) (min^{-1}) $(g/L)^{-m}$**	***n* (reaction order)**	**Standard Error (%)**
Mass Yield	0	5.8361×10^{-9}	3.8741	3.2611
	1	4.3172×10^{-7}	3.6457	1.3024
	3	1.4391×10^{-6}	3.5600	1.4737
	5	4.1854×10^{-6}	3.4800	2.0706
Ea Activation Energy (kJ/mol)			41.1782	
k_0 (min^{-1})			0.3513	
m (reaction order to H^+)			1.4778	
R^2			0.9907	
Standard Error (%)			3.34×10^{-7}	

Average value ± Standard deviation

Ea = 41.1919 ± 0.0982 kJ/mol
k_0 = 0.3632 ± 0.0104 min^{-1}
m = 1.4161 ± 0.0649
n = 3.6307 ± 0.1818

9.3.3 Extracted sugars (total sugars) and reducing sugars (monomers)

The extraction (total sugars) and hydrolysis (reducing sugars) were validated in the same ranges of temperature (110, 120 and 130°C), acid concentration (0, 1, 3 e 5%) and reaction time (0-60 min) and are displayed in **Fig. 9.2** and **Fig. 9.3**. Clearly, at lower temperature (110°C) the amount of total sugars is higher than the reducing sugars measured (**Fig. 9.2A** and **9.3A**, respectively). In this case, it means that the sugars were separated from the biomass matrix but not efficiently converted to monomers. When the temperature increased (120 and 130°C), total and reducing sugars values become closer to each other, thus extraction and hydrolysis can be considered as concomitant processes (extraction and hydrolysis) (**Fig. 9.2B** and **C**, **Fig. 9.3B** and **C**).

At 120°C, more than 90% of reducing sugars were obtained when 3% of sulfuric acid and 30 min of reaction were used: this was considered as the best condition in the range of the experiments performed. In fact, according to literature 90% of biomass was hydrolyzed when 50 g L^{-1} of *Tribonema sp.* was submitted at 121°C and 3% of sulfuric acid for 30 min (Wang et al., 2014). Ashokumar et al. (2015) hydrolyzed 20 g L^{-1} of *Scenedesmus bijugatus* biomass at 130°C and 2% of acid, and obtained around 85% of saccharification. *Dunaliella tertiolecta* LB999 (50 g L^{-1}) at 121°C and 3.73% of sulfuric acid for 15 min provided a hydrolysis yield of 44.31%, but here time was probably limiting (Lee et al., 2013). *Scenedesmus obliquus* (50 g L^{-1}, 120°C and 5% of sulfuric acid for 30 min) provided > 90% of saccharification yield (Miranda et al., 2012). *Chlorella vulgaris* JSC-6 (120 g L^{-1}, 121°C and 4-6% of sulfuric acid for 20 min) (Wang et al., 2016), *Scenedesmus obliquus* CNW-N (10-40 g L-1, 121°C and 1.5-2% of sulfuric acid for 20 min) (Ho et al., 2013) and *Chlamydomonas reinhardtii* (50 g L^{-1}, 120 °C, 3% of sulfuric acid for 30 min) (Nguyen et al., 2009) reached a saccharification yield between 90-100%. All these optimized conditions from the literature agree with the experimental results obtained in our work, so that the presently developed model for *Chlorella vulgaris* could be assumed to be suitable for most of industrial microalgal species considered in the literature. In addition, no significant degradation processes were verified in the variables range used.

From **Table 9.3**, we note that most of extracted sugars was solubilized with higher acid concentrations (3 and 5%), but the kinetic constant did not increase as a function of temperature (see 120° and 130°C with respect to 110°C), probably due the reduced

sugars content on the biomass, because > 90% of sugars were already extracted (**Fig. 9.2**). As an example, with 5% of acid, *k* reduced from 1.612 to 1.391 and 1.378 at 110, 120 and 130°C, respectively. On the other hand, kinetic constants for reducing sugars increased as a function of temperature and acid concentration in all experiments inside the range studied and more than 90% of hydrolysis was reached (**Table 9.3** and **Fig. 9.3**).

According to the assumption $[S] = [Pol]^n[H^+]^m$, also K_M can be expressed including $[H^+]$ in its expression, and a value of the half-saturation mass yield (Pol_{KM}) can be calculated by:

$$[Pol]_{KM} = \left(\frac{KM}{[H^+]^m}\right)^{\frac{1}{n}} \quad (9.19)$$

Interestingly, it was found that the value of Pol_{KM} is practically independent of acid concentration, with an average of 42.02 ± 1.75 g/L (**Table 9.3**), thus the assumption made in the modified equation is reasonable. In this value of mass yield, around 80% of sugars were saccharified what justify the significantly reduction of the hydrolysis constant (*k*), which to the model is half of the maximum (k_{max}).

Furthermore, it is interesting to discuss selectivity values, this variable allows to evaluate the selection of best hydrolysis condition because it evaluates both the substrate (*Pol*) conversion and the product yield (Hydrolyzed Sugars). By looking at **Figure 9.4**, it is perceived that selectivity increased as a function of acid concentration and temperature up to the condition with 3% and 120°C, respectively, where more than 90% of saccharification yield was obtained, confirming the best condition mentioned before.

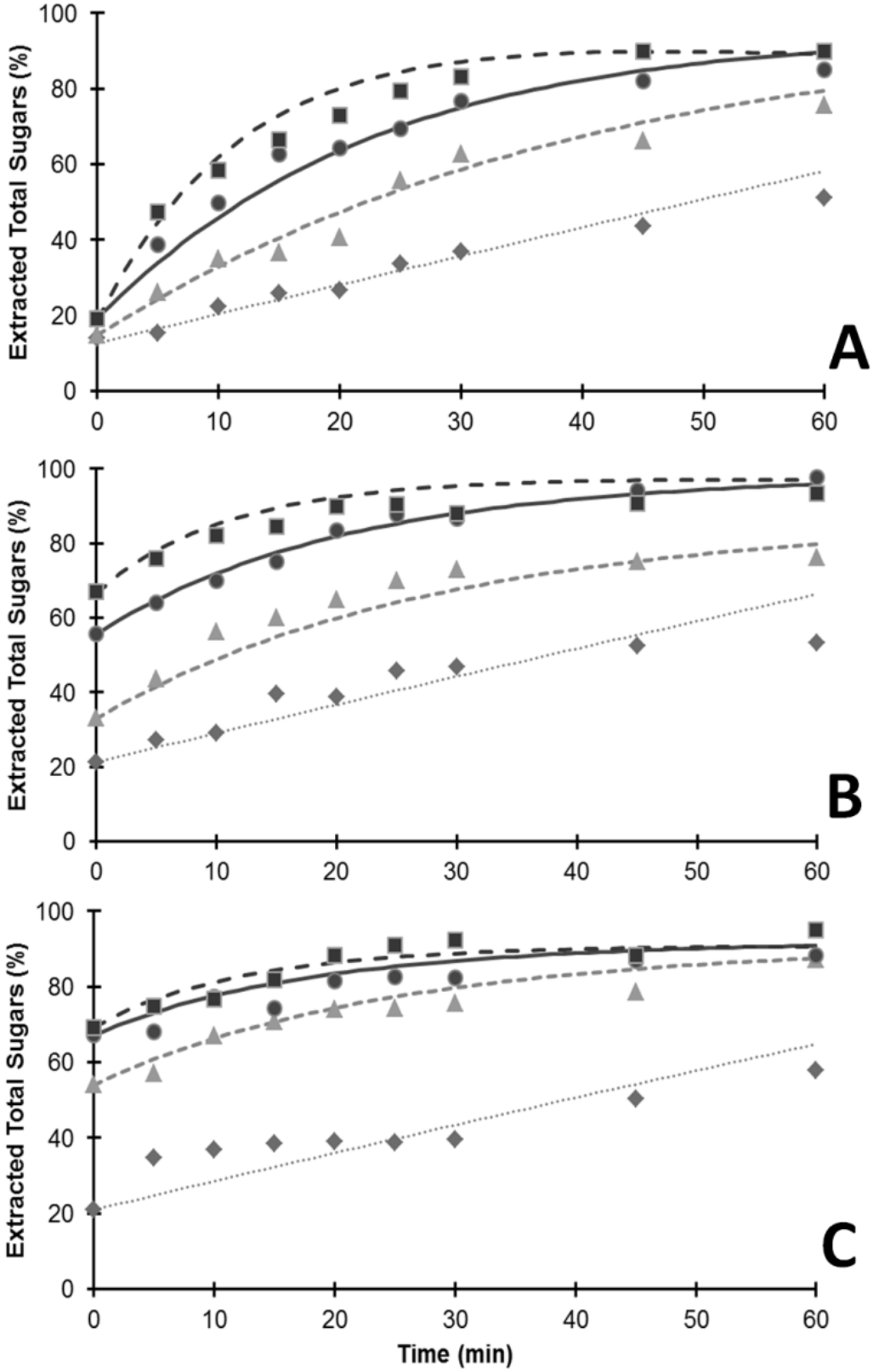

Figure 9.2: Total sugars versus time. A – 110 °C, B – 120 °C and C – 130 °C. (♦) 0, (▲) 1% (●) 3% and (■) 5% (v/v) of H_2SO_4. Lines represent model prediction. Standard deviation < 4%.

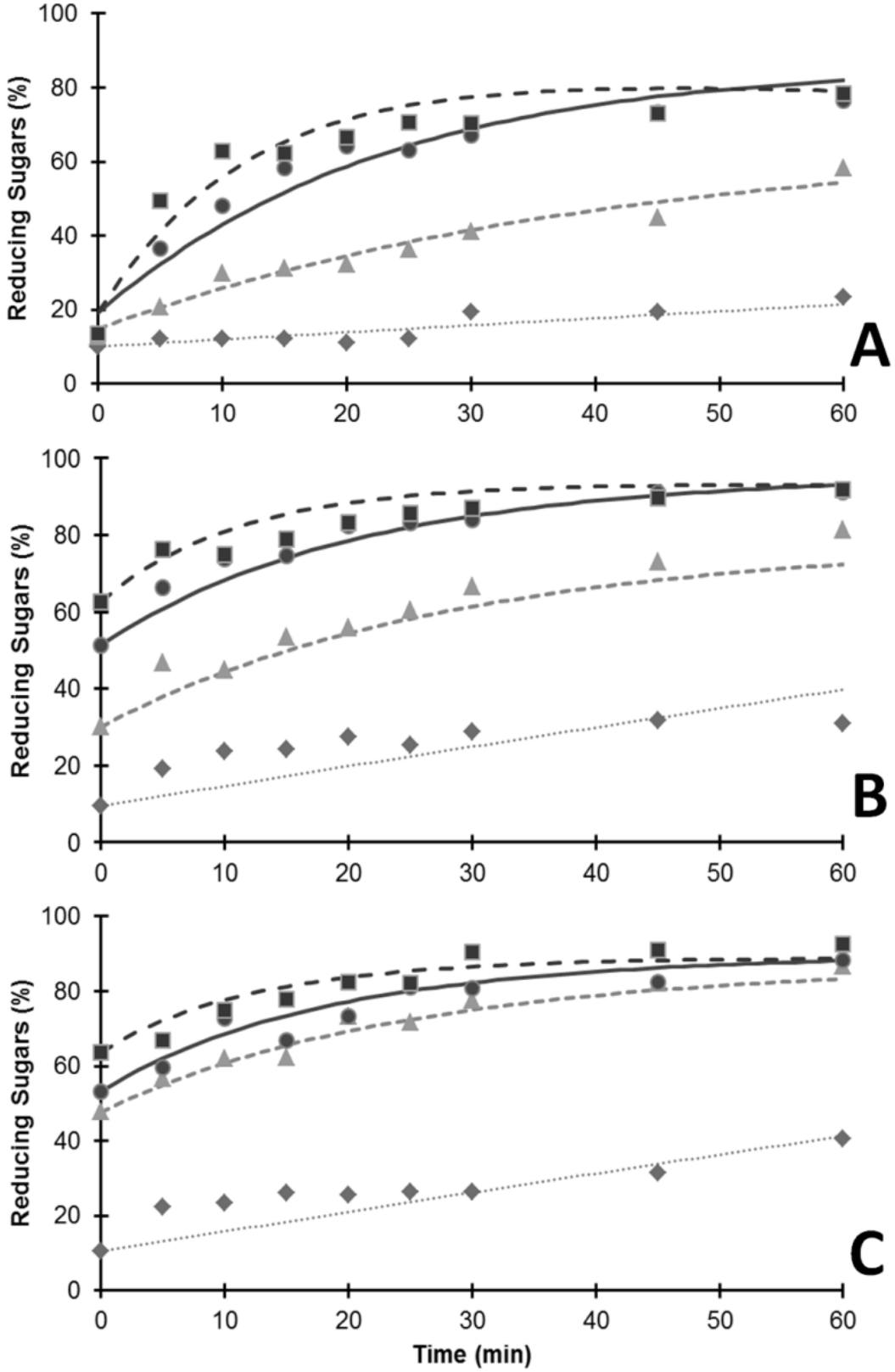

Figure 9.3: Reducing sugars (monomers) versus time. A – 110 °C, B – 120 °C and C – 130 °C. (♦) 0, (▲) 1% (●) 3% and (■) 5% (v/v) of H_2SO_4. Lines represent model prediction. Standard deviation < 7%.

Table 9.3: Kinetic constants at different temperatures to sugars solubilization in acidic hydrolysis.

110°C	Acid Concentration (% v v^{-1})	*k* (min^{-1})	**Standard Error (%)**
Extracted Total Sugars	0	0.2000	2.8090
	1	0.5376	6.1345
	3	0.8312	12.2784
	5	1.6120	11.4015
120°C	Acid Concentration (% v v^{-1})	*k* (min^{-1})	**Standard Error (%)**
Extracted Total Sugars	0	0.2101	0.9519
	1	0.6512	1.6721
	3	0.8613	2.8233
	5	1.3912	1.9537
130°C	Acid Concentration (% v v^{-1})	*k* (min^{-1})	**Standard Error (%)**
Extracted Total Sugars	0	0.2130	3.0718
	1	0.6600	7.0591
	3	0.7513	3.3769
	5	1.3781	14.2573
110°C	Acid Concentration (% v v^{-1})	*k* (min^{-1})	**Standard Error (%)**
Reducing Sugars	0	0.0500	1.9692
	1	0.3276	2.1678
	3	0.7400	12.9241
	5	1.3815	6.8101
120°C	Acid Concentration (% v v^{-1})	*k* (min^{-1})	**Standard Error (%)**
Reducing Sugars	0	0.1003	5.2345
	1	0.5912	6.7966
	3	0.8915	4.6584
	5	1.3900	3.1307
130°C	Acid Concentration (% v v^{-1})	*k* (min^{-1})	**Standard Error (%)**
Reducing Sugars	0	0.1502	6.4838
	1	0.7008	3.4356
	3	1.1112	8.6658
	5	1.6120	4.4052
		Acid Concentration (% v v^{-1})	KM (g/L)
		0	10,557.0
		1	268,920.5
		3	556,314.8
		5	764,521.5
Remembering: $KM = [Pol]^{n}_{KM}[H^{+}]^{m}$			
$[Pol]_{KM}$ (g/L)			42.02 ± 1.75

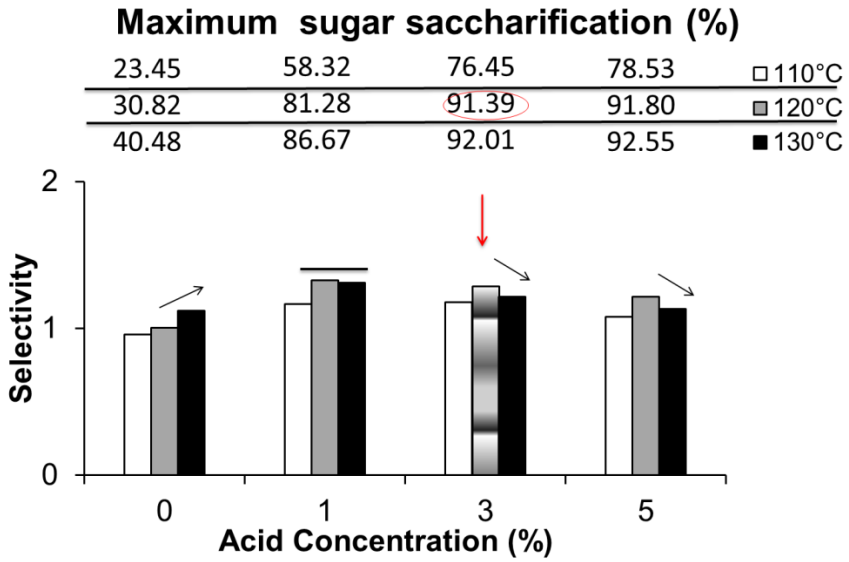

Figure 9.4: Selectivity versus acid concentration at different temperature. The maximum sugars recovery is reported above the graph to be correlate with the selectivity. The best condition was considered 3% of acid concentration and 120 °C, in evidence.

9.3.4 Ethanolic fermentation

Fermentation of the hydrolyzed *Chlorella* biomass was carried out using *S. cerevisiae*, leading to the results presented in **Fig. 9.5**. Here, it can be seen that the fermentation was fast and reached a sugars consumption of 75% in 24 hours. If we consider pentose-excluding sugars (hexoses) only, the reduction was 94.2%, indicating a good performance. The ethanol to sugar factor was 0.307, when the maximum stoichiometric value is 0.5111 (Gay-Lussac stoichiometry), but this is normal because a lower yeast inoculum concentration was used, and part of the carbohydrates are metabolized to cellular multiplication. Similar values are reported by other authors (Lee et al., 2013; Markou et al., 2013; Cabral et al., 2016). On the other hand, when a high inoculum concentration (10% m v^{-1}) is used, this yield is increased to values about 95% of sugars consumption, and more than 80% of ethanol yield can be achieved (Laurens et al., 2015), whereas our work, it was 60.6% (**Table 9.4**).

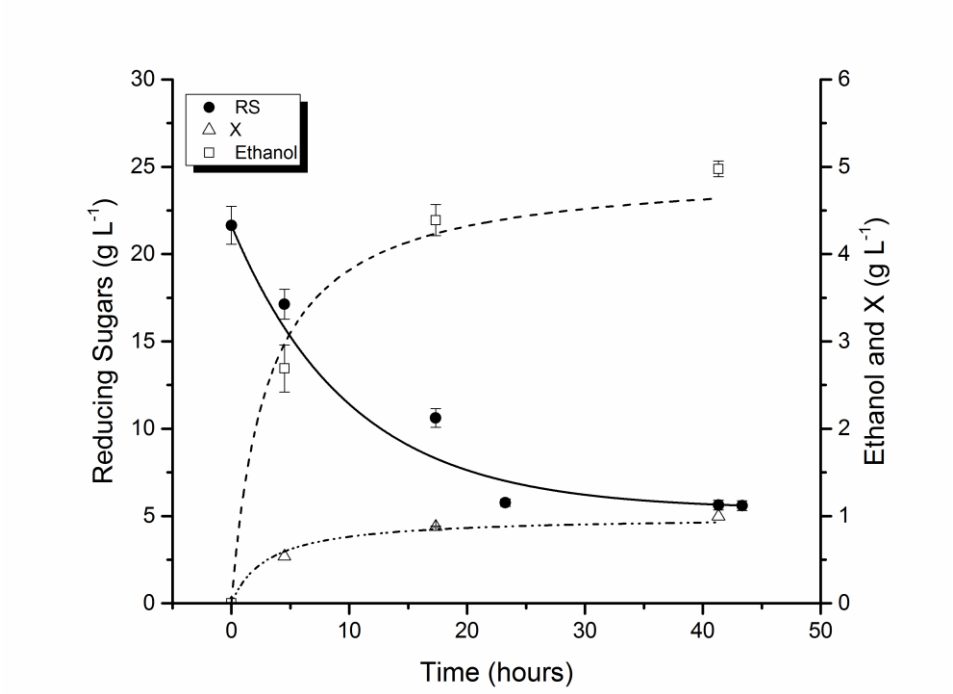

Figure 9.5: Ethanolic fermentation from *Chlorella* hydrolyzed. RS – Reducing sugars and X – yeast concentration.

Table 9.4: Fermentation parameters.

Experiment	% Sugars consumption	Final Ethanol concentration (g/L)	$Yield_{Process}$ (%)	$Yield_{Fermentation}$ (%)	$Y_{X/S}$	$Y_{E/S}$	$Y_{X/E}$
3% of acid at 120°C for 30 min	74.2 (94.2) *	4.97 ± 0.09	45.0	60.6	0.080	0.307	0.250

*Excluding pentose, because 21.56% (Table 1) of sugars are pentose: xylose + arabinose (not naturally fermented for *S. cerevisiae*). $\mu = 0.2311 \pm 0.03$ $hour^{-1}$.

Literature values of ethanol/biomass yields are 0.163 $g_{ethanol}/g_{biomass}$ (*Arthrospira platensis* – chemical hydrolysis) (Markou et al., 2013), 0.140 $g_{ethanol}/g_{biomass}$ (*Dunaliella tertiolecta* - chemeoenzimatic) (Lee et al., 2013) and 0.214-0.233 $g_{ethanol}/g_{biomass}$ (*Chlorella vulgaris* FSP-E - enzymatic and chemical hydrolysis, respectively) (Ho et al., 2013). In this work, a value of 0.150 $g_{ethanol}/g_{biomass}$ was achieved, using low yeast inoculum concentration < 0.1 g L^{-1} of yeast and considering a biomass with 50% of carbohydrates). The stoichiometrically maximum value considering a biomass with 50% of carbohydrates is 0.26.

9.3.5 Nutrient recovery and industrial process development

Acidic hydrolysis, as aforementioned, is a non-specific process and all biomass components are attached and can be dissolved. A special attention was paid to the protein content accounting for most of N fraction in the biomass and ash (mineral content, in particular P content), because N and P salts are the main nutrient requirements for microalgae cultivation (apart of carbon which comes from CO_2), and consequently, they are crucial in determining cultivation costs.

The repetition of the experiments (with a 1 L – scale reactor) at 120°C with 3% of acid (in quadruplicate) showed the same mass and saccharification yield reported before, confirming the reproducibility of the process (**Fig. 9.6A**). In view of ethanol production within a biorefinery approach, the acidic thermochemical process proved to be efficient in the solubilization of protein and ash fractions too: as shown in **Figure 9.6B**, the liquid phase obtained in the best conditions (120°C, 3% of acid and 30 min) contained around 80% of the ash and 70% of the proteins present in the initial biomass.

Nutrient recovery is a 'hot topic' in order to recycle the maximum of these nutrients in the process of microalgae cultivation so that to minimize the consumption of these nutrients (Kumar and Gupta, 2008; Garcia-Moscovo et al., 2013; Marques et al., 2013; Barreiro et al., 2015; Moraes et al., 2015; Silva and Abud, 2016)**.** This possibility was checked with respect to algae cultivation in several standard mediums, which are recipes providing an optimized mixture of nutrients to support their growth (Barreiro et al., 2015). In our currently proposed process, most of solubilized nutrients go to the fermentation, thus helping the yeast growth. After that, ethanol is distilled, yeast is centrifuged and recirculated, and the effluent remaining (stillage/vinasse) has the major concentration of nitrogen and phosphorous, among other nutrients. Therefore, the recycling/recovery of this effluent is mandatory. In addition, the solid waste from hydrolysis process account for around 30% in mass of the initial biomass and its components can be recovered too. To this scope, the most efficient processes to recover the nutrients and increase energy efficiency are, hydrothermal liquefaction (HTL), flash hydrolysis and anaerobic digestion.

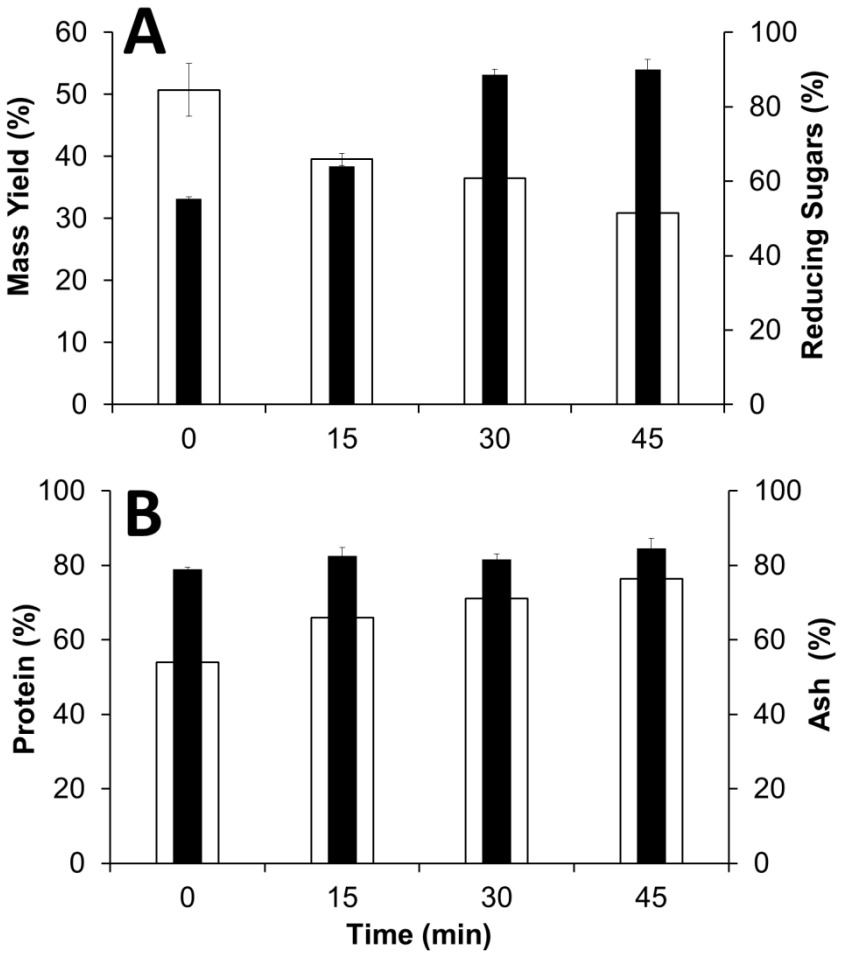

Figure 9.6: Repetition of the acidic hydrolysis experiment at 120°C using 3% of acid concentration. A) Mass yield (White) and reducing sugars (Black). B) Protein (White) and ash (Black) released in the liquid fraction (%).

For instance, HTL with *Arthrospira platensis* at 190-210°C for 2-4 hours was able to recover 78-90% of nitrogen present in biomass (Yao et al., 2016). The main disadvantage of HTL is its high-energy duty, caused by the rather high temperature and pressure operating conditions. *Scenedesmus obliquus* was grown in the hydrolysate obtained by flash hydrolysis obtained from the same specie for flash hydrolysis at 280°C and 9s of residence time with a protein recovery of 65% in the liquid phase (Garcia-Moscovo et al., 2013). This species obtained better performance in batch cultivation than in the standard medium for autotrophic growth, thanks to the combination of heterotrophy (mixotrophy). In continuous cultivation mode, the productivities ranged between 0.62-0.72 g/(L day), showing satisfactory performances (Barbera et al., 2016). When anaerobic digestion is used for nutrient recycling, it is

necessary to discuss about liquid phase (biofertilizer), because several non-gasifiable nutrients in the operation conditions, such as N and P, remain in mineral conditions in the final effluent, known as digestate, especially as ammonium and phosphate salts (Moraes et al., 2015; Silva and Abud, 2016). Anaerobic digestion provides a liquid biofertilizer that can be also used for the cultivation of microorganisms (nutrient recycling) with an increase in sustainability and autonomy of the process; and is already integrated in an ethanol biorefinery (Moraes et al., 2015). For instance, *Chlorella vulgaris* was cultivated in sugarcane stillage anaerobically biodigested with the consumption of a great amounts of N and P of the effluent (Marques et al., 2013).

Economic and energetic analysis will confirm the real applicability of this technology because even with these promising numbers, cultivation costs of microalgae are still high in comparison with other crops (Silva and Bertucco, 2016). Some points that need to be developed to increase the process feasibility are: solid fraction recycling, yeast recycling, stillage utilization, pentose fermentation and lipid fraction destination.

9.4 CONCLUSIONS

In this work it was shown that the acidic treatment of microalgal biomass is effective to solubilize biomass and hydrolyze the biomass sugars (by more than 90% present in *Chlorella vulgaris*). A model of *n* order for biomass solubilization and a modified Michaelis-Menten equation were able to simulate efficiently the experimental hydrolysis data, acid concentration with *m* order kinetic is included in this model, and showing an activation energy lower than for lignocellulosic biomass. After the thermochemical process, most of the proteins and ash present in the biomass are released in the liquid-phase and can be used in the ethanolic fermentation step. It was also shown that *S. cerevisiae* fermented satisfactorily most of the sugars. The simplicity and efficiency of the process make this arrangement promising and a block flow diagram of an industrial process was eventually proposed.

REFERENCES

AOAC – Association of Analytical Chemists. Official Methods of Analysis of the Association of Official Analytical Chemists, 17th ed., Gaithersburg: Ed. William Horwitz, 2002.

Ashokumar, U., Salom, Z., Tiwari, O.N., Chinnasamy, S., Mohamed, S., Ani, F.N., 2015. An integrated approach for biodiesel and bioethanol production from *Scenedesmus bijugatus* cultivated in a vertical tubular photobioreactor. Energy Conversion and Management 101, 778-786.

Barbera, E., Sforza, E., Kumar, S., Morosinotto, T., Bertucco, A., 2016. Cultivation of *Scenedesmus obliquus* in liquid hydrolysate from flash hydrolysis for nutrient recycling. Bioresource Technology 207, 59-66.

Barreiro, D.L., Bauer, M., Mornung, U., Posten, C., Kruse, A., Prens, W., 2015. Cultivation of microalgae with recovered nutrients after hydrothermal liquefaction. Algal Research 9, 99-106.

Belkacemi, K., Abatzaglou, N., Overend, R.P., Chornet, E., 1991. Phenomenological kinetics of complex systems: mechanistic considerations in the solubilization of hemicelluloses following aqueous/steam treatments. Ind. Eng. Chem. Res. 3, 2416-2425.

Biller, P., Ross, A.B., Skill, S.C., Lea-Langton, A., Balasundaram, B., Hall, C., Riley, R., Leewellyn, C.A., 2012. Nutrient recycling of aqueous phase for microalgae cultivation from the hydrothermal liquefaction process. Algal Research 1, 70-76.

Cabral, M.M.S., Abud, A.K.S., Silva, C.E.F., Almeida, R.M.R.G., 2016. Bioethanol from coconut husk fiber. Ciencia Rural 46(10), 1872-1877.

Chen, C., Zhao, X., Yen, H., Ho, S., Cheng, C., Lee, D., Bai, F., Chang, J., 2013. Microalgae-based carbohydrates for biofuel production. Biochemical Engineering Journal 78, 1-10.

Choi, S.P., Nguyen, M.T., Sim, S.J., 2010. Enzymatic pre-treatment of *Chlamydomonas reinhardtii* biomass for ethanol production. Bioresource Technology 101, 5330-5336.

Chum, H.L., Johnson, D.K., Black, S.K., Overend, R.P., 1990. Pretreatment-catalyst effects and the combined severity parameter. Applied Biochemistry and Biotechnology 24/25, 1-14.

Chisti, Y., 2007. Biodiesel from microalgae. Biotechnology Advances 25, 294-306.

Deichmann, U., Schuster, S., Mazat, J., Comish-Bowden, A., 2014. Comemorating the 1913 Michaelis-Menten paper Die Kinetik der Invertinwikiring: three perspectives. the FEBS Journal 281, 435-463.

Ding, L., Cheng, J., Xia, A., Jacob, A., Voelklein, M., Murphy, J.D., 2016. Co-generation of biohydrogen and biomethane through two-stage batch co-fermentation of macro- micro-algal biomass. Bioresource Technology 218, 224-231.

Garcia-Moscovo, J.L., Obeid, W., Kumar, S., Hatcher, P.G., 2013. Flash hydrolysis of microalgae (*Scenedesmus sp.*) for protein extraction and production of biofuels intermediates. J. Supercrit. Fluids 82, 183-190.

Hernandez, D., Riano, B., Coca, M., Garcia-Gonzalez, M.C., 2015. Saccharification of carbohydrates in microalgal biomass by physical, chemical and enzymatic pre-treatmens as aprevious step for bioethanol production. Chemical Engineering Journal 262, 939-945.

Ho, S., Huang, S., Chen, C., Hasunuma, T., Kondo, A., Cheng, J., 2013. Bioethanol production using carbohydrate-rich microalgae biomass as feedstock. Bioresource Technology 135, 191-198.

Jacobsen, S.E., Wyman, C.E., 2000. Cellulose and hemicellulose hydrolysis models for application to current and novel pretreatment processes. Applied Biochemistry and Biotechnology 84-86: 81-96.

Jang, Y., Park, J.M., Choi, S., Choi, Y.J., Seung, D.Y., Cho, J.H., Lee, S.Y., 2012. Engineering of microorganisms for the production of biofuels and perspectives based on systems metabolic engineering approaches. Biotechnology Advances 30, 989-1000.

Kuhad, R.C., Gupta, R., Khasa, Y.P., Singh, A., Zhang, Y.H.P., 2011. Bioethanol production from pentose sugars: current status and future prospects. Renewable and Sustainable Energy Reviews 15(9), 4950-4962.

Kumar, S., Gupta, R.B., 2008. Hydrolysis of microcrystalline cellulose in subcritical and supercritical water in a continuous flow reactor Ind. Eng. Chem. Res. 47(23), 9321-9329.

Kumar, G., Sivagurunathan, P., Thi, N.B.D., Zhen, G., Kobayashi, T., Kim, S., Xu, K., 2016. Evaluation of different pretreatments on organic matter solubilization and hydrogen fermentation of mixed microalgae consortia. International Journal of Hydrogen Energy 41, 21628-21640.

Laurens, L.M.L., Nagle, N., Davis, R., Sweeney, N., Van Wychen, S., Lowell, A., Prenkos, P.T., 2015. Acid-catalyzed algal biomass pretreatment for integrated lipid and carbohydrate-based biofuels production. Green Chemistry 17, 1145-1158.

Lee, O.K., Kim, A.L., Seong, D.H., Lee, C.G., Jung, Y.T., Lee, J.W., Lee, E.Y., 2013. Chemeo-enzymatic saccharification and bioethanol fermentation of lipid-extracted residual biomass of the microalga, Dunaliella tertiolecta. Bioresource Technology 132: 197-201.

Lee, O.K., Oh, Y., Lee, E.Y., 2015. Bioethanol production from carbohydrate-enriched residual biomass obtained after lipid extraction of *Chlorella sp.* KR-1. Bioresource Technology 196, 22-27.

Marques, S.S.I., Nascimento, I.A., Almeida, P.F., Chinalia, F.A., 2013. Growth of Chlorella vulgaris on sugarcane vinasse: the effect of anaerobic digestion pretreatment. Applied Biochemical and Biotechnology 171, 1933-1943.

Markou, G., Angelidaki, I., Nerantzis, E., Georgakakis, D., 2013. Bioethanol production by carbohydrate-enriched biomass of *Antrospira (Spirulina) platensis*. Energies 6, 3937-3950.

Markovsky, I., Huffel, S.V., 2007. Overview of total least squares methods. Signal processing 87, 2283-2302.

Miller, J.G., 1959. Use of dinitrosalicyclic acid reagent for determination of reducing sugars. Analytical Chemistry 31(3), 426-428.

Miranda, J.R., Passarinho, P.C., Gouveia, L., 2012. Pre-treatment optimization of *Scenedesmus obliquus* microalga for bioethanol production. Bioresource Technology 104, 343-348.

Moraes, B.S., Zaiat, M., Bonomi, A., 2015. Anaerobic digestion of vinasse from sugarcane ethanol production in Brazil: Challenges and perspectives. Renewable and Sustainable Energy Reviews 44, 888-903.

Mosier, N., Wyman, C., Dale, B., Elander, R., Lee, Y.Y., Holtzapple, M., Landisch, M., 2005. Features of promising technologies for pretreatment of lignocellulosic biomass. Bioresource Technology 96(6), 673-686.

Negahdar, L., Delidovich, I., Palkovits, R., 2016. Aqueous-phase hydrolysis of cellulose and hemicellulose over molecular acidic catalysis: Insights into the kinetics and reaction mechanism. Apllied Catalysis B: Environmental 184, 285-298.

Nguyen, M.T., Choi, S.P., Lee, J., Lee, J.H., Sim, S.J., 2009. Hydrothermal acid pretreatment of *Chlamydomonas reinhardtii* for ethanol production. Journal of Microbiology and Biotechnology 19(2), 161-166.

Overend, R.P, Chronet, E., 1987. Fractionation of lignocellulosics by steam-aqueous pretreatments. Phil. Trans. R. Soc. Lond. A 321, 523-536.

Rocha, M.S.R.S., Pratto, B., Junior, R.S., Almeida, R.M.R.G., Cruz, A.J.G., 2017. A kinetic model for hydrothermal pretreatment of sugarcane straw. Bioresource Technology 228, 176-185.

Saeman, J.F., 1945. Kinetics of wood saccharification: hydrolysis of cellulose and decomposition of sugars in dilute acid at higher temperature. Industrial and Engineering Chemistry, 43-52.

Silva, C.E.F., Gois, G.N.S.B., Silva, L.M.O., Almeida, R.M.R.G., Abud, A.K.S., 2015. Citric waste saccharification under different chemical treatments. Acta Scientiarum Technology 37(4), 387-395.

Silva, C.E.F., Bertucco, A., 2016. Bioethanol from microalgae and cyanobacteria: a review and technological outlook. Process Biochemistry 51, 1833-1842.

Silva, C.E.F., Sforza, E., 2016. Carbohydrate productivity in continuous reactor under nitrogen limitation: effect of light and residence time on nutrient uptake in *Chlorella vulgaris*. Process Biochemistry 51, 2112-2118.

Silva, C.E.F., Abud, A.K.S., 2016. Anaerobic biodigestion of sugarcane vinasse under mesophilic conditions using manure as inoculum. Ambiente & Agua – An Interdisciplinary Journal of Applied Science 11(4), 763-777.

Silva, C.E.F., Sforza, E., Bertucco, A., 2017. Effects of pH and carbon source on *Synechococcus* PCC 7002 cultivation: biomass and carbohydrate production with different strategies for pH control. Appl. Biochem. Biotechnol. 181, 682-698.

Song, L., Yu, H., Ma, F., Zhang, X., 2013. Biological pretreatment under non-sterile conditions for enzymatic hydrolysis of corn stover. Bioresources 8(3), 3802-3816.

Tercero, E.A.R., Domenicali, G., Bertucco, A., 2014. Autotrophic production of biodiesel from microalgae: An updated process and economic analysis. Energy 76, 807-815.

Trevelyan, W.E., Harrison, J.S., 1952. Studies on yeast metabolism. 1. Fractionation and microdetermination of cell carbohydrates. Biochem. J. 50(3), 298-303.

Vitova, M., Bisova, K., Kawano, S., Zachleder, V., 2015. Accumulation of energy reserves in algae: from cell cycles to biotechnological applications. Biotechnology Advances 33, 1204-1218.

Wang, Y., Guo, W., Lo, Y., Chang, J., Ren, N., 2014. Charactherization and kinetics of bio-butanol production with *Clostridium acetobutylicum* ATCC 824 using mixed sugar medium simulating microalgae-based carbohydrates. Biochemical Engineering Journal 91, 220-230.

Wang, Y., Guo, W., Cheng, C., Ho, S., Chang, J., Ren, N., 2016. Enhancing bio-butanol production from biomass of *Chlorella vulgaris* JSC-6 with sequential alkali pretreatment and acid hydrolysis. Bioresource Technology 200, 557-564.

Yang, J., Xu, M., Zhang, X., Hu, Q., Sommerfeld, M., Chen, Y., 2011. Life-cycle analysis on biodiesel production from microalgae: water footprint and nutrients balance. Bioresource Technology 102, 159-165.

Yao, C., Wu, P., Pan, Y., Lu, H., Chi, L., Meng, Y., Cao, X., Xue, S., Yang, X., 2016. Evaluation of the integrated hydrothermal carbonization-algal cultivation

process for enhanced nitrogen utilization in *Arthrospira platensis* production. Bioresource Technology 216, 381-390.

Zhou, N., Zhang, Y., Wu, X., Gong, X., Wang, Q., 2011. Hydrolysis of Chlorella biomass for fermentable sugars in the presence of HCl and $MgCl_2$. Bioresource Technology 102, 10158-10161.

Chapter 10

Severity factor as an efficient control parameter to predict biomass solubilization and saccharification during acidic hydrolysis of microalgal biomass

In this chapter, the acidic pretreatment of microalgal biomass is investigated, and the solubilized biomass and hydrolyzed sugars were evaluated. The process is analyzed through the severity factor approach (acidic combined severity factor – ACSF). A suitable kinetic model is developed and applied, and it is shown that the severity factor theory works. A discussion and comparison are presented with respect to the literature methods, which are mainly related to lignocellulosic biomass. In the case of microalgae, reaction orders for biomass and acid are shown to be the main parameters, and no other assumptions are needed. Two regions of the acidic treatment process have to be evaluated: low and high reactivity regions. Furthermore, a suitable experimental design is required in order to provide a suitable reaction spectrum to obtain a good estimation of the kinetic parameters. A logarithmic severity factor range (ln ACSF) between 5–6 is able to solubilize around 80% of biomass and to hydrolyze more than 90% of sugars present in the biomass•.

•*Part of this chapter was submitted in BioEnergy Research, 2017.*

10.1 INTRODUCTION

Fractionation of lignocellulosic biomass is an important issue for a biorefinery as its efficiency relies on the possibility to recover all biomass components, generally represented by cellulose, hemicellulose and lignin (Negahdar et al., 2016). In this field, micro and macroalgae have gained space in the last decade, mainly due to the limitations expressed by saccharide/starch-based biomasses (food vs fuel) and lignocellulosic biomasses (high recalcitrance and difficulty/cost to recovery all sugars) (Silva and Bertucco, 2016).

Several processes are used to de-structure/pretreat biomass and dilute acidic biomass is among the most tested pretreatments due to its simplicity, high reactivity with hemicellulose, reduced reaction time and moderate pretreatment temperature, providing high recovery rates of sugars and efficiency to prepare biomass for enzymatic hydrolysis (cellulose accessibility) (Mosier et al., 2005; Nguyen et al., 2009; Zhou et al., 2011; Zoulikha et al., 2015; Temiz and Akpinar, 2017). In terms of kinetics, the main operating variables in acidic pretreatment/hydrolysis are: heating time, acid concentration and temperature. However, studying these variables separately requires an excessive number of experiments (i.e., larger time) and the use of derived variables can help to evaluate and model the process faster. This is the case of the severity factor (ACSF).

Initially, the concept of dilute acidic treatment of lignocellulosic biomass was discussed by Saeman (1945), who modified the classical Arrhenius equation and included the acid concentration as an additional variable of the process. Significant contributions to this concept were made by Overend and Chornet (1987), Chum et al. (1990a), Belkacemi et al. (1991) and Jacobsen and Wyman (2000). ACSF parameter is mainly a result of a combination of heating time, acid concentration and holding temperature. As examples of lignocellulosic biomasses to which this approach was applied are wood (Saeman, 1945), *Populus tremuloides*, *Betula popyrifera*, corn stalks, *Stipa tenacissima* (Chum et al., 1990a; Belkacemi et al., 1991), corn stover (Lloyd and Wyman, 2005), cellulose fiber (Jacquet et al., 2011), poplar and switchgrass (Esteghlalian et al., 1997), pinewood and aspenwood (Janga et al., 2012a; Janga et al., 2012b), wheat straw (Zoulikha et al., 2015), rice husk and straw (Temiz and Akpinar, 2017).

Although the use of the ACSF idea has been applied successfully (mainly at industrial level), simplifications are adopted according to the type of biomass. Unfortunately, a good correlation between biomass solubilization and sugars hydrolysis for any combination of the parameters used with a significant number of levels for time, temperature and acid concentration is generally not achieved (Belkacemi et al., 1991; Lloyd and Wyman, 2000; Pedersen and Meyer, 2010; Zhou et al., 2011). For this reason, some pseudokinetic terms are included in the kinetic equations in order to facilitate graphic adjustment under limited condition ranges (Chum et al., 1990a; Chum et al., 1990b; Jacquet et al., 2011; Janga et al., 2012a; Temiz and Akpinar, 2017). Microalgae had already been previously tested, but a satisfactory correlation between saccharification extension and severity factor was not achieved, i.e., only the trend could be reproduced, indicating that some kinetic considerations were probably misinterpreted (Nguyen et al., 2009; Zhou et al., 2011).

In this chapter, a discussion regarding the definition of the severity factor in the case of a saccharification process from microalgal biomass (*Chlorella vulgaris*) is presented. Reference parameters and transient heating/cooling times are also evaluated. Furthermore, the adoption of reaction orders *n* for biomass solubilization, and *m* for acid concentration, lead to a different analysis, exhibiting a significant contribution in the severity factor sensitivity, and reaching a good correlation between experimental data and simulated function.

10.2 THEORETICAL BACKGROUND AND ASSUMPTIONS

Severity factor (R_0) can be conceptualized as a variable that represents the combination of time and temperature (for a given catalyst), being related with the extent of the reaction from a starting kinetic model (e.g. the Arrhenius equation). The inclusion of the catalyst concentration in the model for acidic process is fundamental, being called, in this case, acidic combined severity factor (*ACSF* or R_0').

Generally, severity factor definitions proposed in the literature are:

$$R_0 = e^{\frac{E_a}{R}\frac{(T-T_r)}{T_r^2}} t \qquad \text{(for hydrothermal treatment)} \qquad (10.1)$$

$$R_0' = e^{\frac{E_a}{R}\frac{(T-T_r)}{T_r^2}} [H^+]t \qquad \text{(for acidic treatment)} \qquad (10.2)$$

where R_0 is the severity factor based on the temperature and time contribution, E_a is the reaction activation energy, R is the gas constant, T is the holding temperature of the process, T_r is the reference temperature (100 °C) and t is the holding time. R_0' is the severity factor with the inclusion of the acidic catalyst and $[H^+]$ is the acid concentration.

From equations, (1) and (2) a correlation between the severity factor value and the reaction extent can be found (both for biomass solubilization and sugars extracted), which is qualitatively represented in **Figure 10.1**. Degradation processes were not addressed in our work, but they can be combined with a severity factor approach as well to obtain other products such as 5-HMF, furfural and formic, acetic, fumaric acid (Chen et al., 2007).

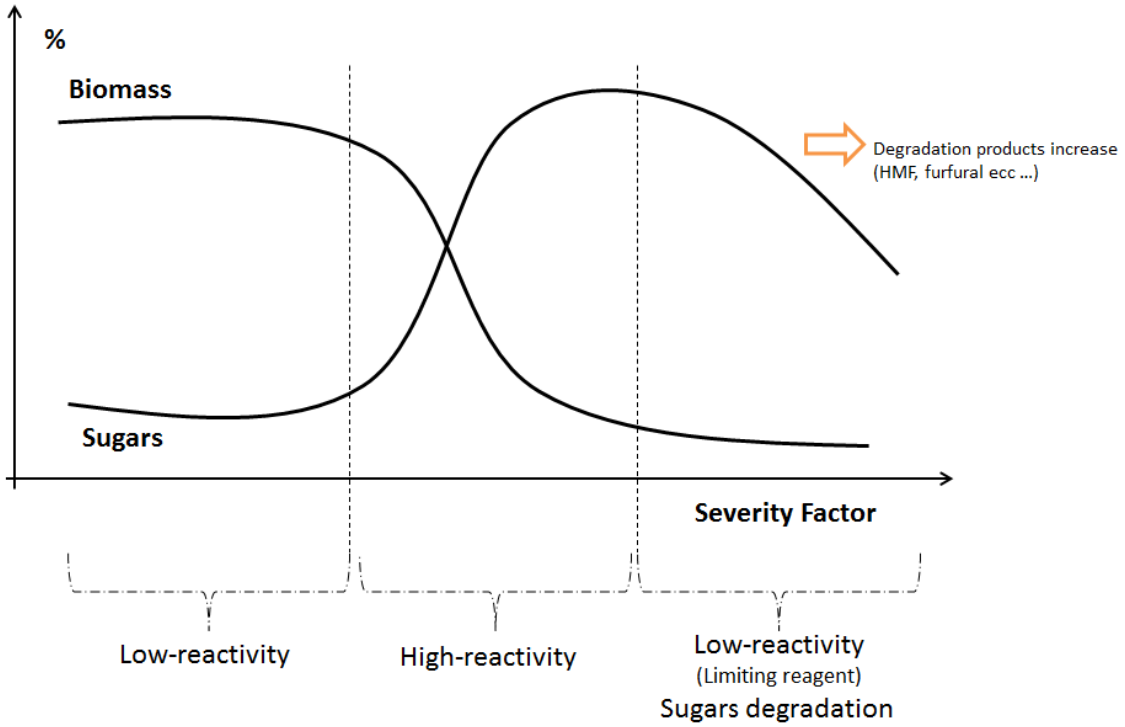

Figure 10.1: Theoretical correlation between biomass solubilization, sugars hydrolysis and severity factor.

The severity factor, namely its logarithmic value is a useful parameter for analyzing the extent of reaction during acidic hydrolysis and can simplify the prediction of sugar yields (Janga et al., 2012a). Log R_0 is used for hydrothermal treatment without acid, whereas for acidic treatment (Equation 10.2), it can be derived:

$$log(R_0') = log(R_0) + \log[H^+] \text{ (acidic treatment)} \quad (10.3)$$

Therefore, for acidic treatment, the same value of R'_0 can be obtained with any combination of time, temperature and acid concentration. However, available data from published papers do not provide a uniform curve, probably due to the fact that some kinetic considerations were not taken into account, or were possibly wrong.

It is important to mention that the severity factor can be used for any thermochemical process, such as hydrothermal pretreatment (Rubio et al., 1998; Jacquet et al., 2011), organosolv (Chum et al., 1990a; Chum et al., 1990b), alkaline (Montané et al., 1994; Pedersen et al., 2010), chemical impregnation – SO_2 (Bura et al., 2003) and subcritical hot water extraction (Kim et al., 2014), i.e., not only for acidic treatment. However, the severity factor values are different as the reaction rate changes from one process to the other (Pedersen and Meyer, 2010). For example, hydrothermal treatment and acidic explosion are generally performed at high temperatures (170-220°C), while alkaline and acidic treatment are carried out at temperatures between 110-150°C due to the additional catalyst effect. Furthermore, the biomass structure or type can also influence in the process. A comparison between the severity factors in the solubilization of different biomasses is only possible if the kinetic model associated is adequately set, which is not so often done in the literature. In fact, main simplifications that can be found are:

10.2.1 First-order reaction

Several papers consider first order reaction models for biomass solubilization and acid concentration (Chum et al., 1990a; Belkacemi et al., 1991; Nguyen et al., 2009; Zhou et al., 2011), but this assumption is not valid for all biomass types. At least for catalyst concentrations, reaction order values of 1.34 (sulfuric acid) (Saeman, 1945), 0.849 (sulfuric acid) and 3.90 (sodium hydroxide) (Silverstei et al., 2007) have been verified. Using a reaction order different from 1 can significantly change the calculation of the severity factor which should be correctly performed. Otherwise a comparison between different biomasses cannot be done.

10.2.2 Assuming that $[H^+]$ is obtained by a pH measurement

The role and applicability of pH value in the kinetic equations is still unclear, especially in the case of a heterogeneous reaction, as it happens for biomass solubilization and

polysaccharides hydrolysis. In order to facilitate the representation of catalyst concentration, some authors use the pH measure to represent the acid concentration of the kinetic model (Chum et al., 1990a; Chen et al., 2007; Zhou et al., 2011; Zoulikha et al., 2015; Temiz and Akpinar, 2017).

Some papers studied the effect of pH on both the pretreatment and enzymatic hydrolysis of biomass (Pedersen and Meyer, 2010; Pedersen et al., 2010; Pedersen et al., 2011). Even though these data suggest a significant influence of the pH on the reaction yield, indicating that best values are both low (1-3) and high (10-13) pH with respect to intermediate values (4-9) (characteristic of acidic and alkaline treatments), it is not confirmed that pH is the right variable to use, because it is well known that applying acidic and alkaline solutions at high concentrations leads to higher process efficiency than expected on the base of Equation 10.2.

For this reason, it has been seen as inappropriate to numerically associate the pH with the kinetic model. In fact, some speculations are made with respect to the pH measure to calculate the severity factor as the interaction between the acid solution, and a biomass which is composed by several fractions, could alter this value (Jacobsen and Wyman, 2000). Two questions mainly arise: "what is the valid range for which pH and acid concentration in a heterogeneous catalysis can be interrelated?" and "is such a correlation correct?". In this article, acid concentration of the initial solution, instead of pH, was used in all kinetic expressions.

10.2.3 Use of pseudo-parameters

Phenomenological kinetics is widely used in heterogeneous catalysis, and it is an important aid in reactor design. It is based on some simplifying assumptions, such as: it neglects the role of fluctuations, it assumes that there is no correlation with the location of reactants on the surface and it considers the reacting mixture to be an ideal solution (Temel et al., 2007). In particular, the severity factor is an approach to describe the phenomenological kinetics of a complex reactive system (in this case, a heterogeneous system for biomass) from basic kinetic principles (Montané et al., 1994).

In some cases, adjustment parameters are proposed, such as ω, β, γ, δ and λ (Chum et al., 1990a; Montané et al., 1994; Janga et al., 2012a). In practical terms, they are useful as they help the severity function to efficiently fit the experimental data, but in most

cases, they change according to the biomass type and operational range, and are not able to explain the basic nature of the process.

An example is parameter ω which accounts for the effect of temperature and is related to the activation energy. It is highly applied in severity factor correlations to approxime the dependency of the Arrhenius equation to the experimental data (Chum et al., 1990a). In general, this parameter is equal to 14.75 (hydrothermal treatment of hardwood, bagasse and plant residues – xylose solubilization) (Overend and Chornet, 1987), with almost all subsequent studies with lignocellulosic and microalgal biomass having adopted this value (Nguyen et al., 2009; Lloyd and Wyman, 2005; Silverstei et al., 2007; Jacquet et al., 2011; Zhou et al., 2011; Temiz and Akpinar, 2017), even for hexose hydrolysis and delignification processes (with both acidic and alkaline treatment). However, some authors suggest that ω can assume other values depending of the biomass, process, catalyst or product desired. In fact, values between 14.3-33.4 are listed by Janga et al. (2012a) (pinewood and aspenwood – acidic hydrolysis), 39.4 by Montané et al. (1994) (wood – alkaline delignification) and 10-12 (aspenwood – hemicellulose hydrolysis) by Chum et al. (1990a).

The severity factor approach must simplify the kinetic representation and adequately predict the experimental data. If the data and the function are not coherently correlated, it means that some kinetic considerations were probably misinterpreted, with the use of pseudo-kinetic parameters inhibiting the visualization of errors. For this reason, this approach must be carefully analyzed before its application and utilized only if the classic kinetic equations cannot be used.

In this article, we propose a detailed analysis regarding the application of the severity factor on biomass solubilization and sugars hydrolysis, in this case of microalgae. *Chlorella vulgaris* was submitted to several reaction times, temperatures and acid concentrations, results are presented and discussed, and a different representation of the severity factor is eventually proposed and checked on the experimental data.

10.3 MATERIAL AND METHODS

10.3.1 Strain and biomass characterization

Chlorella vulgaris biomass powder was produced by Neoalgae® (Micro seaweed products B-52501749). The characterization included the determination of moisture

(method 934.01), ash (method 942.05), protein (method 2001.11) and lipid content (method 2003.05), as well as carbohydrates and monomers (HPLC) (AOAC, 2002).

10.3.2 Biomass solubilization and sugars hydrolysis

Acidic hydrolysis was performed with 10% of solids load (microalgal biomass), in autoclave (Autoclave vapour-line^{eco} VWR®), using temperatures between 100-130°C (P ~ 1 atm), and evaluating the concentration of the catalyst (H_2SO_4 – 98% Sigma®) (0, 1, 3 and 5% v/v) and the reaction time (0-60 mins) to find the kinetic constants required to efficiently simulate the severity factor (see **section 3.3**). Mass yield as well as extracted (total) and reducing (monomers) sugars were evaluated at the end of the reaction.

The mass yield (MY) of the process was measured by gravimetry as the dry weight after the thermochemical treatment, using cellulose acetate filters of 0.45μm (Whatman®) at 105°C for 2 hours. Filters were pre-dried for 10 mins at 105°C to remove any moisture. The relation between solubilized biomass and mass yield is expressed by:

$$[Solubilized\ Biomass]\ (\%) = \frac{Initial\ biomass\ Load\ \left(\frac{g}{L}\right) - Mass\ yield\left(\frac{g}{L}\right)}{Initial\ biomass\ Load\ \left(\frac{g}{L}\right)} \bullet 100 \qquad (10.4)$$

Total extracted sugar (TS) was determined by the Anthrone method (Trevelyan and Harrison, 1952), with the DNS method being used for reducing sugar (monomers) (RS) (Miller, 1959). So, the % of sugars extracted/hydrolyzed can be calculated according to:

$$[Sugar]\ (\%) = \frac{Sugar\ concentration\ \ in\ the\ liquor\ \left(\frac{g}{L}\right)}{Initial\ biomass\ load\ \left(\frac{g}{L}\right) \bullet\ Carbohydrates\ content} \bullet 100 \qquad (10.5)$$

where the carbohydrate content is given as a relative value between 0-0.6, generally the maximum of carbohydrate accumulation in microalgae and cyanobacteria is 0.6 = 60%, expressed in dry weight basis (Silva and Bertucco, 2016; Silva and Sforza, 2016; Silva et al., 2017).

10.3.3 Severity factor analysis

The heating curve of temperature versus time is the starting point to evaluate a thermochemical treatment (**Figure 10.2**). There are three ranges to be considered: 1–$t_{heating}$, 2–$t_{holding}$ and 3–$t_{cooling}$, with the reference temperature (T_r) being set to 100°C. The heating rates used in this work are as follow: 1) until T_r of 6.12, 7.65 and

9.59°C/min, 2) between T_r and $T_{holding}$ of 2.5, 3.3 and 3.6°C/min and 3) between $T_{holding}$ and T_r, of -0.75, -0.78 and -1.12°C/min for 110, 120 and 130°C, respectively.

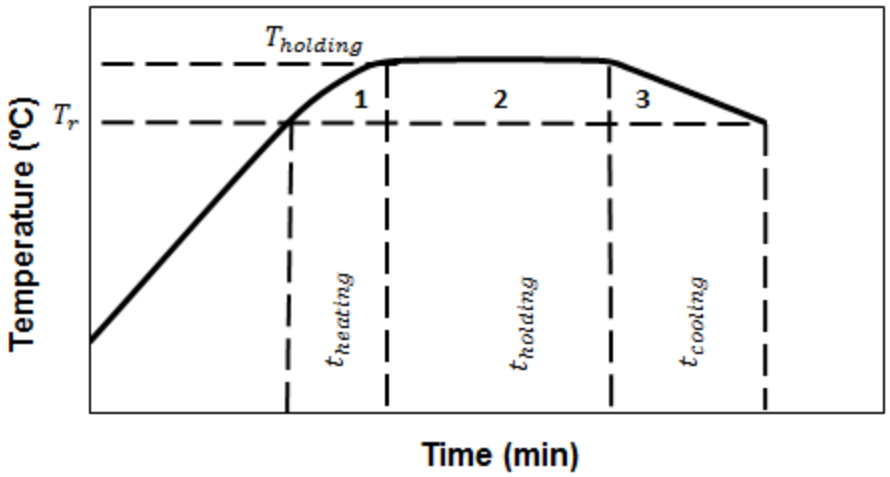

Figure 10.2: Heating curve of the process.

The biomass concentration (Pol – g/L) decreased as an effect of treatment time according to:

$$\frac{dPol}{dt} = [\frac{dPol}{dt}]_2 + [\frac{dPol}{dt}]_1 + [\frac{dPol}{dt}]_3 \quad (10.6)$$

where only the first term has been considered in the literature so far.

The reactions leading to biomass solubilization depend on all the three contributions, i.e. on the transitory heating/cooling times as well. Thus, the biomass solubilized results to be the sum of its transitory heating/cooling times and holding time frations.
The contribution of the holding time can be calculated as a function of time only, as temperature and acid are constant:

$$\frac{dPol}{dt_2} = kPol^n \qquad (T \text{ and } [H]^+ \text{ constant}) \quad (10.7)$$

where

$$k = k_0[H^+]^m e^{\frac{-E_a}{RT}} \text{ (Modified Arrhenius equation)} \quad (10.8)$$

where k is the reaction rate considering the dependency of the modified Arrhenius equation (min^{-1} g L^{-1}), k_0 is the reaction constant (min^{-1}), n is the reaction order of the biomass and m is the reaction order of the acid.

Utilizing a two-terms Taylor expansion of Equation 10.8 as a function of temperature (T) and using T_r = 100 °C as reference temperature, it is possible to find that:

$$k = k_0 e^{\frac{-E_a}{RT_r}} e^{\frac{E_a}{R}\left(\frac{T-T_r}{T_r^2}\right)} [H^+]^m \quad (10.9)$$

and from Equations 10.7 and 10.9, it can be obtained:

$$\frac{Pol^{1-n} - {Pol_0}^{1-n}}{n-1} = k_0 e^{\frac{-E_a}{RT_r}} e^{\frac{E_a}{R}\left(\frac{T-T_r}{T_r^2}\right)} [H^+]^m t_2 \quad (10.10)$$

where *Pol* and Pol_0 are the final and initial biomass concentration and t_2 is the holding reaction time (min).

A combination of these three terms (temperature, time and acid concentration) from the right part of Equation 10.10 is conceptualized as the acidic combined severity factor (ACSF):

$$ACSF = e^{\frac{E_a}{R}\left(\frac{T-T_r}{T_r^2}\right)} [H^+]^m t_2 \quad (10.11)$$

Using the logarithmic form of Equation 10.10, it is possible to highlight a linear relationship between the biomass solubilized (differential) and the ACSF value:

$$\ln\left(\frac{Pol^{1-n} - {Pol_0}^{1-n}}{n-1}\right) = \ln\left(k_0 e^{\frac{-E_a}{RT_r}}\right) + \ln(ACSF) \quad (10.12)$$

Since a correlation between the products of the reaction (sugars) and biomass solubilized can be found:

$$Sugars = f_1(Pol) \quad (10.13)$$

and

$$Pol = f_2(ACSF) \quad (10.14)$$

A dependency of the sugars parameter on the severity factor can also be obtained:

$$\Rightarrow Sugars = f_3(ACSF) \quad (10.15)$$

This relationship is quite complex and cannot be analytically expressed.

Finally, considering the $t_{heating\text{-}1}$ and $t_{cooling\text{-}3}$ of **Figure 10.2**, they effect in biomass solubilization and can be evaluated together, by means of an experiment without the holding time. Generally, this part is not considered in the calculation of the severity factor in the literature, but in this chapter, it is analyzed and discussed (see **section 10.4.4**).

10.4 RESULTS

The biochemical characterization of *Chlorella vulgaris* powder yielded (in % of dry weight): 49.5 ± 0.29 (proteins), 6.3 ± 0.15 (lipids), 23.0 ± 2.0 (carbohydrates), 7.18 ± 0.01 (ash), 5.41 ± 0.05 (moisture) and 8.61 (other). The composition of carbohydrates was found to be (in % of total sugars): 70.15 (glucose), 10.65 (xylose), 10.91 (arabinose), 5.73 (rhamnose) and 2.56 (other). This composition of sugars (around 20% of pentose – xylose and arabinose) correlates with the results published in other papers (Lee et al., 2015; Wang et al., 2016).

10.4.1 100°C as reference temperature

In the following, sometimes it is preferred to represent the results in terms of mass yield (percentage of the final biomass concentration respect to the initial biomass concentration), which is defined by:

$$Mass\ Yield\ (\%) = \frac{Pol_0 - Pol_{solubilized}}{Pol_0} . 100 \qquad (10.16)$$

In **Figure 10.3**, the mass yield was evaluated from room temperature (30°C) until up to 100°C, in order to validate the reference temperature of the model. A part of biomass powder is soluble, with the additional moisture content being then subtracted (12-28% of total biomass). The presence of acid helped the solubilization of a smaller fraction (5-7%) at 30°C. However, between 30-100 °C all experiments reached up to 80% of mass yield, a clear indication that this is the insoluble part, not significantly affected/reacted. Thus, the consideration of 100°C as a reference temperature was correctly accounted for the initial biomass concentration in the reaction, which is 80 g L^{-1}.

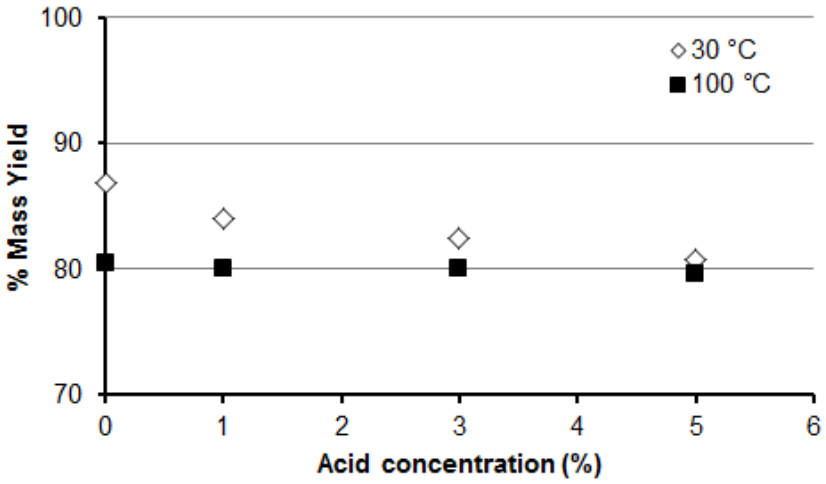

Figure 10.3: Reference temperature. Standard deviation < 3%.

10.4.2 Severity factor and biomass solubilization

Kinetic parameters were estimated from more than 140 independent experiments. Accordingly, these values are presented in **Table 10.1** together with their standard deviation. The estimation was based on the method of least squares which was considered as effective (Markovsky and Huffel, 2007), and the experimental data published (Silva and Bertucco, 2017).

Table 10.1: Constants used in the severity factor analysis.

Constant	Value
Ea (kJ/mol)	41.1919 ± 0.0982
$k_{0\,(}min^{-1}_{)}$	0.3632 ± 0.0104
m	1.4161 ± 0.0649
n	3.6307 ± 0.1818

As aforementioned, a linear correlation between a function of biomass solubilization and the severity factor allows a preliminary evaluation of the results' validity, which is theorethically represented by:

$$\frac{dPol}{Pol^n} = \frac{Pol^{1-n} - Pol_0^{1-n}}{n-1} \Rightarrow \ln\left(\frac{Pol^{1-n} - Pol_0^{1-n}}{n-1}\right) = \ln\left(k_0 e^{\frac{-E_a}{RT_r}}\right) + \ln(ACSF) \qquad (10.17)$$

As shown in **Figure 10.4**, a linear correlation of the experimental data was satisfactorially achieved at all the temperatures considered.

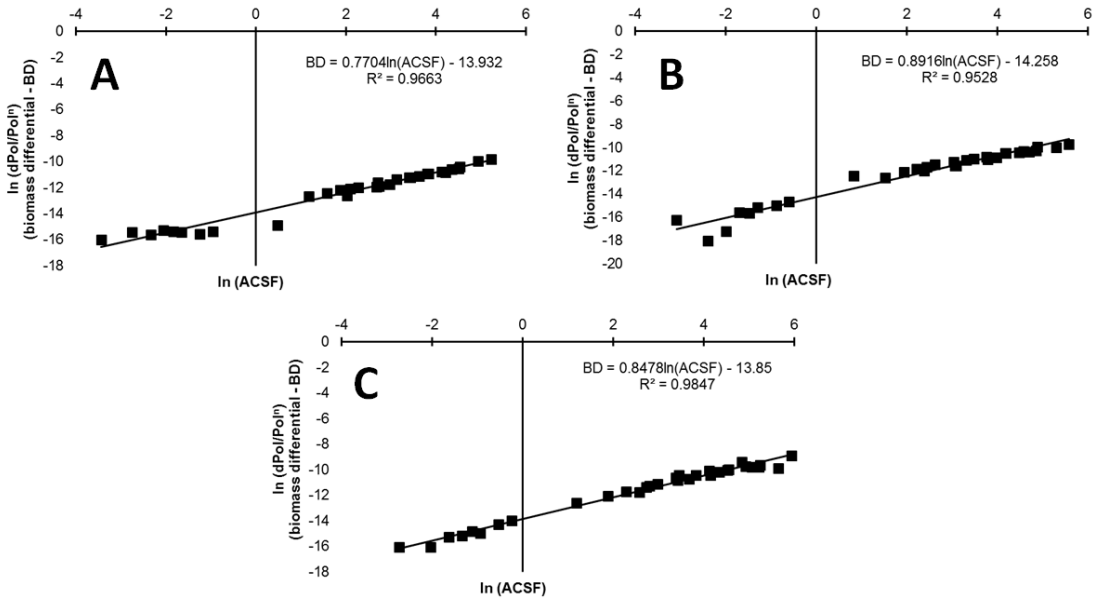

Figure 10.4: Biomass differential as a function of ACSF (severity factor). A – 110, B – 120 and C – 130°C.

Thus, the profile of biomass solubilization as a function of severity factor was seen as appropriate, showing that a variation of 5% in mass yield was sufficient to describe the kinetic behavior for each temperature (**Figure 10.5A-C**). On the other hand, when all temperature data were plotted together, the dispersion increased, but most experimental results could be predicted by the model considering a variation of 10% (**Figure 10.5D**). This behavior demonstrates that the theory was respected.

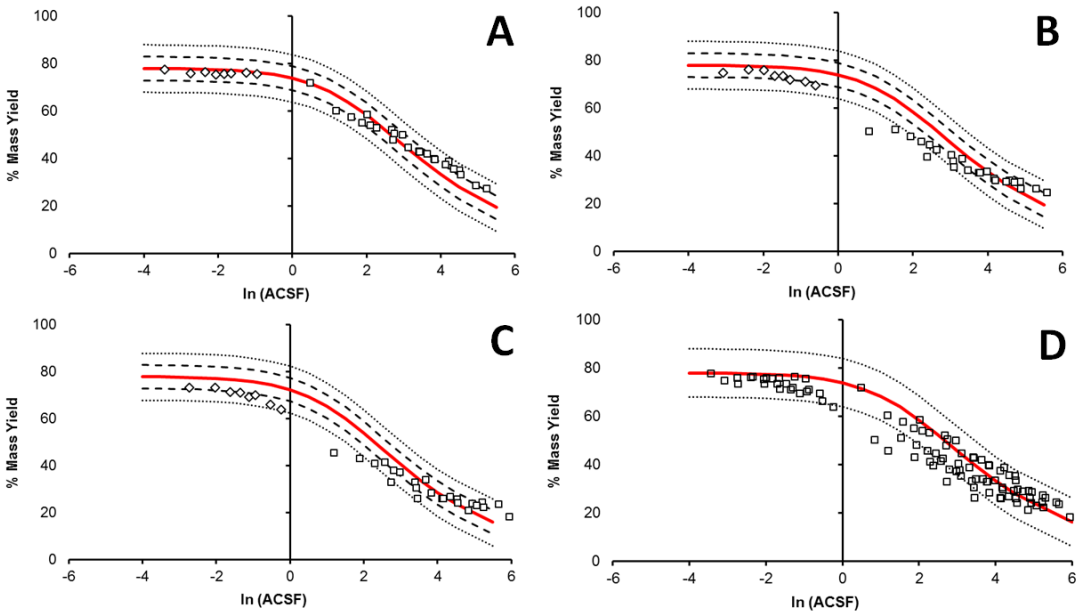

Figure 10.5: Biomass solubilization as a function of ACSF (severity factor). A – 110, B – 120, C – 130°C and D – All experimental data. Red line refers to the severity factor simulation, large-dotted lines considering 5% of deviation and small-dotted lines for 10%. Points indicate the average values of triplicate independent experiments, with a standard deviation of < 3%.

10.4.3 Severity factor and sugars hydrolysis

The total extracted sugars are represented in **Figure 10.6**. It is possible to verify two distinct regions: low-reactivity (white data points) and high-reactivity (black data points). They probably refer to two mechanisms of sugars extraction (**Figure 10.6A-B**), obtained for 0 and 1-5% of acid concentration, respectively. An excellent linear dependency with the severity factor is shown, with these two regions being closer to each other when the temperature was increased (**Figure 10.6C**).

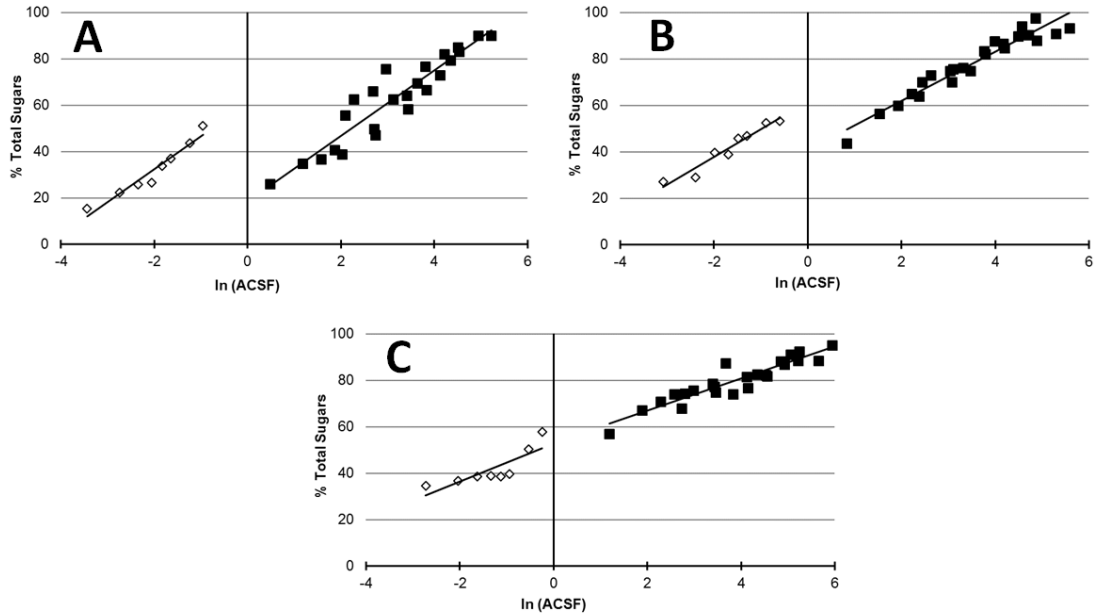

Figure 10.6: Correlation between the yield of biomass solubilization and hydrolized sugar. (♦) 0 and (■) 1, 3 and 5% of acid concentration. A – 110, B – 120 and C – 130°C.

As mentioned in Equation 10.15, if biomass solubilization and hydrolized sugars are correlated, then hydrolyzed sugars can be related with the severity factor. As verified in **Figure 10.7**, a linear function is sufficient to describe sugars hydrolysis and biomass solubilization at a given temperature. As shown in **Figure 10.8**, starting from the functions obtained in **Figure 10.7**, hydrolized sugars and the severity factor could be correlated between each other, despite the higher dispersion in comparison to the biomass solubilization for which the linear correlation of these functions was better. The values of R^2 for solubilizaed sugars were between 0.91 – 0.95, with the trend being respected.

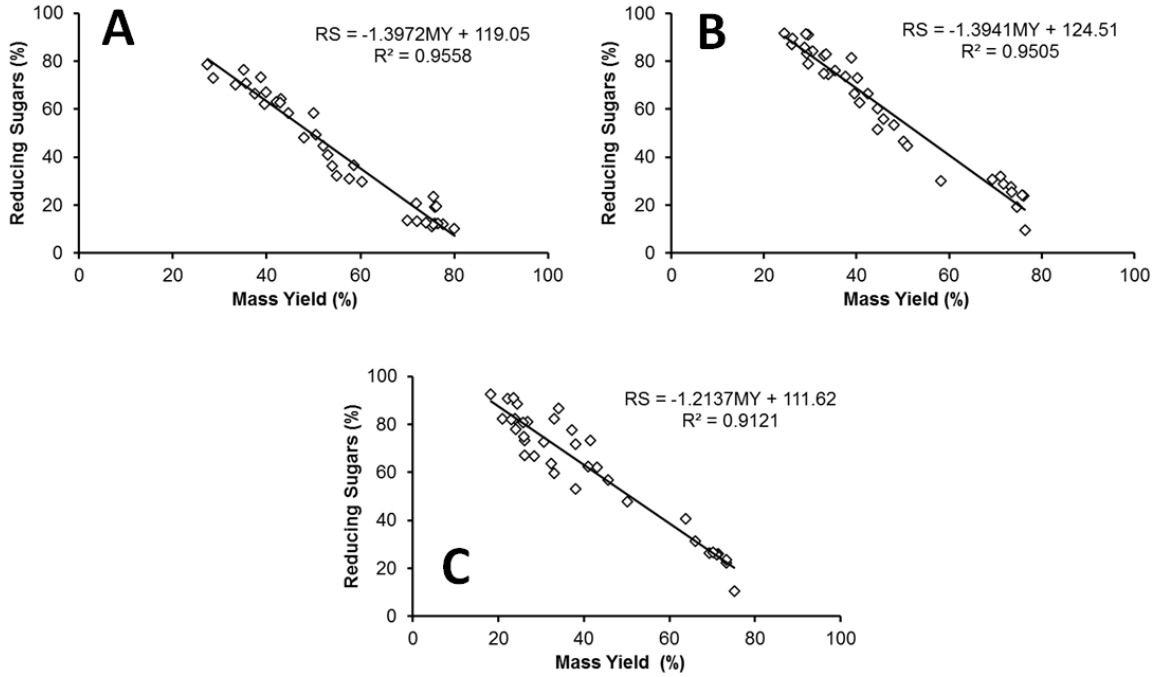

Figure 10.7: Correlation between biomass yield and hydrolized sugar. A – 110°C, B – 120°C and C – 130 °C.

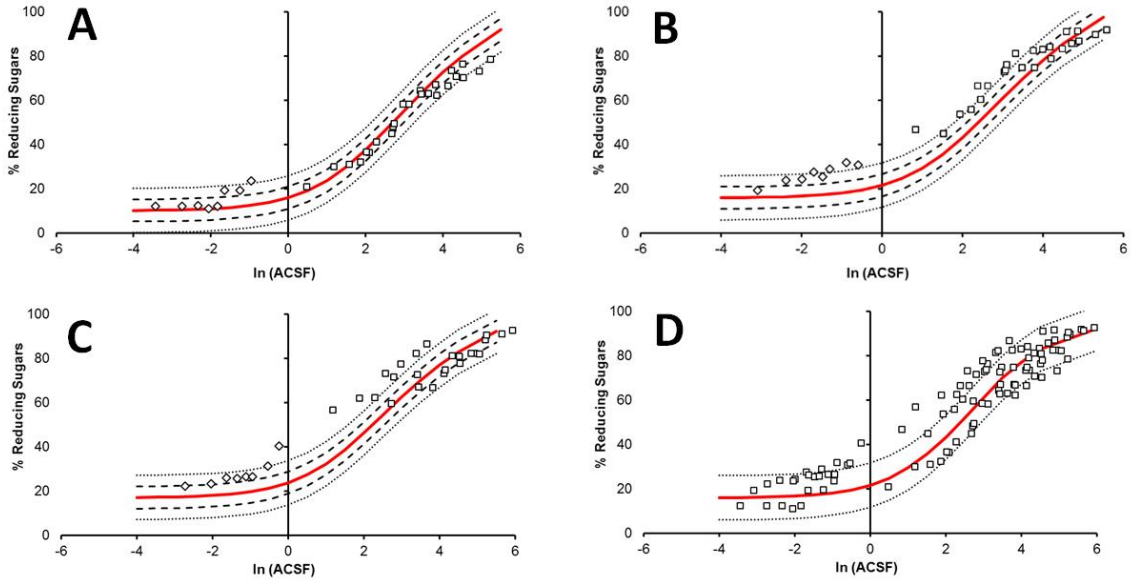

Figure 10.8: Sugars hydrolysis as a function of ACSF (severity factor). A – 110, B – 120, C – 130°C and D – All experimental data. Red line refers to severity factor simulation, large-dotted lines considering 5% of deviation and small-dotted lines for 10%. Points indicate average values of triplicate independent experiments, with a standard deviation of < 7%.

10.4.4 Transient time effects (heating and cooling)

In **Figure 10.9**, linear fitting curves among temperature, transient heating/cooling time, acid concentration and mass yield are shown. These correlations confirm that biomass solubilization and, consequentely, hydrolyzed sugars can be efficiently related with the severity factor using the holding time value (range 2 – **Figure 10.2**). These results may serve as a support to understand the effect of heating/cooling and to calculate the amount of biomass solubilized during the holding time. The fitting equations (18-29) are:

$$T = 0.7419t + 100 \ (R^2 = 0.9451) \quad \text{Fig.10.8A} \quad (10.18)$$

$$MY = -1.8436[H^+] + 78.281 \ (110°C - R^2 = 0.8012) \quad \text{Fig.10.8B} \quad (10.19)$$

$$MY = -6.1764[H^+] + 68.549 \ (120°C - R^2 = 0.8998) \quad \text{Fig.10.8B} \quad (10.20)$$

$$MY = -7.141[H^+] + 63.977 \ (130°C - R^2 = 0.8488) \quad \text{Fig.10.8B} \quad (10.21)$$

$$MY = -0.4974T + 134.81 \ (0 \ [H^+] - R^2 = 0.9458) \quad \text{Fig.10.8C} \quad (10.22)$$

$$MY = -1.1462T + 198.11 \ (1\% \ [H^+] - R^2 = 0.9836) \quad \text{Fig.10.8C} \quad (10.23)$$

$$MY = -1.5559T + 238.42 \ (3\% \ [H^+] - R^2 = 0.9561) \quad \text{Fig.10.8C} \quad (10.24)$$

$$MY = -1.7413T + 256.13 \ (5\% \ [H^+] - R^2 = 0.9496) \quad \text{Fig.10.8C} \quad (10.25)$$

$$MY = -0.4043t + 86 \ (0 \ [H^+] - R^2 = 0.9839) \quad \text{Fig.10.8D} \quad (10.26)$$

$$MY = -0.9103t + 85.189 \ (1\% \ [H^+] - R^2 = 0.957) \quad \text{Fig.10.8D} \quad (10.27)$$

$$MY = -1.2419t + 85.2361 \ (3\% \ [H^+] - R2 = 0.9395) \quad \text{Fig.10.8D} \quad (10.28)$$

$$MY = -1.3953t + 84.834 \ (5\% \ [H^+] - R2 = 0.9405) \quad \text{Fig.10.8D} \quad (10.29)$$

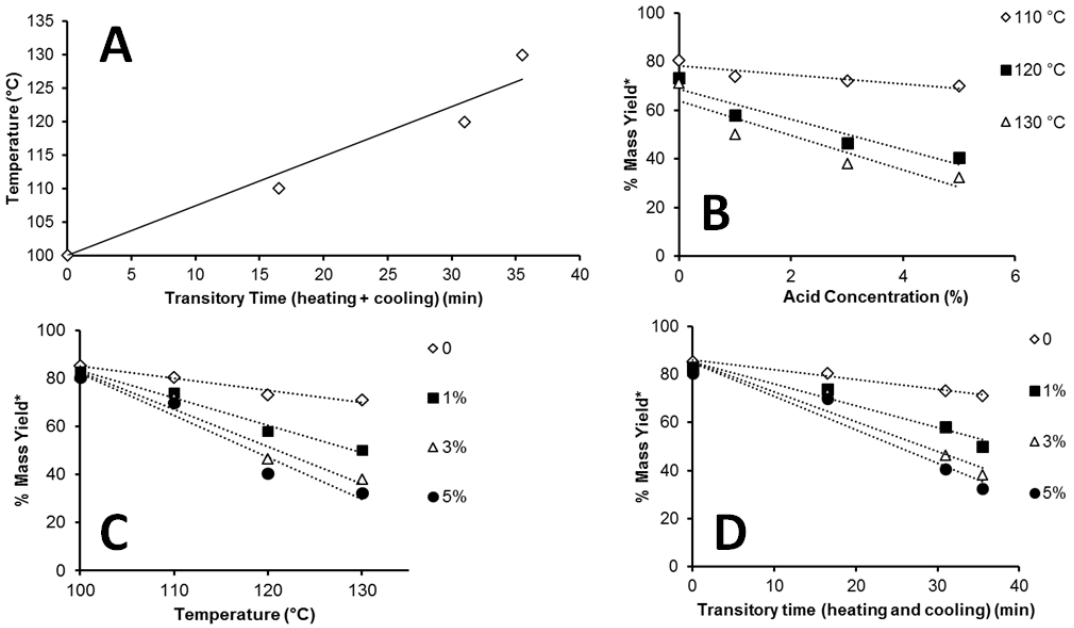

Figure 10.9: Influence of acid concentration and temperature during transitory time (heating and cooling) to biomass solublization. *Means that the mass yield was measured at the end of the transitory time (heating and cooling).

10.4.5 Order n variation

According to **Table 10.1**, both *n* and *m* have relative deviations of about 5%, however, the sensitivity of the mass yield and hydrolyzed sugars prediction was much higher with respect to n, as shown in **Figure 10.10**: where the effect of the variation of *n* was plotted, which corresponded to values between 3.48 and 3.87, almost all points from more than 140 independent average values (triplicate experiments) were embraced by the curves, showing the efficacy to provide an approximation of the combined severity parameter to represent biomass solubilization (**Figure 10.10A**) as well as sugars hydrolysis (**Figure 10.10B**). Thus, the variation of the *n* parameters needs to be considered in the function prediction.

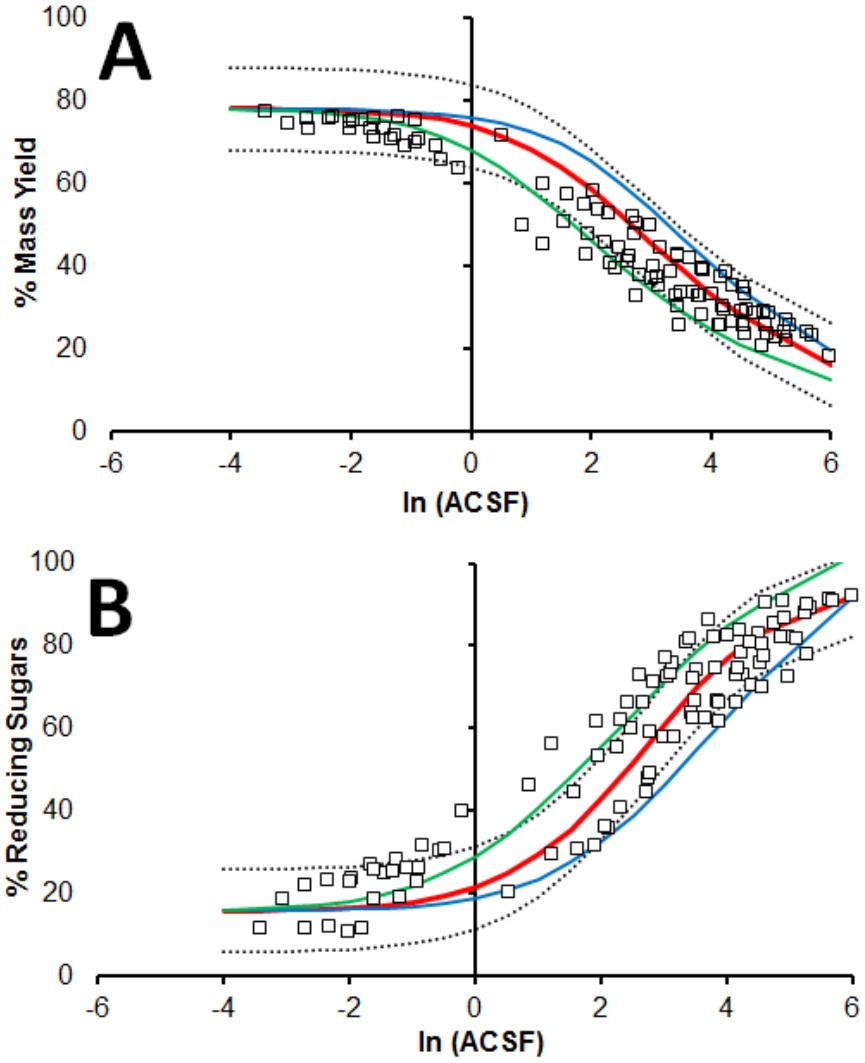

Figure 10: Sensitivity of the severity factor curve as a function of n. Red line – n = 3.63 (experimental average), blue line – n = 3.48 (lower experimental value) and green line – n = 3.87 (higher experimental value). A – Mass yield and B – Reducing sugars. Dotted-lines represent a variation of 10% from the predicted curves (the red lines).

It was verified that *n* decreased when the acid concentration increased, i.e., a lower reaction order between biomass and acid concentration was observed. Accordingly, an exponential relation better represented this behavior (**Figure 10.11** and Equation 10.30).

$$[H^+](\%) = 6.10^{17} e^{-11.54n} \qquad (10.30)$$

This result cannot be easily explained, given that the reaction order for H^+ was the same in all experiments (m = 1.4161 ± 0.0649) and that the biomass solubilization was higher when the acid concentration was increased.

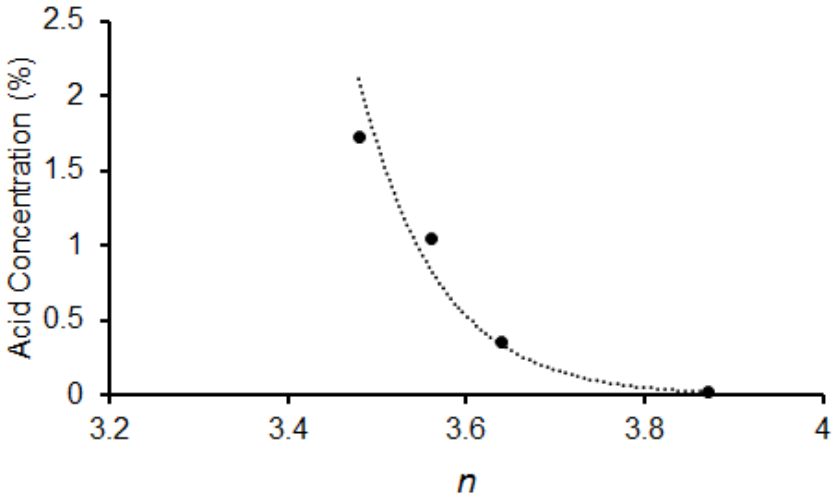

Figure 10.11: *n* as a function of acid concentration.

10.5 DISCUSSION

10.5.1 Reference temperature

The boiling temperature of water has been taken as a reference in previous works (Vroom, 1957; Overend and Chornet, 1987; Chum et al., 1990a; Jacobsen and Wyman, 2000), and conceptualized as the temperature above which the biomass has significantly increased reactivity and is effectively solubilized. In this paper, it is shown that this indeed happens. Additionally, a part of microalgal powder was soluble and/or contained moisture, thus the reaction started to be effective with 80% of mass yield (80 g/L).

10.5.2 Biomass solubilization and sugars hydrolysis

Variations between the severity factor curves for biomass solubilization and sugars hydrolysis have been found when acid concentration changed (Chum et al., 1990b; Belkacemi et al., 1991). The behavior of biomass solubilization we reported was the same as in the hydrothermal treatments of lignocellulosics which considers time and temperature (Overend and Chornet, 1987; Rubio et al., 1998).

It is considered more adequate to apply acid concentration in the kinetic model instead of the liquid suspension pH. In this paper, the values of -log $[H^+]_{initial}$ and the suspension pH of the liquor were remarkably different (higher), mainly when the acid concentration was low, thus significantly altering the calculated value of the severity factor. In fact, pH is frequently considered as a variable in the kinetic model (Pedersen and Meyer, 2010; Pedersen et al., 2010; Pedersen et al., 2011), but its dependency in the process was not demonstrated, reinforcing that it is a consequence of the presence of chemicals, and that is more suitable to include their concentration values in the kinetic model.

The fact that two mechanisms were present in the extraction of the sugars at lower and higher reactivity was already visualized for lignocellulosics, as well as for slow/fast hemicellulose and easily/resistant cellulose, indicating that these saccharides can exhibit different forms in the same polymer (Belkacemi et al., 1991; Jacobsen and Wyman, 2000).

A linear correlation between the solubilized biomass and hydrolyzed sugars shown in this study was already verified for lignocellulosics (Overend and Chornet, 1987). As aforementioned, degradation processes can happen for several fractions of polyssacharides in biomass, and are specially reported in the literature for xylose given its sensibility to acidic treatment (Saeman, 1945; Overend and Chornet, 1987; Rubio et al., 1998; Jacobsen and Wyman, 2000; Lloyd and Wyman, 2005; Zoulikha et al., 2015; Temiz and Akpinar, 2017). They can also be correlated with a severity factor function (Chen et al., 2007; Lee and Jeffries, 2011).

Table 10.2 summarized published papers and their best range of severity factors. It is possible to see that lignocellulosics values are between 0.5–2 and 2–3, for xylose and glucose solubilization, respectively. For microalgae, this range was between 1–2.5. Despite these values being close, they are compressed in a logaritimic scale and the real value can change greatly, as for example: between 1–2.5, the value of the severity factor changes from 10 to 316, a 30-fold difference. In this paper the range of ACSF to obtain more than 90% of hydrolysis was between 5–6 (ln ACSF), which corresponds to 2.17–2.60 (log ACSF), and 147–398 (ACSF), a difference of two times, showing less scatter.

In summary, to represent an efficient e detailed severity factor curve:

- the reaction order for biomass and acid are essential and assumptions should be rarely used. As shown, a variation of 5% in the n order caused a significant deviation of the severity factor curve;
- the pseudoparameters values are process-specific and limit the studies, despite the possibility of graphical adjustment;
- the experimental design must have a number of levels compatible with a reasonable range of temperature and time values, although the acid concentration is required to be higher, since it is charactheristic of the process (acidic treatment); this enables the evaluation of the process from lower to higher reactivity, with an adequate estimation being plotted (in this paper, were used: 110-130°C, 0-60 min and 0–5% of acid concentration, ln ACSF between -2 and 6);
- the model presented in this paper with general orders n and m can be applied for any type of biomass.

Table 10.2: Dilute acid treatment of several biomasses and the respective severity factor used.

Biomass	**Acid Concentration (%)**	**Temperature (°C)**	**Time (min)**	**Log R'$_0$ (ACSF)** (Best range)	**Solubilization/ Hydrolysis**	**Reference**
Corn stover (100 g L^{-1})	-	95-100	-	1-2	75-98% of xylan removal	(Chum et al., 1990a)
Stipa t. Corn stalk *Betula p. Populus t.*	0.4-2.0	-	-	6-7	80% of biomass solubilization	(Belkacemi et al., 1991)
Corn stover (50 g L^{-1})	1.2-2.5	140-200	2-120	0.9-1.6 (1^{st} step) 1.2-2.2 (2^{nd} step)	1^{st} step: 25.8-34-5 % of xylose and 3.1-4.3 of glucose 2^{nd} step: 44.5-57.7% of glucose and 0-4.7% of xylose	(Lloyd and Wyman, 2005)
Chlamydomonas biomass (Microalgae) (50 g L^{-1})	1-5	100-120	15-120	1-1.8	95% of sugars recovery	(Nguyen et al., 2009)
Chlorella biomass (Microalgae) (200 g L^{-1})	0.5-6.5	120-180	10-60	1.8-2.5	80% of sugars recovery	(Zhou et al., 2011)
Pinewood Aspenwood (200 g L^{-1})	65-80	35-70	60-180	1.3-1.7 1.7-2.6	For xylose For glucose (almost 100% of recovery)	(Janga et al., 2012a)
Wheat straw (200 g L^{-1})	0.7-2.2	133-165	5-40	0.5-1.5	From a ACSF of 0.5 xylose starts degradation	Zoulikha et al., 2015)
Rice husk and straw (100 g L^{-1})	0.3-3.7	86-153	6-74	1-2	Pratically all xylose was solubilized and 5-30% of glucose	(Temiz and Akpinar, 2017)

10.5.3 Transient time

Final mass differential is a combination of the transient time and the holding time, both depending on temperature, time and acid concentration. If during the transitory time the biomass variation changes linearly with these three variables, knowing that the biomass solubilization during the holding time is correlated with a function of ACSF (acidic combined severty factor), it is concluded that the difference in biomass during the transitory time is proportional to a function of ACSF, as represented in **Figure 10.12**. This result corroborates with the good correlations shown in **Figure 10.9** and suggests that biomass fractions and the severity factor of area 2 can be correlated easily, thus avoiding the need to include the heating and cooling times in the kinetic proposal, as already has been wrongly proposed (Viegas, 2013).

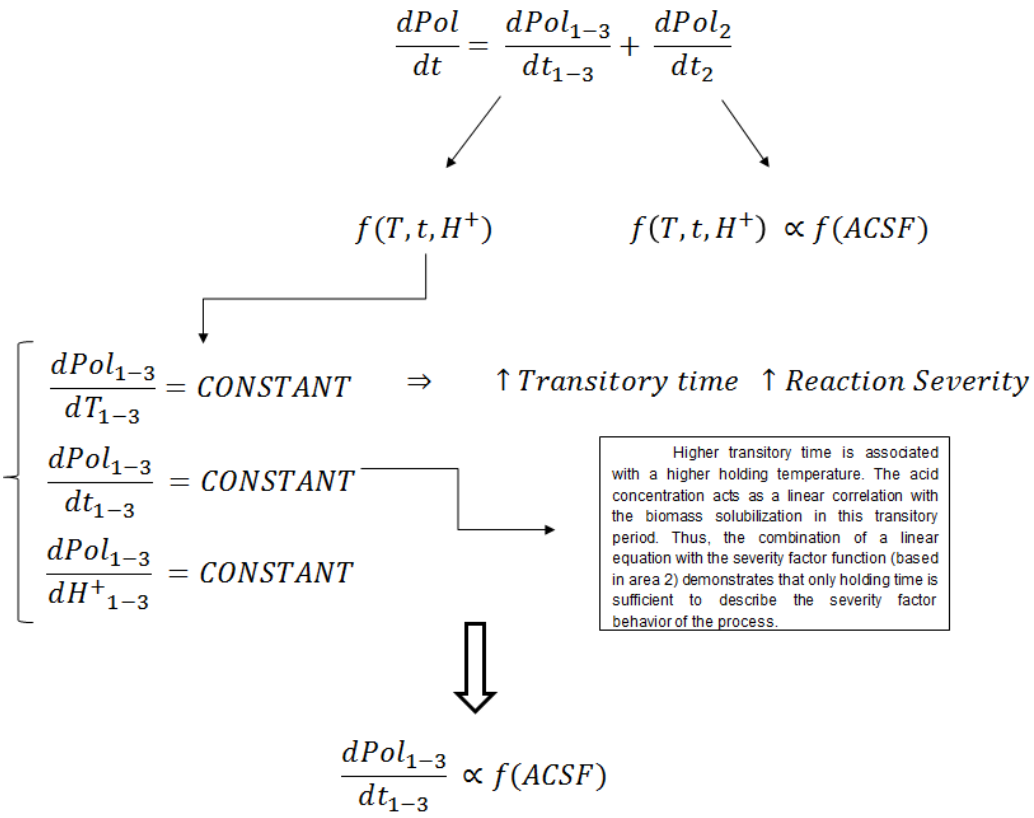

Figure 10.12: Transitory heating/cooling time analysis.

10.5.4 n order variation

A possible explanation regarding the change of *n* when acid concentration is increased is the role of H^+ in the reaction. This occurs because as assumed before, it participates

as a catalyst but also as a reactant, as confirmed by the kinetic relations, as well as by the fact that the respective reaction order was the same, indicating that this variation is due to the biomass properties.

As the same acid order is required to provide an efficient reaction, the possible explanation can be based on the catalytic effect, i.e., more acid in solution provides a higher proton concentration and increases the interaction with biomass, which can exhibit a higher catalytic effect and solubilize more biomass, even though a lower n is shown. A summary of this explanation is presented in **Figure 10.13**.

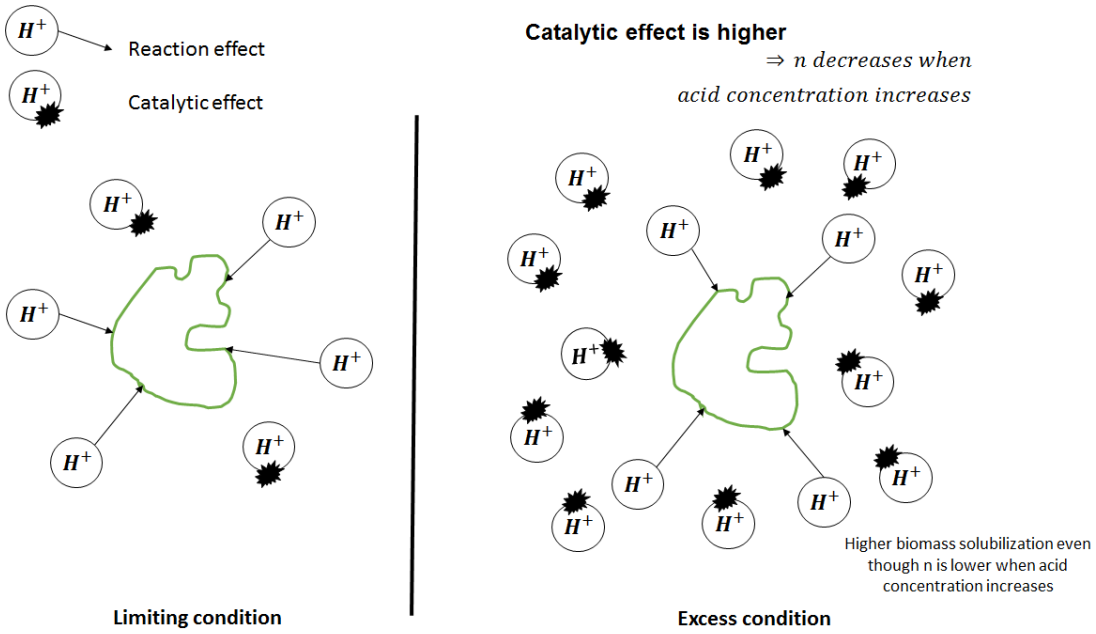

Figure 10.13: Reaction vs catalytic effect when acid concentration is increased.

In this chapter, an improvement of the severity factor application as a real parameter was discussed instead of the actual literature approach (first-order reaction, the use of pH to characterize acid concentration and pseudoparameters). In this way, it can be adequately applied to estimate mass solubilization and sugars hydrolysis from microalgal biomass as a combination of temperature, reaction time and acid hydrolysis. It was proved that the theory is suitable when kinetic aspects are adequately used. An analysis of the transitory heating/cooling time was also made, showing a linear correlation/dependency between this intermediate time and the severity factor which does not influence the direct use of ACSF calculated in the holding time of the reaction.

Particularly for microalgae powder biomass, it is important to mention that diffusion effects are lower than for lignocellulosic biomasses (e.g. wood chips, leaf and stalks), similarly to lignin, thus making the polysaccharides structure in biomass simpler and resulting in a higher susceptibility to the acidic treatment.

REFERENCES

AOAC – Association of Analytical Chemists. Official Methods of Analysis of the Association of Official Analytical Chemists, 17th ed., Gaithersburg: Ed. William Horwitz, 2002.

Belkacemi, K., Abatzaglou, N., Overend, R.P., Chornet, E., 1991. Phenomenological kinetics of complex systems: mechanistic considerations in the solubilization of hemicelluloses following aqueous/steam treatments. Ind. Eng. Chem. Res. 3, 2416-2425.

Bura, R., Bothast, R.J., Mansfield, S.D., Saddler, J.N., 2003. Optimization of SO_2-caralyzed steam pretreatment of corn fiber for ethanol production. Applied Biochemistry and Biotechnology 105-108, 319-335.

Chen, S., Mowery, R.A., Chambliss, C.K., Peter, G., Walsum, P.V.L., 2007. Pseudo reaction kinetics of organic degradation products in dilute-acid.catalyzed corn stover pretreatment hydrolisates. Biotechnology and Bioengineering 98(6), 1135-1145.

Chum, H.L., Johnson, D.K., Black, S.K., Overend, R.P., 1990. Pretreatment-catalyst effects and the combined severity parameter. Applied Biochemistry and Biotechnology 24/25, 1-14. (a)

Chum, H.L., Johnson, D.K., Black, S.K., 1990. Organosolv pretreatment for enzymatic hydrolysis of poplars. 2. Catalyst effects and the combined severity parameter. Ind. Eng. Chem. Res. 29(2), 156-162. (b)

Esteghlalian, A., Hashimoto, A.G., Fenske, J.J., Penner, M.H., 1997. Modeling and optimization of the dilute-sulphuric-acid pretreatment of corn stover, poplar and switchgrass. Bioresource Technology 59, 129-136.

Jacobsen, S.E., Wyman, C.E., 2000. Cellulose and hemicellulose hydrolysis models for application to current and novel pretreatment processes. Applied Biochemistry and Biotechnology 84-86, 81-96.

Jacquet, N., Quiévy, N., Vanderghem, C., Janas, S., Blecker, C., Wathelet, B., Devaux, J., Paquat, M., 2011. Influence of the steam explosion on the thermal stability of cellulose fibers. Polymer Degradation and Stability 96, 1582-1588.

Janga, K.K., Oyaas, K., Hertzberg, T., Moe, S.T., 2012. Application of a pseudo-kinetic generalized severity model to the concentrated sulfuric acid hydrolysis of pinewood and aspenwood. Bioresources 7(3), 2728-2741. (a)

Janga, K.K., Hagg, M., Moe, S.T., 2012. Influence of acid concentration, temperature, and time on decrystallization in two-stage concentrated sulfuric acid hydrolysis of pinewood and aspenwood: a statistical approach. Bioresources 7(1), 391-411. (b)

Kim, Y., Kreke, T., Mosier, N.S., Landisch, M.R., 2014. Severity factor coefficients for subcritical liquid hot water pretreatment of hardwood chips. Biotechnol Bioeng. 11(2), 254-263.

Lee, J., Jeffries, T.W., 2011. Efficiencies of acid catalysts in the hydrolysis of lignocellulosic biomass over a range of combined severity factors. Bioresource Technology 102(10), 5884-5890.

Lee, O.K., Oh, Y., Lee, E.Y., 2015. Bioethanol production from carbohydrate-enriched residual biomass obtained after lipid extraction of *Chlorella sp.* KR-1. Bioresource Technology 196, 22-27.

Lloyd, T.A., Wyman, C.E., 2005. Combined sugar yields for dilute sulfuric acid pretreatment of corn stover followed by enzymatic hydrolysis of the remaining solids. Bioresource Technology 96, 1967-1977.

Markovsky, I., Huffel, S.V., 2007. Overview of total least squares methods. Signal Processing 87, 2283-2302.

Miller, J.G., 1959. Use of dinitrosalicyclic acid reagent for determination of reducing sugars. Analytical Chemistry 31(3), 426-428.

Montané, D., Salvadò, J., Farriol, X., Jollez, P., Chornet, E., 1994. Phenomenological kinetics of wood delignification: application of a time-dependent rate constant and a generalized severity parameter to pulping and correlation of pulp properties. Wood Science and Technology 28, 387-402.

Mosier, N., Wyman, C., Dale, B., Elander, R., Lee, Y.Y., Holtzapple, M., Landisch, M., 2005. Features of promising technologies for pretreatment of lignocellulosic biomass. Bioresource Technology 96(6), 673-686.

Negahdar, L., Delidovich, I., Palkovits, R., 2016. Aqueous-phase hydrolysis of cellulose and hemicellulose over molecular acidic catalysis: Insights into the kinetics and reaction mechanism. Apllied Catalysis B: Environmental 184, 285-298.

Nguyen, M.T., Choi, S.P., Lee, J., Lee, J.H., Sim, S.J., 2009. Hydrothermal acid pretreatment of *Chlamydomonas reinhardtii* for ethanol production. Journal of Microbiology and Biotechnology 19(2), 161-166.

Overend, R.P., Chronet, E., 1987. Fractionation of lignocellulosics by steam-aqueous pretreatments. Phil. Trans. R. Soc. Lond. A 321, 523-536.

Pedersen, M., Meyer, A.S., 2010. Lignocellulose pretreatment severity – relating pH to biomatrix opening. New Biotechnology 27(6), 739-750.

Pedersen, M., Vikso-Nielsen, A., Meyer, A.S., 2010. Monosaccharide yield and lignin removal from wheat straw in response to catalyst type and pH during mild thermal pretreatment. Process Biochemistry 45, 1181-1186.

Pedersen, M., Johassen, K.S., Meyer, A.S., 2011. Low temperature lignocellulose pretreatment effects and interactions of pretreatment Ph are critical for maximizing enzymatic monosaccharide yields from wheat straw. Biotechnology for Biofuels 4(11), 1-10.

Rubio, M., Tortosa, J.F., Quesada, J., Gomez, D., 1998. Fractionation of lignocellulosics. Solubilization of corn stalk hemicellulases by autohydrolysis in aqueous medium. Biomass and Bioenergy 15(6), 483-491.

Saeman, J.F., 1945. Kinetics of wood saccharification: hydrolysis of cellulose and decomposition of sugars in dilute acid at higher temperature. Industrial and Engineering Chemistry 43-52.

Silva, C.E.F., Sforza, E., 2016. Carbohydrate productivity in continuous reactor under nitrogen limitation: effect of light and residence time on nutrient uptake in *Chlorella vulgaris*. Process Biochemistry 51, 2112-2118.

Silva, C.E.F., Bertucco, A., 2016. Bioethanol from microalgae and cyanobacteria: a review and technological outlook. Process Biochemistry 51, 1833-1842.

Silva, C.E.F., Sforza, E., Bertucco, A., 2017. Effects of pH and carbon source on *Synechococcus* PCC 7002 cultivation: biomass and carbohydrate production with different strategies for pH control. Appl. Biochem. Biotechnol. 181, 682-698.

Silva, C.E.F., Bertucco, A., 2017. Dilute acid hydrolysis of microalgal biomass for bioethanol production: an accurate kinetic model of biomass solubilization, sugars hydrolysis and nitrogen/ash balance. Reaction Kinetics, Mechanisms and Catalysis, in Press.

Silverstei, R.A., Sharma-Shivappa, R.R.S., Boyette, M.D., Osborne, J., 2007. A comparison of chemical pretreatment methods for improving saccharification of cotton stalks. Bioresource Technology 98, 3000-3011.

Temel, B., Mekine, M., Reuter, K., Seheffler, M., Metiu, H., 2007. Does phenomenological kinetics provide na adequate description of heterogenous catalytic reaction? The Journal of Chemical Physics 126, 204711-1-12.

Temiz, E., Akpinar, O., 2017. The effect of severity factor on the release of xylose and phenolics from rice husk and rice straw. Waste Biomass Valor 8(2), 505-516.

Trevelyan, W.E., Harrison, J.S., 1952. Studies on yeast metabolism. 1. Fractionation and microdetermination of cell carbohydrates. Biochem. J. 50(3), 298-303.

Viegas, M.R., 2013. Avaliação de métodos de pré-tratamento na gaseificação da biomassa. (Master Thesis). Biotechnology of Natural Products, University Nova de Lisboa, 84 pp.

Vroom, K.E., 1957. The 'H' factor: a means of expressing cooking times and temperatures as a single variable. Pulp paper Mag. Con. 58(3), 228-231.

Wang, Y., Guo, W., Cheng, C., Ho, S., Chang, J., Ren, N., 2016. Enhancing bio-butanol production from biomass of Chlorella vulgaris JSC-6 with sequential alkali pretreatment and acid hydrolysis. Bioresource Technology 200, 557-564.

Zhou, N., Zhang, Y., Wu, X., Gong, X, Wang, Q., 2011. Hydrolysis of Chlorella biomass for fermentable sugars in the presence of HCl and $MgCl_2$. Bioresource Technology 102, 10158-10161.

Zoulikha, M., Thierry, M., Quiyu, Z.J., Nouviaire, A., Sid-Ahmed, R., 2015. Combined steam-explosion toward vacuum and dilute-acid spraying of wheat straw. Impact of severity factor on enzymatic hydrolysis. Renewable Energy 78, 516-526.

Chapter 11

Ultrasonication intensity in the enzymatic hydrolysis of microalgal sugars

Microalgal biomass has been considered as a possible alternative source of carbohydrates and lipids in fermentative/reactional processes, called third generation of biofuels. Carbohydrates from microalgae are mostly composed by glucose and some pentose-derived polymers that must be hydrolyzed to be efficiently used. When enzymatic hydrolysis is applied a pretreatment is required. Sonication/ultrasonication is one of the most promising methods, and in this chapter, the influence of pretreatment time, sonication intensity and biomass concentration was validated, and the energy consumed in the process compared as well. Sonication intensity had the major role on the enzymatic accessibility. Pretreatment time can be used to decrease hydrolysis time. More of 90% of hydrolysis efficiency was reached when higher amplitude (sonication intensity) and pretreatment time were used. The applied energy does not influence directly the hydrolysis process. The best saccharification/energy relation was reached when 50% of amplitude for 25 min was applied, obtaining 91% of hydrolysis yield and spending 2.4 MJ/Kg of dry biomass•.

•*Part of this chapter was submitted in Fuel, 2017.*

11.1 INTRODUCTION

Microalgal carbohydrates have been showed as an interesting alternative to conventional fermentative processes, thus contributing to third generation of biofuels which has several advantages in comparison to the two first ones: it avoids the food vs fuel competition as well as recalcitrant lignocellulosic problems (Silva and Bertucco, 2016). Ethanol (Silva and Bertucco, 2016), methane (Ding et al., 2016), hydrogen (Kumar et al., 2016) and buthanol (Wang et al., 2014a) can be cited as promising applications. Most sugars present in microalgal biomass are glucose polymers (cellulase, starch or glycogen, the last for cyanobacteria), but to be efficiently fermented this sugar content needs to be hydrolyzed (Chen et al., 2013; Vitova et al., 2015).

Among the algal hydrolysis methods, dilute acidic and enzymatic procedures exhibit better efficiencies. Acidic hydrolysis is a non-specific reaction generally performed with acid concentration between 1-10% and temperatures of 110-140 °C (Agbogbo et al., 2006; Logothetis et al., 2007; Nguyen et al., 2009; Nasser and Moghaz, 2010; Miranda et al., 2012; Ho et al., 2013; Lee et al., 2013; Wang et al., 2014b; Ashokumar et al., 2015; Wang et al., 2016), but has as bottlenecks the need of high amount of chemicals during the hydrolysis, a pH adjustment prior to the fermentation step and a high amount of salt formation which has inhibiting action against yeasts (Agbogbo et al., 2006; Logothetis et al., 2007; Nasser and Moghaz, 2010; Casey et al., 2013). On the other hand, enzymatic processes, besides of the high cost of enzymes, provides a more specific process at middle temperature and pressure, resulting in lower heating costs, and decrease the possibility for degradation processes to occur. However, to apply this last method, a pretreatment to improve the accessibility of carbohydrates to the enzymatic attack is necessary (Silva and Bertucco, 2016).

Several methods for algal cell disruption have been evaluated so far: ultrasonication, bead beating, microwave, osmotic shock (NaCl) and autoclaving (at 121 °C), and the results are different (Jeon et al., 2013; McMillan et al., 2013; Kurokawa et al., 2016). Sonication has the advantage of being able to disrupt the cells at relatively low temperatures (lower than microwave and autoclaving), faster extraction, suitability for all cell types, and it does not require beads or chemicals thus decreasing production costs (Jeon et al., 2013; McMillan et al., 2013; Byreddy et al., 2015; Kurokawa et al., 2016). Generally, it is divided in two ranges: low frequency non-focused ultrasound

(LFNFU), at 20 – 50 kHz, and high-frequency focused ultrasound (HFFU), at 1-3 MHz; the first range is more suitable to heterogenous and enzymatic catalysis of biomass (Wang et al., 2014c). The high-energy impact and corrosion by high-intensity ultrasound to the biomass system contributes more easily to pretreat, fractionate and react with biomass under mild conditions, resulting in a higher yield of reaction and catalytic activity over thermochemical methods (Luo et al., 2014).

So far, ultrasonication has been used to prepare microalgal biomass, generally often, without verifying the intensity or energetic efficiency of the process (for carbohydrate extraction and hydrolysis efficiency). For instance, *Chlamydomonas fasciata* was submitted to 30 W and 20 kHz for 30 min and extracted practically all intracellular starch (Asada et al., 2012), *Chlorococcum* using 130 W and 40 kHz for 25 min, reached 62.8% of glucose hydrolysis yield (Harun and Danquah, 2011a); *Chlorella vulgaris* at 24 kHz and 40% amplitude for 15 min achieved 75% of sugars recovery (Kim et al., 2014), in contrast to *Chlorella sp.* KR-1, with 27.4% of hydrolyzed sugars (Lee et al., 2015) and *Chlorella homosphaera* (both unpretreated biomass) with 47% of total glucose in biomass (Rodrigues et al., 2015), showing the importance of the pretreatment. Actually, seeking for the most energy efficient pretreatment for algal materials by parameter optimization is a research need (Luo et al., 2014).

Additionally, the sugars enzymatic hydrolysis process from microalgal biomass has shown lower yield in comparison with acidic treatment, and longer hydrolysis time are required (considering an acceptable value of biomass concentration in view of large scale exploitation), as for example, 27.4 instead of 93.3% for *Chlorella sp.* (50 $g_{dry\ biomass}\ L^{-1}$ and 3 h) (Lee et al., 2015), 64 compared to 96% for *Chlorella vulgaris* FSP-E (40 $g_{dry\ biomass}\ L^{-1}$ and 2-3 days) (Ho et al., 2013) and 62.8 instead of 100% for *Chlorococcum* (10-15 $g_{dry\ biomass}\ L^{-1}$ and 12 h) (Harun and Danquah, 2011a; Harun and Danquah, 2011b). These results emphasize two probable problems of the experiments: ineffective pretreatment and/or specificity/concentration of the enzymes.

For this reason, this chapter is focused on the pretreatment using ultrasonication changing the time, intensity of ultrasound and biomass concentration, and verifying the relation between them and the energy consumption to saccharify *Scenedesmus obliquus* biomass.

11.2 MATERIAL AND METHODS

11.2.1 Microalgal biomass

Scenedesmus Obliquus 276.7 (SAG- Goettingen) biomass was obtained by continuous cultivation in photobioreactor at 23 ± 1 °C, and maintained in a modified BG11 [30] with nitrogen limitation to promote the accumulation of carbohydrates (Silva et al., 2017), using 180 mg L^{-1} of N-nitrogen and 100 mg L^{-1} of P-phosphorous, being the rest of nutrients provided in double concentration.

The continuous cultivation was performed in a vertical flat-plate polycarbonate CSTR (continuous stirred tank reactor) PBR (photobioreactor) with a working volume of 700 mL, a depth of 1.2 cm, and the irradiated surface measures 30 cm (length) and 19.5 cm (width).

CO_2 in excess was provided by a CO_2–air mixture (5% v/v) bubbling at the reactor bottom (1 L h^{-1} of total gas flow rate), which also provided mixing. A magnetic stirrer was used as well to prevent any deposition of biomass and thus ensuring a good mixing of the reactor. The fresh medium was fed at a constant rate by a peristaltic pump (Watson-Marlow sci400). The flowrate was regulated to obtain a residence time $\tau = 2.3 \pm 0.3$ day.

Light was provided by a LED lamp (Photon System Instruments, SN-SL 3500-22) and fixed at 650 µmol photons m^{-2} s^{-1}. Photon Flux Density (PFD) was measured on both the reactor front and back panels using a photoradiometer (HD 2101.1 from Delta OHM), which quantifies the photosynthetically active radiation (PAR). Biochemical characterization included the determination of moisture (method 934.01), ash (method 942.05), protein (method 2001.11), lipid content (method 2003.05), carbohydrates and monomers by HPLC (AOAC, 2002).

11.2.2 Enzymatic hydrolysis and analytical procedures

Enzymatic hydrolysis was performed using citrate buffer 50 mM, pH 5.0 at 50 °C. Enzymes mix was composed by Viscozyme® L (Novozymes cellulases mixture with ≥ 100 FBGU/g – betaglucanase units), AMG 300 L (amyglucosidase from Aspergillus niger with 260 U/mL) and Pectinex Ultra SP-L (pectinase from Aspergillus aculeans with ≥ 3,800 U/mL). All of these were produced by Novozymes® and purchased from Sigma-Aldrich®.

Enzyme concentrations per gram of biomass were fixed since the experiments must validate the effect of ultrasonication on extraction and saccharification of microalgal sugars. The concentrations were: Viscozyme L® – 20 U/$g_{biomass}$, AMG 300 L® – 100U/$g_{biomass}$ and PectineX Ultra SP-L® – 1000U/$g_{biomass}$. Operating conditions were based on published papers been the environmental conditions able to permit each enzyme to work with a sufficient activity to perform the hydrolysis adequately (Harun and Danquah, 2011a; Asada et al., 2012; McMillan et al., 2013; Kim et al., 2014; Lee et al., 2015). Sodium azide was used in a concentration of 0.02% (w/v) to prevent contamination.

Saccharification efficiency is given by:

$$\%\, Saccarification = \frac{M\,(\frac{g}{L})}{DCW\,(\frac{g}{L}) \bullet CC} \bullet 100 \qquad (11.1)$$

where *M* is the yield of monosaccharides, *DCW* is the initial dry cell weight and *CC* is the carbohydrate content, generally between 0.1-0.6.

Dry cell weight was measured by gravimetry using cellulose acetate filters of 0.45 μm (Whatman®) at 105 °C and 2 h. Filters were pre-dried for 10 min at 105 °C in order to remove any moisture. Carbohydrate content (CC) in biomass was determined by Anthrone method (Trevelyan and Harrison, 1952). Monomers (M) were determined by DNS method (Miller, 1959; Silva et al., 2015).

11.2.3 Preliminary experiments

Preliminary experiments to confirm the advantages of ultrasonication with respect to a control condition were carried out. The negative control condition used the microalgal biomass without any treatment and the positive control (exploded cells) utilized biomass suspension after autoclaving at 121°C for 20 min (vapour-line^{eco} VWR®). Ultrasonication was done by using an Ultrasonic generator (cylindrical, AA–WG1–800W – SN 154, Aktive Arc Sarl, Switzerland) with different amplitude/offset and time options. The parameters were set to 50% of amplitude, 25% of offset for 40 min, providing an energy consumption of 30 W, on the base of previous works (Harun and Danquah, 2011a; Asada et al., 2012; McMillan et al., 2013; Kim et al., 2014; Lee et al., 2015). Sonication was applied in continuous (non-pulsed) mode with constant

amplitude. The combination between amplitude/offset and time results in the energy consumed of the process (given by the generator at the end of the treatment process – input energy) and will be discussed in **section 11.3.3**. Biomass concentration in all experiments was 10 g/L and optical microscopic visualization was verified before and after the pretreatments with a magnification of 75x.

11.2.4 Experimental design and statistical treatment

Ultrasonication assays were carried out according to a factorial experimental design 2^3 with three central point (2^n where n is the number of variables), totalizing 11 experiments. The variables studied were time (min), intensity of sonication (amplitude/offset) and biomass concentration (g/L) and the levels of the experimental design are summarized in **Table 11.1**.

Table 11.1: Levels of the factorial experimental design.

Variable	**-1**	**0**	**+1**
Time (min)	5	15	25
Amplitude/Offset (%)*	50/-40	60/-10	70/25
Biomass Concentration (g/L)	10	55	100

All statistical analysis was performed by the software Statistica® for factorial design analysis assuming $p < 0.05$ (95% of significance), considering the variables and their linear interactions.

The efficiency of the process was compared also with respect to the energy consumed per gram of biomass, to verify if it is the intensity and the energy applied by ultrasonication can provide higher accessibility of biomass to the enzymatic hydrolysis.

11.3 RESULTS AND DISCUSSION

Scenedesmus obliquus steady-state cultivation achieved a cell dry weight of 3.97 ± 0.09 g L^{-1}. Biochemical characterization (% of dry matter) resulted in 33.63 ± 4.15 of proteins, 44.9 ± 4.5 of carbohydrates, 25.34 ± 0.64 of lipids and 6.83 ± 0.01 of ash. The profile of monosaccharides (% of carbohydrate content) was composed by 79.78 ± 3.96 of glucose, 16.14 ± 0.11 of xylose and 4.08 ± 0.31 of other monomers.

11.3.1 Preliminary experiments

In **Figure 11.1**, preliminary results with and without pretreatment are shown. It is possible to conclude that sonication improved at least by 30% the saccharification yield in comparison with the negative and positive controls (without pretreatment and autoclaving pretreatment). In fact, these reached around 70% while with sonication all carbohydrate content was practically hydrolyzed in monosaccharides.

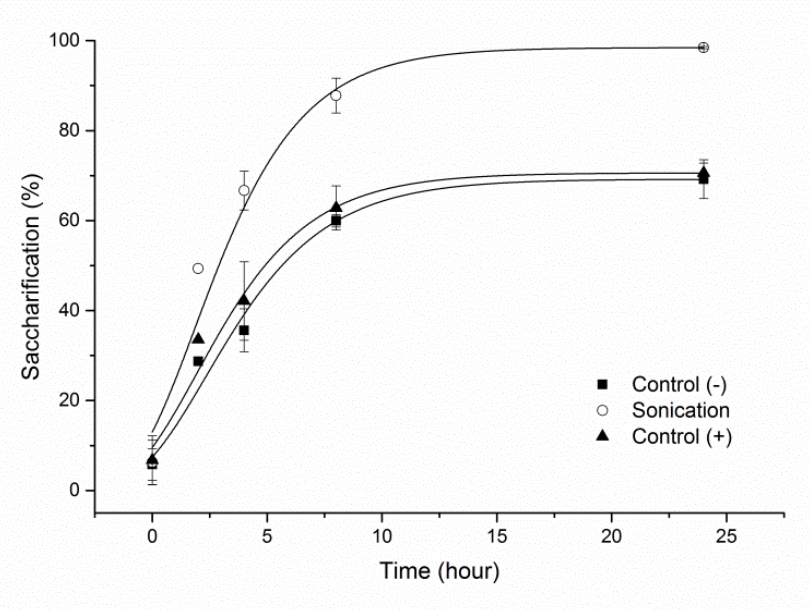

Figure 11.1: Saccharification of the preliminary experiments. Control (-) - whitout treatment; Sonication – 40% amplitude, 40 kHz for 40 min and Control (+) – autoclaving at 121 °C for 20 min.

This result is quite interesting in comparison to heat treatment. As can be seen in **Figure 11.2**, autoclaving microalgal biomass promotes the completely cell explosion/de-structuration, but does not improved enzyme accessibility, probably because diffusion effects were limited by biomass aggregation (**Fig. 11.2C**). This is also in contrast with some comparisons made in the literature, which mention heating methods as more effective to cell disruption and considered as best method to separate biomass fractions and promote enzymatic hydrolysis (McMillan et al., 2013). On the other hand, after sonication an apparently not significant cell volume reduction as likely to occur (**Fig. 11.2B**), a good volume dispersion (homogenization). Sonication promotes fissures and cracks on algal cell surface and consequently enhances enzyme accessibility (jeon et al., 2013), and a reduction of cell volume can or not occur (Kurokawa et al., 2016). In **Fig.**

11.2D, an 'apparently' cell reduction is observed after enzymatic hydrolysis, a behavior which was already observed for *C. homosphaera* (Rodrigues et al., 2015).

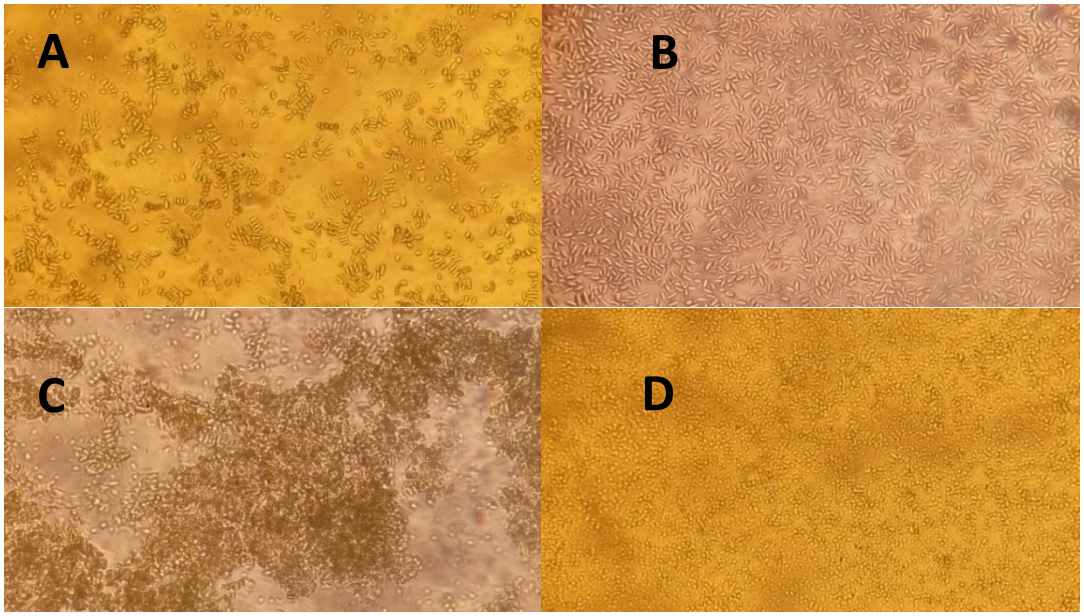

Figure 11.2: Optical visualization after the pretreatments. A) - Control (without treatment), B) Sonication, C) + Control (Autoclave) and D) Sonication experiment after enzymatic hydrolysis. 10 g/L of biomass concentration and optical magnification of 75x.

11.3.2 Experimental design and statistical analysis

As aforementioned, pretreatment time, sonication intensity (amplitude) and biomass concentration were validated by a factorial design of the experimental runs. The enzymatic hydrolysis was very successful, with some experiments achieving more than 90% of sugars recovery as monomers. As can be seen in **Table 11.2**, the best runs were those with higher sonication intensity, higher pretreatment time and lower biomass concentration (5 and 6), which exhibited values near to 95% of saccharification, reaching almost 90% in 4 hours of hydrolysis.

In fact, in the Pareto charts represented in **Figure 11.3** for each hydrolysis time considered in this paper, it is possible to see that at the beginning (**11.3A**) no influence of the variables in the pretreatment was observed, i.e., the sugars concentration starts with approximately the same value. This is important, because the temperature in some experiments remained with a maximum value of 40°C while other reached 90°C (details are reported in **section 11.3.3**). After, all experiments were influenced positively by

sonication intensity (amplitude) and negatively for the linear interaction of sonication intensity and biomass concentration (2L by 3L), i.e., higher sonication intensity promoted more enzyme accessibility and, consequently, hydrolysis, and lower biomass concentration was better pretreated. However, with respect to biomass concentration, it is unfeasible to maintain an industrial process with 10 g/L of biomass, which is generally accounted to be at least 100 g/L. Another detail is the energy consumption of the process and how much the hydrolysis yield is influenced by the energy used in the pretreatment process, a point later discussed in **section 11.3.3**.

Table 11.2: Saccharification results of all experiments and hydrolysis time.

Assay	Time (min)	Sonication parameter Amplitude/Offset (%)	Biomass Concentration ($g.L^{-1}$)	Saccharification (%)*				
				Time (h)				
				0	2	4	8	24
1	5	50/-40	10	13.00±1.41	32.18±1.19	36.02±2.01	62.26±4.16	79.08±5.06
2	25	50/-40	10	10.50±0.71	37.54±1.19	40.70±0.74	82.24±6.24	83.71±0.89
3	5	50/-40	100	10.97±0.14	66.33±2.74	67.85±1.95	70.00±4.05	79.09±1.35
4	25	50/-40	100	9.00±1.41	65.83±0.08	77.87±0.38	83.06±0.97	90.90±0.08
5	5	70/25	10	11.00±1.41	81.23±6.69	86.66±2.34	92.58±4.46	92.89±5.51
6	25	70/25	10	10.50±0.71	88.50±2.12	89.62±9.29	93.04±0.74	96.38±1.96
7	5	70/25	100	9.89±1.09	65.31±7.20	68.65±2.02	74.21±2.40	79.67±9.52
8	25	70/25	100	12.65±0.04	67.82±4.46	81.26±0.53	85.29±0.23	87.67±8.54
9	15	60/-10	55	8.83±0.45	74.72±4.61	71.55±0.40	74.02±5.89	88.48±7.48
10	15	60/-10	55	9.19±0.05	70.32±2.94	73.06±1.87	75.17±2.14	88.38±5.48
11	15	60/-10	55	8.57±0.19	77.65±0.74	75.12±2.01	74.15±6.42	86.78±5.35

*average ± standard deviation. n = 2. Carbohydrate content (% dry cell weight): 44.9 ± 4.5.

Additionally, an interesting consideration was found in the experiments with 4 and 8 hours of hydrolysis: the pretreatment time influenced positively, i.e., if a faster hydrolysis time is required, higher pretreatment time can be used.

We are not aware any sonication intensity study (amplitude) applied to algal pretreatment for sugars hydrolysis in the literature. But some information is provided by sonication frequency sensitivity to disrupt algal cells: *Chaetoceros gracilis*, *Chaetoceros calcitrans* and *Nannochloropsis sp.*, treated with frequencies between 0.02-4.3 MHz, demonstrated the values of 2.2-4.3 MHz as efficient in cell reduction (%) – a parameter used to evaluate the process efficiency (Kurokawa et al., 2016). *Scendesmus dimorphus* and *Nannochloropsis oculata* treated with 20 kHz and 3.2 MHz (low and high frequency) to evaluate chlorophyll and lipid fluorescence and

consequently extraction, demonstrated no differences in lipid recovery, even though the combination of high and low frequencies could decrease the pretreatment time (Wang et al., 2014c).

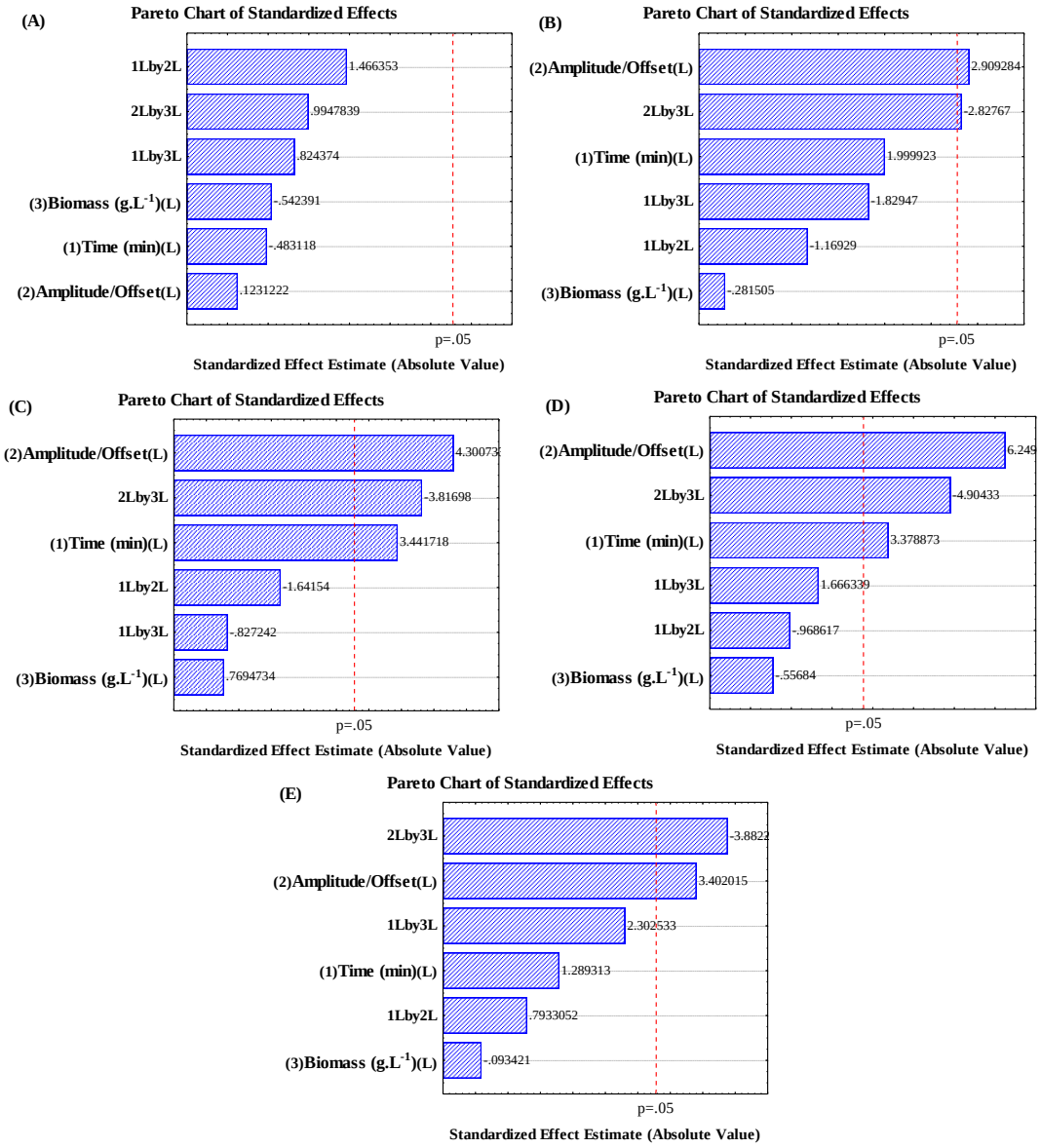

Figure 11.3: Effect of the variables on enzymatic yield for each hydrolysis time. A) 0, B) 2, C) 4, D) 8 and E) 24 h.

Wang et al. (2014c) also verified that the pretreatment time influenced significantly the lipid extraction, proportionally between 1-5 min, reaching value from 50 to 100% of lipid extraction. In dark fermentation of ethanol, volatile fatty acids (VFA) and hydrogen, the pretreatment time was a key-point to promote bioaccessibility/bioavailability of microalgal biomass (*Scenedesmus obliquus* YSW15)

in microbial fermentation reducing the cell surface hydrophobicity and increase ethanol and VFA production (Jeon et al., 2013). Thus, the additional positive influence of the pretreatment time was expected and confirmed.

The regression curves and coefficients of the variables effects on saccharification yield are presented in Equations 11.2-5, and their surface graphs are in **Figure 11.4**, showing more specifically the visual representation of these effects.

$$SY\ (\%) = -92.01 + 2.39.\mathrm{Amp} - 0.0185.\mathrm{Amp}.C_{biom} \quad (2\ h) \qquad (11.2)$$

$R^2 = 0.8632$

$$SY\ (\%) = -92.34 + 3.095.\mathrm{Time} + 2.473.\mathrm{Amp} - 0.0184.\mathrm{Amp}.C_{biom} \quad (4\ h) \qquad (11.3)$$

$R^2 = 0.9243$

$$SY\ (\%) = -22.27 + 0.856.\mathrm{Time} + 0.164.\mathrm{Amp} - 0.013.\mathrm{Amp}.C_{biom} \quad (8\ h) \qquad (11.4)$$

$R^2 = 0.9515$

$$SY\ (\%) = 31.12 + 0.96.\mathrm{Amp} - 0.012.\mathrm{Amp}.C_{biom} \quad (24\ h) \qquad (11.5)$$

$R^2 = 0.8954$

where: SY – Saccharification yield (%), Time – pretreatment time (min), Amp – Amplitude/Offset (%) and $C_{biomass}$ – biomass concentration (g/L).

The complete Analysis of Variance and all statistical parameters (ANOVA) are reported in the **Appendix**.

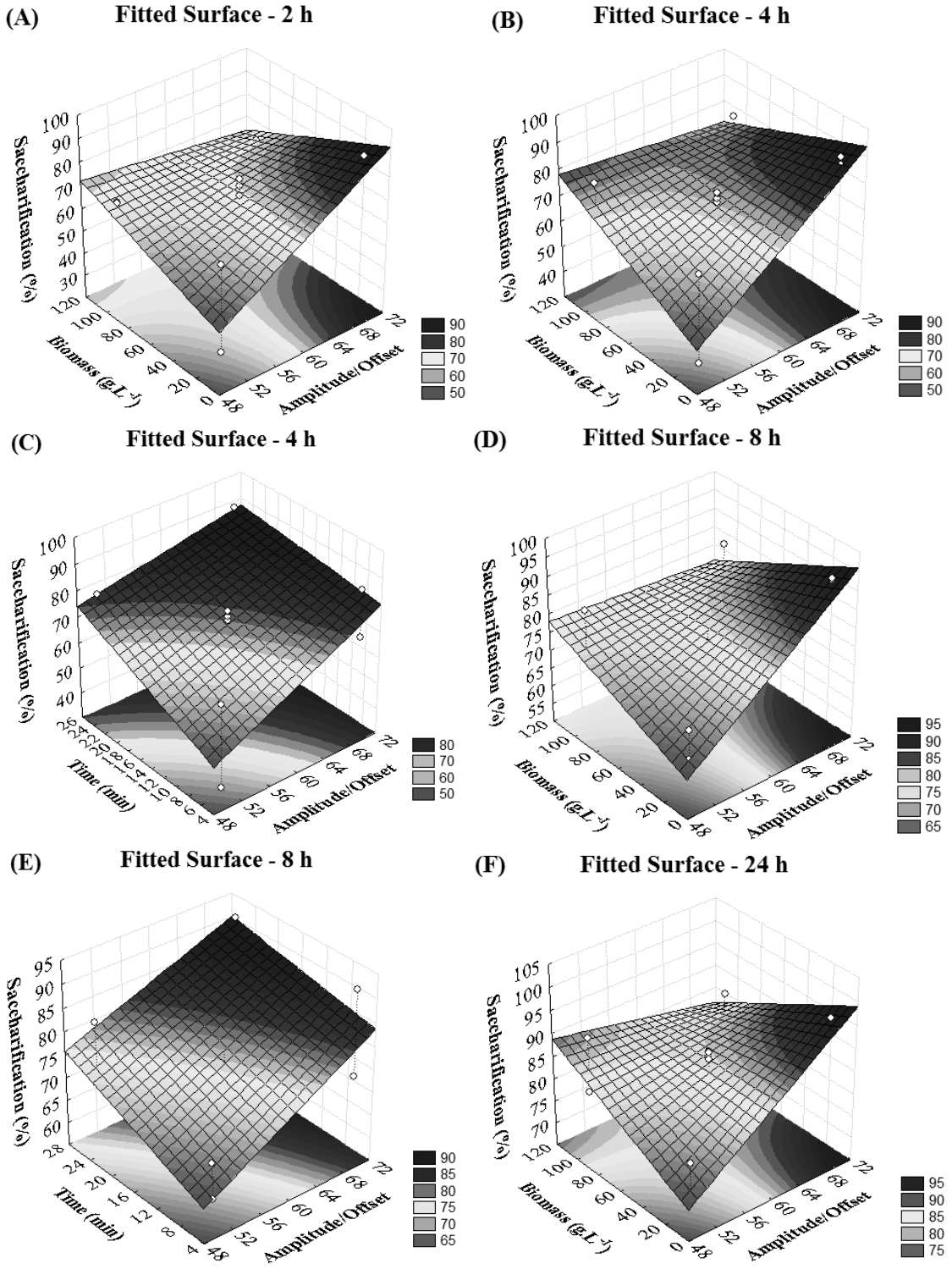

Figure 11.4: Surface graphs of the models obtained by the experimental design.

11.3.3 Energy analysis

The energy analysis of the process is important towards an industrial application. Energy duty is often a bottleneck of sonication treatment, thus, optimizing the energy required to provide an efficient saccharification is a must. As reported in **Table 11.3**, the ratio energy/biomass changed a lot. Experiments 5 and 6, which reached around 95% of hydrolysis yield spent a considerable amount of energy and make this choice unfeasible. On the other hand, experiment 4, reached 90% of hydrolysis and 83% after 8 hours but using between 30-100 times less energy, i.e., 2.4 $MJ/kg_{biomass}^{-1}$.

Some literature values of energy consumption for microalgal pretreatment using sonication are: 70.6 MJ/kg for *Scenedesmus obliquus* YSW15 (Jeon et al., 2013); 1200 MJ/kg for *Thraustochytrid* strains (Byreddy et al., 2015) and 44-132 kJ/kg (extrapolated) for *Nannochloropsis oculata*, but this reduced value demonstrated much lower efficiency in comparison with microwave oven, blender and laser treatments (McMillan et al., 2013). Thus, the value of 2.4 $MJ/kg_{biomass}$ represents a promising value, mainly considering the energy content of microalgal biomass which is generally between 20-22 MJ/kg (Sforza et al., 2014).

In **Figure 11.5**, a plot between the energy consumed and % of saccharification for each hydrolysis time is displayed. It can be concluded that the hydrolysis efficiency does not depend on the energy input, but on the intensity of amplitude mainly, emphasizing the message of our study.

Ultrasound is a mechanical acoustic wave with the frequency range from roughly 10 kHz to 20 MHz. It imparts high energy to reaction medium by cavitation and secondary effects (physical and chemical) (Luo et al., 2014). When the ultrasonication is used to break cells, it is important to determine the energy intensity (experimentally represented by a combination of amplitude-power generated and time) and population of active cavitation to promote the specific reactivity with cells and increase the accessibility to substrate (Kurokawa et al., 2016). In this paper, the validation was based on enzymatic hydrolysis of microalgal biomass, and, in fact, the intensity of sonication showed to be important, but not directly linked to the energy consumed in the pretreatment process. Specifically, this indicates that physical and chemical changes can be achieved by ultrasound which are sufficient to perform enzymatic hydrolysis.

Table 11.3: Energy consumption during sonication pretreatment.

Assay	Power (W)	Total Energy Consumption (kJ)	Energy/Volume (kJ/mL)	Energy/Biomass ($MJ/kg_{biomass}$)	Final Temperature (°C)	Maximum Yield of Sugars (%)**
1	2-4	0.98	0.049	4.90	30	79.08
2	2-4	6.02	0.301	30.10	42	83.71
3	2-4	0.92	0.046	0.46	32.1	79.09
4*	2-4	4.79	0.240	2.40	37.9	90.90
5	34-55	13.00	0.650	65.00	90.2	92.90
6	29-58	43.20	2.160	216.00	89.5	96.38
7	36-50	11.30	0.565	5.65	90.2	79.67
8	37-59	46.90	2.345	23.45	93.2	87.67
9	13-21	12.60	0.630	11.45	85	88.48
10	9-20	11.60	0.580	10.54	83.9	88.38
11	9-19	11.60	0.580	10.54	83.2	86.78

*25 min, 50% of amplitude and 100 g/L of biomass. **24 h hydrolysis yield.

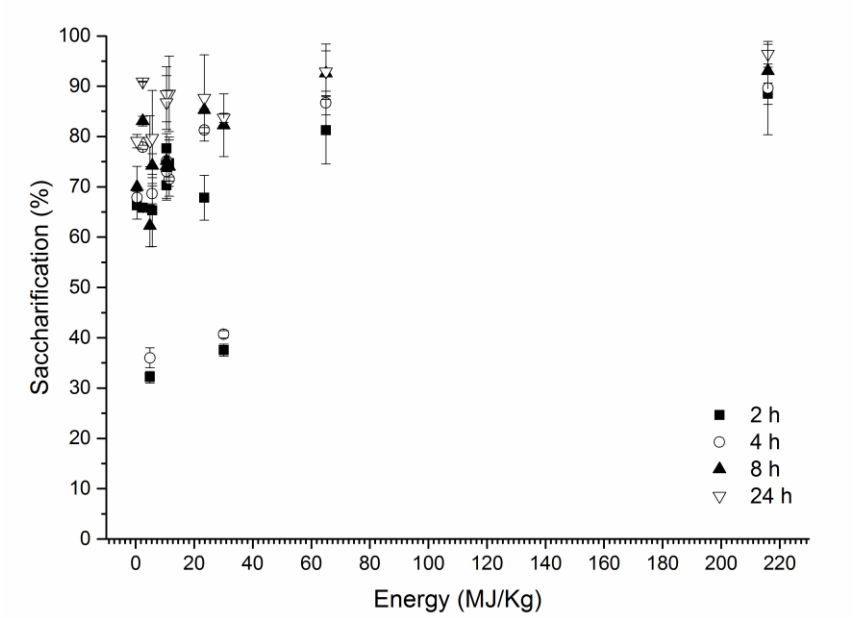

Figure 11.5: Energy consumption versus % saccharification of the experiments.

11.4 CONCLUSIONS

The profitability of performing enzymatic hydrolysis of the sugars contained in *Scenedesmus obliquus* by ultrasonication was addressed with respect to wave intensity, treatment time and biomass concentration. Ultrasonication was effective to treat

microalgal biomass guarantying an excellent enzymatic hydrolysis performance which can compete with chemical methods, as for example, dilute acid treatment. Sonication intensity and pretreatment time had positive importance to enzyme accessibility to reach more than 90% of hydrolysis yield with a limited and acceptable energy duty. The sugars obtained by this way are available to several fermentative possibilities.

REFERENCES

Agbogbo, F.K., Wenger, K.S., 2006. Effect of pretreatment chemicals on xylose fermentation by *Pichia stipitis*. Biotechnol. Lett. 28, 2065-2069.

AOAC – Association of Analytical Chemists. Official Methods of Analysis of the Association of Official Analytical Chemists, 17th ed., Gaithersburg: Ed. William Horwitz, 2002.

Asada, C., Doi, K., Sasaki, C., Nakamura, Y., 2012. Efficient extraction of starch from microalgae using ultrasonic homogenizer and its conversion into ethanol by simultaneous saccharification and fermentation. Natural Resources 3, 175-179.

Ashokumar, U., Salom, Z., Tiwari, O.N., Chinnasamy, S., Mohamed, S., Ani, F.N., 2015. An integrated approach for biodiesel and bioethanol production from *Scenedesmus bijugatus* cultivated in a vertical tubular photobioreactor. Energy Conversion and Management 101, 778-786.

Byreddy, A.R., Gupta, A., Barrow, C.J., Puri, M., 2015. Comparison of cell disruption methods for improving lipid extraction from *Thraustochytrid* strains. Mar. Drugs 13, 5111-5127.

Casey, E., Mosier, N.S., Adamec, J., Stockdale, Z., Ho, N., Sedlak, M., 2013. Effect of salts on the co-fermentation of glucose and xylose by a genetically engineered strain of *Saccharomyces cerevisiae*. Biotechnology for Biofuels 6:83, 1-10.

Chen, C., Zhao, X., Yen, H., Ho, S., Cheng, C., Lee, D., Bai, F., Chang, J., 2013. Microalgae-based carbohydrates for biofuels production. Biochemical Engineering Journal 78, 1-10.

Ding, L., Cheng, J., Xia, A., Jacob, A., Voelklrin, M., Murphy, J.D., 2016. Co-generation of biohydrogen and biomethane through two-stage batch co-fermentation of macro- micro-algal biomass. Bioresource Technology 218, 224-231.

Harun, R., Danquah, M.K., 2011. Enzymatic hydrolysis of microalgal biomass for bioethanol production. Chemical Engineering Journal 168, 1079-1084. (a)

Harun, R., Danquah, M.K., 2011. Influence of acid pre-treatment on microalgal biomass for bioethanol production. Process Biochemistry 46(1), 304-309. (b)

Ho, S., Huang, S., Chen, C., Hasunuma, T., Kondo, A., Cheng, J., 2013. Bioethanol production using carbohydrate-rich microalgae biomass as feedstock. Bioresource Technology 135, 191-198.

Jeon, B., Choi, J., Kim, H., Hwang, J., Abou-Singh, R.A., Dempsey, B.A., Regan, J.M., Kim, J.R., 2013. Ultrasonic disintegration of microalgal biomass and consequent improvement of bioaccessibility/bioavailability in microbial fermentation. Biotechnology for Biofuels 6:37, 1-9.

Kim, K.H., Choi, I.S., Kim, H.H., Wi, S.G., Bae, H., 2014. Bioethanol production from the nutrient stress-induced microalga *Chlorella vulgaris* by enzymatic hydrolysis and immobilized yeast fermentation. Bioresource Technology 153, 47-54.

Kumar, G., Sivagurunathan, P., Thi, N.B.D., Zhen, G., Kobayashi, T., Kim, S., Xu, K., 2016. Evaluation of different pretreatments on organic matter solubilization and hydrogen fermentation of mixed microalgae consortia. International Journal of Hydrogen Energy 41, 21628-21640.

Kurokawa, M., King, P.M., Wu, X., Joyce, E.M., Mason, T.J., 2016. Effect of sonication frequency on the disruption of algae. Ultrasonics Sonochemistry 31, 157-162.

Lee, O.K., Kim, A.L., Seong, D.H., Lee, C.G., Jung, Y.T., Lee, J.W., Lee, E.Y., 2013. Chemeo-enzymatic saccharification and bioethanol fermentation of lipid-extracted residual biomass of the microalga, *Dunaliella tertiolecta*. Bioresource Technology 132 (2013) 197-201.

Lee, O.K., Oh, Y., Lee, E.Y., 2015. Bioethanol production from carbohydrate-enriched residual biomass obtained after lipid extraction of *Chlorella sp.* KR-1. Bioresource Technology 196, 22-27.

Logothetis, S., Walker, G., Nerantzis, E.T., 2007. Effect of salt hyperosmotic stress on yeast cell viability. Proc. Nat. Sci. 113, 271-284.

Luo. J., Fang, Z., Smith Jr., R.L., 2014. Ultrasound-enhanced conversion of biomasss to biofuels. Progress in Energy and Combustion Science 41, 56-93.

McMillan, J.R., Watson, I.A., Ali, M., Jaafar, W., 2013. Evaluation and comparison of algal cell disruption methods: Microwave, waterbath, blender, ultrasonic and laser treatment. Applied Energy 103, 128-134.

Miller, J.G., 1959. Use of dinitrosalicyclic acid reagent for determination of reducing sugars. Analytical Chemistry 31(3), 426-428.

Miranda, J.R., Passarinho, P.C., Gouveia, L., 2012. Pre-treatment optimization of *Scenedesmus obliquus* microalga for bioethanol production. Bioresource Technology 104, 343-348.

Nasser, A., Moghaz, E., 2010. Comparative study of salt tolerance in *Saccharomyces cerevisiae* and *Pichia pastoris* yeast strains. Advances in Bioresearch 1(1), 169-176.

Nguyen, M.T., Choi, S.P., Lee, J., Lee, J.H., Sim, S.J., 2009. Hydrothermal acid pretreatment of *Chlamydomonas reinhardtii* for ethanol production. Journal of Microbiology and Biotechnology 19(2), 161-166.

Rodrigues, M.A., Teixeira, R.S.S., Ferreira-Leitao, V.S., Bom, E.P.S., 2015. Untreated *Chlorella homosphaera* biomass allows for high rates of cell wall glucan enzymatic hydrolysis when using exoglucanase-free cellulases. Biotechnology for Biofuels 8:25, 1-16.

Rippka, R., Deurelles, J., Waterburry, J.B., Herdman, M., Stainer, R.Y., 1979. Generic assignments, strain histories and properties of pure cultures of cyanobacteria. J. Gen. Microb. 111, 1-61.

Sforza, E., Gris, B., Silva, C.E.F., Morosinotto, T., Bertucco, A., 2014. Effects of light on cultivation of *Scenedesmus obliquus* in batch and continuous flat plate photobioreactor. Chemical Engineering Transactions 38, 211-216.

Silva, C.E.F., Bertucco, A., 2016. Bioethanol from microalgae and cyanobacteria: a review and technological outlook. Process Biochemistry 51, 1833-1842.

Silva, C.E.F, Sforza, E., Bertucco, A., 2017. Stability of carbohydrate production in continuous microalgal cultivation under nitrogen limitation: effect of irradiation regime and intensity on *Tetradesmus obliquus*. Journal of Applied Phycology, in Press.

Silva, C.E.F., Gois, G.N.S.B., Silva, L.M.O., Almeida, R.M.R.G., Abud, A.K.S., 2015. Citric waste saccharification under different chemical treatments. Acta Scientiarum Technology 37(4), 387-395.

Trevelyan, W.E., Harrison, J.S., 1952. Studies on yeast metabolism. 1. Fractionation and microdetermination of cell carbohydrates. Biochem. J. 50(3), 298-303.

Vitovà, M., Bisova, K., Kawano, S., Zachleder, V., 2015. Accumulation of energy reserves in algae: From cell cycles to biotechnological applications. Biotechnology Advances 33, 1204-1218.

Wang, Y., Guo, W., Lo, Y., Chang, J., Ren, N., 2014. Charactherization and kinetics of bio-butanol production with *Clostridium acetobutylicum* ATCC 824 using mixed sugar medium simulating microalgae-based carbohydrates. Biochemical Engineering Journal 91, 220-230. (a)

Wang, H., Li, C., Bi, S., Zhou, P., Chen, L., Liu, T., 2014. Joint production of biodiesel and bioethanol from filamentous oleaginous microalgae *Tribonema sp.* Bioresource Technology 172, 169-173. (b)

Wang, M., Yuan, W., Jiang, X., Jing, Y., Wang, Z., 2014. Disruption of microalgal cells using high-frequency focused ultrasound. Bioresource Technology 153, 315-321. (c)

Wang, Y., Guo, W., Cheng, C., Ho, S., Chang, J., Ren, N., 2016. Enhancing bio-butanol production from biomass of *Chlorella vulgaris* JSC-6 with sequential alkali pretreatment and acid hydrolysis. Bioresource Technology 200, 557-564.

APPENDIX

ANOVA – Analysis of Variance

Hydrolysis Time – 2 hours

Effect Estimates; Var.:**2 h**; R-sqr=.86326; Adj:.65815 (Sonication) 3 factors, 1 Blocks, 11 Runs; MS Residual=69.31591 DV: **2 h**

	Effect	Std.Err.	t(4)	p	-95.%	+95.%	Coeff.	Std.Err.	-95.%	+95.%
Mean/Interc.	69.0796	2.510268	27.51883	0.000010	62.1100	76.04926	69.07964	2.510268	62.1100	76.04926
(1)Time (min)(L)	11.7738	5.887101	1.99992	0.116127	-4.5715	28.11896	5.88687	2.943550	-2.2857	14.05948
(2)Amplitude/Offset(L)	17.1273	5.887101	2.90928	0.043709	0.7820	33.47246	8.56363	2.943550	0.3910	16.73623
(3)Biomass (g.L$^{-1)(L)}$	-1.6573	5.887101	-0.28151	0.792286	-18.0025	14.68796	-0.82863	2.943550	-9.0012	7.34398
1L by 2L	-6.8838	5.887101	-1.16929	0.307210	-23.2290	9.46146	-3.44188	2.943550	-11.6145	4.73073
1L by 3L	-10.7703	5.887101	-1.82947	0.141315	-27.1155	5.57496	-5.38513	2.943550	-13.5577	2.78748
2L by 3L	-16.6468	5.887101	-2.82767	0.047457	-32.9920	-0.30154	-8.32338	2.943550	-16.4960	-0.15077

Regr. Coefficients; Var.:**2 h**; R-sqr=.86326; Adj:.65815 (Sonication) 3 factors, 1 Blocks, 11 Runs; MS Residual=69.31591 DV: **2 h**

	Regressn	Std.Err.	t(4)	p	-95.%	+95.%
Mean/Interc.	-92.0073	39.33909	-2.33883	0.079480	-201.230	17.21548
(1)Time (min)(L)	3.3120	1.82628	1.81352	0.143957	-1.759	8.38256
(2)Amplitude/Offset(L)	2.3899	0.64111	3.72780	0.020336	0.610	4.16997
(3)Biomass (g.L$^{-1)(L)}$	1.2709	0.40981	3.10116	0.036181	0.133	2.40868
1L by 2L	-0.0344	0.02944	-1.16929	0.307210	-0.116	0.04731
1L by 3L	-0.0120	0.00654	-1.82947	0.141315	-0.030	0.00619
2L by 3L	-0.0185	0.00654	-2.82767	0.047457	-0.037	-0.00034

ANOVA; Var.:**2 h**; R-sqr=.86326; Adj:.65815 (Sonication) 3 factors, 1 Blocks, 11 Runs; MS Residual=69.31591 DV: **2 h**

	SS	df	MS	F	p
(1)Time (min)(L)	277.242	1	277.2424	3.999694	0.116127
(2)Amplitude/Offset(L)	586.685	1	586.6854	8.463936	0.043709
(3)Biomass (g.L$^{-1)(L)}$	5.493	1	5.4930	0.079245	0.792286
1L by 2L	94.772	1	94.7720	1.367248	0.307210
1L by 3L	231.997	1	231.9966	3.346946	0.141315
2L by 3L	554.229	1	554.2286	7.995691	0.047457
Error	277.264	4	69.3159		
Total SS	2027.682	10			

Hydrolysis Time – 4 hours

Effect Estimates; Var.:4 h; R-sqr=.92436; Adj:.8109 (Sonication a) 3 factors, 1 Blocks, 11 Runs; MS Residual=37.45685 DV: 4 h

	Effect	Std.Err.	t(4)	p	-95.%	+95.%	Coeff.	Std.Err.	-95.%	+95.%
Mean/Interc.	72.5135	1.845310	39.29609	0.000003	67.3901	77.63686	72.51345	1.845310	67.3901	77.63686
(1)Time (min)(L)	14.8945	4.327635	3.44172	0.026252	2.8791	26.90994	7.44725	2.163817	1.4395	13.45497
(2)Amplitude/Offset(L)	18.6120	4.327635	4.30073	0.012638	6.5966	30.62744	9.30600	2.163817	3.2983	15.31372
(3)Biomass (g.L$^{-1)(L)}$	3.3300	4.327635	0.76947	0.484533	-8.6854	15.34544	1.66500	2.163817	-4.3427	7.67272
1L by 2L	-7.1040	4.327635	-1.64154	0.176029	-19.1194	4.91144	-3.55200	2.163817	-9.5597	2.45572
1L by 3L	-3.5800	4.327635	-0.82724	0.454595	-15.5954	8.43544	-1.79000	2.163817	-7.7977	4.21772
2L by 3L	-16.5185	4.327635	-3.81698	0.018827	-28.5339	-4.50306	-8.25925	2.163817	-14.2670	-2.25153

Regr. Coefficients; Var.:**4 h**; R-sqr=.92436; Adj:.8109 (Sonication) 3 factors, 1 Blocks, 11 Runs; MS Residual=37.45685 DV: **4 h**

	Regressn	Std.Err.	t(4)	p	-95.%	+95.%
Mean/Interc.	-92.3459	28.91835	-3.19333	0.033111	-172.636	-12.0557
(1)Time (min)(L)	3.0947	1.34251	2.30517	0.082469	-0.633	6.8221
(2)Amplitude/Offset(L)	2.4729	0.47129	5.24705	0.006310	1.164	3.7814
(3)Biomass (g.L$^{-1)(L)}$	1.1979	0.30125	3.97642	0.016450	0.361	2.0343
1L by 2L	-0.0355	0.02164	-1.64154	0.176029	-0.096	0.0246
1L by 3L	-0.0040	0.00481	-0.82724	0.454595	-0.017	0.0094
2L by 3L	-0.0184	0.00481	-3.81698	0.018827	-0.032	-0.0050

ANOVA; Var.:**4 h**; R-sqr=.92436; Adj:.8109 (Sonication) 3 factors, 1 Blocks, 11 Runs; MS Residual=37.45685 DV: **4 h**

	SS	df	MS	F	p
(1)Time (min)(L)	443.692	1	443.6923	11.84543	0.026252
(2)Amplitude/Offset(L)	692.813	1	692.8131	18.49630	0.012638
(3)Biomass (g.L$^{-1)(L)}$	22.178	1	22.1778	0.59209	0.484533
1L by 2L	100.934	1	100.9336	2.69466	0.176029
1L by 3L	25.633	1	25.6328	0.68433	0.454595
2L by 3L	545.722	1	545.7217	14.56934	0.018827
Error	149.827	4	37.4568		
Total SS	1980.799	10			

Hydrolysis Time – 8 hours

Effect Estimates; Var.:**8 h**; R-sqr=.95154; Adj:.87886 (Sonication) 3 factors, 1 Blocks, 11 Runs; MS Residual=11.444 DV: **8 h**

	Effect	Std.Err.	t(4)	p	-95.%	+95.%	Coeff.	Std.Err.	-95.%	+95.%
Mean/Interc.	77.6158	1.019982	76.09527	0.000000	74.7839	80.44774	77.61582	1.019982	74.78389	80.44774
(1)Time (min)(L)	8.0825	2.392070	3.37887	0.027814	1.4410	14.72395	4.04125	1.196035	0.72052	7.36198
(2)Amplitude/Offset(L)	14.9490	2.392070	6.24940	0.003343	8.3075	21.59045	7.47450	1.196035	4.15377	10.79523
(3)Biomass (g.L$^{-1)(L)}$	-1.3320	2.392070	-0.55684	0.607321	-7.9735	5.30945	-0.66600	1.196035	-3.98673	2.65473
1L by 2L	-2.3170	2.392070	-0.96862	0.387587	-8.9585	4.32445	-1.15850	1.196035	-4.47923	2.16223
1L by 3L	3.9860	2.392070	1.66634	0.170974	-2.6555	10.62745	1.99300	1.196035	-1.32773	5.31373
2L by 3L	-11.7315	2.392070	-4.90433	0.008019	-18.3730	-5.09005	-5.86575	1.196035	-9.18648	-2.54502

Regr. Coefficients; Var.:**8 h**; R-sqr=.95154; Adj:.87886 (Sonication) 3 factors, 1 Blocks, 11 Runs; MS Residual=11.444 DV: **8 h**

	Regressn	Std.Err.	t(4)	p	-95.%	+95.%
Mean/Interc.	-22.2672	15.98442	-1.39306	0.236030	-66.6471	22.11263
(1)Time (min)(L)	0.8556	0.74206	1.15305	0.313102	-1.2047	2.91593
(2)Amplitude/Offset(L)	1.6382	0.26050	6.28847	0.003267	0.9149	2.36141
(3)Biomass (g.L$^{-1)(L)}$	0.7009	0.16651	4.20905	0.013597	0.2385	1.16318
1L by 2L	-0.0116	0.01196	-0.96862	0.387587	-0.0448	0.02162
1L by 3L	0.0044	0.00266	1.66634	0.170974	-0.0030	0.01181
2L by 3L	-0.0130	0.00266	-4.90433	0.008019	-0.0204	-0.00566

ANOVA; Var.:**8 h**; R-sqr=.95154; Adj:.87886 (Sonication) 3 factors, 1 Blocks, 11 Runs; MS Residual=11.444 DV: **8 h**

	SS	df	MS	F	p
(1)Time (min)(L)	130.6536	1	130.6536	11.41678	0.027814
(2)Amplitude/Offset(L)	446.9452	1	446.9452	39.05499	0.003343
(3)Biomass (g.L$^{-1)(L)}$	3.5484	1	3.5484	0.31007	0.607321
1L by 2L	10.7370	1	10.7370	0.93822	0.387587
1L by 3L	31.7764	1	31.7764	2.77669	0.170974
2L by 3L	275.2562	1	275.2562	24.05245	0.008019
Error	45.7760	4	11.4440		
Total SS	944.6928	10			

Hydrolysis Time – 24 hours

Effect Estimates; Var.:**24 h**; R-sqr=.89542; Adj:.73855 (Sonication) 3 factors, 1 Blocks, 11 Runs; MS Residual=15.22445 DV: **24 h**

	Effect	Std.Err.	t(4)	p	-95.%	+95.%	Coeff.	Std.Err.	-95.%	+95.%
Mean/Interc.	85.3928	1.176453	72.58499	0.000000	82.1265	88.65917	85.39282	1.176453	82.12646	88.65917
(1)Time (min)(L)	3.5572	2.759026	1.28931	0.266793	-4.1030	11.21754	1.77862	1.379513	-2.05152	5.60877
(2)Amplitude/Offset(L)	9.3862	2.759026	3.40202	0.027227	1.7260	17.04654	4.69312	1.379513	0.86298	8.52327
(3)Biomass (g.L$^{-1)(L)}$	-0.2578	2.759026	-0.09342	0.930062	-7.9180	7.40254	-0.12888	1.379513	-3.95902	3.70127
1L by 2L	2.1887	2.759026	0.79331	0.472002	-5.4715	9.84904	1.09437	1.379513	-2.73577	4.92452
1L by 3L	6.3528	2.759026	2.30253	0.082708	-1.3075	14.01304	3.17638	1.379513	-0.65377	7.00652
2L by 3L	-10.7112	2.759026	-3.88226	0.017807	-18.3715	-3.05096	-5.35562	1.379513	-9.18577	-1.52548

Regr. Coefficients; Var.:**24 h**; R-sqr=.89542; Adj:.73855 (Sonication) 3 factors, 1 Blocks, 11 Runs; MS Residual=15.22445 DV: **24 h**

	Regressn	Std.Err.	t(4)	p	-95.%	+95.%
Mean/Interc.	31.12179	18.43651	1.68805	0.166673	-20.0662	82.30975
(1)Time (min)(L)	-0.86699	0.85590	-1.01296	0.368374	-3.2433	1.50936
(2)Amplitude/Offset(L)	0.95973	0.30046	3.19418	0.033084	0.1255	1.79395
(3)Biomass (g.L$^{-1)(L)}$	0.60534	0.19206	3.15186	0.034452	0.0721	1.13858
1L by 2L	0.01094	0.01380	0.79331	0.472002	-0.0274	0.04925
1L by 3L	0.00706	0.00307	2.30253	0.082708	-0.0015	0.01557
2L by 3L	-0.01190	0.00307	-3.88226	0.017807	-0.0204	-0.00339

ANOVA; Var.:**24 h**; R-sqr=.89542; Adj:.73855 (Sonication) 3 factors, 1 Blocks, 11 Runs; MS Residual=15.22445 DV: **24 h**

	SS	df	MS	F	p
(1)Time (min)(L)	25.3081	1	25.3081	1.66233	0.266793
(2)Amplitude/Offset(L)	176.2034	1	176.2034	11.57371	0.027227
(3)Biomass (g.L$^{-1)(L)}$	0.1329	1	0.1329	0.00873	0.930062
1L by 2L	9.5813	1	9.5813	0.62933	0.472002
1L by 3L	80.7149	1	80.7149	5.30166	0.082708
2L by 3L	229.4618	1	229.4618	15.07192	0.017807
Error	60.8978	4	15.2245		
Total SS	582.3000	10			

Chapter 12

A systematic study regarding hydrolysis and ethanol fermentation from microalgal biomass

In this chapter, acidic and enzymatic hydrolysis were carried out with *Chlorella vulgaris* and *Scenedesmus obliquus*, and a systematic evaluation of the yeast inoculum optimization (*Saccharomyces cerevisiae* and *Pichia stipitis*) during the hydrolysates fermentation was made. Acidic hydrolysis with 3% of sulphuric acid at 121°C and 30 min of reaction time (50-100 g/L of biomass) was found as best condition, and more than 90% of sugars recovery in the liquid phase was achieved even though *S. obliquus* is more sensible to thermal degradation than *C. vulgaris*. On the other hand, during the enzymatic hydrolysis, ultrasonication showed to be an effective method of biomass pretreatment to provide higher enzyme accessibility and a combination between amylases, cellulase/hemicellulase mix and pectinases, and to achieve more than 90% of sugars recovery in 8 hours of hydrolysis time. Thus, both treatments could recover efficiently the sugars present in microalgae. After inoculum optimization (concentration and consortium between *S. cerevisiae* and *P. stipitis*) and saline influence on yeast performance were evaluated, the fermentation of microalgal hydrolysate exhibited very different profiles in comparison with the control conditions and ethanol biochemical yield changed between 45-61%, emphasizing the importance to optimize this last but not less important step of ethanol production•.

•*Part of this chapter was submitted in Biocatalysis and Agricultural Biotechnology, 2018.*

12.1 INTRODUCTION

Ethanol is the main biofuel worldwide and its demand has been increased in the last decade (Gupta and Verna, 2015). However, first generation crops exploitation such as sugarcane and corn are saturated in terms of arable land (Silva and Bertucco, 2016). In addition, lignocellulosic biomass has found some problems to consolidated large-scakle processes due to the recalcitrance of biomass, mainly (Mosier et al., 2005; Negahdar et al., 2016).

Microalgae as a third-generation of biomass source has been studied as a promising application for biofuel production due to some reasons: growth rate is high, arable land is not necessary, carbohydrate content can achieve up to 60% of dry cell weight, sugars profile is simpler than lignocellulosics, water required is lower than higher plants, and de-structuration of microalgal biomass (hydrolysis) can be performed in only one-step (Chen et al., 2013; Vitovà et al., 2015; Silva and Bertucco, 2016).

In this context, before a real application of microalgal biomass, some steps such as cultivation, hydrolysis and ethanolic fermentation have to be validated at lab-scale. Cultivation processes already showed that microalgae can compete with traditional and lignocellulosics crops in terms of productivity (Acién et al., 2012; Silva et al., 2017a). For hydrolysis processes, acidic and enzymatic methods have been used for several microalgal species: *Scenedesmus spp.* (Ho et al., 2013a; Pancha et al., 2016), *Chlorella spp.* (Ho et al., 2013b; Kim et al., 2014; Rodrigues et al., 2015; Lee et al., 2015; Silva and Bertucco, 2017), *Chlamydomonas spp.* (Nguyen et al., 2009; Choi et al., 2010; Asada et al., 2012), *Tribonema sp.* (Wang et al., 2014), *Dunaliella tertiolecta* (Lee et al., 2013) and *Synechococcus sp.* (Mollers et al., 2014). Acidic process is simpler and requires less treatment time reaching in most cases (optimized conditions) between 80-95% of sugars recovery (Wang et al., 2014; Lee et al., 2015; Ashokkumar et al., 2015; Shokrka et al., 2017). On the other hand, enzymatic hydrolysis has shown lower sugars recovery than acidic one with the same microalgal biomass, reaching a sugars recovery between 30-90% (Harun and Danquah, 2011 a,b; Ho et al., 2013a,b; Lee et al., 2015), even with enzymes having a higher specificity than the acidic attack, and in spite of the several enzymes tested, such as pectinases, cellulases, hemicellulases and amylases.

Fermentation processes generally are used to test the broth obtained from hydrolysis process. Few works have been dedicated specifically to the fermentation process

optimization of microalgal hydrolysates so far (Kuratay et al., 2016; Shokrka et al., 2017), obtaining values of ethanol biochemical yield between 40-98%. This large difference is difficult to be confronted because of different ways of expressing yields (for example, calculation of the efficiency process based on glucose, only), fermentative strains, inoculum and sugars concentration and lacking of a control condition (Choi et al., 2010; Kim et al., 2014; Ho et al., 2013a; Lee et al., 2015; Shokrka et al., 2017).

In this chapter, a careful procedure was developed and carried out to evaluate hydrolysis (acidic and enzymatic) of *Chlorella vulgaris* and *Scenedesmus obliquus*, trying to understand the main bottlenecks of these processes. Also, the fermentation step was carried out based on the consortium of *Saccharomyces cerevisiae* and *Pichia stipitis* to optimize the inoculum concentration, to evaluate the influence of salinity, and to compare a real performance between a microalgal hydrolysates and a control condition. In this way, it is expected to give a contribution to an uniformization of the ethanol fermentation studies from this type of biomass.

12.2 MATERIAL AND METHODS

12.2.1 Microalgal biomass

The microalgae studied were *Chlorella vulgaris* and *Scenedesmus Obliquus*. *Chlorella vulgaris* biomass powder was provided by Neoalgae® (Micro seaweed products B-52501749). *Scenedesmus Obliquus* 276.7 (SAG- Goettingen) biomass was cultivated in a continuous flat-plate photobioreactor (PBR) at 23 ± 1 °C, fed with a modified BG11 in order to provide nutrient limitation (specifically nitrogen) and promote the accumulation of carbohydrates with a residence time τ = 2.3 ± 0.3 days and light intensity of 650 µmol m^{-2} s^{-1} (Silva et al., 2017b). Light was provided by a LED lamp (Photon System Instruments, SN-SL 3500-22). Photon Flux Density (PFD) was measured by a photoradiometer (HD 2101.1 from Delta OHM), which quantifies the photosynthetically active radiation (PAR).

12.2.2 Yeast strains

Yeast species were *Saccharomyces cerevisiae* (Cameo S.p.A.) and *Pichia stipitis* (ATCC 58785). The cultures were maintained in YPD-Medium: 10 g/L of yeast extract, 20 g/L of peptone and 20 g/L of glucose.

For all control fermentations, YPD medium was employed with glucose concentrations of 20 (YPD-20) and 50 (YPD-50) g/L. Generally, 50-100 g/L of algae in the hydrolysis processes were used, with a high carbohydrate content (between 40-50%) which corresponds to a final sugars concentration of 20-25 and 40-50 g/L, respectively. The synthetic medium based on YPD medium was necessary to understand the real potentiality of the yeasts and can make a proper comparison of their performance during the microalgal hydrolysates fermentation step.

11.2.3 Growth analysis

For each experiment, the cellular concentration was monitored through the measurement of dry cell weight and cellular count. Measuring the dry cell weight allows to know the amount of mass per unit volume. First, a known volume of culture is taken. To separate the aqueous bulk from the biomass, nitrocellulose filters (Whatman®) with pore size of 0.45 μm were used. These filters were first dried up to eliminate the absorbed humidity, then they were weighed to measure the tare (Initial filter weight) on an analytical balance (Atilon Acculab Sartorius Group®, sensibility of 10^{-4} g). Phase separation was achieved by suction of the liquid volume of culture through the filter, performed by a vacuum flask. After that the filter with the wet biomass was kept in the oven for 1.5 h at 105°C to eliminate the intracellular water. Then, the final weight of the filter was measured.

Cell concentration was directly measured by counting the cells at the optical microscope using a Bürker® chamber and the result expressed in cells/mL. Growth rate was calculated based on the increasing of the cell concentration in time (during exponential growth phase):

$$\ln \frac{N}{N_0} = \mu t \qquad (12.1)$$

where N_0 and N are the initial and final cellular concentration, respectively, μ is the growth rate and t is the cultivation time.

12.2.4 Sugars hydrolysis and fermentation products analysis

Total sugars were determined by Antrone method (Trevelyan and Harrison, 1952) and reducing sugars by DNS method (Miller, 1959; Silva et al., 2015). Ethanol during the standard fermentations (with YPD medium) was determined by the dichromatic method after distillation (AOAC, 2002). The specific analysis of glucose, xylose, glycerol, acetic acid and ethanol during the hydrolysates fermentation were performed with HPLC (high performance liquid chromatography) according Favaro et al., (2017).

12.2.5 Biochemical characterization of microalgal biomass

Biochemical characterization of microalgal biomass included the determination of moisture (official method 934.01), ash (official method 942.05), protein (official method 2001.11), lipid content (official method 2003.05), carbohydrates and monomers (HPLC) (AOAC, 2002).

12.2.6 Acidic hydrolysis

Acidic hydrolysis was performed with 50 (*Scenedesmus obliquus*) and 100 g/L (*Chlorella vulgaris*) of solids load (biomass), in autoclave (Autoclave vapour-lineeco VWR®), using temperatures between 100-130 °C (P ~ 1 atm), and changing the catalyst concentration (H_2SO_4 – 98% or HCl – 37% - Sigma®, at 0-5% v/v, respectively) and the reaction time (0-60 min). Measures of dry weight, total sugars and reducing sugars were verified. The relation between solubilized biomass and mass yield is given by:

$$[Solubilized\ Biomass](\%) = \frac{Initial\ Biomass\left(\frac{g}{L}\right) - Mass\ yield\left(\frac{g}{L}\right)}{Initial\ biomass\ Load\ \left(\frac{g}{L}\right)} \bullet 100 \qquad (12.2)$$

The amount of total extracted sugars (TS) and reducing sugars (monomers, RS) were represented by the % of sugars extracted/hydrolyzed, respectively, which were calculated by:

$$[Sugar](\%) = \frac{Sugar\ concentration\ in\ the\ liquor\ \left(\frac{g}{L}\right)}{Initial\ biomass\ load\ \left(\frac{g}{L}\right) \bullet Carbohydrates\ content} \bullet 100 \qquad (12.3)$$

where the carbohydrate content is represented by the cellular fraction of this component, generally between 0.1-0.6 depending of the cultivation conditions (Silva and Sforza, 2016; Silva et al., 2017c).

12.2.7 Enzymatic hydrolysis

Enzymatic hydrolysis was performed using citrate buffer 50 mM, pH 5.0 at 50 °C. The enzyme mix was composed by: Viscozyme® L (C - Novozymes cellulases mixture with ≥ 100 FBGU/g – betaglucanase units); AMG 300 L (A - amyglucosidase from *Aspergillus niger* with 260 U/mL) and Pectinex Ultra SP-L (P - pectinase from *Aspergillus aculeans* with ≥ 3,800 U/mL). All of them were produced by Novozymes® and purchased from Sigma-Aldrich®. The amount of enzyme per gram of biomass was fixed, because the experiments were intended to validate the effect of ultrasonication on extraction and saccharification of microalgal sugars.

The enzymatic concentrations were: Viscozyme L® – 20U/$g_{biomass}$; AMG 300 L® – 100U/$g_{biomass}$ and PectineX Ultra SP-L® – 1000U/$g_{biomass}$. All experimental conditions were based on published papers (Harun and Danquah, 2011a; Asada et al., 2012; McMillan et al.,2013; Kim et al., 2014; Lee et al., 2015), and the environmental conditions were able to permit each enzyme to work with a sufficient activity to perform the hydrolysis adequately. Sodium azide was used at concentration of 0.02% (w/v) to prevent contamination (except for the experiments to be fermented).

Biomass pretreatment was carried out using ultrasonication by an ultrasonic generator (AA–WG1–800W – SN 154, Aktive Arc Sarl, Switzerland). The parameters were set to 50% of amplitude and -40% of offset for 25 min and 100 g/L of biomass concentration.

Two sets of experiments were performed:

1) A first one to verify the concentration of the enzymatic mix aforementioned using 100, 50 and 10% of the enzymatic mix, to determine the kinetic profile for 24 hours.

2) After, the specificity of the enzymes during the hydrolysis and all combinations of these three enzymes complexes were used (C, A, P, C + A, C + P, P + A, C + P + A), totalizing 7 experiments and being reported as % of the qualitative enzyme presence in a triangular graph (24 hours of experiment).

All enzymatic hydrolysis experiments were validated by measurements of reducing sugars since the monomers concentration is the final result of the enzyme action and represented as saccharification yield (similar to the % sugars represented by Equation 12.3).

12.2.8 Ethanolic fermentation

Fermentation experiments were performed with two yeasts: *Saccharomyces cerevisiae* (Cameo S.p.A.®) and *Pichia stipitis* (ATCC 58785). Inoculums were stored in liquid and solid YPD medium. All the experiments were carried out at 30 ± 2°C.
Process and fermentation (biochemical) yields are evaluated as:

$$Process\ Yield\ (\%) = \frac{Ethanol\ produced}{0.511 * Initial\ Sugars} 100 \quad (12.4)$$

$$Biochemical\ Yield\ (\%) = \frac{Ethanol\ produced}{0.511 * \Delta Sugars} 100 \quad (12.5)$$

where 0.511 is the glucose-ethanol conversion factor according to the stoichiometry of Gay-Lussac, and *ΔSugars* is the difference between the initial reducing sugars and the final reducing sugars concentrations.

The ethanol productivity is determined by:

$$Productivity\ (\frac{g}{L\ h}) = \frac{\Delta Ethanol}{\Delta t} \quad (12.6)$$

where *ΔEthanol* is the difference between the initial and the final concentration of ethanol (ethanol produced), and *Δt* is the time required to reach the maximum concentration value of ethanol.

In this step, four sets of experiments were carried out:
1) First, the efficiency of each strain (*S.cerevisiae* and *P. stipitis*) and inoculum concentration (0.1, 0.5, 2.5 and 12.5 g/L) were validated in terms of ethanol productivity. The strains were cultivated in YPD-20 (20 g/L of glucose, 20 g/L Peptone and 10 g/L of yeast extract) and YPD-50 (50 g/L of glucose, 20 g/L peptone and 10 g/L of yeast extract).
2) Then, the presence of xylose (20% of sugars present in the medium – generally the pentose fraction in microalgal biomass), and the best consortium combination (*Saccharomyces cerevisiae* and *Pichia stipitis* in different percentages) were validated. Using a consortium *Saccharomyces* + *Pichia* can possibly increase the fermentation productivity since *P. stipitis* is a species able to ferment pentose sugars (*Saccharomyces* is not). The modified culture medium has the following composition: YPD-20 (16 g/L of glucose, 4 g/L of xylose, 20 g/L peptone and 10 g/L of yeast extract) and YPD-50 (40 g/L of glucose, 10 g/L of xylose, 20 g/L peptone and 10 g/L of yeast extract).

3) The third step evaluated the influence of salinity in the fermentation process. During the acidic hydrolysis after neutralization of the broth, salts are formed in a concentration range of 10-50 g/L, which can significantly influence the ethanol productivity. The strains used were the same as for the previous point, with addition of a certain concentration of NaCl or Na_2SO_4.

4) Finally, acidic and enzymatic hydrolysates were fermented under the best conditions of inoculum concentration and consortium as determined in the preliminary experiments, and a comparison between the standard medium and microalgal broth was made.

12.3 RESULTS AND DISCUSSION

A systematic study starting from the acidic/enzymatic hydrolysis of *Chlorella vulgaris* and *Scenedesmus obliquus* (low and high carbohydrate content biomass, respectively) was performed. After that, the fermentation step was investigated to optimize the inoculum concentration and using a consortium between *Saccharomyces cerevisiae* and *Pichia stipitis*. *Pichia stipitis* is able to ferment pentose sugars which are present in microalgae biomass. Additionally, the effect of salinity and microalgal hydrolysates was addressed.

12.3.1 Biochemical characterization of microalgal biomass

The biochemical composition of *Chlorella vulgaris* and *Scenedesmus obliquus* are shown in **Table 12.1.** These species presented quite a different composition in terms of protein, carbohydrate and lipid content. It is important to remember that microalgae display a biochemical plasticity able to change their composition according to the nutritional and environmental factors, and with a relatively fast dynamic (Silva and Sforza, 2016). Specifically, for these microalgae, nitrogen availability, residence time and light intensity allowed to accumulate more or less carbohydrate in *Chlorella vulgaris* and *Scenedesmus obliquus* (Chen et al., 2013; Silva and Sforza, 2016; Silva et al., 2017b). *Chlorella vulgaris* was cultivated in excess of nutrients, and for this reason it showed a high protein content.

Table 12.1: Macrocomponents and sugars profile in *Chlorella vulgaris* and *Scenedesmus obliquus*.

Components	***Chlorella vulgaris***	***Scenedesmus obliquus***
	% of dry cell weight	
Protein	49.5 ± 0.29	33.63 ± 4.04
Lipid	6.3 ± 0.15	25.34 ± 0.64
Carbohydrates	23.0 ± 2.0	45.9 ± 4.5
Glucose*	**70.15**	**79.78**
Xylose*	**10.65**	**16.14**
Arabinose*	**10.91**	**-**
Rhamnose*	**5.73**	**-**
Other*	2.56	4.08
Ash	7.18 ± 0.01	6.83 ± 0.01
Moisture	5.41 ± 0.05	7.05 ± 0.01

*% respect to the carbohydrate content. The values are represented by average ± standard deviation.

Carbohydrates in microalgae are present as both cell wall components (generally cellulose and soluble hemicellulose) and plastids (mainly in the form of starch) (Chen et al., 2013). Glucose was found as the predominant monosaccharide in the biomass, which accounts for more than 70% of total sugars, together with xylose (10.65% for *Chlorella*, 16.14% for *Scenedesmus*), arabinose (10.91% for *Chlorella*) and rhamnose (5.73%, *Chlorella*). Similar compositions were found in the literature for these species. *Chlorella sp KR1* (36.1% of carbohydrate content where 82% glucose, 18% pentose) (Lee et al, 2015) and *Chlorella sorokiniana* (18.2% of carbohydrate content where 70.8% glucose, 21.5% pentose and 7.7% other) (Hernandez et al, 2015). *Scenedesmus obliquus* with 50% of carbohydrate content exhibited a monosaccharide profile composed by 80% glucose and 20% xylose (Ho et al., 2013a). *Scenedesmus almeriensis* with 14.5% of carbohydrate content exhibited a sugars composition of 52.2% of glucose, 33.4% of xylose, 15.4 others (Hernandez et al., 2015). Miranda et al. (2012) verified *Scenedesmus obliquus* biomass composed by 65% of glucose and 35% other monosaccharides.

12.3.2 Acidic hydrolysis

12.3.2.1 Effect of acid concentration and reaction time for *Chlorella vulgaris*

A number of experiments already showed 120°C as best temperature for acidic hydrolysis (Silva and Bertucco, 2017). As shown in **Figure 12.1**, higher acid

concentration and reaction time lead to a higher sugars recovery. Sugar extracted (total Sugars) were saccharified into reducing sugars with a high efficiency.

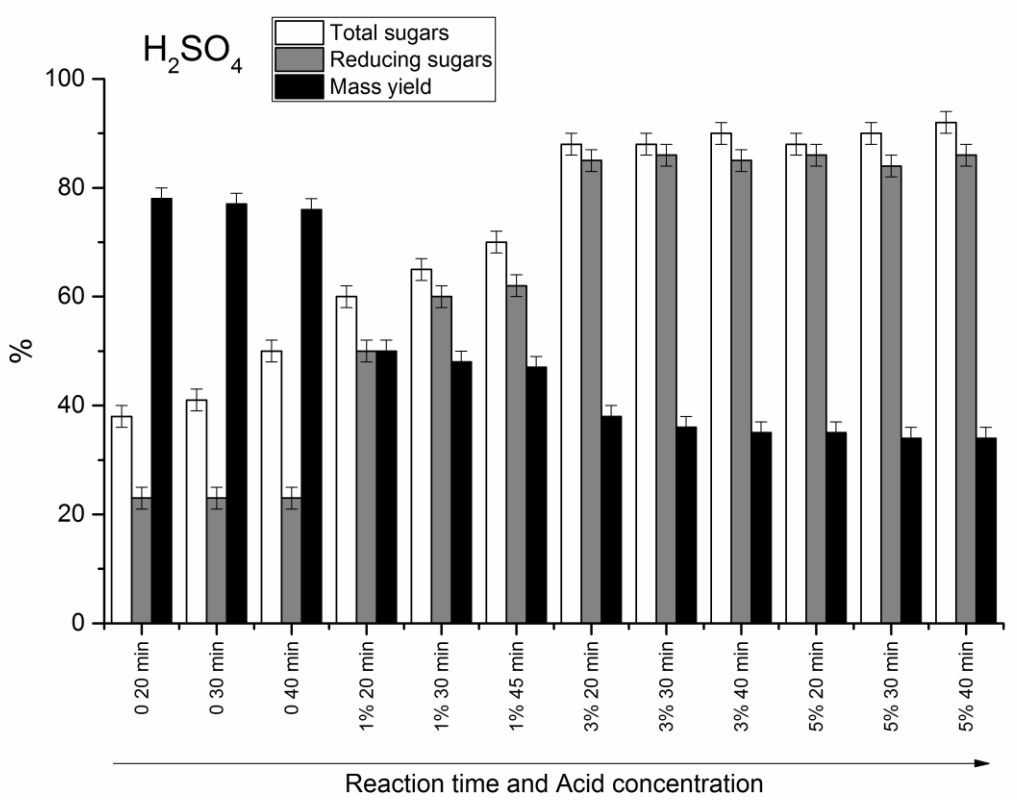

Figure 12.1: Acid hydrolysis for *Chlorella vulgaris* performed at T = 120°C and 100 g/L of biomass load.

At 120 °C, more than 90% of reducing sugars were obtained when 3% H_2SO_4 and 30 min of reaction time were applied. This was considered as the best condition in the range of the experiments performed. In fact, according to literature, 90% of biomass has been hydrolyzed when 50 g/L of *Tribonema* sp. was submitted at 121 °C and 3% of sulfuric acid for 30 min (Wang et al., 2014). *Chlorella vulgaris* JSC-6 (120 g/L), at 121°C and 3% of sulfuric acid for 20 min reached a saccharification yield of 90% (Wang et al., 2016). Ho et al. (2013b) for *Chlorella vulgaris* (53% of carbohydrate content) with 1% of acid concentration, 20 min of reaction time and 60 g/L of biomass at 121°C reached almost 95% of saccharification yield. *Dunaliella tertiolecta* LB999 (50 g/L) at 121 °C and 0.5N of hydrochloric acid for 15 min achieved a hydrolysis yield of 56.7% (Lee et al., 2015).

12.3.2.2. Comparison between sulphuric and chloride acid for *Chlorella vulgaris*

As seen in **Figure 12.2**, H_2SO_4 gives better carbohydrate conversion into reducing sugars than HCl, confirming as best condition 3% of acid concentration and 30 min of reaction time at 120°C. This check was necessary since Lee et al. (2015) found better performance for *Chlorella* using HCl 0.5N with 15 minutes of treatment at 121°C and 50 g/L of biomass concentration, reaching 98% in comparison with sulphuric acid (0.5N, 121°C, 15min), i.e. as 80% of yield for maximum sugars recovery. Lee et al. (2013) also found better saccharification with HCl in comparison with H_2SO_4 (121°C, 15 min, 50 g/L and 0.5N of acid) reaching 56.7 and 29.4% of saccarification yield, respectively. With the conditions used in **Figure 12.2** sulphuric acid 3%v/v showed be more suitable for acidic hydrolysis, in disagreement these paper cited above.

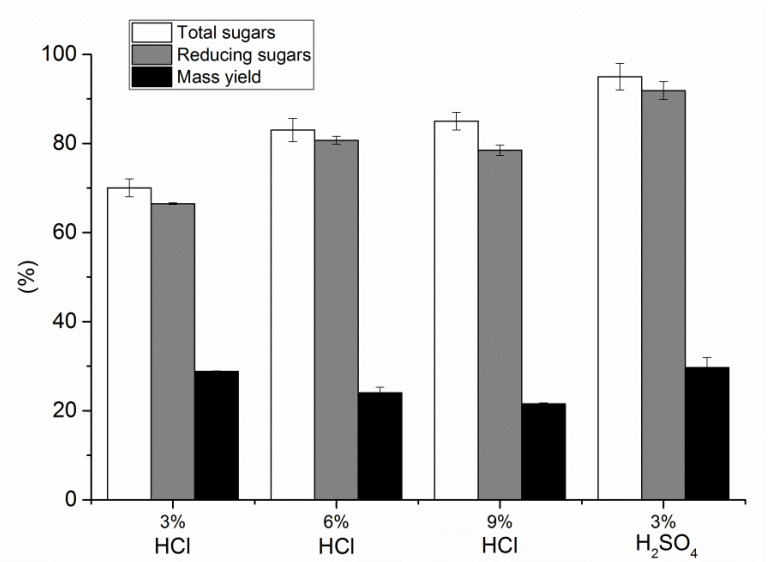

Figure 12.2: Comparison between the performance with HCl and H_2SO_4. *Chlorella vulgaris* (100 g/L) with 30 min at 120 °C.

12.3.2.3. Effect of acid concentration and reaction time for *Scenedesmus obliquus*

These experiments were performed with 50 g/L of biomass at 120°C and 3% of acid concentration. Initially, reaction time was 30 min, according to the best condition found for *Chlorella vulgaris*. But this was not sufficient for *Scenedesmus obliquus* which reached 90% of sugars extraction and 64% of saccharification yield (reducing sugars – monomer) as visualized in **Figure 12.3**.

Biomass concentration was set to 50 g/L because viscosity problems occurred with 100 g/L, differently of *Chlorella vulgaris*. A decrease of the saccharification yield is already demonstrated in the literature when biomass concentration is high and increases significantly the viscosity (Ho et al., 2013a). Maximizing biomass concentration is important from an industrial point of view.

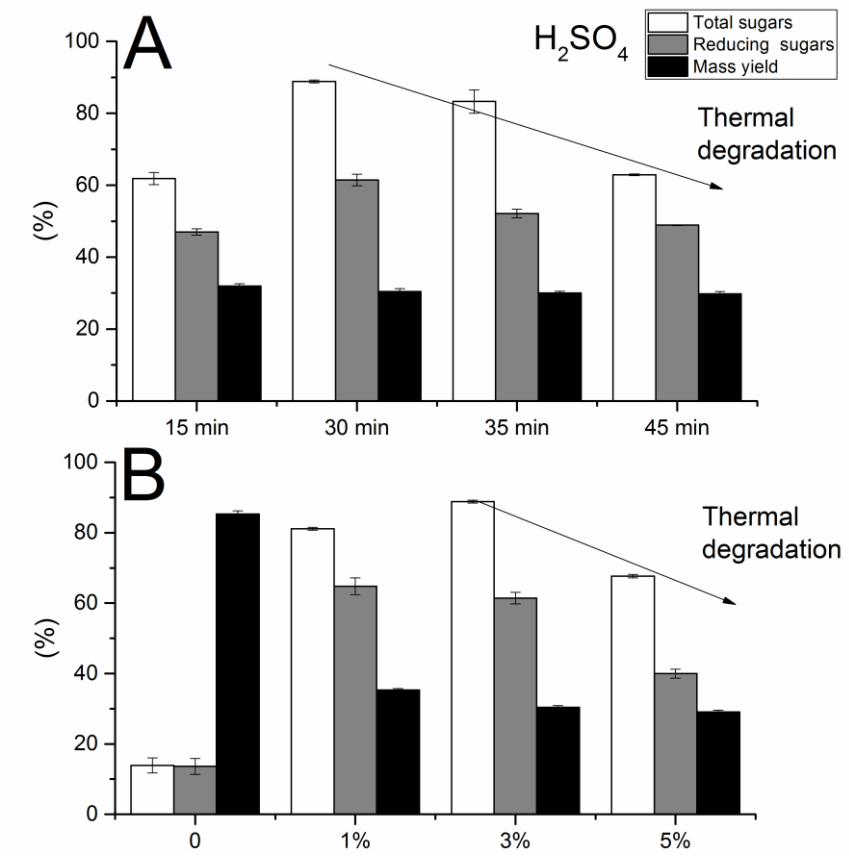

Figure 12.3: Acid hydrolysis for *Scenedesmus obliquus* (50 g/L) at 120 °C. A) Influence of reaction time with 3% of acid v/v. B) Influence of H_2SO_4 concentration with 30 min of reaction time.

The results of **Figure 12.3A** are in agreement with literature. *Scenedesmus obliquus* hydrolyzed (50 g/L) at 120 °C and H_2SO_4 5% v/v for 30 min, provided 90% of saccharification yield (Miranda et al., 2012). Ashokkumar et al. (2013) hydrolyzed 20 g/L of *Scenedesmus bijugatus* biomass at 130 °C, 45 min of reaction time and 2% of acid v/v obtained around 85% of saccharification. Ho et al., (2013a) with *Scenedesmus obliquus* CNW-N, 10–40 g/L, at 121 °C and with different concentrations of H_2SO_4 (1.5–2% v/v) for 20 min reached 95% of sugars recovery.

With H_2SO_4 5% v/v it was visualized a significant sugars degradation from 87 to 70% (**Figure 12.3A**). As a slight increase of acid concentration caused degradation of the sugars, it was decided to study the effect of the reaction time with H_2SO_4, varying it between 0-45 min at 120°C and 3% of acid **(Figure 12.3B**). Increasing the reaction time (35 and 45 min) a linear degradation process of the sugars was noted, showing high sensitivity; as well, none advantages were obtained.

Sugars degradation at high temperatures and catalyzed by acids is well known in literature, and depends of the biomass type, catalyst and operating conditions (biomass concentration, reaction time and temperature). It was evidenced for *Tribonema sp*. with H_2SO_4 3% v/v, biomass concentration of 70 g/L at 121°C in the treatment time range of 15-90 minutes. It was found a maximum saccharification of 81.2% at 35 minutes, after that the sugars yield decreased fast, because at 60 minutes the saccharification yield was 65% and at 75 minutes of 40% (Wang et al., 2014). Also, degration processes was highlighted by Ashokkumar et al. (2013) (*Scenedesmus bijugatus*) when acid concentration or temperature increased (2 to 3% v/v and 130 to 160°C), a decreasing of hydrolysis yield was evidenced from 83 to 35 and 35%, respectively. Miranda et al., (2012) with *Scenedesmus obliquus* studied the effects of H_2SO_4 concentration (0.05-10 N) performed at 120°C for 30 minutes. The maximum yield obtained was 91% with H_2SO_4 2 N. For acid concentration > 2 N the sugars yield decreased faster.

In conclusion, comparing the results of the two different microalgae during the acidic hydrolysis, *Scenedesmus obliquus* resulted to be apparently more sensitive to thermal degradation than *Chlorella vulgaris*.

12.3.3 Enzymatic hydrolysis

12.3.3.1. Enzyme mix concentration

For *Chlorella vulgaris* biomass, purchased as dried and milled, no pretreatment was required, i.e., enzymes were able to react directly with the biomass because the cells were already broken during the drying treatment. The experiments were carried out with 100 g/L of microalgal biomass. The enzymatic mix (x) was used in the concentrations of 1x, 0.5x and 0.1x in order to study the effect of enzymes, as show in **Figure 12.4A**. The enzymatic hydrolysis with enzyme concentration 1x reached the maximum value of

92% of saccharification in 4 hours. With 0.5x a sugars recovery of 60% after 10 hours was obtained. For 0.1x only 25% was saccharified. This behavior depends on the polysaccharides type present in the biomass. Each enzyme is specialized to saccharify specific polysaccharides.

Scenedesmus obliquus biomass (100 g/L) was also contacted with to different concentration of enzymatic mix (as made with *Chlorella vulgaris*), i.e., 1x, 0.5x and 0.1x. The biomass was pretreated by ultrasonication. From **Figure 12.4B**, it was noticed that the maximum saccharification level is reached faster by increasing the enzymes concentration. In the concentration 1x the maximum saccharification was 95% reached after 8 hours of enzymatic hydrolysis. With the other concentrations (0.5x and 0.1x), the sugars yield was as high as 90% and 75% after 24 hours, respectively. Thus, it is a two-variable system saccharification time and enzyme concentration. It is important to mention that the enzymatic mix was based on literature data but the influence of the specific enzyme and its concentration has still to be optimized.

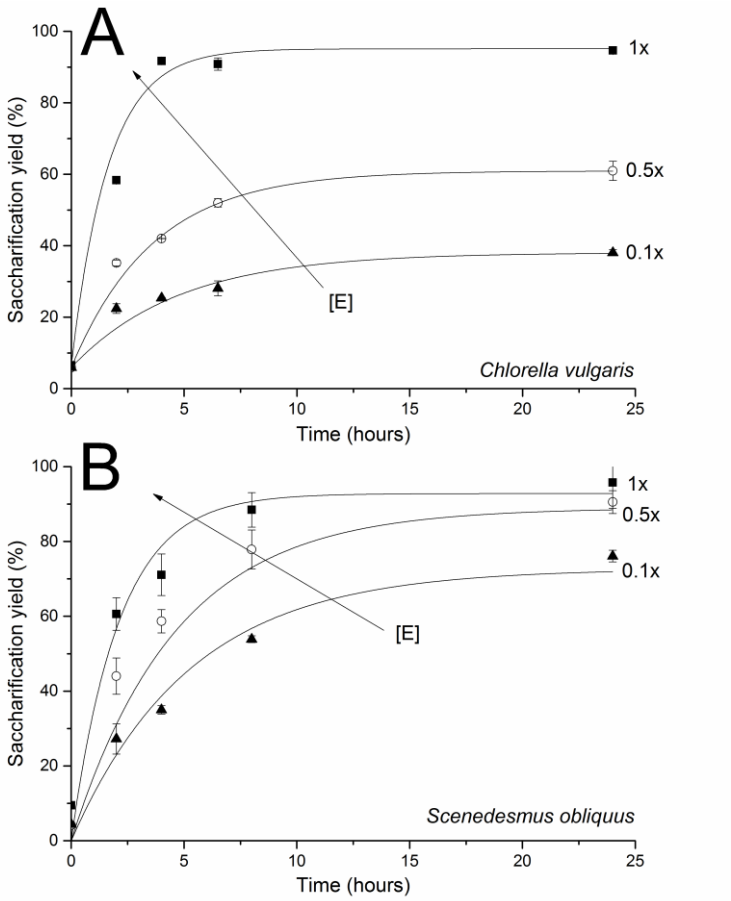

Figure 4: Enzymatic hydrolysis of microalgal biomass: effect of enzymatic mix concentration. A) *Chlorella vulgaris* and B) *Scenedesmus obliquus* (x = Viscozyme L: 20 U/$g_{biomass}$, AMG: 100U/$g_{biomass,}$ Pectinex Ultra SP-L: 1000U/$g_{biomass}$).

12.3.3.2. Type of enzyme

As the results showed different behavior of the enzymatic mix between these two microalgal species, it means that the sensibility of these biomasses to the enzymes present in the mix are different. So, some additional experiments using the enzymes alone, and the combination between them were performed and the results are shown below in **Figure 12.5**. Both species were more susceptible to cellulase and amylase complex mix, reaching more than 90% of saccharification yield. On the other hand, pectinase did not demonstrate a fundamental importance.

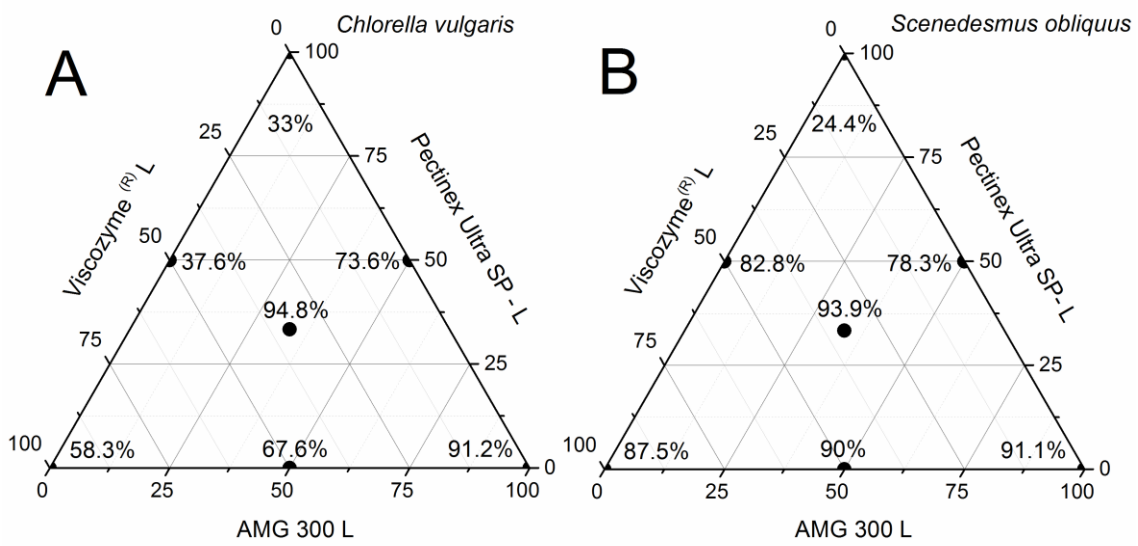

Figure 12.5: Effect of the enzymes on saccharification yield. A) *Chlorella vulgaris* and B) *Scenedesmus obliquus*. The values of the diagram are qualitatively cumulative in %. For example, the point P + A + C is signalized as 33.3% of each enzyme and P, A or C alone represent 100% of each enzyme. Numbers inside the triangles represent saccharification yield after 8 hours of hydrolysis. Standard deviation < 7%.

12.3.3.3. Discussion regarding the enzymatic hydrolysis results

According to our results acid hydrolysis showed high efficiency in terms of sugars recovery, mainly for *Chlorella vulgaris* where degradation processes were not clearly viewed. On the other hand, this process for *Scenedesmus obliquus* must be carefully used, because the sensitivity of biomass to degradation of sugars was highly evidenced.

According to literature, enzymatic hydrolysis from microalgal biomass ensured lower yield in comparison with acidic treatment and required longer hydrolysis time when a acceptable biomass concentration value in view of industrial application is considered.

For example, it was found 27.4 instead of 93.3% for *Chlorella sp.* (50 g /L and 3 h) (Lee et al., 2015) 64 instead of 96% for *Chlorella vulgaris* FSP-E (40 g /L and 2-3 days) (Ho et al., 2013b) and 62.8 instead of 100% for C*hlorococcum* (10-15 g /L and 12 h) (Harun and Danquah, 2011a,b). However, it has to be considered that these results could be affected at least by two problems: ineffective pretreatment and/or inadequate specificity/concentration of the enzymes.

Kim et al., (2014) tested different enzymes (cellulase, pectinase, xylanase, β-glucosidale, amylase, chitinase, lysozyme and sulfatase) for the enzymatic hydrolysis of *Chlorella vulgaris* (KMMCC-9; UTEX 26 – 16% of carbohydrate content), and in this case pectinase was the only one to reach a saccharification yield of 78%, the other enzymes being less than 20%. Also, Lee et al. (2015) using *Chlorella sp*. KR-1 (36.1% of carbohydrate content) confirmed Pectinex Ultra-SP-L (pectinase) as more efficient in the enzymatic hydrolysis reaching more than 90% of saccharification yield. Unfortunately, for the species studied in this paper the effect of pectinase was synergic with the other enzymatic complex (Vyscozyme L and AMG 300L), but when alone, it was not more than 35% of saccharification yield was reached.

A study investigated the hydrolysis of *Chlorella pyrenoidosa* using cellulase with a biomass concentration of 20 g/L at 50°C and a saccharification yield of 60% was obtained after 24 hours (Fu et al., 2010). Interestingly, Rodrigues et al. (2015) using exoglucanases-free cellulases to saccharify *Chlorella homosphoera* reached a maximum hydrolysis yield of 50%. The maximum values found in these works were lower than ours.

The use of enzymatic mix is important since the components in microalgal biomass can change a lot as the result of environmental/nutritional condition or species-dependent. Shokrkar et al., (2017) studied an enzymatic hydrolysis of microalgal biomass mix with β-glucosidase/cellulose, α-amylase and amyglucosidase was carried out. A synergy of these enzymes was observed and almost 100% of sugars recovery was reached, indicating that an enzymatic mix is more efficient than the application of simple enzymes, and confirming our results. Pancha et al. (2016) studied the effect of enzymes concentration on *Scenedesmus obliquus CCNM 1077* de-oiled biomass (45.23% carbohydrate content). The enzymes were amylase, Viscozyme-L and cellulase, in the concentration range 5-50 $U/g_{biomass}$. The best condition after 24 hours was the ones with

Viscozyme-L 50 U/$g_{biomass}$, with a saccharification efficiency of 77.4%, but still insufficient for industrial purposes. They mentioned that this efficiency (in comparison with amylase and cellulase alone) was attributed to the complex mix of Viscozyme L, which is composed by arabanase, cellulase, beta-glucanase, hemicellulose and xylanase. *Chlorella vulgaris* FSP-E (53% of carbohydrates) hydrolyzed by a mixture of endoglucanase, beta-glucosidase and amylase reached between 80-90% of saccharification yield (Ho et al., 2013b). In this paper, more than 90% of sugars recovery was obtained, and it was also demonstrated that by increasing the enzymes concentration, the saccharification yield obtained is higher with less hydrolysis time.

In our work, we also have demonstrated that enzymatic hydrolyses can compete in terms of sugar recovery with acidic treatment since more than 90% of saccharification was achieved in both treatments, using ultrasonication as biomass pretreatment and an enzymatic mix composed by pectinase, cellulase/hemicellulase mix and amylases.

12.3.4 Ethanolic fermentation

12.3.4.1. Inoculum optimization

In this experimental part, the focus was to find out the best initial inoculum ensuring a viable ethanol productivity, defined as the ethanol produced per unit volume, in g L^{-1} h^{-1}. Remember that sugarcane broth industrial fermentation in Brazil generally provides ethanol productivity between 5-10 g L^{-1} h^{-1}. Two yeasts, *Saccharomyces cerevisiae* and *Pichia stipitis*, were studied separately. The fermentations were performed in YPD-20 and YPD-50 with different initial inoculums: 0.1 g/L, 0.5 g/L, 2.5 g/L and 12.5 g/L.

In **Figure 12.6**, sugars consumption, ethanol production and cell growth for *S. cerevisiae* are reported. The fermentations reached the stationary phase faster when the initial inoculum concentration was higher. Both YPD-20 and YPD-50 achieved a stationary phase in less than 6 hours for inoculums concentration larger than 2.5 g/L. A lag phase of at least 2 hours was required to adapt the microorganisms in the medium conditions.

Final sugars concentration was practically the same in all experiments, between 2-4 g/L. This emphasizes that the capabilities of the cells to metabolize changed the assimilation time, i.e., the higher the inoculum concentration, the faster the sugar consumption (**Figure 12.6A** and **D**). In **Figure 12.6B** and **E** ethanol concentration profiles along the

time are shown. The larger is the inoculum, the faster is the ethanol production as well. The inoculum with 12.5 g/L reached the maximum ethanol concentration in less than 2.5 hours, those with 0.1 g/L and 0.5 g/L needed at least 12 hours. Final ethanol concentrations were practically the same for all the experiments. Increasing the initial inoculum, the rate at which the maximum concentration of ethanol is reached increases. Growth curves achieved the stationary phase in less than 6 hours for all fermentations (**Figure 12.6C** and **F**). Inoculum concentration optimization is one of the most known techniques to improve the efficiency of the fermentation process (Shokrkar et al., 2017). Unlike *Saccharomyces cerevisiae*, *Pichia stipites* showed a considerable lag time in all the experiments. The time required by this strain to adapt was at least 20 hours. Observing the growth curves reported in **Figure 12.7C** and **F**, it can be noted that at high inoculum concentrations the difference between initial and final dry cell weight is negligible. The sugars were consumed slowly during the lag time, and slower after the adaptation time depending on the inoculum concentration (12.5 g/L versus 0.1 and 0.5 g/L, for example). See **Figure 12.7A** and **D** for details. This was more evident for YPD-50 because the glucose concentration was high (50 g/L) and the yeast required a longer period of adaptation, exhibiting also an influence on the sugars concentration. This evidence was also reported by Silva et al. (2016), who reported that *P. stipitis* in a culture medium with 20 g/L xylose, 3 g/L of glucose and 6.7 g/L YNB (yeast nitrogen base) with the inoculum of 0.1 g/L consumed only 57.5% of sugars after 72 hours. Ethanol concentration was low during the first hours of fermentation as well and after 24 hours the ethanol production rate remarkably increased (**Figure 12.7B** and **E**).

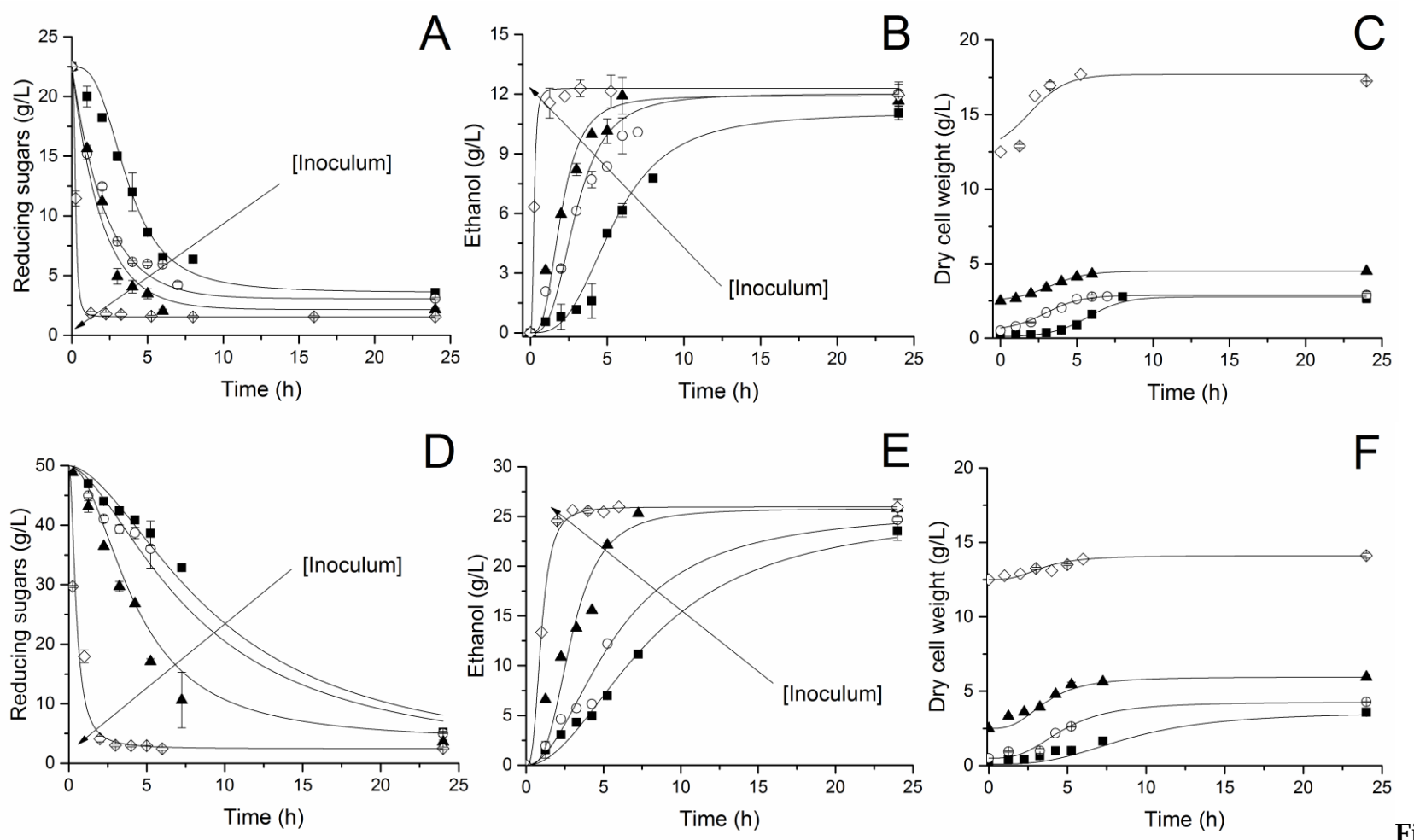

Figure 12.6: Ethanolic fermentation with *Saccharomyces cerevisiae*. A, B and C using YPD-20. D, E and F using YPD-50. (■) 0.1, (○) 0.5, (▲) 2.5 and (◊) 12.5 g/L of inoculum concentration.

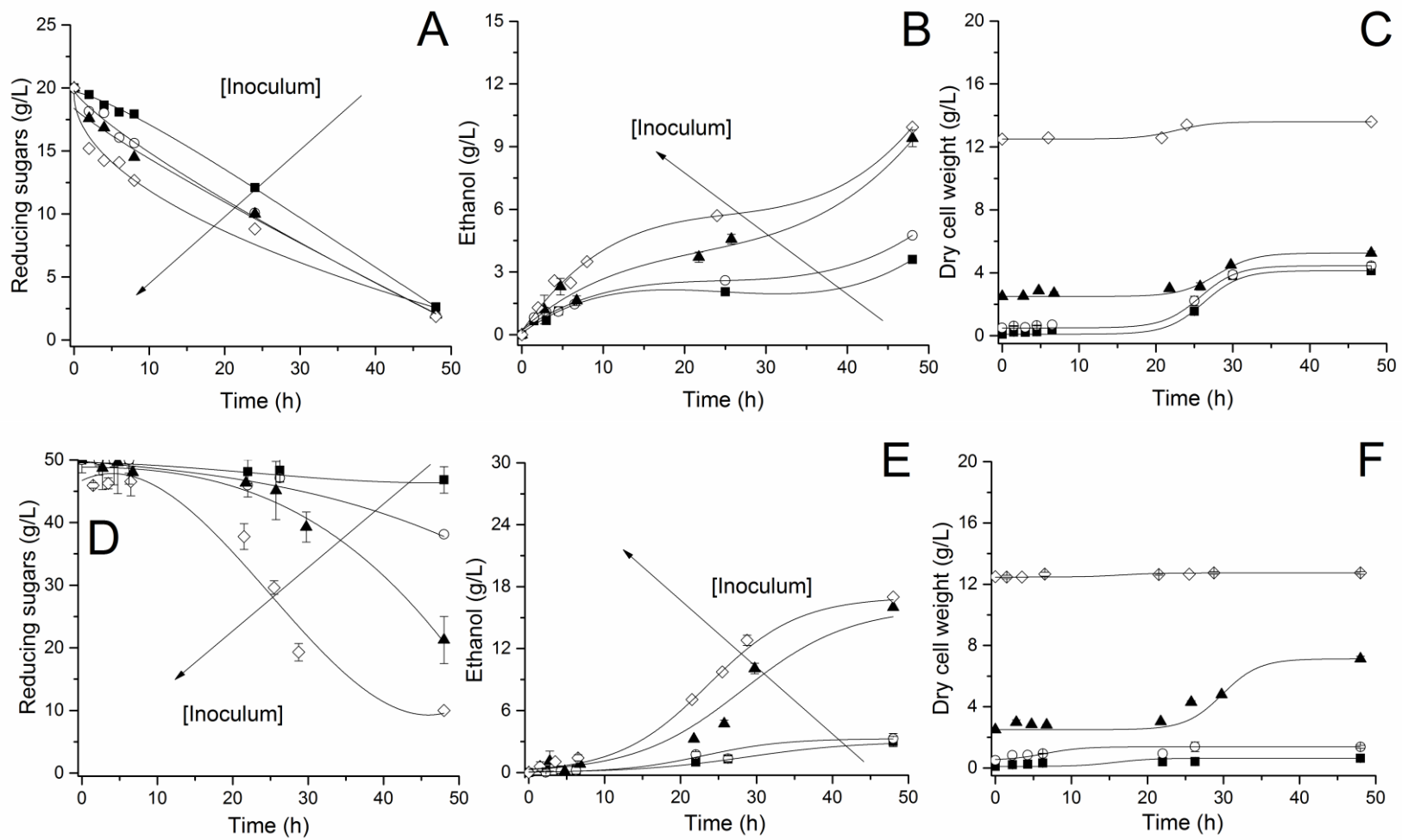

Figure 12.7: Ethanolic fermentation with *Pichia stipitis*. A, B and C using YPD-20. D, E and F using YPD-50. (■) 0.1, (○) 0.5, (▲) 2.5 and (◊) 12.5 g/L of inoculum concentration.

Two important considerations can be done, about: 1) growth rate and 2) ethanol productivity. In **Figure 12.8A** growth rates of the *S. cerevisiae* experiments are displayed. When increasing the initial inoculum concentration, yeast's growth rate decreased. The values ranged from 0.57 h^{-1} with 0.1 g/L of inoculum to 0.1 h^{-1} when 12.5 g/L was used. Higher sugar concentration provided higher growth rates as well. For *P. stitpitis*, growth rates are not shown because in 48 hours they were < 0.1 h^{-1}. Thus, a fermentation using only *P. stipitis* is not feasible, but as aforementioned it is able to ferment pentose and a consortium between *Saccharomyces* and *Pichia* can be formulated.

Ethanol productivities for *S. cerevisiae* e *P. stipitis* are displayed in **Figure 12.8B** and **C**. *Saccharomyces cerevisiae* showed a linearly correlation between ethanol productivity and inoculum concentration which was dependent of the sugars concentration as well. It is possible to conclude that this microorganism is not inhibited by sugars concentration in the range studied. On the other hand, *P. stipitis* showed an ethanol productivity much lower than *S. cerevisiae* and an additional negative influence of the sugars concentration, confirming the unfeasibility of this microorganism to be used alone.

Günan Yücel and Aksu (2015) studied the fermentation with *Pichia stipitis* (NRRL Y-7124) using sugars obtained from beet pulp hydrolysate. They observed low ethanol productivities (0.06 – 0.494 g L^{-1} h^{-1}) and long fermentation time (50-75 hours) to reach a maximum ethanol concentration of 37.1 g/L (culture medium with 75.1 g/L of xylose). On the other hand, *Pichia stipitis* (NRRL Y-7124), with inoculum concentration of 7.5 g/L, fermented a culture medium with 20 g/L of xylose, 3 g/L of glucose and 6.7 g/L of YNB (yeast nitrogen base) and an ethanol productivity of 0.03 g L^{-1} h^{-1} after 72 hours was achieved, with a maximum ethanol concentration of 4 g/L (Silva et al., 2016).

From an industrial point of view, the ethanol produced per unit time is of crucial importance. The yeast inoculum concentration was selected as 7.5 g/L since between 3-7.5 g L^{-1} h^{-1} (for YPD-20 and 50, respectively) of ethanol productivity can be achieved. In fact, Wanderley et al. (2014) studied the effect of *Saccharomyces cerevisiae* concentration (UFPEDA 1238 and UFPEDA 1324) for ethanol production from sugar cane broth (inoculum concentration of 0.4, 4 and 8 g/L). The found maximum ethanol productivity (3.1 g L^{-1} h^{-1}) starting from a strain with 40 g/L of sugars and 8 g/L of

inoculum. The biochemical conversion for *S. cerevisiae* of sugars to ethanol was higher than 90%, evidencing that this strain is able to efficiently use the energy produced during the process in the fermentation pathway.

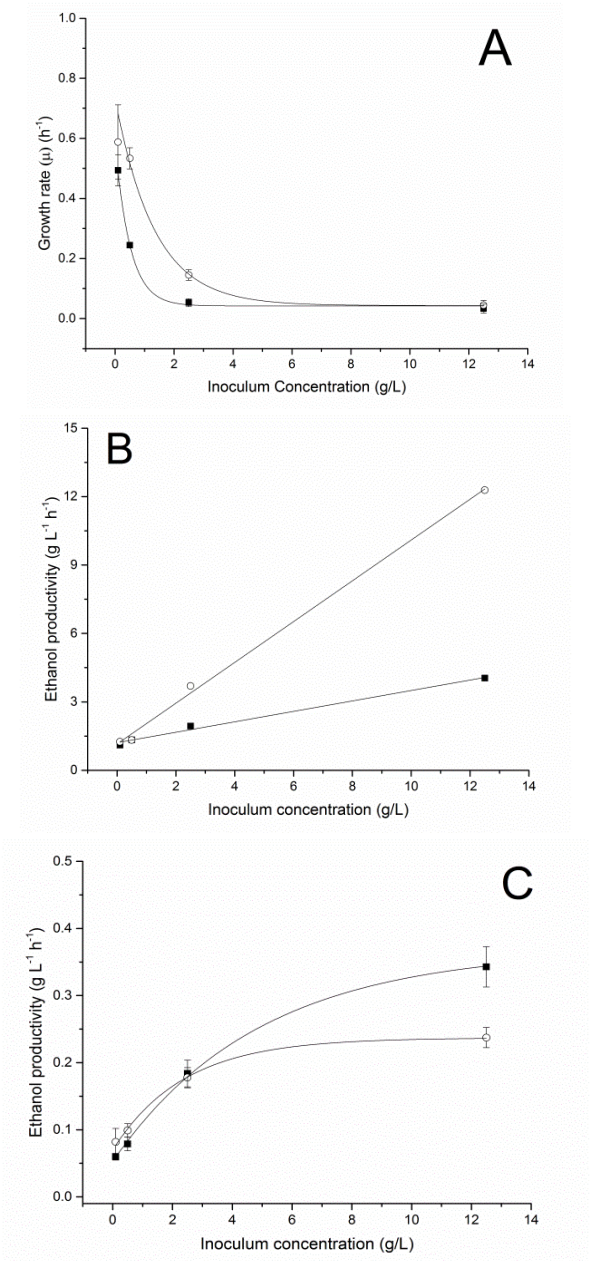

Figure 12.8: Growth rate and ethanol productivities during the standard fermentations with *S. cerevisiae* and *P. stipitis*. A) Growth rate for *S. cerevisiae* fermentations. Ethanol productivity for B) *S. cerevisiae* and C) *P. stipitis*. (■) YPD-20 and (○) YPD-50.

12.3.4.2. Consortium optimization

The biochemical characterization of microalgal biomass highlighted the presence of xylose and other C-5 sugars (**section 12.3.1**), with pentose ≈ 20% of total sugars, in addition to glucose (70-80% of cell carbohydrate dry weight). As *Saccharomyces cerevisiae* is not able to ferment pentose sugars, a lower sugars consumption and process yield are expected (Silva and Bertucco, 2017).

On the other hand, *Pichia stipitis* is naturally able to ferment pentose sugars. However, as seen in the previous step, it reached a remarkably lower ethanol productivity than *Saccharomyces cerevisiae.* The aim of this second part of the fermentation study was to optimize a *Saccharomyces-Pichia* consortium in order to maintain a high ethanol productivity and simultaneously maximize the sugars consumption (both hexose and pentose). The adapted culture mediums were YPD-20* (16 g/L of glucose, 4 g/L of xylose, 20 g/L peptone and 10 g/L of yeast extract) and YPD-50* (40 g/L of glucose, 10 g/L of xylose, 20 g/L peptone and 10 g/L of yeast extract). The inoculum concentration optimized in the first experiments was used (7.5 g/L), where it was able to consume sugars in less than 8 hours. Several fractions of *S. cerevisiae* and *P. stipitis* were tested: 100% *S. cerevisiae* and 0% *P. stipitis*, 75% *S.cerevisiae* and 25% *P.stipitis*, 50% *S. cerevisiae* and 50% *P. stipitis*, 25% *S.cerevisiae* and 75% *P.stipitis*, 0% *S.cerevisiae* and 100% *P.stipitis*.

In **Figure 12.9,** process yield and ethanol productivity for the consortium are shown, since they are the most important to determine the fermentation efficiency. The **Figure 12.9** confirm that the best consortium was the one composed by 75% of *S. cerevisiae*, and a positive contribution of *P. stipitis* to pentose fermentation is shown. This increased process yield/ethanol productivity to 95-100%, 4.91 g L^{-1} h^{-1} for YPD-20* and 6.36 g L^{-1} h^{-1} for YPD-50*, respectively. The velocity of the fermentation process was proportional to the *S. cerevisiae* percentage, and as expected the worst performance was the experiment with 100% *P. stipitis*.

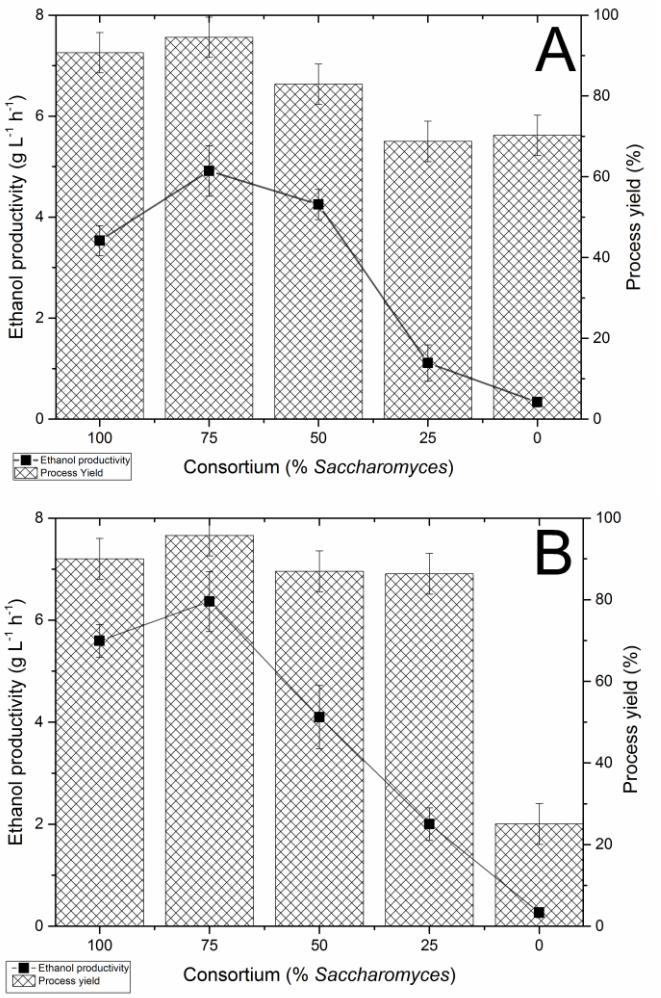

Figure 12.9: Process yield (bars) and ethanol productivity (squares) for the consortiums in YPD-20* (A) and YPD-50* (B). The percentage of *S. cerevisiae* is summed with the % of *P. stipitis* to reach 100%.

Our results are in agreement with those of Ciolfi et al. (2012) who studied the influence of *Pichia guilliermondii* on fermentation for alcohols production, performed with *Saccharomyces cerevisie* and *Saccharomyces uvarum*. Different consortiums were tested (100% *S. cerevisiae* and *S. uvarum*; 100% *P. guilliermondii*; 10% *S. cerevisiae* and *S. uvarum* and 90% *P. guilliermondii*; 50% *S. cerevisiae* and *S. uvarum* and 50% *P. guilliermondii*; 90% *S. cerevisiae* and *S. uvarum* and 10% *P. guilliermondii*), in a synthetic medium with 200 g/L of sucrose (pH=3.20) and initial inoculum of $2 \bullet 10^6$ cells/mL. The best consortium was the one made with 90% *S. cerevisiae* and *S. uvarum* and 10% *P. guilliermondii*, which reached the highest alcohols concentration and productivity. The other consortiums tested showed a decrease of alcohols productivity when the *Pichia guilliermondii* fraction increased in the inoculum initial concentration.

The advantages of a consortium were shown using an inoculum composed by 50% *S. cerevisiae* ATCC 26603 and 50% *P. stipitis* KCCM 12009 for the fermentation of woody biomass (Kalyani et al., 2013). The hydrolysate with 50 g/L of sugars was neutralized to pH 5 and added with 5 g/L of yeast extract, 10 g/L $(NH_4)_2SO_4$, 4.5 g/L KH_2PO_4, and 1 g/L $MgSO_4.7H_2O$ (yeast inoculum was equal to 2% v/v). A sugars consumption of 70% for the fermentation with *S. cerevisiae* was founded, 62.2% with *P. stipitis* and 88% for the consortium. The process yield (based on ethanol) measured was 65% for *S. cerevisiae*, 52% with *P. stipitis* and 84% with the consortium (Kalyani et al., 2013).

12.3.4.3 Effect of salinity

After acidic hydrolysis, the broth needs to be neutralized to a pH between 5-6, generally to provide an efficient yeast cultivation/fermentation. NaOH was used in this work, so Na_2SO_4 (if acid hydrolysis has been performed with H_2SO_4) or NaCl (if acid hydrolysis has been performed with HCl) are produced.

In **Figures 12.10A-11A** and **12.10D-11D** the sugars concentration of the YPD-20* and YPD-50* are reported. Compared to the fermentations without salt addition (control condition) it was evident that salts inhibited sugars assimilation, which was slower when salt concentration was increased. The same effect was observed on the ethanol production (**Figures 12.10B-11B** and **12.10E-11E**). The maximum ethanol concentration (end of fermentation) was obtained in few hours (≈ 5 hours) and was lower than the one without salts, even if the sugars were almost completely consumed, thus indicating that a part of energy produced by the sugars metabolism was used in other cellular processes instead of ethanol production.

Fermentations with *Saccharomyces cerevisiae* under salinity stress was studied by several authors, who demonstrated that salts stress is caused by two different phenomena: osmotic stress and ion toxicity. In osmotic stressed condition *S. cerevisiae* tends to accumulate osmolytes like polyols (glycerol, for example) by wasting energy and consuming sugars present in the fermentation broth (Blomberg, 2000; Logothetis et al., 2007). For this reason, the ethanol produced resulted lower even though most of sugars were consumed. A similar behavior probably is occurring in our work.

From the growth curves reported in **Figures 12.10C-11C** and **12.10F-11F**, it was noticed a decreasing of dry cell weight during the first 5 hours in all the experiments.

Probably part of the cells died due to the osmotic shock. Alternatively, during the adaption time, the morphology/physiology can change causing an increasing/decreasing of the cellular density (Logothetis et al., 2007). In addition, it was demonstrated that the presence of sodium ions in excess are toxic to yeast (Arino et al., 2010; Casey et al., 2013).

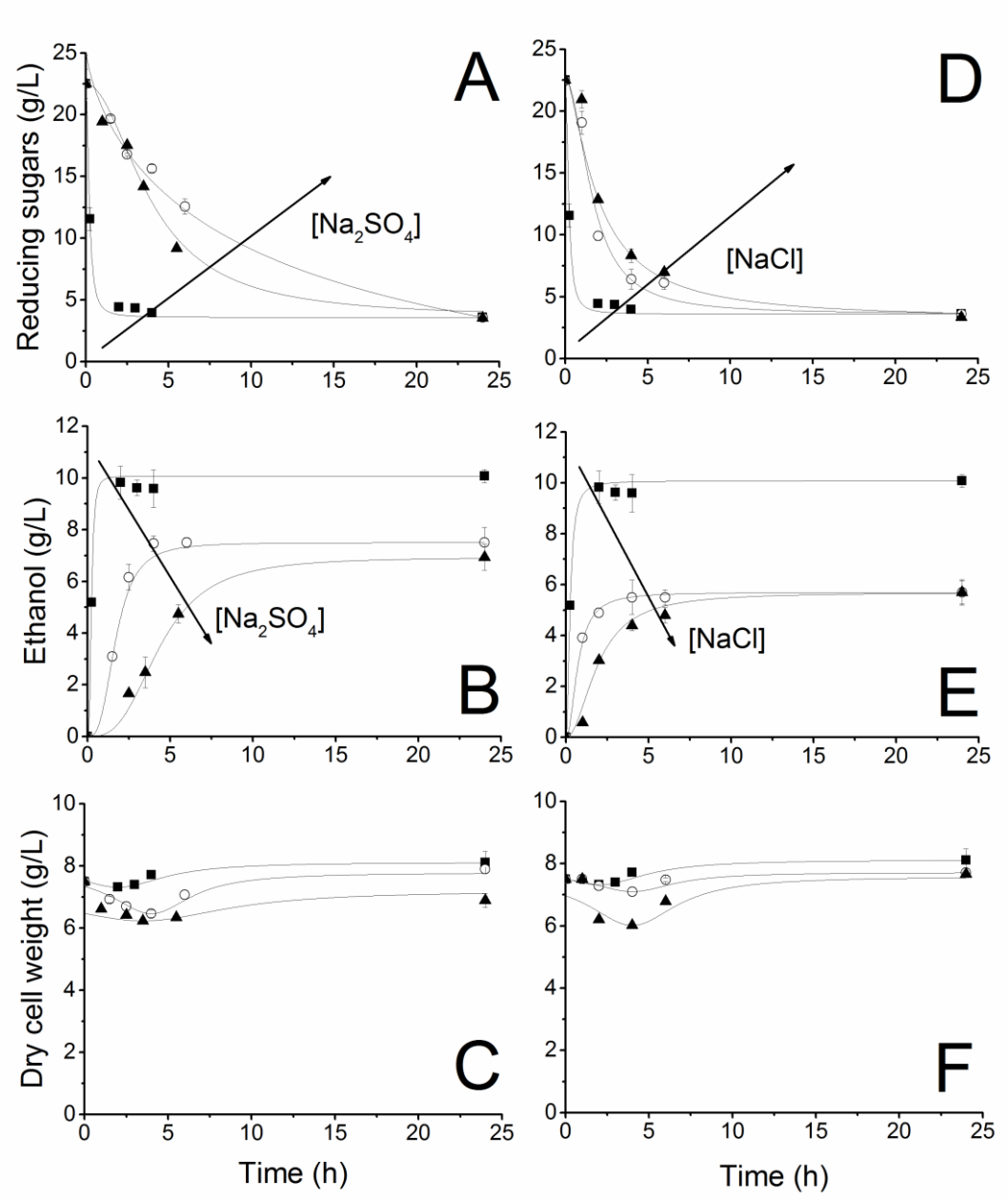

Figure 12.10: Fermentation curves of YPD 20* – A, B and C for Na_2SO_4 and D, E and F for NaCl. (■) no salts, (○) 10 g/L and (▲) 30 g/L.

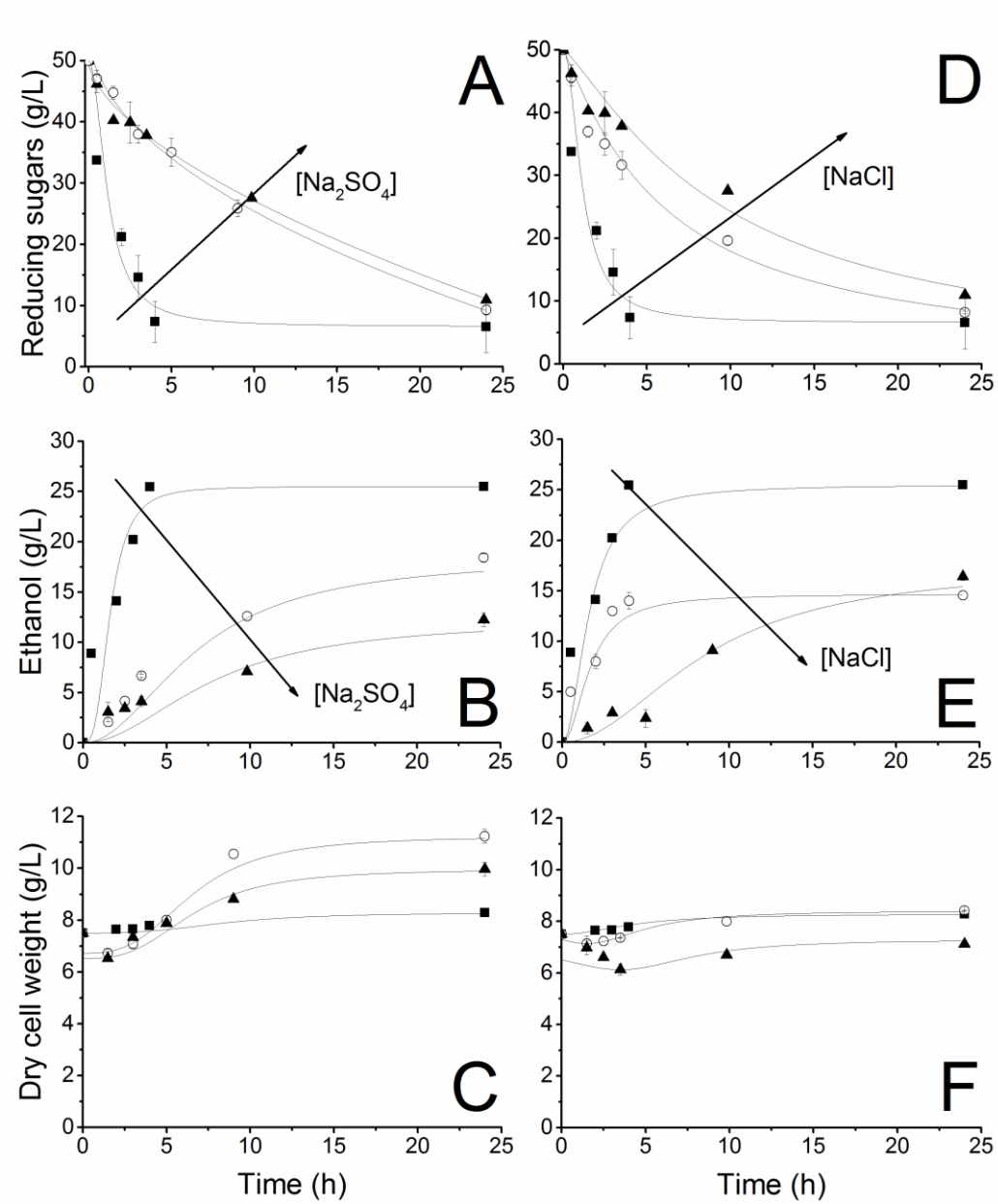

Figure 12.11: Fermentation curves of YPD 50* – A, B and C for Na_2SO_4 and D, E and F for NaCl. (■) no salts, (○) 10 g/L and (▲) 30 g/L.

In **Figure 12.12** the process yield and ethanol productivity for the fermentations under salinity stress are reported. Process yield values between 50 and 75% were achieved, with respect to 90-95% in the control (no salts), despite the sugars have been consumed. Also, ethanol productivity decreased, as a consequence of the slower sugars consumption probably caused by the cellular adaptation to the osmotic environment. For YPD-20* the maximum ethanol production was reached after 4 hours for the experiments with 10 g/L of NaCl and Na_2SO_4, exhibiting values of 1.37 and 1.86 g L^{-1} h^{-1}, respectively. The fermentations with 30 g/L of salt decreased more the ethanol

productivity, confirming inhibition due the osmotic stress. The productivities values (after 24 hours of fermentation) were 0.237 for NaCl and 0.288 g L^{-1} h^{-1} for Na_2SO_4. On the other hand, for YPD-50*, the ethanol productivities found were 0.77 and 0.51 g L^{-1} h^{-1} for 10 g/L and 30 g/L Na_2SO_4, 0.70 and 0.65 for 10g/L and 30 g/L of NaCl, respectively. These significant reductions of ethanol productivity are not desirable from an economic and industrial point of view and further studies to improve cultivation techniques and strains are necessary.

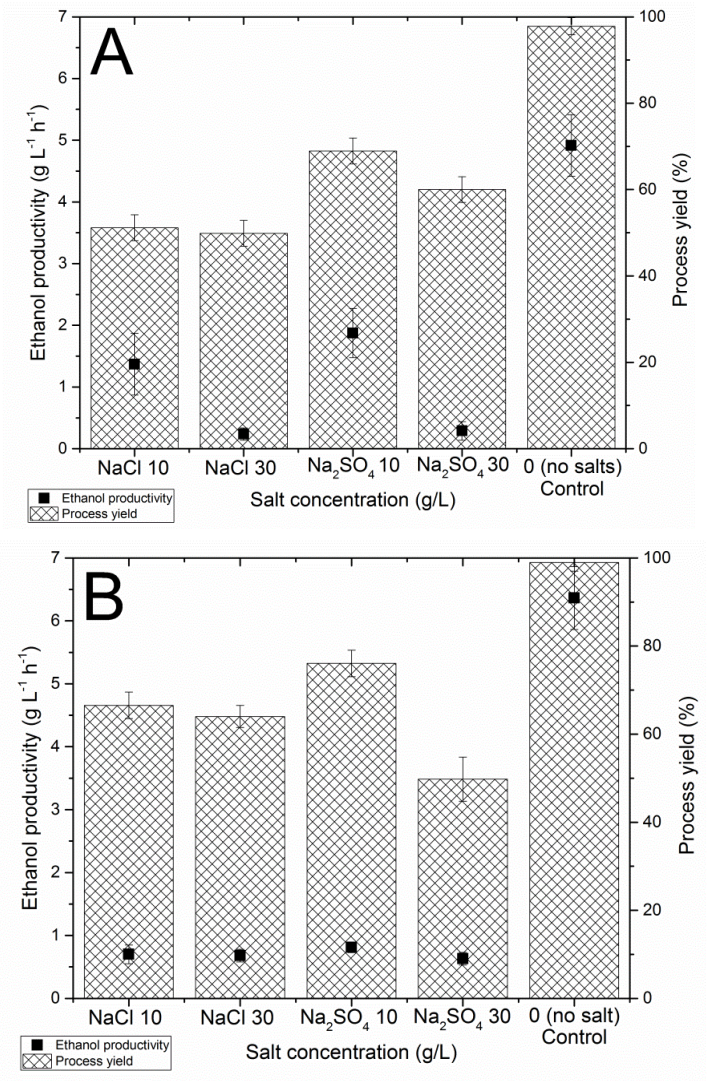

Figure 12.12: Process yield (bars) and ethanol productivity (squares) for the fermentations under saline stress. A) YPD-20 and B) YPD-50.

12.3.4.4 Fermentation of microalgal hydrolysate

The purpose of this last step of the work was to evaluate the performance of ethanol production with real microalgal hydrolysates. All hydrolysis conditions used in this section were defined as best ones during hydrolysis processes (acidic and enzymatic). In acidic hydrolysate fermentation the growth curves of the yeasts exhibited the same profile as those with saline influence (**section 12.3.4.3**) with an initial decreasing of the dry weight and a slightly final growth. On the other hand, for enzymatic hydrolysate the growth curve did not show an extended lag-phase (data not shown).

A positive point was the sugars consumption which demonstrated that almost all sugars can be used by the yeast consortium, mainly in the case of enzymatic hydrolysis. However, ethanol concentration was lower in both cases than the theoretical biochemical conversion value (**Figure 12.13**).

This is a potential problem since a lot of works are dedicated in the hydrolysis process, but if a fermentation process is such lower (around 40%) than a control condition, significative losses in terms of productivity and process efficiency were verified and can invalidate this type of biomass for biofuel applications. Process operating parameters are summarized in **Table 12.2**.

As demonstrated by acidic hydrolysate fermentation from *Chlorella vulgaris* and *Scenedesmus obliquus*, inhibition was found during ethanol fermentation. Enzymatic hydrolysate fermentation was slower than the control condition as well, but faster with respect to acidic hydrolysis, even though the conversion rate were lower In addition, a strange detail was verified, i.e. a significative formation of glycerol. This emphasize that the biomass matrix influences the performance of the strains and further experiments are necessary to understand/improve these aspects. We repeat that together with biomass cultivation and hydrolysis, the fermentation process is of fundamental importance. In literature, contrasting results are found as summarized in the following:

Kim et al. (2014) investigated the fermentation of *Chlorella vulgaris* after enzymatic hydrolysis. The fermentation process was done in continuous (fed with 0.03 mL/min, residence time of 5.55 hours) with *Saccharomyces cerevisiae* at 30°C. At steady state condition 89% of sugars conversion was reached and an ethanol yield and productivity of 78% and 0.11 g L^{-1} h^{-1}, respectively; but considering hexoses sugars (called fermentable sugars in the article). Shokrkar et al. (2017) performed the fermentations of

acid and enzymatic hydrolysates of a biomass of an algae mix. For the enzymatic hydrolysate with 13.5 g/L of reducing sugars obtained a process yield 89.5% after 24 hours of fermentation with a maximum ethanol concentration of 6.2 g/L. From the acid hydrolysate (13 g/L of sugars content), 4.96 g/L of ethanol were produced with a process yield of 75% after 24 hours. Practically all sugars were consumed. Ho et al. (2013b) fermented *C. vulgaris* hydrolysate (acidic and enzymatic) with *Zymomonas mobilis* (ATTC 29191) at 30°C. Enzymatic and acidic fermentation obtained an ethanol process yield og 65.7 and 87%, respectively. In addition, a control fermentation was done with a culture medium containing the same concentration of the hydrolysate total sugars and a faster sugars consumption and ethanol production were verified Thus it was concluded that microalgal hydrolysates are fermented slower than simple sugars obtained from traditional crops. Silva and Bertucco (2017) fermenting *Chlorella vulgaris* acidic hydrolysate (120°C, 3% of acid sulphuric, 30 min of reaction time and 100 g/L of biomass) found an ethanol biochemical yield of 60.6%. Ashokkumar et al. (2015) after acid hydrolysis of *Scenedesmus bijugatus* obtained 100 g/L of reducing sugars which were fermented with *Saccharomyces cerevisiae* (0.01 g/L as initial inoculum). The sugars conversion after 24 hours was 30% (due to the small inoculum used) and after 120 hours was 70%. The process yields were 39% and 72% after 24 and 120 hours, respectively. *Scenedesmus obliquus* acid hydrolysate (16.5 g/L of sugars) fermented with 0.7 g/L of *Zymomonas mobilis* (ATCC 29191) (30°C) achieved an ethanol concentration of 8.55 g/L after 4 hours with an ethanol productivity of 2.13 g L^{-1} h^{-1} (practically all the sugars were consumed and an ethanol yield of 99.8% considering glucose – 80% considering all sugars) (Ho et al., 2013a).

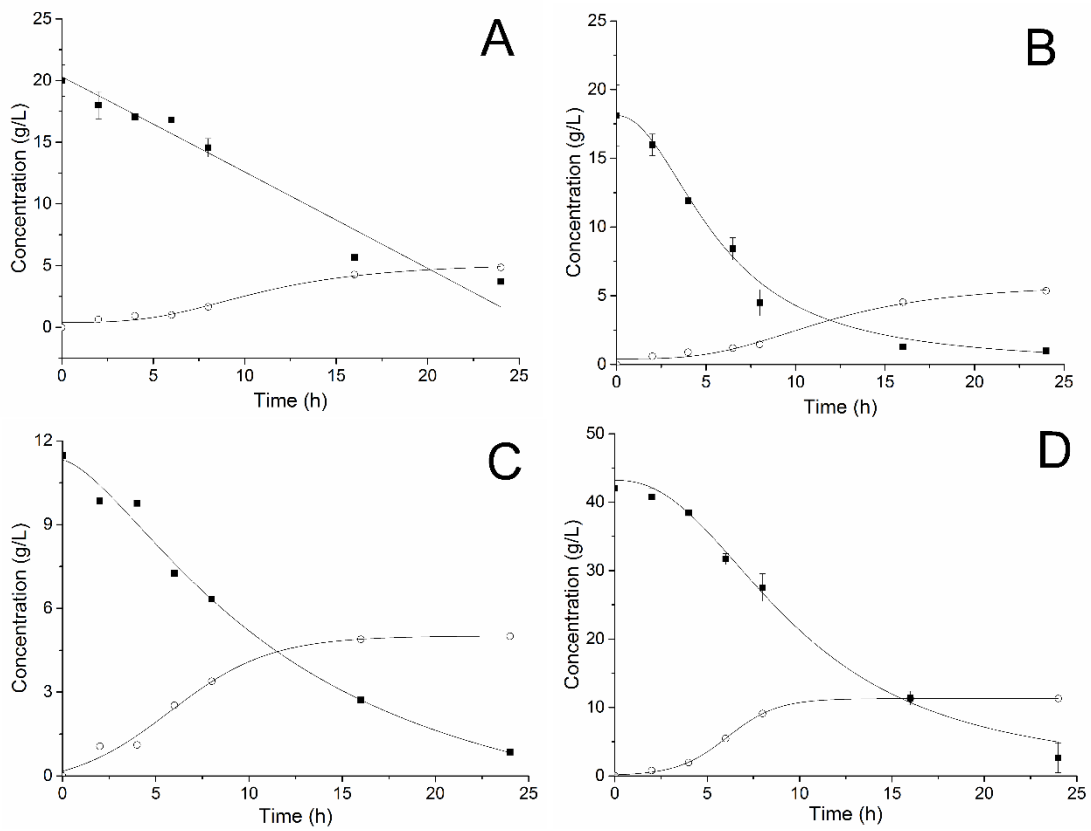

Figure 12.13: Sugars consumption and ethanol production during microalgal hydrolysate fermentation. *Chlorella vulgaris*: A) acidic hydrolysis (100 g/L of biomass, 120°C, 3% of H_2SO_4 and 30 min of reaction time). B) Enzymatic hydrolysate (100 g/L of biomass). *Scenedesmus obliquus*: C) acidic hydrolysis (50 g/L of biomass, 120°C, 3% of H_2SO_4 and 30 min of reaction time). D) Enzymatic hydrolysate (100 g/L of biomass pretreated by ultrasonication and using the enzymatic mix – x). Squares represent sugars and circles are with respect to ethanol concentrations. (■) Reducing sugars and (○) ethanol.

These literature data and the results obtained in our work claim for an uniformization of fermentation representation, and a higher importance and proper discussion of this step, because it is quite of the difficult to understand if it is a problem of yeast acclimation or hydrolysate characteristics, or both and how this aspect can be improved. Sugars consumption, ethanol productivity and biochemical and process yield are the most important parameters to understand the efficiency of the process and must be always compared with respect to a control condition performed with the same microorganism. It is highlighted that biochemical/process yield (ethanol) higher than 95% for a complex biomass hydrolysate is not common. In addition, the effect of process parameters must be discussed with respect to the entire carbohydrates in biomass, and not only glucose, because in a biorefinery approach all carbohydrate fractions are important in view of a biofuel application.

Table 12.2: Fermentation process parameters.

Microorganism	Type of Hydrolysis	Sugars Consumption (%)	Biochemical Yield (%)	Process Yield (%)	Ethanol productivity ($g\ L^{-1}\ h^{-1}$)	Glycerol* (g/L)	Acetic acid* (g/L)
Chlorella vulgaris	Acidic	81.47 ± 6.37	60.68 ± 3.49	49.03 ± 5.21	0.215 ± 0.056	0.75 ± 0.12	1.12 ± 0.08
	Enzymatic	93.04 ± 2.03	53.09 ± 0.68	49.36 ± 0.51	0.234 ± 0.01	8.72 ± 0.16	0.63 ± 0.02
Scenedesmus obliquus	Acidic	92.60 ± 4.35	94.35 ± 2.27**	87.21 ± 5.55**	0.392 ± 0.083	1.32 ± 0.06	0.69 ± 0.06
	Enzymatic	91.71 ± 7.17	44.76 ± 1.82	40.90 ± 1.52	0.425 ± 0.045	8.30 ± 1.45	1.24 ± 0.17

*Final concentration (24 h). **For *Scenedesmus obliquus* the hydrolysis was incomplete (calculus based on reducing sugars) obtaining around 60% of the sugars present in biomass which was remarkably different of *Chlorella vulgaris* that reached more than 90% of sugars recovery.

12.4 CONCLUSIONS

Both acidic and enzymatic methods of microalgal biomass hydrolysis can be used to recover more than 90% of sugars. Biomass pretreatment and enzyme specificity are required to perform the enzymatic process. It was shown that a consortium between *S. cerevisiae* and *P. stipitis* was able to ferment efficiently a mixture between hexoses and pentoses. Salinity influence decreased ethanol biochemical yield and increases the fermentation time, reducing significantly ethanol productivity. Acidic and enzymatic hydrolysates achieved lower process yield in comparison with the control optimized conditions (even though sugars had been almost completely consumed), revealing an additional influence of the biomass matrix. Therefore, further studies in the development of strategies to understand specifically these aspects are necessary.

REFERENCES

Acién, F.G., Fernandez, J.M., Magan, J.J., Molina, E., 2012. Production cost of a real microalgae production plant and strategies to reduce it. Biotechnol. Adv. 30, 1344-1353.

AOAC – Association of Analytical Chemists. Official Methods of Analysis of the Association of Official Analytical Chemists, 17th ed., Gaithersburg: Ed. William Horwitz, 2002.

Asada, C., Doi, K., Sasaki, C., Nakamura, Y., 2012. Efficient extraction of starch from microalgae using ultrasonic homogenizer and its conversion into ethanol by simultaneous saccharification and fermentation. Natural Resources 3, 175-179.

Ashokkumar, U., Salom, Z., Tiwari, O.N., Chinnasamy, S., Mohamed, S., Ani, F.N., 2015. An integrated approach for biodiesel and bioethanol production from *Scenedesmus bijugatus* cultivated in a vertical tubular photobioreactor. Energy Convers. Manage. 101, 778–786.

Arino, J., Ramos, J., Sychrova, H., 2010. Alkali metal cation transport and homeostasis in yeasts. Microbiol Molecular Biology Reviews 74, 95–120.

Blomberg, A., 2000. Methabolic surprises in *Saccharomyces cerevisiae* during adaption to saline conditions: questions, some answers, and model. FEMS Microbiology Let. 182, 1-8.

Casey, E., Mosier, N.S., Adamec, J., Stockdale, Z., Ho, N., Sedlak, M., 2013. Effect of salts on the co-fermentation of glucose and xylose by a genetically engineered strain of *Saccharomyces cerevisiae*. Biotechnology for Biofuels 6(83), 1-10.

Chen, C., Zhao, X., Yen, H., Ho, S., Cheng, C., Lee, D., Bai, F., Chang, J., 2013. Microalgae-based carbohydrates for biofuel production. Biochemical Engineering Journal 78, 1-10.

Choi, S.P., Nguyen, M.T., Sim, S.J., 2010. Enzymatic pretreatment of *Chlamydomonas reinhardtii* biomass for ethanol production. Bioresource Technology 101, 5330-5336.

Ciolfi, C.,Favale, S., Pietromarchi, P., 2012. Production of volatile compounds by mixed culture of *Pichia guilliermondii* and *Saccharomyces cerevisiae*. Vitis 51(4), 191-194.

Favaro, L., Cagnin, L., Basaglia, M., Pizzocchero, V., van Zyl, W.H., Casella, S., 2017. Production of bioethanol from multiple waste streams of rice milling. Bioresource Technology 244, 151-159.

Fu, C.C., Hung, T.C., Chen, J.Y., Su, C.H., Wu, T.W., 2010. Hydrolysis of microalgae cell walls for production of reducing sugar and lipid extraction. Bioresource Technology 101, 8750–8754.

Günan Yücel, H., Aksu, Z., 2015. Ethanol fermentation characteristics of *Pichia stipitis* yeast from sugar beet pulp hydrolysate: Use of new detoxification methods. Fuel 158, 793-799.

Gupta, A., Verna, J.P., 2015. Sustainable bio-ethanol production from agroresidues: a review. Renew. Sust. Energ. Rev. 41, 550 – 567.

Harun, R., Danquah, M.T., 2011. Enzymatic hydrolysis of microalgal biomass for bioethanol production. Chemical Engineering Journal 168(3), 1079-1084. (a)

Harun, R., Danquah, M.T., 2011. Influence of acid pre-treatment on microalgal biomass for bioethanol production. Process Biochemistry 46(1), 304-309.

Hernandez, D., Riano, B., Coca, M., Garcia-Gonzalez, M.C., 2015. Saccharification of carbohydrates in microalgal biomass by physical, chemical and enzymatic pre-treatments as a previous step for bioethanol production. Chemical Engineering Journal 262, 939-945.

Ho, S.H., Li, P.J., Liu, C.C., Chang, J.S., 2013. Bioprocess development on microalgae-based CO_2 fixation and bioethanol production using *Scenedesmus obliquus CNW-N*. Bioresource Technology 145, 142-149. (a)

Ho, S.H., Huang, S.W, Chen, C.Y, Hasunuma, T., Kondo, A., Chang, J.S, 2013. Bioethanol production using carbohydrate-rich microalgae biomass as feedstock. Bioresource Tecnhology 135, 191-198. (b)

Kalyani, D., Lee, M., Kim, T.S., Li, J., Dhiman, S.S., Kang, Y.C., Lee, J.K., 2013. Microbial consortia for saccharification of woody biomass and ethanol fermentation. Fuel 107, 815–822.

Kim, K.H., Choi, I.S., Kim, H.M., Wi, S.G., Bae, H.J., 2014. Bioethanol production from the nutrient stress-induced microalga *Chlorella vulgaris* by enzymatic hydrolysis and immobilized yeast fermentation. Bioresource Tecnhology 153, 47-54.

Lee, O.K., Kim, A.L., Seong, D.H., Lee, C.G., Jung, Y.T., Lee, J.W., Lee, E.Y., 2013. Chemeo-enzymatic saccharification and bioethanol fermentation of lipid-extracted residual biomass of the microalga,*Dunaliella tertiolecta*. Bioresource Technology 132, 197–201.

Lee, O.K., Oh, Y., Lee, E.Y., 2015. Bioethanol production from carbohydrate-enriched residual biomass obtained after lipid extraction of *Chlorella sp.* KR-1. Bioresource Technology 196, 22-27.

Logothetis, S., Walker, G., Nerantzis, E.T., 2007. Effect of salt hyperosmotic stress on yeast cell viability. Proc. Nat. Sci. 113, 271-284.

McMillan, J.R., Watson, I.A., Ali, M., Jaafar, W., 2013. Evaluation and comparison of algal cell disruption methods: Microwave, waterbath, blender, ultrasonic and laser treatment. Applied Energy 103, 128-134.

Miller, J.G., 1959. Use of dinitrosalicyclic acid reagent for determination of reducing sugars. Analytical Chemistry 31(3), 426-428.

Miranda, J.R., Passarinho, P.C., Gouveia, L., 2012. Pre-treatment optimization of *Scenedesmus obliquus* microalga for bioethanol production. Bioresource Technology 104, 343-348.

Mosier, N., Wyman, C., Dale, B., Elander, R., Lee, Y.Y., Holtzapple, M., Landisch, M., 2005. Features of promising technologies for pretreatment of lignocellulosic biomass. Bioresource Technology 96(6), 673-686.

Negahdar, L., Delidovich, I., Palkovits, R., 2016. Aqueous-phase hydrolysis of cellulose and hemicellulose over molecular acidic catalysis: Insights into the kinetics and reaction mechanism. Apllied Catalysis B: Environmental 184, 285-298.

Nguyen, M.T., Choi, S.P., Lee, J., Lee, J.H., Sim, S.J., 2009. Hydrothermal acid pretreatment of *Chlamydomonas reinhardtii* biomass for ethanol production. J. Microbiol. Biotechnol. 19(2), 161-166.

Pancha, I., Chokshi, K., Maurya, R., Bhattacharya, S., Bachani, P., Mishra, S., 2016. Comparative evaluation of chemical and enzymatic saccharification of mixotrophically grown de-oiled microalgal biomass for reducing sugars production. Bioresource Technology 204, 9-16.

Rodrigues, M.A., Teixeira, R.S.S., Ferreira-Leitao, V.S., Bon, E.P.S., 2015. Untreated *Chlorella homosphaera* biomass allows for high rates of cell wall glucan enzymatic hydrolysis when using exoglucanase-free cellulases. Biotechnology for Biofuels 8:25, 1-16.

Shokrkar, H., Ebrahimi, S., Zamani, M., 2017. Bioethanol production from acid and enzymatic hydrolysates of mixed microalgae culture. Fuel 200, 380-386.

Silva, C.E.F., Gois, G.N.S.B., Silva, L.M.O., Almeida, R.M.R.G., Abud, A.K.S., 2015. Citric waste saccharification under different chemical treatments. Acta Scientiarum Technology 37(4), 387-395.

Silva, S.A., Júnior, A.M.O., Silva, C.E.F., Abud, A.K.S., 2016. Inhibitors Influence on Ethanol Fermentation by *Pichia Stipitis*. Chemical Engineering Transaction 46, 367-372.

Silva C.E.F., Sforza E., 2016. Carbohydrate productivity in continuous reactor under nitrogen limitation: Effect of light and residence time on nutrient uptake in *Chlorella vulgaris*. Process Biochemistry 51, 2112-2118.

Silva C.E.F., Bertucco A., 2016. Bioethanol from microalgae and cyanobacteria: A review and tecnhological outlook. Process Biochemistry 51, 1833-1842.

Silva, C.E.F., Sforza, E., Bertucco, A., 2017. Continuous cultivation of microalgae as an efficient method to improve carbohydrate productivity and biochemical stability. 25th European Biomass Conference and Exhibition, Stockholm, Sweden. (a)

Silva, C.E.F., Sforza, E., Bertucco, A., 2017. Stability of carbohydrate production in continuous microalgal cultivation under nitrogen limitation: effect of irradiation regime and intensity on *Tetradesmus obliquus*. Journal of Applied Phycology, in Press. doi: 10.1007/s10811-017-1252-x (b)

Silva, C.E.F., Sforza, E., Bertucco, A., 2017. Effects of pH and carbon source on *Synechococcus* PCC 7002 cultivation: biomass and carbohydrate production

with different strategies for pH control. Appl. Biochem. Biotechnol. 181, 682-698. (c)

Silva, C.E.F., Bertucco, A., 2017. Dilute acid hydrolysis of microalgal biomass for bioethanol production: an accurate kinetic model of biomass solubilization, sugars hydrolysis and nitrogen/ash balance. Reaction Kinetics, Mechanisms and Catalysis, in Press. doi.: 10.1007/s11144-017-1271-2

Trevelyan, W.E., Harrison, J.S., 1952. Studies on yeast metabolism. 1. Fractionation and microdetermination of cell carbohydrates. Biochem J. 50(3), 298-303.

Vitovà, M., Bisova, K., Kawano, S., Zachleder, V., 2015. Accumulation of energy reserves in algae: from cell cycles to biotechnological applications. Biotechnol. Adv. 6, 1204-1218.

Wanderley, M.C.A, Soares, M.L., Gouveia, E.R., 2014. Selection of inoculum size and *Saccharomyces cerevisiae* strain for ethanol production in simultaneous saccharification and fermentation (SSF) of sugar cane bagasse. African Journal of Biotechnology 13, 2762-2765.

Wang H., Chunli J., Shenglei B., Zhou P., Chen L., Liu T., Joint production of bioethanol from filamentous oleaginous microalgae *Tribonema sp*., *Bioresource Technology* 172, 169-173, 2014.

Wang Y., Guo W., Cheng C., Ho S., Chang J., Ren N., Enhancing bio-butanol production from biomass of *Chlorella vulgaris* JSC-6 with sequential alkali pretreatment and acid hydrolysis, *Bioresource Technology* 200, 557-564, 2016.

Conclusions

In this PhD project the potentials of microalgae/cyanobacteria as a biomass source for fermentation applications were addressed, with particular attention to bioethanol production. A process based on the biorefinery concept aimed to maximize biofuel throughput was proposed without considering high-value products. It was shown that this type of biomass can be integrated with the traditional process routes, i.e., those based on sugarcane, corn and lignocellulosics crops. The main process steps investigated were the microalgal cultivation to ascertain the real carbohydrate productivity and the hydrolysis and fermentation to optimize the extraction and conversion of the sugars present in the biomass. Regarding the cultivation step, it was demonstrated that microalgae can accumulate up to 60% of carbohydrates content. *Chlorella vulgaris*, *Scenedesmus obliquus* and *Synechococcus* PCC 7002 were studied. *Synechococcus* exhibited sensitivity to organic buffers and its stability during the entire period of cultivation in batch mode was improved by using an inorganic CO_2-bicarbonate buffer. As a result, a biomass with 60% of carbohydrate content was produced. In addition, continuous cultivation using nitrogen limitation was able to ensure higher productivities in comparison with batch operation mode, and achieved very good results in terms of ethanol productivity with respect to both the traditional and lignocellulosic biomass sources. Values between 2 and 5 times higher were obtained for *Chlorella vulgaris* and *Scenedesmus obliquus*. Also, when outdoor conditions were simulated (day-night cycles) it was possible to produce a carbohydrate-rich biomass, thus helping the feasibility and energetic balance of the process. During the sugars extraction and hydrolysis steps, both acidic and enzymatic methods were shown to able to recover more than 90% of the carbohydrates present in the biomass. Acidic sugars hydrolysis was efficiently modeled with a modified Michaelis-Menten equation, and the severity factor was applied to represent the process as well. Enzymatic hydrolysis was improved thanks to the pretreatment by ultrasonication, thus proposing a promising method in terms of simplicity and energy consumption. Finally, it was possible to consume practically all microalgal sugars by yeasts with a *Saccharomyces* and *Pichia* consortium, even though further experiments are necessary to optimize the fermentation step. Therefore, the potentiality of using microalgae/cyanobacteria for obtaining bioethanol was demonstrated in terms of biomass production and sugars hydrolysis and conversion, but the feasibility of the process and the

life-cycle assessment of all the nutrients used in the cultivation step need additional investigation before achieving a real industrial application.